Towards novel antimicrobials

Chiara Maria Costanzo

School of Chemistry

Swansea University

A thesis submitted to Swansea University in fulfilment of the requirements for the Degree of Doctor of Philosophy

2023

Supervisor: Dr Joel Loveridge

Abstract

The widespread use of antimicrobials has led to the development of resistance to most known active compounds. This has led to the necessity to discover new drugs or adopt new strategies in order to overcome resistance. Benzimidazole is a building block commonly found in pharmaceuticals. It is well known for its antimicrobial, antiviral, anticancer and antiulcer properties as well as antihistaminic, anticoagulant and anti-inflammatory activity. In order to overcome bacterial resistance to β-lactam antibiotics, an *in-silico* screening of the designed benzimidazoles was undertaken leading to a library of compounds with good predicted binding affinity for lytic transglycosylases, a group of enzymes involved in the induction of β-lactamases. Strategies for extending the benzimidazole nucleus were developed, leading to the synthesis of 150 compounds. The synthetic strategies explored led to the discovery of a N_1 / C_2 competition with the recovery of two products in a one pot synthesis. This allowed formation of N_1-alkylated and 2-phenyl analogues as well as 2-pyrrole and 2-thiophene derivatives. The consolidation of the most suitable synthetic method for extending the core in position number 2 furtherly led to bis-benzimidazoles and indole-benzimidazole hybrids. The benzimidazoles synthesized were screened against *E. coli*, *S. aureus* and *P. aeruginosa*, leading to the identification of hit compounds with antibacterial effect, one of them having a comparable activity to ampicillin. Furthermore, as benzimidazoles are well known for targeting tubulin, an attractive target for antiparasitic drugs, the effect of the benzimidazoles against *S. mansoni* was investigated in order to establish their activity against parasitic worms. A hit compound was selected for affecting both phenotype and motility in adult worms. Structure-activity relationship considerations have been proposed and the most promising core modifications leading to antibacterial or antiparasitic activity have been highlighted. Overall, this work has identified new antibacterial and antihelminthic hit compounds that can form the basis for future work to improve potency, confirm the compounds' targets, and investigate other important medicinal chemistry considerations such as selectivity and ADME properties.

Declarations

This work has not previously been accepted in substance for any degree and is not being concurrently submitted in candidature for any degree.

████████████████

Signed...

Date..31/03/2023...

This thesis is the result of my own investigations, except where otherwise stated. Other sources are acknowledged by footnotes giving explicit references. A   bibliography   is appended.

████████████████

Signed...

Date.. 31/03/2023...

I hereby give consent for my thesis, if accepted, to be available for electronic sharing **after expiry of a bar on access approved by the Swansea University.**

████████████████

Signed...

Date.. 31/03/2023...

The University's ethical procedures have been followed and, where appropriate, that ethical approval has been granted.

████████████████

Signed...

Date.. 31/03/2023...

Table of contents

Acknowledgements

Abbreviations

DNA	deoxyribonucleic acid
RNA	ribonucleic acid
9BBN	9-borabicyclo[3.3.1]nonane
Ac_2O	acetyl anhydride
Ala	Alanine
Amp	ampicillin
Arg	arginine
Asn	asparagine
AUR	auranofin
BZI	benzimidazole
DHP	3,4-dihydropyran
DMAP	4-(dimethylamino)pyridine
DMSO	dimethyl sulfoxide
EtOH	ethanol
GlcNAc	N-acetylglucosamine
Gln	glutamine
Glu	glutamic acid
Gly	glycine
Gram-	Gram negative bacteria
Gram+	Gram positive bacteria
HAS	albumine
HCl	hydrochloric acid
HEWL	lysozyme
His	Histidine
HY	Hybrid
LBDD	Ligand-Based Drug Design
LiAlH4	lithium aluminium hydride
LT	Lytic transglycosylases
MeOH	methanol
Met	Methionine
MurNAc	N-acetylmuramic acid
NaBH4	sodium borohydride
NAG	N-acetylglucosamine
NAM	N-acetylmuramic acid
p-TsCl	p-toluenesulfonyl chloride
Phe	phenylalanine
PZQ	praziquantel
SBDD	Structure-Based Drug Desing
Ser	serine
TEA	triethylamine
TMSCl	trimetylsilyl chloride
Tyr	tyrosine
VS	Virtual Screening

Chapter 1

Introduction

1 Introduction

1.1 Microbes

Microbes are microorganisms that can be distinguished into prokaryotic (bacteria and archaea), eukaryotic (protists, fungi and algae) and viruses. They play a critical role in nutrition and human health.[1,2,] Many microorganisms, mainly bacteria but also viruses, fungi and protozoa, live in the human gastrointestinal tract. Gut microbes contribute to the maintenance of a healthy condition being involved in several key processes in the body and modulating key aspects such as immune and metabolic response.[1,3,4] Despite their positive effects, microbes can be harmful leading to diseases.

Changes in the population of gut microbes as well as pathogenic infections can harm the health condition.[5] Pathogens are microorganism that invade and use the human/animal body to sustain, reproduce and colonize themself.[6] Microbes need to penetrate into the body, reach their target cells or a favorable environment for their growth and replication. They can access the body through oral/urethral cavities, skin or eyes, suppress defense mechanisms from the body and finally acquire the necessary substances for their survival. Microbes can colonize cells or use substances from the host, interact with specific protein and alter host cellular mechanisms. The microbial invasion can lead to several alterations of the host's health condition such as cell dysfunction, cell death and inflammation.

In order to combat microbial infections and restore the health condition, antimicrobial agents have been developed for over 100 years.[7,8] Antimicrobials are therapeutic agents used in the treatment of microbial infections. They aim to kill, damage or limit the growth of microorganisms. Due to the structural and biochemical difference between prokaryotic and eukaryotic cells, antimicrobial agents target different structures/mechanisms depending on the microbe they target.

1.2 Antibacterials

Antibiotics are compounds used for the treatment of bacterial infections. Bacteria are unicellular prokaryotic microorganisms consisting of a simple cell and no nucleus with the genetic material having no specific location into the cell. Some bacteria can also have plasmids, circular DNA that

replicates insentiently from the chromosome. They have different size and shape (spherical-shaped bacteria are known as *cocci*; spiral-shaped are known as *spirilla* while rod-shaped bacteria are known as *bacilli*), they usually have a flagellum that allows motility and can have pili. Bacteria have a cell wall (peptidoglycan is the major constituent) and a plasma membrane allowing transport of molecules. They are distinguished in Gram positive (Gram+) and Gram negative (Gram-) on the basis of their different colors when treated with Gram stain.[9] This is connected to their structural differences: Gram+ bacteria have a thick layer of peptidoglycan, the main component of the bacterial cell membrane, which avoids the removal of the typical compounds of the Gram stain from the cytoplasm giving a blue/violet coloration of cells on light microscope.

Bacteria invade the host and alter critical intracellular pathways, such as apoptosis,[10] for the survival. Antibiotics[11,12] have been introduced since long time in order to contrast bacterial infections. Antibacterial agents can inhibit bacterial growth interfering with bacterial DNA replication or general cellular metabolism without directly producing cell death (bacteriostatic activity) or they can kill bacteria (bactericidal activity). The difference between prokaryotic and eukaryotic cells leads to advantages in the treatment of human conditions with antibiotics: targets are either not present in human/mammalian cells or they are significantly different. Due to this, antibiotics are selective for bacterial cells and don't have impact on eukaryotic cells even if they can have side effects. Multiple pathways can be targeted by antimicrobial agents. They can inhibit the synthesis of bacterial nucleic acid and protein as well as cell wall.

Antifolates,[13] such as sulfonamides and trimethoprim, inhibit the synthesis of tetrahydrofolate which is involved in the synthesis of amino acids and nucleobases. Sulfonamides (sulfadiazine, sulfadoxine, and sulfisoxazole; Figure 1.1A-C) inhibit dihydropteroate synthase while trimethoprim (Figure 1.1D) inhibits dihydrofolate reductase, two key enzymes involved in the synthesis of tetrahydrofolate. This induces inhibition of DNA synthesis and bacterial cell lysis. A further class of critical antibiotics is given by quinolones, such as ciprofloxacin (Figure 1.1E).[14] They stabilize the gyrase-DNA complex, during the bacterial DNA reproduction, stopping the synthesis of DNA in bacteria and leading to cell lysis. Quinolones also target topoisomerase IV in Gram+ bacteria, inhibiting DNA decatenation followed by DNA replication or introduction of positive DNA supercoils. Rifampin[15] targets a different pathway. It inhibits RNA polymerase which is an enzyme able to bind DNA sequences called promoters and initiate the DNA transcription. This leads to the inability to produce a RNA molecule complementary to the DNA strand giving incorrect gene transcription and bacterial cell death. Tetracyclines (Figure 1.1F),[16]

aminoglycosides, such as streptomycin (Figure 1.1G), and macrolides, such as azithromycin (Figure 1.1J) inhibit the protein synthesis in bacteria binding the 30S or 50S subunit of ribosome. This gives non-functional proteins compromising the bacterial cell. One of the most important targets for antimicrobials is the cell wall synthesis.
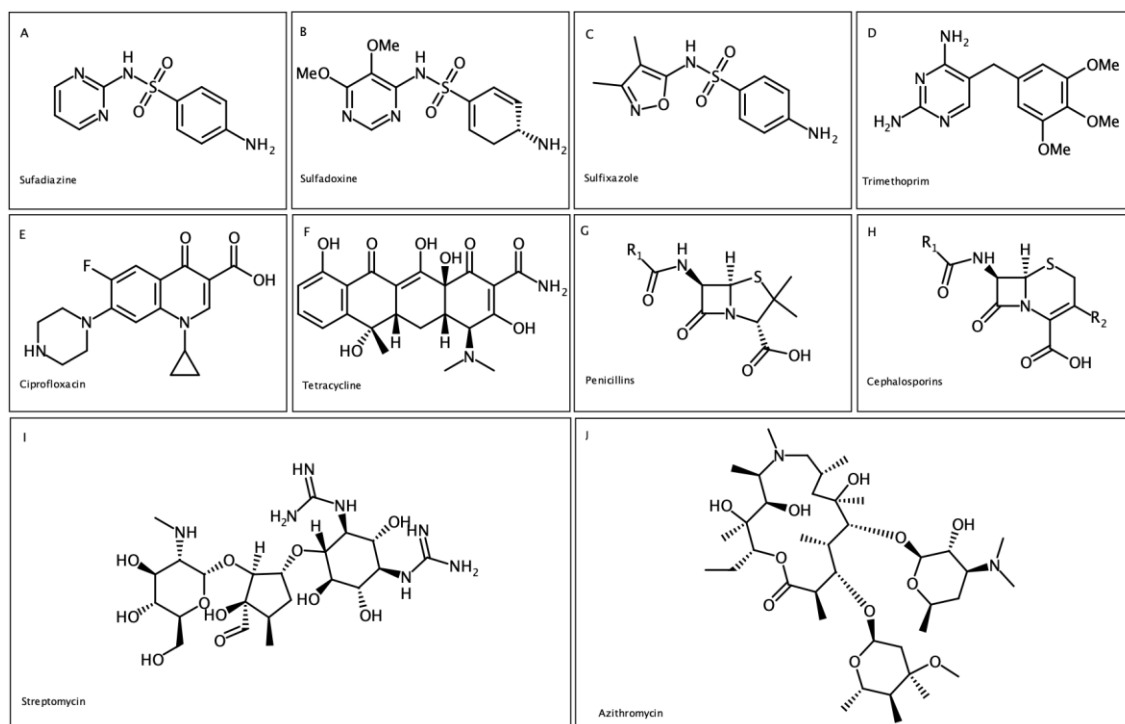

Figure 1. 1: Representative antibiotic structures.

β-lactams,[17] such as penicillins and cefalosporins (Figure 1.1 G-H), inhibit the transpeptidation reaction used by bacteria to form cross-linking between different peptidoglycan strands. This destabilizes the bacterial cell wall leading to osmotic lysis. Vancomycin and bacitracin also target cell wall synthesis, but by different mechanisms of action. Vancomycin binds the acyl-D-ala-D-ala portion of the peptide chain in peptidoglycan, which prevents the cross-linking between stands. Bacitracin interferes with the dephosphorylation of membrane carrier molecules, which are involved in transporting building blocks critical in peptidoglycan synthesis.[18,19]

1.3 Antifungals and antiparasitics

Protists and fungi are eukaryotic organisms. Fungi can be unicellular or multicellular, they have a defined nucleus containing genetic material and membrane-bound organelles. Fungi have a cell wall containing chitin and glucan. They also have a plasma membrane having ergosterol[20] as

4

main sterol component. Ergosterol plays a critical role preserving cell stability and integrity and it represents one of the main targets for antifungal drugs. Fungi have an important role as they break down organic matter but they can also be pathogenic invading a host and leading to the development of fungal infections.[21] Fungal infections can be skin located or systemic. *Candida albicans* is a common fungal pathogen causing candidiasis.[22] If not controlled, candida can cause several health issues such as infections in the organs (kidney, hearth or brain) leading to candidemia, a life-threatening condition.[23] Fluconazole (Figure 1.2A) and itraconazole are antifungal drugs commonly used for treating candida.[24]

Like fungi, protists are microbes having nuclei and membrane bound organelles. Parasites[25] are microbes that live inside a host and benefit from the hosts resources. They can be distinguished in protozoa, helminths and ectoparasites. Protozoa,[26] such as *Trypanosoma cruzi* and *Plasmodium* parasites, are unicellular microbes. *T. cruzi* is a parasite causing Chagas' disease, a life threatening disease[27,28] that leads to cardiopathy and gastrointestinal tract complications. Malaria is a further example of a life-threatening condition. It is caused by *Plasmodium* parasites.[29] Malaria generally gives high fever and it can progress leading to respiratory, kidney and liver failure as well as cardiovascular collapse and shock. Chloroquine[30] (Figure 1.2B) is the first choice for the treatment of malaria. Helminths are parasitic worms with flat or round bodies.[31] Their life is characterized by different stages: eggs, larvae and adult worms. They are distinguished into trematodes, cestodes and nematodes and cause several extraintestinal or intestinal diseases. Ectoparasites[32] are microbes that live on the host skin causing severe pruritis, dermatitis and disease such as scabies[33] which is caused by *Sarcoptes scabiei*.
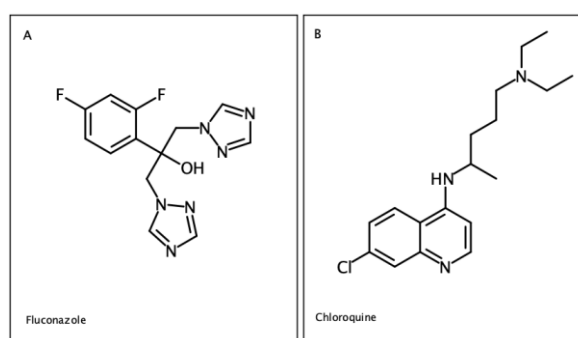

Figure 1. 2: Representative antifungal and antiparasitic structures.

Antiparasitic drugs[25] have multiple mechanism of actions. They usually aim to kill the parasite's eggs or directly the parasite, to stop the parasite growth or to inhibit its motility in order to avoid the attachment of the parasite to the host which now can't use the host's resource for surviving. Paromomycin is a drug used in the treatment of leishmaniasis[34] while nifurtimox or benznidazole

are trypanocide drugs able to contrast the infections mediated by *T. cruzi*.[35] Anthelmintic drugs can aim to kill the worms (vermicides) or they can remove the worms from the body during their life-time (vermifuges). Albendazole, a benzimidazole-based compound, is a common antiparasitic drug used in the treatment of nematode infections.[36] It is known for blocking the microtubule system.

Tubulin is an attractive target for antifungal and antiparasitic drugs. It a protein able to polymerize forming microtubules which are the main component of the cytoskeleton. Microtubules are structures involved in several critical cell processes such as cell division, intracellular transport of substances as well as cell motility.[37] Tubulin is a dimer composed of α- and β-tubulin which polymerize forming microtubules. Tubulin is a dynamic structure, constantly subjected to depolymerization and polymerization processes which are GTP mediated.[37] Due to the critical role played by tubulin in key cellular processes, it represents a fascinating target for antifungal and antiparasitic drugs.[37] Tubulin inhibitors disrupt the dynamic of microtubules harming critical processes in the cell such as cell division and intracellular trafficking. Several tubulin targeting agents are already used as antifungal and antiparasitic drugs, such as colchicine, or albendazole and mebendazole (Figure 1.3A-C) which are benzimidazole-based compounds.[37]
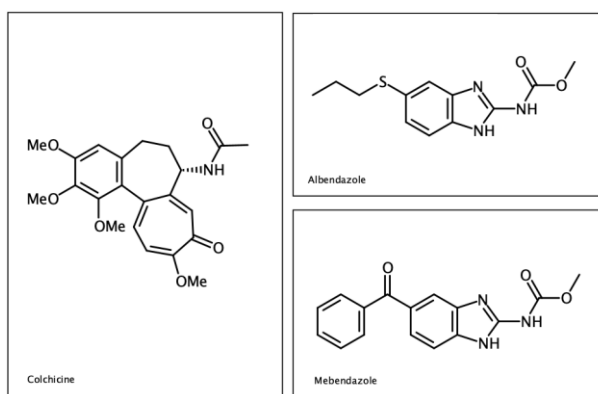
Figure 1. 3: Representative tubulin inhibitors. A) colchicine, B) albendazole, C) mebendazole.

Colchicine is an alkaloid extracted from *Colchicum autumnale* while albendazole and mebendazole are methyl-1H-benzimidazole-2-yl-carbamates holding a substituent in position 5 of the benzene moiety. It is possible to distinguish three tubulin binding sites, named colchicine, vinblastine and taxol sites. Benzimidazoles are known for binding β-tubulin (colchicine binding site) and several studies have been undertaken in order to identify the key interactions leading to the target inhibiton.[38,39]

Mebendazole creates a network of interactions in complex with tubulin (Figure 1.4; PDB 7OGN).[40] The N-H hydrogen atoms of both the benzimidazole and the amide form hydrogen bonds with the carboxyl group of Glu200 while the oxygen atom of the carbamate moiety interacts with Asn167.
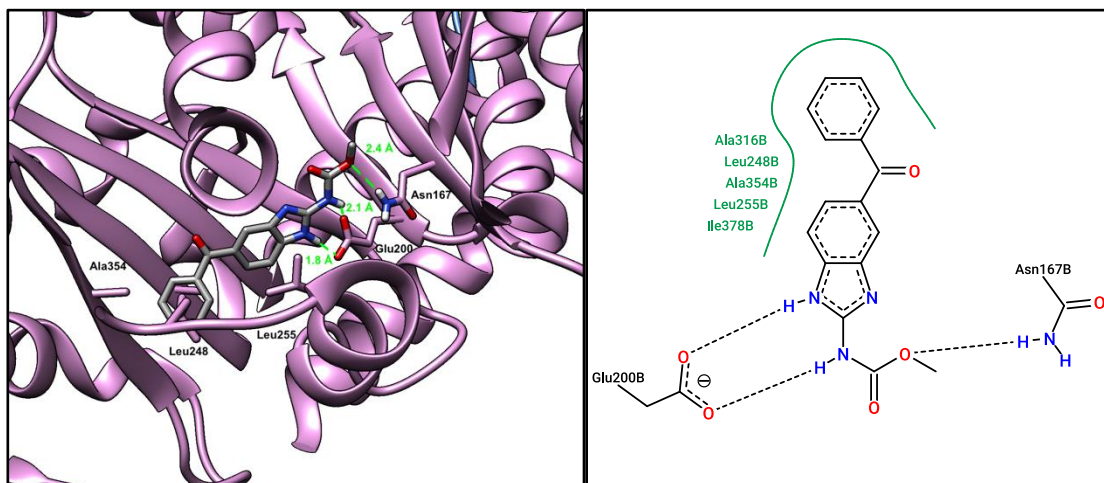

Figure 1. 4: Left- Cartoon representation of tubulin (purple) in complex with mebendazole (shown as sticks) (PDB 7OGN). Right- 2D diagram of tubulin-mebendazole interactions.

In addition, mebendazole is able to form hydrophobic contacts with several active site residues (Ale316, Leu248, Ala354, Leu255 and Ile378) located in a hydrophobic pocket of the tubulin active site. This non polar moiety of the ligand seems to play a critical role in the binding as well as the imidazole part of the benzimidazole core which hold a C_2-extension.

1.4 Antimicrobial resistance

The widespread use of antimicrobials led to the development of resistance to most known active compounds.[41, 42] This in turn has led to the necessity of discovering new drugs or adopting new strategies in order to overcome the resistance.[43] For example, *Candida auris* is a new emergent fungal strain, which has been identified on every continent except Antarctica since its discovery in 2009, and which is well known for its resistance to drugs that usually work on *Candida*.[44,45] It is considered a multidrug resistant strain with intrinsic resistance to fluconazole and limited sensitivity to other azole antifungal drugs including amphotericin B, echinocandins and 5-flucytosine. Resistance among protists such as malaria is also a big concern. Malarial strains resistant to aminoquinolones, antifolates and artemisinin-based drugs represent a major challenge to the treatment of malaria.[46] Drug resistance is also a problem in multicellular parasites.[47] Resistance to antimicrobials occurs through multiple mechanisms including cellular

efflux pumps to actively expel antimicrobials from the cell, changes in membrane permeability leading to the antimicrobials' inability to enter the cell, changes in drug receptors that prevent drug binding or decreased expression of drug target molecules, as well as, in fungi, alterations in sterol biosynthesis.[48] The development of bacterial resistance and inactivation of the known active compounds led to the urgent necessity of new strategies for fighting bacterial infections.[49] Combination therapy[50,51] is given by the association of multiple drugs having different mechanisms of action. This can harm multiple key paths in the bacterial cells representing one of the most promising options in the fight against bacteria resistance. The association between β-lactam antibiotics and β-lactamases inhibitors[52] is an important example. One mechanism of resistance to β-lactams is the production of β-lactamases, enzymes that are able to covalently bind the antibiotic and break its structure, deactivating it.[53] The co-administration of β-lactamase inhibitors is a strategy adopted for combatting β-lactam resistance. The inhibition of β-lactamases leads to the enhancement of the antibiotic life-time. A further example of combination therapy is given by co-administration of sulfonamides and trimethoprim.[54] These drugs inhibit two enzymes of the synthesis of tetrahydrofolate, strongly disrupting this cellular path. The introduction of new active compounds as well as the reintroduction of "old" antimicrobials [55] represent further promising strategies for combatting the bacteria resistance.

1.4.1 Bacterial cell wall recycling silently connected to bacterial resistance

The bacterial cell wall is a key structure that protects the bacterial cell from the high internal pressure and confers the typical shape. Being a dynamic structure, it is able to mediate bacterial cell growth and division. Peptidoglycan (PG, also called murein) is the main component of the cell wall.[56] It is a polymer made of a repetition of the dimer N-acetylglucosamine (NAG) and N-acetylmuramic acid (NAM), with a peptide appended to the lactyl moiety of NAM (Figure 1.5). These peptide chains are connected by a transpeptidase reaction creating a cross linkages between neighboring strands of peptidoglycan and generating a structure critical for the stability of the bacteria cell wall. The cell wall mediates bacterial cell growth and division throughout a constant process of remodeling guided by degrading and synthesizing enzymes. This allows the recycling of old peptidoglycan as well as the insertion of new cell wall material.[57]

The peptidoglycan recycling process plays a role in the resistance to β-lactam antibiotics.[58] Lytic transglycosylases (LTs) are critical murein-degrading enzymes in Gram negative bacteria. They

are space makers, being able to catalyze the cleavage of the β-1,4-glycosidic bond between NAM and NAG residues in peptidoglycan, (like lysozyme), but with the concomitant formation of a 1,6-anhydro bond between the O6 and C1 atoms in the NAM residue (unlike lysozyme, which catalyzes a direct hydrolysis). The product deriving from their activity, 1,6-anhydromuropeptide, is then internalized into the bacterial cell and used in the recycling process. In presence of β-lactams, the anhydromuropeptides can induce AmpC β-lactamase production leading to β-lactam resistance.
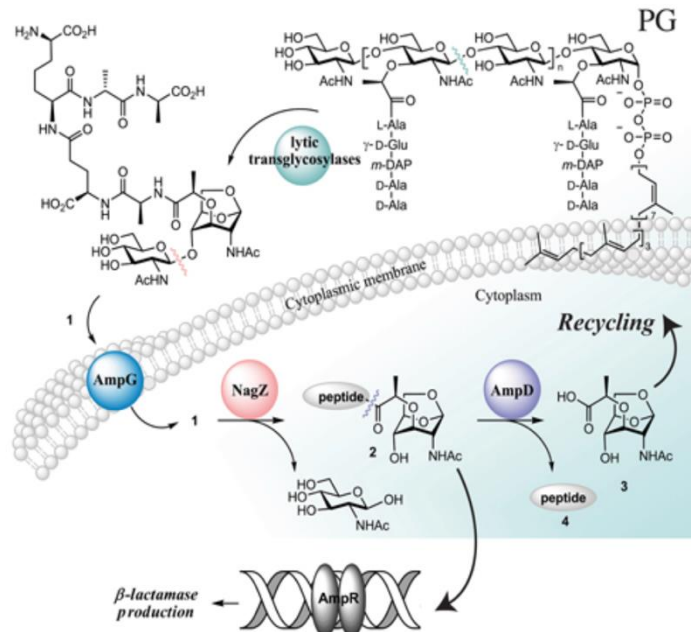
Figure 1. 5: The link between bacterial cell wall recycling and β-lactamase production.[58]

The inhibition of LT could directly harm the peptidoglycan recycling process, compromising the cell wall integrity. Moreover, in combination with a β-lactam, LT inhibitors could inhibit the β-lactamase production and so overcome the resistance to β-lactam antibiotics. Inhibition of lytic tranglycosylases could represent a promising synergistic strategy for enhancing the activity of β-lactams and avoiding their inactivation.

1.4.2 Lytic transglycosylases and lysozyme

Lytic transglycosylases (LT)[59,60,61] and lysozyme[62] are both classes of enzyme involved in peptidoglycan structure breakage. Their mechanism of action is similar, but the final step differs leading to different products (Figure 1.6). Lysozyme hydrolyzes the glycosidic bond between

NAM and NAG residues in peptidoglycan leading to the formation of MurNAc and GlcNAc residues while LTs perform an intramolecular glycosyl transfer reaction resulting in the formation of 1,6-anhydromuropeptide and GlcNAc residue.
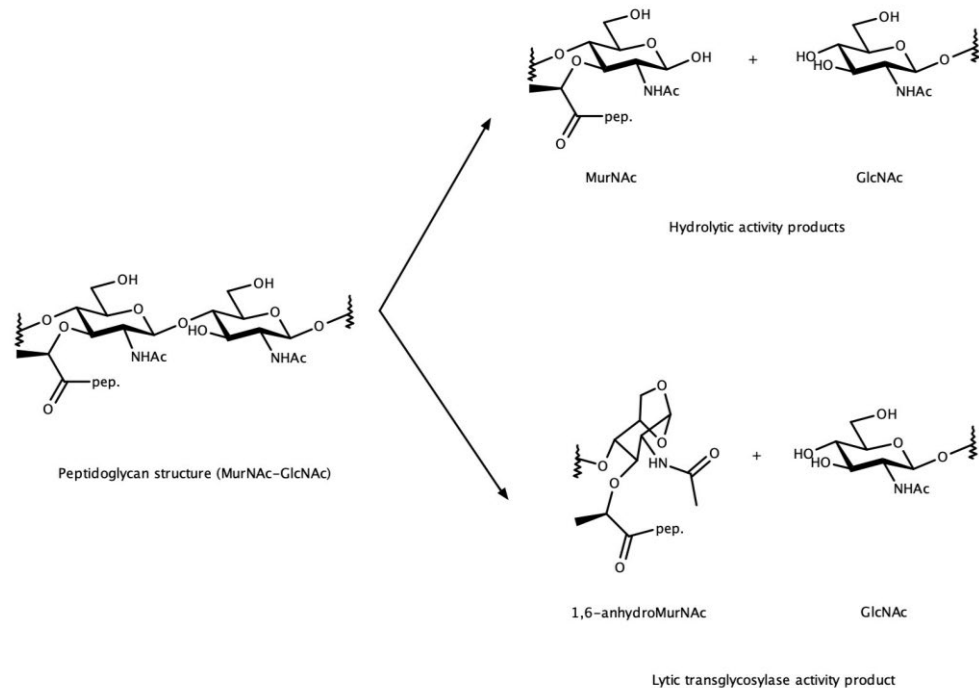
Figure 1. 6: Key differences in the lytic action of lysozymes and lytic transglycosylases.

The products deriving from their activity are different due to their catalyzed mechanism. In the first step of the lysozyme-catalyzed reaction, the catalytic glutamic acid residue (Glu35) donates a proton to the oxygen atom of the glycosidic bond (Figure 1.7). This leads to the breakage of this bond giving the formation of the oxocarbenium intermediate ion which is favored and stabilized by steric distortion of the NAM residue from a low-energy chair conformation toward a higher energy half chair or sofa conformation and by the electrostatic interaction with the carboxylate group of the catalytic aspartate (Asp52). The first product obtained from this step then diffuses away and it is replaced into the active site by a water molecule. The water,

activated by the Glu35, attacks the C_1 carbon atom of the oxocarbenium ion giving the second product of the lysozyme mechanism.
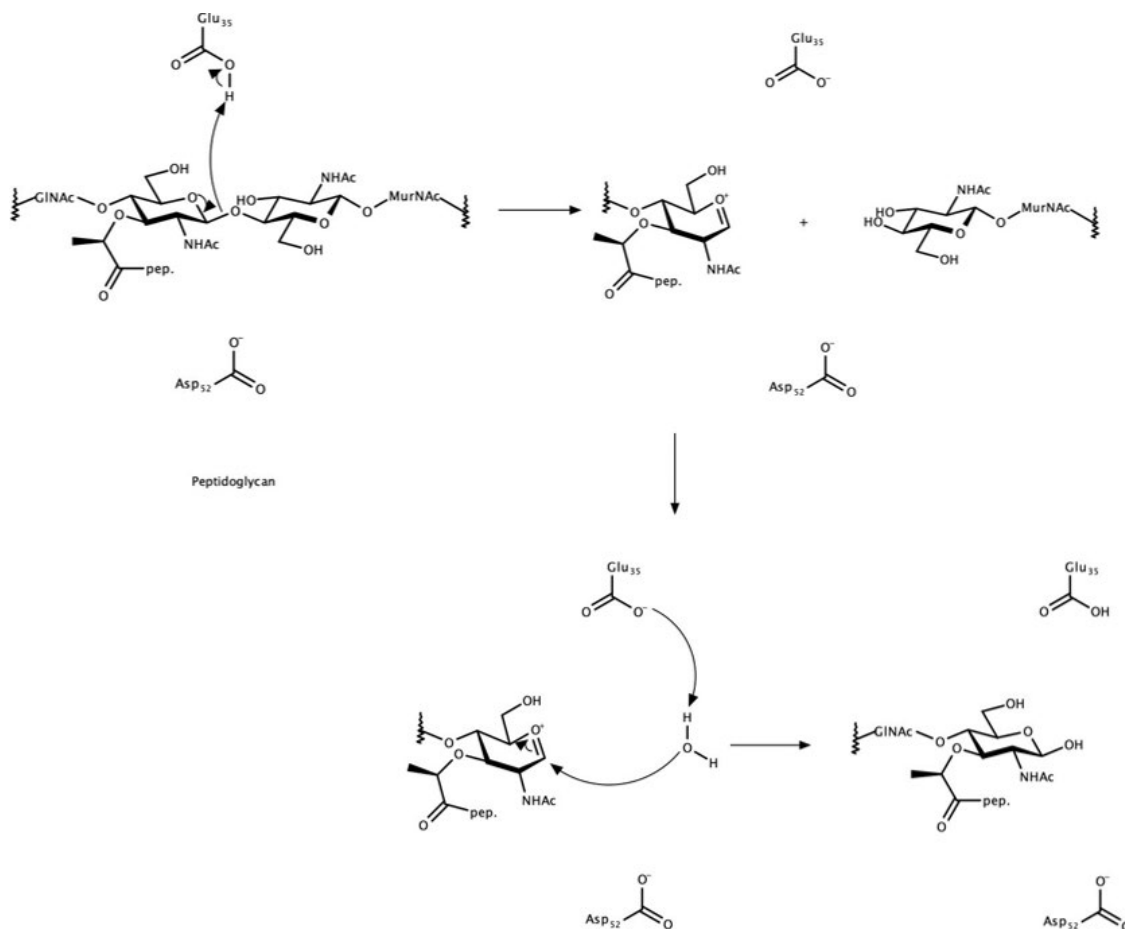
Figure 1. 7: Mechanism of peptidoglycan hydrolysis catalysed by lysozymes.

The first step of the lytic transglycosylase catalytic reaction (Figure 1.8) is similar to that of lysozyme.[63,64, 65] The catalytic glutamic acid residue acts as acid and leads to the breakage of the glycosidic bond with the formation of the first product and the oxocarbenium intermediate ion. In the second step of the reaction, an oxazolinium ion is formed by anchimeric assistance from the acetamido group, which attacks the C_1 atom of the sugar ring. This step should be driven by formation of a more stable oxazolinium species having a positive charge shared between the nitrogen and the oxygen atoms. Then, instead of a water molecule attacking C_1, the catalytic glutamic acid acts as a base, activating the oxygen atom of the C_6-hydroxyl group of the NAM residue, which performs an intramolecular nucleophilic attack on the C_1 carbon to form the 1,6-anhydromuropeptide product. In order to have an optimal interaction between the C_6-hydroxyl

group and the C_1 carbon, the glycosidic ring must adopt a distorted conformation with the hydroxymethyl group in an axial position.
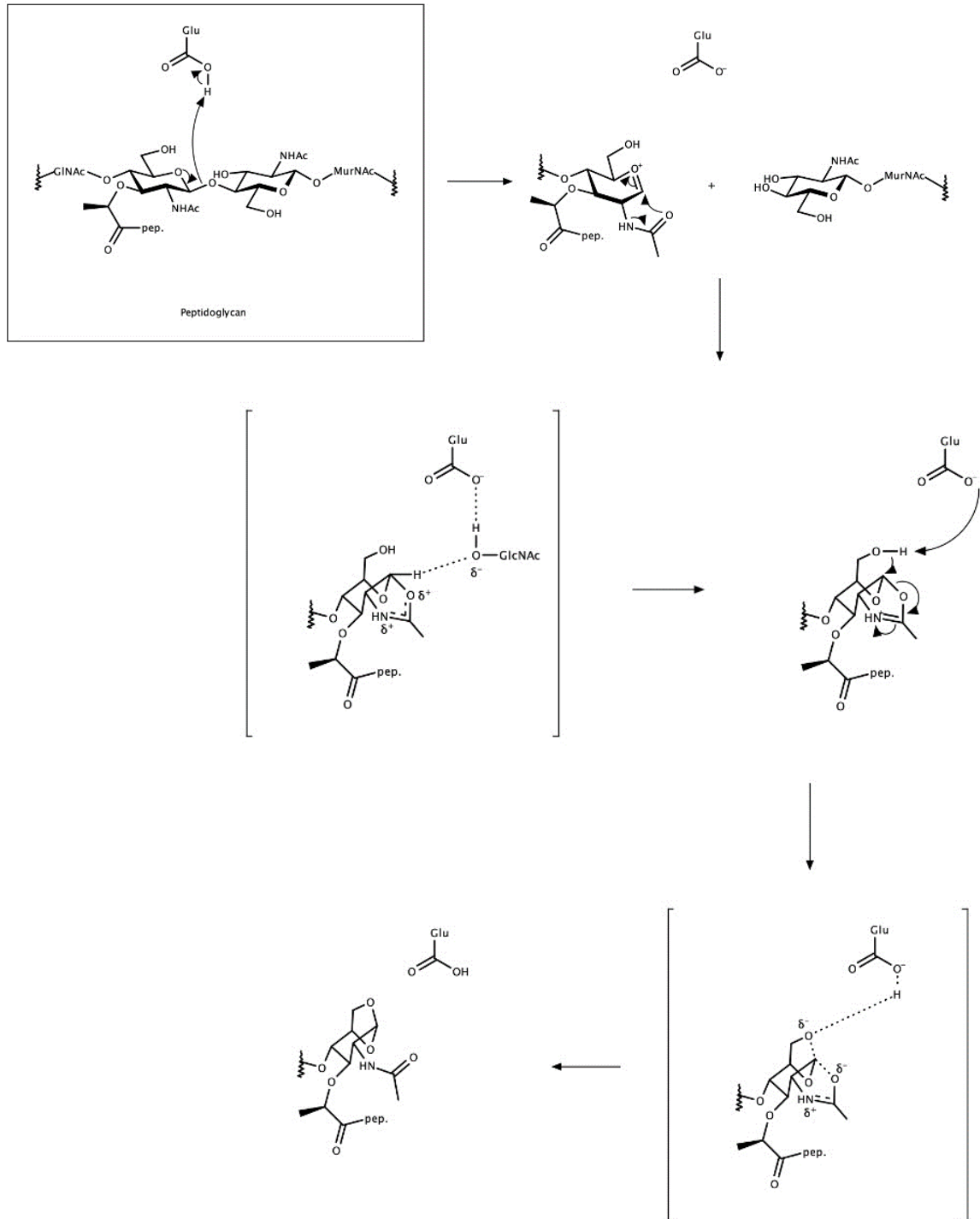
Figure 1. 8: Mechanism of peptidoglycan breakdown catalysed by lytic transglycosylases.

The favorable interaction between the carbonyl oxygen atom of the substrate N-acetyl group and some residues of the enzyme, which may assist the catalysis, guide the stabilization of the intermediate. Moreover, a reorientation of enzyme domains is possible, which could narrow the peptidoglycan binding groove prohibiting the access of water molecules close to the C_1 carbon atom of the oxocarbenium ion intermediate leading so to the formation of the 1,6-anhydro product instead of the lysozyme product.

Following this catalytic mechanism, LTs act as zippers during the cell division and peptidoglycan recycling process. *Escherichia coli* encodes eight LTs named Slt70, MltA, MltB, MltC, MltD, MltE, MltF, MltG. The first is a soluble enzyme located in the periplasmic space while the others are bound to the inner leaflet of the outer cell membrane. They differ in size and shape but they all catalyze the same reaction. Slt35, a naturally occurring fragment of MltB formed when the first 39 residues are cleaved, has been considered a model LT structure.[66,67]

1.4.3 Known LT inhibitors

Due to the critical role that LT inhibitors could have in the overcoming of bacteria resistance when in combination therapy with a β-lactam, the analysis of the structure of known LT inhibitors is critical. They are all competitive inhibitors, replacing the natural substrate into the LT active site.
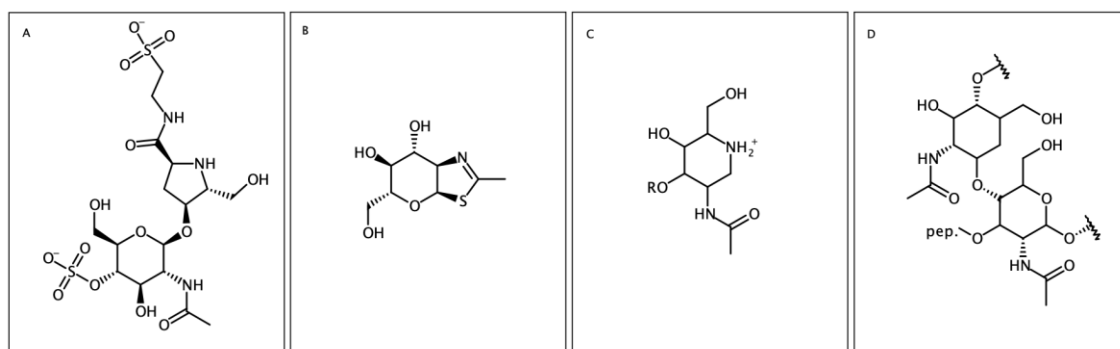
Figure 1. 9: Known lytic transglycosylase inhibitors. A) Bulgecin A, B) NAG-thiazoline, C-D) iminosaccharides.

One of the most studied inhibitors is Bulgecin A (Figure 1.9A).[68,69] It is an O-sulfated glycopeptide produced by *Pseudomonas acidophila* and *Pseudomonas mesoacidophila*, which lacks any antibacterial activity by itself but has a synergistic effect in combination with β-lactams, enhancing their antibacterial activity. N-Acetylglucosamine thiazoline (NAG-thiazoline; Figure 8B), is a further LT inhibitor which mimics an intermediate in the LT-catalyzed reaction.[70] Finally, some iminosaccharides (Figure 1.9C-D) have been found to bind MltB and so inhibit its activity.

1.4.4 Binding of bulgecin A to Slt35

Investigations on the forces driving binding to the LT active site are a key step in developing inhibitors. The analysis of interactions between the known inhibitor Bulgecin A and the Slt35 has been critical to design ligands which could mimic the structure of Bulgecin. The crystal structure of Slt35 in complex with bulgecin A has been solved (PDB 1D0L).[67] Bulgecin A is able to strongly inhibit Slt35 forming a complex network of hydrogen bonds with the LT active site residues (Figure 1.10).
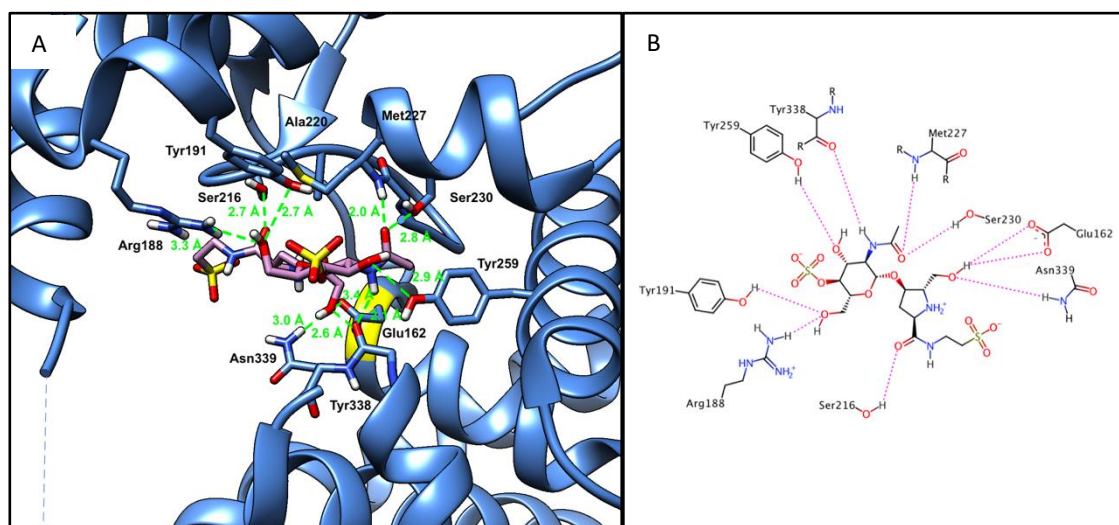
Figure 1. 10: A) Cartoon representation of Slt35 (blue) in complex with the known inhibitor bulgecin A (pink sticks) (PDB 1D0L).[67] The catalytic Glu162 residue is shown with yellow ribbon while hydrogen bonds are shown as dashed light green lines. B) 2D diagram of interactions between Slt35 and bulgecin A, showing hydrogen bonds (dashed lines).

The GlcNAc residue of bulgecin occupies the same site region of the active site as the GlcNAc residue of muropeptides, forming hydrogen bonds with the side chains of Ser230, Tyr259, Tyr191 and Arg188. The proline part of bulgecin is bound at the adjacent enzyme subsite with its hydroxymethyl group mimicking the hydroxyl moiety in C_6 of the MurNAc and it is involved

in hydrogen bond formation with the Glu162, which is the catalytic residue of the enzyme, and also (through its oxygen atom) with Asn339. Moreover, Ser216 interacts with the carbonyl oxygen of the taurine part of bulgecin A. On the other hand, no strong interactions occur between the enzyme and the taurine or sulfate parts of bulgecin A, suggesting that it is not necessary to mimic these parts of the molecule being not critical for binding the target and so not required in the structure of new inhibitors. Further evidence that the taurine and sulfate parts of bulgecin A don't have a critical role in binding LT is given by the structure of bulgecin B and C. The sulfate group attached to the taurine ring is not present in bulgecin B while bulgecin C lacks of both sulfate and taurine moiety.[71] Other bulgecins produced by *Chromobacterium violaceum* have also longer peptide chains attacked to the bulgecinine moiety demonstrating that this part of bulgecin is not essential for the inhibitor-target interaction.[72] Conversely, the GlcNAc residue and the proline nucleus of bulgecin, with their amide and hydroxyl groups seem to play a critical role in binding. Especially the hydrogen bond between the bulgecinine hydroxymethyl group and the catalytic Glu162 could be a key binding interaction, being the catalytic residue critical for the target activity and closely conserved in the active enzyme. The positive charge on the nitrogen atom of the proline ring, mimicking the oxocarbenium intermediate ion, could also lead to the achievement of the right ligand conformation and optimize the interaction with the target.[73]

1.5 Benzimidazole and its pharmacological effects

1.5.1 Benzimidazole and Its chemical properties

Benzimidazole is a heterocyclic aromatic compound with unique chemical properties. It is one of the oldest nitrogen heterocycles, first synthesized in the late 1800s,[74] and is a fusion of benzene and imidazole. The two nitrogen atoms, in the imidazole moiety, are separated by a carbon and numbered N_1/N_3, with a hydrogen atom bound to the nitrogen in position-1. Like imidazole, 1-H-benzimidazole tautomerizes, with the structures (1a) and (1b) interconverting (Figure 1.11). The N_1-H proton, in structure (1a), can be transferred to the nitrogen in position-3, giving back 1-H-benzimidazole (1b). The numbering changes in structure (1b), referring to the nitrogen binding the H-atom as N_1 and not anymore as N_3. Thus, the unsubstituted benzimidazole can be represented by two different structures.

Conversely, if the nitrogen-1 binds a different substituent than hydrogen, tautomerism doesn't occur and different isomers exist.
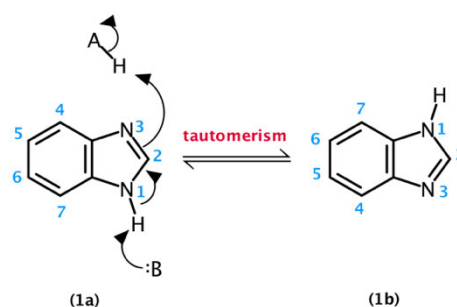
Figure 1. 11 Tautomeric forms of 1-H-benzimidazole.

All the carbon atoms are sp^2 hybridized with one unpaired electron in a p orbital, perpendicular to the ring. These electrons are shared among all the atoms of the ring, giving electron delocalization through a conjugated π-system. The lone pair of electrons on the N_1 atom is also involved in the aromatic structure, meaning that this is not a basic site. It resembles the nitrogen atom of pyrrole. Conversely, the N_3 atom of benzimidazole has a free lone pair located in a sp_2 orbital perpendicular to the p orbitals plane, so it is unable to participate to the π-system and can act as nucleophile. This is a typical characteristic of the nitrogen atom in pyridine.

1.5.2 Synthetic routes

One of the most appealing chemical characteristics of benzimidazole is the feasibility of the core synthesis. A retrosynthetic approach (Figure 1.12A) identifies simple precursors o-phenylenediamine (2) and a carbon donor species (3), obtained by disconnection between the N_1-C_2 and C_2-N_3 atoms of the benzimidazole nucleus (1). This evidence the feasibility of benzimidazoles preparation through a straightforward 1-step synthesis. The first benzimidazole synthesis dates back in 1872. It was prepared by Hoebrecker[74] by reduction of 2-nitro-4-methyl acetanilide (4) followed by dehydration to form 2,5-dimethylbenzimidazole (Figure 1.12B).

Over the years, a wide variety of methods for preparing benzimidazoles have been developed, mostly involving the condensation between o-phenylenediamine and a corresponding carbon donor agent such as carboxylic acids, aldehydes or acid chlorides.[75]

For synthesizing extended benzimidazoles, the paths considered can be also undertaken using suitably substituted starting precursors (Table 1.1).
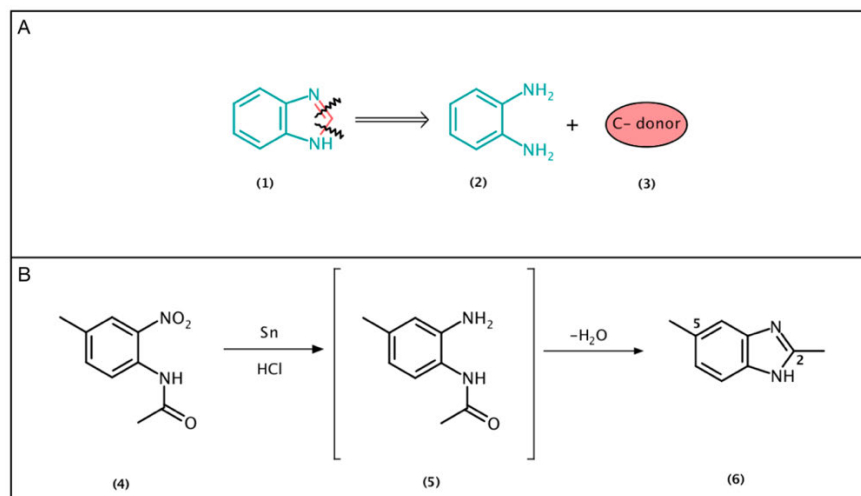
Figure 1. 12: A) Retrosynthetic approach. B) Synthetic route for the first benzimidazole synthesized.[74]
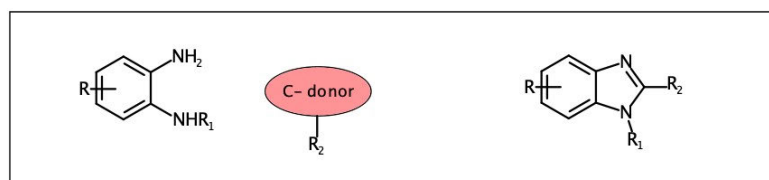
Diamine	C– donor	Conditions
	Carboxylic acid	–Philip's method: HCl (conc), heating –EtOH, NH$_4$Cl, heating
	Aldehyde	–Oxidative conditions such as Water and cupric acetate or air solvent while refluxing
	Acid chloride	–Refluxing or heating in presence of pyridine
	Acid anhydride	–Heating or in 4N HCl
	Ester	–Heating and diamine hydrochloride
	Ketone	–Heating
	Nitrile	–Mixing in aqueous suspension using diamine monohydrochloride
	Amide	–Heating using diamine hydrochloride

Table 1. 1: Multiple methods for synthesizing benzimidazole based derivatives.[76,77,78,79,75,] Compound 1 is obtained when R=R$_1$=R$_2$= H.

An alternative route for preparing extended benzimidazoles involves firstly the core synthesis, followed by its functionalization (Figure 1.13). In light of benzimidazole's chemical properties, multiple sites of this privileged structure could be extended, leading to a variety of derivatives (Figure 1.13). Binding a proton and sharing its lone pair with the conjugated π-system, the N_1 atom of benzimidazole doesn't represent an extensible site of the core. Conversely, owing to its free lone pair, the N_3 atom is able to perform a nucleophilic attack on electrophilic species, representing a good site for potential extensions of this heterocyclic nucleus leading to N-alkyl or acyl derivatives. Compound (10) is an alkyl-derivative obtained by reacting benzimidazole (1) with an alkyl chloride (Figure 1.13). The nucleophilic attack performed by the N_3 atom of benzimidazole on the activated carbon atom of the alkyl chloride leads to the product formation giving the displacement of chlorine[80]. A further extensible position of the BZI core is given by the carbon atom in position-2. This carbon, being located in between two electronegative nitrogen atoms, has a partial positive charge and It represents an electrophile site, which is able to undergo the attack from Nu species. Functionalization of the nucleus in position 2 has been repeatedly undertaken. 2-Aryl benzimidazoles (11) have been synthesised using palladium as catalyst (Figure 1.13).[81] Furthermore, the benzene moiety of this heterocycle is a good substrate for electrophilic aromatic substitution (S_EAr). Extensions at positions 4 and 7 of the nucleus are more challenging as they are not activated, unless pre-functionalized with halogens. Conversely, the extension of benzimidazole at the positions 5 and 6 is more feasible. N-Bromosuccinimide has been used as bromine source for halogenating the benzimidazole in position 5 (12) (Figure 1.13).[82]
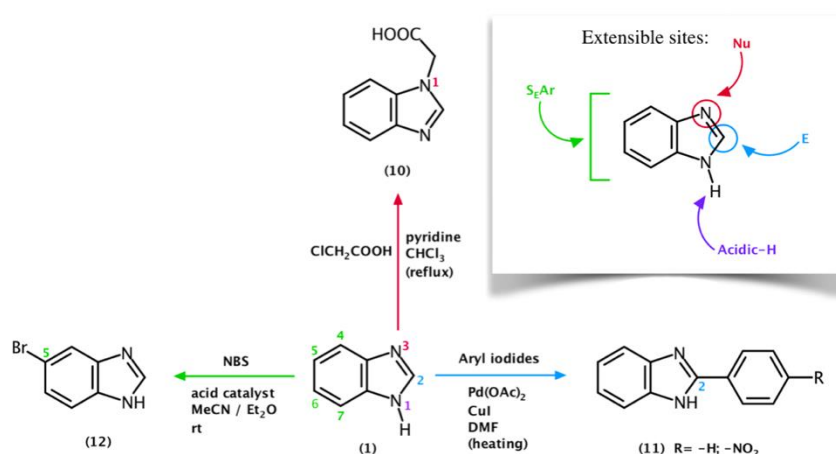
Figure 1. 13: Scheme of reactions for the extension of the benzimidazole core.

The singular chemical properties of this bicyclic compound and the multiple extensible sites make benzimidazole a promising core for originating complex multiply-substituted derivatives.

This gives the chance to access a variety of benzimidazole-based compounds which can reflect a wide range of pharmacological activities. Due to this versatility, benzimidazole is commonly used as a scaffold for modeling drug-like molecules.

1.5.3 Benzimidazole moiety in nature

Nitrogen based compounds represent critical structures in nature, being involved in key biological functions. Heterocycles are one of the main examples of nitrogen containing scaffolds essential for life. The critical role of this building blocks as biological components is shown by their presence in nucleic bases, vitamins and coenzymes.[83] Nucleobases, elementary units of nucleic acids (DNA and RNA), are heterocyclic compounds. They are distinguished into pyrimidines, which are analogues of pyridine, and purines, which contain a pyrimidine ring fused to an imidazole moiety. The benzimidazole core, as first observed by Woolley in 1944,[84] is an analogue of purines (Figure 1.14A-B), where the pyrimidine moiety is substituted by a benzene ring. This analogy is believed to lead the antimicrobial activity of benzimidazole derivatives which, competing with purines, inhibit microbial nucleic acid synthesis.[85,86] A further role of the benzimidazole moiety as a biological entity was following identified by Brink.[87] This scaffold was found to be part of vitamin B12 (Figure 1.14C), also called cobalamine, which has a critical role in cells metabolism, nervous system health and blood cell formation.[88,89] The structure of vitamin B12 is given by a tetrapyrrole moiety coordinating a cobalt ion, which is further linked to the N-3 atom of a 5,6-dimethylbenzimidazole. This nucleus represents the lower ligand of this essential biological entity.
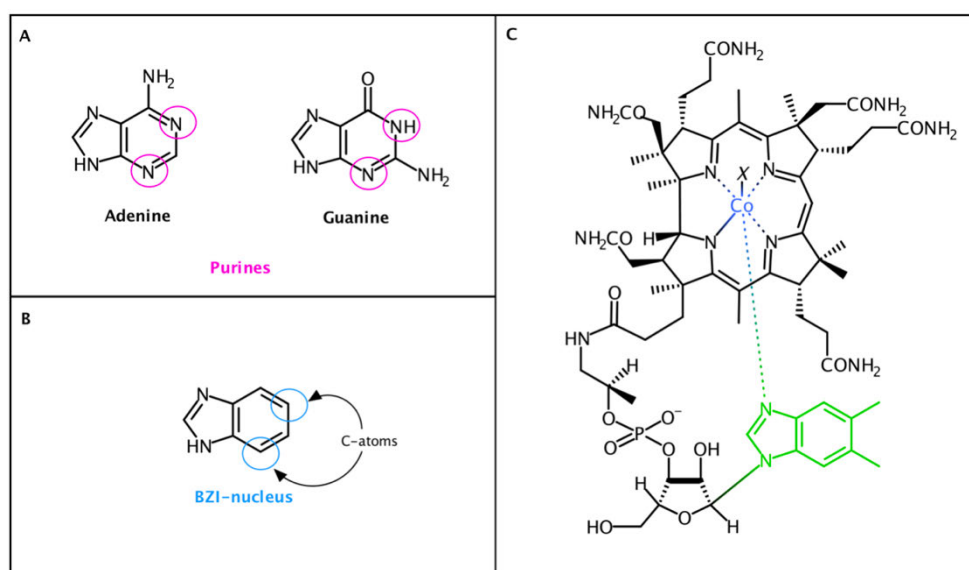
Figure 1. 14: A) purine structures; B) benzimidazole nucleus as an analogue of purines; C) vitamin B12 structure containing the BZI derivative (in green).

The structural analogy of benzimidazoles to purines and the presence of the benzimidazole nucleus in essential natural products could lead to pharmacologically active compounds with low toxicity for the host due to interactions naturally occurring between biostructures and N-containing heterocyclic compounds. The feasibility of synthetic approaches aimed to prepare benzimidazoles and their established pharmacological activities, suggest the promising role of this scaffold as pharmacophore in the design of a wide variety of active compounds.

1.5.4 Pharmacological activities of benzimidazoles

In the early 1990s a 2-extended benzimidazole derivative was synthesized and identified as pharmacologically active.[90] It was a 2-(2'-benzimidazolyl)-amino-4-methyl-thiazole and it was evidenced for Its antiulcer and gastroprotective effect. This has led to an increase in attention to the benzimidazole moiety. Over the years, several core modifications have been designed, leading to compounds with a wide range of pharmacological activities (Figure 1.15).[91,92,93,94,95]
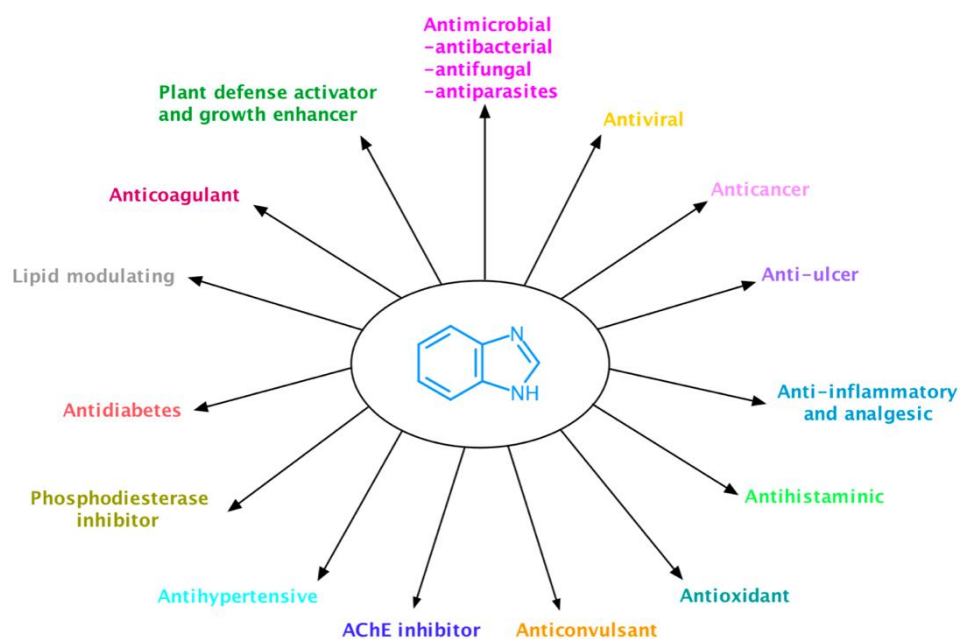
Figure 1. 15: Pharmacological uses of benzimidazole-based compounds.

Benzimidazoles are well known for their antimicrobial, antiviral and antiulcer properties. Moreover, they seem to play a key role as anti-inflammatory, antihypertensive, anticonvulsant, antioxidant and anticancer drugs. The pharmacological effect of benzimidazoles varies depending by the relative functionalization of the nucleus. Mono-extended derivatives such as 1-substituted and 1-H-2-substituted benzimidazoles have been identified as active compounds. Di-extended compounds such as 1,2-disubstituted benzimidazoles, which can also include fused ring systems, have been further evidenced.
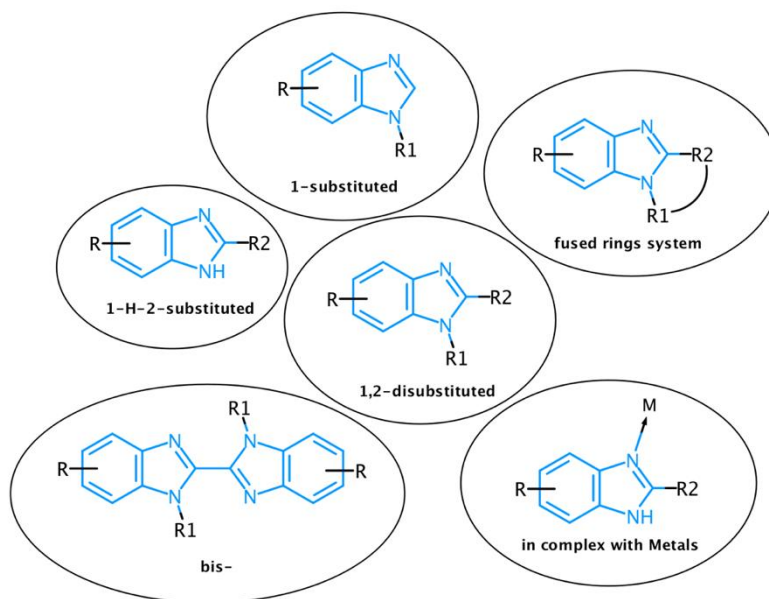
Figure 1. 16: Multiple functionalization of the benzimidazole nucleus.

Bis- (or tris-) benzimidazoles, having multiple benzimidazole nuclei linked, are also commonly identified as active compounds. Each of these extensions can then be combined with the presence of substituents on the benzene ring (-R group in Figure 1.16).[91,92,93,94,95]

1.5.5 Antimicrobial BZIs

The benzimidazole moiety is a commonly used scaffold for antibiotics and anti-fungal drugs as shown by the multiple BZI-based formulations currently available on the market. Ridinazole (13) is a bis-benzimidazole antibacterial compound (Figure 1.17), currently under investigation, where the two benzimidazole nuclei are linked at position 5. It has been distinguished for being active against *Clostridium difficile* infections,[96] which represent a serious healthcare issue. *C. difficile* is an anaerobic Gram+ bacterium able to infect the intestine, causing diarrhea, fever and nausea. Vancomycin represents the standard therapy. Despite an existing treatment, recurrence seems to be a critical issue often encountered by infected patients. Ridinilazole has been found

to be a promising active compound and it is currently undergoing phase III clinical trials for treating *Clostridium difficile* infections.[96,97] The mechanism leading to Its activity has not been fully elucidated, but it seems to inhibit cell division causing bacterial death. The investigation of the antibacterial effects of the benzimidazole moiety is a brand new area. This, as well as lack of specificity and therefore toxicity in mammals, explain the lack of currently marketed benzimidazole-based antibiotics. Despite this, literature studies strongly suggest its key role in fighting bacteria as shown by Its revealed activity against multiple strains. [96,97]

Ridinilazole (13) – antibacterial

Chlormidazole (14) – antifungal

Benomyl (15) – antifungal

Fuberidazole (16) – antifungal
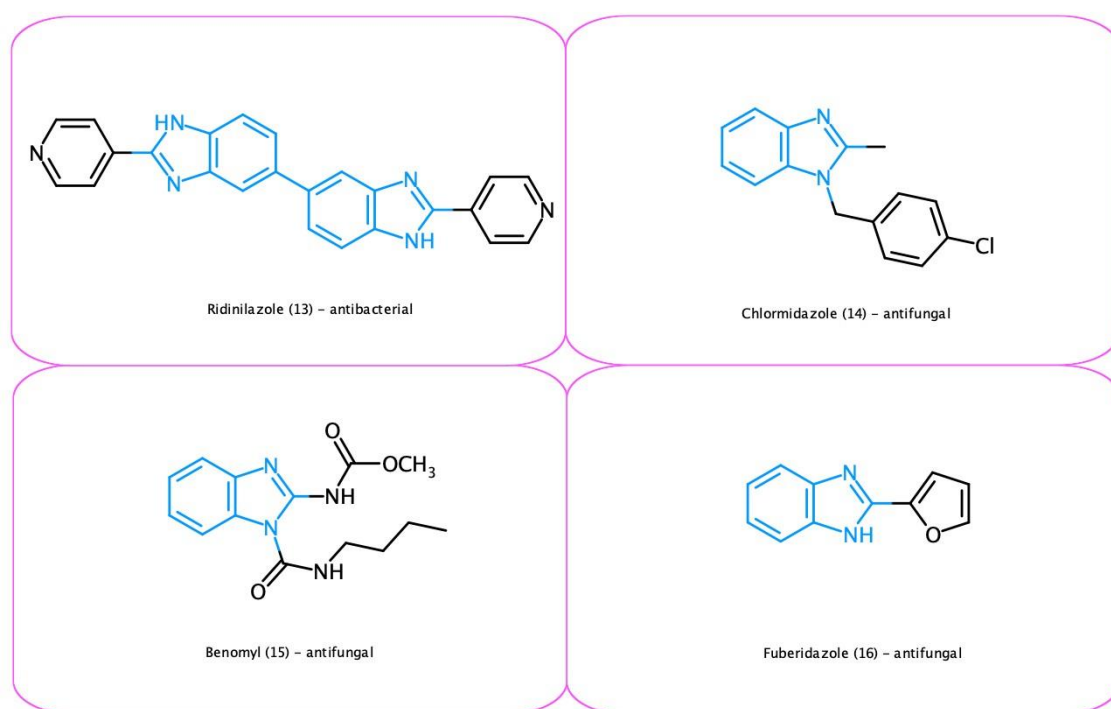
Figure 1. 17: Antibacterial and antifungal benzimidazoles available on the market.

Conversely, a wide variety of antifungal formulations containing the benzimidazole core are currently on the market (Figure 1.17). Chlormidazole (14) is the first azole antimycotic introduced during the late 1950s.[98,99,100] Its discovery represents the turning point for the development of multiple azole drugs, largely used for combatting fungal infections, such as chlortrimazole, miconazole and econazole.[100,101,102] Chlormidazole is a 1,2-disubstituted BZI derivative used in the therapy of topic mycosis such as nail and skin infections.[100,103] The mechanism of action, typical of all the azole derivatives, is given by the inhibition of CYP51A demethylase, a critical enzyme involved in ergosterol synthesis. This compromises the stability of the fungal cell membrane.[100,104] Benomyl (15) is a fungicidal 1,2-disubstituted benzimidazole, having the N_1 nitrogen atom making part of an urea group. It is active against a broad range of fungi inhibiting the polymerization of tubulin and compromising so critical cellular pathways.[105]

It is mainly used for contrasting fungicidal infections in plants, due to Its metabolite toxicity observed on mammals.[106,107] A further example of a benzimidazole-based agrochemical compound is given by fuberidazole, a benzimidazole holding a furan ring on position-2 of the core. It is a fungicide able to inhibit, like benomyl, the polymerization of tubulin.[108]

The already commercialized antibacterial and antifungal benzimidazoles are the outcome deriving from initial interest of scientists towards this moiety. Over the years, the increased attention to all the possible modification of the benzimidazole nucleus has led to the synthesis of a variety of derivatives, widely reported in literature, which suggest the incredible role that this heterocyclic could play in drug development, laying the foundations for its promising future in medicinal chemistry. Literature studies report multiple benzimidazole extensions leading to antibacterial and antifungal activity. Different core extensions lead to changes in activity. Generally, 1-substituted benzimidazoles have been found to have low activity against microbes.[92] Conversely extension of the benzimidazole nucleus on position-2 generally leads to an increase in activity. The combination of these two modifications of the core leads to 1,2-disubstituted benzimidazoles which exhibit a strong antimicrobial effect. Bis-benzimidazoles typically have strong activity against fungi.

1-H-2-substituted-derivatives:

Compound (17) (Figure 1.18) has been found to be active against *Campylobacter pylori*.[92] It has a sulfone group in position-2 which connects the benzimidazole core to an extended pyridine ring. Changing the sulfone to a thioether creates the 2-mercapto-benzimidazoles, which seems to give promising active derivatives. Benzimidazoles having the 2-sulfur group which holds a chain containing a β-lactam ring have been reported for their antibacterial and antifungal activity.[92] Compound (18a) has been found strongly active against *Bacillus subtilis*, while compound (18b) has shown activity against *Escherichia coli* and *Staphylococcus aureus.* Both derivatives have given comparable activity to the standard streptomicin.[93,109]

Derivative (19a) is a further 2-mercaptobenzimidazole. It is more active than the standard cefadroxil against *E. coli*, *B. subtilis* and *Pseudomonas aeruginosa*. This derivative has also antifungal properties against *C. albicans* and *Aspergillus niger.* Changing the position of methoxy-substituents on the phenyl extension influences the activity. Compound (19b) has higher activity against *B. subtilis* and *P. aeruginosa* than the analogue (19a).[93] In the category of 1-H-2-substituted benzimidazoles, compound (20a) showed antibacterial activity against species

such as *P. aeruginosa*, *E. coli*, *Klebsiella pneumonia* and *S. aureus,* leading to a higher effect than the standard ofloxacin and metronidazole. It has a 2-methylamine moiety which holds a 1,3,4-thiazole ring. Compound (20b), having a slightly different extension to (20a), has a strong antifungal effect against *Candida albicans*, *Aspergillus niger* and *Fosarium oxysporium*, and has stronger activity than the standard fluconazole.[93,110] The o-aminophenyl extension, leading to compound (21), has given a promising benzimidazole, with higher activity against *S. aureus* than the standard gentamicin.[111] The concomitant 2,5-substitution, such as in (22a) and (22b) resulted in derivatives having activity against Gram+ bacteria such as *S. aureus*, *Streptococcus faecalis* and *B. subtilis*.[112] A 2,5,6-trisubstituted benzimidazole (22c) has a potent effect against drug-resistant *S. aureus*.[92]

(17)

(18a) : R₁= H; R₂= NO₂
(18b) : R₁= Cl; R₂ = H

(19a)

(19b)

(20a)

(20b)
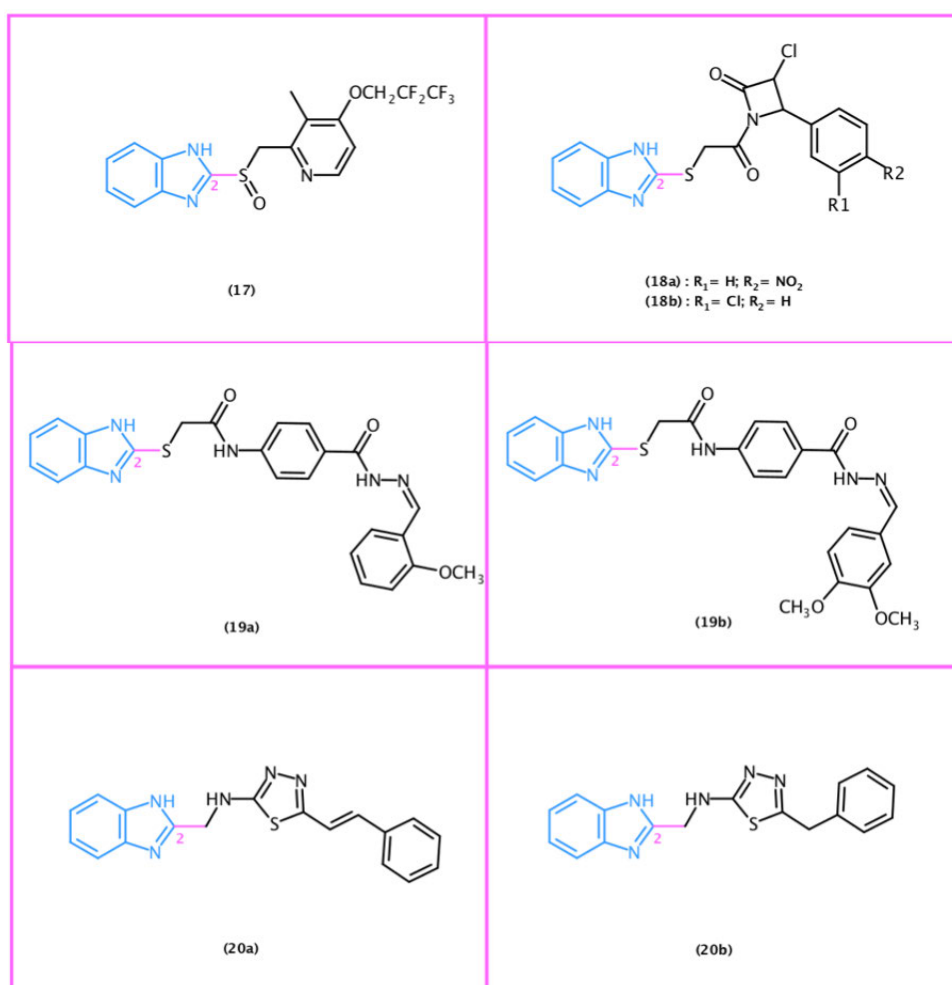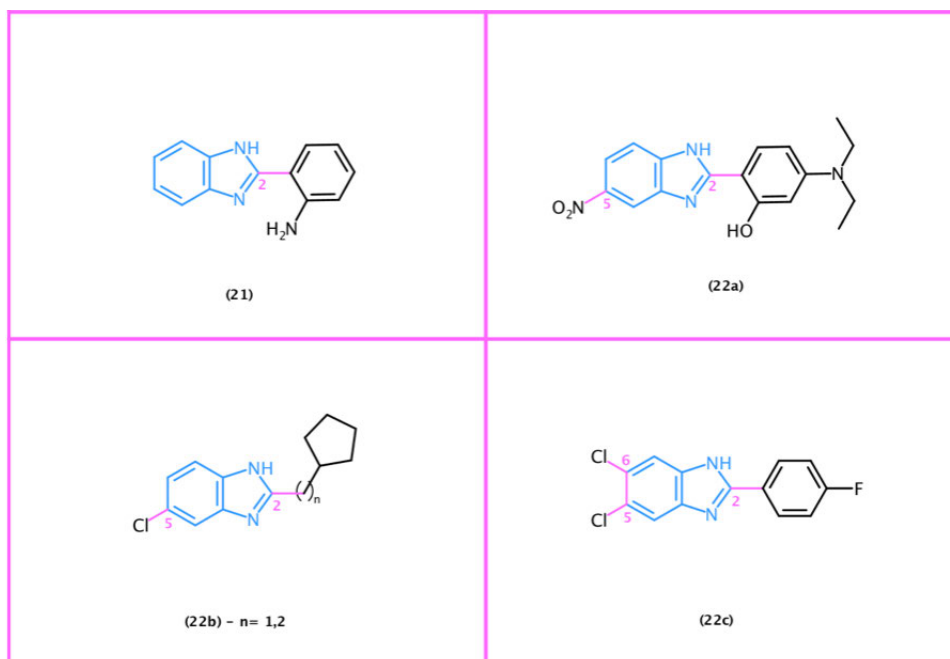
Figure 1. 18: 1-H-2-substituted benzimidazoles reported in literature for their antibacterial and/or antifungal properties.

1,2-disubstituted-benzimidazoles:

A concomitant extension in position-1 and -2 of the benzimidazole core has been found to lead to excellent antimicrobial derivatives (Figure 1.19). A series of 2-methylbenzimidazoles having a 1,3,4-thiazole ring between the benzimidazole nucleus and different chains have been revealed to be good antimicrobials. In compound (23) the thiazole moiety connects the benzimidazole to a phenyl ring through an imine while derivative (24) has a β-lactam ring as tail. Benzimidazole (23) has an antibacterial effect against *B. subtilis* and antifungal activity against *C. albicans*, *A. niger* and *Aspergillus flavus* while compound (24) has been found active against *E. coli*.[93,113] Compound (25), a further 2-methylbenzimidazole, has been revealed to be a strong bactericidal.[92] It is characterized by a complex N_1 extension carrying a heterocyclic ring which contains N- and O-atoms and a m-methoxyphenyl tail. Generally, the insertion of heterocycle-based extensions is a promising strategy for obtaining antibacterial and antifungal benzimidazoles such as compound (26a) and (26b).[92] A series of 1,2-phenyl extensions, such as in compound (27), have led to antimicrobial derivatives, active against different bacteria such as *E. coli*, *Vibrio cholera* and *S. aureus*.[113,114]

A benzyl moiety in position 2 of the benzimidazole nucleus has also been investigated, leading to derivatives having effect against *S. aureus* and *P. aeruginosa*. Compounds (28a) and (28b), which differ in the N$_1$-extension, have both been found to have higher activity than the standard gentamicin.[111]
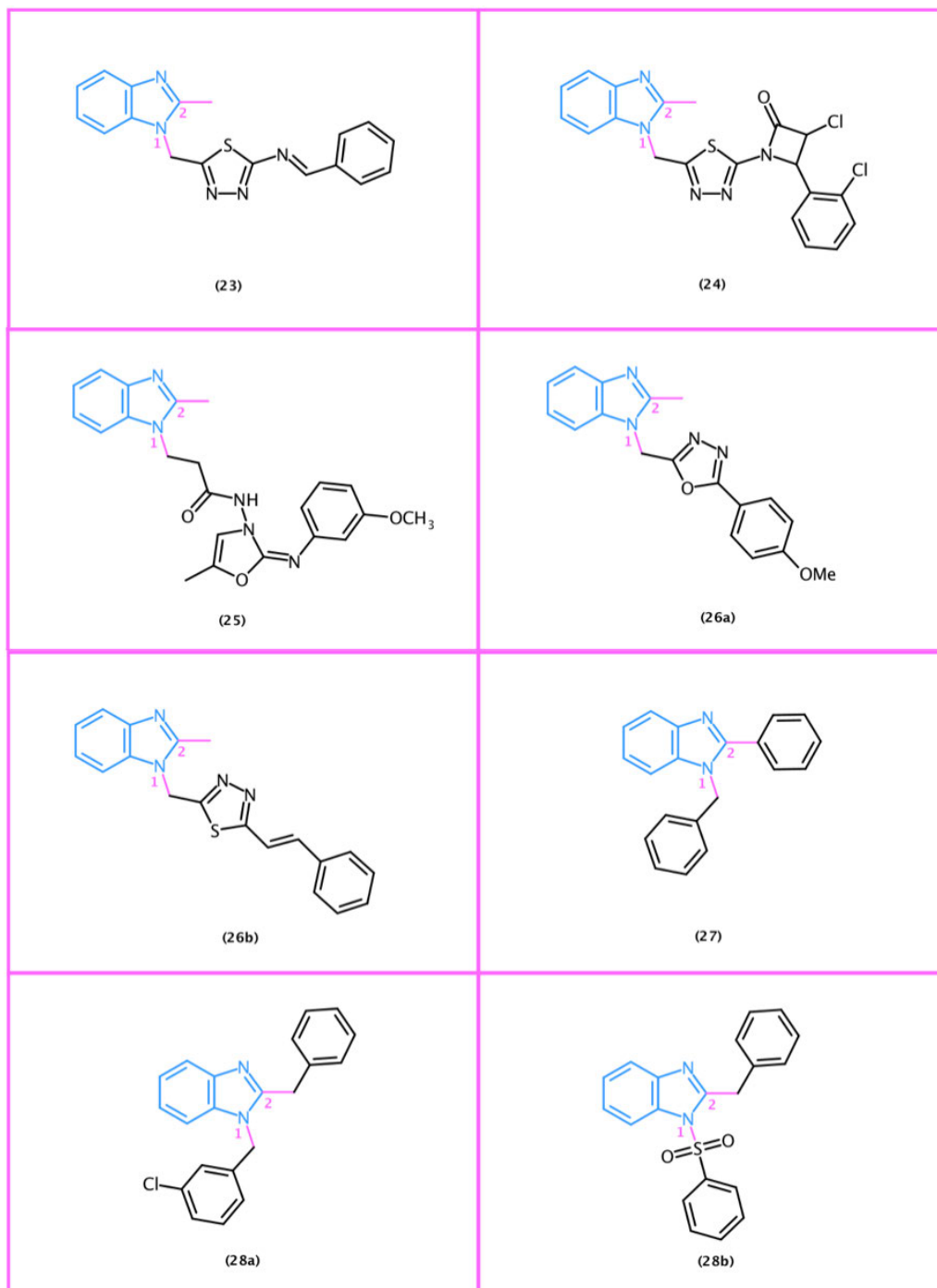
Figure 1. 19: 1,2-extended benzimidazoles reported in literature studies for their antibacterial/antifungal activity.

Some 1,2-extended benzimidazoles contain fused systems (Figure 1.20). Often this structure is combined with the insertion of other pharmacologically active moieties. This strategy is commonly used in drug design and it seem particularly promising in benzimidazole-based formulations. In this category, compound (29a) has been found to be a strong antibacterial agent while (29b) has showed antifungal properties.[115] The 1,2-fused benzimidazole bears an extended coumarin scaffold where variation in the halogen substituents reflects different pharmacological activity. A series of condensed systems containing an isoindoline-1,3-dione nucleus, such as compound (30), has also been found extremely active against microorganisms such as *A. flavus* and *A. niger*.[93]

A further series of fused systems has been screened for antimicrobial effects revealing promising results. In this category, derivative (31) has been found to be a good antimicrobial, active against *B. subtilis*, *E. coli*, *V. cholerae* and *C. albicans*. It has a methyl group in position 5 while the 1,2-fused extension form a 6 membered ring with an o-amino substituent, m-nitrile and p-pyrazole moiety giving a complex extended benzimidazole. Compound (31) has been further evidenced for Its potent effect against *S. typhi*. The activity seems to closely depend by the substituent in position 5 of the benzimidazole nucleus (-R_3) and the group attached to the ether moiety of the pyrazole.[116] 1,2,5-extended benzimidazoles seem also to lead to antimicrobial effects. Compound (32) is a 1,2-substituted-BZI having the BZI-core extended in position 5, which is active against *S. aureus* and *S. epidermidis*.[117]
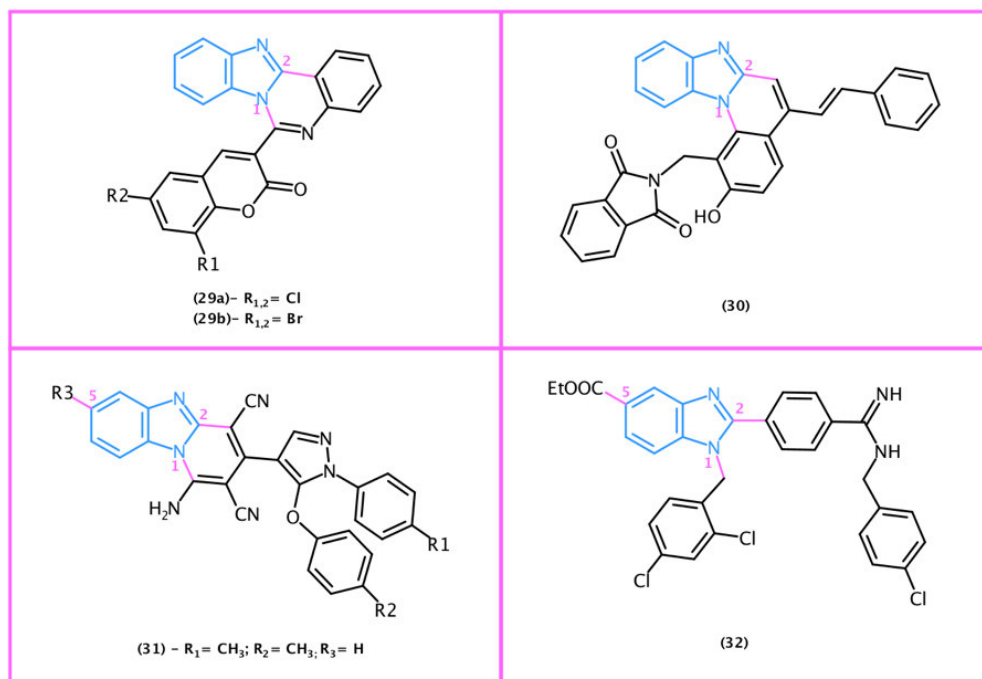
Figure 1. 20: 1,2- extended benzimidazoles, originating fused ring, and 1,2,5-extended benzimidazoles reported in literature studies for their antibacterial/antifungal activity.

Bis- and tris-benzimidazoles

Compounds containing two benzimidazole nuclei, directly attached or connected by a linker (Figure 1.21), have been investigated for their antimicrobial properties leading to promising results.
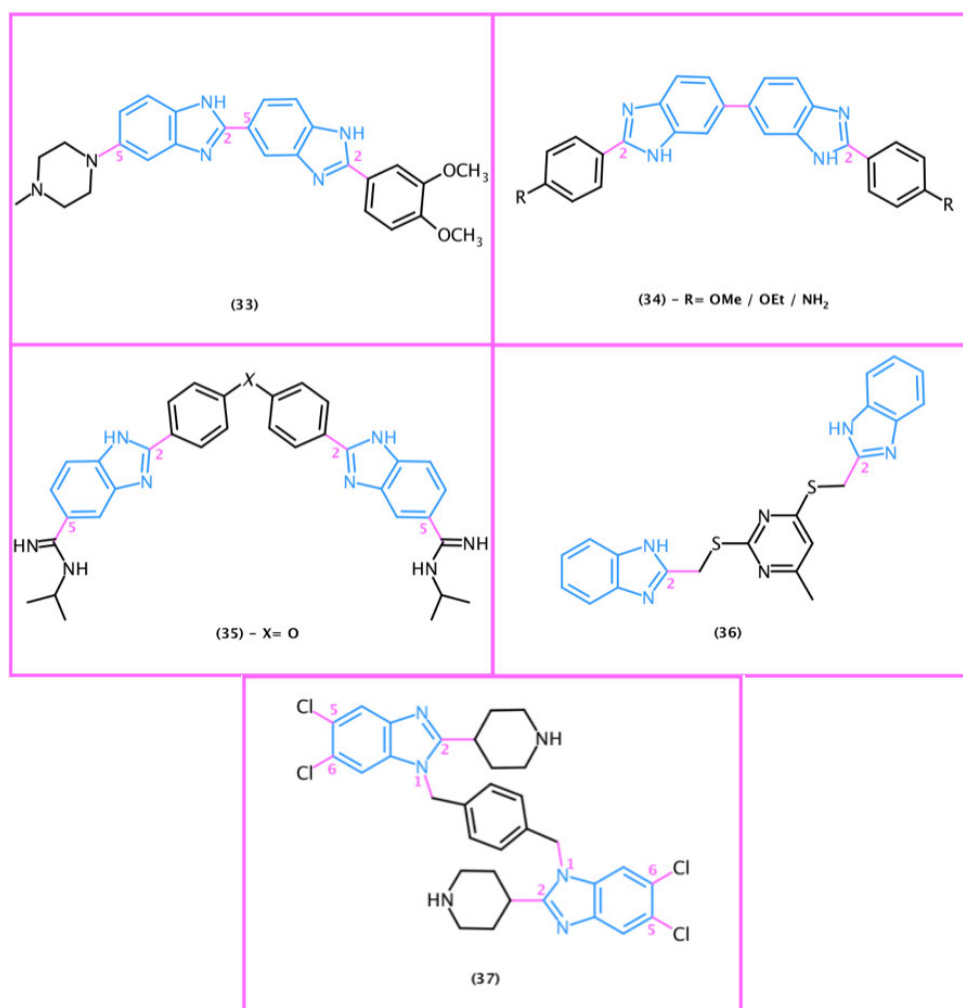
Figure 1. 21: Bis-benzimidazoles reported in literature studies for their antibacterial/antifungal activity.

They seem to interact with the DNA minor groove and inhibit DNA replication in bacteria, without causing toxicity in mammalian cells. In this category, compound (33) has been distinguished for its activity against *E coli* through inhibition of topoisomerase I.[92, 118] It is a bis-benzimidazole, having the position 2 of one nucleus directly connected to the position 5 of the other BZI moiety. A series of symmetric bis-benzimidazoles connected in position 6 of the nucleus, such as derivatives (34), have been screened for their antimicrobial activity.[119] They have potent effects against Gram positive bacteria, such as methicillin-resisitant *S. aureus* (MRSA), vancomycin-intermediate *S. aureus* (VISA) and vancomycin-resistant *Enterococci* (VRE), being so promising in fighting the drug-resistant bacteria. No activity has been observed against

Gram negative bacteria. A further symmetric combination of benzimidazole moieties is shown in derivative (35). The two benzimidazole moieties are linked in position 2 by phenyl rings connected to an oxygen atom while position 5 of the cores is substituted with alkylated-amidine chains. Benzimidazole (35) has been distinguished for its antimicrobial activity against MRSA and VRE.[120] The electronegativity of the linker (X) seems to be a critical aspect for the antimicrobial effect. Compound (36) has been found to be an extremely active antibacterial against *S. aureus* and *Penicillium chrysogenum*. The two thio-benzimidazole moieties are linked by a pyrimidinyl nucleus.[121] A further active bis-benzimidazole is given by compound (37).[119] In this derivative, the benzimidazole nuclei are 1,2,5,6-extended. The two moieties are N_1-connected by a benzyl linker, position 2 bears a piperidine ring, and chlorine atoms are located in position 5 and 6 of the core.

Tris-benzimidazoles have also been revealed to lead antimicrobial activity (Figure 1.22). In this category, compound (38a) and (38b) have three 5-substituted benzimidazole nuclei connected in position 2 by a tripodal-linker based on 1,3,5-triazine moiety (Figure 12). Substituted triazines are well known for their pharmacological activity as antimalarial, antiviral and anticancer.[122] The combination of this pharmacophore with benzimidazole, giving compounds (38), leads to potent antibacterial effect against *E. coli*, *S. aureus* and *B. subtilis*.[123]

(38) – a : R= –Cl
–b : R= –NO2
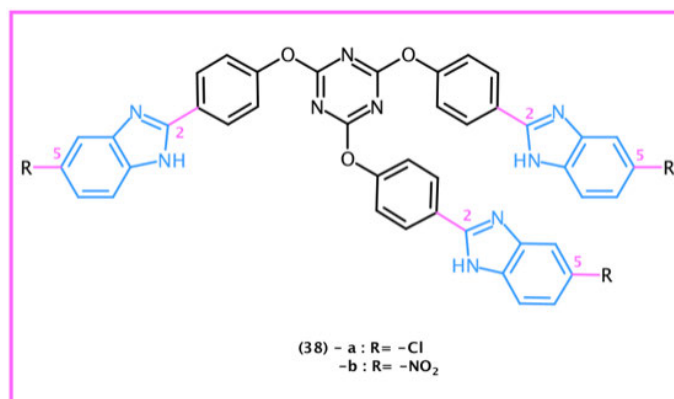
Figure 1. 22: Tris-benzimidazoles reported in literature studies for their antimicrobial activity.

Benzimidazole in complex with metals

A further functionalization of the benzimidazole moiety is given by complexation (Figure 1.23). Metals have an important role in nature, being involved in important biological processes and they are sometimes inserted in drug structures.[124] Ag(I), Zn(II) and Fe(III) complexes seem to have promising antimicrobial effect. Metal complexes containing the benzimidazole moiety have been repeatedly prepared and found to be promising antibacterial and antifungal compounds. Derivative (39) is an Ag(I) complex with potent antibacterial activity against a wide

variety of bacteria. The Zn complex (40) had effect against Gram negative bacteria such as *K. pneumoniae* and Gram positive such as *S. aureus* and *S. epidermidis* while compound (41) was found to inhibit *E. coli*, *K. pneumoniae* and *S. aureus*.[125]
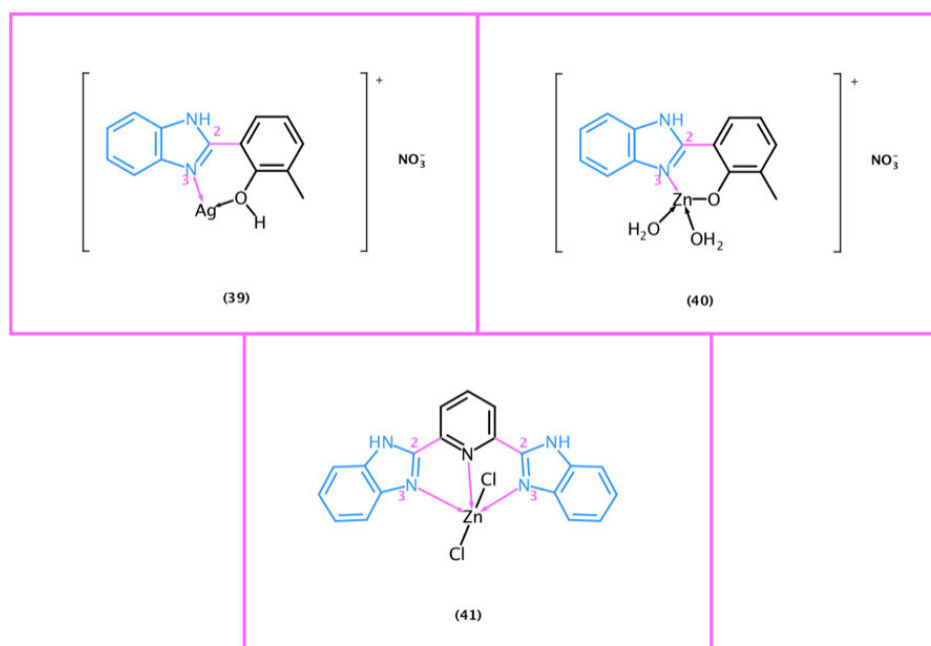
Figure 1. 23: Benzimidazoles in complex with metals reported in literature studies for their antimicrobial activity.

Derivative (41) is a bis-benzimidazole in complex with $ZnCl_2$ that has been revealed to be a promising antibacterial and antifungal compound. It has higher antibacterial activity than the standard gentamicin against *S. aureus* and *P. vulgaris* and a stronger antifungal effect than the standard nystatin against *C. albicans* and *K. fragilis*.

1.5.5.1 Antimycobacterial benzimidazoles

Despite the absence of already marketed antitubercular benzimidazoles, multiple benzimidazole-based compounds have been synthesised and found to be active against *Mycobacterium tuberculosis* (Figure 1.24) Literature studies suggest that 2-extended benzimidazoles generally lead to active compounds. The concomitant functionalization in position 1 and 2 of the core seems to increase the antimycobacterial activity. Despite this, compound (42), which is a 1,5-extended benzimidazole, has been found active against *M. tuberculosis*. It targets MmL3, a critical mycobacterial protein involved in the transport of mycolic acid, affecting the stability of the bacterial membrane and potentially leading to contrast mycobacterial resistance.[126] Imidazo-thiadiazole is an important scaffold in drug design, well known for its multiple pharmacological activities. The combination of this moiety with

benzimidazole, giving compound (43a) as result, has been found to be remarkably active against *M. tuberculosis*.[127] Compound (43b) belongs to the same category of benzimidazoles but holds a concomitant extension on position 5 of the core. Derivative (44) is a 2,-6-extended benzimidazole carrying a nitrofuran moiety in position 2 and a carbodihydrazide group, which holds a p-chlorophenyl group, in position 6. It is active against *M. tuberculosis,* compromising β-hematin formation.[128] Literature studies have revealed that when the carbodihydrazide carries a 3-hydroxy-2-naphtyl moiety instead of the p-chlorophenyl, activity against resistant strains of mycobacterium is observed.
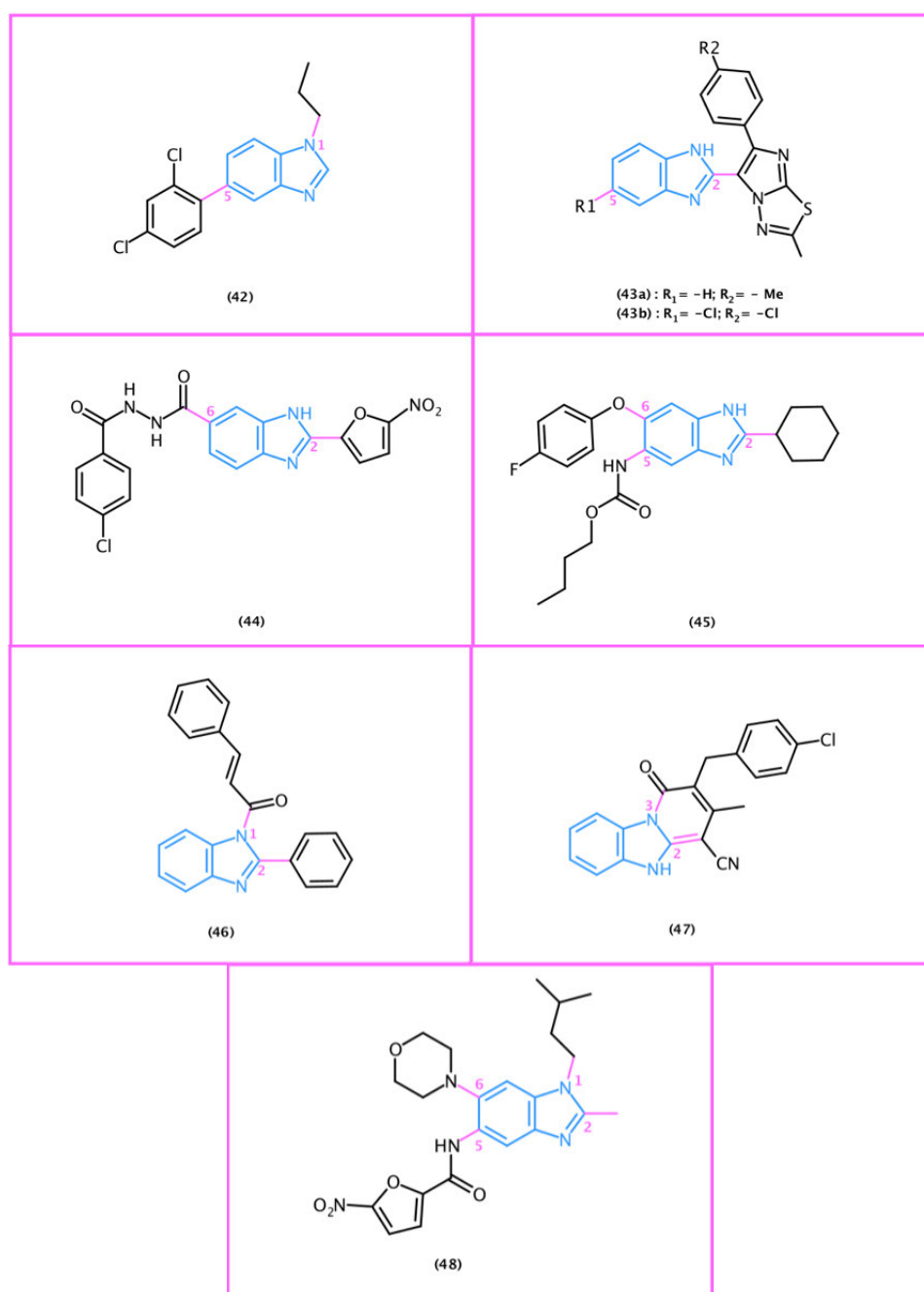
Figure 1. 24: Benzimidazoles reported in literature studies for their antimycobacterial activity.

The trisubstituted benzimidazole (45) seem also to be a favorable core extension, leading to potent antimycobacterials.[129] The extension in position 6 of the core has been revealed to be a key modification, with the ether- or thio- group as promising linker. Compound (46) is a 1,2-extended benzimidazole, having a phenyl moiety in position 2 of the core while N_1 is extended forming an amide. As evidenced previously, the 1,2-disubstituted nuclei could form fused systems. Compound (47) is an example of fused BZI-based antimycobacterial. It is a 1-H-2,3-fuctionalized derivative carrying a pyridine moiety. It has been found to be active against resistant tuberculosis, and SAR studies evidenced the need for a para-substituent on the phenyl ring in order for activity.[130] An example of fully extended benzimidazole having antimycobacterial activity is given by compound (48). It is a 1,2,5,6-substituted derivative, having alkyl groups on positions 1 and 2 while morpholine and nitrofuran moieties are in positions 5 and 6. Both compounds (47) and (48) have been found to be active against *M. tuberculosis*.[128]

2.5.5.2 Antiparasitic benzimidazoles

Multiple antiparasitic formulations containing the benzimidazole scaffold have been marketed (Figure 1.25).[131] Thiabendazole (49), the first benzimidazole based antihelmintic drug, was introduced in 1960.[132,133] It is a 1-H-2-substituted benzimidazole carrying a thiazole moiety, with a similar structure to fuberidazole (16).

Thiabendazole – (49)

Albendazole – (50a) : R= –COC$_6$H$_5$
Mebendazole – (50b) : R= –SCH$_2$CH$_3$

Cambendazole – (51)
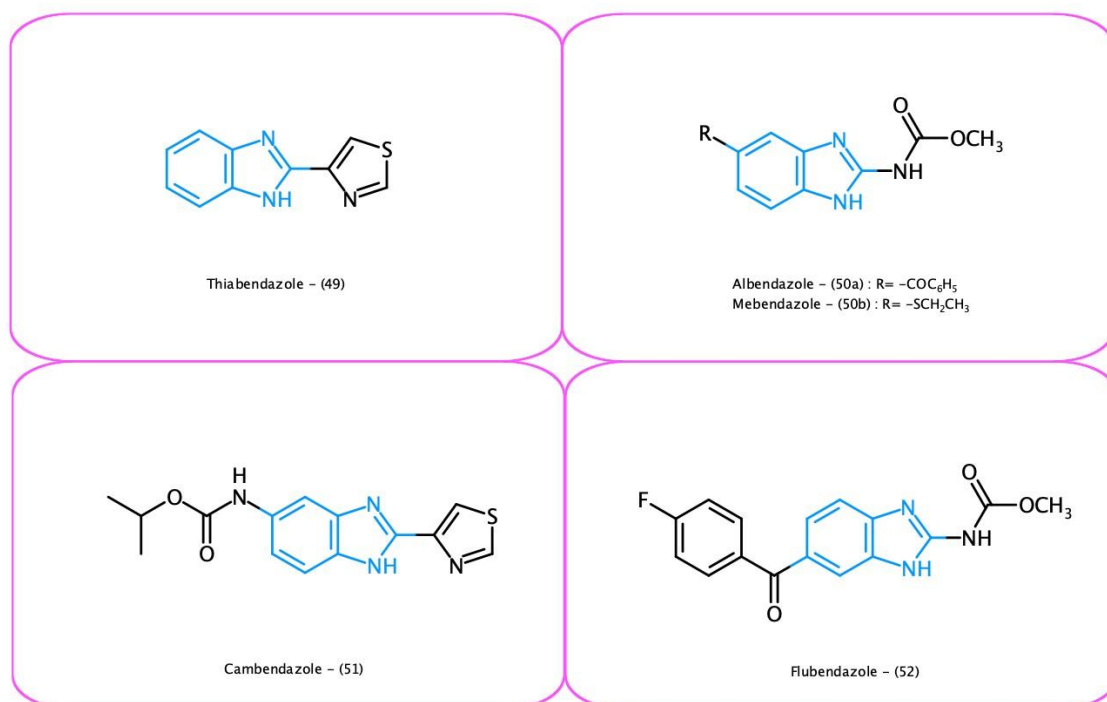
Flubendazole – (52)

Figure 1. 25: Antiparasitic benzimidazoles available on the market.

Thiabenazole is commonly used as a pesticide, as it has both antifungal and antiparasitic activity.[134] Currently albendazole (50a) and mebendazole (50b) are clinically used antihelminthic drugs containing the benzimidazole moiety,[135,136,137] as are cambendazole (51) and flubendazole (52).[138] Cambendazole (51) is an analogue of thiabendazole (49), holding an amide extension at position 5 of the benzimidazole core. Flubendazole (52), as albendazole (50a) and mebendazole (50b), is a 2-carbamate-benzimidazole. It differs from the analogues by having the extension at position 6.

Multiple benzimidazole-based compounds have been evidenced by literature studies for their antiparasitic properties (Figure 1.26), suggesting the critical role played by this scaffold. In the category of 1-extended benzimidazoles, compound (53) demonstrated to have good antihelmintic and antiprotozoal properties. It is active against *Trichinella spiralis* larvae and *Paramaecium caudatum*.[139] A series of 1-H- and 1-extended-benzimidazoles, fully substituted on the benzene ring of the core, such as (54a) and (54b), have been evidenced for their antiprotozoal effect against *Acanthamoeba castellanii*.[140] Multiple active derivatives bear a sulfur group in position 2 which links the core with the relative extension. In this category, compound (55), which has chlorine atoms in position 4 and 6, has been found to be more potent than the standards albendazole against *Giardias intestinalis* and *Trichomonas vaginalis*.[141] Compound (56), which has a methoxycarbonyl group in position 5 and chlorine in 6, is active against *Trypanosoma cruzi*.[142] The sulfur in position 2 holds a chain having a terminal pyrazin-2-yl moiety. In the category of 1,2-extended benzimidazoles, compound (57), a 1-methyl-2-mercaptobenzimidazole, has been found to be active against *Giardia duodenalis*, a parasite which infects the small intestine causing diarrhea.[143] Multiple 2-trifluoromethylbenzimidazoles, such as compound (58), have been evidenced for their promising role in fighting parasitic infections. Compound (58) is a 1,2-extended derivative bearing a methyl chain in position 1, as compound (57), but unlike its analogue, (58) bears a trifluoromethyl group in position 2 and is functionalized in position 5 of the benzene moiety. It has been found to be active against adult stage of a wide variety of protozoa such as *Trichinella spiralis*.[144] Multiple 2-carbamate-benzimidazoles extended on the benzene ring, such as compound (59), have been evidenced for their anti-parasitic activity. Derivative (59) is a 1,2-extended benzimidazole bearing a thioether chain in position 5 and an α-naphthyl ether in 6. It is an analogue of albendazole and has been found to be more active than albendazole against *Toxocara canis*.[145]

A further combination of benzimidazoles moieties, leading to anti parasitic activity, is given by amino bis-benzimidazoles.
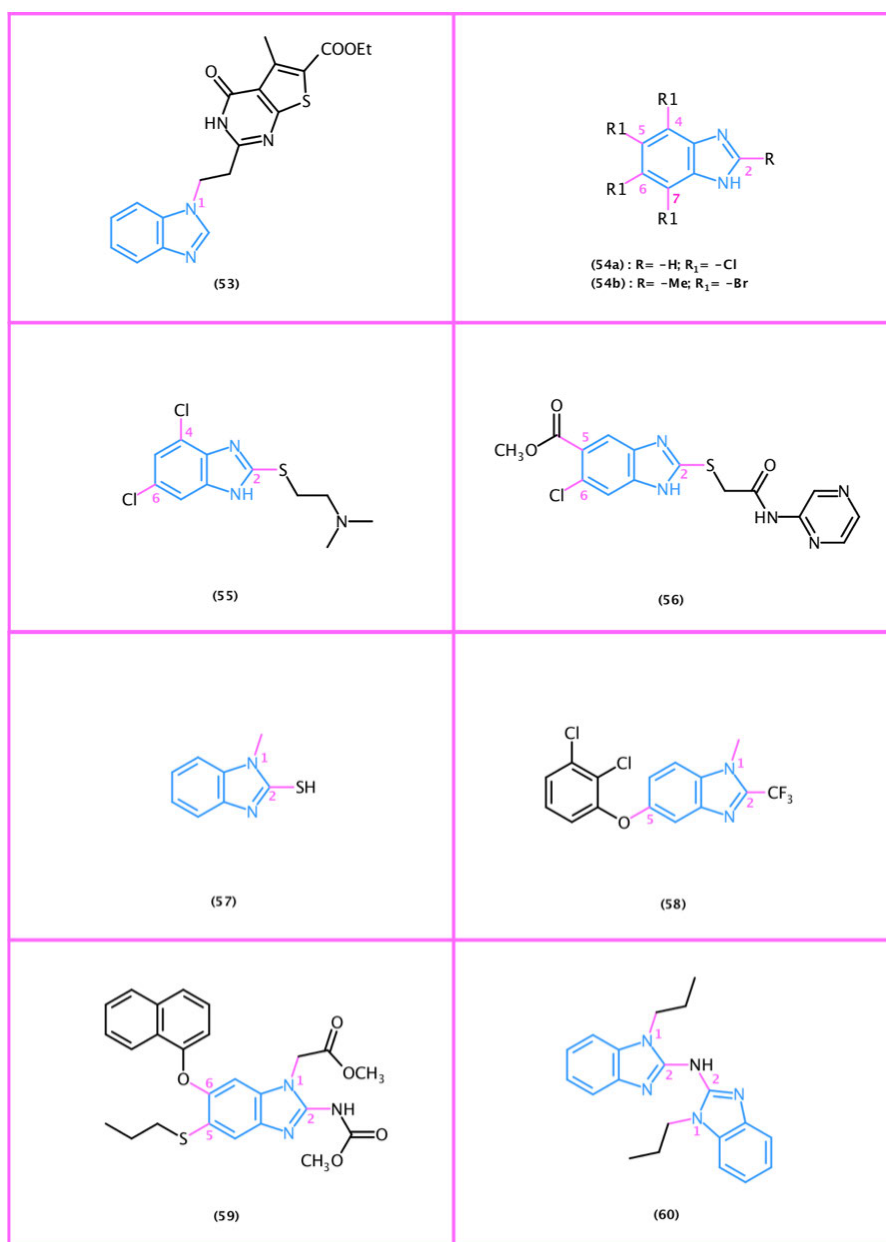
Figure 1. 26: Benzimidazoles reported in literature studies for their antiparasitic activity.

In this category, compound (60) has the two benzimidazole moieties linked in position 2 by an amine group and further extended in position 1. It has been distinguished for Its higher activity than the standard albendazole against *T. spiralis* larvae.[146]

A series of benzimidazole N-oxides, such as compound (61), have been found to be active against *T. cruzi* and *T. vaginalis* (Figure 1.27).[147] Compound (61) is a 3-N-oxide-5-nitrobenzimidazole

derivative, bearing an amide moiety in position 2 of the core. The increase in lipophilic character, shown in compound (62), where the NO- moiety is extended with a lipophilic chain, leads to higher anti protozoal activity.
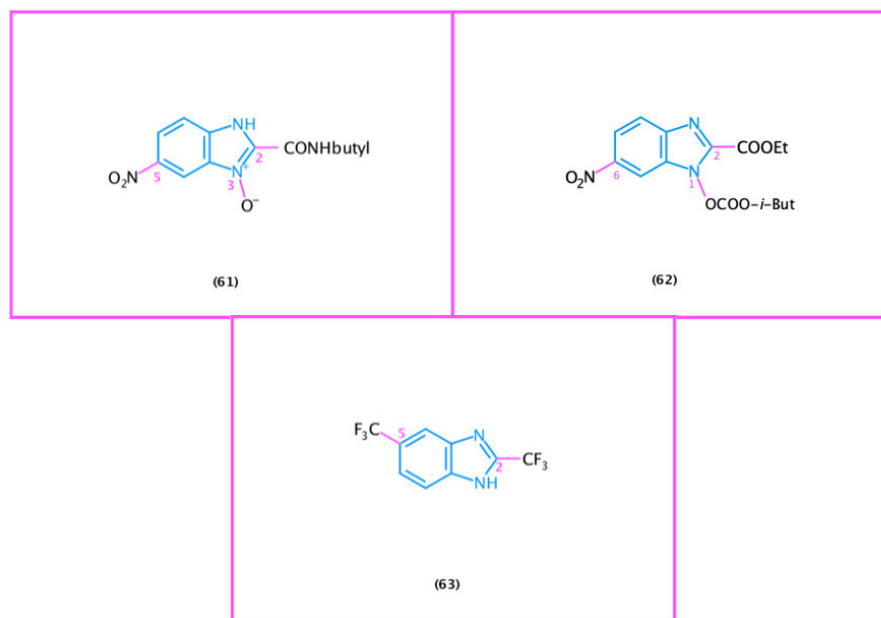
Figure 1. 27: Benzimidazole N-oxides and $C_{2,5}$-substituted benzimidazole reported in literature studies for their antiparasitic activity.

Plasmodium malaria and *P. falciparum* are protozoa causing malaria, an infectious disease which provokes many deaths. Chloroquine has been largely used in the malaria treatment. Despite this, the development of resistance lead to the needing of new active compounds.[30] Several benzimidazole derivatives have been identified as active against different species of P*lasmodium.* Compound (63), a 1-H-2-trifluoromethylbenzimidazole bearing a further trifluoromethyl group in position 5, has been evidenced for its antimalarial effect.[148]

1.5.6 Non-antimicrobial benzimidazoles

Benzimidazole is further commonly used as building block for non-antimicrobial drugs. Multiple marketed formulations contain this moiety (Figure 1.28). Enviroxime (64) is a benzimidazole-based antiviral. It is a non-nucleoside analogue, active against RNA viruses, known for inhibiting the replication of enteroviruses and rhinoviruses.[149] Enviroxime (64) is a 2-aminobenzimidazole bearing a sulfone in position 1 and a benzophenone oxime moiety in 6. Benzimidazole based compounds are also well known anticancer agents. They target critical processes for the cancer cell, harming its stability.[150] Veliparib (65), which is a 2,6-extended derivative bearing a methyl-

pyrrolidine moiety in position 2, inhibits poly-(ADP ribose) polymerase (PARP), a critical enzyme involved in DNA repair. It sensitizes cancer cells to cytotoxic agents, leading to DNA damage by lower expression of PARP.[151] This results in a promising co-administration of veliparib and different chemotherapeutic agents such as carboplatin and paclitaxel, followed by veliparib maintenance.[152]

Omeprazole (66) is the first of a large series of potent benzimidazole-based antiulcer agents.[153] It is a proton pump inhibitor (PPI), largely used for treating gastric damage deriving from an altered secretion of acids. Omeprazole is a 1-H-benzimidazole carrying a methoxy group in position 6 of the core and a 4-methoxy-pyridine moiety linked in position 2 by a sulfur.
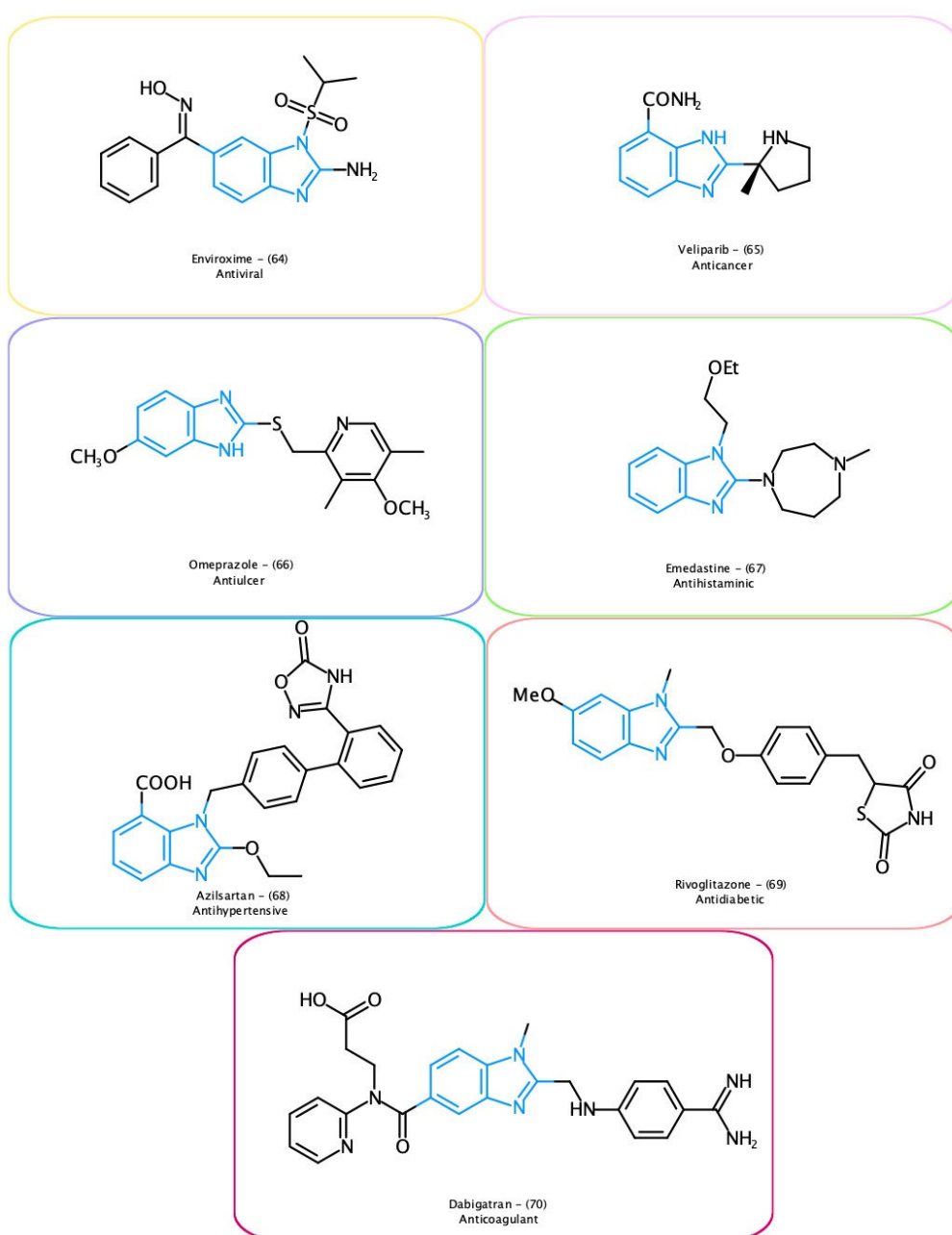
Figure 1. 28: Non-antimicrobial marketed benzimidazoles.

Emedastine (67) is an antihistaminic medication containing the benzimidazole moiety. It is a selective H1-receptor antagonist used for the treatment of allergic aversions, especially conjunctivitis.[154] Emedastine is a 1-alkyl-benzimidazole having a 1,3-diazepine nucleus in position 2. Azilsartan (68) is a benzimidazole-based antihypertensive drug.[155,156] It is an angiotensin II blocker, able to restore the normal blood pressure. Azilsartan is commonly administrated as prodrug formulation, named azilsartan medoxomil, which once in the gastro-intestinal tract releases the active compound. Rivoglitazone (69) is commonly used for the treatment of type II diabetes.[157,158] It is a 1,2,6-extended benzimidazole bearing a methyl in position 1, a thiazolidinedione containing chain in position 2 and a methoxy group in 6. Dabigatran (70) is an anticoagulant benzimidazole used to treat blood clots.[159] It a 1-methyl derivative holding a p-aminobenzamidine moiety in position 2 and an amide in 5 which is connected to a pyrimidine and a propanoic acid chain.

Literature studies strongly evidenced the versatile character of benzimidazole derivatives, suggesting its critical role in drug design and development of non-antimicrobials (Figure 1.29). Some benzimidazole-based compounds bearing a benzotriazolyl moiety, such as derivative (71), have been found to be active against a wide variety of viruses.[160] The benzimidazole moiety has also been revealed to be a promising scaffold for anticancer drugs.[150] Derivatives bearing oxadiazole moiety, such as compound (72), have shown good anticancer effect.[161] Compound (73) has been found to be a potent antiulcer agent if compared with omeprazole, being a potential H^+/K^+ ATPase inhibitor.[162] It is a benzimidazole-pyrazole hybrid bearing a sulfur group in position 2 which seems to be critical for the activity. Some 2-methylaminobenzimidazoles have been revealed promising derivatives leading to potent analgesic and anti-inflammatory effect.[163] Compound (74) has been distinguished for its analgesic activity, comparable to the standard nimesulide, while compound (75) was found to be a potent anti-inflammatory derivative. They are 2-extended benzimidazoles carrying a m-chloroaniline scaffold. Compound (76) has been found to be a promising histamine H1-receptor antagonist, leading to potent anti-allergic effect.[164] Antioxidants containing benzimidazole moiety have been repeatedly studied for their structural analogy to melatonin, a compound well known for its antioxidant properties.

Some benzimidazole-2-thiones, such as compound (77), have demonstrated antioxidant properties.[165] (77) seems to be able to act as radical scavenger, fighting the oxidative damage provoked by lipid peroxidation. Benzimidazole derivatives have also been identified as anticonvulsant agents. Compound (78), a 2-extended benzimidazole having a sulfur group in

position 2 which bears a 4-thiazolidinone moiety, is promising in the treatment of epilepsy.[166]

Benzimidazole seems further to be a critical scaffold in the treatment of Alzheimer disease.

(71) – R= Homolupinyl

(72)

(73)

(74) : R₁=−H
(75) : R₁=−Br

(76)

(77)

(78)

(79)

(80)

(81)
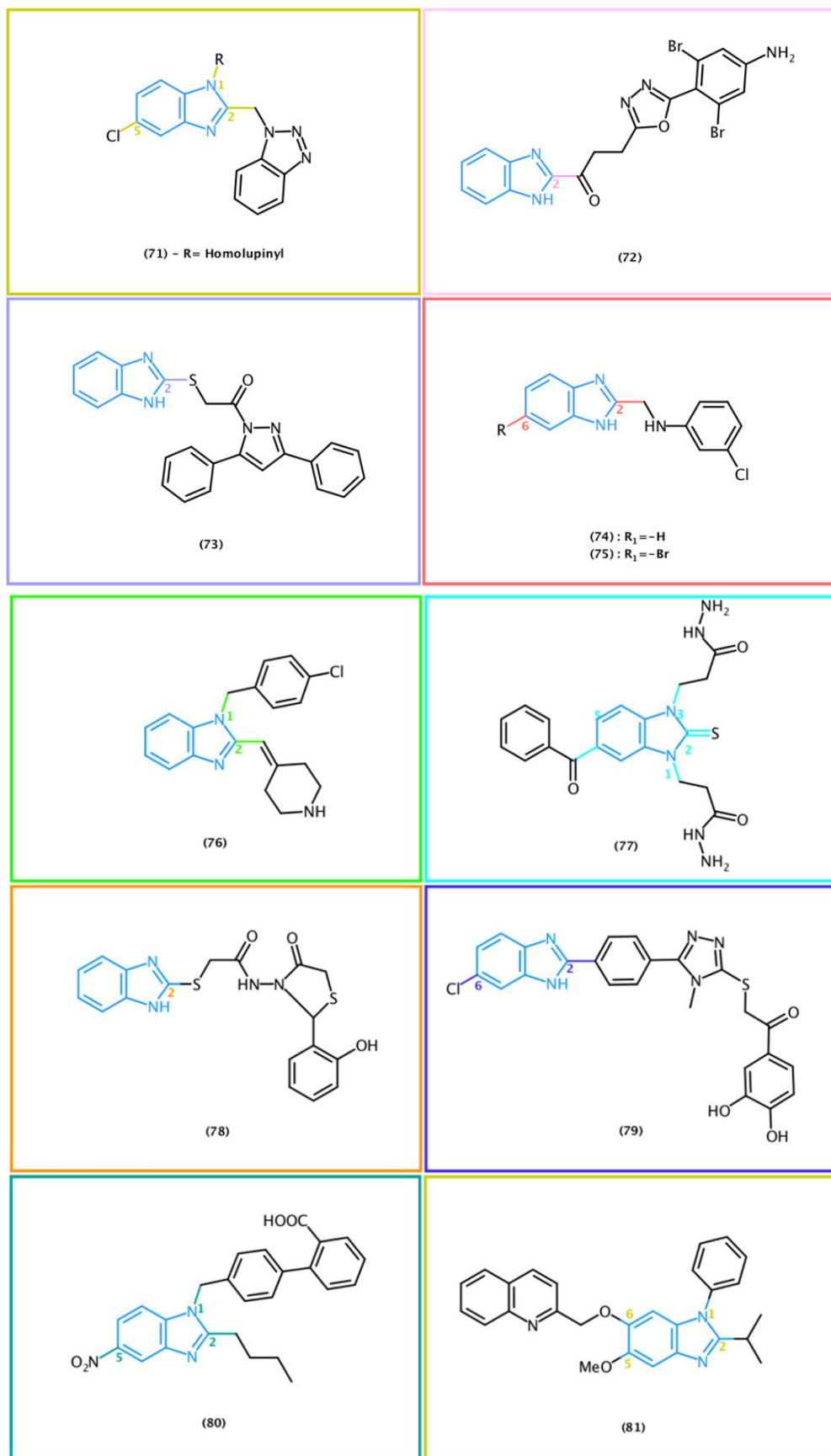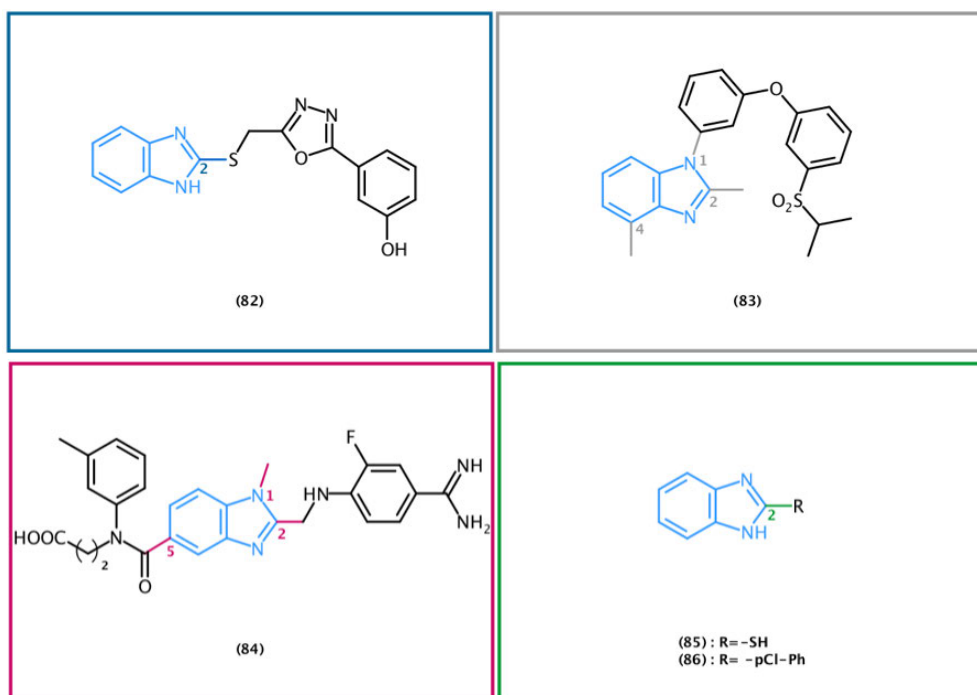
Figure 1. 29: Non-antimicrobial benzimidazoles reported in literature studies.

Multiple derivatives, such as compound (79), have been found to act as acetylcholinesterase inhibitors leading to an increase of the relative neurotransmitter level and fighting the loss of communication between neuronal cells.[167] Compound (80) has an antihypertensive effect, being a potential angiotensin II receptor antagonist as suggested by docking studies.[168] Benzimidazoles also found application in the treatment of psychiatric disorders such as schizophrenia. Compound (81) has been evidenced for its potential role in inhibiting phosphodiesterase 10A (PDE10A), leading to the restoration of second messengers (cAMP/cGMP) levels in schizophrenic patients.[169] It is 1,2,5,6-extended benzimidazole bearing a quinoline moiety in position 6.

Compound (82) is a 2-mercaptobenzimidazole having potent antidiabetic activity.[166] A further activity of benzimidazole derivatives is given by lipid modulation. Compound (83) has been evidenced for its affinity to liver X receptor which regulates lipid efflux, avoiding accumulation and preventing atherosclerosis.[170] The nucleus is 1,2,4-extended and the aryloxyaryl moiety, in position 1, bears a sulfone group. Compound (84) was found to have higher anticoagulant effect than the standard argatroban and it has been considered a potential antithrombin benzimidazole.[171] The benzimidazole core is 1,2,5-extended and bears a fluorinated carbamimidoyl-phenylamino moiety. Benzimidazole derivatives, such as compound (85) and (86), have been identified as critical priming agents, and used for improving seed parameters and crop production.[172]

1.6 Previous Efforts

Previous work in the Loveridge group[173,174] has been focused on lytic tranglycosylases (LT) as a potential target for fighting the bacteria resistance to β-lactam antibiotics. Owing to the variability of LTs, the analysis of the known LT structures and their mechanism of action has been deeply studied. Alignment of their amino acid sequences showed a close conservation of the main active site residues involved in the binding of substrates and known inhibitors. This led to the understanding of the key interactions required to bind the enzyme (Fig1). Bulgecin is able to strongly interact with LT forming a complex network of H-bonds. The hydroxymethyl group of the proline moiety interacts with the catalytic Glu162 and it is believed to be a key structure for new LT inhibitors. Potential benzimidazole-based LT inhibitors have been designed (Figure 1.30A-B), based on the interactions between LT and Bulgecin A,[175,176] a known enzyme inhibitor which is hard to synthesise and isolate. The designed compounds have been manually modeled into the LT active site giving promising results. In the modeled compounds, the proline moiety of bulgecin is replaced with the imidazole ring of a benzimidazole. Then the core is extended (Figure 1.30A-B) on its N_1-atom with amino acid chains through and acyl- or alkyl- bonds.
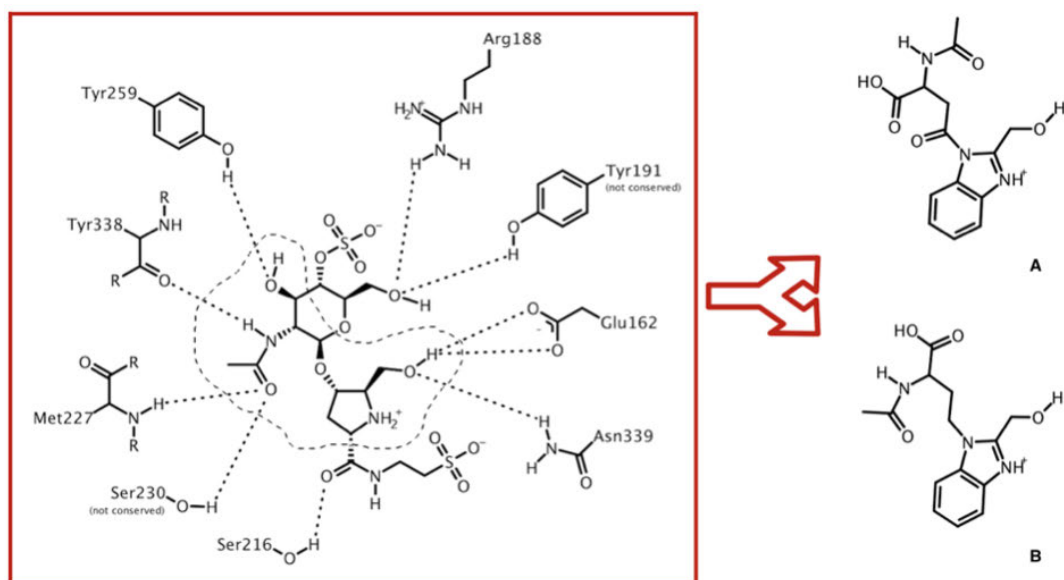
Figure 1. 30: 2D diagram of interactions between Slt35 and the known inhibitor Bulgecin A. The non-conserved residues are indicated. A and B represent early potential LT inhibitors designed in the previous work.

Due to the complex structure of the designed benzimidazole-based compounds, and the uncertainty about the feasibility of synthetic routes needed for preparing them, simpler

benzimidazole-based derivatives have been designed. Model reactions have been performed in order to investigate the feasibility of the BZI nucleus extension (Figure 1.31).
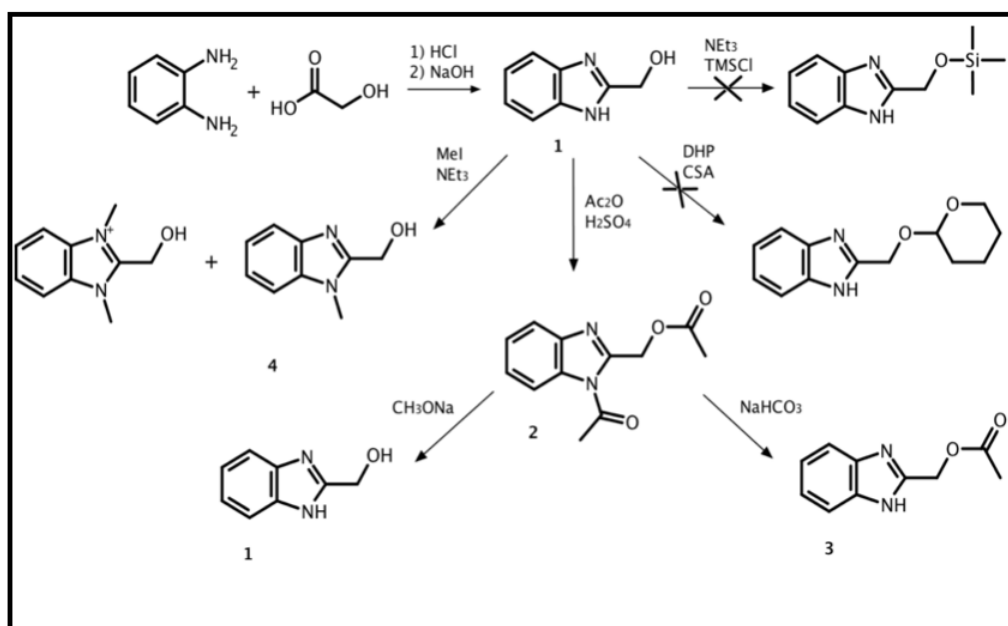
Figure 1. 31: Model synthetic routes undertaken in the previous work.

1H-Benzimidazole-2-methanol (1 in Figure 1.31) has been previously synthesized but was found to lack activity against *E. coli*.[177] Previous work in the Loveridge group investigated its activity against LT, but it was found not to bind the target. However, it was still considered a promising starting point for development of LT inhibitors.[173]

1H-Benzimidazole-2-methanol was therefore synthetized from o-phenylenediamine and glycolic acid with 83% yield for use in further investigations. In order to avoid competitivity between the N_3- nitrogen and the oxygen atoms, hydroxyl group protection was attempted using trimethylsilyl chloride (TMSCl) or 3,4-dihydropyran (DHP) without success. A double acetylation has been successfully performed leading to (1-acetylbenzimidazole-2-yl)methyl acetate (2 in Figure 1.31) with 53% yield. Attempts to perform a selective deacetylation[178] using a strong base (CH₃ONa) were unsuccessful as both the acetyl groups were removed using these conditions, giving 1H-Benzimidazole-2-methanol (1 in Figure 1.31). On the contrary, using a weak base (NaHCO₃), a selective N-deacetylation was successfully obtained leading to (1-H-benzimidazole-2-yl)methyl acetate with 46% yield. This demonstrated that the amide on the N1 nitrogen atom is more reactive than the ester part of benzimidazole derivative. In addition to this, an N_1 alkylation was attempted obtaining a mixture of the mono- and di-methylated 2-hydroxymethylbenzimidazole (4 in Fig1.31). The protection strategies might not be needed if

the relative reactivity of the oxygen and the nitrogen atoms is taken into account at early stages of the benzimidazole-based compounds.

The compounds synthesized have been tested against *E. coli* JM109 cells by disk diffusion assay. One of the model compounds synthesised in this work, (1-acetyl-benzimidazole-2-yl)methyl acetate (2 in Fig2), showed antimicrobial activity (Figure 1.32) with an inhibition zone of 16.0 ± 3.6 mm from 300 μg compound. This is considerably weaker than the strong inhibition typical of ampicillin (19.7 ± 6.7 mm inhibition zone from 30 μg compound),) , but demonstrates that 1-H-hydroxymethylbenzimidazole can be developed into an active antimicrobial with only minor modification.
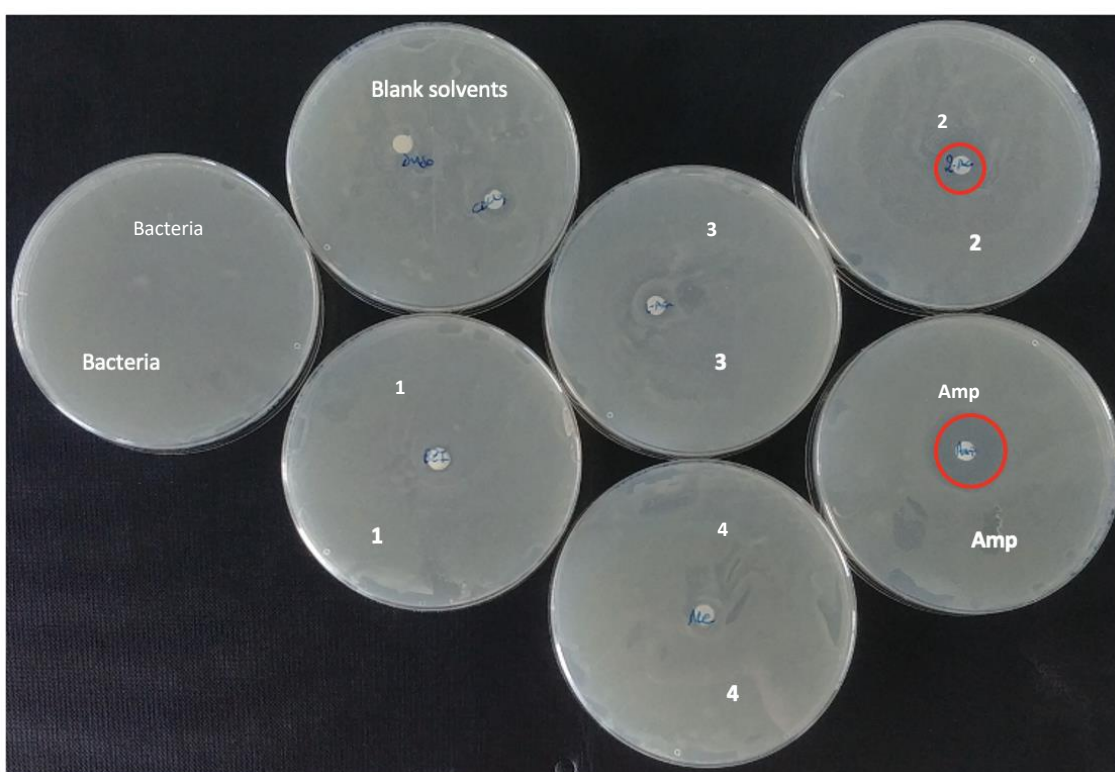
Figure 1. 32: Disk diffusion assays performed in the previous work.[174]

Despite the activity of the diacetyl- derivative was found to be weaker than the positive control Ampicillin, Its activity needs to be investigated. It could target LT or Its activity could purely be a chance discovery. However, It could be that the parent 1-H-hydroxymethyl-benzimidazole (1 in Figure 1.31) is active against bacteria but unable to penetrate the cell membrane whereas the acetylated derivative (2 in Fig1.31) could act as prodrug, penetrate the cell and then be hydrolyzed to release the active compound.

1.7 Aims of the work

Overall, the main aim of this work was to develop antimicrobial compounds based on benzimidazoles. The need for new antibiotics, and more in general antimicrobial agents, has been highlighted above. Lytic transglycosylase (LT) has been considered a promising target for overcoming the resistance to β-lactam antibiotics due to its critical role in activating the production of β-lactamases. The co-administration of a LT inhibitor and a β-lactam antibiotic could directly harm the stability of the bacteria call wall as well as enhance the activity of the β-lactam by inhibiting its inactivation.

The first aim of this work was therefore to design extensions of the benzimidazole nucleus leading to antimicrobial activity. Benzimidazole is a common building block in drug design and discovery. Based on the structure of already marketed benzimidazoles and the most promising analogues highlighted by literature studies, combined with information about the active site of lytic transglycosylases, novel benzimidazoles would be designed and investigated by *in silico* screening to determine whether affinity for the designed target is feasible.

Once suitable benzimidazoles were designed, the second aim was identification of suitable synthetic routes for preparing these compounds in order to build a library of synthetic derivatives. The results presented in previous works evidenced the possibility to acetylate both the nitrogen and the oxygen atoms of the 1-H-2-hydroxymethyl-benzimidazole, showing a competitivity between these atoms of the nucleus. Alkylating the benzimidazole core selectively on the nitrogen atom was unsuccessful leading to a mixture of mono- and di-alkylated benzimidazole. Therefore a critical aim of this work was to find an alternative synthetic path in order to selectively extend the benzimidazole on its N-atom as well as extend the nucleus on its different sites.

Once a library of benzimadazoles was available, the final aim of this work was to investigate their antimicrobial effect and their binding to protein targets. Based on these results, structure-activity relationships could be investigated with a view to improving the potency and other drug-like properties of the hit compounds identified here.

Chapter 2

Design of benzimidazole-based ligands and *in-silico* studies

2. Design of benzimidazole-based ligands and *in-silico* studies

2.1. Introduction: drug discovery/development

Developing a new drug from initial investigations to its actual market introduction is a complex process which usually takes up to 10-15 years, cost over a million of pounds and involves multiple critical research workers such as medicinal and organic chemists, biochemists and pharmacologists.[179,180] Due to the high time/ resources consuming associated with drug discovery, 'Preclinical' studies play a critical role in order to select and optimize highly promising drug-like compounds, limiting drug failure during the following clinical phases.

Early phases of 'drug discovery', aim to identify molecules potentially active against a designed target. Computational approaches[181,182] have a critical role at this stage by reducing the number of promising candidates and leading to the design of a small library of hit-molecules with high affinity for the biological target.[180] Once identified active compounds (Lead identification) and considered their potential effects in living being, the following 'Preclinical stage' aims to identify the drug toxicity level on the base of in vitro and in vivo testing (Lead optimization).[183]

Candidates having efficacy and safety on animals, undergo 'clinical research' stage. Clinical trial studies involve four phases and lead to the launch of new drugs if the candidate successfully passes each phase, demonstrating to be safe and effective.[184]

An overall of just 25% of drugs is believed to move from Phase III to IV leading to a time/ resources wasting when drugs fail in the late clinical trials.[185] Drugs fail mainly due to their inactivity or toxicity when administered.[186] Accurate preclinical studies are a key step in drug discovery process leading to the selection of hits having high probability to successfully pass the following clinical trials and limiting late failures.

2.1.1 Virtual Screening

Computational approaches have been introduced since long time.[187] In silico drug design (Computer Aided Drug Design, or CADD) is commonly used in the early stages of drug discovery for the identification and selection of new compounds which could potentially bind a desired target. It aims to reduce the number of drug-like candidates leading to the design of a small library of compounds with high probability to be active against the target. It involves Virtual Screening (VS).[188,189] The ligand design process is a computational path that involves a Ligand Based[190] and Structure-Based Drug Design[191] (LBDD and SBDD). The LBDD approach, also called pharmacophore study, is commonly used when the 3D target structure is not available. It selects potential candidates on the base of structural frames (pharmacophores) present in known ligands and believed to lead to biological activity[192]. Conversely, SBDD, also known as drug-target docking, is based on the knowledge of the target 3D structure, and it is the most common computational approach. Molecular docking predicts the orientations (poses) and relative interactions of a ligand in complex with a protein or an enzyme target.[193]

2.1.2 Ligand-receptor complex formation

Different interactions drive the molecular recognition and the complex formation[194] leading to a stable ligand-receptor association. The contribute given by the relative forces employed is critical in drug design leading to the understanding of the requirements needed by new drug-like molecules.

Docking programs use algorithms for predicting the energetics of the ligand-receptor complex. The stability associated with the complex formation is reflected by the binding free energy (ΔG; Gibbs free energy) which is given by two thermodynamic factors, changes in enthalpy (ΔH) and entropy (ΔS),[195,196] following the equation (1).

$$\Delta G = \Delta H - T\Delta S \qquad (1)$$

Systems physiologically evolve towards a minimum of energy, which means stability, leading to a decrease of the ΔG value. Considering an enzyme binding its ligand, the binding enthalpy is given by the loss of interactions (H-bonds) with displaced solvent molecules and following replacement of these H-bonds with complementary groups of the ligand. The replacement of water interactions given by ligand groups, with are highly complementary to the active site, gives

stability to the complex leading to a negative enthalpy change value. The entropy factor considers the displacement of solvent molecules from the active site and the loss of conformational freedom, reflecting disorder and the disruption of interactions, leading to a positive entropy value. Thus, the contribute given by these two thermodynamic entities result in a final negative binding free energy which represents a stable complex.

The ligand-receptor interaction can be seen as a binding reaction given by an equilibrium between the dissociated entities (un-bonded ligand [L] and receptor [R]) and the complex [RL] given by the relative associated units, as shown from equation (2). The forward and reverse paths are regulated by the relative kinetic constants (K_{on} for the forward and K_{off} for the reverse path).

$$[R] + [L] \rightleftarrows [RL] \qquad (2)$$

The complex formation starts when a low concentrated ligand successfully binds the relative receptor. The increasing of ligand availability leads to a rise of the complex formation, until the reaching of a steady state given by the equilibrium. At this stage, the complex formation and dissociation proceed with the same speed. The kinetic parameters, K_{on} and K_{off}, are concentration-dependent, as shown from equation (3). They can be used for obtaining the binding affinity constant (K_a), which regulates the complex formation. K_a is equal to the reverse of K_d (dissociation constant), which modulates the complex breakage, leading to the releasing of unbounded entities following equation (3) and (4).

$$K_{on} [R] [L] = K_{off} [RL] \qquad (3)$$

$$K_a = K_{on} / K_{off} = [RL] / [R] [L] = 1 / K_d \qquad (4)$$

The complex formation between a general inhibitor [I] and an enzyme [E], could be studied by considering the dissociation phenomenon[197] as shown from equation (5).

$$[EI]_{aq} \rightleftarrows [E]_{aq} + [I]_{aq} \qquad (5)$$
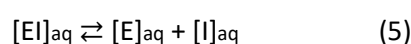
The complex is considered being in equilibrium with the dissociated patterns and the equilibrium shifting depends on the binding free energy (ΔG).
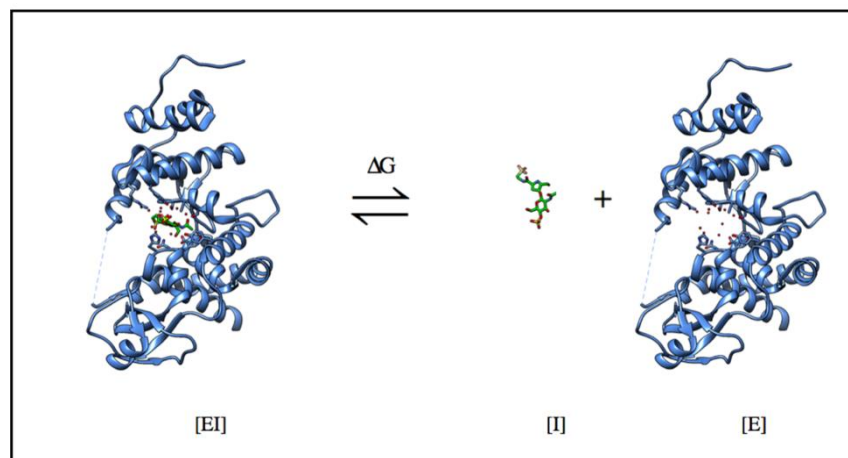
Figure 2. 1: Cartoon representation of the protein-ligand complex in equilibrium with the relative dissociated forms.

The ΔG energy value is directly correlated to the binding affinity constant (K_a), following equation (6). Being K_a equal to the reverse of K_d (dissociation constant) and depending on the concentration of the [EI] complex following equation, the different equations for ΔG can be easily obtained.

$$\Delta G = -RT \ln K_a = -RT \ln 1/K_d = -RT \ln [EI] / [E] [I] \qquad (6)$$

It is not possible to obtain the K_a binding constant values, which is the factor reflecting the binding affinity using classic docking programs. K_a is usually obtained in the last step of preclinical studies, performing specific ligand binding assays[198]. Despite this, computational approaches aim to predict the binding energy on the base of a sum of different factors which strongly contribute to the complex formation such as interactions, protein flexibility, solvation and protonation. The more factors considered, the more accurate the results will be, but also more expensive, more challenging and more time consuming.

2.1.3 Molecular Docking

As mentioned, docking aims to identify potential new ligands/inhibitors having high affinity for the target. One of the main distinctions in between ligands is given by reversible or irreversible enzyme inhibitors. In sight of this, the docking approach could be distinguished in Non-covalent docking, used for selecting promising inhibitors associated to the target through non covalent interactions (mainly H-bonds), and Covalent molecular docking which simulates covalent bonds between a suicidal irreversible inhibitor and the target.[199,200,201,202,203] Despite covalent inhibitors having well known advantages, the limited use of irreversible drugs, mainly for safety reasons, makes this computational branch not fully explored and still challenging. This work is focused on selecting reversible/competitive inhibitors on the base of non-covalent molecular docking studies and so focused only on a non-covalent computational approach.

Different approaches have been in depth studied and improved over the years trying to overcome the initial issues of computational programs which were leading to results with pour accuracy. Critical factors influencing the accuracy of computational analysis are given by flexibility, X-ray crystallography methods, solvation and protonation.[204] Computational analysis should consider the multiple factors involved in the ligand-receptor complex formation in order to improve the accuracy of docking results. Despite the importance given by each factor, considering all forces employed in ligand association is a challenging goal to achieve and would require complex computational methods.

A critical factor is given by flexibility. The docking programs initially developed were based on the "lock and key" theory, introduced by Fisher in 1894, and considered both ligand and receptor as rigid structures leading to results with poor accuracy.[205] The ligand was considered to perfectly fit into the receptor binding pocket, like lock and key, on the base of their complementarity. Although the "lock and key" approach properly explains the ligand-receptor affinity, it lacks critical considerations about their structures. In fact, both ligand and enzyme are naturally dynamic molecules able to readapt their conformation forming a stable complex. Thus, their flexibility is an intrinsic property, which needs to be considered when predicting the ligand binding affinity. The later "induced-fit" theory, introduced by Koshland,[206] was based on a continuously remodeling active site when the receptor is interacting with a ligand, suggesting a flexible context. Nevertheless, this approach doesn't fully reproduce the real ligand-receptor interaction, not reflecting the physiological protein behavior. Simulating the protein and ligand behavior represents one of the biggest problems in computational drug design[207]. Different

algorithms have been developed over the years in order to consider protein flexibility and overcome the initial difficulties, giving a full representation of the ligand-target complex.[208] "Soft docking" was one of the earliest computational approaches considering local protein flexibility.[209] It was based on a 'soft lock and key' theory, accounting minor receptor conformational changes.

Molecular Dynamics (MD),[210] a more accurate approach recently developed in order to consider the flexibility of both ligand and receptor, is time consuming and is not the most convenient strategy in the early drug design stage. MD considers the receptor structure as the sum of different conformations reproducing a full spectrum of possible protein structures interacting with the ligand. This method is challenging and requires advanced/expensive software and so is only used in the latest steps of preclinical research, once the selected drug-like molecule has been revealed as active against the designed target. It is generally used for confirming the ligand conformation/location into the receptor binding pocket.

The best compromise between accuracy and time/resources considers a flexible ligand interacting with a rigid receptor which is the strategy adopted in this work. Multiple docking programs have been developed over the years in order to increase the accuracy of the ligand pose prediction into the receptor binding pocket. Autodock Vina is one of the latest docking tools bringing several improvements in VS analysis such as higher speed, if compared with the previous AutoDock4, and accuracy in the binding pose prediction.[211]

2.1.4 Limitation of "early-stage" computational approaches

Despite their critical role in the development of new drugs, as previously mentioned, most common Virtual Screening (VS),[188,189] programs don't account all factors influencing the ligand-receptor complex formation (such as receptor flexibility and solvent effect), leading to a partial method reliability and limited accuracy associated with this computational approach. Considering all effects contributing to the ligand binding requires complex algorithms, expensive software and long time of analysis. Despite these disadvantages, the most common docking approach represents the best option in predicting the potential affinity of new drug-like molecules for the target, at early stages of drug discovery. An additional limitation of *in-silico* drug design is the sole attribution of drug's effects to one target as this doesn't consider off-target mechanisms.

2.2 Design of benzimidazole-based ligands

2.1.1 1H-Benzimidazole-2-methanol

Observing the main interactions required for binding the target, on the basis of the studies of Slt35 in complex with bulgecin A (section 1.4.4), potential new inhibitors have been designed using the benzimidazole nucleus as scaffold for mimicking the structure of the known inhibitor and so its interaction with the target. In this work, the proline moiety of bulgecin is replaced by the imidazole part of a benzimidazole nucleus (Figure 2.2A), a critical moiety well known for its antimicrobial properties (section 1.5.4). The further modification designed,[173] is the insertion of a hydroxymethyl group in position 2 of the BZI core mimicking the proline-hydroxymethyl of bulgecin and potentially reproducing the interaction with the catalytic Glu162 residue into the LT active site. This modeled core modification led to 1H-benzimidazole-2-methanol (Figure 2.2B) which seems to be a promising scaffold for new LT inhibitors, having the N3- atom potentially protonated, with its positive charge mimicking the oxocarbenium intermediate ion[73] as Bulgecin does, and the hydroxyl group likely able to interact with Glu162 and Asn 339. In order to increase the potential affinity of the 2-hydroxymethyl-benzimidazole nucleus for the LT target, different extensions of the core have also been considered.
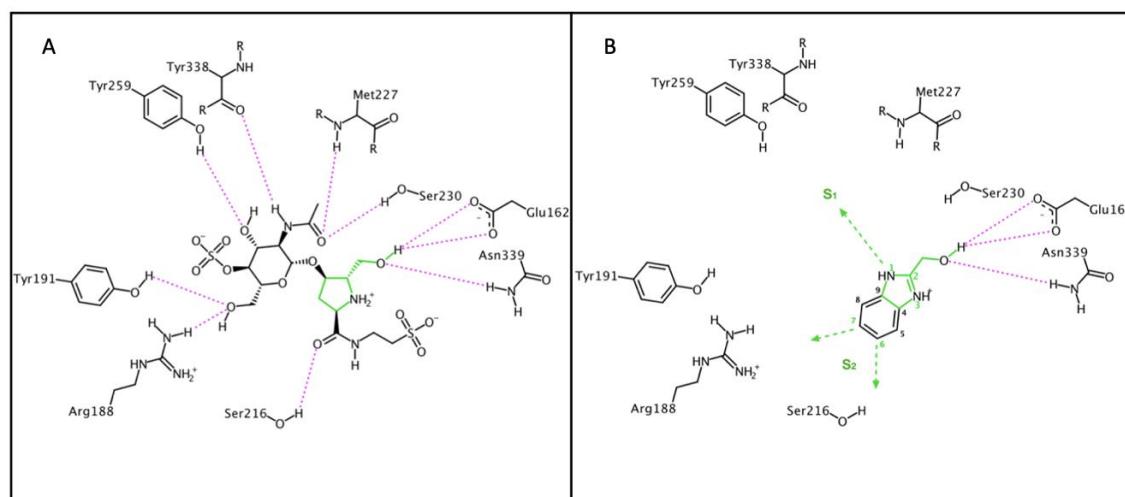
Figure 2. 2: A) Diagram of interactions of Slt3567 in complex with the known inhibitor evidencing its key hydroxymethyl-proline moiety (shown in green) to be mimicked in the design of new LT inhibitors. B) Manually imported 2-hydroxymethyl-benzimidazole core into Slt35, having the imidazole (shown in green) ring mimicking the proline-bulgecin A moiety. The extending strategies (S1 and S2) of the core, planned in order to enhance the ligand affinity for the target are also shown.

Starting from the structure of 1H-benzimidazole-2-methanol, extensions on the N-1 atom of BZI seem to be a promising strategy (strategy1 or S_1 in Figure 2.2B) that could mimic the GlcNAc residue of Bulgecin and reproduce the network of interactions with the side chains of Ser230, Try 259 and/or Tyr191.

In addition, extending the core on the benzene ring (strategy2 or S_2 in Figure 2.2B), on its C_6/C_7 atoms, has also been considered in order to improve the affinity between the ligand and the target reproducing the H-bonds with Arg188, Tyr191 and/or Ser216 residues that bulgecin creates. Early active site considerations revealed available active site space on the benzene side (C_6/C_7 atoms) of 1H-benzimidazole-2-methanol. The benzimidazole was manually imported into the Slt35 crystal structure (PDB 1D0L).[67] Bulgecins was replaced by 1H-benzimidazole-2-methanol with its N-atom in the same location than the nitrogen atom of the proline moiety of the known inhibitor. Considerations on the active site pocket with the benzimidazole replacement indicated a hydroxymethyl group close to the protein surface, suggesting lack of possibility for extensions on this site of the ligand. Conversely, available space on the N_1-atom and benzene ring sides were observed suggesting possibility to extend these parts of the ligand (Figure 2.3A).
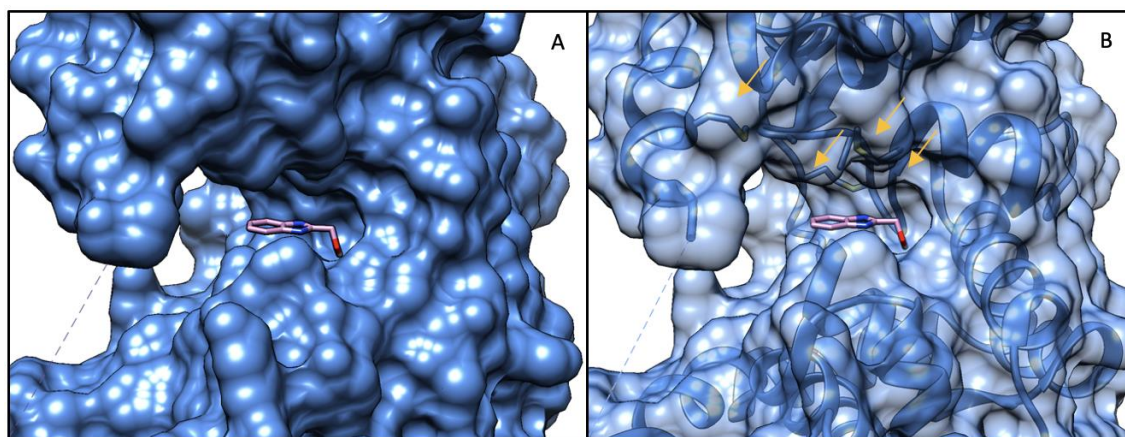
Figure 2. 3: A)Cartoon representation of Slt35 (1D0L) in complex with 1H-Benzimidazole-2-methanol (in pink). The protein surface is shown in blue. B) Cartoon representation of Slt35 (1D0L) in complex with 1H-Benzimidazole-2-methanol (in pink). The protein ribbons and hydrophobic residues (indicated by yellow arrows) have been partially shown.

The benzene ring of the ligand is into a hydrophobic pocket with Met and Ala residues which could generate hydrophobic contacts (Figure 2.3B). This suggests that insertion of non-polar extensions on C_6/C_7 atoms of the benzimidazoles could lead to interactions with the target.

The combination of the two strategies (S_1+S_2 in Figure 2.2B), extending the benzimidazole nucleus on both sides, could finally lead to a hit molecule potentially able to form a complex network of interactions with the target and strongly inhibit lytic tranglycosylases. In this work, most promising benzimidazole extensions have been introduced and analyzed in depth.

2.1.2 N_1-extended benzimidazole-2-methanol

Multiple extensions on the nitrogen N_1 atom have been considered. The effect of non-polar chains, able to generate hydrophobic interactions into the LT active site, as well as the insertion of polar chains, able to form H-bonds with the active site residues of the target, has been deeply analyzed.

N-acylation and N-alkylation have been examined as the two model extensions of the BZI nucleus on the N1 position. As evidenced before (section 1.5.1), the benzimidazole core has unique chemical properties which need to be analyzed when designing possible nucleus modifications. The lone pair of electrons on the nitrogen N1 atom is involved in the π system giving a non basic N-atom as result which could discourage the extension on this side of the molecule (Figure 2.2B- strategy-s1). Conversely the lone pair of the N3 nitrogen atom of benzimidazole is not involved in the aromatic system, being in an sp^2 orbital which is perpendicular to the plane of the p orbitals. This lone pair on the N3, not being involved in the π system, is available to perform nucleophilic attack and to act as a base leading to a feasible N-extension of the benzimidazole core.
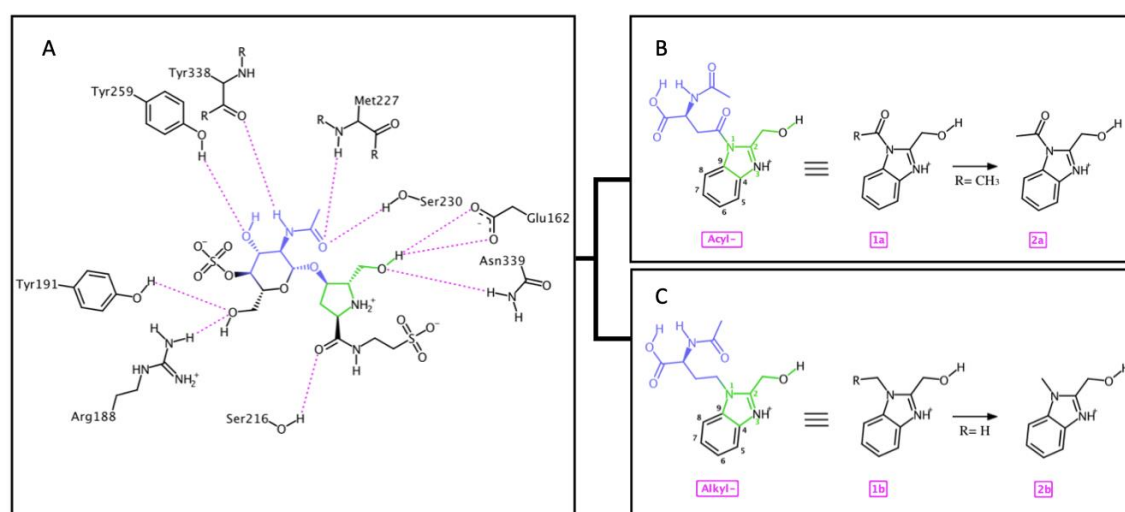
Figure 2. 4: A) Diagram of interactions of Slt35 in complex with the known inhibitor evidencing its key hydroxymethyl-proline moiety (shown in green) and its GlcNAc moiety to be mimicked. B) Model N-Acyl and C) Model N-Alkyl benzimidazole derivatives modeled in early stage of the work.

Considering acylation and alkylation as promising N-extensions of the nucleus, two compounds have been designed in the early stage of this work and considered promising candidates for mimicking the GlcNAc residue of Bulgecin (violet in Figure 2.4). Both of them are given by a 2-hydroxymethyl-benzimidazole extended on the N atom with amino acid chains. Amino acids are readily available reagents, potentially able to form H-bonds into the active site due to multiple functional groups present in their chains. In the acyl-derivative (Figure 2.4B) a L-aspartic acid chain is connected, through its side chain, to the benzimidazole nucleus by an amide bond, while the alkyl benzimidazole (Figure 2.4C) has a L-homoserine as N-extension forming an alkylated derivative. Both of them have the main chain free, able to interact with the target. The modeled benzimidazole derivatives (Figure 2.4B-C) have been manually imported into the Slt35 active site using Chimera in order to verify their orientation. The 2-hydroxymethyl-imidazole part has been superimposed to the proline moiety of Bulgecin and the N-extension located in the same subsite as the GlcNAc residue of the known inhibitor and seems to preserve the interactions given by the hydroxymethyl group with Glu162 and Asn339. The modeled extensions have multiple polar groups which seem to be at H-bond distance with the main active site residues involved in the binding of the GlcNAc part of the known inhibitor. This is only an early investigation on properties required by the BZI N-extensions for mimicking the Bulgecin structure and the results will be confirmed by docking studies before to be considered reliable.

Due to the complexity of the early designed ligands, the potential variability of their orientation into the LT active site and the competitive reactivity that their multiple functional groups could have when considering synthetic approaches, simpler compounds have been modeled (section 1.6) and their potential affinity has been investigated through docking study providing a library of promising ligands.

A further extension on the nitrogen-1 atom considered in this work is given by substituted benzyl moieties. Multiple substituents (such as methyl, chlorine, bromine, nitro or hydroxyl groups) on the N1- benzyl ring have been considered and their potential role in interacting with the target has been analyzed (Figure 2.5).

R_1= –H , –NO$_2$, –OH
R_2= –H , –NO$_2$, –OH , –OCH$_2$CH$_3$
R_3= –H , –CH$_3$, –Br , –Cl , –F, –NO$_2$, –OH , –OCH$_3$
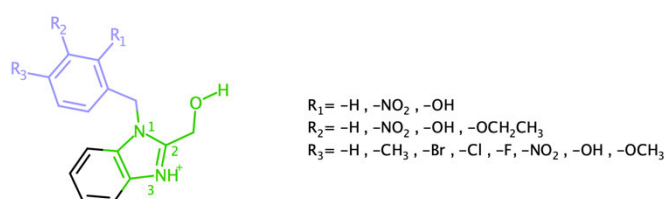
Figure 2. 5: General structure of 1-benzyl-2-hydroxymethyl benzimidazoles designed in this work. The 2-hydroxymethyl-imidazole moiety is in green color while the N$_1$ benzyl extension is in purple color (R$_1$, R$_2$ and R$_3$ vary).

The phenyl moiety of these ligands could form hydrophobic interactions with active site residues, the insertion of halogen substituents on the benzene ring could lead to the formation of non-bonding interactions with the target[212] while hydroxyl groups could form H-bonds with active site residues. This modification of the benzimidazole core could increase the affinity of this class of BZI-based ligands for the LT target by reproducing critical interactions with the main active site residues involved in the binding of the GlcNAc part of the known inhibitor Bulgecin A.

2.1.3 Alternative C_2-extensions of the benzimidazole core

Literature studies evidenced the critical pharmacological role played by benzimidazoles extended on the C_2 atom of the nucleus (section 1.5). In addition, early docking studies suggest an alternative orientation of the 1H-benzimidazole-2-methanol into the Stl35[67] active site.
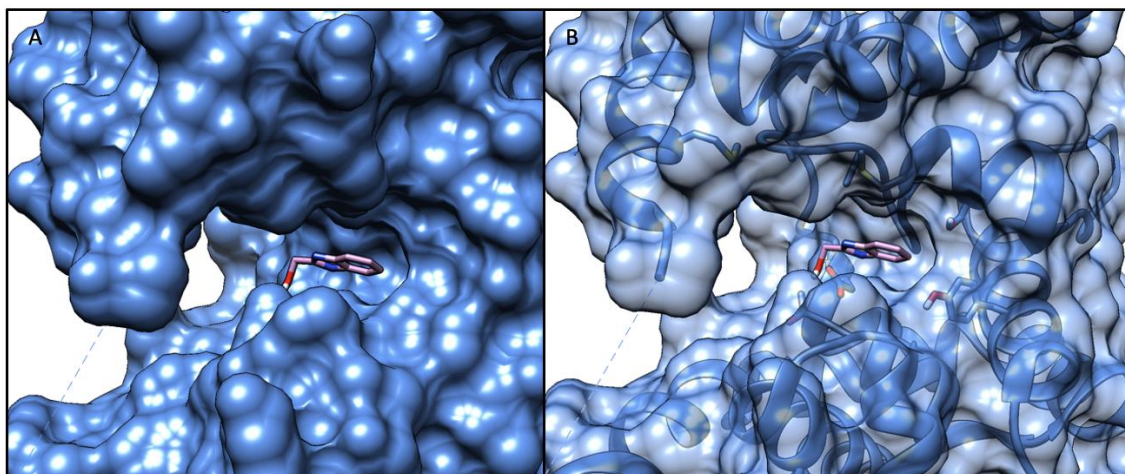
Figure 2. 6: A) Cartoon representation of docking results when Slt35 (1D0L) is in complex with 1H-Benzimidazole-2-methanol (in pink). The protein surface is shown in blue. B) Cartoon representation of Slt35 (1D0L) in complex with 1H-Benzimidazole-2-methanol (in pink). The protein ribbons and hydrophobic residues (indicated by yellow arrows) have been partially shown.

The predicted binding pose (Figure 2.7) showed the benzimidazole in a flipped orientation compared to the one obtained by manually importing the ligand into the active site and replacing bulgecin (Figure 2.3).

Despite this, molecular docking confirmed its predicted affinity for the target revealing a potential good ligand-receptor interaction. Its hydroxyl group is involved in H-bond formation (light green color in Figure 2.7A; dashed lines in Figure 2.7B) with the catalytic Glu162 and, through its oxygen atom, with Asn339 residue.
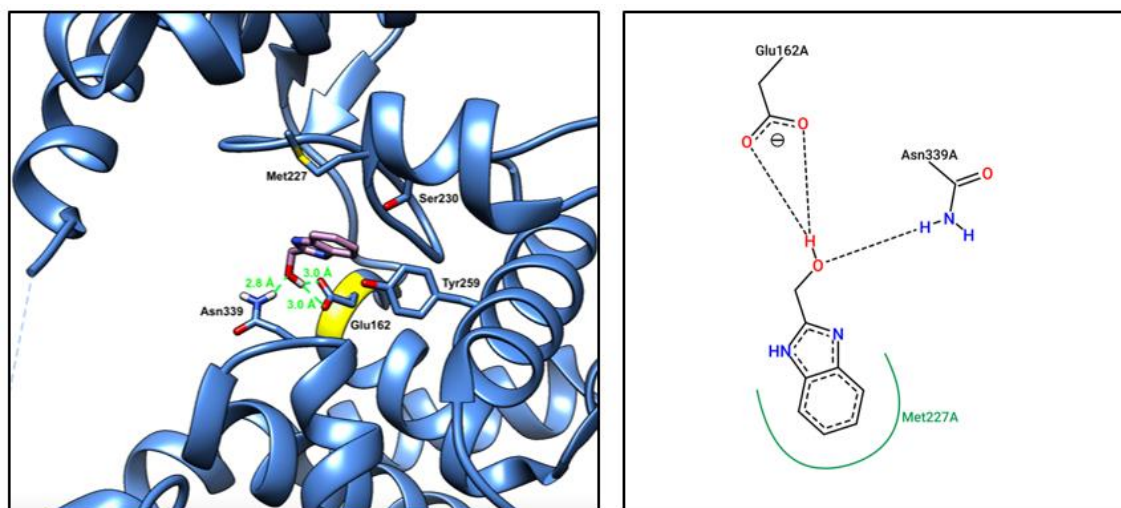
Figure 2. 7: A) cartoon representation of Slt35 (blu color -PDB 1D0L) in complex with 1H-benzimidazol-2-ylmethanol (BZI-1) (pink color). The catalytic Glu162 residue is shown using yellow ribbon color while H-bonds are in dashed light green lines. B) 2D diagram of interactions showing H-bonds (dashed lines) and hydrophobic interactions in spline dark green color.

Docking analysis also revealed hydrophobic contact (spline section in B) between the benzene ring of the BZI core and Met227 residue, as showed in the 2D diagram of interactions. The ligand affinity for the target confirms the critical role this benzimidazole scaffold could potentially have in mimicking the bulgecin structure and so binding the LT active site.

This revealed the possibility to extend the nucleus on the C_2-part (Figure 2.6A). In this predicted orientation, the hydrophobic pocket with Met and Ala residues could generate hydrophobic contacts with benzene rings at C_2-position of the benzimidazole. Therefore, a further category of ligands has been designed. They are substituted 2-phenyl-1H-benzimidazoles and bis-benzimidazoles.

Multiple substituents, new or already known, on the 2-phenyl ring have been designed and their potential interactions with the 1D0L active site residues considered (Figure 2.8). The C_2-benzene could generate hydrophobic contacts while substituents (R1, R2, R3) could generate additional interactions with Arg188 and Tyr191.

$R_1 = -H, -NO_2, -OH$
$R_2 = -H, -NO_2, -OH, -OCH_2CH_3$
$R_3 = -H, -CH_3, -Br, -Cl, -F, -NO_2, -OH, -OCH_3$
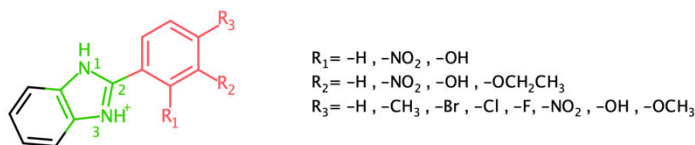
Figure 2. 8: General structure of 2-phenyl-1H-benzimidazoles designed in this work. The imidazole moiety is in green color while the C_2 benzene extension is in red color (R_1, R_2 and R_3 vary).

The phenyl- C_2 extension has very different chemical and physical properties than the 2-hydroxymethyl chain and so it could lead to a different ligand orientation into the LT active site. This category of ligands could create a strong network of interactions with the LT active site residues and potentially inhibit lytic tranglycosylases.

Bis-benzimidazole are compounds given by the connection of two benzimidazole nuclei. In this work 2,6-bis-BZIs are considered as LT ligands. In this class of compounds one BZI nucleus, through Its position 2, is connected to the C_6 atom of the second benzimidazole moiety (Figure 2.9).
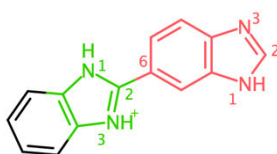
Figure 2. 9: General structure of 2,6-bis-benzimidazole designed in this work. The imidazole moiety of the first BZI-nucleus is in green color while the C_2 BZI extension (second nucleus of benzimidazole) is in red color.

The benzene moieties of the two benzimidazole nuclei could form hydrophobic interactions into the LT active site as well as represent good substrate for electrophilic aromatic substitution leading to potential extension sites. The N_3-, with its lone pair, and the N_1-H atoms could create H-bonds with the active site residues. Moreover, the nitrogen atoms could represent good sites for extension (such as N-acylation or N-alkylation).

2.1.4 Thiabendazole analogues

Thiabendazole is a marketed C_2-extended benzimidazole with anthelmintic activity (review chapter). It is composed of a benzimidazole moiety having a thiazole extension in position 2 of the BZI-nucleus (Figure 2.10).
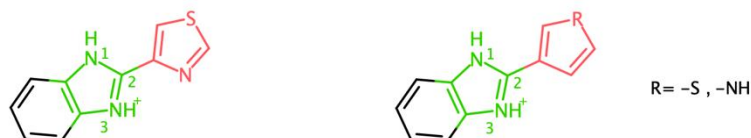
Figure 2. 10: Left) structure of thiabendazole. Right) general structure of thiabendazole analogues designed in this work. The imidazole moiety of the BZI-nucleus is in green color while the C_2 extension is in red color and the benzene moiety is in black.

Thiabendazole is an example of active molecules having antimicrobial activity which are given by the combination of heterocycles (section 2.5.5.2). Due to the critical role played by these molecules, in this work, several thiabendazole analogues, obtained by connecting two heterocyclic nuclei, have been designed. In these compounds the BZI moiety has been extended in position 2 with a thiophene or a pyrrole ring.

2.1.5 Benzene extensions

Owing to its structure, the benzene ring should be easily extensible being a good substrate for electrophilic aromatic substitution. Multiple extensions on the C_6 or/and C_7 carbon atom, having different chemical properties, have been considered (such us methyl or carboxylic groups, halogens or carbon chains) leading to mono- or di-substituted derivatives (Figure 2.11).

$R= -CH_2OH , -C_6H_5 , -C_7H_5N_2 , -C_4H_3S , -C_4H_4N$
$R_1 = -H , -CH_3$
$R_2 = -H , -CH_3 , -Cl , -NO_2 , -COOH , -C_8H_5O , -F$
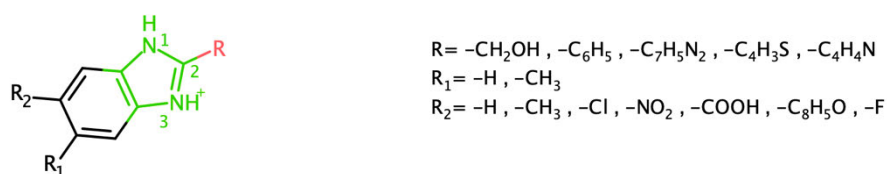
Figure 2. 11: General structure of 5,6-substituted-1H-benzimidazoles designed in this work. The imidazole moiety is in green color while the C_2 benzene extension is in red and the benzene moiety is in black color (R_5, R_6 vary).

Polar groups in position 5 and 6 of the benzene ring could be able to form H-bonds with Arg188, Tyr191 and/or Ser216 residues in the LT active site (Figure 2.4) while non polar chains could create electric forces and maybe optimize the ligand-receptor interaction orienting the ligand in a favorable pose. The analysis of the effects created by different substituents in these positions of the ring could lead to the understanding of the ligand properties required for binding the target.
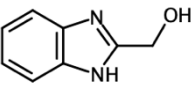
This core modification has also been combined with N_1 and/ or C_2-extenasions in order to fully investigate the extensibility of the BZI nucleus and the relative effect on the ligand affinity for the target. Substituents on the benzene side of the molecule could be critical for binding LT or could enhance the affinity of a N_1-extended benzimidazole for the target when considering a combination of the two extending strategies (S_1+S_2 in Figure 2.2).
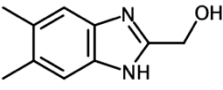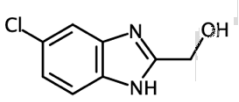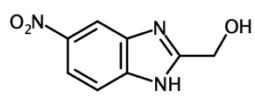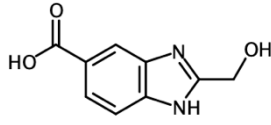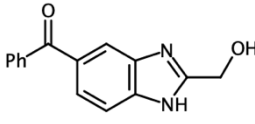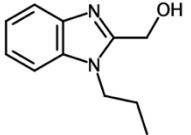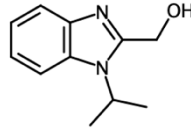
2.2 Molecular Docking of the designed benzimidazoles (BZI)
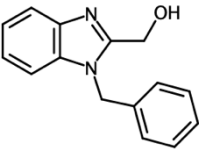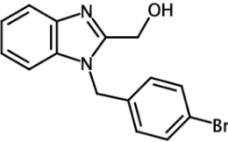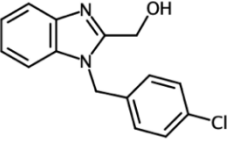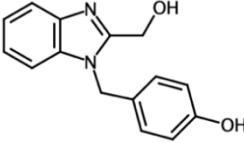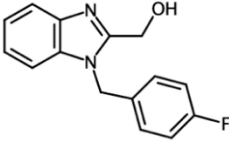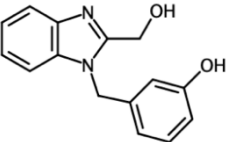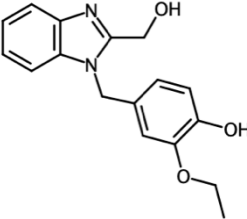
This section is focused on molecular docking as computational approach for predicting the poses of designed benzimidazole-based compounds bound to a biological target (Lytic transglycosylases). The final aim is to create a library of hit compounds with high affinity for the receptor and so potentially active against the target. Benzimidazoles have been imported into UCSF Chimera[213] and docked using AutoDock Vina.[213] Ligand-receptor interactions have been evaluated in order to select potential target inhibitors.
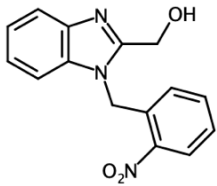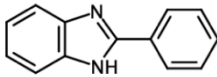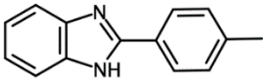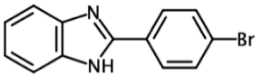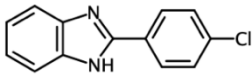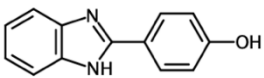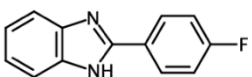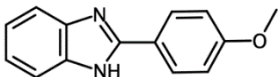
2.2.1 Lytic transglycosylases (LT) as target for BZIs
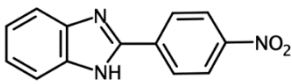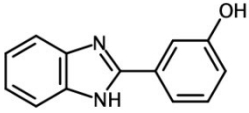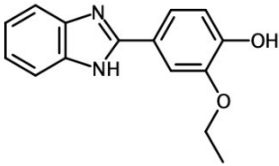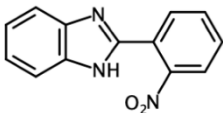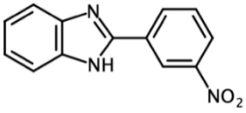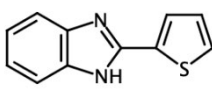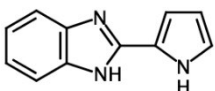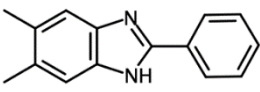
Slt35 crystal structure has been used as model LT target. 150 benzimidazole ligands have been docked into the Slt35 active site (PDB 1D0L),[214] based on the location of the co-crystallized Bulgecin A. The structure and relative ligand-receptor interactions have been reported in the following table. The score value associated with the ligand pose is noted. Scoring functions are mathematic functions used in order to predict the binding affinity for ligand-receptor complex, when performing docking analysis. Calculating the binding free energy by computational approach would be demanding and would require complex algorithms in order to include all interactions, effects and factors involved in the complex formation. Scoring functions are commonly used for distinguish binding poses and especially for simplifying the prediction of the ligand affinity for the target.[215] They give a predicted examination of favorable and unfavorable effects involved in the ligand-receptor complex formation considering multiple factors such as H-bonds and hydrophobic contacts. Despite the critical role of score values in comparing different ligand poses they don't reflex the binding constant. Score values only compare different orientation of the docked ligand. The reported ligand-receptor interactions have been retrieved from the 3D and 2D analysis of the complex. These interactions are based on atoms types, geometry and distance criteria. The H-bonds have been observed in UCSF Chimera while hydrophobic interactions have been retrieved from 2D analysis, using Proteins*Plus* web server.[216] The noted predicted affinity is a reflection of the ligand- protein interaction obtained by observing the number of H-bonds generated as well as the ligand location into the 1D0L[214] active site.
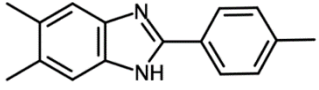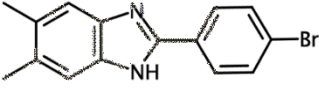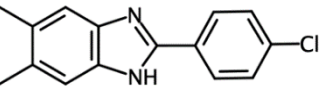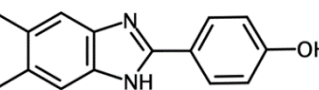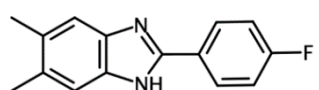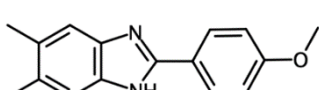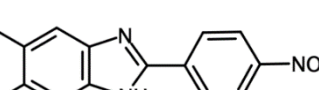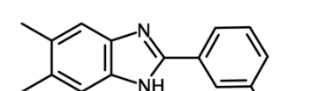
Compound ID	Structure	Score	H-bonds/ Hydrophobic interactions	Predicted affinity
BZI-1		-5.1	2 present	✓
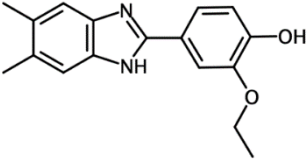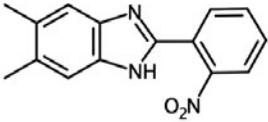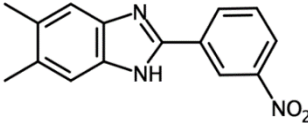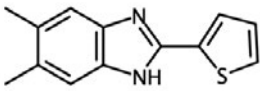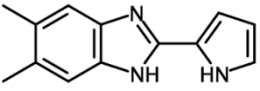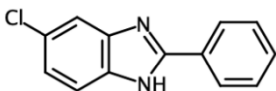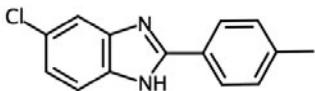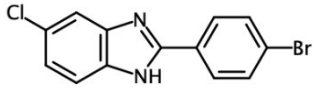
BZI-2		-5.4	3 present	✓
BZI-3		-5.4	2 absent	✓
BZI-4		-6.1	4 absent	✓
BZI-5		-6.0	4 absent	✓
BZI-6		-6.4	4 present	✓
BZI-7		-5.3	3 present	✓
BZI-8		-5.2	3 present	X
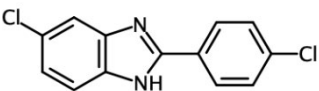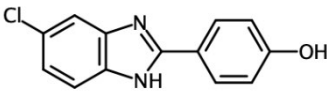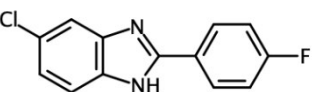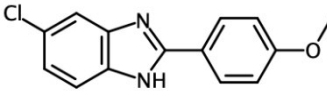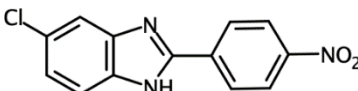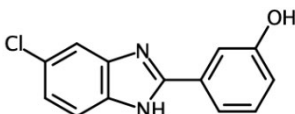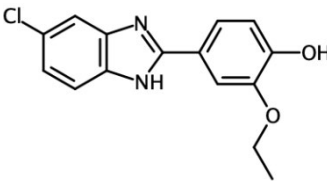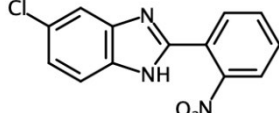
ID	Structure	Binding energy	H-bonds	Pass
BZI-9		-5.8	3 present	✓
BZI-10		-5.1	2 present	✓
BZI-11		-5.8	2 present	✓
BZI-12		-6.1	6 present	✓
BZI-13		-6.0	3 present	✓
BZI-14		-5.9	2 present	✓
BZI-15		-5.5	1 absent	X
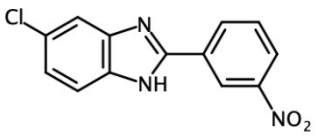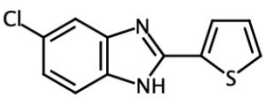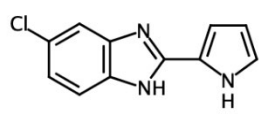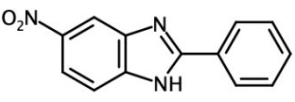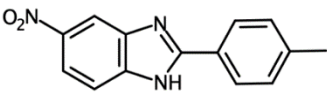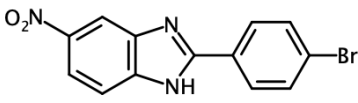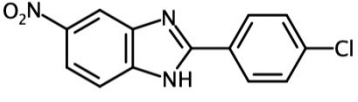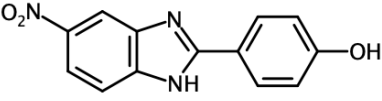
BZI-16		-6.6	3 present	✓
BZI-17		-6.2	1 present	✓
BZI-18		-6.4	1 present	✓
BZI-19		-6.4	1 present	✓
BZI-20		-6.3	1 present	✓
BZI-21		-6.2	1 present	✓
BZI-22		-6.4	1 present	✓
BZI-23		-6.4	2 present	✓
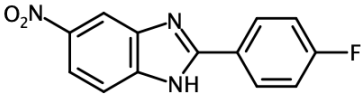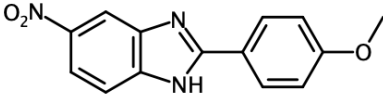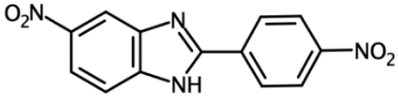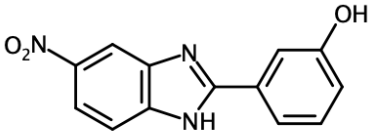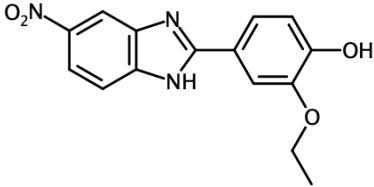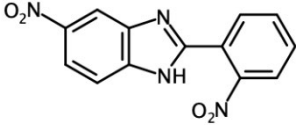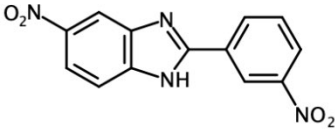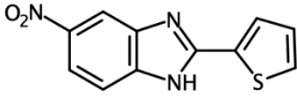
BZI-24		-6.8	2 present	✓
BZI-25		-6.5	2 present	✓
BZI-26		-6.5	2 present	✓
BZI-27		-6.9	3 present	✓
BZI-28		-6.6	2 present	✓
BZI-29		-5.6	1 present	✓
BZI-30		-5.6	1 present	✓
BZI-31		-5.9	1 present	✓
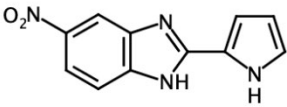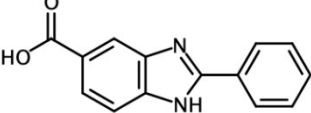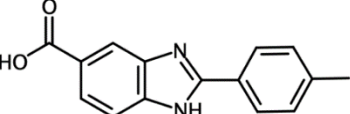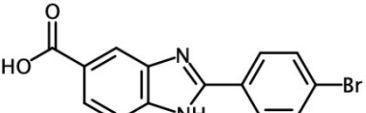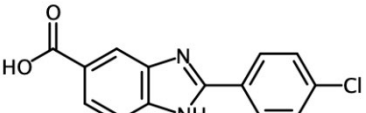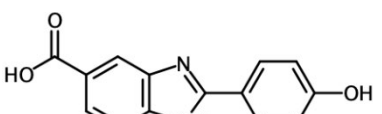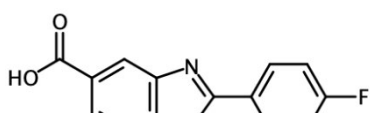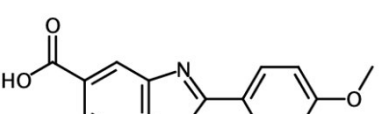
BZI-32		-6.8	2 present	✓
BZI-33		-6.7	0 absent	X
BZI-34		-7.1	0 absent	X
BZI-35		-7.6	1 present	✓
BZI-36		-6.5	1 absent	✓
BZI-37		-6.7	1 present	✓
BZI-38		-7.5	2 present	✓
BZI-39		-6.5	2 present	✓
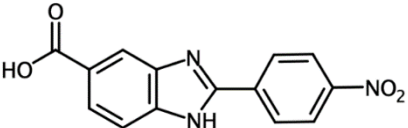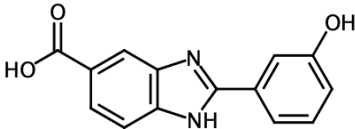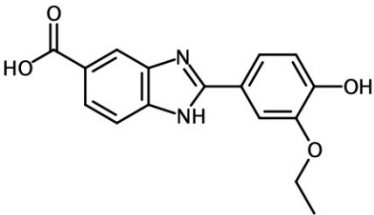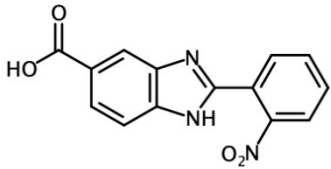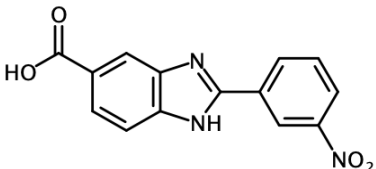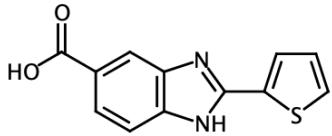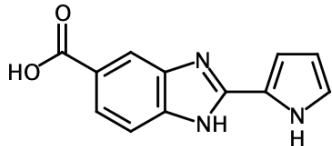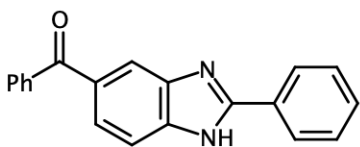
BZI-40		-6.7	1 present	✓
BZI-41		-7.3	2 present	✓
BZI-42		-7.6	4 present	✓
BZI-43		-7.6	1 present	✓
BZI-44		-6.4	1 present	✓
BZI-45		-6.1	2 present	X
BZI-46		-6.1	1 present	✓
BZI-47		-6.6	2 present	✓
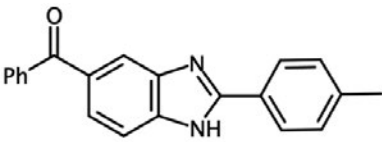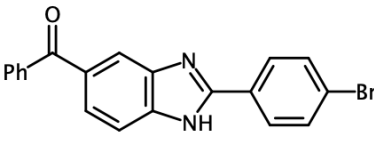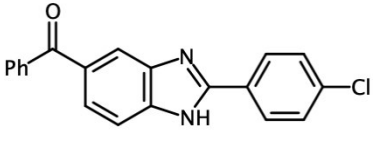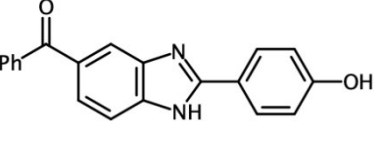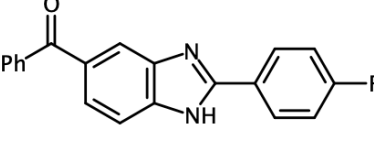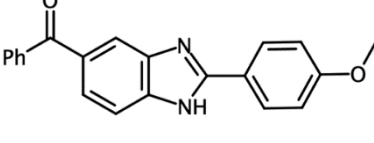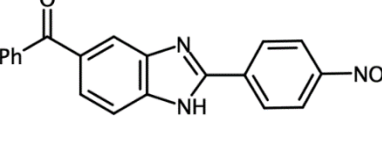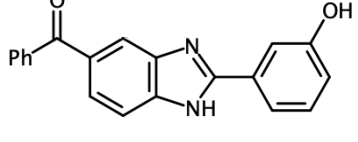
BZI-48		-6.2	1 present	✓
BZI-49		-6.2	1 present	✓
BZI-50		-6.0	1 present	✓
BZI-51		-6.5	1 present	X
BZI-52		-7.0	2 present	✓
BZI-53		-6.5	2 present	✓
BZI-54		-7.2	2 present	✓
BZI-55		-6.5	2 present	✓
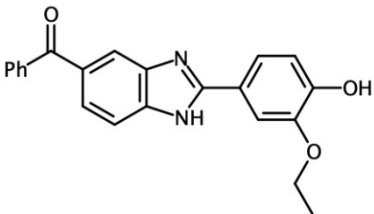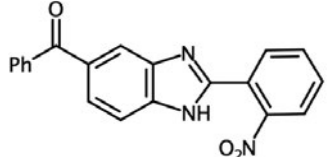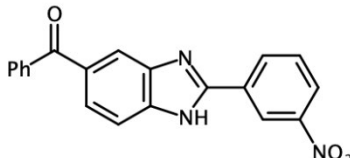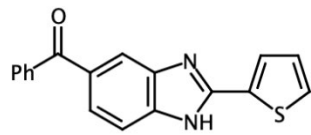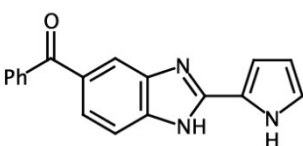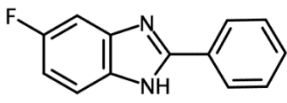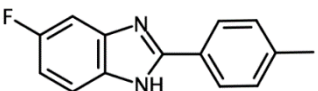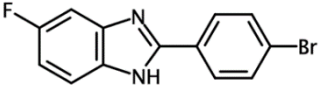
BZI-56		-6.9	2 present	✓
BZI-57		-5.7	2 present	✓
BZI-58		-5.8	2 present	✓
BZI-59		-7.4	2 present	✓
BZI-60		-7.2	3 present	✓
BZI-61		-7.4	3 present	✓
BZI-62		-6.7	1 present	✓
BZI-63		-7.1	2 present	✓
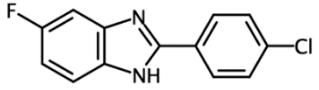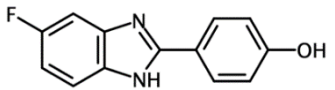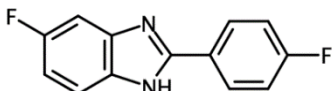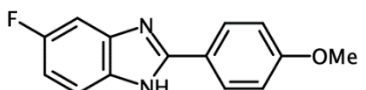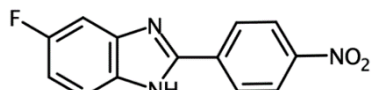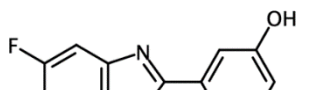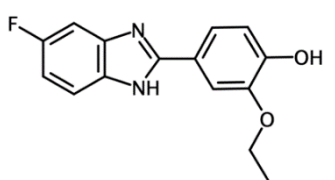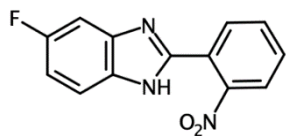
BZI-64		-7.1	2 present	✓
BZI-65		-6.4	2 present	✓
BZI-66		-7.0	2 present	✓
BZI-67		-7.0	3 present	✓
BZI-68		-7.0	1 present	✓
BZI-69		-6.9	4 present	✓
BZI-70		-7.4	2 present	✓
BZI-71		-6.5	4 present	✓
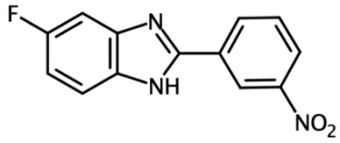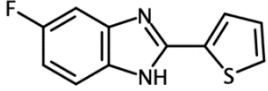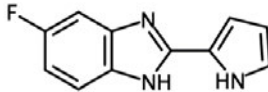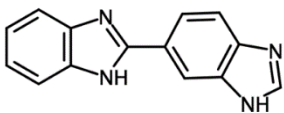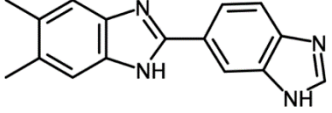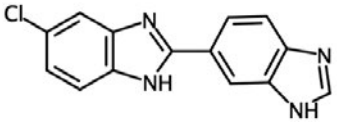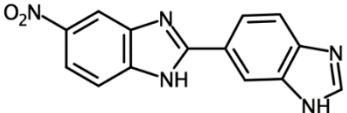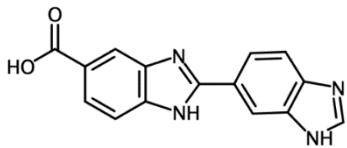
Code	Structure	Binding Energy		
BZI-72		-6.4	2 present	✓
BZI-73		-6.9	2 present	✓
BZI-74		-6.9	1 present	✓
BZI-75		-6.5	2 present	✓
BZI-76		-6.4	2 present	✓
BZI-77		-7.0	5 absent	✓
BZI-78		-7.3	3 present	✓
BZI-79		-6.7	3 present	✓
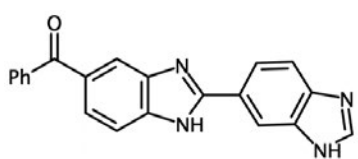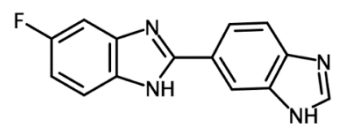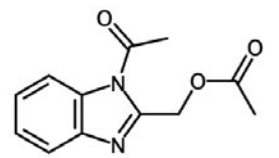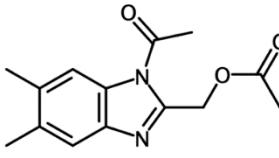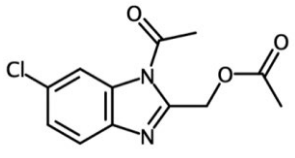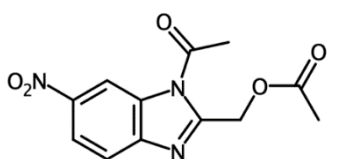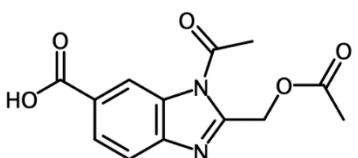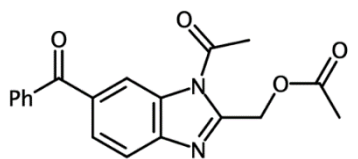
BZI-80		-7.4	2 present	✓
BZI-81		-7.0	3 present	✓
BZI-82		-7.5	2 present	✓
BZI-83		-7.3	2 absent	✓
BZI-84		-6.9	5 present	✓
BZI-85		-6.5	4 present	✓
BZI-86		-6.5	3 present	✓
BZI-87		-7.3	1	✓

BZI-88		-8.1	2 present	✓
BZI-89		-7.5	1 present	✓
BZI-90		-7.9	1 present	✓
BZI-91		-7.6	1 present	✓
BZI-92		-7.5	1 present	✓
BZI-93		-7.8	2 present	✓
BZI-94		-8.1	1 present	✓
BZI-95		-7.8	2 present	✓

BZI-96		-8.6	1 present	✓
BZI-97		-8.4	1 present	✓
BZI-98		-7.9	1 present	✓
BZI-99		-7.1	2 present	✓
BZI-100		-7.6	1 absent	✓
BZI-101		-6.4	2 present	✓
BZI-102		-6.4	1 present	✓
BZI-103		-6.3	1 absent	✓

BZI-104		-6.0	1 absent	✓
BZI-105		-6.1	1 present	✓
BZI-106		-6.5	1 present	✓
BZI-107		-6.4	1 present	✓
BZI-108		-7.0	2 present	✓
BZI-109		-6.2	1 present	✓
BZI-110		-6.8	2 present	✓
BZI-111		-6.9	1 present	✓

BZI-112		-7.5	1 present	✓
BZI-113		-7.2	1 present	✓
BZI-114		-6.2	2 present	✓
BZI-115		-7.2	2 present	✓
BZI-116		-7.3	2 present	✓
BZI-117		-7.0	1 absent	✓
BZI-118		-7.1	1 absent	✓
BZI-119		-7.0	1 absent	✓

BZI-120		-8.8	2 absent	✓
BZI-121		-7.5	2 absent	✓
BZI-122		-7.6	2 present	✓
BZI-123		-6.9	1 present	✓
BZI-124		-6.5	1 present	✓
BZI-125		-7.3	2 present	✓
BZI-126		-7.0	2 present	✓
BZI-127		-6.9	1 present	✓
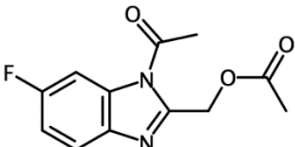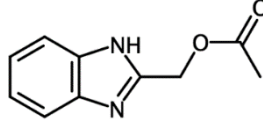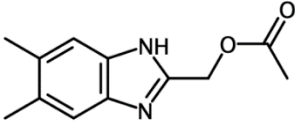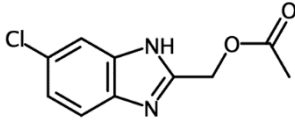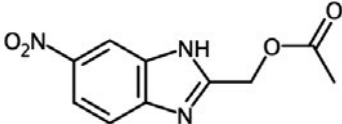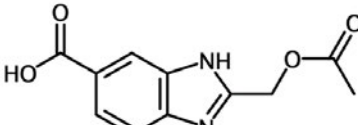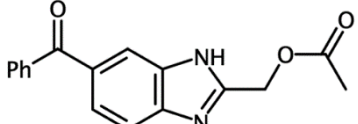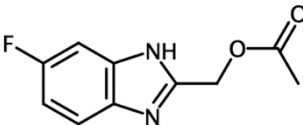
BZI-128		-7.5	1 present	✓
BZI-129		-7.1	2 present	✓
BZI-130		-7.4	1 present	✓
BZI-131		-7.0	2 present	✓
BZI-132		-6.8	2 absent	✓
BZI-133		-7.0	2 present	✓
BZI-134		-7.3	2 present	✓
BZI-135		-6.9	1 present	✓

Table 2. 1: Docking results for the benzimidazole based compounds in complex with Slt35 (PDB 1D0L).[214]

2.2.1.1 Analogues of 1H-Benzimidazole-2-methanol

The 6-chloro derivative (BZI-3) gave identical network of interaction to the non extended BZI-1 (Figure 2.7) while BZI-2 -4 -5 -6 shown additional linkages. The dimethylbenzimidazole (BZI-2) conserved the main H-bonds with the catalytic Glu162 (light green color in Figure 2.12A; dashed lines in Figure 2.12B) and Asn339 (not revealed by the 2D diagram) as well as the hydrophobic interaction with Met227. In addition to this, BZI-2 is able to form the further hydrogen bond between Its N_1-H and the carboxyl oxygen atom of the Gln225-Phe226 main chain.
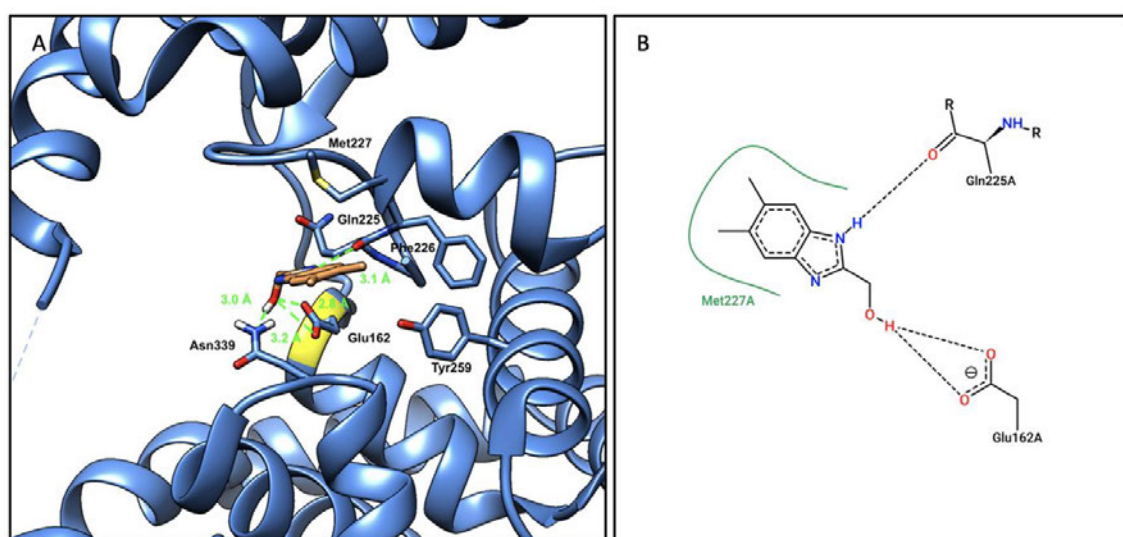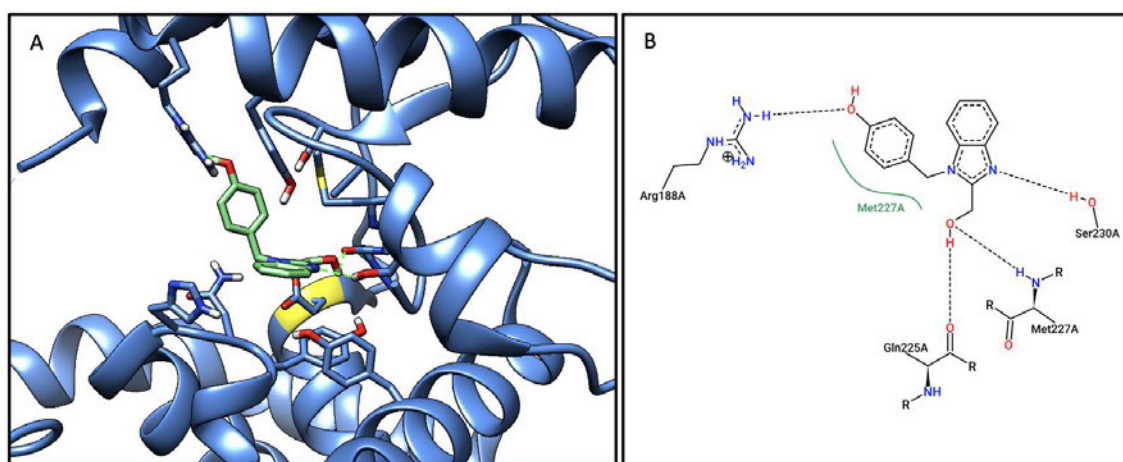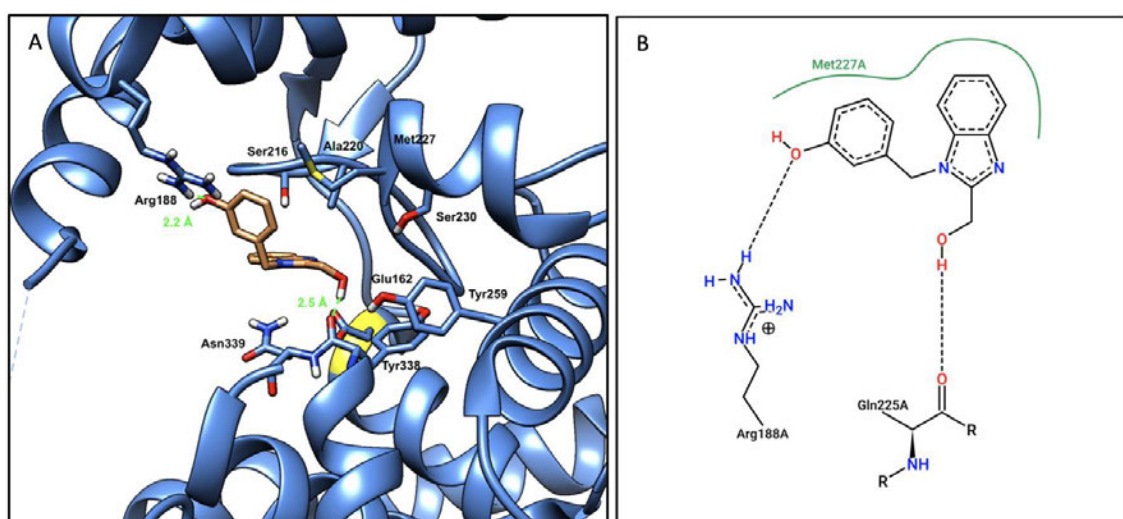

Figure 2. 12: A) cartoon representation of Slt35 (1D0L-blu color) in complex with (5,6-dimethyl-1H-1,3-benzodiazol-2-yl)-methanol (BZI-2, orange color). The catalytic Glu162 residue is shown using yellow ribbon color while H-bonds are in dashed light green lines. B) 2D diagram of interaction showing H-bonds (dashed lines) and hydrophobic interactions in spline dark green color.

The hydrophobic contact with Met227 has also been revealed when the non extended core (BZI-1) is in complex with the target, but the two methyl groups are likely to orient the ligand in a slightly different pose leading to the different H-bond formed. The network of interaction between the benzimidazole ligand and Slt35 expands when a nitro- (BZI-4; Figure2.13), carboxyl- (BZI-5) or benzophenone- (BZI-6) group are present on the benzene core of the 2-hydroxymethyl-benzimidazole. BZI-4 creates a complex network of H-bonds into the LT active site. The critical interactions of Its 2-hydroxymethyl group with the catalytic Glu162 and Asn339 are closely conserved while Its nitro group, in position 5 of the benzene ring, makes H-bond with Ser230 (not revealed in 2D diagram of interactions) and Tyr259. No hydrophobic contacts have

been revealed for this ligand. The interactions showed by docking analysis demonstrate the potential high affinity of BZI-4 for the receptor which makes of this benzimidazole derivative a good candidate as LT inhibitor. Similar ligand orientation and relative interactions with the active site residues have been revealed for BZI-5 having a carboxyl moiety in position 5 of the ring.

On the contrary BZI-6, which has a benzophenone substituent on the benzene moiety of the benzimidazole core, has not revealed good interactions with the target when in a similar orientation to previous benzimidazole derivatives (hydroxymethyl group close to the catalytic residue), as the benzoyl group is too large to occupy the usual site behind the benzimidazole ring.
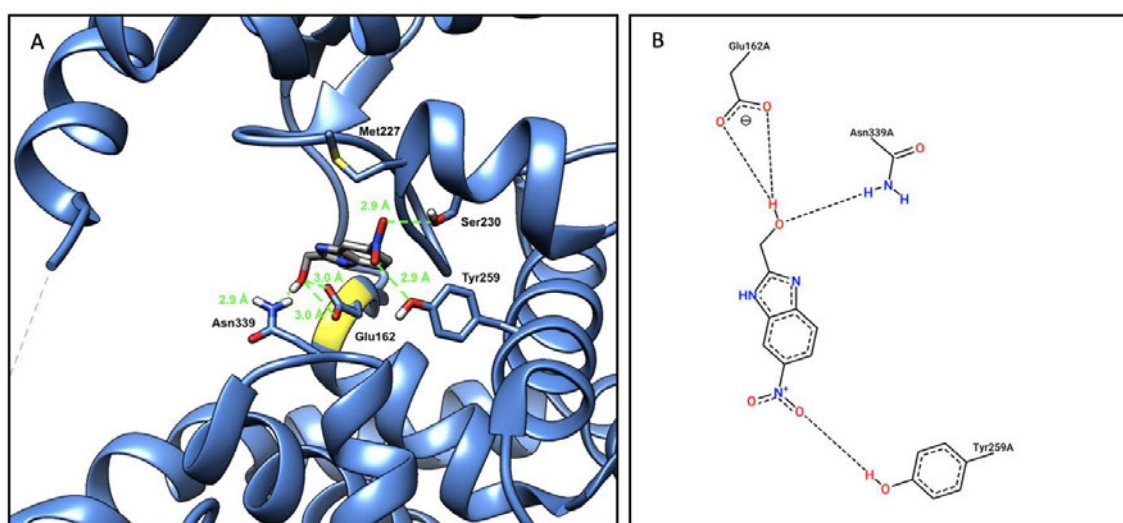
Figure 2. 13: A) cartoon representation of Slt35 (1D0L-blu color) in complex with (6-nitro-1H-benzimidazol-2-yl)methanol (BZI-4, grey color). The catalytic Glu162 residue is shown using yellow ribbon color while H-bonds are in dashed light green lines. B) 2D diagram of interaction showing H-bonds (dashed lines) and hydrophobic interactions in spline dark green color.

Despite this, a different BZI-6 orientation has been found leading to the formation of multiple hydrogen bonds. The hydroxymethyl group, through its oxygen atom, interacts with the Ser230 (and with Tyr259 in the diagram of interactions), the N_1-H forms a H-bond with the carbonyl oxygen of the Gly224-Gln225 main chain while the carbonyl oxygen atom of the benzophenone moiety interacts with Ser216. Hydrophobic contacts with Ala220 and Met227 have been

detected. Despite the typical interactions of the ligand hydroxymethyl group with the catalytic Glu162 and Asn339 are not conserved but the complex network of H-bonds generated by BZI-6 in complex with Slt35 makes of this ligand a good candidate as LT inhibitor.

Docking analysis showed that, in the series of benzimidazole-2-methanol derivatives, the 2-methanol benzimidazole core is mostly able to mimic the interactions generated by proline part of Bulgecin A into the Slt35 active site.
This lead to the potential critical role of this core molecule to represent a good candidate for inhibiting this biological target.
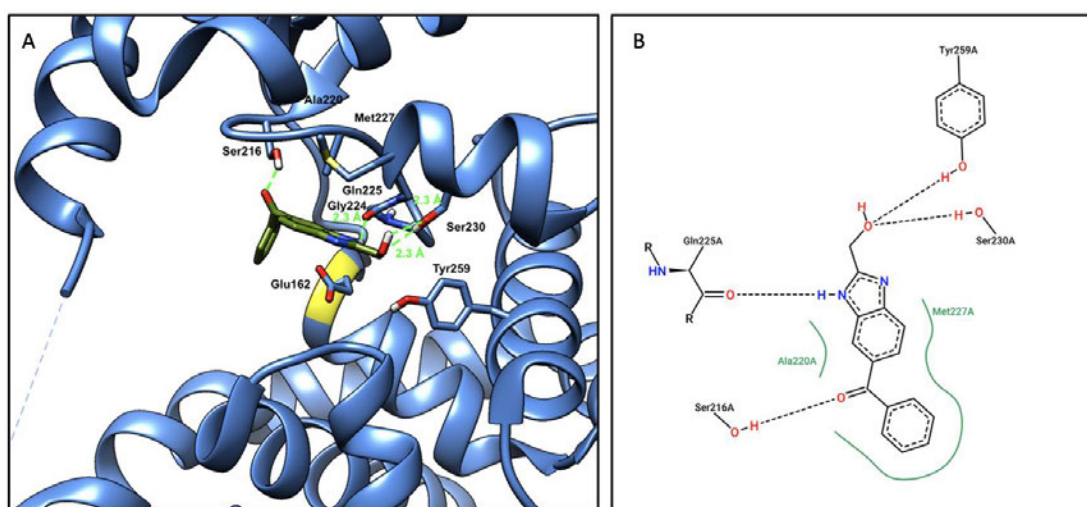
Figure 2. 14: A) cartoon representation of Slt35 (1D0L-blu color) in complex with 2-(hydroxymethyl)-3H-benzimidazole-5-carboxylic acid (BZI-6, olive green color). The catalytic Glu162 residue is shown using yellow ribbon color while H-bonds are in dashed light green lines. B) 2D diagram of interaction showing H-bonds (dashed lines) and hydrophobic interactions in spline dark green color.

2.2.1.1 N_1-aliphatic extensions of benzimidazole-2-methanol

The second class of benzimidazole-based molecules is given by 2-methanol-BZIs having an aliphatic chain as extension on the N_1 atom. Docking analysis of BZI-7, which has a propyl moiety as N-extension, revealed the conserved interactions between Its hydroxymethyl group and the catalytic Glu162 as well as Asn339.

In addition to this, hydrophobic contacts of the benzene and propyl moieties with Met227 and Tyr338 have been revealed (Figure 2.15-B).
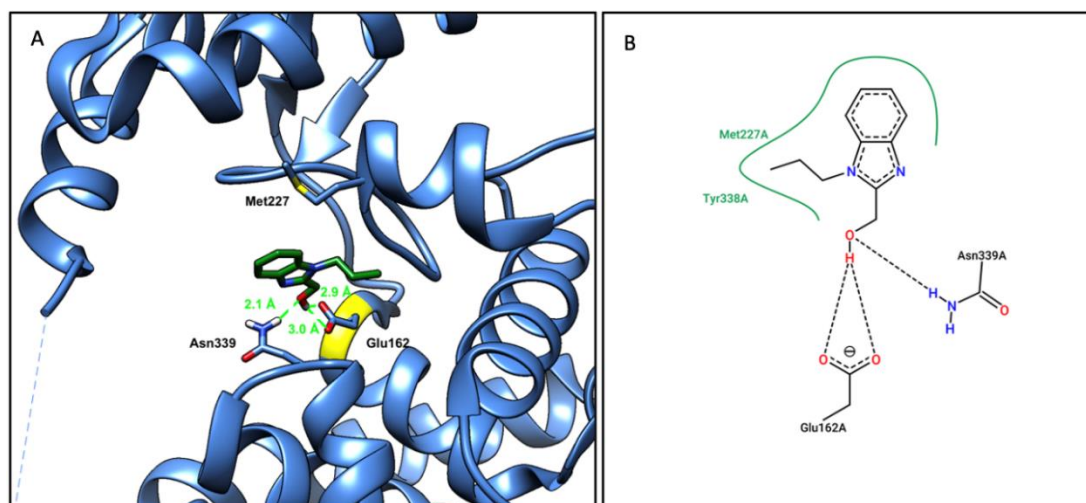
Figure 2. 15: A) cartoon representation of Slt35 (1D0L-blu color) in complex with (1-propylbenzimidazol-2-yl)methanol (BZI-7, green color). The catalytic Glu162 residue is shown using yellow ribbon color while H-bonds are in dashed light green lines. B) 2D diagram of interaction showing H-bonds (dashed lines) and hydrophobic interactions in spline dark green color.

The orientation of BZI-8 is slightly shifted into the active site. Its hydroxymethyl group forms H-bonds with His340 (not revealed in the 2D diagram of interactions) as well as the carbonyl oxygen atom of the Arg337-Tyr338 main chain. Moreover, the N_3 atom of the benzimidazole core is involved in H-bond formation with Tyr259. BZI-8, similarly to BZI-7, generates hydrophobic interaction with Met227.
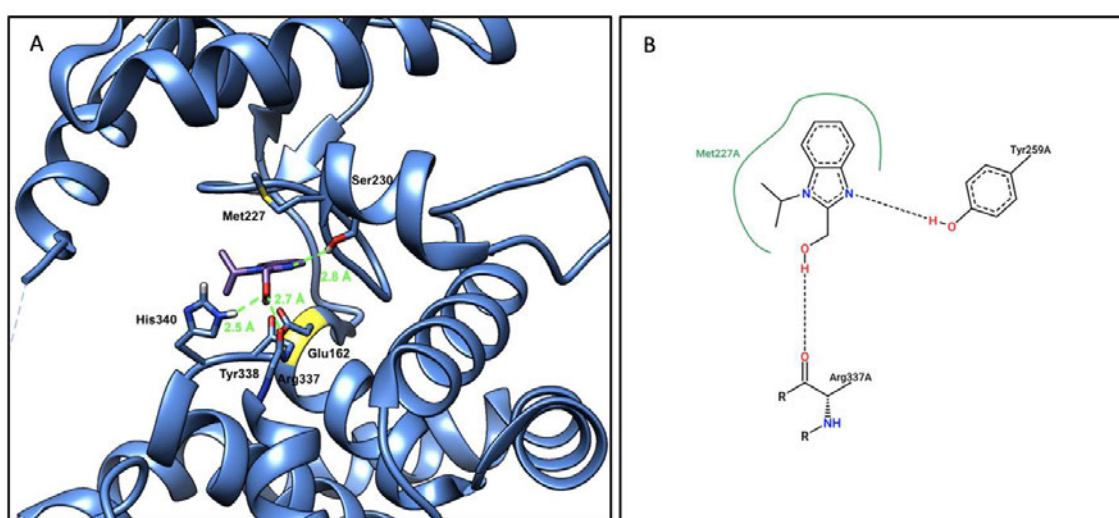
Figure 2. 16: A) cartoon representation of Slt35 (1D0L-blu color) in complex with (1-propan-2-ylbenzimidazol-2-yl)methanol (BZI-8, dark pink color). The catalytic Glu162 residue is shown using yellow ribbon color while H-bonds are in dashed light green lines. B) 2D diagram of interaction showing H-bonds (dashed lines) and hydrophobic interactions in spline dark green color.

Docking studies showed that the presence of a simple, linear propyl N-extension closely conserves the interactions of the BZI derivative with the catalytic Glu162 and Asn339 while the changing of the N-extension with an isopropyl chain leads to a change in the ligand orientation into the active site.

This gives a loss of the key interactions that the proline moiety of Bulgecin A forms in the Slt35 pocket. Despite this, BZI-8 seems to be able to create H-bonds with different active site residues representing a good predicted LT inhibitor.

2.2.1.2 N_1-benzyl extension of benzimidazole-2-methanol

The further N_1-extension designed in this work is given by non-substituted, mono- or di-substituted benzyl moiety. In this series of benzimidazole-based compounds, the non-substituted benzyl-derivative (BZI-9) closely conserves the main interactions between its hydroxyl- group and the catalytic Glu162 as well as Asn339. Hydrophobic contacts with Asn339 and Met227 have been revealed (as shown in the 2D diagram of interactions).
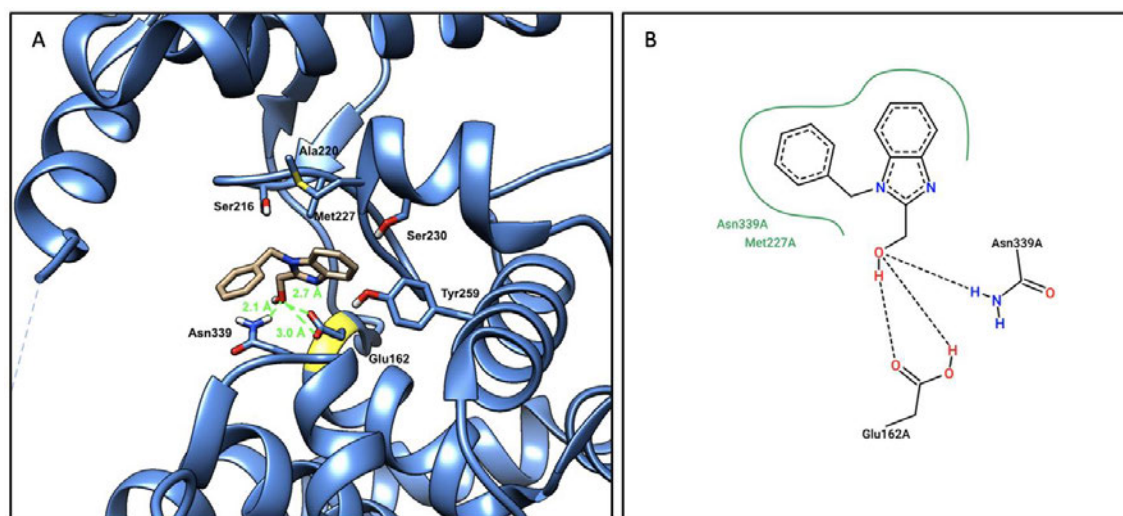
Figure 2. 17: A) cartoon representation of Slt35 (1D0L-blu color) in complex with (1-benzylbenzimidazol-2-yl) methanol (BZI-9, sand color). The catalytic Glu162 residue is shown using yellow ribbon color while H-bonds are in dashed light green lines. B) 2D diagram of interaction showing H-bonds (dashed lines) and hydrophobic interactions in spline dark green color.

The insertion of a p-hydroxyl substituent on the N-benzyl moiety leads to BZI-12 which creates a complex network of interactions with the 1D0L active site residues. This makes of BZI-12 a promising Slt35 inhibitor. Its hydoxymethyl group interacts, through the H-atom, with the Gln225 and the mainnchain of Met227 and it is close in space to the catalytic Glu162 (it is at H-

bond distance). Its p-hydroxyl oxygen atom forms H-bond with Arg188. In addition to this, the nitrogen in position 3 of the BZI core interacts with Ser 230.

Figure 2. 18: A) cartoon representation of Slt35 (1D0L-blu color) in complex with 4-{[2-(hydroxymethyl)-1,3-benzodiazol-1-yl]methyl}phenol (BZI-12, pink color). The catalytic Glu162 residue is shown using yellow ribbon color while H-bonds are in dashed light green lines. B) 2D diagram of interaction showing H-bonds (dashed lines) and hydrophobic interactions in spline dark green color.

Changing the hydroxyl- group location on the benzyl moiety to meta position (BZI-14) leads to a slight ligand shifting into the active site and the loss of interactions with the catalytic Glu162. The hydroxymethyl moiety of the benzimidazole core forms H-bond with the carbonyl oxygen atom of Tyr338-Asn339 main chain (not revealed in the 2D diagram) while the m-hydroxyl group interacts with Arg188.

Figure 2. 19: A) cartoon representation of Slt35 (1D0L-blu color) in complex with 3-{[2-(hydroxymethyl)-1,3-benzodiazol-1-yl]methyl}phenol (BZI-14, light orange color). The catalytic Glu162 residue is shown using yellow ribbon color while H-bonds are in dashed light green lines. B) 2D diagram of interaction showing H-bonds (dashed lines) and hydrophobic interactions in spline dark green color.

2.2.1.3 C$_2$-extended benzimidazoles

Multiple benzene-based C$_2$-extensions have been considered in this work. These core modifications have also been analyzed in combination with the presence of substituents on the benzene moiety of the benzimidazole core.

2.2.1.3.1 Benzene ring as C$_2$-extension

The first class of extension in position 2 of the benzimidazole core analyzed is given by a non-substituted benzene ring. In this category of ligands, BZI-17 has a non substituted benzene ring as C$_2$-extension while R$_1$ and R$_2$ are given by H-atoms.
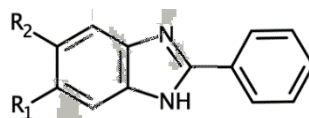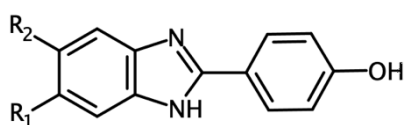

Figure 2. 20: General chemical structure of C$_2$-phenyl benzimidazole. In position 2 of the BZI core a non-substituted benzene ring is present while R$_1$ and R$_2$ vary.

Docking studies revealed that BZI-17 doesn't interact with the catalytic residue or Asn339. Its N$_1$-H atom forms a hydrogen bond with the carbonyl oxygen atom of the Gln225-Phe226 main chain (Figure 2.21A1). Hydrophobic interactions with both Met227 and Ala220 have been observed (Figure 2.21B1).

If compared to BZI-1, docking analysis showed that BZI-17 has lost the critical interactions that the proline moiety of bulgecin A forms into the active site but It's still able to potentially bind the target by forming a H-bond and two hydrophobic interactions. The presence of a nitro substituent in position 5 of the benzene moiety of the BZI core leads to the formation of an additional H-bond between the oxygen atom of the nitro group and the H-atom of Ser230 residue (Figure 2.21A2-B2).

Hydrophobic contact with Met227 and Ala220 as well as Ser230 have been observed.
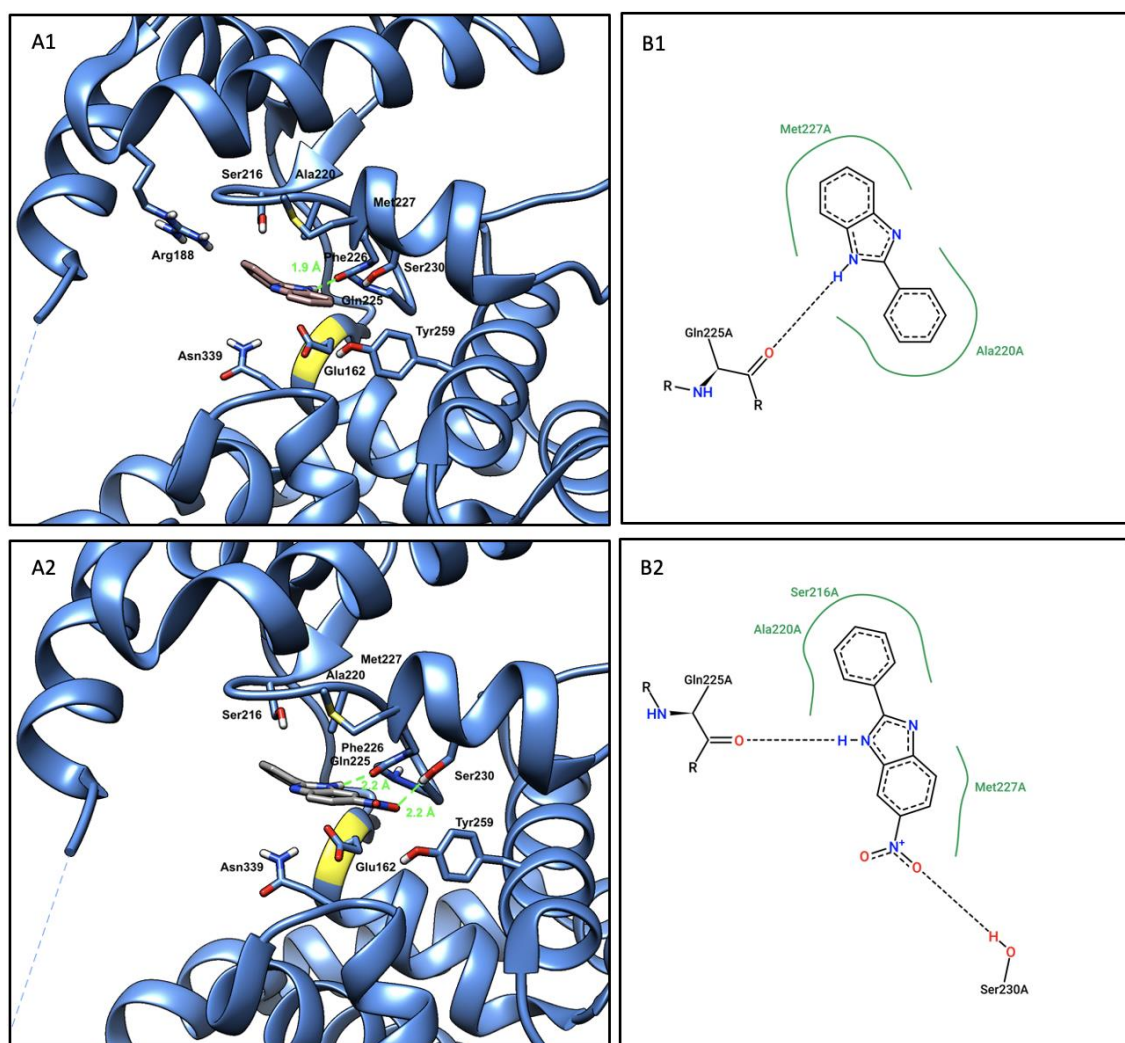
Figure 2. 21: A) cartoon representation of Slt35 (1D0L-blu color) in complex with 2-phenyl-1H-benzimidazole (A1-BZI-17, sand color) and 6-nitro-2-phenyl-1H-benzimidazole (A2-BZI-59, grey color). The catalytic Glu162 residue is shown using yellow ribbon color while H-bonds are in dashed light green lines. B) 2D diagram of interaction showing H-bonds (dashed lines) and hydrophobic interactions in spline dark green color.

2.2.1.3.2 p-methyl-benzene ring as C_2-extension

The effect of a p-methyl benzene in position 2 of the BZI core has been analyzed by docking studies.
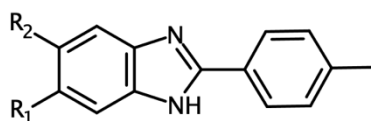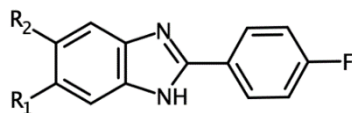

Figure 2. 22: General chemical structure of C_2-p-methylphenyl benzimidazole. In position 2 of the BZI core a p-methyl-benzene ring is present while R_1 and R_2 vary.

BZI-18 reproduces the same interactions than BZI-17 showing no effect of the p- methyl group. On the contrary, BZI-32, which is given by a p-methylbenzene substituent in position 2 of the BZI core combined with the insertion of two methyl groups in position 5 and 6, leads to additional ligand interaction.
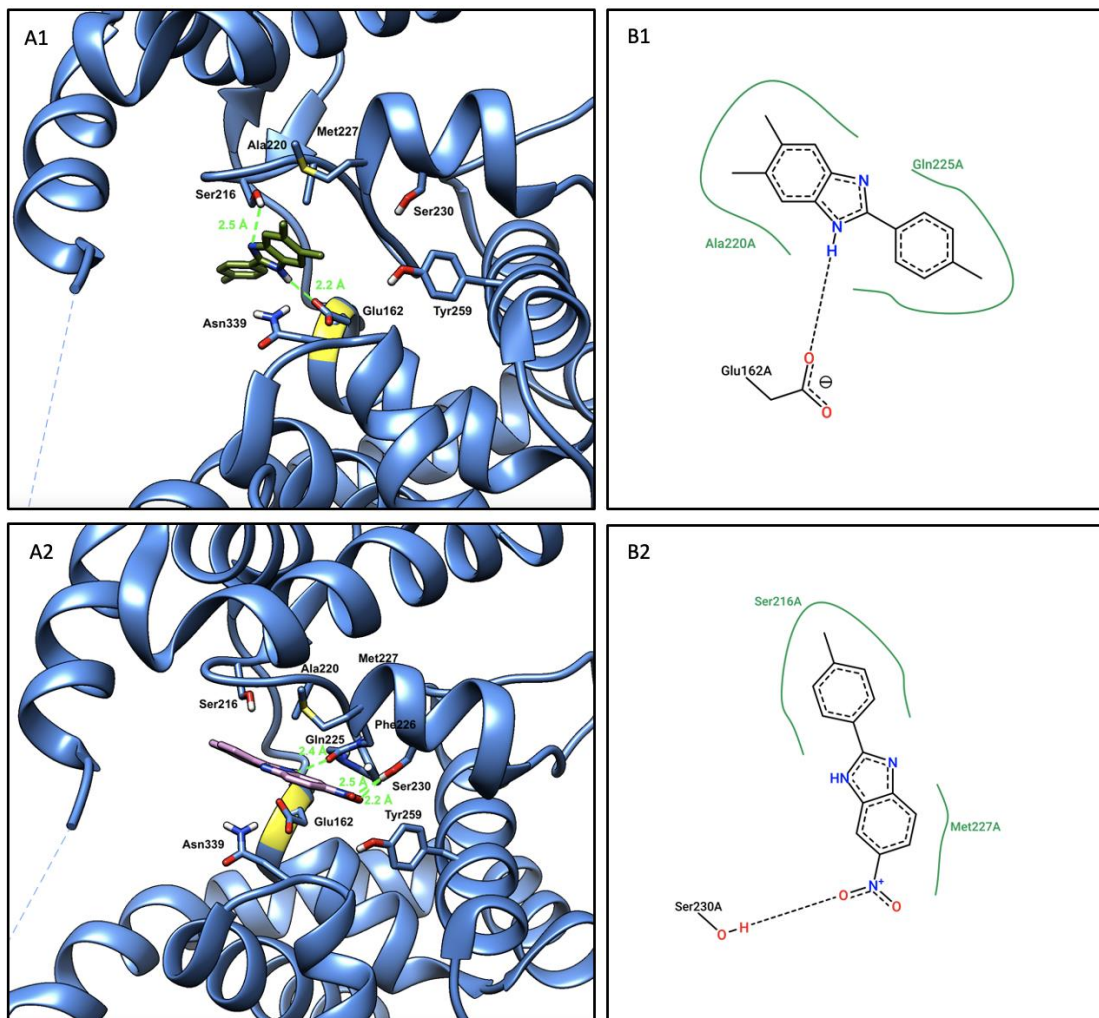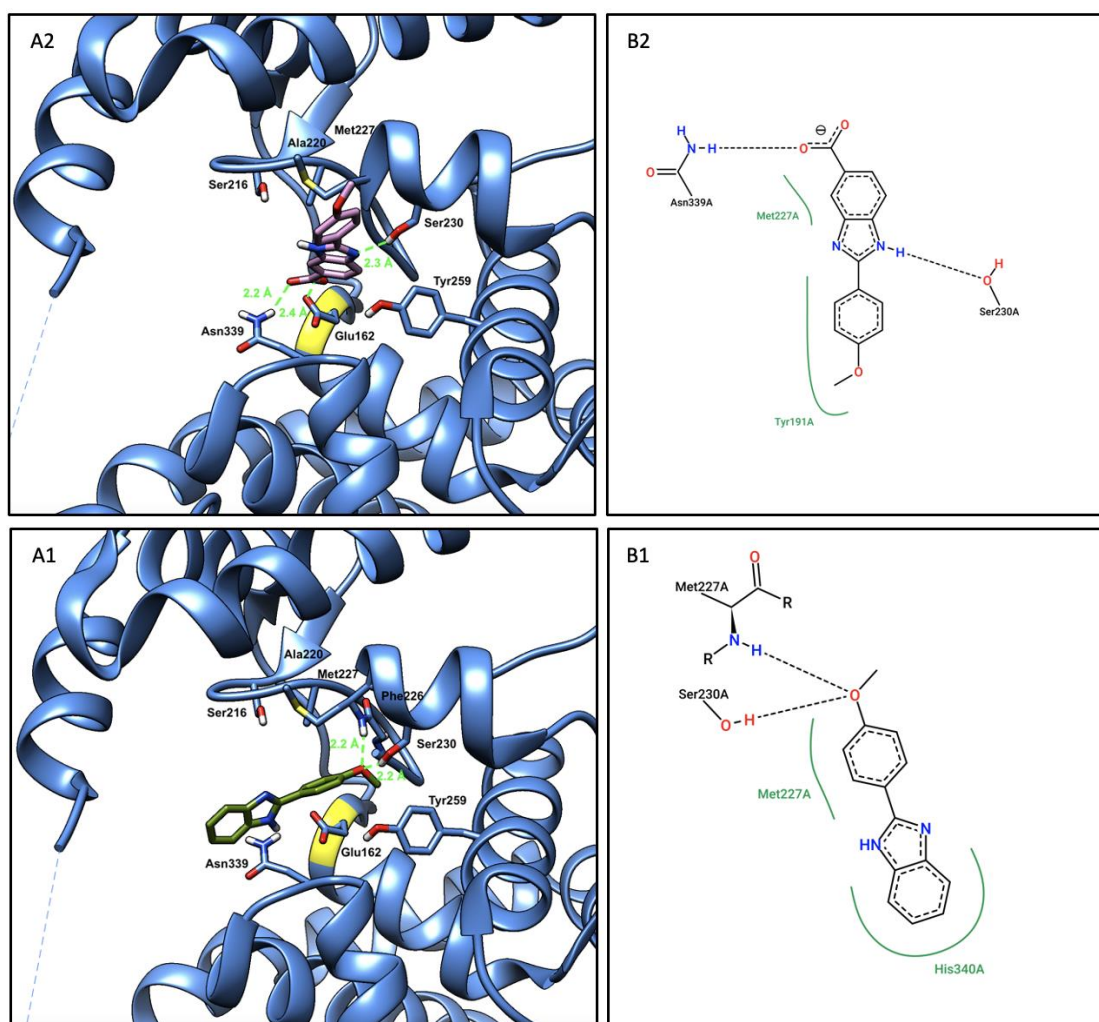

Figure 2. 23: A) cartoon representation of Slt35 (1D0L-blu color) in complex with 5,6-dimethyl-2-(4-methylphenyl)-1*H*-benzimidazole (BZI-32, green color) and 2-(4-methylphenyl)-6-nitro-1*H*-benzimidazole (BZI-60, plum color). The catalytic Glu162 residue is shown using yellow ribbon color while H-bonds are in dashed light green lines. B) 2D diagram of interaction showing H-bonds (dashed lines) and hydrophobic interactions in spline dark green color.

Its N_1-H hydrogen atom interacts with the catalytic Glu162 while the nitrogen atom in position 3 of the nucleus forms hydrogen bond with Ser216 (not revealed in the 2D diagram of interaction- Figure 2.23). Hydrophobic interactions with Ala220 and Gln 225 residues have been observed.

Docking analysis revealed a similar orientation of BZI-88 into the active site to BZI-60. The N_1-hydrogen atom interacts with Gln225-Phe226 main chain while Its carbonyl oxygen atom forms

hydrogen bonds with Ser230. Hydrophobic contact of the ligand benzene moieties with Ser216 and Met227 have been observed in the 2D diagram of interactions.
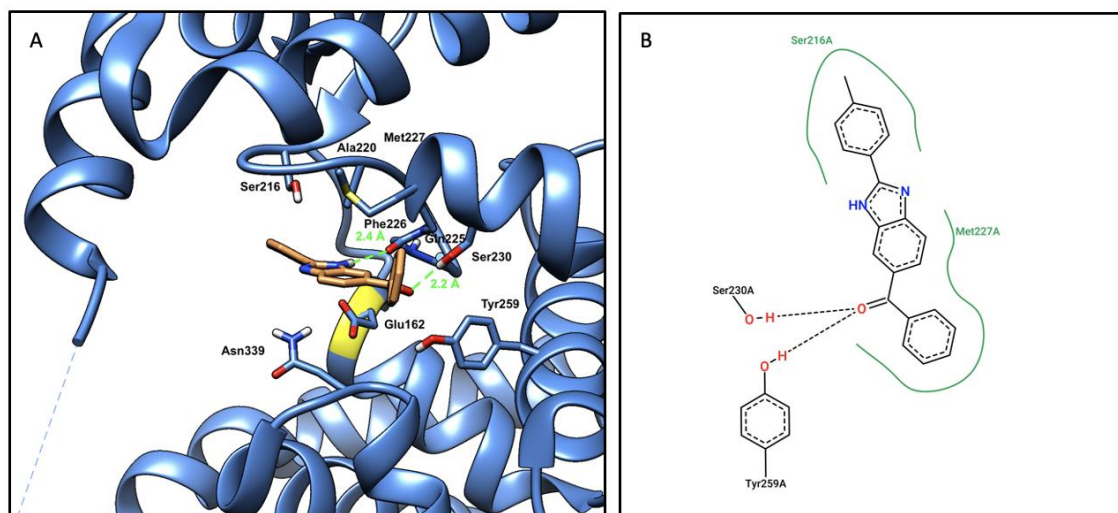
Figure 2. 24: A) cartoon representation of Slt35 (1D0L-blu color) in complex with [2-(4-methylphenyl)-3*H*-benzimidazol-5-yl]-phenylmethanone (BZI-88, orange color). The catalytic Glu162 residue is shown using yellow ribbon color while H-bonds are in dashed light green lines. B) 2D diagram of interaction showing H-bonds (dashed lines) and hydrophobic interactions in spline dark green color.

2.2.1.3.3 p-bromo-benzene ring as C_2-extension

The Insertion of a p-bromo substituent in para position of the C2-benzene ring lead to the category of 2-(4-bromophenyl)-1*H*-benzimidazoles.
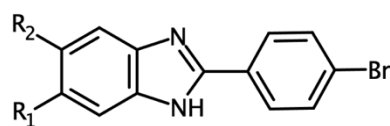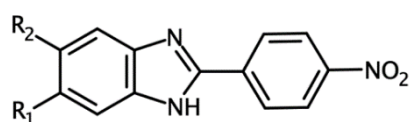

Figure 2. 25: General chemical structure of C_2-p-bromophenyl benzimidazole. In position 2 of the BZI core a p-bromo-benzene ring is present while R_1 and R_2 vary.

In this category of ligands, BZI-19, having hydrogen atoms as R_1 and R_2, appear to be shifted into the active site. Its N1 hydrogen atom interacts with Tyr259 while the N3 atom forms H-bond with Tyr191 (not revealed in the 3D analysis). The benzene ring of the BZI core is slightly exposed outside the active site. Hydrophobic contacts with Met227 have been revealed. Identical interactions and ligand location into the LT active site have been reveled for BZI-47, with the chlorine in position number 5 of the benzimidazole core not having effect on the ligand affinity

for the target. On the contrary, BZI-61, having a nitro group in position 5 of the BZI nucleus, interacts, through Its N_1-hydrogen atom, with the Gln225-Phe226 main chain and through the nitro group with Ser230, reproducing the same interactions formed by BZI-60.
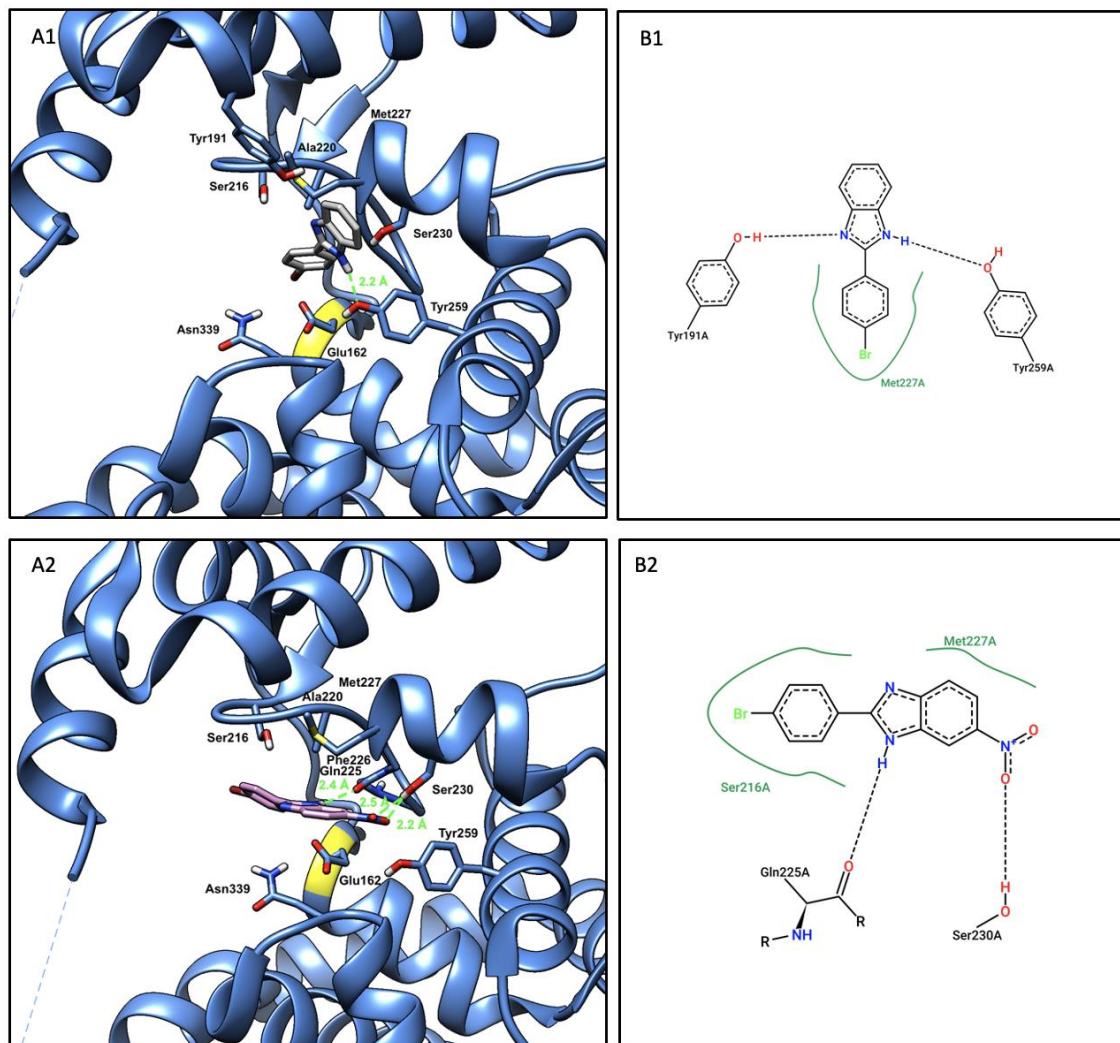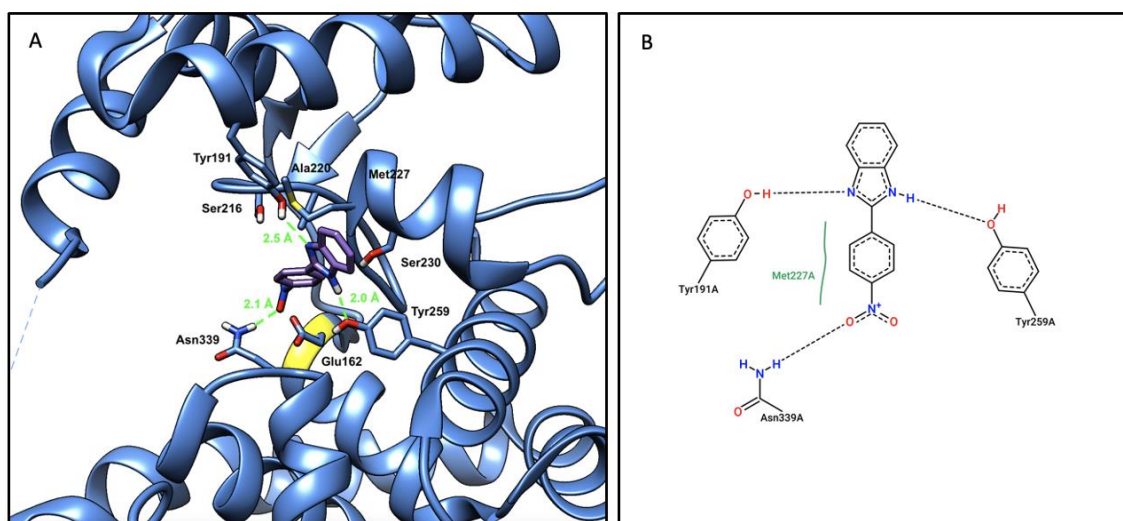

Figure 2. 26: A) cartoon representation of Slt35 (1D0L-blu color) in complex with 2-(4-bromophenyl)-1H-benzimidazole (BZI-19, grey color) and 2-(4-bromophenyl)-6-nitro-1H-benzimidazole (BZI-61, plum color). The catalytic Glu162 residue is shown using yellow ribbon color while H-bonds are in dashed light green lines. B) 2D diagram of interaction showing H-bonds (dashed lines) and hydrophobic interactions in spline dark green color.

This shows that the p-methyl and the p-bromo benzene substituent in position 2 of the BZI nucleus similarly orient the ligand into the LT active site.

2.2.1.3.4 p-chloro-benzene ring as C_2-extension

The effect of a p-chloro benzene in position 2 of the BZI core has been analyzed by docking studies.
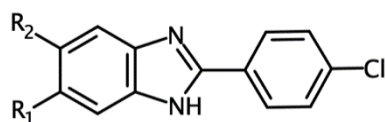
Figure 2. 27: General chemical structure of C_2-p-chlorophenyl benzimidazole. In position 2 of the BZI core a p-chloro-benzene ring is present while R_1 and R_2 vary.

In this category BZI-20, having H-atoms as R_1 and R_2, represents the ligand non extended on the benzene moiety of the benzimidazole core. Similarly to BZI-17, Its N1-hydrogen atom interacts with the carbonyl oxygen of the Gln225-Phe226 main chain. Hydrophobic contact with Met227 and Ala220 have been observed. This ligand reproduces the interactions between BZI-17 and the target showing that a chlorine in para position of the benzene C_2-extension doesn't change the ligand location into the LT active site.
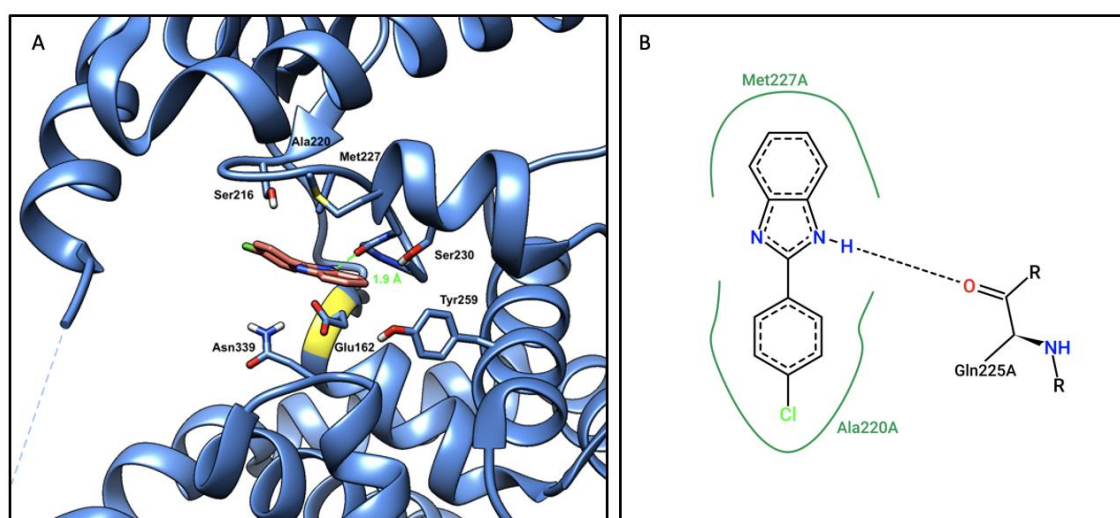
Figure 2. 28: A) cartoon representation of Slt35 (1D0L-blu color) in complex with 2-(4-chlorophenyl)-1H-benzimidazole (BZI-20, salmon color). The catalytic Glu162 residue is shown using yellow ribbon color while H-bonds are in dashed light green lines. B) 2D diagram of interaction showing H-bonds (dashed lines) and hydrophobic interactions in spline dark green color.

BZI-62 and BZI-90, having relatively a nitro and a benzophenone group in position 5 of the benzimidazole core, give similar ligand-target interactions if compared with the non modified BZI-20.

On the contrary, BZI-76, which has a carboxylic substituent on C_5, has Its N_3 atom forming H-bond with Ser230 while the carboxyl group interacts through Its carbonyl oxygen atom, with Asn339 (not revealed in the 2D diagram of interactions). Hydrophobic contact between the benzene moiety of the benzimidazole core and Met227 has been observed.
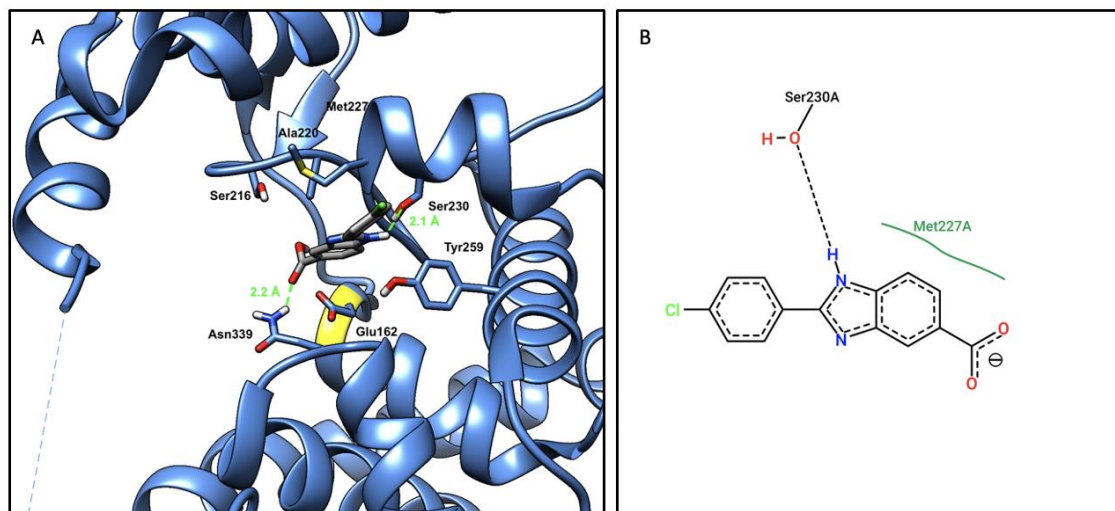
Figure 2. 29: A) cartoon representation of Slt35 (1D0L-blu color) in complex with 2-(4-chlorophenyl)-3H-benzimidazole-5-carboxylic acid (BZI-76, grey color). The catalytic Glu162 residue is shown using yellow ribbon color while H-bonds are in dashed light green lines. B) 2D diagram of interaction showing H-bonds (dashed lines) and hydrophobic interactions in spline dark green color.

2.2.1.3.5 p-hydroxy-benzene ring as C_2-extension

Reaplcement of the p-chloro group with a p-hydroxy group gives the next category of ligands analyzed in this work.
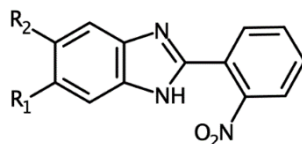

Figure 2. 30: General chemical structure of C_2-p-hydroxylphenyl benzimidazole. In position 2 of the BZI core a p-hydroxy-benzene ring is present while R_1 and R_2 vary.

The BZI-21, having a non modified benzimidazole core and a p-hydroxy benzene in position 2, has been found in a similar location to BZI-20 into the LT active site. BZI-21 reproduces the interaction with the carbonyl oxygen atom of the Gln225-Phe226 main chain showing no different interaction if compared with the 2-(4-chlorophenyl)-1H-benzimidazole (BZI-20) and no effect of a hydroxyl group in para position. BZI-77, having a carboxyl group in position 5 of the nucleus, represents the most promising candidate of this category of benzimidazoles. Its

carboxylic substituent forms H-bonds with the Phe226-Met227 main chain as well as with Ser230. The N3-atom interacts with Asn339 while the oxygen atom of the p-hydroxy benzene moiety interacts with Gln98.
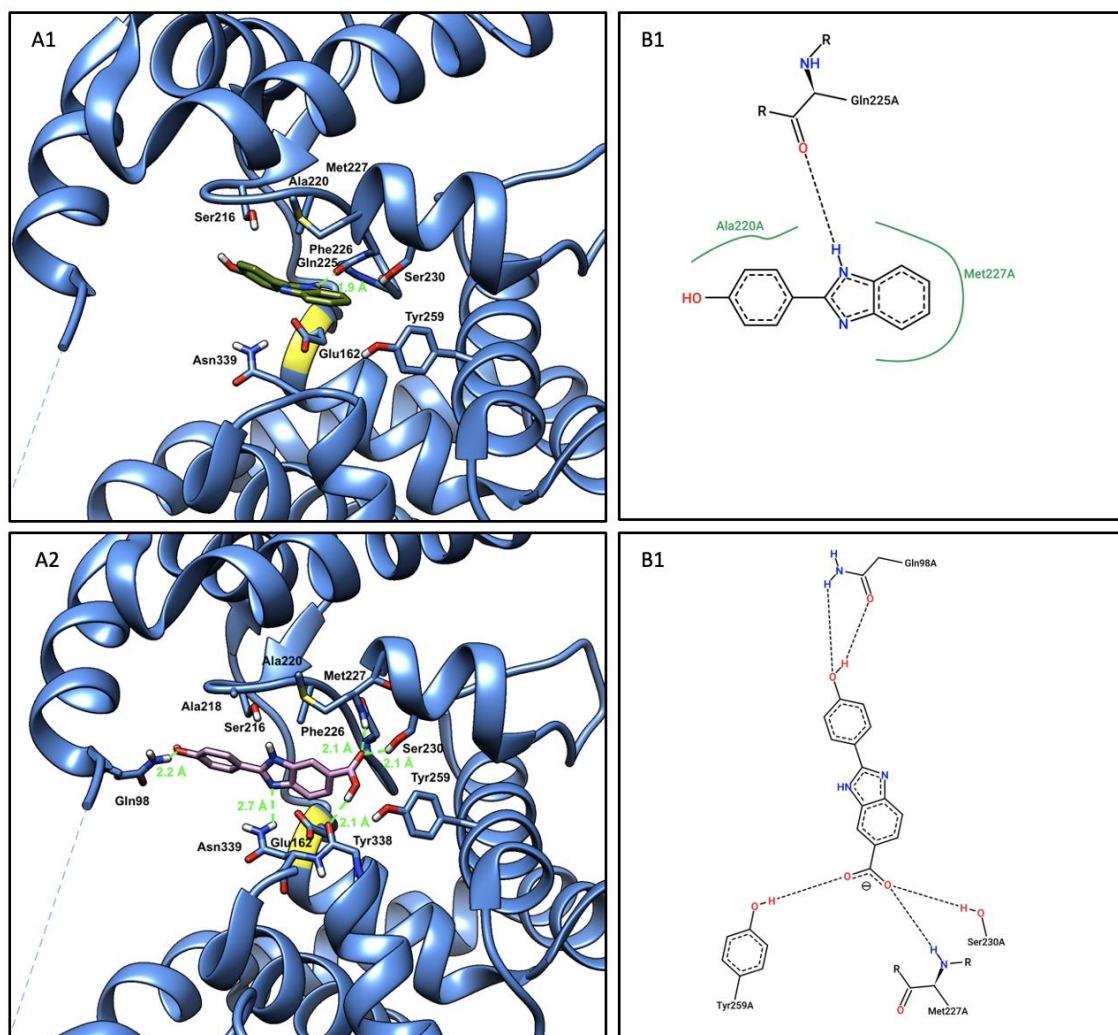
Figure 2. 31: A) cartoon representation of Slt35 (1D0L-blu color) in complex with 4-(1H-benzimidazol-2-yl)phenol (BZI-21, green color) and 2-(4-hydroxyphenyl)-3H-benzimidazole-5-carboxylic acid (BZI-77, plum color). The catalytic Glu162 residue is shown using yellow ribbon color while H-bonds are in dashed light green lines. B) 2D diagram of interaction showing H-bonds (dashed lines) and hydrophobic interactions in spline dark green color.

2.2.1.3.6 p-fluoro-benzene ring as C_2-extension

In the category of 4-fluorophenyl-1-H-benzimidazoles, BZI-22 has hydrogen atoms as R_1 and R_2. This ligand closely conserves the interaction observed for the non extended BZI-17 (Fig2.21).

Figure 2. 32: General chemical structure of C_2-p-fluorophenyl benzimidazole. In position 2 of the BZI core a p-fluoro-benzene ring is present while R_1 and R_2 vary.
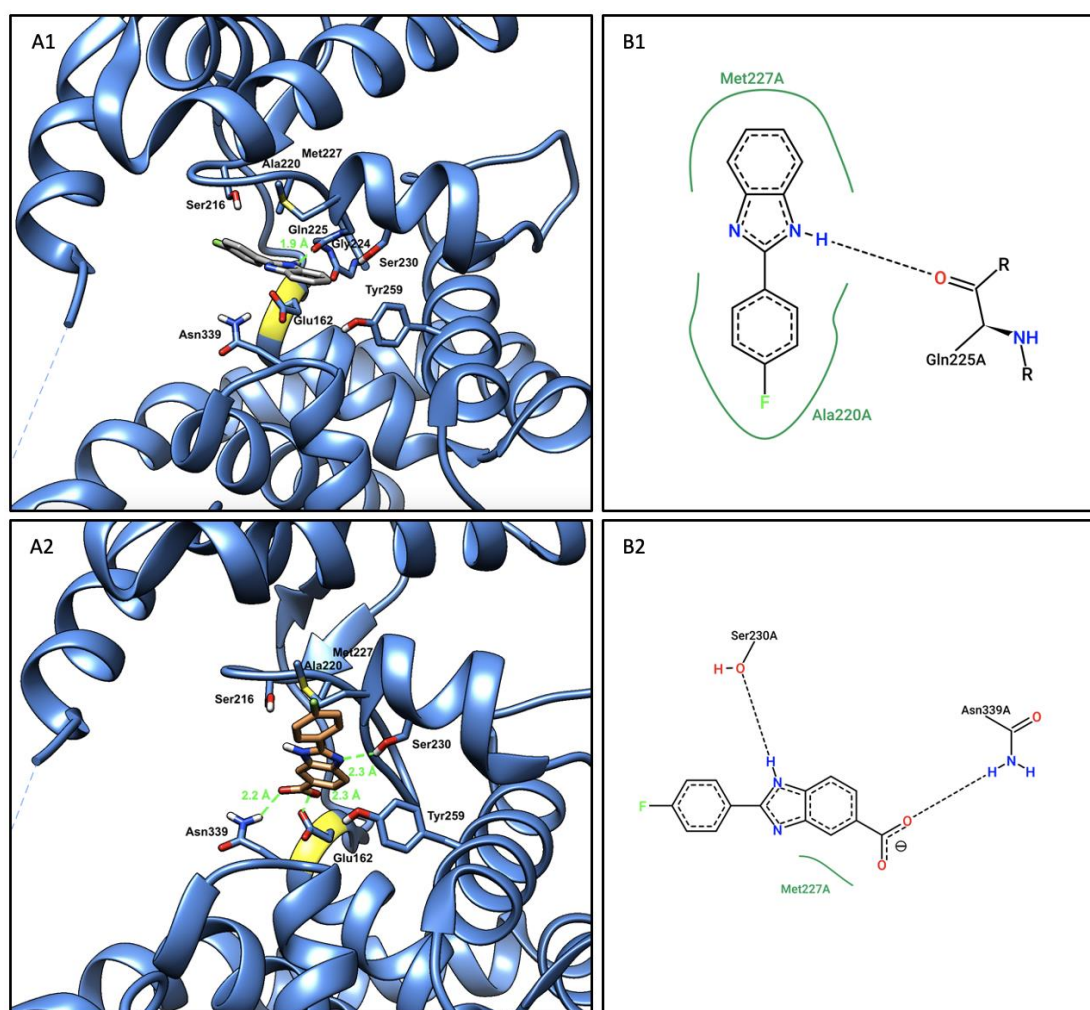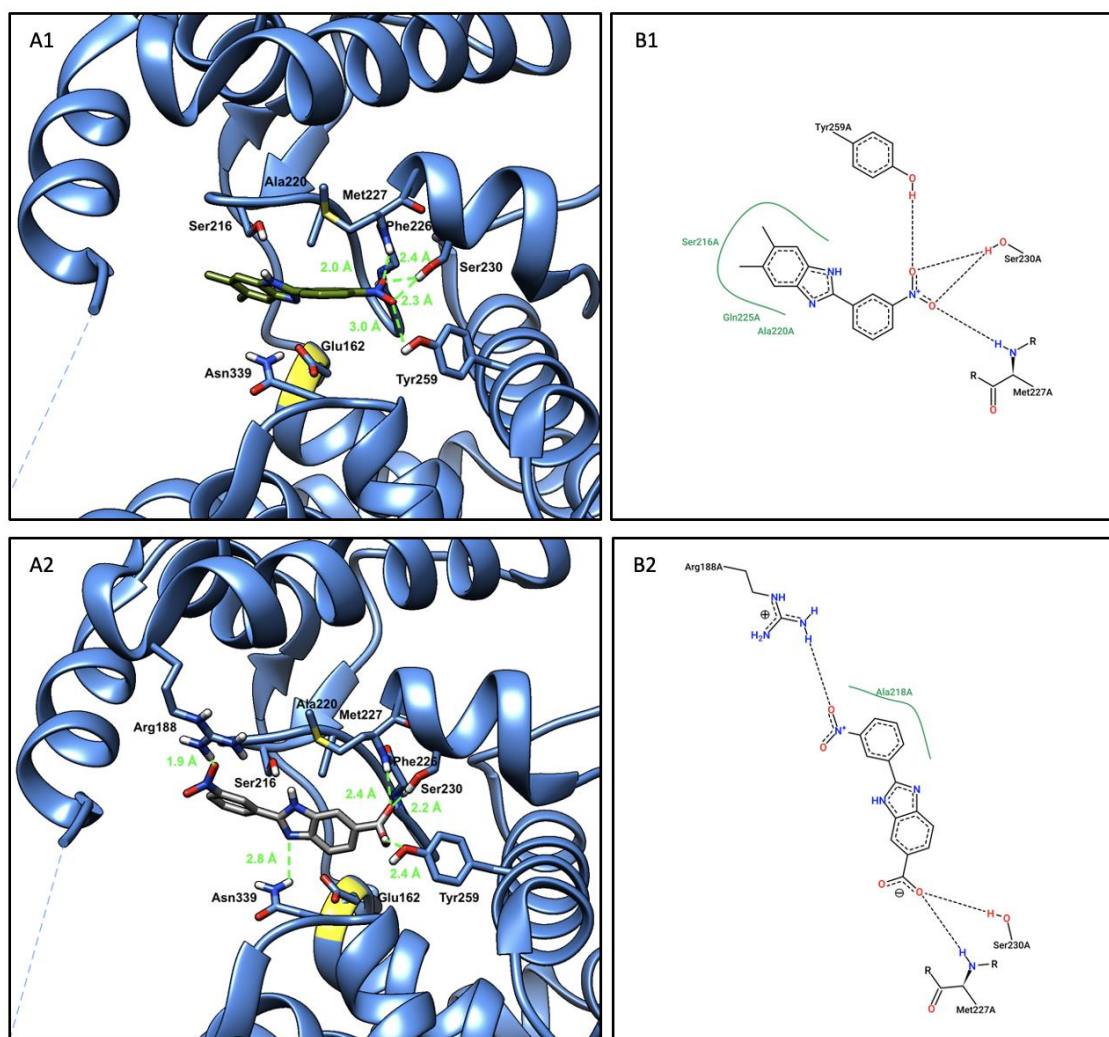

Figure 2. 33: A) cartoon representation of Slt35 (1D0L-blu color) in complex with 2-(4-fluorophenyl)-1H-benzimidazole (BZI-22, grey color). The catalytic Glu162 residue is shown using yellow ribbon color while H-bonds are in dashed light green lines. B) 2D diagram of interaction showing H-bonds (dashed lines) and hydrophobic interactions in spline dark green color.

Its N_1-H atom forms H-bond with the Gly224-Gln225-Phe226 main chain (the carbonyl oxygen atom of Gln225). Hydrophobic contacts with Met227 have been observed. The introduction of a carboxylic substituent in position 5 of the benzene moiety of the nucleus (BZI-78) leads to a change of the ligand orientation into the LT active site.

2.2.1.3.7 p-methoxy-benzene ring as C_2-extension

A para-methoxy substituent on the C_2-benzene extension of the benzimidazole core leads to the category of 2-(4-methoxyphenyl)-1*H*-benzimidazoles.
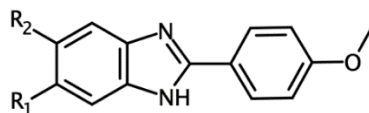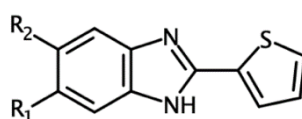

Figure 2. 34: General chemical structure of C_2-methoxyphenyl benzimidazole. In position 2 of the BZI core a p-methoxy-benzene ring is present while R_1 and R_2 vary.

In this group of ligands, docking studies revealed that BZI-23, which has hydrogen atoms as R_1 and R_2 groups, has a different location than the other benzimidazoles into the LT active site.
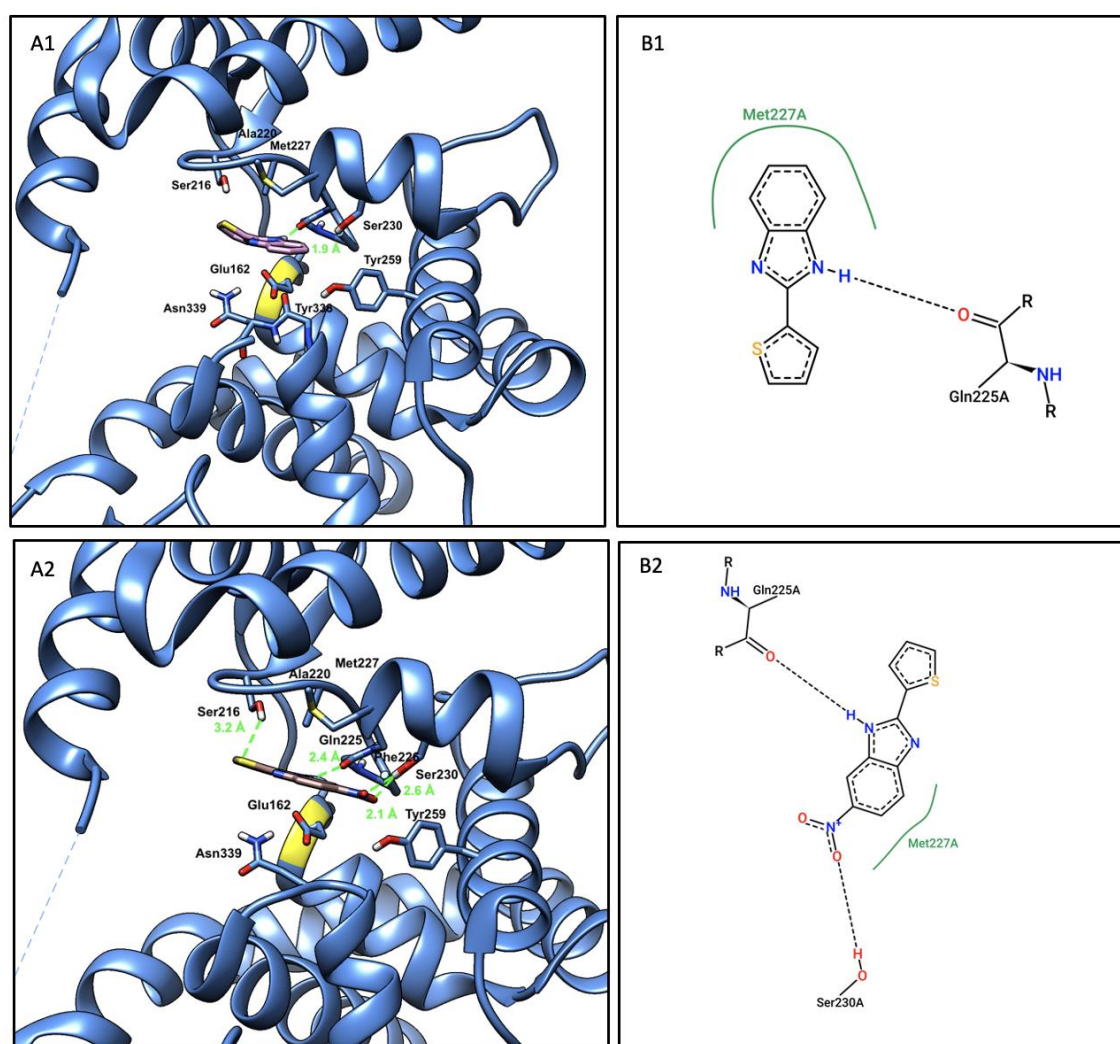

Figure 2. 35: A) cartoon representation of Slt35 (1D0L-blu color) in complex with 2-(4-methoxyphenyl)-1*H*-benzimidazole (BZI-23, green color) and 2-(4-methoxyphenyl)-3*H*-benzimidazole-5-carboxylic acid (BZI-79, plum color). The catalytic Glu162 residue is shown using yellow ribbon color while$ H-bonds are in dashed light green lines. B) 2D diagram of interaction showing H-bonds (dashed lines) and hydrophobic interactions in spline dark green color.

Its methoxy oxygen atom forms H-bonds with Ser230 as well as the amino hydrogen of the Phe226-Met227 main chain. In this category of ligands, BZI-79 is the most promising candidate for binding Slt35. Its carboxyl group in position 5 of the nucleus interacts with both the catalytic Glu162 and Asn339 while its N_1 atom forms H-bond with Ser230. Hydrophobic contacts with Met227 and Tyr191 have also been revealed by docking studies.

2.2.1.3.8 p-nitro-benzene ring as C_2-extension

In the series of 2-(4-nitrophenyl)-1H-benzimidazoles (Fig2.36), BZI-24 represent the best candidate for binding Slt35.

Figure 2. 36: General chemical structure of C_2-extended benzimidazole. In position 2 of the BZI core a p-nitro-benzene ring is present while R_1 and R_2 vary.
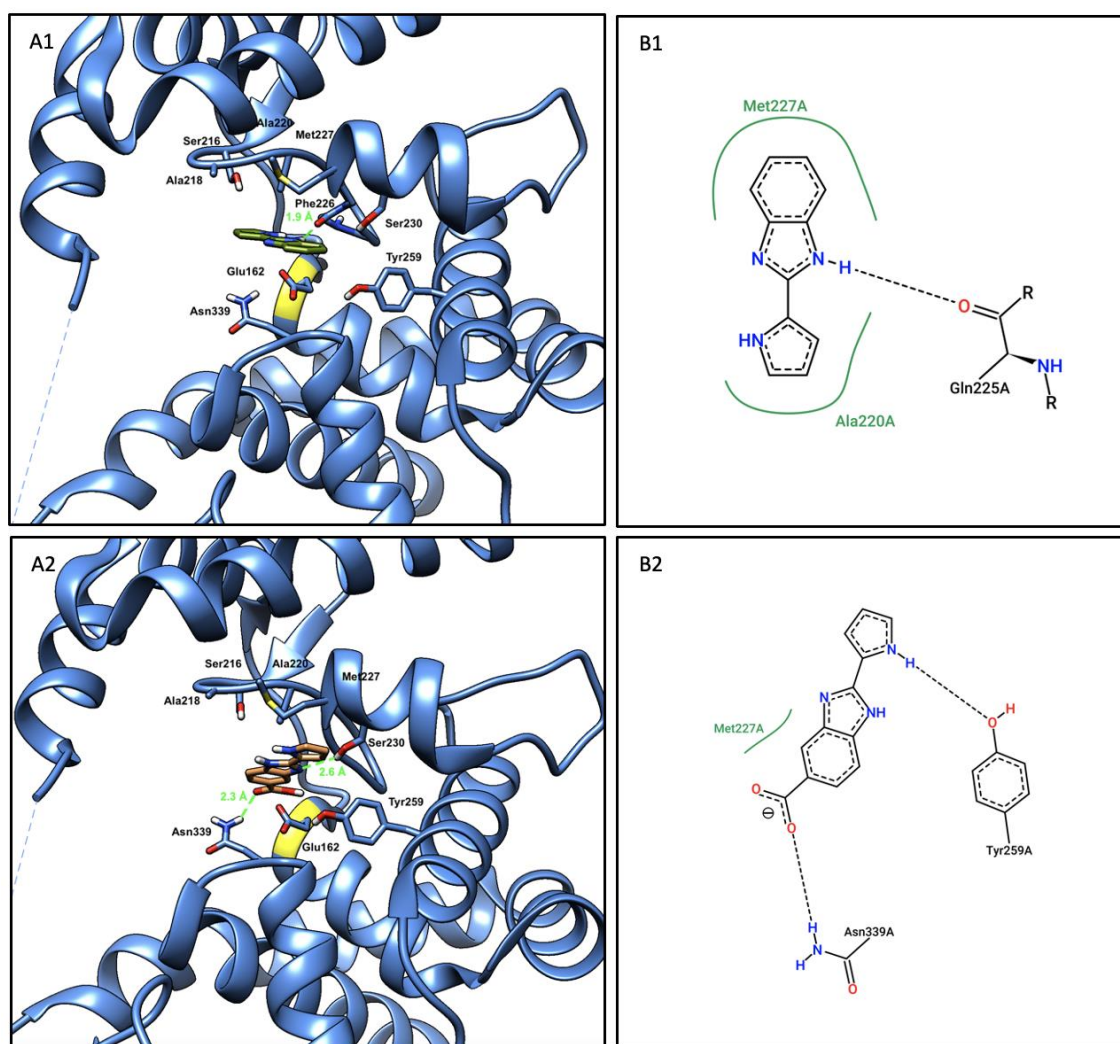

Figure 2. 37: A) cartoon representation of Slt35 (1D0L-blu color) in complex with 2-(4-nitrophenyl)-1H-benzimidazole (BZI-24, violet color). The catalytic Glu162 residue is shown using yellow ribbon color while H-bonds are in dashed light green lines. B) 2D diagram of interaction showing H-bonds (dashed lines) and hydrophobic interactions in spline dark green color.

Its N_1-hydrogen atom forms H-bond with Tyr259 while the N_3-nitrogen atom interacts with Tyr191. In addition to this, the nitro group in para position of the C2-benzene substituent forms H-bonds with Asn339. Hydrophobic contacts with Met227 have also been revealed.

2.2.1.3.9 m-hydroxy-benzene ring as C_2-extension

An hydroxyl group in meta position of the C2-benzene substituent of the benzimidazole core leads to the class of 3-(1*H*-benzimidazol-2-yl)phenol.
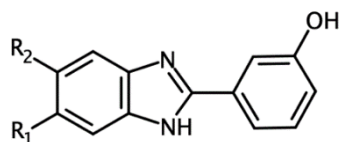
Figure 2. 38: General chemical structure of C_2-m-hydroxyl-phenyl benzimidazole. In position 2 of the BZI core a m-hydroxy-benzene ring is present while R_1 and R_2 vary.

BZI-25, the simplest ligand of this benzimidazole category, forms, through its N1-hydrogen atom, H-bond with the carbonyl oxygen atom of the Phe226-Met227 main chain while Its m-hydroxyl group interacts with the catalytic Glu162. Hydrophobic contacts with Ala220 and Met227 have been revealed.
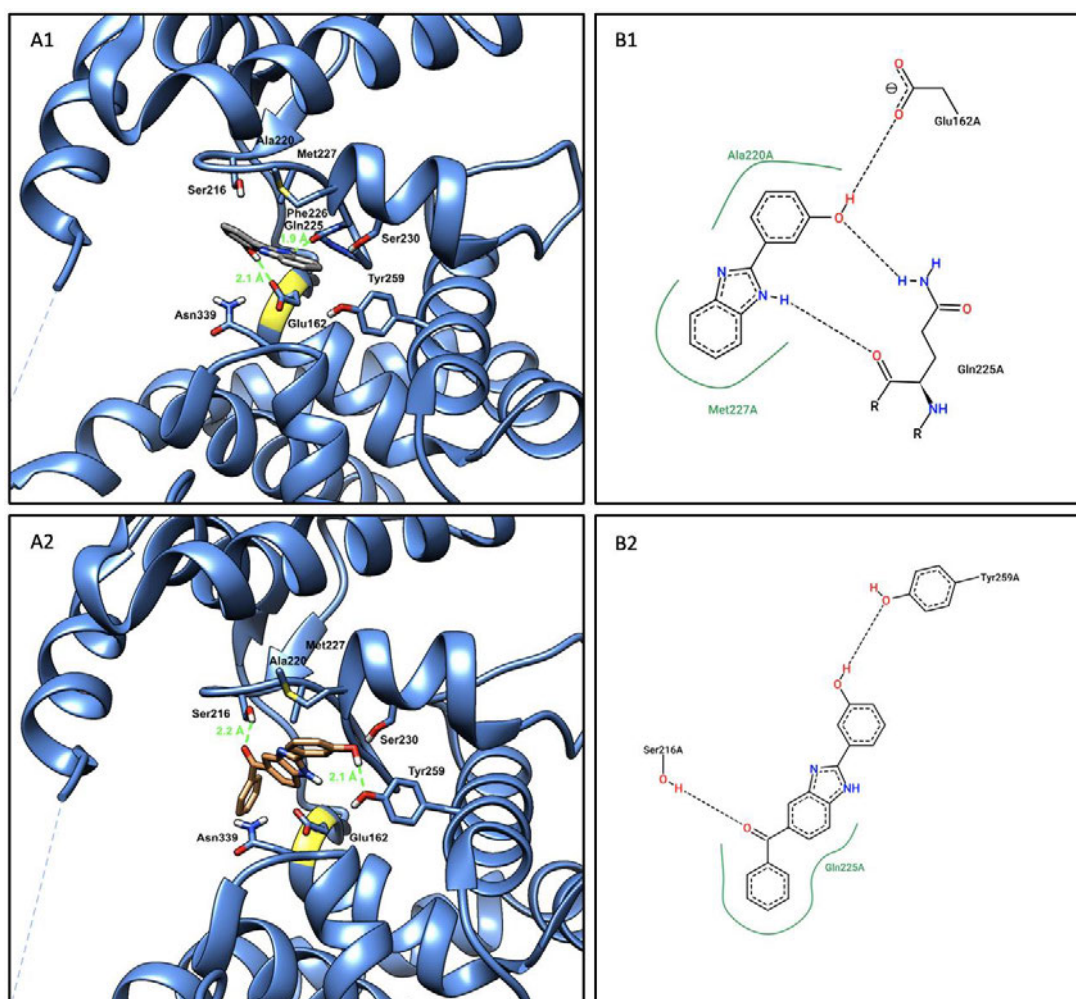
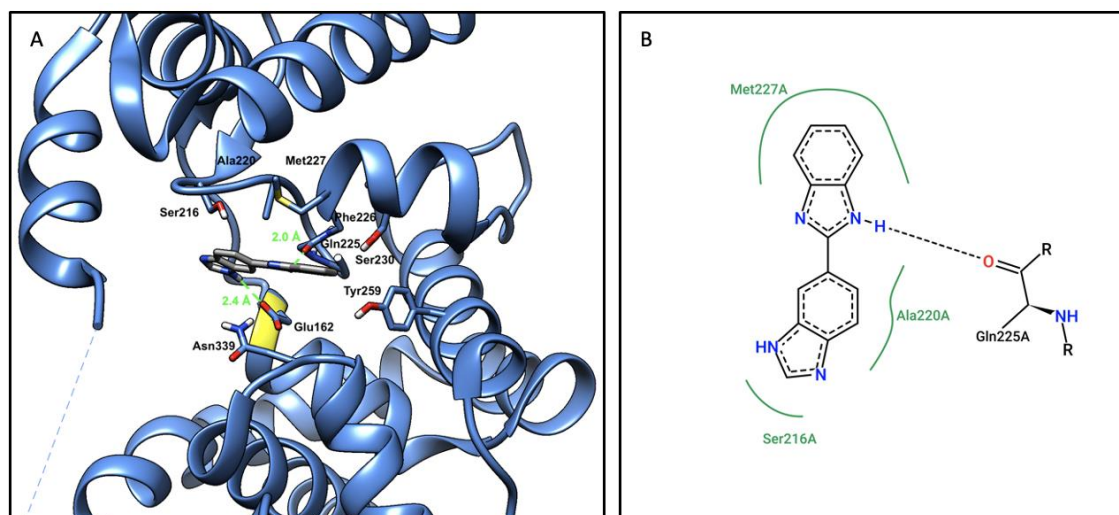Figure 2. 39: A) cartoon representation of Slt35 (1D0L-blu color) in complex with 3-(1*H*-benzimidazol-2-yl)phenol (BZI-25, grey color) and 3-(5-benzoyl-1H-1,3-benzodiazol-2-yl)phenol (BZI-95, sand color). The catalytic Glu162 residue is shown using yellow ribbon color while H-bonds are in dashed light green lines. B) 2D diagram of interaction showing H-bonds (dashed lines) and hydrophobic interactions in spline dark green color.

The presence of a benzophenone substituent in position 5 of the benzimidazole core leads to BZI-95. Docking studies revealed a different ligand location into the LT active site for the 3-(5-benzoyl-1H-1,3-benzodiazol-2-yl)phenol. The ligand is reversed into the active site if compared to BZI-25, with Its 5-substituent located close to the Ser216. The carbonyl oxygen atom forms H-bonds with the Ser216 while the C2- benzene m-hydroxyl group interacts with Tyr259.

2.2.1.3.10 Ethoxyphenol ring as C_2-extension

A m-ethoxy-p-hydroxy benzene ring in position 2 of the benzimidazole core leads to the category of ligands named 4-(1H-benzimidazol-2-yl)-2-ethoxyphenols.
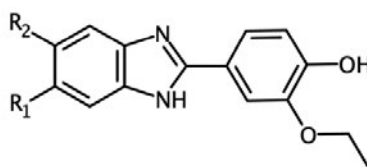
Figure 2. 40: General chemical structure of C_2-p-ethoxyphenyl benzimidazoles. In position 2 of the BZI core a m-ethoxy-p-hydroxy benzene ring is present while R_1 and R_2 vary.

In this group, BZI-26 conserves the interaction between the N1-hydrogen atom and the carbonyl oxygen of the Gln225-Phe226 main chain, typical of many C_2-benzimidazoles. Furthermore, Its methoxy-oxygen atom forms H-bond with Ser216 residue. Hydrophobic interaction between the benzene moiety of the benzimidazole core and Met227 as well as the ethyl group and Ala218 residue have been observed. Also, the benzene ring of the phenol portion generates hydrophobic contact with Ala220.
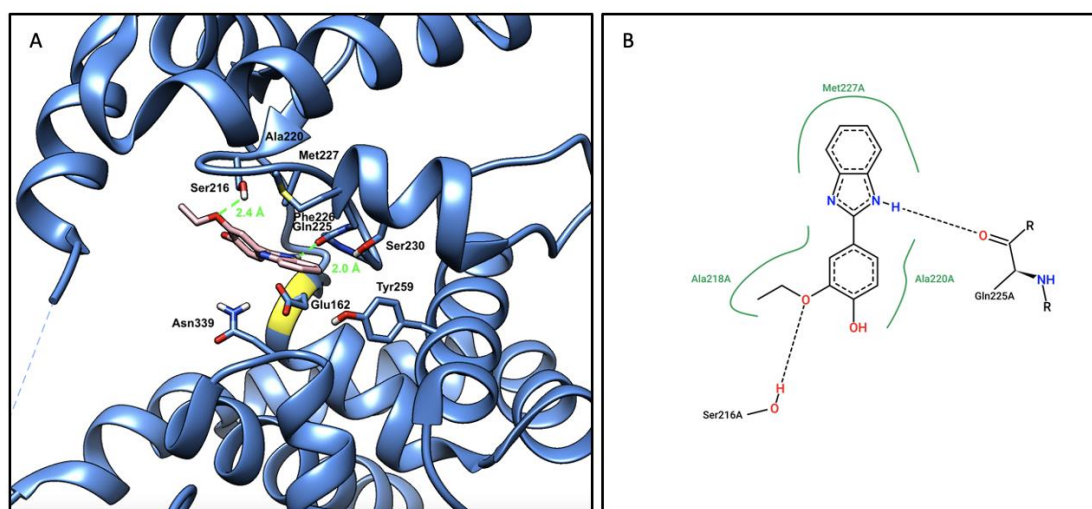
Figure 2. 41: A) cartoon representation of Slt35 (1D0L-blu color) in complex with 4-(1H-benzimidazol-2-yl)-2-ethoxyphenols (BZI-26, pink color). The catalytic Glu162 residue is shown using yellow ribbon color while H-bonds are in dashed light green lines. B) 2D diagram of interaction showing H-bonds (dashed lines) and hydrophobic interactions in spline dark green color.

2.2.1.3.11 o-nitro-benzene ring as C₂-extension

In the class of 2-(2-nitrophenyl)-1H-benzimidazoles, BZI-27 has hydrogen atoms as R_1 and R_2 groups (Fig2.42).

Figure 2. 42: General chemical structure of C_2-o-nitrophenyl benzimidazole. In position 2 of the BZI core an o-nitro benzene ring is present while R_1 and R_2 vary.
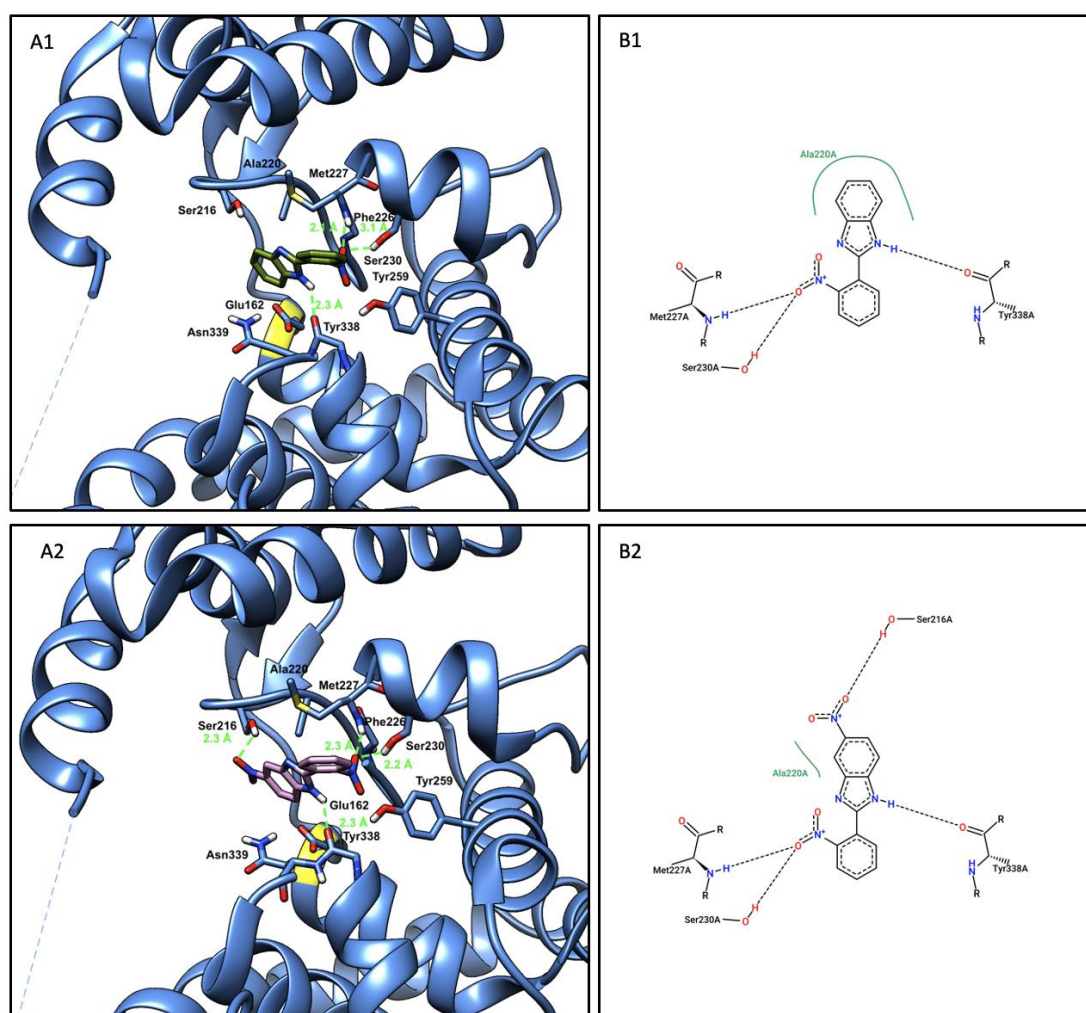
Figure 2. 43: A) cartoon representation of Slt35 (1D0L-blu color) in complex with 2-(2-nitrophenyl)-1H-benzimidazoles (BZI-27, olive green color) and 6-nitro-2-(2-nitrophenyl)-1*H*-benzimidazole (BZI-69, plum color). The catalytic Glu162 residue is shown using yellow ribbon color while H-bonds are in dashed light green lines. B) 2D diagram of interaction showing H-bonds (dashed lines) and hydrophobic interactions in spline dark green color.

Its N_1 hydrogen atom interacts with the carbonyl oxygen atom of the Tyr338-Asn339 main chain while the nitro group of the C2-benzene extension forms H-bonds with Ser230 as well as the N-H atom of the Phe226-Met227 main chain. Hydrophobic contacts with Ala220 have also been revealed. The insertion of a nitro group in position 5 of the benzimidazole core leads to BZI-69 which shows a complex network of H-bonds with the target. It reproduces the same interactions given by BZI-27 with an additional H-bond between the nitro group in position 5 and Ser216 residue.

2.2.1.3.12 m-nitro-benzene ring as C_2-extension

The effect of a nitro group in meta position of the C_2-benzene substituent has also been analyzed.
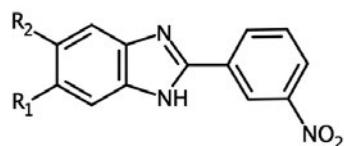
Figure 2. 44: General chemical structure of C_2-m-nitrophenyl benzimidazoles. In position 2 of the BZI core an m-nitro benzene ring is present while R_1 and R_2 vary.

In this class of ligands, BZI-28, which has hydrogen atoms as R_1 and R_2 substituents, gave the same interactions than BZI-27 in complex with Slt35 (Figure 2.45). Additional interactions have been revealed by docking studies when BZI-42 interacts with the target. Its m-nitro group forms H-bonds with Phe226-Met227 main chain as well as Ser 230 and Tyr 259 residues while Its 2-methyl-benzene moiety gives hydrophobic interactions with several active site residues (Ser216, Ala220 and Gln225) representing a good potential candidate as LT inhibitor.

The presence of a carboxylic group in position 5 of the benzimidazole core leads to BZI-84. 3D docking analysis revealed a complex network of H-bonds between this ligand and the target. The nitro group of its C_2-benzene substituent interacts with Arg188 while the N_3 atom forms H-bond with Asn339.

The 5-carboxylic group, through Its carbonyl oxygen atom, interacts with the N-hydrogen atom of the Phe226-Met227 main chain as well as the hydrogen atom of Ser230 and, through Its -OH hydrogen atom with Tyr 259. Hydrophobic interactions with Ala218 have also been revealed.

Figure 2. 45: A) cartoon representation of Slt35 (1D0L-blu color) in complex with 5,6-dimethyl-2-(3-nitrophenyl)-1*H*-benzimidazole (BZI-42, olive green color) and 2-(3-nitrophenyl)-3*H*-benzimidazole-5-carboxylic acid (BZI-84, grey color). The catalytic Glu162 residue is shown using yellow ribbon color while H-bonds are in dashed light green lines. B) 2D diagram of interaction showing H-bonds (dashed lines) and hydrophobic interactions in spline dark green color.

2.2.1.3.13 thiazole-moiety as C$_2$-extension

The effect of a thiazole ring in position 2 of the benzimidazole nucleus, leading to the category of 2-thiophen-2-yl-3H-benzimidazoles, has also been investigated by docking studies.

Figure 2. 46: General chemical structure of C$_2$-thiophenyl benzimidazoles. In position 2 of the BZI core a thiazole ring is present while R$_1$ and R$_2$ vary.

In this group of ligands, BZI-29, through Its N_1-hydrogen atom, interacts with the carbonyl oxygen atom of the Gln225-Phe226 main chain and, through Its benzene moiety, creates hydrophobic contacts with Met227 residue. BZI-71, having a nitro group in position 5 of the benzimidazole core, conserves all interactions given by BZI-29 with the additional formation of H-bond between the nitro substituent and Ser230 residue.

Figure 2. 47: A) cartoon representation of Slt35 (1D0L-blu color) in complex with 2-thiophen-2-yl-1H-benzimidazole (BZI-29, pink color) and 6-nitro-2-thiophen-2-yl-1H-benzimidazole (BZI-71, sand color). The catalytic Glu162 residue is shown using yellow ribbon color while H-bonds are in dashed light green lines. B) 2D diagram of interaction showing H-bonds (dashed lines) and hydrophobic interactions in spline dark green color.

2.2.1.3.14 pyrrole-moiety as C$_2$-extension

The class of 2-(1H-pyrrol-2-yl)-1H-benzimidazole a pyrrole moiety in position 2 of the BZI-core.
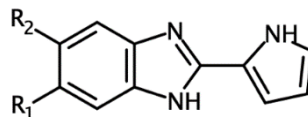
Figure 2. 48: General chemical structure of C$_2$-pyrrol-2-yl benzimidazoles. In position 2 of the BZI core a pyrrole ring is present while R$_1$ and R$_2$ vary.

Figure 2. 49: A) cartoon representation of Slt35 (1D0L-blu color) in complex with 2-(1H-pyrrol-2-yl)-1H-benzimidazole (BZI-30, olive green color) and 2-(1H-pyrrol-2-yl)-1H-benzimidazole-5-carboxylic acid (BZI-86, orange color). The catalytic Glu162 residue is shown using yellow ribbon color while H-bonds are in dashed light green lines. B) 2D diagram of interaction showing H-bonds (dashed lines) and hydrophobic interactions in spline dark green color.

In this category of ligands, BZI-30, having hydrogen atoms as R_1 and R_2 substituents, interacts with the carbonyl oxygen atom of the Gln225-Phe226 main chain. Hydrophobic contacts between the benzene moiety and Met227 as well as the aromatic pyrrole moiety and Ala220 have been revealed. A carboxylic group in position 5 of the BZI core leads to BZI-86 which, though Its pyrrole N-hydrogen atom, interacts with Tyr 259 while its carboxylic groups forms H-bond with Asn339.

2.2.1.3.14 Bis-benzimidazoles

Bis-benzimidazoles are given by the combination of two BZI-nuclei. In this work the affinity of 2,6-bis-benzimidazoles for the target has been investigated by docking studies.
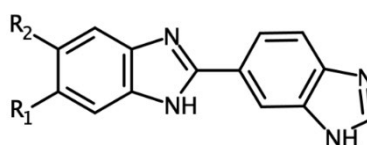
Figure 2. 50: General chemical structure of 2,6-bis-benzimidazoles. R_1 and R_2 vary.

Figure 2. 51: A) cartoon representation of Slt35 (1D0L-blu color) in complex with 2-(1H-1,3-benzodiazol-6-yl)-1H-1,3-benzodiazole (BZI-115, grey color). The catalytic Glu162 residue is shown using yellow ribbon color while H-bonds are in dashed light green lines. B) 2D diagram of interaction showing H-bonds (dashed lines) and hydrophobic interactions in spline dark green color.

In this category of ligands, BZI-115, having hydrogen atoms as R_1 and R_2 substituents, interacts, thought its N_1 hydrogen atom, with the carbonyl oxygen atom of the Gln225-Phe226 main chain. Hydrophobic interactions between the benzene moiety of one BZI nucleus and Met227 as well as the benzene moiety of the second nucleus and Ala220 have been revealed. All benzimidazole derivatives in this category of ligands creates similar interactions to BZI-115 into the Slt35 active site.

2.3 Conclusion

Multiple extensions of the benzimidazole nucleus have been designed and the effect that different substituents could have on the ligand-target binding properties has been analyzed. The analysis of the interactions between the known inhibitor bulgecin A and Slt35 led to the identification of critical interactions required for binding the target. Bulgecin structure has been used as model for designing benzimidazole based ligands which could potentially show affinity for Slt35. Early studies on the possible extensible sites of the benzimidazole core led to the design and selection of a library of desirable compounds. Their affinity for the LT active site has then been investigated by docking studies. The benzimidazole derivatives shown previously have been designed as antibacterial agents (potential LTs inhibitors).

Based on computational studies undertaken in this work, a library of benzimidazole-based compounds showing potential high affinity for the LT target has been built. The 2-hydroxymethyl moiety represents a promising C_2-extension having the hydroxyl group interacting, for most of analogues in this class of ligands, with the LT catalytic Glu162 residue. This mimics the hydroxymethyl group in the proline core of the known inhibitor Bulgecin A representing a promising core modification. The insertion of a benzyl chain in position number 1 of the benzimidazole nucleus generally leads to an increase of ligand-receptor interactions giving a stronger ligand predicted affinity for the target. Both the categories of benzimidazoles having a benzene substituent or the analogues having a second benzimidazole nucleus in position 2 of the benzimidazole nucleus seem to lead to compounds having high predicted affinity for the LT active site and so they represent good inhibitor candidates.

Chapter 3

Synthetic approaches

3. Synthetic approaches

3.1 Introduction

The compounds designed in the previous work consist of benzimidazole core having a 2-hydroxymethyl chain in position 2 and an aminoacidic chain on the N_1-atom. Based on results obtained from model reactions performed in the previous work,[174] the stability of acyl derivatives of benzimidazole is likely to be low. The acyl bond is weak probably because breakage of this bond generates a very stable benzimidazole anion in which the negative charge is shared between the two nitrogen atoms and delocalized by the aromatic system (Figure 3.1).
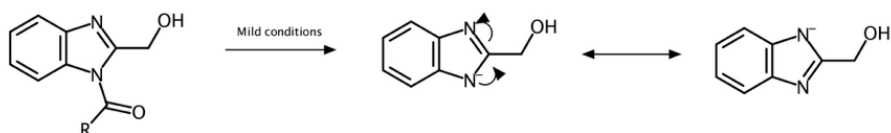
Figure 3. 1: Acyl-BZI instability in mild conditions found in the previous work[174] and resonance structure of the anion formed.

This work focuses on the identification of a suitable path for the synthesis of target molecules A and B (Figure 3.2) which are N-alkylated benzimidazoles. These are derived from the amino acids homoserine, aspartic acid and serine.
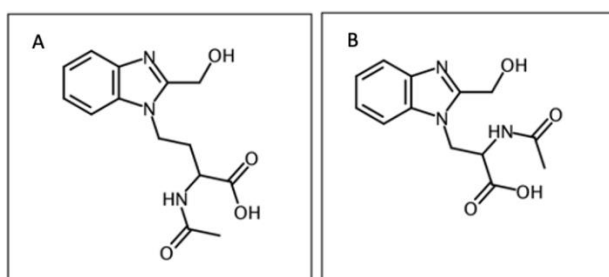
Figure 3. 2: Structure of potential LT inhibitors designed.

Amino acids are critical compounds as they are building blocks of proteins/polypeptides and regulate key metabolic processes which are critical in the growth and maintenance of a health condition.[217]
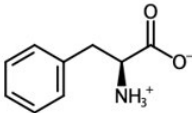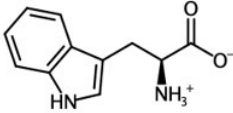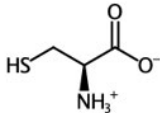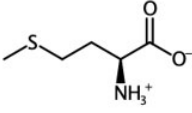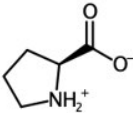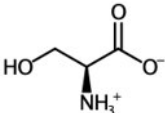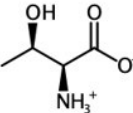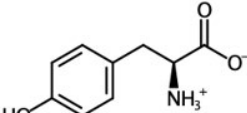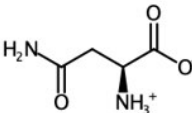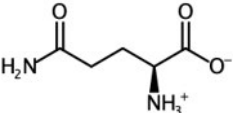
The structure of amino acids is given by a main chain having both amino and acid groups. All of them, except glycine (Figure 3.3A), have an asymmetric (chiral) carbon atom which binds a typical side chain (Figure 3.3B).

Figure 3. 3: General structure of A) glycine and B) asymmetric amino acids.

Owed to the variability of this chain and the properties of the functional groups present, amino acids exhibit different biological and chemical properties (Table 3.1). Their side chain can be distinguished into non-polar, polar or charged. Non-polar side chains can furtherly be distinguished into aliphatic (glycine, alanine, isoleucine, leucine, valine and proline), aromatic (phenylalanine and tryptophan) and sulfur-containing (cysteine and methionine). Amino acids containing polar side chains are divided into hydroxylic (serine and threonine), aromatic (tyrosine) and amidic (asparagine and glutamine). Finally, amino acids containing charged side chain are distinguished into positively (histidine, arginine and lysine) and negatively charged (glutamic and aspartic acid).

Amino acid	Structure	Side chain properties
Glycine (Gly)		Non-polar Aliphatic
Alanine (Ala)		Non-polar Aliphatic
Isoleucine (Ile)		Non-polar Aliphatic
Leucine (Leu)		Non-polar Aliphatic
Valine (Val)		Non-polar Aliphatic

Phenylalanine (Phe)		Non-polar Aromatic
Tryprophan (Trp)		Non-polar Aromatic
Cysteine (Cys)		Sulfur-containing
Methionine (Met)		Sulfur-containing
Proline (Pro)		Non-polar Aliphatic
Serine (Ser)		Polar Hydroxylic
Threonine (Thr)		Polar Hydroxylic
Tyrosine (Tyr)		Polar Hydroxylic
Asparagine (Asn)		Polar Amidic
Glutamine (Gln)		Polar Amidic
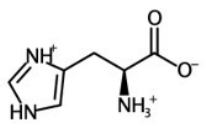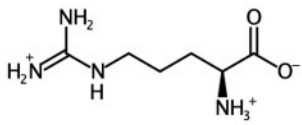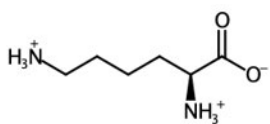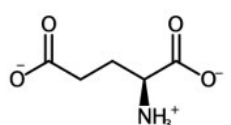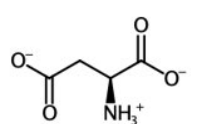
Histidine (His)		Polar	Charged
Arginine (Arg)		Polar	Charged
Lysine (Lys)		Polar	Charged
Glutamic acid (Glu)		Polar	Charged
Aspartic acid (Asp)		Polar	Charged

Table 3.1: Structure of the 20 essential amino acids and their side chain properties.

The insertion of amino acidic moieties onto the compounds designed in this work aims to generate extensions of the benzimidazole core that could generate H-bonds with the LT active site residues.

3.2 Retrosynthetic analysis of the target molecules

After considerations on the structure of target molecules (potential LT inhibitors designed in the previous work), this study focuses on the retrosynthetic analysis of the desired compounds in order to design a suitable method for their synthesis. Retrosynthesis is a key step when planning a synthetic approach in organic chemistry. It involves working backward from the desired target molecules towards simpler compounds that can be used as starting materials imagining all the possible intermediates and conditions that could give the designed target. A desired functional group can be given by two different approaches in retrosynthesis: the 'interconversion' which is the conversion in a different group or the 'disconnection' which is given by bond breakage. On the contrary the synthetic approach is the forward path which, starting from simple compounds (starting materials), gives the target molecule's formation as result. Only after having completed the retrosynthetic analysis, the forward multistep synthesis can be considered and undertaken. Usually, multiple retrosynthetic approaches can be considered, leading to the possibility of adopting different strategies for the synthesis of the target molecule. The synthetic path to be undertaken is given by a combination of different factors such as the availability of the starting material, suitability of the chosen mechanism of action and the leading to the greatest simplification given by disconnection. Previous work demonstrates the poor suitability of the N_1 extension of benzimidazoles once the nucleus has been closed. Retrosynthetic analysis of the target molecules (compounds A, B in Figure 3.2) has been undertaken in order to design alternative suitable paths for their synthesis.

The routes considered involve selective functional group protection/modification in order to avoid competitive reactions as the target molecules have multiple functional groups that could potentially interfere giving complex mixture of products.

3.2.1 Retrosynthetic approach for compound A

Compound A is an N1-alkylated 2-hydroxymethyl benzimidazole. A suitable retrosynthesis of this target molecule (Figure 3.4) involves the disconnection between the N-1 and the C-2, and between the C-2 and N-3 atoms of BZI giving the breakage of the benzimidazole core and leading to glycolic acid and the o-phenylenediamine, which has appended an amino acid chain (4-[2-aminophenyl)amino]-2-acetaminobutanoic acid). The interconversion of the alkylated phenylenediamine into the next intermediate (imine; 4-[(2-aminophenyl)imino]-2-acetaminobutanoic acid) by oxidation and the further disconnection of the N=C bond gives o-

phenylenediamine and N-acetyl-aspartate semialdehyde (2-acetamido-4-oxobutanoic acid). This aldehyde can be derived from a cyclic anhydride (N-(2,5-dioxooxolan-3-yl)acetamide).
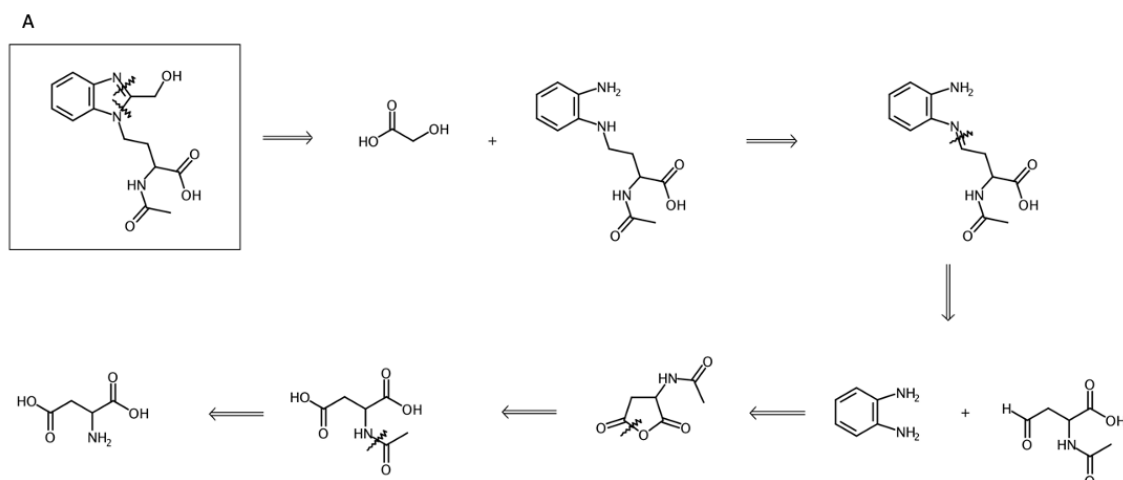
Figure 3. 4: Retrosynthetic scheme proposed in this work for compound A.

The disconnection of the beta C-O bond of the anhydride gives N-acetyl-aspartic acid (2-(carboxyamino)butanedioic acid), then disconnection at the acetyl group gives aspartic acid as starting material. As shown from the retrosynthetic scheme, in order to perform the forward path in the target molecule A, the main chain of the amino acidic part needs to be selectively protected by N-acetylation followed by cyclic anhydride formation, avoiding its reactivity in the following steps.

3.2.1 Retrosynthetic approach for compound B

Target molecule B is another N-1 alkylated 2-hydroxymethyl benzimidazole, with a shorter chain than compound A. A suitable retrosynthetic approach (Figure 3.5) involves the disconnection between the N_1 and the C_2, and between the C_2 and N_3 atoms of BZI giving the breakage of the benzimidazole core with glycolic acid and an extended o-phenylendiamine.

The disconnection of the alkylated phenylendiamine gives N-Ac-serine which has its hydroxyl group and the main chain protected with two different protecting groups (PG).
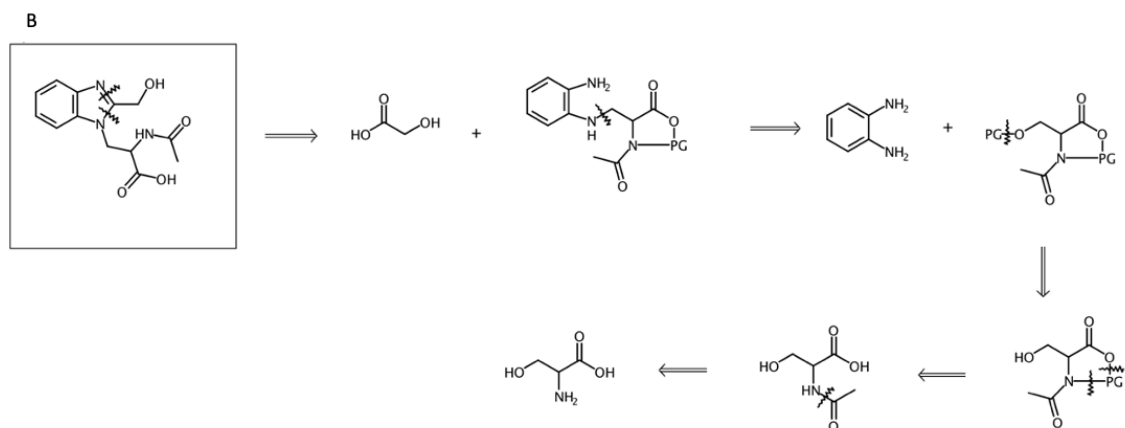
Figure 3. 5: Retrosynthetic scheme proposed in this work for compound B.

A further disconnection between the oxygen and its PG (hydroxyl protective group) gives the N-Ac-serine with a main chain protective group interacting with both the carboxylic and the amidic group. The breakage of this complex and the leaving of the PG gives an N-acetylated amino acid which, after the removal of the acetyl group gives serine as starting material.

Serine is an amino acid having a beta hydroxyl group with the oxygen atom having its lone pairs able to give to the molecule nucleophilic characteristic. The difference in electronegativity between the hydroxyl-oxygen atom and the carbon in beta position determines a polarization of this bond with a partial positive charge on the C atom which could undergo the attack from a nucleophile (diamine) if the hydroxyl group is converted into a better leaving group. In order to have the selective nucleophilic attack on this carbon atom in beta, the main chain (with its carbonyl function) needs to be protected. The disconnection of the extended phenylendiamine gives a protected N-Ac-serine with its hydroxyl group converted in a good LG (tosylate is considered) in order to activate strongly the carbon atom in beta.

3.3 Synthetic plan

As shown from the retrosynthetic analysis of A and B, the starting materials are amino acids. Thus the first synthetic approach taken in this study is given by modifications of aspartic acid and serine in order to investigate their reactivity and the suitability of the synthetic plan to be undertaken.

3.3.1 Amino acids modification and synthetic difficulties

As observed previously, amino acids are made of a main chain having both amine (basic) and carboxylic (acidic) functional groups. An internal hydrogen transfer from the carboxylic acid to the amine group gives a zwitterion (Figure 3.6), which is a species having no overall electrical charge, but containing both a negative and a positive charge, as result. The zwitterion is the prevalent form in which amino acids exist. Modifications of the pH value can give then the ion forms (cation or anion) as shown from the scheme (Figure 3.6). Increasing the pH of a solution of amino acids, adding hydroxide ions, the hydrogen is removed from the amine and the anionic form of the a.a. is formed (A in Figure 3.6). The decreasing the pH of the solution, adding an acid, determinates the cation form formation given by the protonation of the carboxylic group (B in Figure 3.6). It is an important consideration which can explain one of the main difficulties faced when working with amino acids. Due to their chemical properties, amino acids usually insoluble (or poorly soluble) in organic solvents which could make them not react when most common organic reactions are performed.
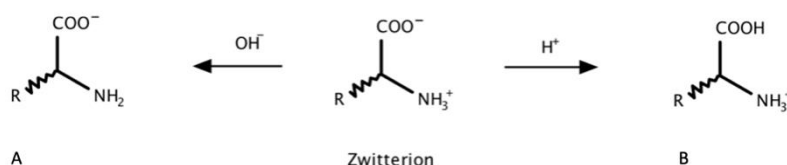
Figure 3. 6: Protonated states of amino acids.

After multiple attempts using organic solvents in order to modify the aminoacidic structure, in this study, water or very polar organic solvents are considered the most suitable solvents to start the modification of aspartic acid or serine.

3.3.2 Synthesis of target molecule A

In order to synthesise compound A, the following synthetic path (Figure 3.7) was attempted in this work. The acetylation of aspartic acid (2-aminobutanedioic acid) is followed by the cyclic N-Ac-anhydride formation (N-(2,5-dioxooxolan-3-yl)acetamide). The selective reduction of the gamma-carbonyl group could give the opening of the ring with the aldehyde formation (2-acetamido-4-oxobutanoic acid), which could undergo the nucleophilic attack by o-phenylenediamine giving an imine intermediate as result (4-[(2-aminophenyl)imino]-2-

acetamidobutanoic acid). The imine reduction could then lead to an alkylated phenylenediamine (4-[(2-aminophenyl)amino]-2-acetamidobutanoic acid) which is able to give the closure of the benzimidazole core by reacting with glycolic acid giving the formation of compound A.
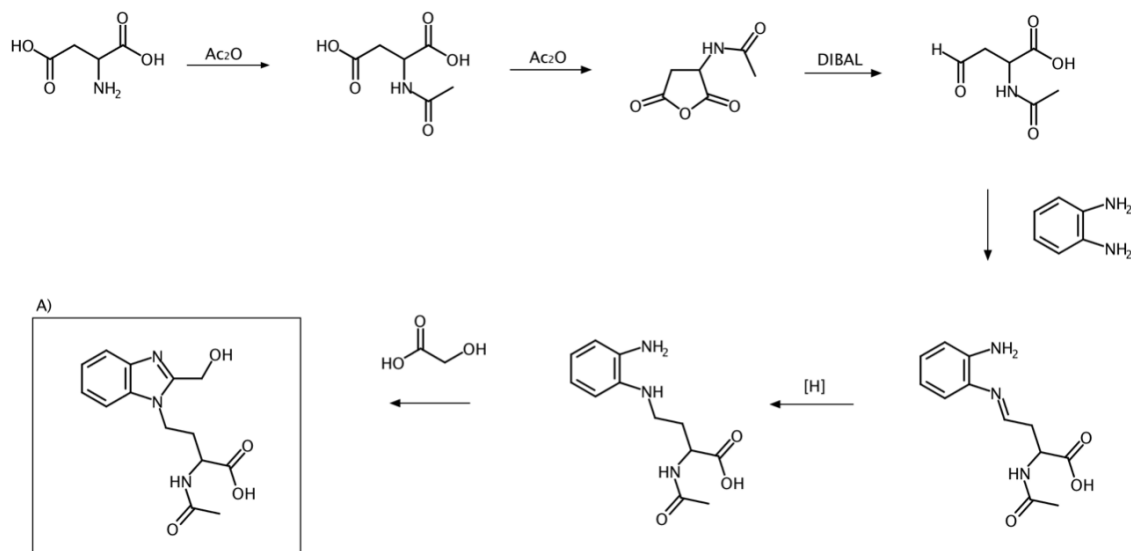
Figure 3. 7: Synthetic path for the preparation of target molecule A proposed in this study.

3.3.2.1 Acetylation of aspartic acid

The insertion of an acetyl group is called acetylation reaction which is the first step considered and undertaken in the synthetic path of compound A. It is given by the nucleophilic attack of an electron rich species (acetyl acceptor) to the carbonyl group of an acetyl source (acetyl donor) such as acetyl chloride (acyl halide) or acetyl anhydride (symmetric anhydride).

The key of both mechanisms of reaction is the presence of a very electronegative atom (such as nitrogen or oxygen) in the acetyl-acceptor compound, which performs a nucleophilic attack on the electrophile carbonyl group of the acetyl-donor.
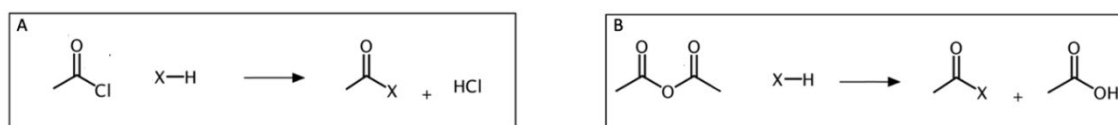
Figure 3. 8: Acylation reaction using A) acetyl chloride or B)acetic anhydride.

The transferring of the acetyl group is faster if acetyl chloride is used as source of acetyl group instead of anhydrides. Halides are usually more reactive than anhydrides, as the halide (chlorine in this case) is more electronegative than the oxygen atom (present in anhydride), bonded to the carbonyl group. This creates a more polarized C-X bond and strongly activates the carbonyl carbon atom. Moreover the chlorine anion is a better leaving group than carboxylate (occurring when anhydrides are used), which increases the reactivity of halides. One of the main differences between the two acetylation methods (A and B in Figure 3.8) is given by the formation of the secondary product occurring in this reaction, which is hydrochloride acid, if acetyl chloride is used, or acetic acid, if acetic anhydride is the acetyl source. Despite the greater reactivity of halides, anhydrides are considered good sources of acetyl groups. They have two acyl groups (acetyl if acetic anhydride is used) bonded to the same oxygen atom which has the lone pair that can be shared by both the carbonyl groups giving a compound highly stabilized by resonance (Figure 3.9).
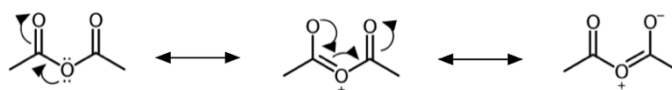
Figure 3. 9: Resonance structures of acetic anhydride.

In this work acetic anhydride is used as source of acetyl group, giving acetic acid as secondary product of reaction which is preferred than hydrogen chloride gas generation (obtained when acetyl chloride is used). Acetic anhydride is a symmetric anhydride where both the acetyl groups are equivalent and able to undergo nucleophilic attacks. In order to find a suitable method for the N-acetylation of aspartic acid (Asp), which could give the N-acetylated intermediate, different methods have been attempted in this work.

Acetic anhydride in large excess (as solvent) and acid catalyst[218,219]

The acidic conditions should protonate the carbonyl oxygen atom of the acetic anhydride (Figure 3.10) giving a more electrophilic carbon atom which can then undergo nucleophilic attack from the nitrogen atom of the amine group of Asp. The trigonal carbonyl carbon atom of the anhydride becomes tetrahedral, giving the acetyl derivative after a deprotonation step followed by the loss of a molecule of acetic acid.
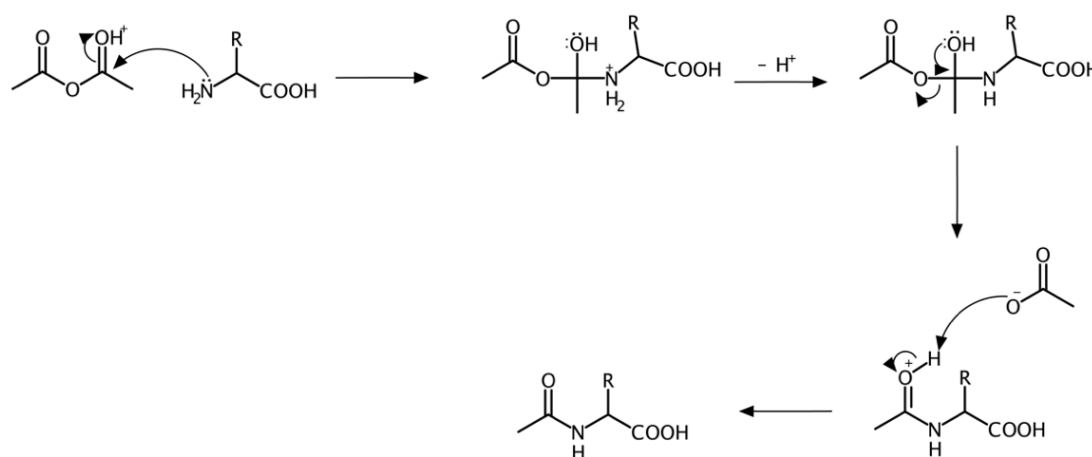
Figure 3. 10: General mechanism for acetylation of amino acids (the stereochemistry is avoided to simplify the scheme) using acetic anhydride and acid catalyst.

Unluckily, under these conditions, reaction was attempted both under reflux and at room temperature without giving the expected product (Figure 3.10). Probably the strong acid conditions protonate the amine group of the aspartic acid making it less reactive as the lone pair of the nitrogen atom is not anymore available to perform the nucleophilic attack.

The reaction was run using different conditions in order to find the most suitable method for acetylating the considered starting materials (Asp). When an equimolar amount (1eq) or 2 equivalent of acetic anhydride were used, starting material was recovered (Figure 3.11).
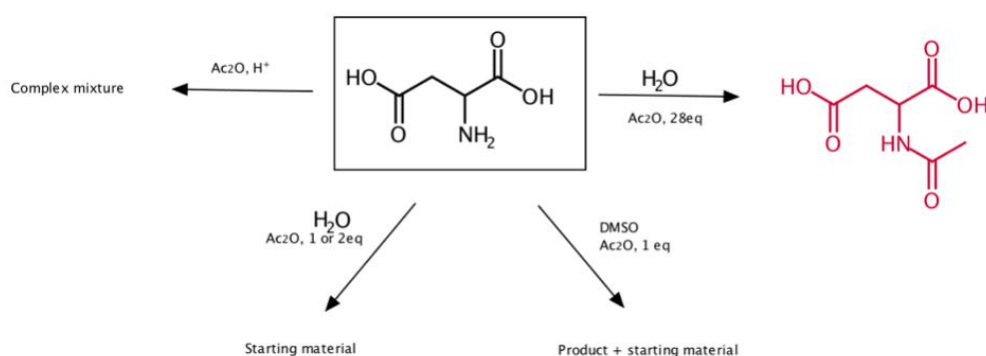
Figure 3. 11: Different strategies attempted in aspartic acid acetylation; the desired product is in red color.

Only using a large excess of acetic anhydride[220] and water as solvent, the expected product was successfully obtained giving N-acetyl-aspartic acid (2-aminobutanedioic acid) with 94% yield. The mechanism proposed is the same showed previously (Figure 3.10) and the acid conditions are given by the generation of acetic acid naturally occurring when acetic anhydride is in water. In fact water hydrolyzes the symmetric anhydride giving acetic acid formation (2 mol).

3.3.2.2 Cyclic anhydride formation

The previously obtained N-acetyl aspartic acid (2-aminobutanedioic acid) was then successfully converted into the corresponding anhydride (N-(2,5-dioxooxolan-3-yl)acetamide) by heating with an excess of acetic anhydride with 61% yield.[220]
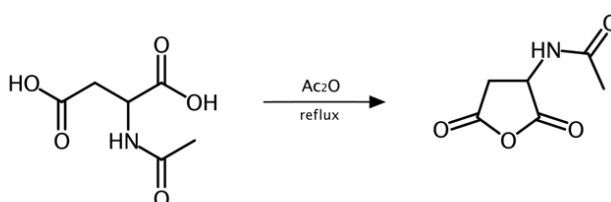
Figure 3. 12: Reaction scheme for the cyclic anhydride formation using N-Ac-Asp as starting material.

The structure of the N-Ac-aspartic anhydride (B in Figure 3.13) resembles the succinic anhydride (A in Figure 3.13) structure which is a symmetric cyclic anhydride obtained using succinic acid as starting material.
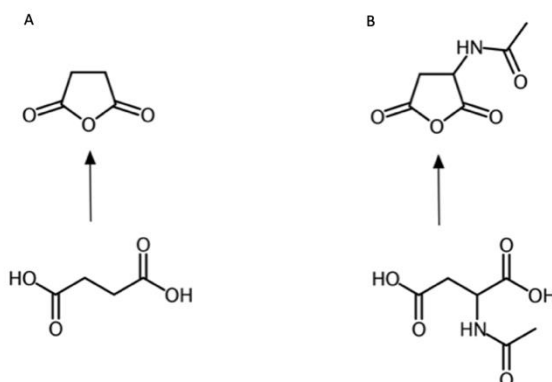
Figure 3. 13: A) succinic acid B) N-Ac-Asp generating the corresponding anhydrides.

Succinic acid is a dicarboxylic acid with its two carboxylic groups which are equal and both can undergo a nucleophilic attack by an electron rich species. When succinic acid reacts with acetic anhydride, the oxygen atom of the Ac_2O, with its lone pair, deprotonates one of the carboxylic group of the succinic acid giving the corresponding carboxylate intermediate which can then attack the electrophile carbon atom of the other carboxyl group giving the closure of the 5 membered ring and a compound with a negative charge on the oxygen atom. The protonated acetic anhydride donates a proton to the anionic cyclic intermediate forming a diol. The following exchange of a hydrogen atom between the hydroxyl groups and the loss of water gives the formation of succinic anhydride. The molecule of water, formed in the reaction, then attacks the carbonyl group of acetic anhydride giving, after its hydrolysis, acetic acid as secondary product of reaction.
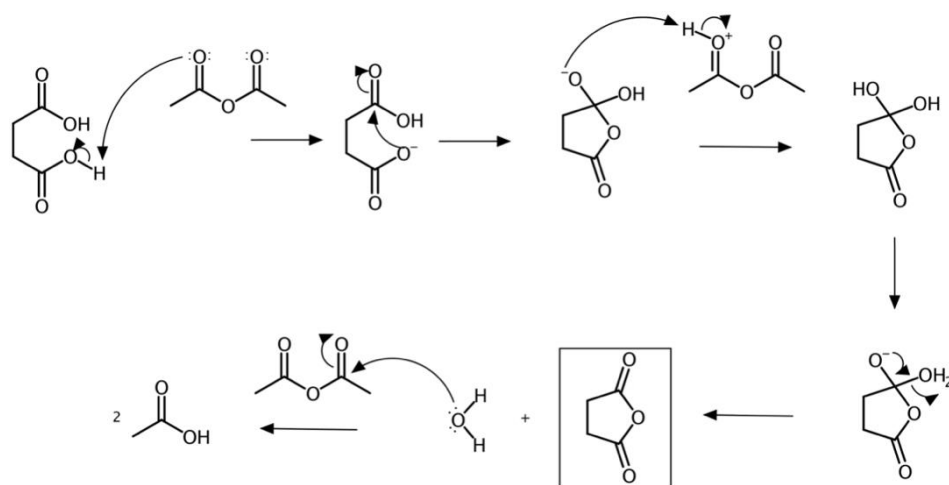
Figure 3. 14: Proposed mechanism considered for succinic anhydride formation.

Unlike succinic acid, N-Ac-Aspartic acid is an asymmetric dicarboxylic acid having an acetylated amino group in alpha. Thus the reactivity of the two carboxyl groups is different. In order to investigate the suitability of the formation of Asp-cyclic anhydride (N-(2,5-dioxooxolan-3-yl)acetamide) and propose a mechanism for this reaction, the reactivity of aspartic acid has been analyzed.[221] A potential mechanism of reaction involves the deprotonation of the beta carboxylic group which can then attack the carbonyl carbon atom of the alpha carboxyl group, closing the ring an giving the corresponding cyclic anhydride formation (like the mechanism considered for the formation of succinic anhydride- Figure 3.14).

3.3.2.3 Anhydride reduction using DIBAL-H

In the synthetic path considered, the anhydride formation is followed by a selective reduction of the carbonyl carbon atom in beta position in order to form an aldehyde group in the side chain of the aspartic acid. Reduction is a class of reactions in which the number of electrons associated with a species is increased by an electron donor. One of the most important classes of reducing agents is the metal hydrides, which are source of hydride based usually on boron or aluminium. Sodium borohydride (NaBH4; A in Figure 3.15) and lithium aluminium hydride (LiAlH$_4$; B in Figure 3.15) are common reducing agents used in carbonyl reduction to the corresponding alcohols.
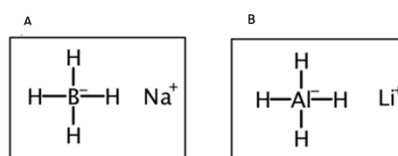
Figure 3. 15: Structure of A) sodium borohydride and B) lithium aluminium hydride.

They have the boron or aluminum atom which is bonded to four hydrogens in a tetrahedral shape.

The general mechanism driving this reaction is based on the activation of the carbonyl group by interaction between the metal and the carbonyl oxygen atom and the nucleophilic attack performed by the hydride (aluminium hydride in Figure 3.16) on the carbonyl carbon atom giving a tetrahedral metal alkoxide complex which generates the aldehyde as intermediate.

A second equivalent of metal hydride then reacts with the aldehyde giving the corresponding alcohol as product (Figure 3.16) occurring after two resulting reduction steps.
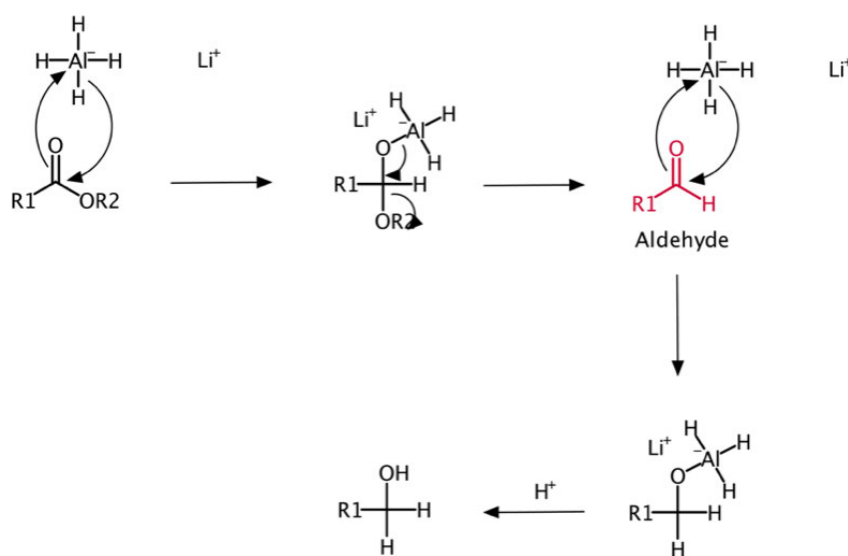
Figure 3. 16: General mechanism of esters reduction using lithium aluminum hydride; the aldehyde intermediate is in red color.

Owed to the higher reactivity of aldehydes than esters or ketones, it is not possible to isolate the aldehyde intermediate when lithium aluminium hydride or sodium borohydride are used. On the contrary, a known reducing agent able to stop the reduction to the aldehyde formation is DIBAL-H (Figure 3.17). It is an organoaluminium reagent having two isopropyl groups bonded to the aluminum atom which has its third sp2 hybrid orbital bonding a hydrogen atom giving a compound without charge as result and, unlike the hydrides considered before (Figure 3.16), it has electrophilic characteristics having an empty p orbital able to interact with a nucleophile.
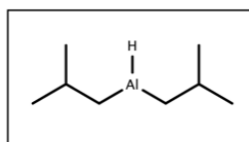
Figure 3. 17: Diisobutyl aluminium hydride (DIBAL-H) structure.

In this work, the reduction of the N-Ac-aspartic anhydride using DIBAL-H was attempted without having success.[222]
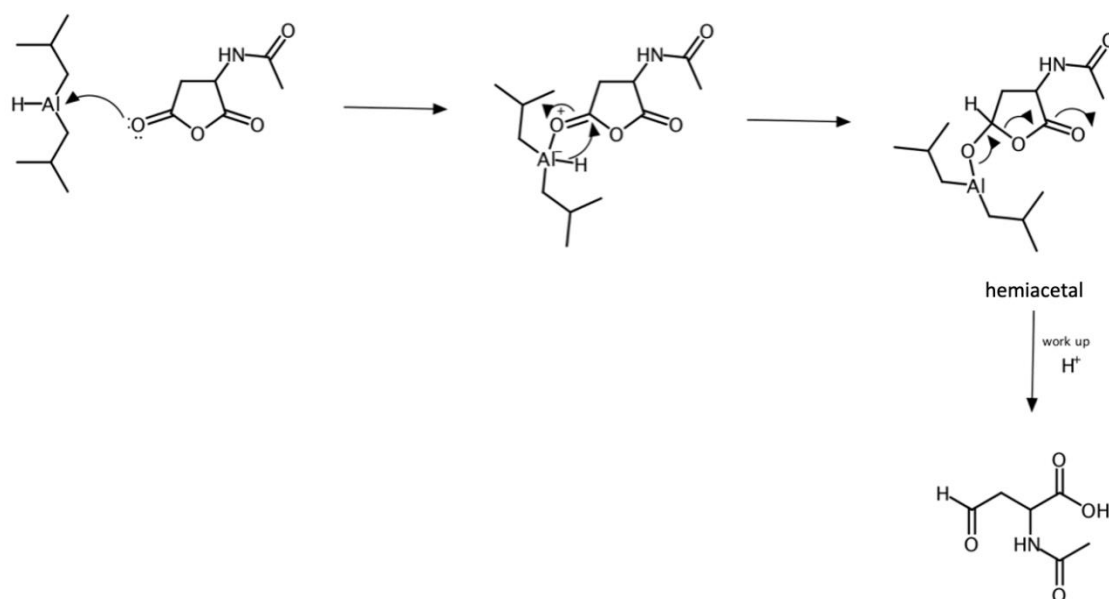
Figure 3. 18: Proposed mechanism of reaction propose in this work for the reduction of the cyclic anhydride using DIBAL-H.

The proposed mechanism of reaction involves the interaction between the carboxylic oxygen atom in beta position and the metal, which has an empty p orbital, followed by the nucleophilic attack of the halide on the electrophile carbonyl carbon atom giving the corresponding hemiacetal, stable at low temperature. The following acidic work up gives the breakage of the bond between the Al and the oxygen atom which forming the aldehydic group gives the opening of the ring as result.

Owed to the failure of this step, it was not possible to proceed with the synthetic path of target molecule A.

3.3.3 Synthesis of target molecule B

Compound B is a N_1-alkylated benzimidazole having serine as extension. The synthetic path considered in this work involves the acetylation of serine followed by the protection of the amino-acidic main chain in order to avoid its reactivity in the further steps (Figure 3.19). Retrosynthetic studies considered serine as starting material and Its acetylation as first step of reaction followed by the main chain protection using 9BBN. Due to the nature of N-acetyl-serine

(wet gum) and the high reactivity of 9-borabicyclo[3.3.1]nonane with water, the main chain protection was directly performed on serine instead of Its acetylated derivative. The acetylation step was anyway performed in order to investigate serine reactivity.
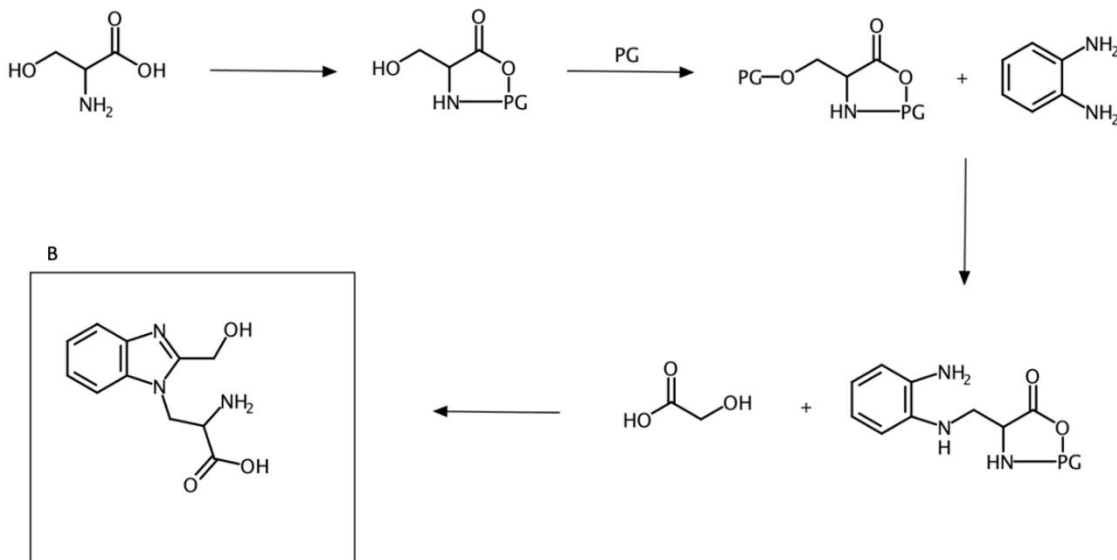
Figure 3. 19: Synthetic path considered in this work for the preparation of target molecule B.

The protected amino acid then reacts with o-phenylenediamine giving the alkylated amine which can then close the benzimidazole ring (and release the protecting group) by reacting with glycolic acid.

3.3.3.1 Acetylation of serine

Acetylation of serine was attempted several time in order to find the most suitable method. This is critical in order to plan the N-acetylation step after the main chain protection, avoiding the reactivity of 9BBn with water. Acetylation was attempt using the same conditions of reaction showed for N-Ac-Aspartic acid preparation (section 3.3.2.1).

N-acetylation of serine using a acetic anhydride in large excess (as solvent) and acid catalyst[218,219]
The reaction was attempted in different conditions (reflux or at room temperature, changing the time of reaction) without giving the expected product, like in synthetic path of target molecule A using Asp a starting material.

Acetic anhydride (equimolar or in excess) and water as solvent at room temperature:
Using an equimolar amount or 2 eq of acetic anhydride product formation didn't occur.

-When a <u>large excess of Acetyl-source (acetic anhydride, 28eq) and water as solvent</u>,[220] a double
acetylation occurred giving the N,O-diacetyl-serine (quantitative yield).
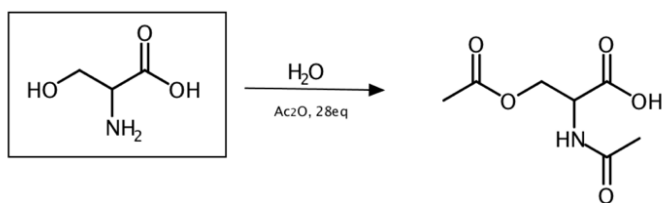
Figure 3. 20: General scheme of reaction for a double acetylation of serine.

The hydroxyl group of serine, with its lone pair, can perform a nucleophilic attack on the carbonyl
atom of the acetic anhydride giving an O-acetylated derivative which can then be acetylated on
the nitrogen atom by a second molecule of acetic anhydride giving a double acetylated amino
acid as result (Figure 3.21).
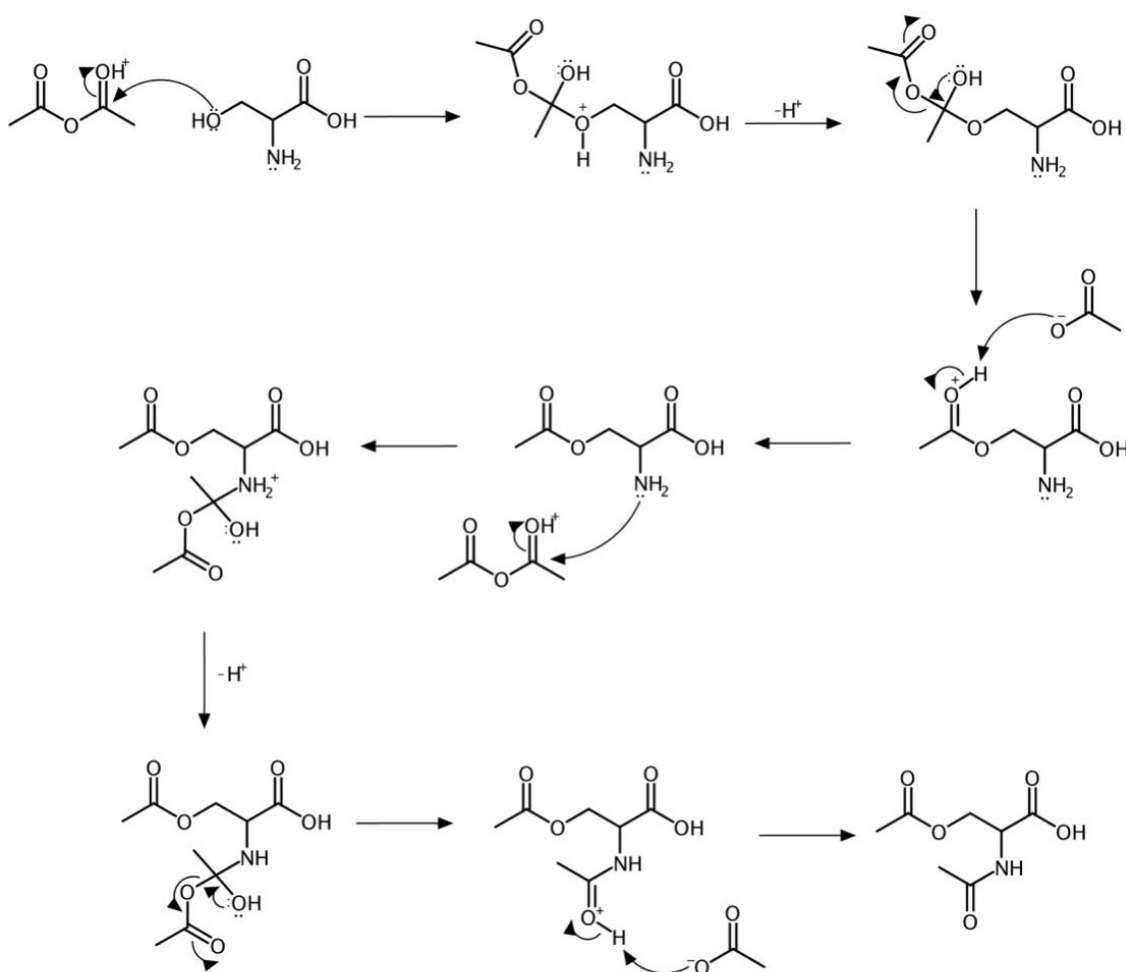
Figure 3. 21: Proposed mechanism for the double acetylation of serine.

-Only when a very <u>polar organic solvent (DMSO) and 1 eq of acetic anhydride</u> were used, the expected product formation occurred (86% yield). The reaction was run for 12 h at room temperature monitored by TLC.
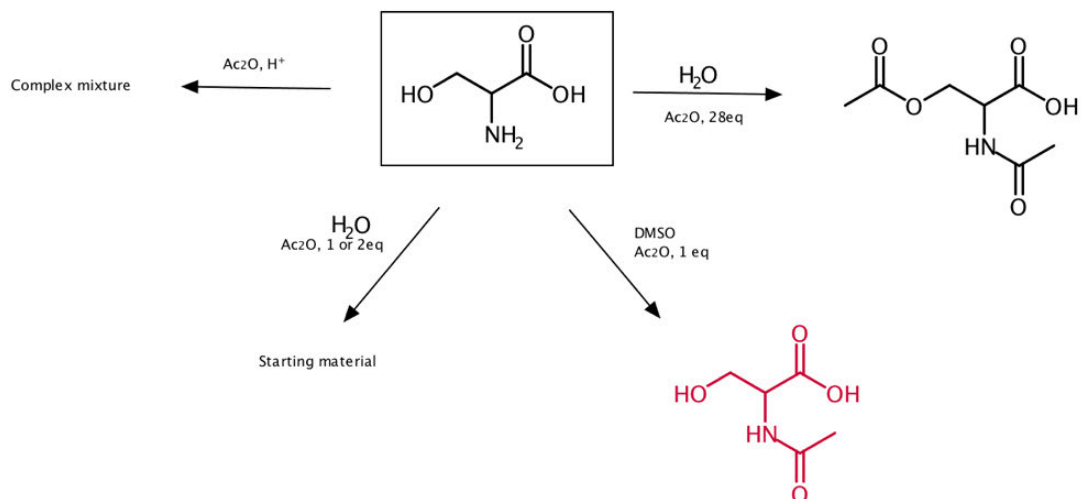
Figure 3. 22: Different strategies attempted in serine acetylation; the desired product is in red color.

3.3.3.2 Main chain protection of serine

The protection of the main chain was attempted using 9-borabicyclo[3.3.1]nonane (9BBN-H) which is an organometallic compound. The boron is bonded to two alkyl groups being part of a hindrance alkyl cyclic chain. The boron atom of BBN is also bonded to and hydrogen atom and has an empty p orbital able to interact with a nucleophile. 9-borabicyclo[3.3.1]nonane, with its highly hindrance chain, is commonly used in the hydroboration-oxidation of alkenes being able to strongly favors the selectively formation of the less substituted alcohol as product.[223] Recently, the role of 9BBN in the main chain protection of few amino acids has also been discovered.[223]

The protection of the main chain of serine using 9BBN-H, unlike the protection of aspartic acid, successfully gave the formation of the expected product (55% yield).
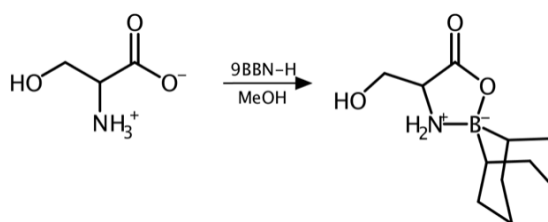
Figure 3. 23: General scheme of reaction for main chain protection of serine using 9BBN.

In this work a mechanism for the protection of amino acids (Figure 3.24) given by BBN-H has been proposed. It involves the nucleophilic attack of the carboxylic oxygen atom of the amino acid to the boron atom of BBN. The resulting hydride deprotonates the amine group of the amino acid giving hydrogen as leaving molecule. The boron atom of BBN has an empty p orbital able to interact with the hydrogen atom of the amine group of the main chain giving a complex with no overall charge but having a positive charge on the nitrogen atom and a negative charged boron atom. Due to this complex formation, the reactivity of the main chain of the amino acid is avoided and modifications of their side chain can be undertaken.
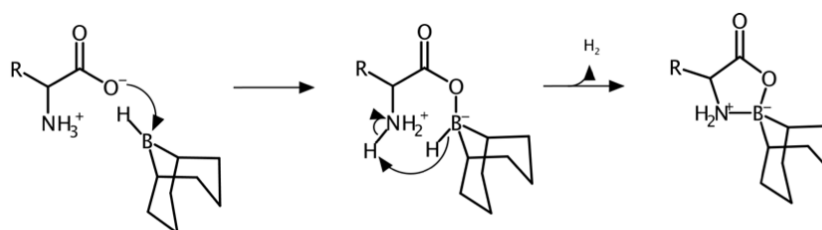
Figure 3. 24: Proposed mechanism for the amino acid main chain protection using BBN.

Having the main chain interacting with the protecting group (PG), modifications of the side chain can be attempted avoiding main chain competitive reactivity.

3.3.3.3 Tosylation of Serine-BBN

The following synthetic step considered in this work is given by the tosylation of the hydroxyl-group of serine followed by the formation of an alkylated diamine. In order to have a successful nucleophilic attack of the o-phenylenediamine on the carbon atom in β position of serine, it is critical to find a suitable method for increasing its electrophilicity. The carbon atom in beta is bonded to a hydroxyl group. Due to the difference in electronegativity between the oxygen and the carbon atoms, this bound is polarized with a partial positive charge on the alkyl-beta-carbon and a partial negative charge on the oxygen atom. Despite the weak electrophilic characteristic of the carbon atom in beta, the hydroxyl- group is a bad leaving group. Its conversion in a better leaving group is thus critical. Tosylation of the alcohol functionality was considered and attempted several times. The p-toluenesulphonate is a good leaving group and the presence of a toluenesulphonyl moiety should also enhance the electrophilicity of the carbon atom in beta position. P-toluene sulphonyl chloride is often used as activating agent for hydroxyl groups and

the mechanism allowing the product formation (Ts-OR) in a S_N2 substitution in which the oxygen atom, with its lone pair, performs a nucleophilic attack on the sulphur atom of the tosyl-Cl giving the leaving of a chloride ion. In order to contrast the acid formation (HCl) occurring in this reaction usually bases are used (pyridine or triethylamine).
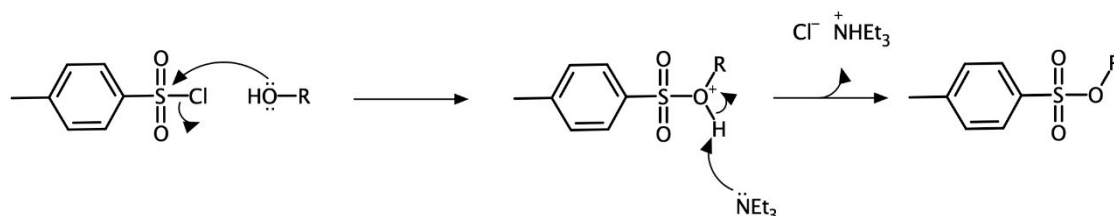
Figure 3. 25: Proposed mechanism for tosylation of alcohols.

Different attempts in the tosylation of Ser-BBN have been undertaken in this work:

-Reaction was run using Ts-Cl and pyridine at 0 ºC for 24 hours, and then at room temperature for 12 hours without giving the expected product.

-The same reaction was run at room temperature for 4 hours and then refluxed for 10 hours unsuccessfully.

-Only using a catalyst (DMAP), adding triethylamine as base and running the reaction at room temperature for 12 hours, the formation of the desired tosylated Ser-BBN was obtained with success (quantitative yield assuming purity). The catalyst is probably needed in order to favour the displacement of the chlorine and create a stable intermediate which can undergo the attack by the Ser-BBN, an alcohol with steric hindrance.
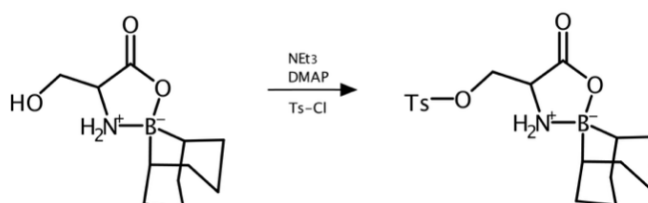
Figure 3. 26: General scheme of reaction for the tosylation of Ser-BBN.

DMAP (4-(dimethylamino)pyridine) is a derivative of pyridine, with a higher basicity than pyridine due to the resonance stabilization given by the dimethylamino group in para position which gives to this compound strong nucleophilic characteristic. It is an excellent catalyst for alcohol acylation/tosylation being able to attack the sulfur atom giving an intermediate cation stabilized by resonance. This intermediate can then undergo the nucleophilic attack by the alcohol giving the protonated tosyl alcohol and the regeneration of the catalyst. Triethylamine then deprotonates the cation obtained determining the product formation and contrasting the acid formation (HCl).
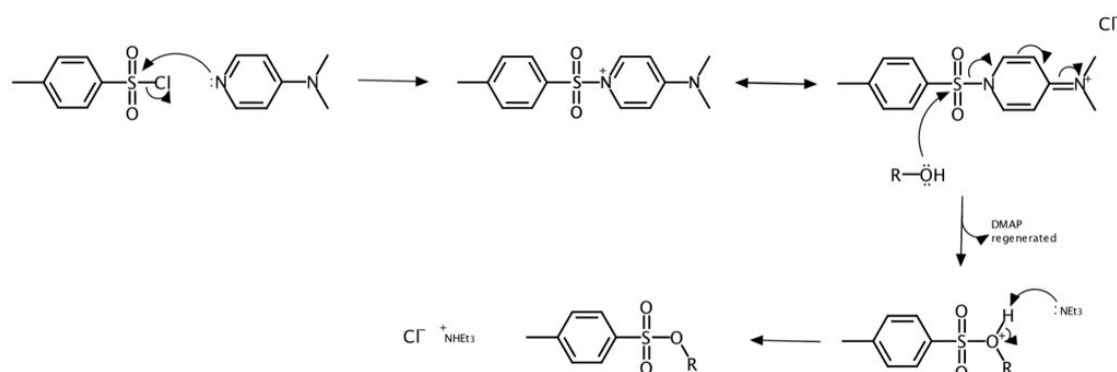
Figure 3. 27: Proposed mechanism for tosylation of alcohols in presence of DMAP as catalyst.

3.3.3.4 Replacement of the tosyl group by nucleophilic attack

In the synthetic path considered, the formation of the tosyl derivative with the activation of the carbon atom in beta position of the protected serine is followed by the replacement of the tosyl group given by the nucleophilic attack performed by the o-phenylenediamine.
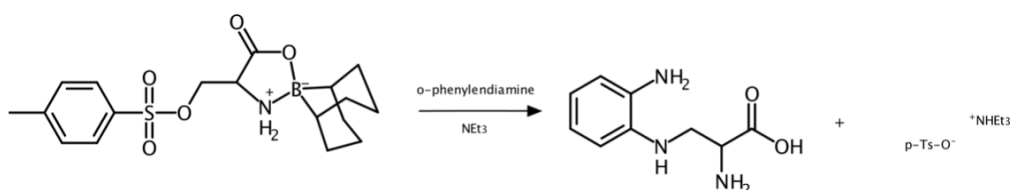
Figure 3. 28: General scheme of reaction for the displacement of tosyl group operated by a nucleophile (o-phenylenediamine).

The reaction was run in presence of triethylamine in order to contrast the formation of p-toluensulphonic acid occurring. The formation of the o-anilin-beta-amino serine as product was

achieved successfully (quantitative yield assuming purity) observing the removal of the BBN chain in these reaction conditions.

As remarked previously, the tosylated ser-BBN has the carbon in beta position with a partial positive charge owed to the polarization of the C-O bond. Moreover the beta-carbon is bonded to a tosyl chain which can easily be removed being tosyl-acid a good leaving group. Thus in presence of a nucleophile (o-phenylendiamine) the tosyl is replaced by a S_N2 reaction giving a protonated beta-amino-[o-anilin]-serine as intermediate (Figure 3.29). The triethylamine can then remove the proton from the positive charged nitrogen giving the product as result.
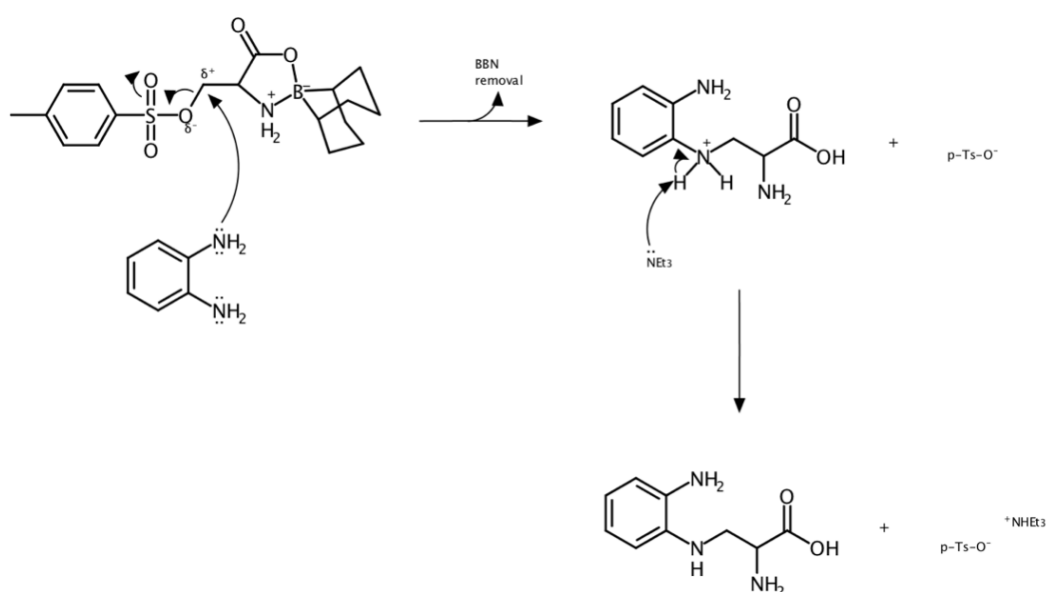
Figure 3. 29: Proposed mechanism for the nucleophilic attack performed by the o-phenylenediamine on the tosylated ser-BBN.

3.3.3.5 Benzimidazole core formation

The last step for the target molecule C synthesis is the formation of the BZI core given by the reaction between the previously obtained beta-amino-[o-anilin]-serine derivative and glycolic acid.

Reaction was run following the same conditions adopted previously for the synthesis of 1-H-2-hydroxy-methylbenzimidazole such as acidic condition and high temperature (3 hours reflux) without observing the product formation.[173,174]
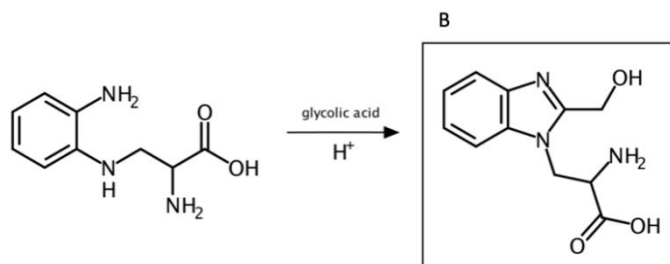
Figure 3. 30: General scheme of reaction for the final step in the synthetic path of compound C.

The acidic conditions could protonate the amine groups making their lone pairs unavailable for the nucleophilic attack and so unable to form the product of reaction. However, from the pKa values of the o-phenylendiamine (<2 and 4.47) it is easy to observe that at pH 2 only one amine is protonated while the other has its lone pair available to perform nucleophilic attack on the electrophilic carbon atom of the carboxyl group of glycolic acid.
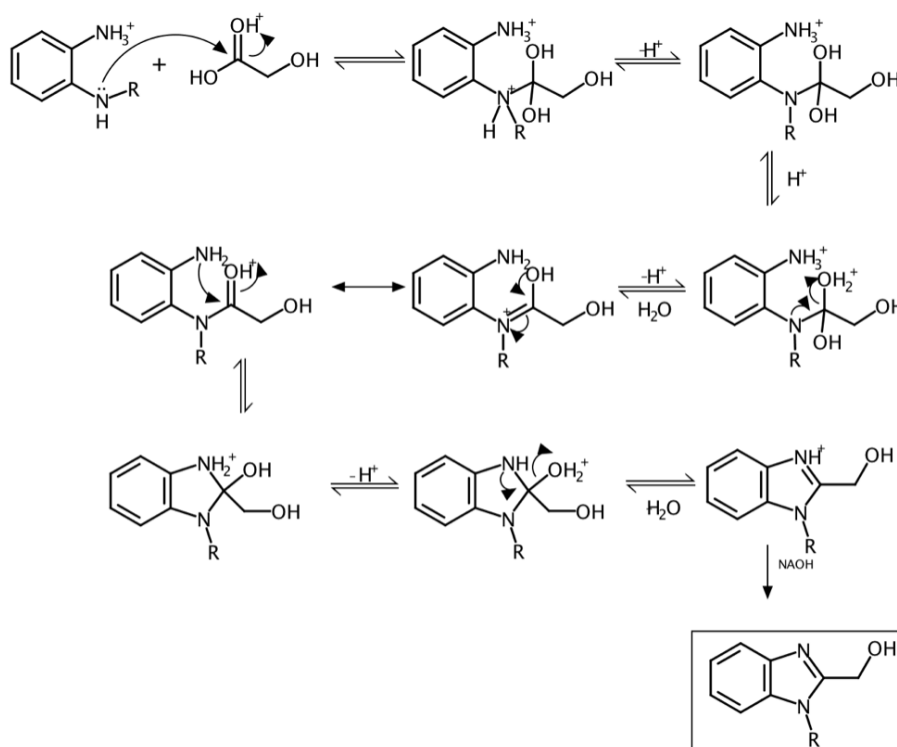
Figure 3. 31: Proposed mechanism for the benzimidazole core formation.

The carbonyl group of the glycolic acid is protonated by the acid catalyst while the unprotonated amine group of the extended phenylenediamine performs a nucleophilic attack on the electrophilic carbon atom of glycolic acid (Figure 3.31). This is followed by proton transfer and dehydration steps. This creates a new electrophilic carbon center which promotes the nucleophilic intramolecular attack performed by the second amine group giving the closure of a five membered ring. The following step evolves towards the formation of the aromatic system, energetically favored, with a concomitant removal of a water molecule. A final deprotonation gives the extended 1-R-2-hydroxymethylbenzimidazole product. The aromatic stabilization is the most important factor driving this reaction towards the product formation.

The synthesis of 1-H-2-hydroxymethylbenzimidazole was successfully achieved in previous work.[173,174] The synthesis of an extended BZI was attempted using the same conditions, without obtaining the expected product. This occurred probably due to the difference of starting materials. Instead of the o-phenylendiamine, an extended diamine is used and more time could be needed to form the product as the substituted amine is less reactive and has steric hindrance. The reaction was then run for longer (12h) without observing the formation of the desired product. Despite the failure in attempting this step, this synthetic path is far to be given up and Loveridge's group will strongly focus in the future in order to find a suitable method to achieve the target molecule B formation. Alternative reagents than glycolic acid, such as aldehydes, could be used in order to close the benzimidazole core.

3.3.4 Carbon chains for N-1 alkylation of benzimidazole

Due to the difficulties faced in this work attempting modifications of the amino acid structures as well as failures in the closure of the benzimidazole ring, model compounds where synthesized. This is critical in order to confirm the suitability of the designed synthetic paths. The extension of o-phenylenediamine followed by the BZI ring formation is essential for formation of an alkylated benzimidazole. An alternative strategy for the synthesis of an N_1-alkylated benzimidazole was considered and undertaken.

3.3.4.1 Alternative strategy

(1-propyl-2-yl)hydroxymethyl benzimidazole synthesis

In order to investigate the failure of the last step of the target molecule B synthetic path (section 3.3.3.5), the same synthetic approach was undertaken using a easier and monofunctional starting materials (1-propanol and 2-propanol).
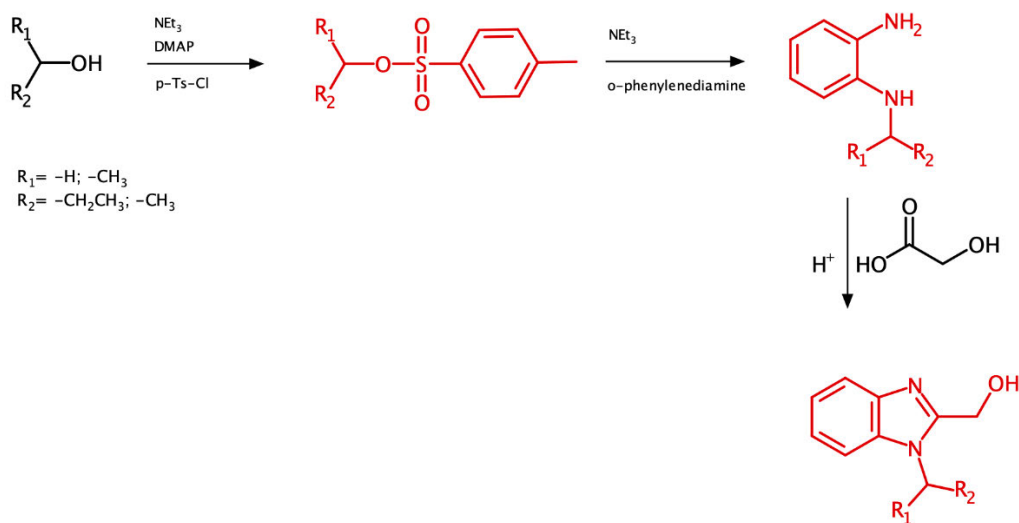
Figure 3. 32: Synthesis of (1-propyl-1H-1,3-benzodiazol-2-yl)methanol and [1-(propan-2-yl)-1H-1,3-benzodiazol-2-yl]methanol.

The reactions and mechanisms considered in this synthetic strategy are the same showed in section 3.3.3.3 and 3.3.3.5 and the compounds successfully synthesised are showed in red color (Figure 3.32).

The starting material (1-propanol and 2-propanol) were successfully tosylated using p-toluensulphonyl chloride and DMAP as catalyst giving the desired products propyl 4-methylbenzene-1-sulfonate (84% yield) and propan-2-yl 4-methylbenzene-1-sulfonate (52% yield).

The tosyl group was then displaced by the nucleophilic attack of o-phenylendiamine. This gave an extended diamine (alkylated) leading to the formation of the expected products N1-propylbenzene-1,2-diamine (71% yield) and N1-(propan-2-yl)benzene-1,2-diamine(6% yield).

The formation of the benzimidazole core was finally attempted using the same condition (acid catalyst, 4 hours reflux) adopted in the previous work for the 1-H-2-hydroxymethylbenzimidazole preparation,[174] giving a mixture of the desired product and starting material, demonstrating that probably more time is needed for the BZI core formation when an extended phenylendiamine is used as starting material.

Only refluxing the mixture for 24 hours the formation of the expected products, (1-propyl-1H-1,3-benzodiazol-2-yl)methanol (95% yield) and [1-(propan-2-yl)-1H- 1,3-benzodiazol-2-yl]methanol (25% yield), successfully occurred (95% yield). This demonstrate that, unlike the free o-phenylendiamine, the extended diamine requires forced conditions to react and close the benzimidazole ring.

The synthetic route leading to the formation of isopropyl-benzimidazole has a lower yield, if compared with the primary alcohol (1-propyl-benzimidazole) as the secondary alcohol is less reactive by S_N2 due to steric hindrance. This makes the attack from the phenylenediamine more difficult. Nevertheless, this work shows that the 2-isopropyl-benzimidazole formation is still achievable using this synthetic strategy.

(1-propyl-2-yl)methyl acetate benzimidazole:
The O-acetylated derivative of the 1-propyl-benzimidazole was successfully synthesised (6% yield) using an access of acetic anhydride and acid catalyst and having (1-propyl-2-yl)methyl acetate benzimidazole as product.[218,219]
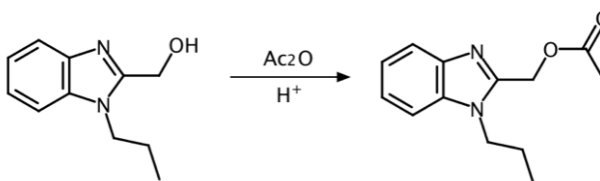
Figure 3. 33: General scheme of reaction for the synthesis of (1-propyl-2-yl)methyl acetate benzimidazole.

In the previous work, the (1-Acetylbenzimidazole-2-yl)methyl acetate, unlike the unacetylated benzimidazole, was found to be active against *E. coli*. Probably the acetyl group on the oxygen atom could be necessary in the antimicrobial structure.[174] Due to this consideration, it was of

primary interest to obtain the acetylated derivative and then compare the antimicrobial activity of both (1-propyl-2-yl)hydroxymethyl benzimidazole and its acetylated derivative.

3.3.4.2 Alkyl-benzimidazole with polar chain as N1-extension

The insertion of polar groups in the N_1 chain has also been investigated. Inspection of LT active site and in-silico docking performed in this work (section 2.2.1) showed that polar groups could generate H-bonds into the target active site optimizing the ligand-receptor interaction. Based on this, three simpler polar N-extensions have been designed.
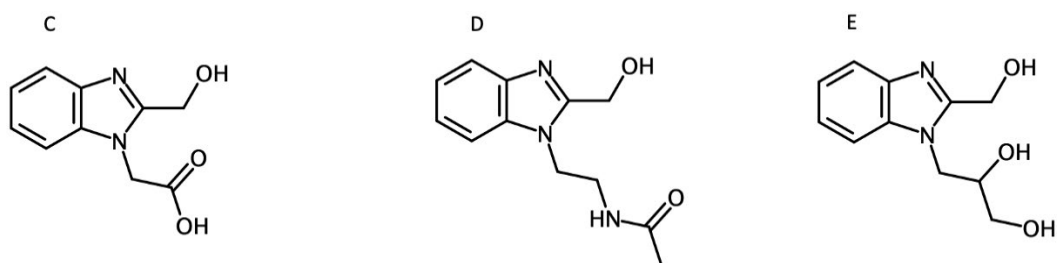
Figure 3. 34: Benzimidazoles designed in this work having polar chains as N_1-extension.

BZI-C has a N-chain given by a carboxylic terminal group, BZI-D has an acetamido group while the N-extension of BZI-E is given by two hydroxyl groups. The strategy undertaken for the synthesis of these three benzimidazoles follows strategy adopted in section 3.3.4.1.

3.3.4.2.1 Synthesis of BZI-C

The synthetic route for preparing BZI-C considers glycolic acid as starting material. The carboxylic group of glycolic acid was successfully protected using alcohols (methanol or ethanol) obtaining methyl-2-hydroxyacetate (85% yield) or ethyl-2-hydroxyacetate (65% yield). This will avoid the reactivity of the carboxylic group in the following synthetic steps. The alcohol group of these derivatives was tosylated and the resulting compounds underwent the nucleophilic attack of o-phenylenediamine on the activated carbon atom. This should give an extended diamine that can then react with glycolic acid forming the benzimidazole nucleus. The following expected

synthetic step is given by the deprotection of the carboxylic group leading to BZI-D as final product (Figure 3.35).
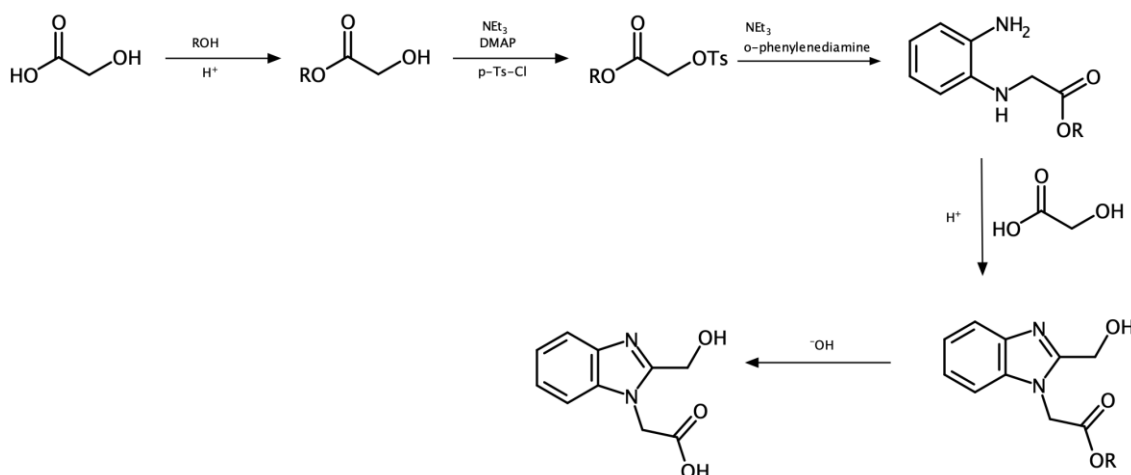
Figure 3. 35: Scheme of reactions for the synthesis of BZI-C. In this work R= -CH$_3$ or -CH$_2$CH$_3$.

3.3.4.2.1.1 Esterification of glycolic acid

The esterification of a carboxylic group, also named Fisher esterification, is a common strategy for protecting carboxylic acids and converting them in ester groups. It is given by the replacement of the -OH with an -OR group. This reaction is carried out using acid catalyst (sulfuric acid) and an excess of alcohol. The alcohol is used in large excess as each step of the mechanism of reaction are reversable. An excess of alcohol shifts the equilibrium toward the ester production following Le Chatelier's principle). The catalyst is needed in in order to obtain the conjugate acid of the alcohol which is now able to act as acid catalyst.
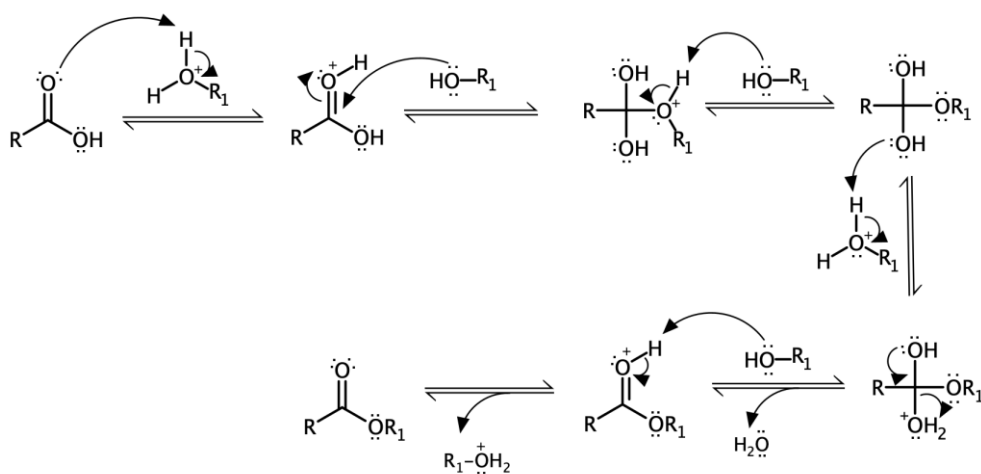
Figure 3. 36: Proposed mechanism for the esterification of carboxylic acids.

The carbonyl oxygen atom becomes protonated and so the electrophilic properties of the carbonyl carbon atom will be strongly enhanced. The alcohol can now perform a nucleophilic attack on the electrophilic specie leading to a tetrahedral carbon atom. Two proton transfer steps are followed by the elimination of a water molecule. Finally, the regeneration of the acid catalyst leads to the formation of the desired product.

In this work glycolic acid was successfully esterified using methanol or ethanol as alcohol and sulfuric acid as catalyst (Figure 3.37) leading to the formation of methyl 2-hydroxyacetate (85% yield) or ethyl 2-hydroxyacetate (65% yield). The protection of the carboxylic group of glycolic acid is critical in order to avoid its reactivity in the following steps of this synthetic path.
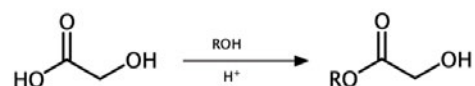
Figure 3. 37: General scheme of reaction for the esterification of glycolic acid. R= R= -CH$_3$ or -CH$_2$CH$_3$.

3.3.4.2.1.2 Tosylation of methyl 2-[(4-methylbenzenesulfonyl)oxy]acetate and ethyl 2-[(4-methylbenzenesulfonyl)oxy]acetate

The esterification of glycolic acid is followed by the tosylation of the -OH group of the previously obtained derivatives (2-[(4-methylbenzenesulfonyl)oxy]acetate and ethyl 2-[(4-methylbenzene sulfonyl)oxy]acetate). This leads to the activation of the carbon atom in alpha position which is now able to undergo the nucleophilic attack from the diamine.

In this work, methyl 2-[(4-methylbenzenesulfonyl)oxy]acetate (74% yield) and ethyl 2-[(4-methylbenzenesulfonyl)oxy]acetate (73% yield) were obtained using DMAP as catalyst and triethylamine (section 3.3.3.3; Figure 3.38).
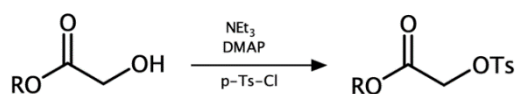
Figure 3. 38: General scheme of reaction for the tosylation of glycolic acid esters. R= R= -CH$_3$ or -CH$_2$CH$_3$.

3.3.4.2.1.3 Amine alkylation

The synthetic route considered in this work for preparing BZI-C involves the nucleophilic attack of the o-phenylenediamine on the activated alpha carbon atom of the glycolic acid ester leading to an extended alkyl-diamine (Figure 3.39).

Figure 3. 39: General scheme of reaction for the alkylation of the o-phenylenediamine. R= R= -CH$_3$ or -CH$_2$CH$_3$.

Unluckily the desired product was not isolated. The reaction was run using MeOH as solvent and TEA was used for contrasting the TsOH formation occurring in this reaction. This reaction led to the formation of 3,4-dihydroquinoxalin-2-ol (45% yield).
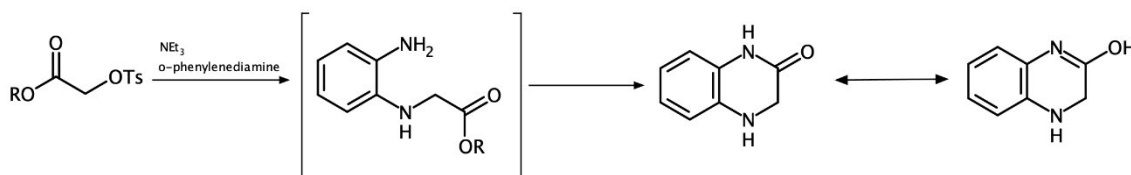
Figure 3. 40: General scheme of reaction for the formation of 3,4-dihydroquinoxalin-2-ol. R= R= -CH$_3$ or -CH$_2$CH$_3$.

The mechanism proposed in this work involves the nucleophilic attack of one of the amine group of the o-phenylenediamine on the activated carbon atom of the methyl 2-[(4-methylbenzenesulfonyl)oxy]acetate or ethyl 2-[(4-methylbenzenesulfonyl)oxy]acetate (Figure 3.41). This leads to an extended diamine as intermediates. The second amine group can now perform a intramolecular nucleophilic attack on the carbonyl-carbon atom leading to the formation of a stable 6-membered ring and leaving of alcohol.

The extended amine intermediate was not isolated as the cyclization step occurs quickly leading to an energetically favorable 6 membered ring.
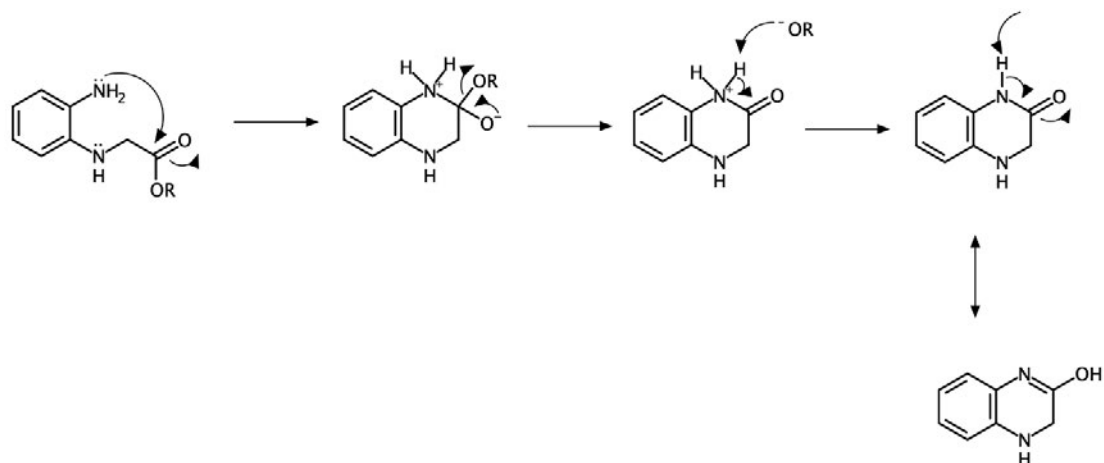
Figure 3. 41: Proposed mechanism for the formation of 3,4-dihydroquinoxalin-2-ol. R= R= -CH$_3$ or -CH$_2$CH$_3$.

The obtained 1,2,3,4-tetrahydroquinoxalin-2-one tautomerizes to the final product 3,4-dihydroquinoxalin-2-ol.

3.3.4.2.2 Synthesis of BZI-D

BZI-D has a N-acetylated ethylamine chain as extension on the N$_1$-atom of the benzimidazole nucleus. The synthetic route for preparing BZI-D considers ethanolamine as starting material (Figure 3.42).
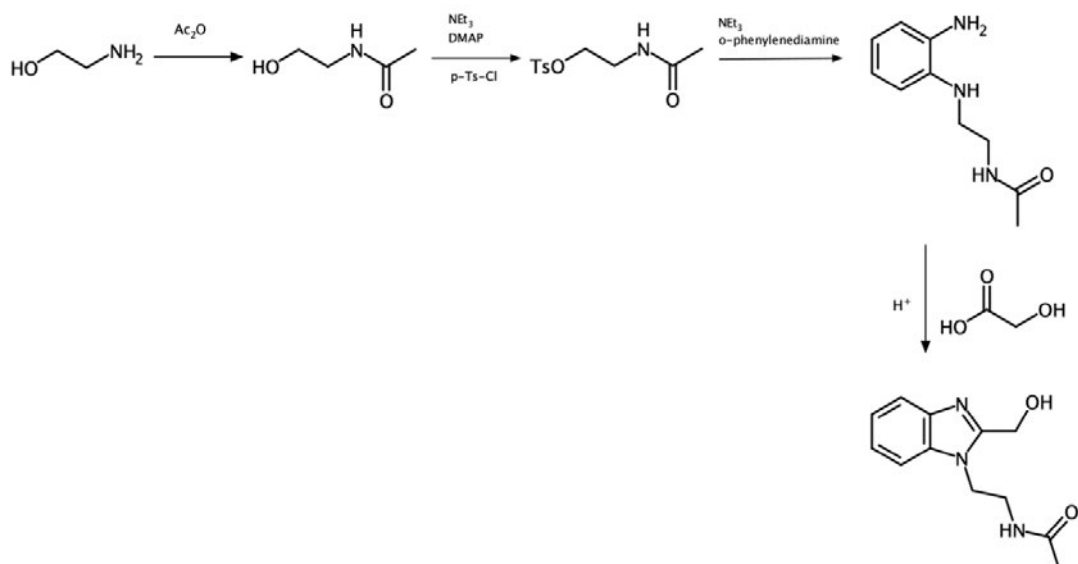
Figure 3. 42: General scheme of reaction for the synthesis of BZI-D.

Its acetylation gives N-(2-hydroxyethyl)acetamide which is then tosylated on its oxygen atom in order to activate the carbon atom. This is now ready to undergo the nucleophilic attack from the o-phenylenediamine giving the displacement of the tosyl group and an extended diamine as result. The last synthetic step involves the closure of the benzimidazole core given by the reaction of the diamine with glycolic acid.

3.3.4.2.2.1 Acetylation of ethanolamine

Ethanolamine has a 2-carbon chain connected to an amine group and a hydroxyl moiety. In order to selectively acetylate the nitrogen atom, leaving the hydroxyl group free, multiple attempts have been undertaken.

-Acetic anhydride (1.2 eq) and water as solvent at room temperature:

When an equimolar amount (1 eq or 1.2 eq) of acetic anhydride was used in presence of water, the desired product was isolated in mixture with starting material and impurities.

-Acetic anhydride (1.2 eq) and DMSO as solvent at room temperature:

Only using 1.2 eq of Acetyl-source (acetic anhydride) and DMSO as solvent, the expected product was successfully obtained giving N-(2-hydroxyethyl)acetamide with 62% yield.

3.3.4.2.2.2 Tosylation of N-(2-hydroxyethyl)acetamide

The N-acetylation of ethanolamine is followed by the tosylation of the hydroxyl group. N-(2-hydroxyethyl)acetamide was successfully tosylated leading to N-{2-[(4-methylbenzenesulfonyl) oxy]ethyl}acetamide (40% yield). The proposed mechanism for this reaction has been previously described (section 3.3.3.1).
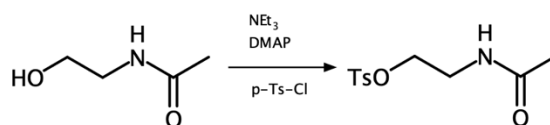
Figure 3. 43: Scheme of reaction for the formation of N-{2-[(4-methylbenzenesulfonyl) oxy]ethyl}acetamide.

3.3.4.2.2.3 Displacement of the tosyl-group

The tosyl group of the N-{2-[(4-methylbenzenesulfonyl) oxy]ethyl}acetamide should then be displaced by the nucleophilic attack of the o-phenylenediamine giving N-{2-[(2-aminophenyl)amino]ethyl}acetamide (Figure 3.44).
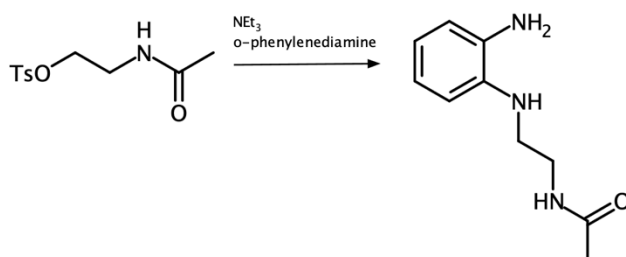
Figure 3. 44: Scheme of reaction for the predicted formation of N-{2-[(2-aminophenyl)amino]ethyl}acetamide.

The proposed mechanism of reaction is the same than section 3.3.3.4. The expected product was not isolated. The 2-aminoethyl 4-methylbenzene-1-sulfonate was instead found to be the reaction product (Figure 3.45). The HMBC showed a clear correlation between the methyl-peak and the aromatic system proving that the tosyl-group has not been displaced while the H-NMR showed the absence of the N-acetyl group. This demonstrates how, under these conditions, the o-phenylenediamine can't displace the tosyl-group. This probably due to hindrance effects of the acetylated intermediate.
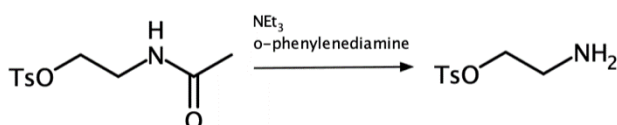
Figure 3. 45: Scheme of reaction for the formation of 2-aminoethyl 4-methylbenzene-1-sulfonate.

Although the displacement of the tosyl groups was not observed when using N-{2-[(4-methylbenzenesulfonyl) oxy]ethyl}acetamide as starting material, the intermediate obtained in the reaction (2-aminoethyl 4-methylbenzene-1-sulfonate) was used in order to force the leaving of the tosyl group and achieve the formation of the extended diamine (Figure 3.46).

Unluckily, the desired product was not isolated. Starting material was recovered from this reaction.
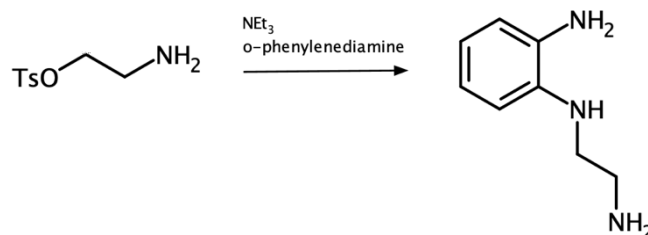
Figure 3. 46: Scheme of reaction for the attempt in forming N1-(2-aminoethyl)benzene-1,2-diamine.

The reaction was also attempted changing solvent conditions (DCM at room temperature) without observing the product formation. This leads to the inability of extending the diamine for this synthetic route and so forming BZI-E.

3.3.4.2.3 Synthesis of BZI-E

The synthetic route for preparing BZI-E considers glycerol as starting material (Figure 3.47). The protection of two hydroxyl groups of glycerol, avoiding their reactivity in the following steps, gives solketal. The tosylation of the remaining free hydroxyl group activates the carbon atom in position 1 which now can undergo the nucleophilic attack of the o-phenylenediamine leading to an alkylated diamine. The final step of this synthetic path involves the closure of the benzimidazole core and the hydrolysis of the ketal moiety. This gives an N_1-extended BZI having an alkyl chain with two free hydroxyls as final compound.
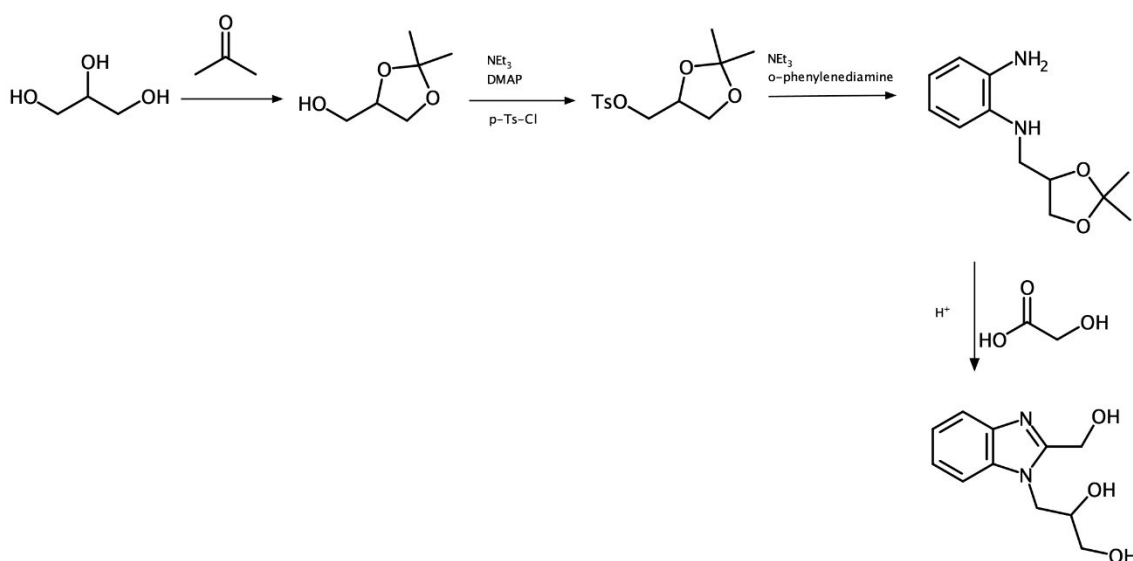
Figure 3. 47: General scheme of reaction for the synthesis of BZI-E.

3.3.4.2.3.1 Synthesis of solketal

Glycerol is given by a three carbon chain molecule having an hydroxyl group bond to each carbon atom. Solketal is an acetal compound formed when glycerol reacts with acetone (Figure 3.48).
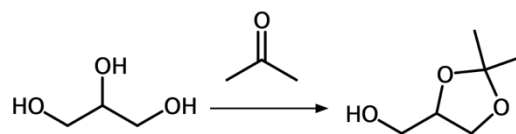
Figure 3. 48: General scheme of reaction for the formation of solketal.

Acetals are derivatives given by the condensation of two molecules of alcohol with a carbonyl compound (e.g. ketone). This reaction is usually carried out using an acid catalyst in order to activate the carbonyl carbon atom. In the first step of this reaction the oxygen atom of the carbonyl compound (acetone in this reaction) becomes protonated. This enhances the electrophilicity of the carbonyl carbon atom. The first molecule of alcohol then performs a nucleophilic attack on the electrophile species leading to a quaternary carbon atom. The following deprotonation gives hemiacetal formation and regeneration of the acid catalyst. The protonation of the alcohol group and following elimination of water gives a protonated carbonyl compound which can undergo the nucleophilic attack of the second molecule of alcohol. The last step is given by the deprotonation of this intermediate and regeneration of the acid catalyst leading to the formation of the acetal.
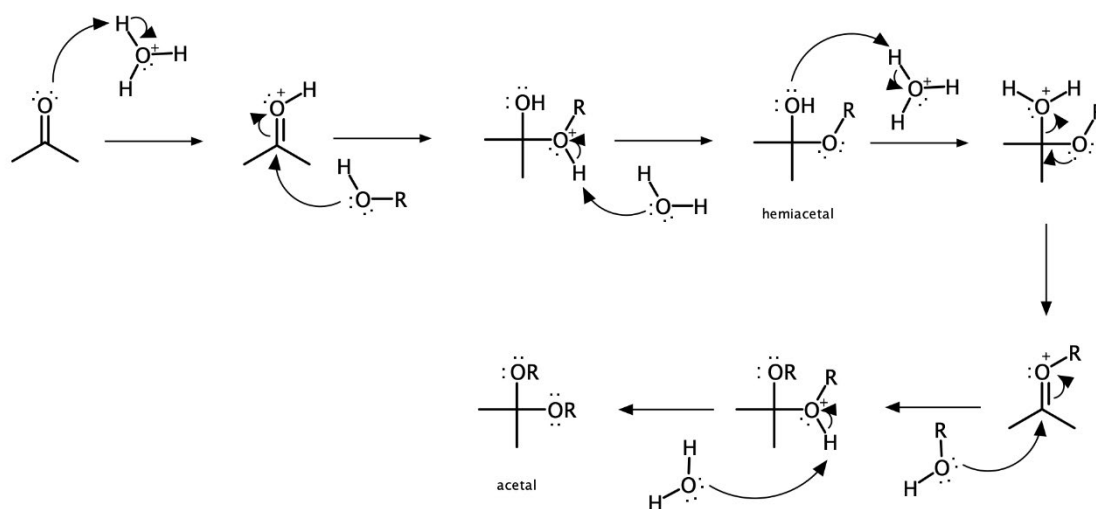
Figure 3. 49: General mechanism of reaction for the formation of acetals using acetone.

Glycerol has multiple hydroxyl groups so after the formation of the hemiacetal, the intramolecular attack of the second hydroxyl group will form a 5 membered ring generating the acetal form. Solketal formation was attempted at different temperatures (on ice, at room temperature and under reflux). The highest yield/purity was obtained when reaction was run on ice (57% yield) for 5h.
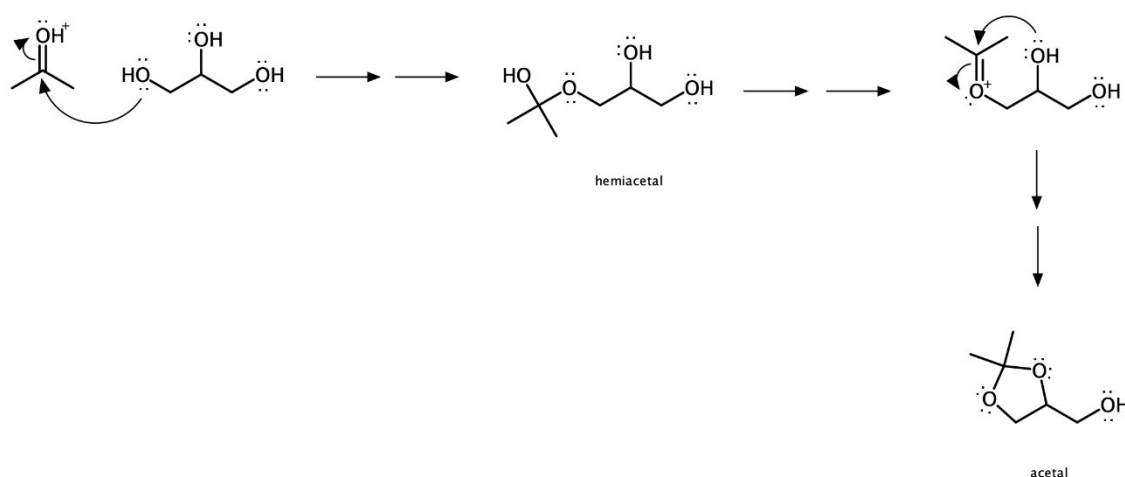
Figure 3. 50: Proposed mechanism of reaction for the formation of solketal.

3.3.4.2.3.2 Tosylation of solketal

The free hydroxyl group of solketal was successfully tosylated forming (2,2-dimethyl-1,3-dioxolan-4-yl)methyl 4-methylbenzene-1-sulfonate (55% yield). The proposed mechanisms been previously described (section 3.3.3.3).

3.3.4.2.3.3 Displacement of tosyl group from (2,2-dimethyl-1,3-dioxolan-4-yl)methyl 4-methylbenzene-1-sulfonate

The synthetic path considered for the synthesis of BZI-E involves the nucleophilic attack of the o-phenylenediamine on the activated carbon atom of (2,2-dimethyl-1,3-dioxolan-4-yl)methyl 4-methylbenzene-1-sulfonate in order to form an alkylated diamine.

The reaction was repeatedly attempted without observing the formation of the desired product. The reaction was run using the usual conditions adopted previously in this work (methanol as solvent and triethylamine for contrasting the formation of HCl occurring in the reaction). Despite the mixture was left reacting for 24h (instead of 7h) the isolation of the product was not achieved. Starting material was recovered.

This leads to the inability to proceed with the synthesis of BZI-E as the amine was not successfully extended.

3.3.5 Alkyl-benzimidazole with aromatic chain as N_1-extension

The inability to form benzimidazoles having saturated polar extension on the N_1 atom of the nucleus, led to a step back. The effect of the insertion of an aromatic moiety on the N_1 extension chain was evaluated and the synthesis of (1-benzyl-1H-1,3-benzodiazol-2-yl) methanol (BZI-9 in table1- section 2.2.1) was undertaken (Figure 3.51).
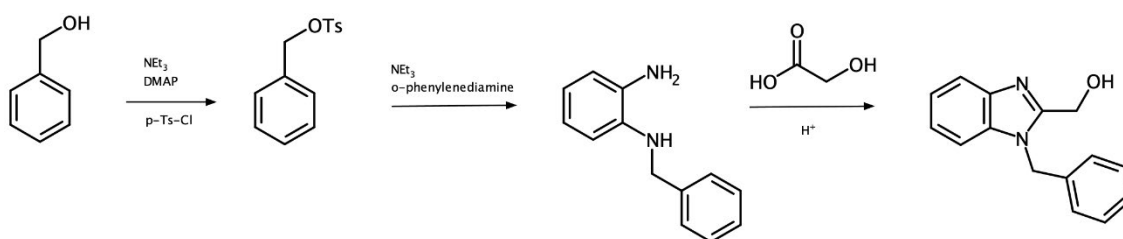
Figure 3. 51: General scheme of reactions for the synthesis of (1-benzyl-1H-1,3-benzodiazol-2-yl)methanol.

Following the synthetic strategy previously described (section 3.3.4.1), the tosylation of phenyl methanol was attempted (Figure 3.51). Surprisingly, the isolation of the expected product, benzyl 4-methylbenzene-1-sulfonate, was not observed.

It is well known that reaction of alcohols and tosyl chloride can lead to the formation of alternative products to the tosylated internediates.[224] The product formed in this reaction was (chloromethyl)benzene (85% yield).
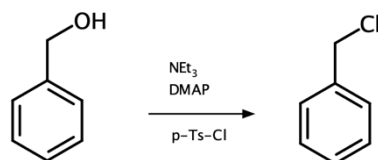
Figure 3. 52: General scheme of reaction for the synthesis of (chloromethyl)benzene.

In this reaction the p-TsCl reacts with the benzyl alcohol forming the corresponding tosylated alcohol (benzyl 4-methylbenzene-1-sulfonate) as intermediate and triethylammonium chloride (Figure 3.52). Then the chlorine ion performs a nucleophilic attack on the activated carbon atom displacing the tosyl group and forming (chloromethyl)benzene. This is due to the electron donating effect of the ring in the transition state of the reaction, which lowers the energy. This leads to the inability to isolate the tosylated intermediates as the substitution takes place quickly.
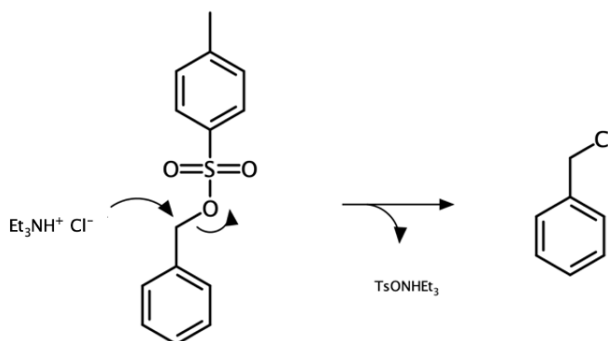
Figure 3. 53: Mechanism proposed for the formation of (chloromethyl)benzene.

The (chloromethyl)benzene obtained was reacted with o-phenylenediamine giving the formation of N1-benzylbenzene-1,2-diamine (33% yield). The reaction of the extended diamine with glycolic acid led to the formation of the desired final compound (BZI-9). The mechanism of reaction for each step of this synthetic path have been previously discussed.

The success of this synthetic path and the suitability in synthesizing N_1-benzyl benzimidazole led to possibility to go further and combine the N_1-extension with the insertion of substituents on the benzene moiety of benzimidazole. Following this synthetic strategy, the previously obtained

(chloromethyl)benzene was reacted with several 4,5-substituted diamines (Figure 3.56). This should lead to the relative alkylated amines. The following formation of the benzimidazole core should give 1,5,6-extended BZIs. Unluckily, when the (chloromethyl)benzene and substituted diamines reacted, the desired product was not isolated. Complex mixture of starting materials and impurities were recovered.
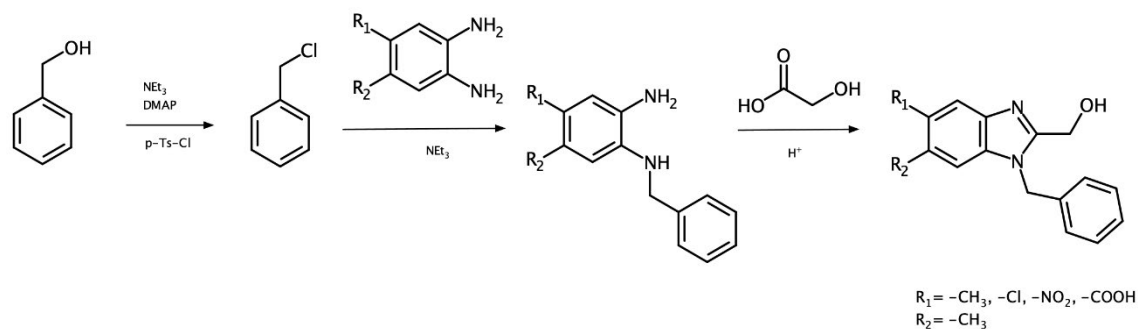
Figure 3. 54: General scheme of reactions for the synthesis of 1,5,6-extended BZIs.

3.3.6 Alternative approach for the synthesis of (1-benzyl-1H-1,3-benzodiazol-2-yl)methanol: reductive amination route

The synthesis of (1-benzyl-1H-1,3-benzodiazol-2-yl)methanol (BZI-9) has been attempted following an alternative synthetic approach (if compared to section 3.3.5) in order to establish the most suitable way to form N_1-benzyl-$C_{5,6}$-extended benzimidazoles. This synthetic path involves the reaction of substituted diamines with aldehydes leading to the formation of a Schiff base (imine). Schiff bases are compounds characterized by the double bond between a carbon and a nitrogen atom (imine). They are well known for their versatility in organic chemistry.[225]

The following reduction of the imine to the relative amine gives an alkylated substituted diamine which then can react with glycolic acid closing the benzimidazole nucleus and forming the desired products.

R$_1$= –H, –CH$_3$, –Cl, –NO$_2$, –COOH, –C$_6$H$_5$CO
R$_2$= –H, –CH$_3$
R$_3$= –H, –CH$_3$, –OH, –Br, –Cl, –F, –OCH$_3$, –NO$_2$
R$_4$= –H, –OH, –NO$_2$, –OCH$_2$CH$_3$
R$_5$= –H, –OH, –NO$_2$
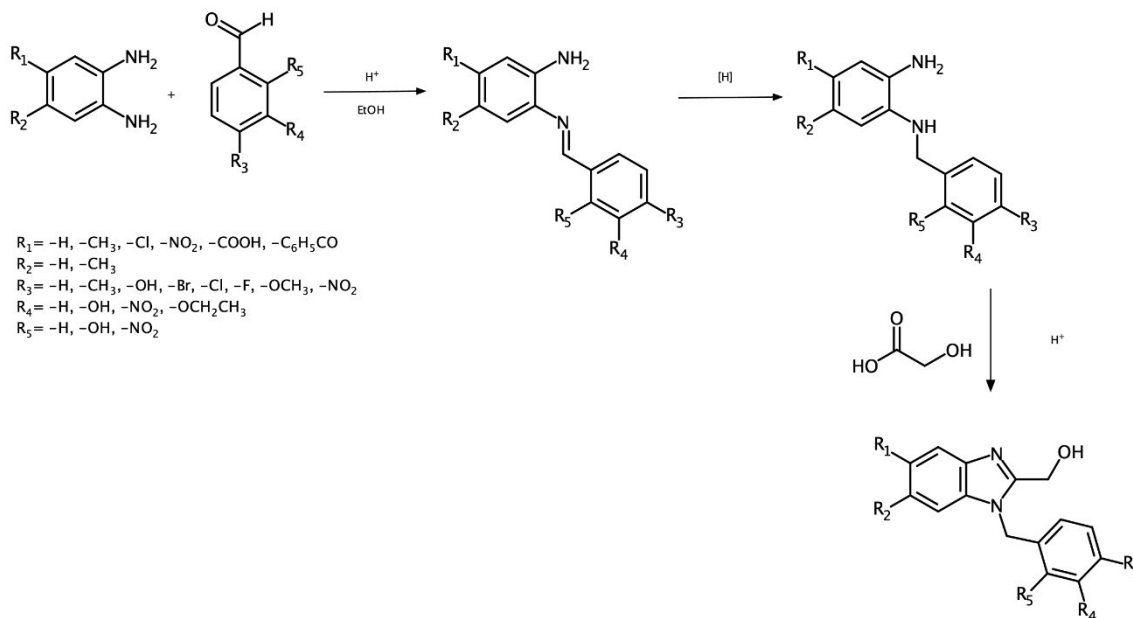
Figure 3. 55: Alternative scheme of reactions for the synthesis of 1,5,6-extended BZIs.

The suitability of this method has been tested in the lab[226] leading to the successful formation of {1-[(4-methylphenyl)methyl]-1H-1,3-benzodiazol-2-yl}methanol (R$_1$=R$_2$=R$_4$=R$_5$= -H; R$_3$= -CH$_3$). In addition, difficulties in isolating the N$_1$-alkylated final products have been encountered in the Loveridge's team when changing the substituents on the aldehyde. Thus, this work has been focused on understanding this synthetic route and the identification of an "unknown" product previously obtained. This led to the possibility to go further and investigate the effect of different substituents on the benzyl moiety as well as combine the N$_1$-extension with the insertion of substituents on the benzene ring of benzimidazole.

Following this synthetic path, in this work, several N$_1$-benzyl-C$_{5,6}$-extended benzimidazoles have been successfully synthesised.

3.3.6.1 Synthesis of Schiff base

In this work, several Schiff bases have been synthesised by reaction between an o-diamine and an aromatic aldehyde using acetic acid as catalyst (Figure 3.56).

$R_1=$ –H, –CH$_3$, –Cl, –NO$_2$, –COOH, –C$_6$H$_5$CO
$R_2=$ –H, –CH$_3$
$R_3=$ –H, –CH$_3$, –OH, –Br, –Cl, –F, –OCH$_3$, –NO$_2$
$R_4=$ –H, –OH, –NO$_2$, –OCH$_2$CH$_3$
$R_5=$ –H, –OH, –NO$_2$
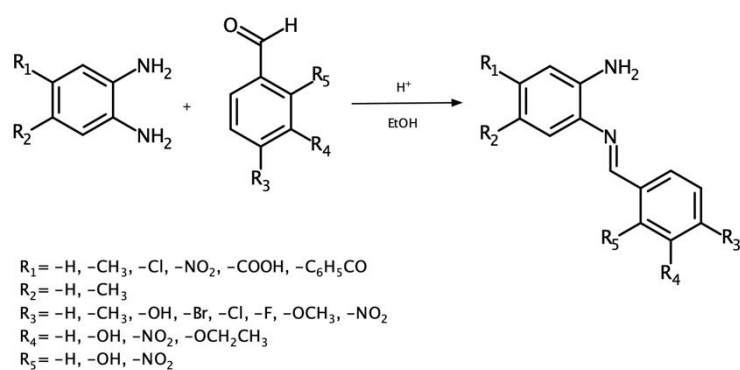
Figure 3. 56: Scheme of reaction for the synthesis of Schiff-bases.

The acid catalyst protonates the carbonyl oxygen atom of the aldehyde which then can undergo the nucleophilic attack by the diamine forming a tetrahedral carbon atom (Figure 3.57).
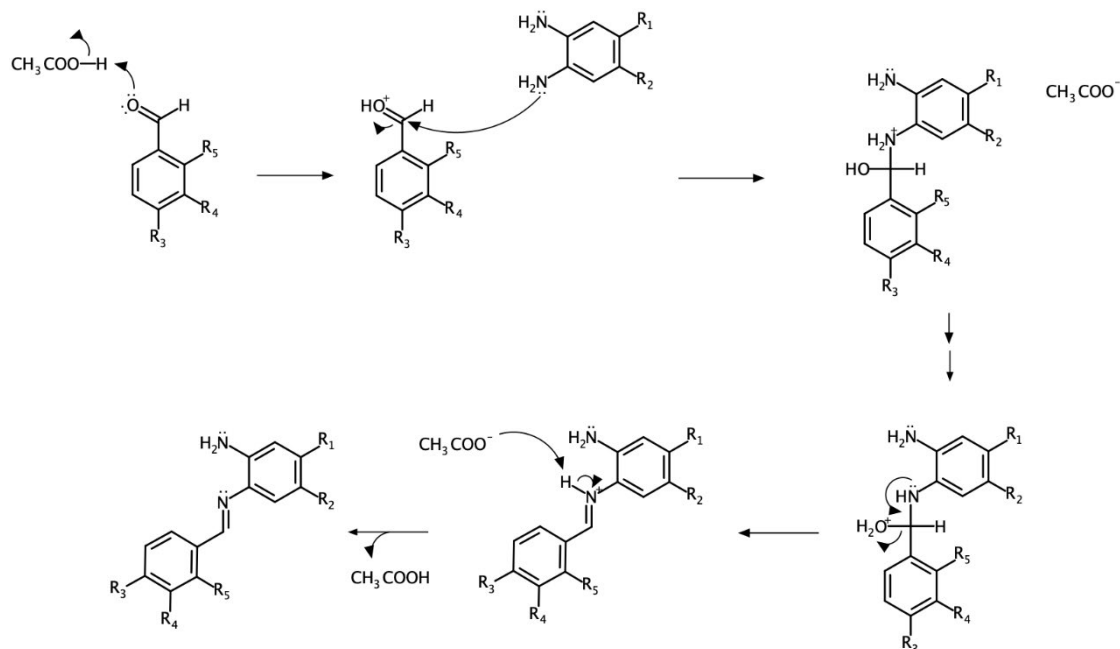
Figure 3. 57: Proposed mechanism of action for the formation of Schiff bases.

Two following steps are needed for the acetate to perform a proton exchange. The nitrogen atom of the resulting intermediate can then form a C=N double bond leading to water elimination. The regeneration of the acid catalyst gives the formation of the Schiff base.

146

Despite the Schiff bases synthesised following this synthetic strategy have been found to be a complex mixture of imine and secondary product, the crude product was used in the following steps.

3.3.6.2 Reduction of the Schiff base

A common reducing agent for imines is sodium borohydride.[227] In this work the imine reduction has been carried out refluxing the Schiff base in ethanol for 1h using sodium borohydride (1eq).

R_1 = –H, –CH$_3$, –Cl, –NO$_2$, –COOH, –C$_6$H$_5$CO
R_2 = –H, –CH$_3$
R_3 = –H, –CH$_3$, –OH, –Br, –Cl, –F, –OCH$_3$, –NO$_2$
R_4 = –H, –OH, –NO$_2$, –OCH$_2$CH$_3$
R_5 = –H, –OH, –NO$_2$
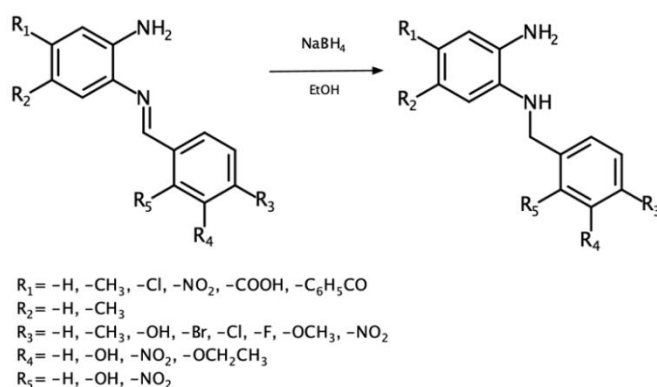
Figure 3. 58: General scheme of reaction for the reduction of imines.

The proposed mechanism of reaction for this step has previously been reported (section 3.3.2.3). The crude product isolated during this step of reaction, like the relative Schiff bases, was found to be in a complex mixture with a secondary product. Despite this, it was used, with no purification, in the subsequent steps of reactions.

3.3.6.3 Formation of the benzimidazole core

The last step of this synthetic path involves the reaction between the alkylated diamine and glycolic acid in order to close the benzimidazole nucleus forming the desired final compound. When this synthetic approach was tested in the lab several issues have been encountered. The desired product was obtained with extremely low yield or isolated in mixture with "unknown impurities".[226] In this work several efforts were undertaken in order to fully investigate this step of reaction and selectively isolate the desired product.

3.3.6.4 Competitivity in N_1 vs C_2

In this work it has been discovered that the reductive amination route generates two products which can be isolated during the last step of reaction. Once the Schiff base has been formed, the second amine group performs an intramolecular nucleophilic attack giving a stable C_2-extended benzimidazole in mix with the imine which is then reduced to the relative amine and can react with glycolic acid forming the N_1-extended benzimidazole (Figure 3.59).

$R_1 = -H, -CH_3, -Cl, -NO_2, -COOH, -C_6H_5CO$
$R_2 = -H, -CH_3$
$R_3 = -H, -CH_3, -OH, -Br, -Cl, -F, -OCH_3, -NO_2$
$R_4 = -H, -OH, -NO_2, -OCH_2CH_3$
$R_5 = -H, -OH, -NO_2$
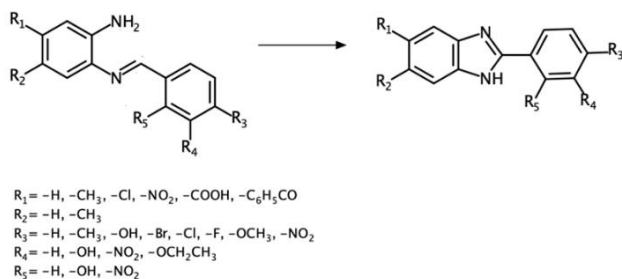
Figure 3. 59: General scheme for the formation of C_2-extended benzimidazoles from the relative imines.

This leads to the discovery of a new synthetic strategy isolating two products in one pot synthesis route (Figure 3.60). The mixture obtained at the latest step of this synthetic path was given by the N_1-extended benzimidazole (minor product) as well as C_2-extended benzimidazole (major product).

$R_1 = -H, -CH_3, -Cl, -NO_2, -COOH, -C_6H_5CO$
$R_2 = -H, -CH_3$
$R_3 = -H, -CH_3, -OH, -Br, -Cl, -F, -OCH_3, -NO_2$
$R_4 = -H, -OH, -NO_2, -OCH_2CH_3$
$R_5 = -H, -OH, -NO_2$
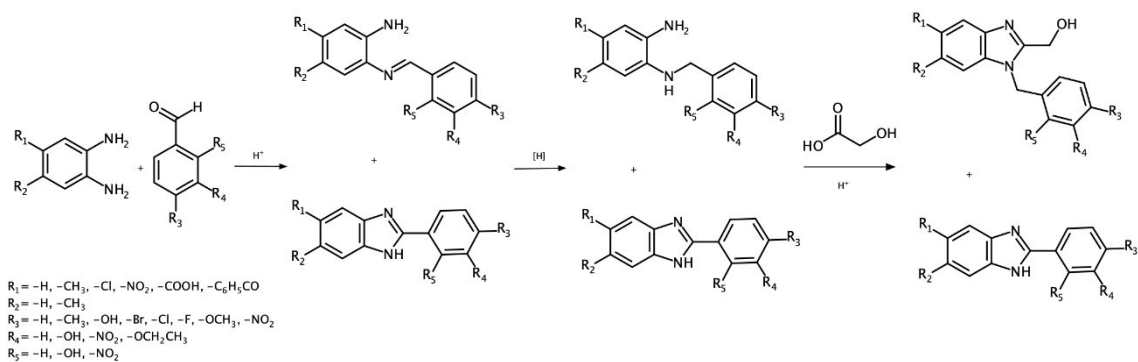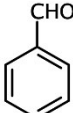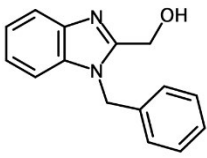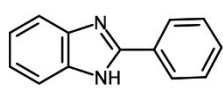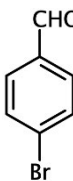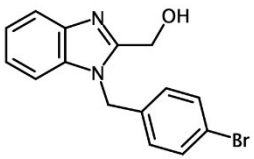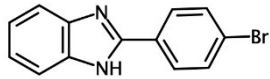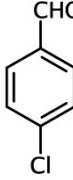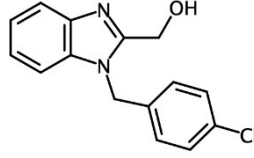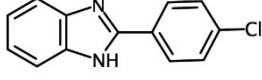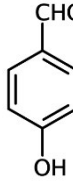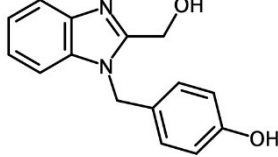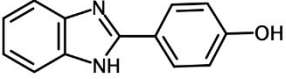
Figure 3. 60: General view of the products obtained undertaking this synthetic route.

Following this synthetic strategy, in this work, 18 further benzimidazoles have been formed. The N_1-extended benzimidazole was found in solution after 24h refluxing while the C_2-extended derivative was found as an insoluble gum at the bottom of the flask. Performing a hot filtration allowed the recovery of the N_1-BZI while the trituration of the gum using ethyl acetate/acetone or petroleum ether led to the isolation of the C_2-BZIs. Despite this success, several C_2-derivatives were soluble in these solvents and their extraction didn't lead to good yield. In this case, the gum was furtherly refluxed in 2 M HCl (24h). The following trituration in petroleum ether led to the isolation of the desired product.

The suitability for the formation of N_1 vs C_2 extended benzimidazole has been analyzed and the results reported in the following table. Generally, it has been observed a large predominance of C_2-product over N_1-product formed. This is due to the rapid cyclization of the imine to form a stable 5 membered ring and leading to the formation of the C_2-extende benzimidazole as major product.

Starting benzaldehyde	N_1-BZI / yield	C_2-BZI/ yield
	 3%	 21%
	 2%	 14%
	 3%	 51%
	 5%	 9%
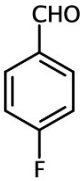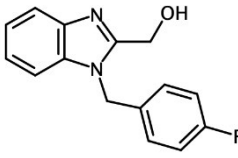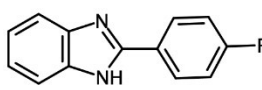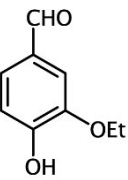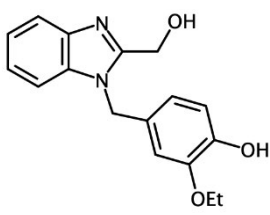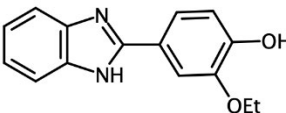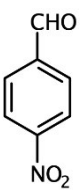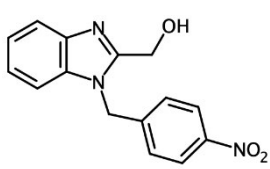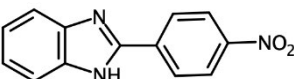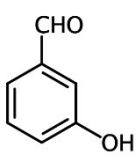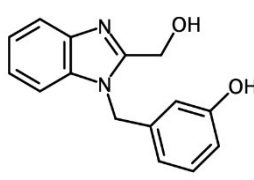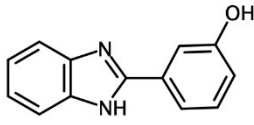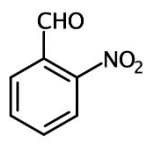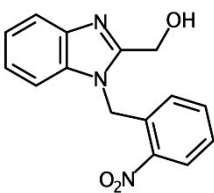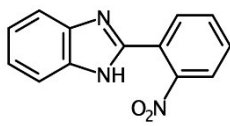
CHO, F	14%	42%
CHO, OEt, OH	1%	2%
CHO, NO$_2$	2%	8%
CHO, OH	5%	61%
CHO, NO$_2$	2%	10%

Table 3. 2: Relative yields for the 1-pot synthesis of N$_1$ vs C$_2$ extended benzimidazoles.

The substituents on the aldehyde strongly influence its reactivity. A resonance electron donor group, such as a hydroxyl- substituent, reduces the electrophilicity of the carbonyl carbon atom of the aldehyde as result of the delocalization of charge across the carbonyl group. The oxygen donates a lone pair to the aromatic ring reducing the electrophilicity of the aldehyde and generating the relative resonance forms (Figure 3.61).

This is reflected by the yields obtained. In case of a hydroxyl group is in para position, while the yields for the N_1-product are comparable ((1-benzyl-1H-1,3-benzodiazol-2-yl)methanol- 3% yield and 4-{[2-(hydroxymethyl)-1H-1,3-benzodiazol-1-yl]methyl}phenol- 5% yield), there is a large difference in the yields for the formation of the relative C_2-product (2-phenyl-1H-1,3-benzodiazole-21% yield vs 4-(1H-1,3-benzodiazol-2-yl)phenol-9% yield).
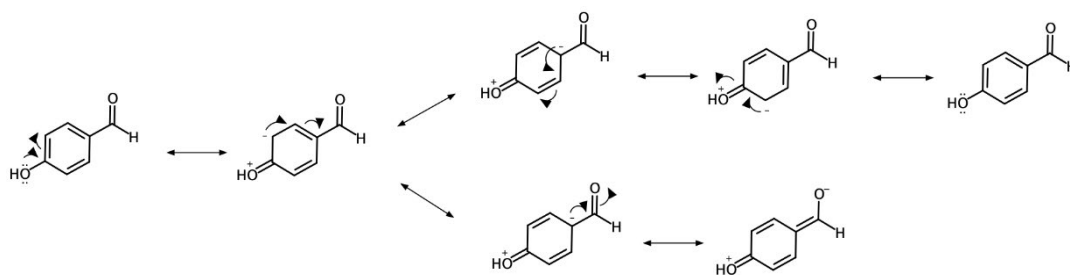
Figure 3. 61: Resonance forms for p-hydroxybenzaldehyde.

Like the hydroxyl group, halogen atoms in para position, such as chlorine, bromine or fluorine, donate electrons to the aromatic ring deactivating the aldehyde function. On the other side, fluorine, followed by chlorine and finally bromine are some of the most electronegative elements, meaning that they are strongly able to draw electron density towards themself. This will increase the electrophilicity of the aldehyde function activating it. This is reflected by the higher yields obtained for the 2-(4-fluorophenyl)-1H-1,3-benzodiazole (42% yield) and 2-(4-chlorophenyl)-1H-1,3-benzodiazole (51% yield) if compared with the (2-phenyl-1H-1,3-benzodiazole) which was obtained with 21% yield. The yields obtained for the synthesis of N_1-extended benzimidazoles also reflect this except for the bromine that gave extremely low yields for both N_1- and C_2-products, probably because the deactivating wins over the activating effects as bromine is not as electronegative as fluorine and chlorine. The 3-(1H-1,3-benzodiazol-2-yl)phenol, obtained using m-hydroxybenzaldehyde as starting material, was isolated in good yield (61%). The deactivating effect of the hydroxyl group is greater in para to the aldehyde and lesser when in meta to the aldehyde. When the hydroxyl is in meta position, the delocalization of charge is not across the carbonyl group and the angle for the nucleophilic attack performed by the o-phenylenediamine is more favorable.

Despite this synthetic route led to the preferred isolation of the C_2- over the N_1-extended product, both have been isolated in low yields and additional work will be done in future in order to optimize the reaction yields. Using more acid could lead to higher yields for the C_2-benzimidazole. Conversely the reaction could be attempted in a minimum presence of acid in order to increase the rate of N_1-product.

3.3.7 Selective formation of C_2-extended BZI: 2-phenyl- 1H-1,3-benzodiazole

The suitability of the synthesis of C_2-alkyl benzimidazoles starting from o-diamines and carboxylic acids has been previously demonstrated in this work. The (1H-1,3-benzodiazol-2-yl)methanol has been successfully synthesised from o-phenylenediamine and glycolic acid using HCl as acid catalyst .[173,174] In Loveridge's team, several attempts were undertaken in order to synthesise C_2-extended benzimidazoles using aromatic acids as starting materials without isolating the desired product.[228]

R₁= –H, –CH₃, –Cl, –NO₂
R₂= –H, –CH₃
R₃= –H, –OH
R₄= –H, –OH
R₅= –H, –OH
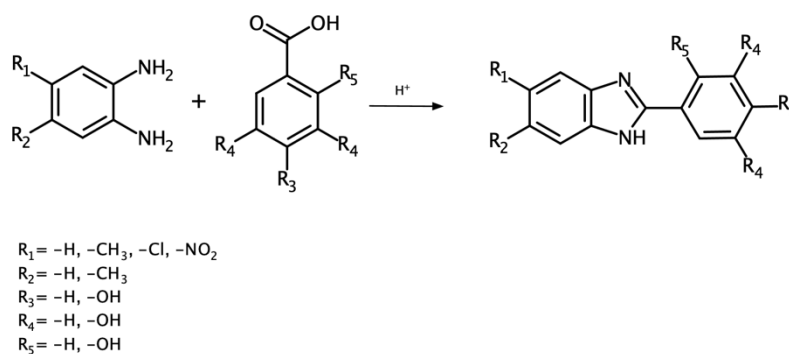
Figure 3. 62: General scheme of reaction for attempting the selective formation of C_2-phenyl-benzimidazoles using aromatic acids.

Due to the failure in forming C_2-phenyl-benzimidazoles using aromatic acids and HCl, an alternative catalyst has been considered. The reactions have been attempted using EtOH as solvent and NH₄Cl as catalyst. The mixture has been refluxed for 5h, 12h or 24h. Unluckily the desired product was not isolated and starting materials have been recovered. The inability to form the desired product using aromatic aldehydes is probably due to the withdrawal effect of

the carboxyl group. It withdraws electron from the ring becoming less electrophilic and so less reactive.

3.3.7.1 Synthesis of C_2-phenyl-benzimidazoles using aromatic aldehydes instead of acids

The selective formation of C_2-phenyl-benzimidazoles was successfully achieved in this work using aromatic aldehydes instead of acids and sodium metabisulfite ($Na_2S_2O_5$) as catalyst (Figure 3.63).[229] Using sodium metabisulfite represents a simple and efficient strategy for forming the desired products.

R_1= −H, −CH_3, −Cl, −NO_2, −COOH, C_6H_5CO, −F
R_2= −H, −CH_3
R_3= −H, −OH, −Br, −Cl, −OH, −F, −OCH_3, −NO_2
R_4= −H, −OH, −OCH_2CH_3, −NO_2
R_5= −H, −OH, −NO_2
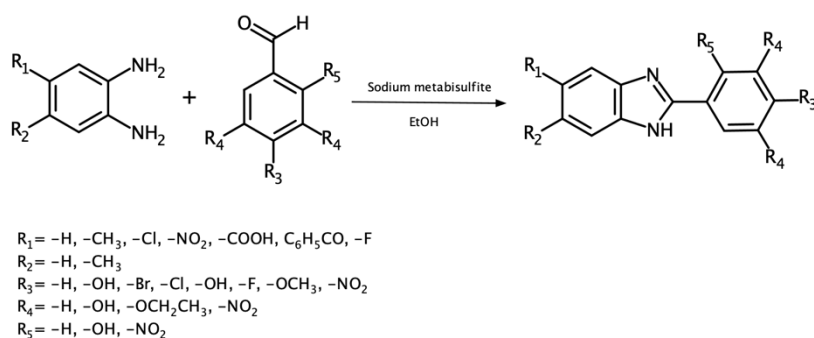
Figure 3. 63: General scheme of reaction for the selective synthesis of substituted C_2-phenyl-benzimidazoles using sodium metabisulfite as catalyst.

Following this synthetic method, 84 substituted C_2-phenyl-benzimidazoles have been synthesised in this work. The reaction has been run in ethanol for 24h and the crude products opportunely purified. The sodium metabisulfite reacts in solution forming sodium and hydrogensulfite ions which then reacts with the aldehyde leading to the formation of an aldehyde-bisulfite adduct (Figure 3.64). Sodium metabisulfite acts as activating agent in this reaction making the carbon atom of the aldehyde more electrophilic. The activated carbon atom can now undergo the nucleophilic attack by one amine group of the phenylenediamine leading to the imine formation.

The second amine group can now perform an intramolecular nucleophilic attack leading to the cyclization and the formation of a 5 membered ring. The last step involves the proton elimination giving the formation of the product.
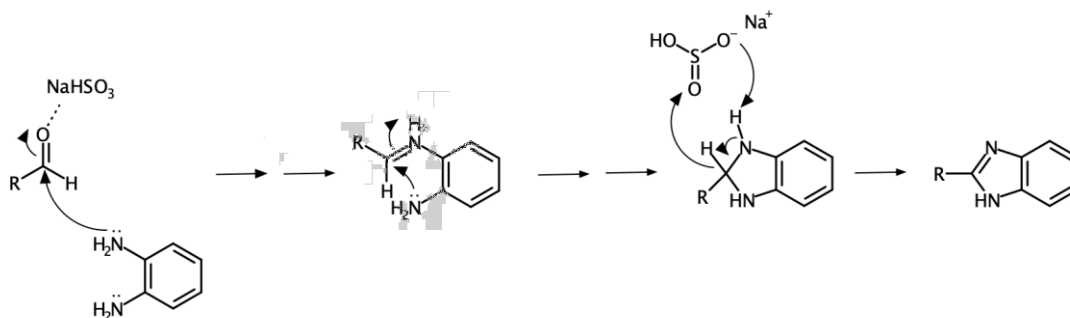
Figure 3. 64: Proposed mechanism for the formation of C_2-phenyl-benzimidazoles using sodium metabisulfite.

The C_2-extended benzimidazoles synthesised are stated in the following table with the relative yields.

Compound ID	R_1	R_2	R_3	R_4	R_5	Yield %
BZI-17	-H	-H	-H	-H	-H	55
BZI-18	-H	-H	-H	-H	-CH$_3$	40
BZI-19	-H	-H	-H	-H	-Br	75
BZI-20	-H	-H	-H	-H	-Cl	65
BZI-21	-H	-H	-H	-H	-OH	45
BZI-22	-H	-H	-H	-H	-F	55
BZI-23	-H	-H	-H	-H	-OMe	25
BZI-24	-H	-H	-H	-H	-NO$_2$	40
BZI-25	-H	-H	-H	-OH	-H	57
BZI-26	-H	-H	-H	-OEt	-OH	25
BZI-27	-H	-H	-NO$_2$	-H	-H	40
BZI-28	-H	-H	-H	- NO$_2$	-H	40
BZI-29	-H	-H	-NO$_2$	-H	-H	40
BZI-33	-CH$_3$	- CH$_3$	-H	-H	-Br	35
BZI-34	-CH$_3$	- CH$_3$	-H	-H	-Cl	60
BZI-35	-CH$_3$	- CH$_3$	-H	-H	-OH	52

BZI-36	-CH$_3$	- CH$_3$	-H	-H	-F	45
BZI-39	-CH$_3$	- CH$_3$	-H	-OH	-H	55
BZI-45	-Cl	-H	-H	-H	-H	56
BZI-46	-Cl	-H	-H	-H	- CH$_3$	47
BZI-47	-Cl	-H	-H	-H	-Br	67
BZI-48	-Cl	-H	-H	-H	-Cl	59
BZI-49	-Cl	-H	-H	-H	-OH	41
BZI-50	-Cl	-H	-H	-H	-F	62
BZI-51	-Cl	-H	-H	-H	-OMe	21
BZI-52	-Cl	-H	-H	-H	-NO$_2$	30
BZI-53	-Cl	-H	-H	-OH	-H	47
BZI-54	-Cl	-H	-H	-OEt	-OH	31
BZI-55	-Cl	-H	-H	-OEt	-OH	20
BZI-56	-Cl	-H	-H	-NO$_2$	-H	37
BZI-59	-NO$_2$	-H	-H	-H	-H	40
BZI-61	-NO$_2$	-H	-H	-H	-Br	43
BZI-62	-NO$_2$	-H	-H	-H	-Cl	56
BZI-63	-NO$_2$	-H	-H	-H	-OH	36
BZI-64	-NO$_2$	-H	-H	-H	-F	57
BZI-65	-NO$_2$	-H	-H	-H	-OMe	21
BZI-67	-NO$_2$	-H	-H	-OH	-H	37
BZI-68	-NO$_2$	-H	-H	-OEt	-OH	23
BZI-69	-NO$_2$	-H	-NO$_2$	-H	-H	20
BZI-70	-NO$_2$	-H	-H	-NO$_2$	-H	15
BZI-73	-COOH	-H	-H	-H	-H	35
BZI-75	-COOH	-H	-H	-H	-Br	45
BZI-76	-COOH	-H	-H	-H	-Cl	42
BZI-77	-COOH	-H	-H	-H	-OH	40
BZI-78	-COOH	-H	-H	-H	-F	45
BZI-79	-COOH	-H	-H	-H	-OMe	30
BZI-80	-COOH	-H	-H	-H	-NO$_2$	30
BZI-81	-COOH	-H	-H	-OH	-H	55
BZI-82	-COOH	-H	-H	-OEt	-OH	31
BZI-83	-COOH	-H	-NO$_2$	-H	-H	37
BZI-84	-COOH	-H	-H	-NO$_2$	-H	41
BZI-87	-C$_6$H$_5$CO	-H	-H	-H	-H	47
BZI-89	-C$_6$H$_5$CO	-H	-H	-H	-Br	51

BZI-90	-C$_6$H$_5$CO	-H	-H	-H	-Cl	51
BZI-91	-C$_6$H$_5$CO	-H	-H	-H	-H	49
BZI-92	-C$_6$H$_5$CO	-H	-H	-H	-F	45
BZI-93	-C$_6$H$_5$CO	-H	-H	-H	-OMe	35
BZI-94	-C$_6$H$_5$CO	-H	-H	-H	-NO$_2$	41
BZI-95	-C$_6$H$_5$CO	-H	-H	-OH	-H	39
BZI-96	-C$_6$H$_5$CO	-H	-H	-OEt	-OH	35
BZI-98	-C$_6$H$_5$CO	-H	-H	-NO$_2$	-H	41
BZI-101	-F	-H	-H	-H	-H	40
BZI-103	-F	-H	-H	-H	-Br	57
BZI-104	-F	-H	-H	-H	-Cl	50
BZI-105	-F	-H	-H	-H	-OH	59
BZI-106	-F	-H	-H	-H	-F	35
BZI-109	-F	-H	-H	-OH	-H	46

Table 3. 3: structure and relative yields for the C$_2$-extended benzimidazoles synthesized.

The desired products have been isolated in good yields following this synthetic method. As mentioned earlier (Table 3.2), the substituent on the aldehyde strongly influenced its reactivity. In fact, the 2-(4-methylphenyl)-1H-1,3-benzodiazole (40% yield) and 4-(1H-1,3-benzodiazol-2-yl)phenol (45% yield) were obtained in lower yields than the 2-phenyl-1H-1,3-benzodiazole (55% yield). Halogens in para position, due to their electronegativity, are strongly able to draw electron density towards themself increasing the electrophilicity of the aldehyde function activating it. This is reflected by the higher yields obtained for 2-(4-fluorophenyl)-1H-1,3-benzodiazole (55% yield) as well as 2-(4-bromophenyl)-1H-1,3-benzodiazole (75% yield) and 2-(4-chlorophenyl)-1H-1,3-benzodiazole (65% yield) if compared with the non substituted 2-phenyl-1H-1,3-benzodiazole (55%). For the synthesis of these analogues, several substituted o-phenylenediamine have been used as starting materials leading to 5,6-substituted-C$_2$-phenyl-benzimidazoles. Substituents on the diamine ring also influence its reactivity and so the reaction yields. Electro withdrawing groups, such as nitro- and carboxyl-, draw electron density out of the π system. This creates electron deficiency on the aromatic ring making the amine less nucleophilic (Figure 3.65).

A carboxyl- group in para of the amine function strongly deactivate its nucleophilicity as its lone pair is delocalized on the aromatic ring due to resonance and it is not available to attack the aldehyde.
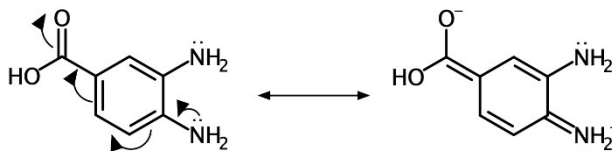
Figure 3. 65: 4-carboxyl-phenylenediamine lone pair delocalization on the aromatic ring.

This is reflected by the yields obtained. The 5-carboxy- and 5-nitro analogues were generally isolated in lower yields if compared to the non substituted 2-phenyl-1H-1,3-benzodiazole. The benzophenone group has the same deactivating effect than the carboxyl as result of the resonance. The nitro deactivating effect, combined with the low reactivity of the p-methoxybenzaldehyde, gave a 2-(4-methoxyphenyl)-5-nitro-1H-1,3-benzodiazole isolated in low yield (21% yield). The methoxy substituents have an electron donating effect due to their lone pairs resonating with the delocalized aromatic system deactivating the aldehyde function in para position.

3.3.8 Alternative C_2-extended benzimidazoles

Following the synthetic strategy previously adopted (section 3.3.7.1), alternative C_2-extensions have been inserted in the benzimidazole nucleus. Using alternative aldehydes (1H-pyrrole and thiophene-2-carbaldehyde) and sodium metabisulfite as catalyst, further benzimidazole analogues have been synthesized (Figure 3.67).

R$_1$= –H, –CH$_3$, –Cl, –NO$_2$, –COOH, C$_6$H$_5$CO, –F
R$_2$= –H, –CH$_3$
X= –NH, –S
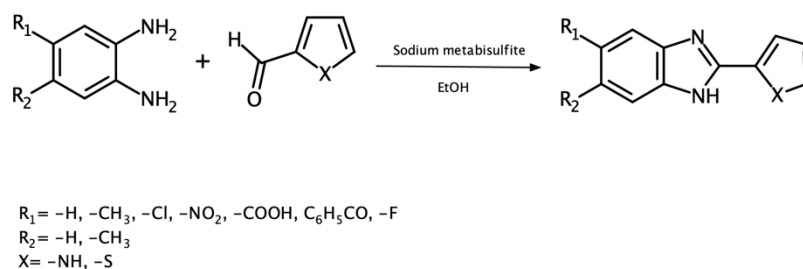
Figure 3. 66: General scheme of reaction for the selective synthesis of substituted C_2-phenyl-benzimidazoles using sodium metabisulfite as catalyst.

157

2-(thiophen-2-yl)-1H-1,3-benzodiazole (81% yield) and 2-(1H-pyrrol-2-yl)-1H-1,3-benzodiazole (80% yield) were isolated in extremely good yield. This is explained by the structural properties of the starting material. Substituents on the o-phenylenediamine slightly affect the reactivity.
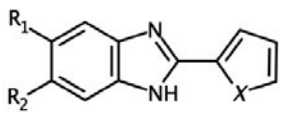
Compound ID	R_1	R_2	X	Yield %
BZI-29	-H	-H	-S	81
BZI-30	-H	-H	-NH	80
BZI-57	-Cl	-H	-S	53
BZI-58	-Cl	-H	-NH	71
BZI-72	-NO$_2$	-H	-NH	59
BZI-85	-COOH	-H	-S	55
BZI-86	-COOH	-H	-NH	59
BZI-99	-C$_6$H$_5$CO	-H	-S	51
BZI-100	-C$_6$H$_5$CO	-H	-NH	65
BZI-114	-F	-H	-NH	58

Table 3. 4: structure and relative yields for further C$_2$-extended benzimidazoles synthesized.

The analogues bearing a chlorine, fluorine, nitro or benzophenone group have been isolated in lower yields if compared to the non substituted 2-(thiophen-2-yl)-1H-1,3-benzodiazole and 2-(1H-pyrrol-2-yl)-1H-1,3-benzodiazole. The analogues bearing a pyrrol- substituent in position 2 of the benzimidazole core have been isolated in higher yields than the derivatives bearing a thiophen- ring (except BZI-29 and BZI-30). This can be explained by the higher electronegativity of the nitrogen atom which is able to pull electron cloud towards itself in a stronger way enhancing the electrophilicity of the aldehyde function.

3.3.9 Bis-benzimidazoles

Bis benzimidazole are compounds given by connection of two BZI nuclei. They can be connected in different position of the core. In this work, multiple 2,6-bis benzimidazoles have been successfully synthesised (Figure 3. 68; synthetic approach in 3.3.7.1).

$R_1 = -H, -Cl, -COOH$
$R_2 = -H$
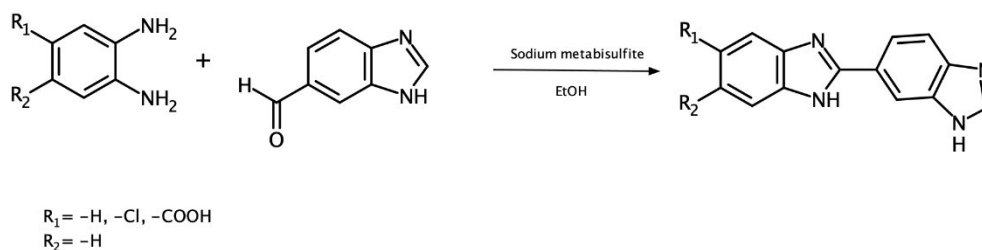
Figure 3. 67: General scheme of reaction for the synthesis of bis-benzimidazoles.

Compound ID	R$_1$	R$_2$	Yield %
BZI-117	-Cl	-H	45
BZI-119	-COOH	-H	37

Table 3. 5: structure and relative yields for the bis-benzimidazoles synthesized.

The bis-benzimidazoles were isolated in good yields. The 2-(1H-1,3-benzodiazol-6-yl)-5-chloro-1H-1,3-benzodiazole was isolated in higher yield (45%) than the analogue 2-(1H-1,3-benzodiazol-6-yl)-1H-1,3-benzodiazole-5-carboxylic acid (37%). This is due to the deactivating effect of the carboxyl- group pf the o-diamine which reduces the nucleophilicity of the amine group in para position, as previously explained (Figure 3.65).

3.3.10 Hybrid derivatives: 2-(1H-indol-3-yl)-1H-1,3-benzodiazoles

Based on the results obtained in this work, a further category of benzimidazoles have been designed. This group of derivatives is given by the connection of a benzimidazole nucleus and an indole core. Using the substituted o-diamines and substituted 1H-indole-3-carbaldehydes, 21 hybrid derivatives have been synthesised in the Loveridge's group.[230]

R_1= –H, –CH$_3$, –Cl, –NO$_2$, –COOH, –C$_6$H$_5$CO, –F
R_2= –H, CH$_3$
R_3= –H, –Br
R_4= –H, –Cl
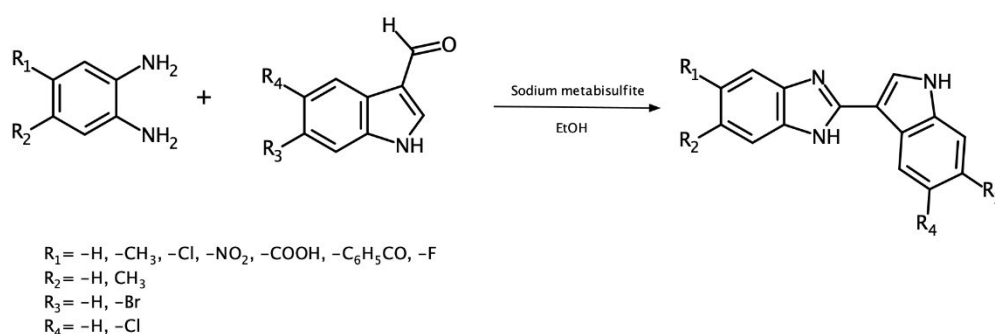
Figure 3. 68: General scheme of reaction for the synthesis of 2-(1H-indol-3-yl)-1H-1,3-benzodiazoles.

Compound ID	R_1	R_2	R_3	R_4	Yield %
HY-1	-H	-H	-H	-Cl	80
HY-2	-H	-H	-H	-H	89
HY-3	-H	-H	-Br	-H	84
HY-5	-Cl	-H	-H	-Cl	80
HY-6	-Cl	-H	-Br	-H	92
HY-7	-Cl	-H	-H	-H	91
HY-8	-C₆H₅CO	-H	-H	-H	87
HY-9	-C₆H₅CO	-H	-H	-Cl	80
HY-10	-C₆H₅CO	-H	-Br	-H	82
HY-11	-F	-H	-H	-H	93
HY-12	-F	-H	-H	-Cl	84

HY-13	-F	-H	-Br	-H	87
HY-14	-COOH	-H	-H	-H	quantitative
HY-15	-COOH	-H	-H	-Cl	86
HY-16	-COOH	-H	-Br	-H	81
HY-17	-NO$_2$	-H	-H	-H	89
HY-18	-NO$_2$	-H	-H	-Cl	69
HY-19	-NO$_2$	-H	-Br	-H	quantitative
HY-20	-CH$_3$	-CH$_3$	-H	-H	80
HY-21	-CH$_3$	-CH$_3$	-Br	-H	85
HY-22	-CH$_3$	-CH$_3$	-H	-Cl	80

Table 3. 6: structure and relative yields for the indole-benzimidazole hybrids synthesized.

The hybrid analogues were isolated in extremely good yields. The substituents on the o-phenylenediamine or on the 1H-indole-3-carbaldehydes do not strongly influence the yields of reaction. The 2-(1H-indol-3-yl)-1H-1,3-benzodiazoles were obtained in higher yields if compared to the relative C$_2$-extended analogues synthesised using different aldehydes. Surprisingly the results obtained in this work identify the 1H-indole-3-carbaldehydes as the more reacting starting materials with a general product yield range between 69 and 93%. The 1H-pyrrole and thiophene-2-carbaldehyde follow in the list with a product yield range of 65-81%. The starting material giving the lowest range of yield seem to be the benzaldehyde with a product range yield of 15-75 %. the presence of heteroatoms in the aldehyde rings could slightly have a opposite effect, pulling away the cloud of electrons from the aldehyde leading to its activation. Conversely the more electron rich aldehydes, such as1H-indole-3-carbaldehydes, should decrease the reactivity of the starting material by mesomeric effect. Despite this, the yields of reactions obtained show that more electron rich aldehydes are able to generate products with the higher yields.
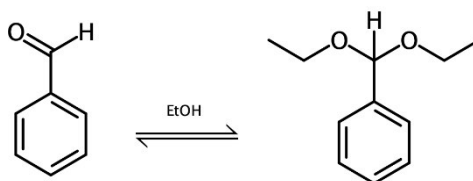
Figure 3. 69: equilibrium between benzaldehyde and its acetal analogue in ethanol.

This could be explained by the equilibrium created when the aldehydes are in ethanol, the reaction solvent. Aldehydes in ethanol can be in equilibrium with their relative acetal form.[231] Electron pour aldehydes, such as benzaldehyde, are more likely to be present in the acetal form. This means that, once in ethanol, some of the aldehyde is converted into the acetal form and is not available for the nucleophilic attack performed by the o-phenylenediamine. This explains the lower yields obtained when electron pour aldehydes are used as starting materials. In case of electron rich aldehydes, the equilibrium is more driven towards the aldehyde form giving more starting material available for the nucleophilic attack of the diamine leading so to higher yields of reaction.

3.3.11 Alternative benzimidazole derivatives

Previous works have investigated the suitability of the synthesis of (1H-1,3-benzodiazol-2-yl)methanol. In this work has been studied the effect of substituents on the benzene ring of benzimidazole derivatives. In this work the two extensions have been combined. A short research project in the team led to the synthesis of (5,6-dimethyl-1H-1,3-benzodiazol-2-yl)methanol as well as (5-substituted-1H-1,3-benzodiazol-2-yl)methanol.[232]

3.3.11.1 Substituents on the benzene ring of (1H-1,3-benzodiazol-2-yl) methanol

Based on the success achieved in the Loveridge's team, in this work further 5,6-substituted-2-hydroxymethyl benzimidazoles have been successfully synthesised in order to complete the set of BZIs designed. Starting from substituted amines and glycolic acid, several benzimidazole derivatives have been successfully obtained (Figure 3.70).
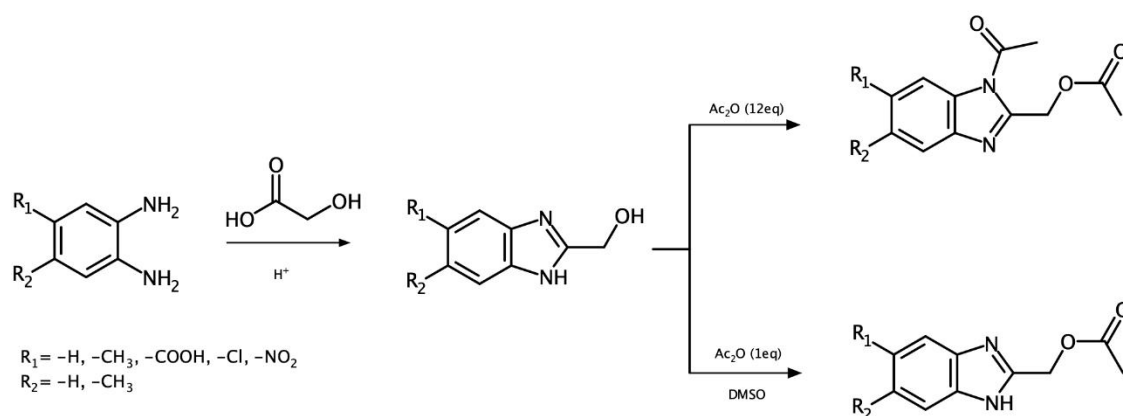
Figure 3. 70: General scheme of reaction for the synthesis of 5,6-substituted-2-hydroxymethyl benzimidazole and relative mono- and di-acetylation.
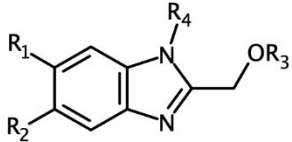
Compound ID	R_1	R_2	R_3	R_4	Yield %
BZI-1	-H	-H	-H	-H	83
BZI-2	-CH$_3$	-CH$_3$	-H	-H	95
BZI-3	-Cl	-H	-H	-H	70
BZI-4	-NO$_2$	-H	-H	-H	95
BZI-5	-COOH	-H	-H	-H	91
BZI-6	-C$_6$H$_5$CO	-H	-H	-H	40
BZI-122	-H	-H	-CH$_3$CO	-CH$_3$CO	53
BZI-129	-H	-H	-CH$_3$CO	-H	46
BZI-132	-NO$_2$	-H	-CH$_3$CO	-H	45
BZI-131	-Cl	-H	-CH$_3$CO	-H	51
BZI-123	-CH$_3$	-CH$_3$	-CH$_3$CO	-CH$_3$CO	41
BZI-124	-Cl	-H	-CH$_3$CO	-CH$_3$CO	55

Table 3. 7: structure and relative yields for the 2-hydroxymethyl-benzimidazole and relative acetylated analogues synthesized.

Due to the activity of (1-acetyl-1H-1,3-benzodiazol-2-yl)methyl acetate, obtained in the previous works,[174] the substituted benzimidazoles have been mono or double acetylated in order to investigate the suitability of this route and set future plans.

3.4 Conclusion

Overall, this work provides optimal strategies for extending the benzimidazole nucleus leading to the synthesis of 150 compounds. The results obtained in previous works[174] have been used in order to develop the synthesis of multiple benzimidazole-based compounds. Several attempts for N-alkylating the benzimidazole core after the closure of the imidazole ring have failed. A different strategy has been developed in order to be able to extend the BZI core on its nitrogen N_1 atom. This work evidences that alkylating the o-diamine and then closing the benzimidazole core represents the best synthetic strategy for achieving the synthesis of N-substituted derivatives. This has been obtained using several alcohols as starting materials. The tosylation

of alcohols followed by the nucleophilic attack of the o-phenylenediamine led to the displacement of tosyl-group forming the desired alkylated amine which them formed the benzimidazole core by reacting with glycolic acid. Unluckily the poor yield in the amine alkylation led to the necessity of finding an alternative synthetic route. A reductive amination route led to the isolation of the desired N_1-alkylated BZIs as minor product. This route gave the formation of 2 products-in-1-pot. The major product of this reaction is the C_2-extended benzimidazole formed by cyclization of the imine intermediate. The N_1/C_2 competition has been deeply analysed in this work and several derivatives successfully synthesised. Unluckily the two products are formed in low yields and additional work will be done in future in order to optimize the yields. A suitable synthetic method for the selective formation of C_2-exteneded benzimidazoles, using sodium metabisulfite as catalyst, have also been identified leading to the synthesis of several derivatives. Based on this approach bis-benzimidazoles have also been obtained. This led the way to a further class of compounds given by the connection of a benzimidazole core and an indole ring (hybrids). Substituents on the benzene ring of the BZI core have also been considered.

Chapter 4

Biological assays

4. Biological assays

The compounds synthesised in this work were screened against bacterial cultures and parasites in order to investigate their antimicrobial effect.

4.1 Antibacterial assay: disk diffusion assay

The antibacterial activity of the benzimidazoles obtained in this work was investigated by performing a disk diffusion assay, also known as agar test,[233] with *E. coli* JM109, a K12 strain bacterium that provides minimized recombination and aids in plasmid stability, as the target bacterium. Bacterial cultures were incubated in a rich culture medium on solid agar. Agar forms a supporting structure and it is composed of agarose (a linear polysaccharide) and a mixture of agaropectins. The benzimidazoles were applied on a disk of filter paper which was then added to the agar plate containing the bacterial culture. In case of positive result (antibacterial activity), a clear inhibition zone was observed around the filter disk where the compound was applied, which indicates that bacteria were unable to grow in this zone. DMSO, used for dissolving the benzimidazoles, was applied on the filter paper and tested in order to demonstrated its negative effect on bacteria while ampicillin was used as positive control.

Benzimidazoles were initially tested at high concentration (30 mg ml^{-1}). Several compounds were found to be active against *E. coli* JM109 (Figure 4.1A-B). The compounds giving the largest inhibition zone were selected as hits (Figure 4.1) and tested at lower concentrations (Figure 4.1-C; Table 4.1).

BZI-21 and BZI-22 as well as BZI-72 (50 in fig) are only active at high concentration (30 mg ml^{-1}). BZI-30 (27 in fig), BZI-58 (39 in fig), BZI-144 (96 in fig) as well as BZI-105 (92 in fig), BZI-122 and BZI-132 were active at all concentrations tested. BZI-144 (96 in Figure 4.1) showed the strongest activity against *E. coli* JM109. At high concentration (30 mg ml^{-1}), its inhibition zone was larger than the inhibition zone of ampicillin and it was still active at the same concentration as ampicillin (3 mg ml^{-1}) (Figure 4.1-C; Table 4.1).

On the contrary BZI-131 has been found to be active at higher concentrations, but its effect was lost at the lowest concentration (3 mg ml^{-1}).
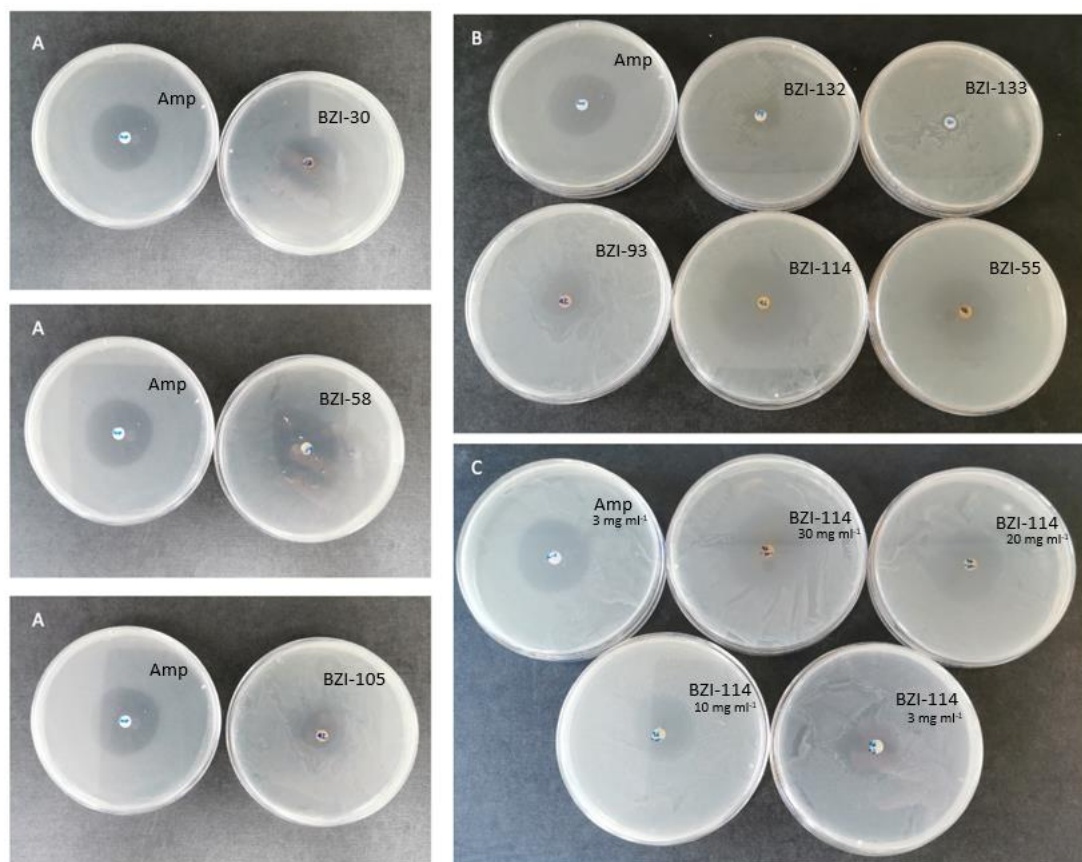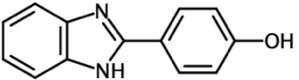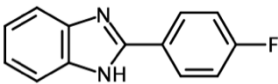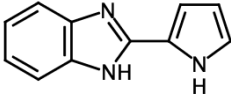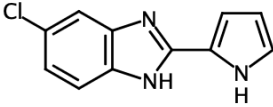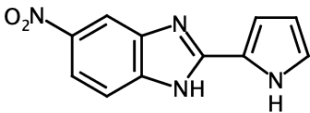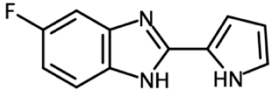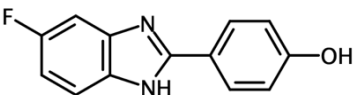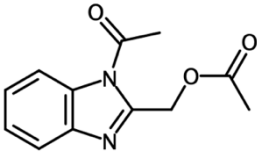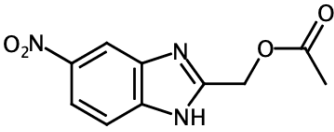
Figure 4. 1: Disk diffusion assays of *E. coli* JM109 with the hit benzimidazoles: A-B: tested at 30 mg ml^{-1}; C-tested at 30 mg ml^{-1}, 20 mg ml^{-1}, 10 mg ml^{-1} and 3 mg ml^{-1}. The numbers in the figure refer to an early numbering system of the benzimidazoles synthesised (the current numbers are shown in black).

Compound ID	Structure	BZI-IZ diameter (30 mg ml^{-1})	BZI-IZ diameter (20 mg ml^{-1})	BZI-IZ diameter (10 mg ml^{-1})	BZI-IZ diameter (3 mg ml^{-1})	Amp-IZ diameter (3 mg ml^{-1})
BZI-21		12 ± 1 mm	X	X	X	30 ± 0 mm

167

BZI-22		11 ± 1 mm	X	X	X	30 ± 0 mm
BZI-30		27 ± 2 mm	26 ± 2 mm	22 ± 1 mm	10 ± 0 mm	30 ± 0 mm
BZI-58		32 ± 1 mm	32 ± 1 mm	23 ± 1 mm	10 ± 0 mm	30 ± 0 mm
BZI-72		12 ± 1 mm	12 ± 1 mm	10 ± 1 mm	7 ± 1 mm	30 ± 0 mm
BZI-114		36 ± 1 mm	30 ± 0 mm	25 ± 0 mm	23 ± 1 mm	30 ± 0 mm
BZI-105		14 ± 1 mm	11 ± 1 mm	10 ± 0 mm	10 ± 0 mm	30 ± 0 mm
BZI-122		10 ± 0 mm	9 ± 0 mm	8 ± 0 mm	8 ± 0 mm	30 ± 0 mm
BZI-132		12 ± 0 mm	10 ± 0 mm	9 ± 0 mm	9 ± 0 mm	30 ± 0 mm

168
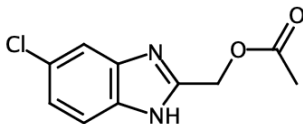
BZI-131		10 ± 0 mm	10 ± 0 mm	7 ± 0 mm	X	30 ± 0 mm

Table 4. 1: Inhibition zones (IZ) for *E. coli* JM109 treated with the hit benzimidazoles at different concentrations. Amp IZ= 30 ± 0 mm. "X" indicates no visible inhibition zone.

The benzimidazoles were also tested in combination with ampicillin in order to investigate potential synergistic effect and verify if the benzimidazoles can enhance the activity of the β-lactam antibiotic. Several active and inactive benzimidazoles have been found to enhance the activity of the β-lactam antibiotic (Figure 4.2).
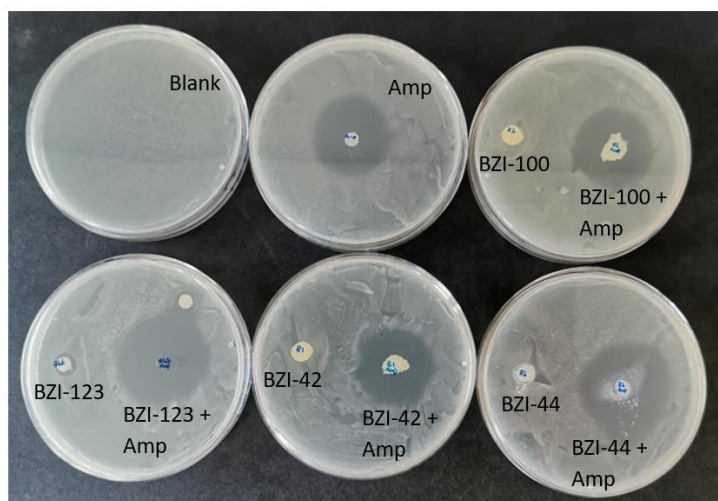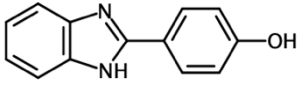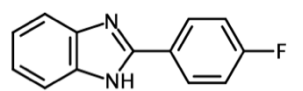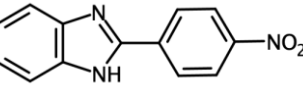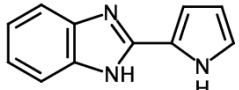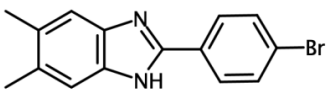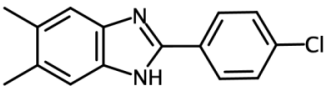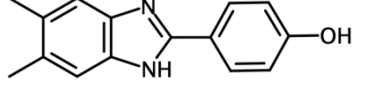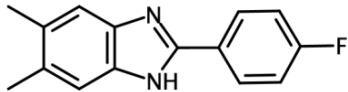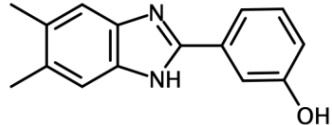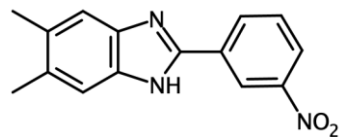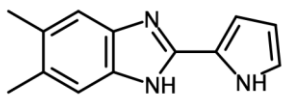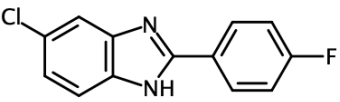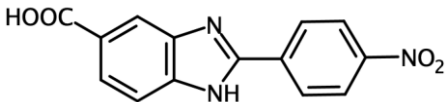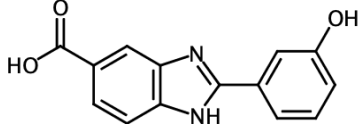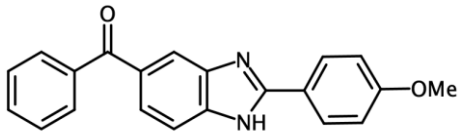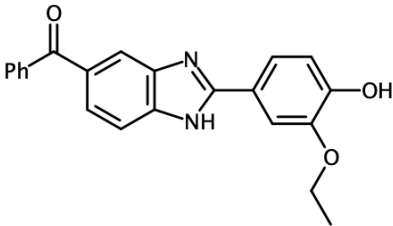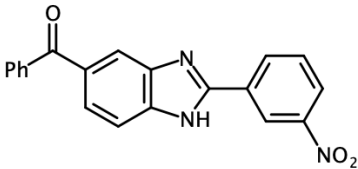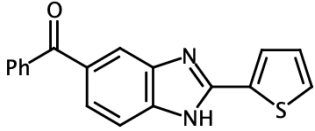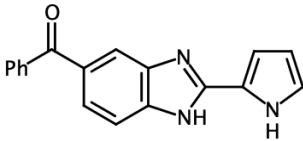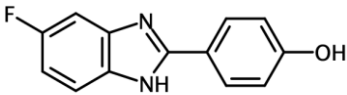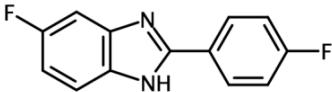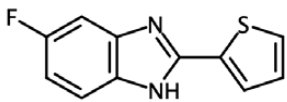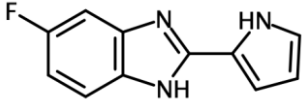
Figure 4. 2: Disk diffusion assays of *E. coli* JM109 with the hit benzimidazoles (at 30 mg ml^{-1}) in combination with ampicillin (3 mg ml^{-1}). The numbers in the picture refers to an early numbering system of the benzimidazoles synthesised (the current numbers are shown in black).

BZI-123 did not show remarkable activity when tested alone on the plate but It showed the greatest activity when in combination with ampicillin. BZI-131 gave good inhibition zones when tested alone but this was enhanced in combination with ampicillin. On the contrary, BZI-114 showed essentially the same inhibition zone regardless of the presence of ampicillin. Despite giving no inhibition zone against *E. coli* JM109 when applied alone, several inactive benzimidazoles (at 30 mg ml^{-1}) were able to increase the diameter of the inhibition zone when tested on the same filter paper as ampicillin, giving a synergistic effect. BZI-105 and BZI-40 gave

the best results when in combination with ampicillin, but BZI-34, -44, -100, -106 and -129 also showed a remarkable synergistic effect.

Compound ID	Structure	IZ-diameter (30mg/ml)	IZ-diameter (30mg/ml) + Amp (3 mg ml^{-1})	Amp-IZ diameter (3 mg ml^{-1})
BZI-21		12 ± 1 mm	37 ± 1 mm	30 ± 0 mm
BZI-22		11 ± 1 mm	38 ± 3 mm	30 ± 0 mm
BZI-24		X	35 ± 0 mm	30 ± 0 mm
BZI-30		27 ± 2 mm	35 ± 3 mm	30 ± 0 mm
BZI-33		X	34 ± 0 mm	30 ± 0 mm
BZI-34		X	39 ± 0 mm	30 ± 0 mm
BZI-35		X	37 ± 0 mm	30 ± 0 mm

BZI-36		X	35 ± 0 mm	30 ± 0 mm
BZI-39		X	40 ± 0 mm	30 ± 0 mm
BZI-42		X	36 ± 2 mm	30 ± 0 mm
BZI-44		X	38 ± 0 mm	30 ± 0 mm
BZI-50		X	36 ± 0 mm	30 ± 0 mm
BZI-80		X	35 ± 0 mm	30 ± 0 mm
BZI-81		X	36 ± 2 mm	30 ± 0 mm
BZI-93		X	32 ± 0 mm	30 ± 0 mm

BZI-96		10 ± 2 mm	38 ± 2 mm	30 ± 0 mm
BZI-98		X	35 ± 2 mm	30 ± 0 mm
BZI-99		X	34 ± 2 mm	30 ± 0 mm
BZI-100		X	39 ± 2 mm	30 ± 0 mm
BZI-105		X	43 ± 3 mm	30 ± 0 mm
BZI-106		X	38 ± 0 mm	30 ± 0 mm
BZI-113		X	35 ± 1 mm	30 ± 0 mm
BZI-114		36 ± 1 mm	37 ± 1 mm	30 ± 0 mm
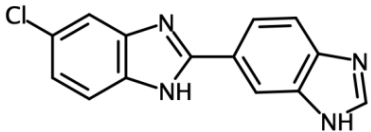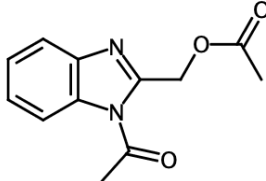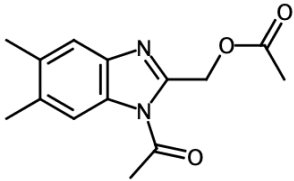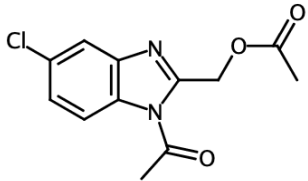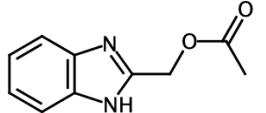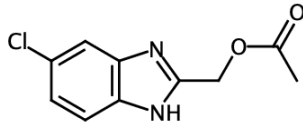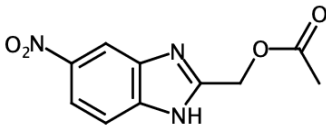
BZI-117		10 ± 0 mm	34 ± 1 mm	30 ± 0 mm
BZI-122		16 ± 1 mm	37 ± 2 mm	30 ± 0 mm
BZI-123		8 ± 1 mm	43 ± 1 mm	30 ± 0 mm
BZI-124		X	32 ± 1 mm	30 ± 0 mm
BZI-129		X	36 ± 3 mm	30 ± 0 mm
BZI-131		20 ± 0 mm	42 ± 1 mm	30 ± 0 mm
BZI-132		16 ± 1 mm	40 ± 0 mm	30 ± 0 mm

Table 4. 2: Inhibition zones (IZ) for *E. coli* JM109 treated with benzimidazoles (30 mg ml^{-1}) in combination with ampicillin (IZ 30 ± 0 mm). "X" indicates no visible inhibition zone.

Further investigation on their synergistic effect will be undertaken in future works in order to identify the mechanism behind their effect and whether they target lytic transglycosylases or this was a chance discovery. The inhibition of Slt35 will be investigated performing a turbidometric assay of Hash as a substrate as previously reported.[234] Turbidity measures the decrease of light transmitted intensity by the effect of particles suspended in solvent. The Hash assay can be used to monitor the time course of peptidoglycan solubilisation when the enzyme is added to the reaction mixture. This leads to the determination of the lytic activity of Slt35. This assay will be critical for determining whether the compounds synthesised in this work are able to inhibit Slt35 or target a different pathway. The compounds synthesised in this work will be tested at different concentrations by the Loveridge's team. In case Slt35 of inhibition, the IC_{50}, the concentration of inhibitor required to reduce the enzyme activity by 50%, will be determined. Running this assay involves protein purification processes and access to adequate labs and resources that it was not possible to obtain in this work (due to COVID pandemic).

The 2-(1H-indol-3-yl)-1H-1,3-benzimidazoles, hybrid (HY) molecules designed in this work and synthesised in a small research project,[230] have also been tested against *E. coli* JM109. HY-2 has been found to be active at high concentration (30 mg ml^{-1}) and a dose-related disk diffusion assay has been undertaken.
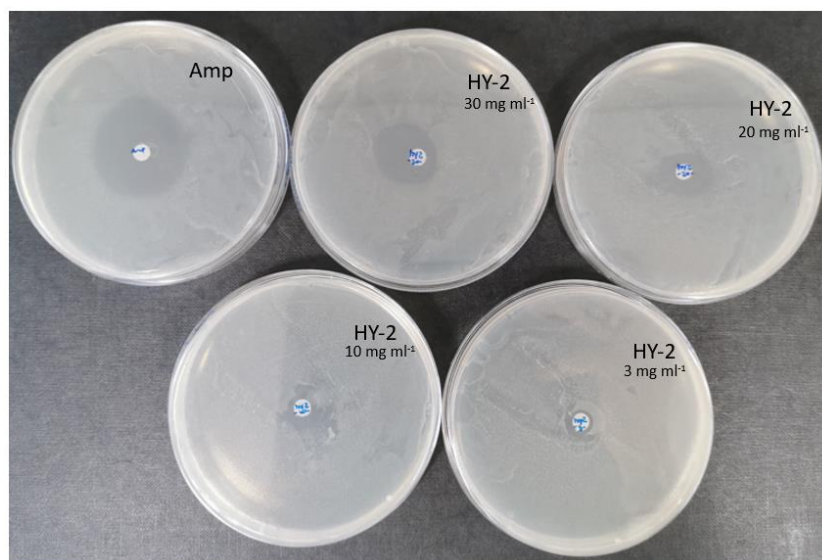
Figure 4. 3: Disk diffusion assays of *E. coli* JM109 treated with HY-2 at 30 mg ml^{-1}, 20 mg ml^{-1}, 10 mg ml^{-1} and 3 mg ml^{-1}.

HY-2 is active at all concentrations tested. At high concentration (30 mg ml^{-1}), Hy-2 has a smaller inhibition zone than the IZ$_{Amp}$. Its activity (IZ) decreases at lower concentration but HY-2 is still active at the same concentration as ampicillin (3 mg ml^{-1}).
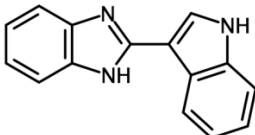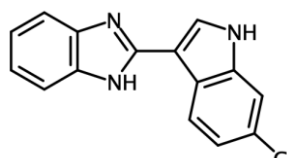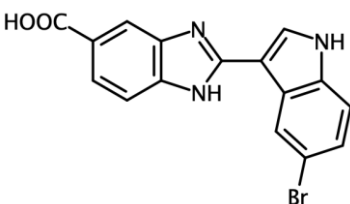
Compound ID	Structure	IZ diameter (30 mg ml^{-1})	IZ diameter (20 mg ml^{-1})	IZ diameter (10 mg ml^{-1})	IZ diameter (3 mg ml^{-1})
HY-2		12 ± 1 mm	10 ± 1 mm	9 ± 1 mm	7 ± 1 mm

Table 4. 3: Inhibition zones (IZ) for *E. coli* JM109 with HY-2 at different concentrations. Amp IZ=30 ± 0 mm. "X" indicates no visible inhibition zone.

Although HY-2 showed activity when tested alone on the plate, it didn't show a synergistic effect when tested in combination with ampicillin. On the contrary, HY-16, -17, -21 and -22 didn't show any activity when alone but they have been found to slightly enhance the effect of ampicillin on *E. coli* JM109. The greatest result has been obtained with HY-22 + Amp.

Compound ID	Structure	IZ diameter (30 mg ml^{-1})	IZ diameter (30 mg ml^{-1}) + Amp (3 mg ml^{-1})	Amp-IZ diameter (3 mg ml^{-1})
HY-1		X	36 ± 1 mm	30 ± 0 mm
HY-16		X	35 ± 2 mm	30 ± 0 mm
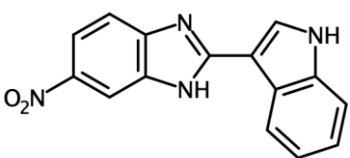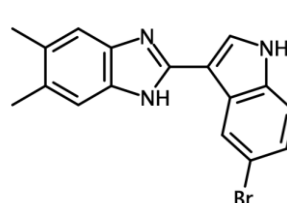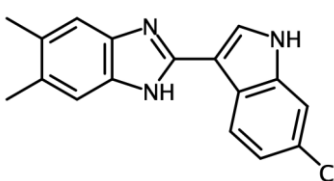
HY-17		X	36 ± 1 mm	30 ± 0 mm
HY-21		X	36 ± 1 mm	30 ± 0 mm
HY-22		X	37 ± 1 mm	30 ± 0 mm

Table 4. 4: Inhibition zones (IZ) for *E. coli* JM109 with the inactive HY (30 mg ml^{-1}) in combination with ampicillin (3 mg ml^{-}1; IZ 30 ± 0 mm). The diameter of the IZs is reported in mm. "X" indicates missing activity.

4.1.1 Minimum inhibitory concentrations

A minimum inhibitory concentration (MIC) assay was run for the hit compounds (benzimidazoles synthesised in this work as well as hybrid molecules) in order to identify the minimum concentration for their antimicrobial activity. MIC correspond to the lowest concentration of active compound leading to inhibition of bacterial growth.[235]

The active benzimidazoles, as well as HY-2, were tested at different concentrations. Ampicillin was used as the positive control.
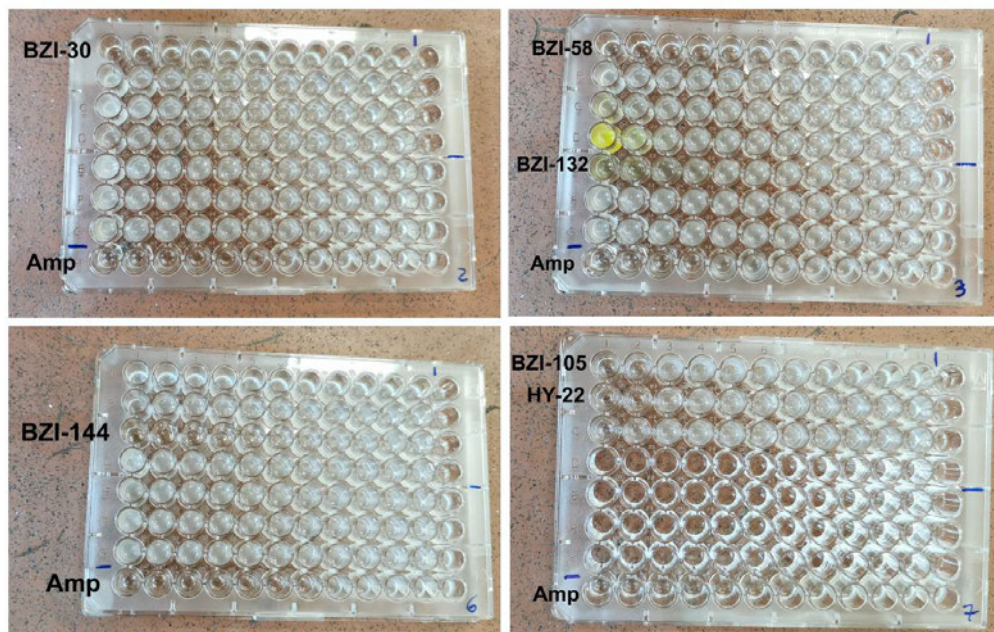
Figure 4. 4: MIC assay of hit benzimidazoles tested at different concentrations against *E. coli* JM109. The active compounds are labelled in green.

BZI-58 has been found to have the same MIC as the positive control, ampicillin, showing a value of 8 µg/ml. It represents a promising drug-like candidate with an activity comparable to the known β-lactam antibiotic. Other benzimidazoles were found to have lower activity (Table 5).

Compound ID	MIC / µg ml^{-1}
Amp	2
BZI-30	64
BZI-58	8
BZI-132	64
BZI-144	32
BZI-105	128
HY-2	128
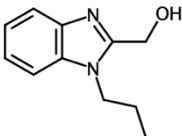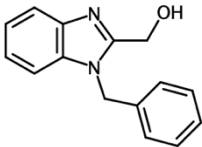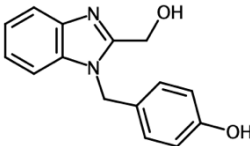
Table 4. 5: MIC values (in µg ml^{-1}) of the hit benzimidazoles against *E. coli* JM109.
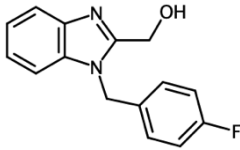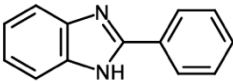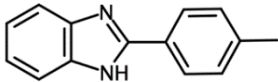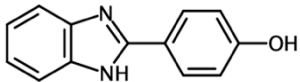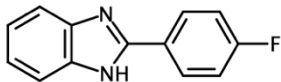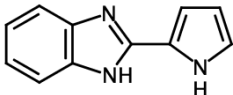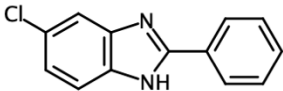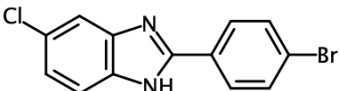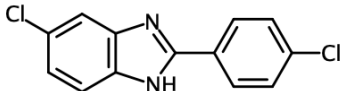
4.2 Further investigations on antimicrobial activity
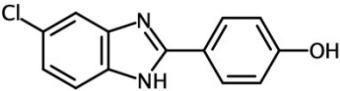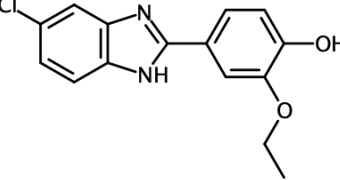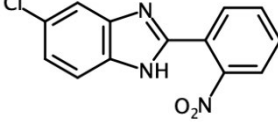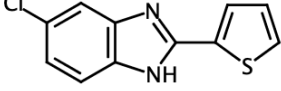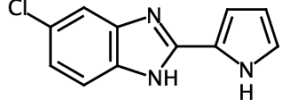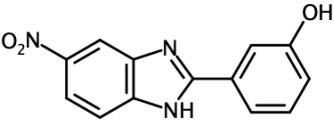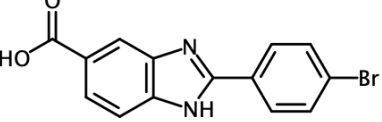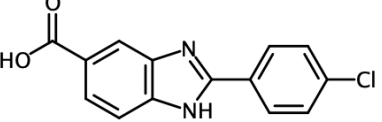
Space and resource limitations led to the inability to test the compounds synthesised in this work against different species of bacteria or investigate their activity against alternative microbes. Thus the benzimidazole- and hybrid-based compounds have been sent to collaborators in order to investigate their spectrum of activity.
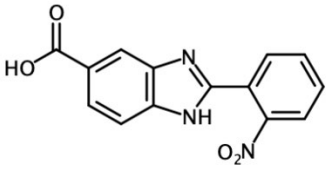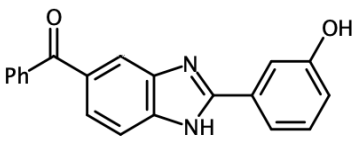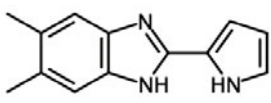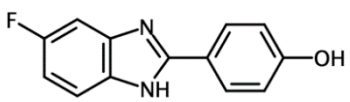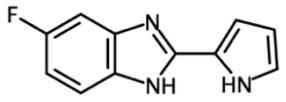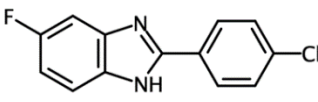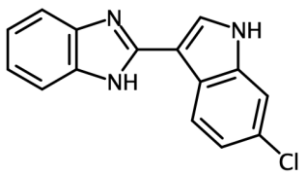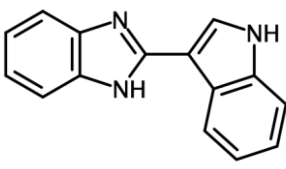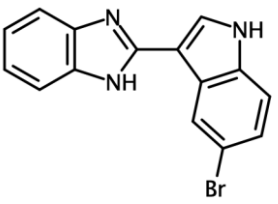
4.2.1 Antibacterial
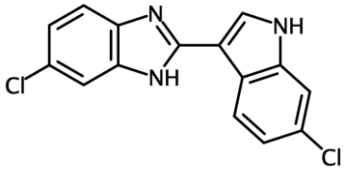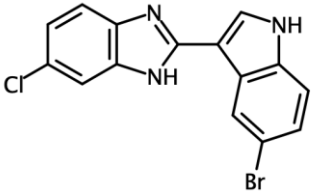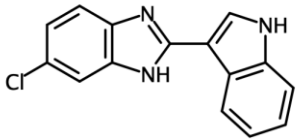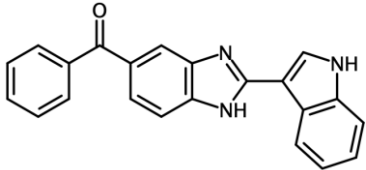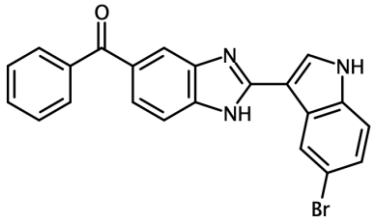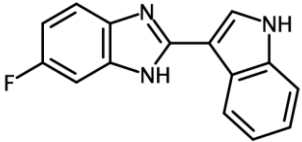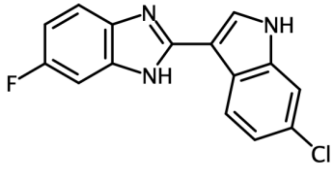
Benzimidazoles and hybrids were screened against a further strain of *E. coli* (ATCC 35218) as well as *Staphylococcus aureus* (NCTC 6571) and *Pseudomonas aeruginosa* (NCTC 950), in the group of Dr Suzy Moody at Kingston University. The antimicrobial activity was investigated performing a disk diffusion assay (as in section 3.1).[233] The molecules showing the greatest inhibition zones were selected and labelled as hits (Table 4.6).
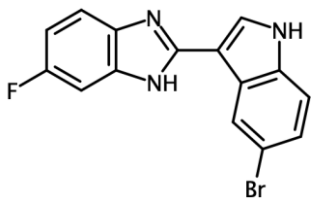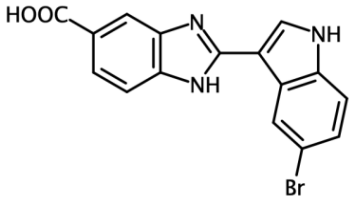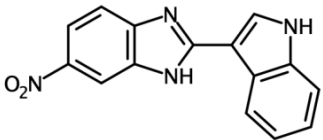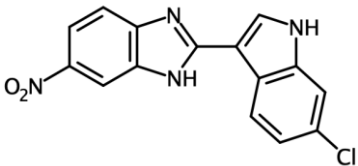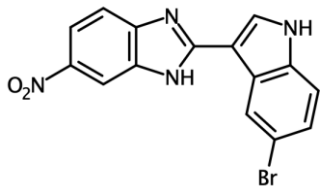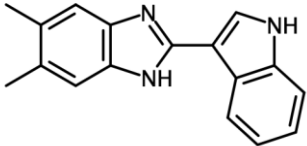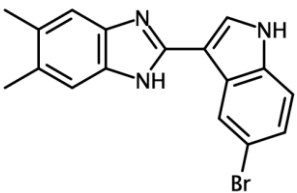
Compound ID	Structure	*E. coli* ATCC 35218	*S. aureus* NCTC 6571	*P. aeruginosa* NCTC 950
BZI-7		X	X	11 ± 1 mm
BZI-9		X	X	15 ± 4 mm
BZI-12		X	X	8 ± 1 mm

BZI-13		X	X	11 ± 1 mm
BZI-17		X	7 ± 1 mm	X
BZI-18		7 ± 1 mm	7 ± 1 mm	X
BZI-21		X	X	10 ± 1 mm
BZI-22		8 ± 1 mm	8 ± 1 mm	11 ± 1 mm
BZI-30		23 ± 1 mm	X	X
BZI-45		8 ± 1 mm	8 ± 1 mm	10 ± 1 mm
BZI-47		X	X	8 ± 1 mm
BZI-48		X	X	9 ± 1 mm

BZI-49		9 ± 1 mm	8 ± 1 mm	9 ± 1 mm
BZI-54		X	8 ± 1 mm	9 ± 1 mm
BZI-55		X	7 ± 1 mm	9 ± 1 mm
BZI-57		X	7 ± 1 mm	X
BZI-58		22 ± 1 mm	9 ± 1 mm	20 ± 1 mm
BZI-67		X	X	14 ± 1 mm
BZI-75		8 ± 1 mm	X	X
BZI-76		8 ± 1 mm	X	8 ± 1 mm

BZI-83		X	X	8 ± 1 mm
BZI-95		X	X	9 ± 1 mm
BZI-44		X	X	13 ± 1 mm
BZI-105		X	X	11 ± 1 mm
BZI-114		16 ± 1 mm	X	9 ± 1 mm
BZI-104		X	X	10 ± 1 mm
HY-1		11 ± 1 mm	X	18 ± 1 mm
HY-2		X	X	13 ± 1 mm
HY-3		10 ± 1 mm	X	18 ± 1 mm

HY-5		X	X	17 ± 1 mm
HY-6		X	X	20 ± 1 mm
HY-7		X	X	19 ± 1 mm
HY-8		X	X	12 ± 1 mm
HY-10		X	X	11 ± 1 mm
HY-11		X	X	16 ± 1 mm
HY-12		X	X	19 ± 1 mm

HY-13		X	X	21 ± 1 mm
HY-16		X	X	7 ± 1 mm
HY-17		X	X	14 ± 1 mm
HY-18		X	X	11 ± 1 mm
HY-19		X	X	15 ± 1 mm
HY-20		X	X	15 ± 1 mm
HY-21		X	X	12 ± 1 mm
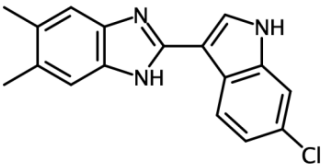
| HY-22 | | X | X | 12 ± 0 mm |

Table 4. 6: Inhibition zones (IZ) for three bacterial strains with the hit benzimidazoles and hybrid compounds (at 10 mg ml⁻¹). IZ for positive controls: ciprofloxacin (10 µg) IZ 34 ± 1 mm; gentamicin (10 µg) IZ 20 ± 0 mm; cefuroxime (30 µg) IZ 25 ± 2 mm; piperacillin/tazobactam IZ 38 ± 0 mm. "X" indicates no visible inhibition zone.

BZI-30 has been found to be the best drug-like candidate against *E. coli* ATCC 35218, but it is not active against *S. aureus* or *P. aeruginosa*. BZI-58 represents one of the best antimicrobial candidates. It is able to inhibit all the microbes included in this study. It is strongly active against *E.coli* (ATCC 35218) (IZ= 22 ± 1 mm) and *P. aeruginosa* (IZ= 20 ± 1 mm). It also inhibits *S.aureus* with an inhibition zone of 9 ± 1 mm, the best inhibition against this bacterium. The greatest antimicrobial effect was observed against *P. aeruginosa*. Several benzimidazoles and the majority of the hybrid compounds were found to inhibit *P. aeruginosa*. BZI-58 showed the greatest activity of the benzimidazoles, while HY-13 and HY-6 represent the best hybrid candidates. HY-1, -3, -7 and -19 also showed activity against *P. aeruginosa*.

4.2.2 Antiparasitics

The benzimidazole and hybrid compounds were tested against *Schistosoma mansoni* in the group of Prof Karl Hoffmann at Aberystwyth University using the Roboworm platform,[236] an automated imaging platform, in order to investigate their activity against parasitic worms.[237,238] Compounds' effects on *Schistosoma mansoni* are detected in terms of motility disturbance (such as paralysis) as well as morphological changes (such as shrinkage).

Each compound (provided as 10 mM DMSO stock solutions) was screened in S. mansoni larvae at both 50 and 10 µM concentration. Auranofin (AUR) and praziquantel (PZQ) were used as positive controls while DMSO was the negative control. Several benzimidazoles and hybrid compounds, such as BZI-47, -48, -62, -87, -95 and -96, as well as HY-7 and -22, showed an effect

on phenotype and motility at 50 µM (Fig4.5). The phenotype score measures how closely the treated larvae morphology resembles the healthy controls of *S. mansoni*, while the motility score measures changes in parasite mobility.
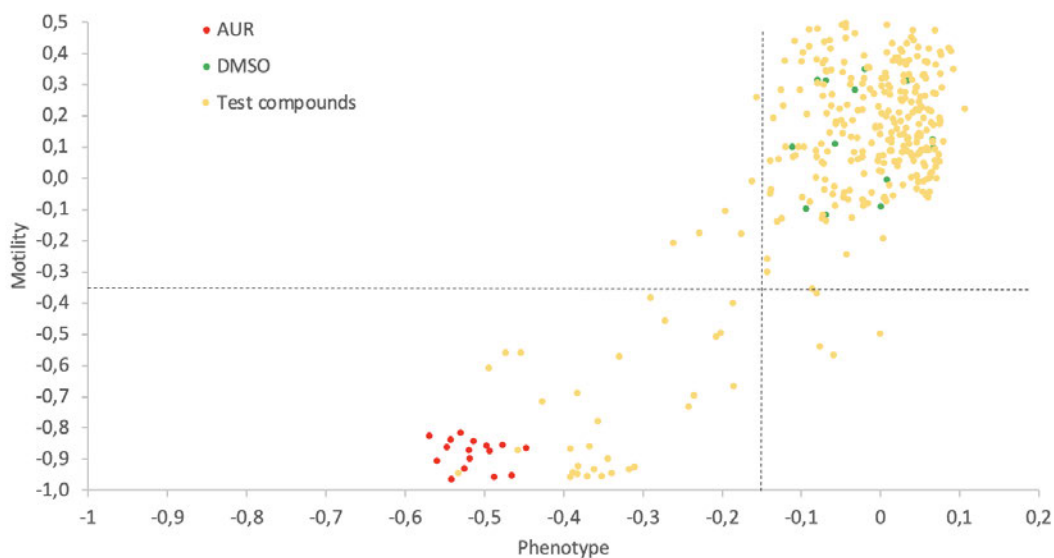
Figure 4. 5: Initial screening against *S. mansoni* larvae. The positive control (AUR) is indicated in red and the solvent (used as negative control) in green, while the test compounds are in orange.

Compounds having a phenotype score less than -0.15 and motility score of less than -0.35 were considered to be consistent hits at 50 µM (BZI-93 as well as HY-1, -3, -5, -6, -8, -9, -10, -12, -13, -18, -19, -20, -21 and HY-22).
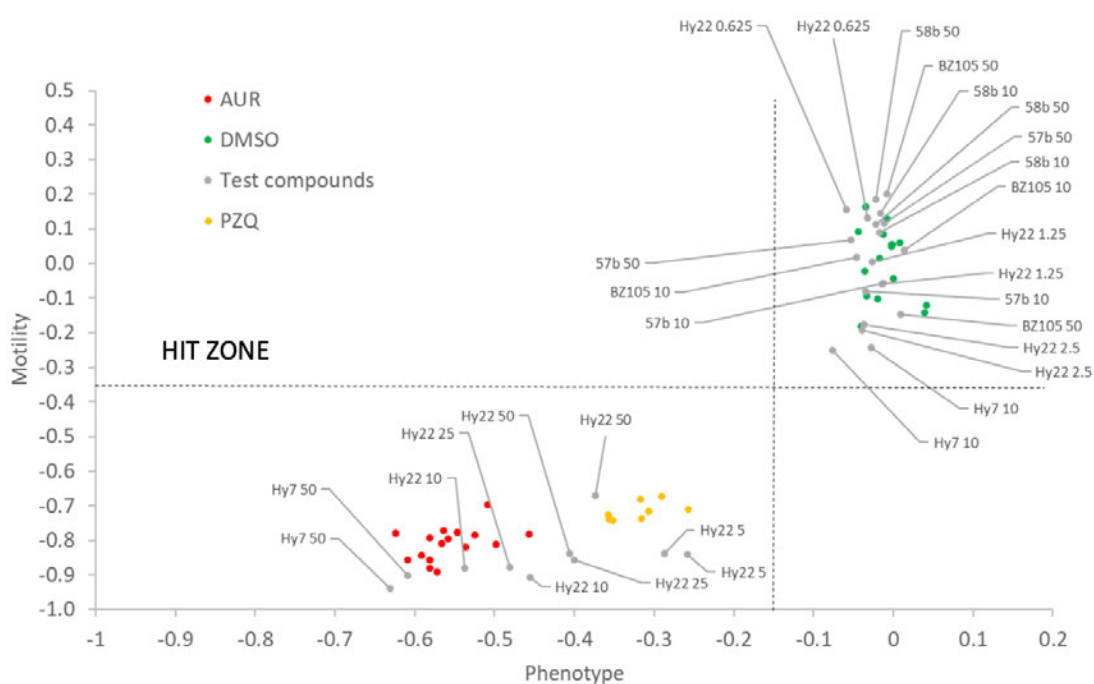
Figure 4. 6: Further screening against *S. mansoni* larvae. The positive controls are indicated in red (AUR) and orange (PZQ), the solvent (used as negative control) in green, while the test compounds are in grey.

HY-22 represent the best candidate at 50 µM as it has a comparable effect to the positive control on the phenotype and motility of *S. mansoni* larvae. Therefore, HY-22 was screened as a dose-titration (50, 25, 10, 5, 2.5, 1.25 and 0.625 µM) (Figure 4.6).

HY-22 was considered sufficiently potent to warrant further testing in adult worms. It was screened in triplicate against adult worm pairs. All worms were scored by eye at 14, 48 h and 72 h by Dr Josephine Forde-Thomas using the WHO-TDR scoring matrix.[239]

HY-22 was found to cause complete loss of movement after 24 h treatment at 20 µM. EC_{50} values were found to be comparable to praziquantel.[240,241,242]

MTT assay against Hep-G2 cells, which are a mammalian liver cell line, was performed. This is a calorimetric assay for detecting cell metabolic activity. 3-(4,5-dimethylthiazol-2-yl)-2,5-diphenyl**tetrazolium** bromide (MTT) is used to detect NAD(P)H dependent oxydoreducteses which reflect the living cells present. MTT can be reduced by these enzyme and form formazan and give purple color. Cytotoxicity assay showed that HY-22 compound selectively kills schistosomes over HepG2 cells.

	Activity on schistosomula (EC_{50}, µM)			Activity on adults worms (EC_{50}, µM)			HepG2 cells Average (CC_{50}, µM)	Selectivity Index (somula)	Selectivity Index (adult)
Compound	Phenotype	Motility	Average	Male	Female	Average			
HY-22	4.59	3.28	3.94	8.66	8.29	8.48	51.14	13.0	6.0
AUR	0.37	0.45	0.41	NR	NR	NR	5.07	12.4	NR
PZQ	1.14	0.88	1.01	NR	NR	0.11	142.8	141.4	1298.2

Table 4. 7: Anti-schistosomal and HepG2 cytotoxic activity data for HY-22 (this work) and positive controls. [236,237,238]

The selectivity for schistosomal cells is measured in terms of selectivity index (SI) which indicates the ratio of the toxic concentration of a drug against its active concentration. The cytotoxicity assay showed that AUR is more potent than HY-22 against somula but also more cytotoxic, having the same SI. PZQ is slightly more potent against somula than HY-22 but much more potent against adults, and also slightly less cytotoxic, giving much better SI values. HY-22 therefore represents a promising hit compound that should be used as a basis for structure-activity relationship studies to improve activity and reduce cytotoxicity.

4.3 Binding assay: STD-NMR

The assays previously mentioned led to the selection of hit molecules having antimicrobial or antiparasitic effects. Although it was not possible to undertake studies on LT, to further elucidate the target the compounds synthesized in this work were interacting with, Saturation Transfer Difference (STD) NMR[243] was used to determine if the benzimidazoles and hybrids can bind lysozyme and albumin. Lysozyme has a similar arrangement of active site residues to LTs and is readily available commercially. Albumin has been investigated as this protein is a critical drug carrier.[244] STD-NMR is a simple technique that requires a low concentration of protein and relies only on the signals produced by the ligand that successfully binds the macromolecule. This technique is based on the nuclear Overhauser effect.[245] An "on-resonance" spectrum of the protein-ligand mixture (selectively irradiated at a ppm value that only contains protein resonances, typically 0.5 to -0.5 ppm, prior to acquisition of the spectrum) is subtracted from an "off-resonance" spectrum (irradiated at a ppm value that contains no resonances prior to acquisition of the spectrum). On-resonance irradiation leads to the transfer of the magnetization to all protons in the protein and finally to the ligand, while off-resonance irradiation does not lead to magnetization transfer. The resulting difference spectrum shows only the ligand resonances that received magnetization transfer from the protein.

Dimethyl sulfoxide (DMSO) has been chosen as an optimal solvent for solubilizing benzimidazoles and hybrid compounds. It is well known that DMSO can induce conformational changes in proteins.[246,247] It can decrease thermal stability and lead to unfolding. Therefore, ^{1}H-NMR spectra of both hen egg white lysozyme (HEWL) and human serum albumin (HSA) were acquired in varying water/DMSO mixtures in order to investigate the stability of the chosen proteins in the organic solvent. The ^{1}H NMR spectra of both proteins were unchanged in 10% and 25% DMSO, while minimal changes were observed at 50% DMSO. When the concentration of DMSO was increased to 60% and 75% the ^{1}H NMR spectra of the proteins was substantially changed. Loss of up-field shifted methyl resonances (the ones below 0 ppm) was observed, showing protein unfolding.

The solubility of the benzimidazoles and hybrid compounds have also been tested in order to find the minimum concentration of DMSO needed for dissolving the ligands and guaranteeing the proteins' stability. The optimal DMSO concentration was found to be 50%. Despite the

observed changes in the proteins' spectra at this concentration of DMSO, they have been considered minimal and necessary in terms of solubility.

In order to only detect the ligand bound to the protein, 0.5 ppm was used as optimal region of the spectrum for selective on-resonance irradiation. The compounds were screened for the binding to HEWL and HSA with a saturation time (D20) of 5.9 seconds and a T_1 relaxation delay of 2 seconds. BZI-72, -100 and -114 have been found to bind lysozyme (Table 4.8) as well as HSA. The STD amplification factors were calculated for the integrated protons following Equation1 in order to identify the protein binding sites.

$$STD_{amp} \text{ of resonance} = (STD_{diff} / STD_{off}) \times \text{ligand excess} \qquad (1)$$

Several protons seem to be mainly engaged in the ligand-protein interaction. In all the selected ligands, the N-H protons of the benzimidazole and the pyrrole (H_1 and H_2 in table 4.8) have the highest STD_{amp} of resonance which means that they receive the most magnetization from the protein and so are probably the most deeply bound into the active site, probably forming H-bonds. In BZI-72 and BZI-100, the protons of the pyrrole seem also to be involved in the interaction, probably generating hydrophobic contacts, with H_6 being the closest to the protein.

Compound\ STD_{amp} of resonance	H_1	H_2	H_3	H_4	H_5	H_6	H_7
BZI-72	61	53	52	/	20	16	20
BZI-100	21	11	8	9	10	10	10
BZI-114	21	9	6	/	3	3	3

Table 4. 8: STD_{amp} resonance for the protons mainly involved in the lysozyme binding.

BZI-100 has the two H_4, which can form hydrophobic interactions, as close to the protein as the pyrrole protons. BZI-72 and BZI-114 didn't show these signals as these protons are not present.

4.4 Structure-activity relationships

Several 2-phenyl-1H-1,3-benzodiazoles have been selected as hits showing activity against all the bacterial species considered in this work. 2-(4-fluorophenyl)-1H-1,3-benzodiazole (BZI-22) as well as 5-chloro-2-phenyl-1H-1,3-benzodiazole (BZI-45), 4-(5-chloro-1H-1,3-benzodiazo l-2-yl)phenol (BZI-49) and 5-chloro-2-(1H-pyrrol-2-yl)-1H-1,3-benzodiazole (BZI-58) all showed good antibacterial activity. 2-(1H-pyrrol-2-yl)-1H-1,3-benzodiazole (BZI-30), 5-chloro-2- (1H-pyrrol-2-yl)-1H-1,3-benzodiazole (BZI-58), as well as 5-fluoro-2-(1H-pyrrol-2-yl)-1H-1,3- benzodiazole (BZI-114) and 4-(5-fluoro-1H-1,3-benzodiazol-2-yl)phenol (BZI-105), were highlighted for their activity against *E. coli* JM109. MIC assays revealed a comparable activity of the 5-nitro-2-(1H-pyrrol-2-yl)-1H-1,3-benzodiazole (BZI-72) to the positive control ampicillin. Several C_2-extended benzimidazoles and most of the indole-benzimidazole hybrids were found to be active against *S. mansoni* larvae at 50 µM while the 2-(6-chloro-1H-indol-3-yl)-5,6- dimethyl-1H-1,3-benzodiazole (HY-22) was active against larvae at 10 µM as well as affecting both phenotype and motility in adult worms. Binding assays highlighted 5-nitro-2-(1H-pyrrol- 2-yl)-1H-1,3-benzodiazole (BZI-72) as well as 5-benzoyl-2-(1H-pyrrol-2-yl)-1H-1,3-benzodiazole (BZI-100) and 5-fluoro-2-(1H-pyrrol-2-yl)-1H-1,3-benzodiazole (114) as lysozyme binders.
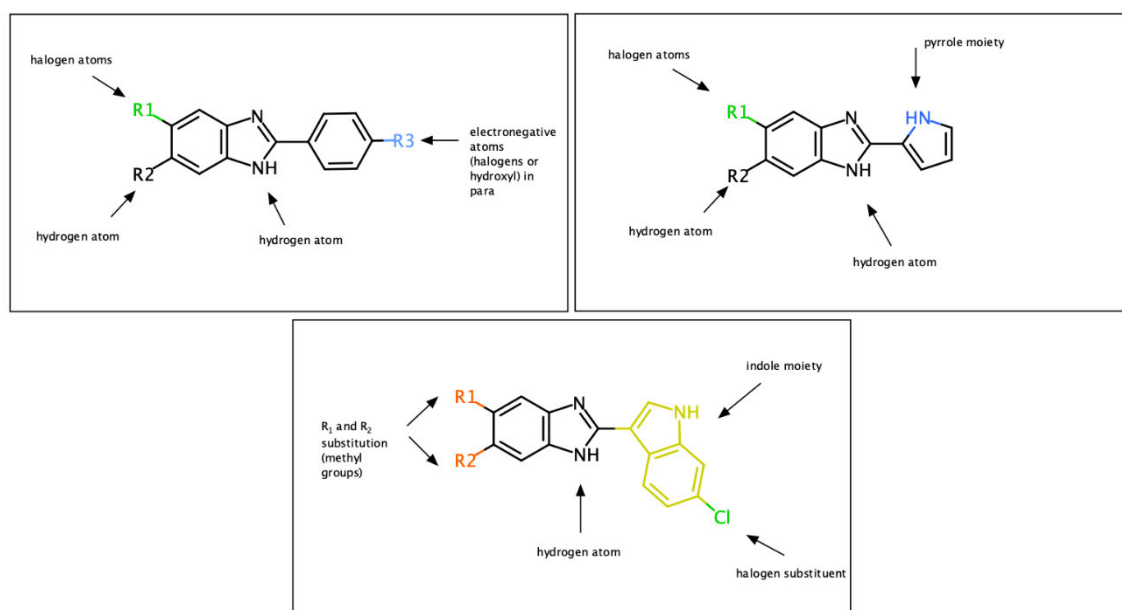
Figure 4. 7: Structure activity relationship showing the benzimidazole extensions leading to antimicrobial activity.

Based on Structure Activity Relationship studies (SAR), the C_2 extension appears to be preferred over the N_1 extension, and the concomitant presence of a substituent in position 5 and 6 (R_1 and R_2 in Figure 4.7) of the benzimidazole core leads to antimicrobial effect. A chlorine or nitro group in position 5, as well as a p-fluorophenyl, p-hydroxyphenyl or pyrrol-2-yl moiety in position 2 of the benzimidazole nucleus seems to be critical for the antibacterial activity. The combination of the indole and benzimidazole moieties was found to be critical for activity against *S. mansoni.* The pyrrole moiety seems to be a key structural requirement for binding lysozyme, which has a similar active site structure to lytic transglycosylases.

4.5 Conclusion

The antibacterial properties of the compounds synthesised were investigated in order to give an overview on their structure-activity relationships. Compounds were screened against *E. coli* JM109, *E. coli* ATCC 35218, *S. aureus* and *P. aeruginosa*. Several hits have been identified. BZI-30 was found to be the best drug-like candidate against *E. coli* ATCC 35218, but it is not active against *S. aureus* or *P. aeruginosa*. BZI-58 represents one of the best antimicrobial candidates as it inhibits all the bacteria species considered in this study. It is strongly active against *E.coli* (ATCC 35218) and *P. aeruginosa* and it also inhibits *S.aureus*, representing the best inhibitor against this bacterium. An indole-benzimidazole hybrid (HY-22) has been highlighted for its activity against adult worms of *S. mansoni.* A structure-activity relationship study identified the core modifications leading to antimicrobial activity. The C_2 extension appears to be preferred over the N_1 extension. The presence of a p-substituted phenyl ring or a pyrrole moiety in position 2 of the benzimidazole nucleus seems to lead to good antibacterial activity. The concomitant presence of a halogen in position 5 of the core increases the antibacterial effect. The presence of a indole as C_2-extension leads to very good the activity against worms. Furtherly, the presence of a chlorine in position 6 of the indole nucleus and the concomitant presence of methyl groups in position 5 and 6 of the benzimidazole moiety leads to activity on adult worms. HY-22 could potentially bind tubulin with a similar pose than mebendazole (Figure 1.4). The N-H of the benzimidazole core as well as the N-H of its indole moiety could recreate the interactions with Glu200 while its non-polar parts could leads to hydrophobic interactions with the hydrophobic pocket into the tubulin active site.

Chapter 5

Conclusions

5. Conclusions

Benzimidazole is a building block commonly found in pharmaceuticals. Changing the substituents in its extensible sites leads to different pharmacological activity. It is well known for its antimicrobial, antiviral, anticancer and antiulcer properties as well as antihistaminic, anticoagulant and anti-inflammatory activity. Based on the overview of already marketed benzimidazoles as well as several promising extensions of the nucleus evidenced by literature studies, new potential antimicrobial benzimidazole-based compounds have been designed.

Lytic transglycosylases (LTs) are critical enzymes involved in the peptidoglycan recycling as well as the induction of β-lactamases. Inhibition of LT could directly harm the cell wall stability, by inhibiting the peptidoglycan recycling, as well as interfere with the synthesis of β-lactamases. Thus, lytic transglycosylases are considered a promising target for overcoming the bacteria resistance. A co-administration of LT inhibitor and β-lactam antibiotics can lead to an enhancement of the β-lactam activity by synergistic effect. Due to the critical role that lytic transglycosylases could play in the fighting to the bacteria resistance, the benzimidazoles were modelled into a Slt35 active site, a model LT. The *in-silico* screening of the designed benzimidazoles led to a library of compounds with good predicted binding affinity for the target. The 2-hydroxymethyl moiety represents a promising C_2-extension having the hydroxyl group interacting, for most of analogues in this class of ligands, with the LT catalytic Glu residue. This mimics key interactions that the known inhibitor bulgecin A generates into the LT active site representing a promising core modification. The insertion of a benzyl chain in position number 1 of the benzimidazole nucleus, giving 1-benzyl-1H-1,3-benzodiazoles, generally leads to an increase of ligand-receptor interactions giving a stronger ligand predicted affinity for the target. Both the categories of 2-phenyl-1H-1,3-benzodiazoles, having a C_2-benzene substituent, or the 2-(1H-1,3-benzodiazol-6-yl)-1H-1,3-benzodiazoles, bis-analogues, seem to lead to compounds having high predicted affinity for the LT active site and so they represent good inhibitor candidates.

Overall, this work provides optimal strategies for extending the benzimidazole nucleus leading to the synthesis of 150 compounds. The identification of suitable routes for extending the benzimidazole nucleus was critical. Based on the previously synthesised 1-H-hydroxymethyl-benzimidazole,[173,177] the synthesis of several 5,6-1-H-hydroxymethyl-benzimidazoles was successfully achieved. This allowed to investigate the effect of substituents on the benzene

moiety of the benzimidazole core. Based on previous work considerations and the inability to selectively extend the 1-H-hydroxymethyl-benzimidazole on its N_1-atom due to a competitivity between the oxygen and the nitrogen,[174] it was critical to identify a suitable synthetic path for producing N_1-substituted benzimidazoles. The alkylation of the o-phenylenediamine followed by the closure of the benzimidazole core was identified as ideal route for extending the benzimidazole on its nitrogen atom, avoiding the competitivity of the oxygen. The low yield and difficulties in the product isolation encountered in the amine alkylation step led to the need of a more suitable route for synthesise N-alkylated derivatives. A reductive amination route was undertaken in order to synthesise several (1-benzyl-1H-1,3-benzodiazol-2-yl)methanol-derivatives. This led to the recovery of 2 products in one pot synthesis: the desired N_1-alkylated and the competitor C_2-extended derivative, which was found to be the major product of this synthetic path. Once the imine is formed, an intramolecular cyclization gives the concomitant formation of the 2-phenyl-1H-1,3-benzodiazole and, as minor product, the desired Schiff base which can be reduced giving the alkylated amine and so form the (1-benzyl-1H-1,3-benzodiazol-2-yl)methanol-derivative as minor product. The N_1/C_2 competition has been deeply analysed in this work and several derivatives successfully synthesised. Unluckily the two products are formed in low yields and additional work will be done in future by the Loveridge's team in order to optimize the yields. A suitable synthetic method for the selective formation of C_2-exteneded benzimidazoles, using benzaldehyde and sodium metabisulfite as catalyst, have also been identified leading to the synthesis of 2-phenyl-1H-1,3-benzodiazoles and 2-(1H-pyrrol-2- yl)-1H-1,3-benzodiazoles. This synthetic strategy led the way to further categories: bis-benzimidazoles and as well as hybrid benzimidazole-imidazole derivatives. The synthetic approaches undertaken give an overview of the most suitable routes for extending the benzimidazole nucleus in its different sites.

The antibacterial properties of the compounds synthesised were investigated in order to give an overview on the structural-activity relationship of the benzimidazoles produced. Compounds were screened against *E. coli* (JM109), *E.coli* (ATCC 35218), *S.aureus* and *P.aeruginosa* performing a disk diffusion assay. Several 2-phenyl-1H-1,3-benzodiazoles have been selected as hits showing activity against all the bacteria species considered in this work. 2-(4-fluorophenyl)-1H-1,3-benzodiazole (BZI-22) as well as 5-chloro-2-phenyl-1H- 1,3-benzodiazole (BZI-45), 4-(5-chloro-1H-1,3-benzodiazol-2-yl)phenol (BZI-49) and 5-chloro-2-(1H-pyrrol-2-yl)-1H-1,3-benzodiazole (BZI-58) showed a good antibacterial activity.

2-(1H-pyrrol-2-yl)-1H-1,3-benzodiazole (BZI-30), 5-chloro-2-(1H-pyrrol-2-yl)-1H-1,3-benzodiazole (BZI-58) , as well as 5-fluoro-2-(1H-pyrrol-2-yl)-1H-1,3-benzodiazole (BZI-114) and 4-(5-fluoro-1H-1,3-benzodiazol-2-yl)phenol (BZI-105), were highlighted for their activity against *E. coli* (JM109). MIC assay revealed a comparable activity of the 5-nitro-2-(1H-pyrrol-2-yl)- 1H-1,3-benzodiazole (BZI-72; 8 µg/ml) to the positive control ampicillin (2 µg/ml). The C_2- over the N_1-extension and the concomitant presence of a substituent in position 5 of the benzimidazole core leads to antimicrobial effect. The chlorine or the nitro in position number 5 as well as the p-F and p-OH phenyl or the pyrrol- moiety in position 2 of the benzimidazole nucleus seem to be critical for the antibacterial activity.

The compounds synthesised were screening against *S. mansoni* in order to investigate their activity against worms. Several benzimidazoles, C_2-extended and most of the imidazole-benzimidazole hybrids, were found to be active at 50 µM while the 2-(6-chloro-1H-indol-3-yl)-5,6-dimethyl-1H-1,3-benzodiazole (HY-22) was selected as hit being active at 10 µM as well as affecting both phenotype and motility in adult worms. The combination of the imidazole and benzimidazole moieties was found to be critical for the activity against *S. mansoni.* Cytotoxicity assay showed that HY-22 compound selectively kills schistosomes over HepG2 cells.

Binding assay highlighted 5-nitro-2-(1H-pyrrol-2-yl)-1H-1,3-benzodiazole (BZI-72) as well as 5-benzoyl-2-(1H-pyrrol-2-yl)-1H-1,3-benzodiazole (BZI-100) and 5-fluoro-2-(1H-pyrrol-2-yl)- 1H-1,3-benzodiazole (114) as lysozyme binders. The pyrrole moiety seems to be a key structural requirement for binding this enzyme, which has a similar active site structure than lytic transglycosylases. Investigation on synergistic effect of these benzimidazole analogues will be undertaken in future works in order to identify the mechanism behind their effect and whether they target lytic transglycosylases or this was a chance discovery.

Future efforts in Loveridge's group will aim to furtherly investigate the activity of the hit-molecules selected in this work. It is critical to deeply explore the binding to lytic transglycosylases as well as investigate the affinity of the synthesised compounds to tubulin, an attracting target for antimicrobials. In addition, the selectivity of 2-(6-chloro-1H-indol-3- yl)-5,6-dimethyl-1H-1,3-benzodiazole (HY-22) for killing schistosomes as well as its cytotoxicity to cells will be investigated. HY-22 could potentially bind tubulin with a similar pose than mebendazole and represent a promising drug-like candidate.

Chapter 6

Methods

6. Methods

6.1: Molecular docking

The receptor (PDB 1D0L) was fetched in UCSF Chimera[248] and prepared by removing existing ligands. Ligand structures were drawn using PubChem Sketcher V2.4[249] and imported into UCSF Chimera. Docking was performed using AutoDock Vina.[250] The grid (center 7; 24; 12. Size 22 x 22 x 22 Å) was prepared using the co-crystallized known bulgecin inhibitor.[251] The best 10 ranked docking poses were visually inspected to evaluate their ability to occupy the receptor active site and the number of interactions formed.[252] The visualization of H-bonds was undertaken using UCSF Chimera[248] while hydrophobic interactions were visualized using ProteinPlus web server.[216]

6.2: TLC assay

Amino acids and their derivatives were separated by TLC, in propanol: acetic acid: water (5: 1: 1). The plate was carefully dried before visualizing the spots using ninhydrin solution (0.3% w/v ninhydrin and 3% v/v glacial acetic acid in 1-butanol).[253] The primary amines gave a purple colored spot while the secondary amines gave a yellow spot.

6.3: Organic synthesis

Chemicals were purchased from Sigma-Aldrich, Fisher Scientific and Fluorochem. NMR spectra were recorded on a Bruker Avance III 500 MHz (^{1}H) NMR spectrometer and are reported as chemical shifts in parts per million. Melting points were recorded using Stuart Melting point machine (SMP30).

6.3.1: 2-Acetamidobutanedioic acid attempt 1
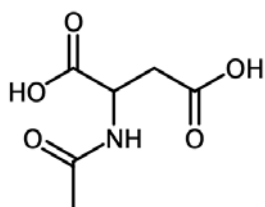
L-Aspartic acid (0.2 g; 1.5 mmol) was added to acetic anhydride (1.7 ml; 17.9 mmol; 12 eq) on ice and the mixture was stirred. Sulfuric acid conc. (4 drops) was then added and the mixture was refluxed (70 ºC) for 1 hour. The solution was cooled to room temperature (on ice) and water (5 ml) was added. The mixture was quenched with ethyl acetate, the two layers separated, the

organic phase was washed with HCl (20 ml, 1 M solution) and dried with Na$_2$SO$_4$. The solvent was evaporated giving an oil (0.1 g). The desired product was not isolated.

6.3.2: 2-Acetamidobutanedioic acid attempt 2

The same reaction was run at room temperature giving an oil (0.1 g). The desired product was not isolated.

6.3.3: 2-Acetamidobutanedioic acid attempt 3

L-Aspartic acid (2.5 g; 18.8 mmol) was dissolved in hot water (50.0 ml). Acetic anhydride (12.5 ml) was then added and the mixture was cooled quickly (on ice). More acetic anhydride (37.5 ml) was added (50 ml in total; 528.0 mmol; 28 eq) and the mixture was stirred at room temperature for 6 hours (cooling if necessary). The mixture was neutralized with NaHCO$_3$ and the solvent evaporated. Starting material was recovered.

6.3.4: 2-Acetamidobutanedioic acid attempt 4

The same reaction was run using NaOH (1 M solution) to neutralize the mixture giving an unknown solid (transparent crystals). Melting point > 240 ºC. ^{1}H-NMR (500 MHz in D$_2$O) δ (ppm): gave no useful peaks.

6.3.5: 2-Acetamidobutanedioic acid attempt 5

The same reaction was run extracting the product in ethyl acetate (30 ml). The organic phase was neutralized with NaHCO$_3$ and dried with MgSO$_4$ without giving the expected product.

6.3.6: 2-Acetamidobutanedioic acid

L-Aspartic acid (5.0 g; 37.6 mmol) was dissolved in hot water (150 ml). Acetic anhydride (25.0 ml) was added to the hot solution of the amino acid and the mixture was cooled quickly (on ice). More acetic anhydride (75 ml) was added and the mixture was stirred at room temperature (cooling) for 6 hours. Evaporation of the solvent gave the desired product as a gum (6.2 g, 94% yield). N-acetyl-aspartic acid was used as a gum, without purification, in the corresponding anhydride synthesis. ^{1}H-NMR (500 MHz, D$_2$O) δ (ppm): 2.01 (s, 3H); 2.83 (m, 2H); 4.75 (t, 1H).

6.3.7: 2-Acetamidobutanedioic acid (in DMSO)

L-Aspartic acid (0.5 g, 4 mmol) was added to dimethyl sulphoxide (25 ml) and the mixture was stirred at first at room temperature and then with a gently heating for 30 minutes. Acetic anhydride (2 eq) was added and reaction was run until completed (monitored by TLC). Water (5

ml) was added and the product was extracted with ethyl acetate (30 ml). The two layers were separated and the organic phase washed with water (15 ml). The solvent was evaporated giving 2-acetamidobutanedioic acid as a white oil (0.4 g, 60%). The product was used in subsequent steps. ^{1}H-NMR (500 MHz, DMSO-d$_6$) δ (ppm): 1.90 (s, 3H); 3.64 (d dd, 2H); 4.26 (m, 1H); 8.00 (d, 1H, N-H).

6.3.8: 3-(Acetyloxy)-2-acetamidopropanoic acid
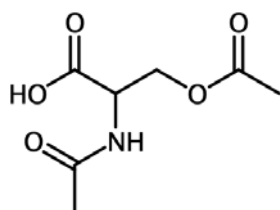
L-Serine (1.0 g, 9.5 mmol) was dissolved in hot water (150 ml). Acetic anhydride (25.0 ml) was added to the hot solution of the amino acid and the mixture was cooled quickly (on ice). More acetic anhydride (75 ml) was added and the mixture was stirred at room temperature (cooling) for 6 hours. Evaporation of the solvent gave 3-(acetyloxy)-2-acetamidopropanoic acid (N,O-diacetyl-L-serine) as a gum (2.0 g, quantitative yield) which was used in subsequent step as crude product.^{1}H-NMR (500 MHz, D$_2$O) δ (ppm): 1.96 (s, 3H); 1.98 (s, 3H); 3.81 (d dd, 2H); 4.41 (t, 1H). ^{13}C-NMR (125 MHz, D$_2$O) δ (ppm): 20.2; 21.6; 54.7; 61.0; 173.3; 174.1; 176.4.

6.3.9: 2-Acetamido-3-hydroxypropanoic acid attempt 1
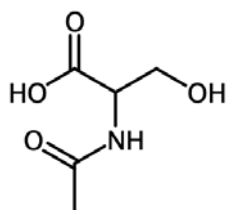
3-(Acetyloxy)-2-acetamidopropanoic acid (0.5 g; 2.1 mmol) was refluxed in MeOH:DCM (50%), the mixture was cooled and filtered. MeONa (4.8 ml; 0.5 eq; 30% solution in methanol) was added dropwise (on ice) to the filtrate which was then washed with HCl (1M). The organic layer was neutralized and evaporate. The desired product was not isolated.

6.3.10: 2-Acetamido-3-hydroxypropanoic acid attempt 2

3-(Acetyloxy)-2-acetamidopropanoic acid (0.5 g; 2.1 mmol) was stirred in MeOH:DCM (50%), the product was extracted with EtOAc and the organic layer washed with HCl (1 M), then with NaHCO$_3$ aq and the organic solvent was evaporated. The expected product was not isolated.

6.3.11: 2-Acetamido-3-hydroxypropanoic acid attempt 3

L-Serine (1.0 g, 9.5 mmol) was solubilized in hot water (60 ml). Acetic anhydride (0.5 ml, 0.5 eq) was added and the mixture was cooled quickly (on ice). More acetic anhydride was added (0.5 ml, 0.5 eq) and the mixture was stirred for 6 hours. The solvent was evaporated and starting material recovered.

6.3.12: 2-Acetamido-3-hydroxypropanoic acid attempt 4

The same reaction was run starting from L-serine (0.5 g, 4.7 mmol) and using 2 equivalent of acetic anhydride. The removal of the solvent gave a gum as final product. Starting material was recovered.

6.3.13: 2-Acetamido-3-hydroxypropanoic acid

L-Serine (0.5 g, 4.7 mmol) was added to dimethyl sulfoxide (25 ml) and the mixture was stirred at first at room temperature and then with gentle heating for 30 minutes. Acetic anhydride (1 ml, 2 eq) was added and reaction was run until completed (monitored by TLC). Water (5 ml) was added and the product was extracted with ethyl acetate (30 ml). The two layers were separated and the organic phase washed with water (15 ml). The solvent was evaporated giving an oil as product (0.6 g, 86% yield). ^{1}H-NMR (500 MHz, DMSO-d$_6$) δ (ppm): 1.88 (s, 3H); 3.64 (d dd, 2H); 4.26 (m, 1H); 8.00 (d, 1H, N-H). ^{13}C-NMR (125 MHz, DMSO-d$_6$) δ (ppm): 22.7; 55.1 ; 6.80; 170.3; 172.5.

6.3.14: N-(2,5-Dioxooxolan-3-yl)acetamide
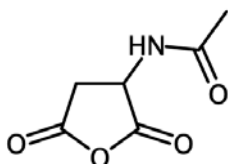
2-Acetamidobutanedioic acid (2.0 g, 11 mmol) was added as a gum to acetic anhydride (12 ml, 11 eq) and heated for 20 minutes (100 ºC). The solution was filtered, reduced to half volume and cooled on ice for 1 hour. The crystals obtained were washed with acetic anhydride, ethyl acetate and petroleum ether (40-60 ºC). N-(2,5-dioxooxolan-3-yl)acetamide, was isolated as

white crystals (1.1 g, 61% yield). The product was used without purification in subsequent steps. Melting point 139-141 ºC. ^{1}H-NMR (500 MHz, DMSO-d$_6$) δ (ppm): 1.88 (s, 3H); 2.85 (dd, 1H); 3.20 (q, 1H); 4.57 (m, 1H); 8.84 (d, 1H, N-H). ^{13}C-NMR (125 MHz, DMSO-d$_6$): 22.1; 35.3; 49.9; 170.8; 172.32.

6.3.15: 3-Acetamido-4-oxobutanoic acid
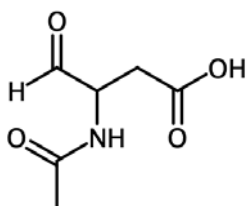
N-(2,5-Dioxooxolan-3-yl)acetamide (0.47 g) was dried and then stirred in dry DCM (20 ml) under nitrogen. The solution was cooled to -78 ºC for 15 minutes and DIBAL-H solution (0.6 ml; 1.0 M sol. in hexanes) was added dropwise. Reaction was run for 2 hours and then the mixture was quenched by the addition of ethyl acetate (20 ml) maintaining the N$_2$ flow. The bath was then removed and sulfuric acid (100 ml, 1 M solution) was added slowly stirring vigorously the mixture for 1 hour. The layers were separated and the aqueous phase was extracted with ethyl acetate (50 ml). The two organic extracts were combined and washed with HCl (50 ml, 1 M solution), NaHCO$_3$ (50 ml, 0.8 M solution) and with brine (50 ml). The organic phase was dried with MgSO$_4$ and the solvent evaporated. The desired product was not isolated.

6.3.16: 4'-(Carboxymethyl)-5'-oxospiro[bicyclo[3.3.1]nonane-9,2'-[1,3]oxazolidin]-3'-ium attempt 1
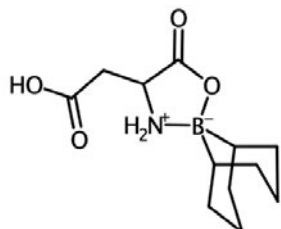
L-Aspartic acid (0.4 g; 3.0 mmol) was solubilized in dry MeOH (20 ml) under inert atmosphere and 9-BBN (6.7 ml, 1 M solution in THF; 1.1 eq) was added dropwise. Reaction was refluxed for 72-120 hours giving a complex mixture of product (TLC; propanol: acetic acid: water (5:1:1)). The

mixture was cooled to room temperature and concentrated in vacuo giving a yellow gum. Hot THF (40 ml) was added and the solvent evaporated. The solid obtained was triturated in hot hexanes (70 ml) giving a light-yellow solid (0.2 g) which was a complex mixture of compounds. The desired product was not isolated.

6.3.17: 4'-(Hydroxymethyl)-5'-oxospiro[bicyclo[3.3.1]nonane-9,2'-[1,3]oxazolidin]-3'-ium
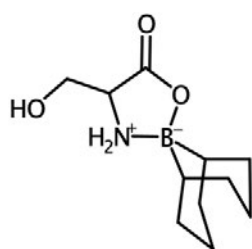
L-Serine (0.3 g; 2.9 mmol) was solubilized in dry MeOH (20 ml) under inert atmosphere and 9-BBN (6.7 ml, 1 M solution in THF; 1.1 eq) was added dropwise. Reaction was refluxed for 24 hours, the mixture was cooled to room temperature and concentrated in vacuo giving a yellow gum. Hot THF (40 ml) was added and the solvent evaporated. The solid obtained was triturated in hot hexanes (70 ml) giving 4'-(hydroxymethyl)-5'-oxospiro[bicyclo[3.3.1]nonane-9,2'-[1,3]oxazolidin]-3'-ium as white powder (0.55 g, 55% yield). Rf 0.90 (propanol: acetic acid: water (5:1:1). Melting point 165-167 ºC. ^{1}H-NMR (500 MHz, DMSO-d_6) δ (ppm): 0.49 (d, 2H); 1.58-1.78 (m, 12H); 3.70 (m, 2H); 5.14 (t, 1H); 5.46 (t, 1H, N-H); 6.53 (t, 1H, N-H). ^{13}C-NMR (125 MHz, DMSO-d_6) δ (ppm): 24.3; 24.7; 31.2; 31.2.

6.3.18: 4'-[(2-Aminophenyl)amino]-5'-oxospiro[bicyclo[3.3.1]nonane-9,2'-[1,3]oxazolidin]-3'-ium attempt 1
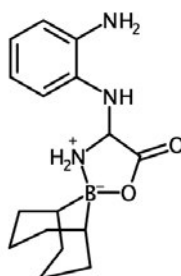
Dry DCM (10 ml) was added to 4'-(hydroxymethyl)-5'-oxospiro[bicyclo[3.3.1]nonane-9,2'-[1,3]oxazolidin]-3'-ium (0.1 g; 0.29 mmol) under N₂, the mixture was placed on ice and pyridine (0.05

ml; 0.58 mmol; 2 eq) was then added. The mixture was stirred for 30 minutes and p-toluene-sulfonyl chloride (0.08g; 0.43 mmol; 1.5 eq) was added. Reaction was monitored by TLC and, after 3 hours, o-phenylendiamine (0.05 g; 0.43 mmol; 1.5 eq) was added without isolating the intermediate. The mixture was stirred for 2 hours , filtered and the organic solution washed with HCl (10 ml, 1M) and then with $NaHCO_3$ (10 ml). The organic phase was dried over Na_2SO_4 and the solvent evaporated giving an oil as result. The desired product was not isolated.

6.3.19:   4'-{[(4-Methylbenzenesulfonyl)oxy]methyl}-5'-oxospiro[bicyclo[3.3.1]nonane-9,2'-[1,3]oxazolidin]-3'-ium attempt 1
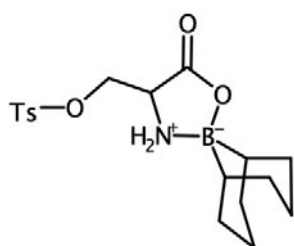
Dry DCM (10 ml) was added to 4'-(hydroxymethyl)-5'-oxospiro[bicyclo[3.3.1]nonane-9,2'-[1,3]oxazolidin]-3'-ium (0.1 g; 0.29 mmol) under N_2, the mixture was placed on ice and pyridine (0.05 ml; 0.58 mmol; 2 eq) was then added. The mixture was stirred for 30 minutes and p-toluene-sulfonyl chloride (0.08g; 0.43 mmol; 1.5 eq) was added. Reaction was run for 24 hours on ice monitoring it by H-NMR. The mixture was then stirred at room temperature for 15 hours and, not being completed, it was refluxed for 24 hours. DCM (5 ml) was added and the organic mixture was washed with $NaHCO_3$ solution (10 ml), then with brine (10 ml) and dried over NaSO4. The solvent was evaporated and analyzed by H-NMR without giving the desired product.

6.3.20:   4'-{[(4-Methylbenzenesulfonyl)oxy]methyl}-5'-oxospiro[bicyclo[3.3.1]nonane-9,2'-[1,3]-oxazolidin]-3'-ium attempt 2

S4'-(hydroxymethyl)-5'-oxospiro[bicyclo[3.3.1]nonane-9,2'-[1,3]oxazolidin]-3'-ium (0.1 g; 0.29 mmol) was stirred in dry DCM under nitrogen for 15 minutes. Triethylamine (0.05 ml; 0.43 mmol; 1.5eq) was added, followed by the addition of DMAP (7 mg; 0.06 mmol; 0.2 eq) at 0 ºC (on ice). A solution of p-toluenesulfonyl chloride (0.66 g; 0.35 mmol; 1.2eq) in dry DCM (5 ml) was added drowse and the mixture was stirred on ice for 30 minutes and then at room temperature for 7 hours monitored by TLC. The organic phase was washed with water (20 ml), then with HCl (1M), with $NaHCO_3$ aq (10 ml x 2) and finally with brine. The organic layer was dried over Na_2SO_4 and

the solvent evaporated giving 4'-{[(4-methylbenzenesulfonyl)oxy]methyl}-5'-oxospiro[bicyclo[3.3.1]nonane-9,2'-[1,3]oxazolidin]-3'-ium, as a yellow oil (0.21 g, quantitative yield). Rf 0.85 (ninhydrin assay: propanol: acetic acid: water (5:1:1)) . ^{1}H-NMR (500 MHz, CDCl$_3$) δ (ppm): 2.40 (s, 3H), 4.37 (q, 1H); 4.46 (dd, 1H); 4.85 (t, 1H, N-H); 5.57 (t, 1H, N-H); 7.32 (d, 2H,); 7.70 (d, 2H).

6.3.22: 4'-[(2-Aminophenyl)amino]-5'-oxospiro[bicyclo[3.3.1]nonane-9,2'-[1,3]oxazolidin]-3'-ium attempt
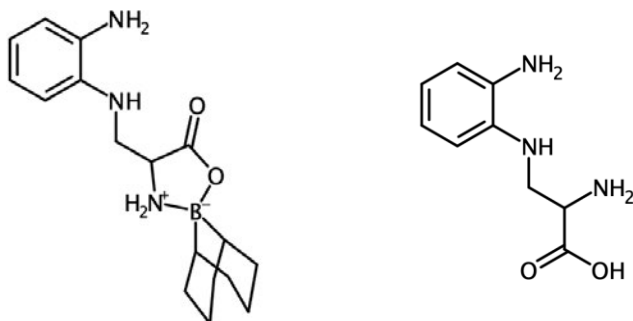
4'-{[(4-Methylbenzenesulfonyl)oxy]methyl}-5'-oxospiro[bicyclo[3.3.1]nonane-9,2'-[1,3]-oxazolidin]-3'-ium (0.1 g; 0.2 mmol) was solubilized in dry MeOH (20 ml) under dried conditions. Triethylamine (0.03 ml; 0.2 mmol; 1 eq) was added, followed by the addition of a solution of o-phenylenediamine (5 ml; 0.02 g in dry MeOH; 0.2 mmol; 1 eq) dropwise. The mixture was gently heated (40 ºC) for 9 hours and then refluxed for 15 hours monitored by TLC. The mixture was cooled, it was diluted with water (5 ml) and then DCM (20 ml) was added. The evaporation of the aqueous layer gave 2-amino-2-[(2-aminophenyl)amino]acetic acid (0.05 g, quantitative yield assuming purity) and the loss of the protecting group. Rf 0.97 (propanol: acetic acid: water (5:1:1)). ^{1}H-NMR (500 MHz, D$_2$O) δ (ppm): 2.59 (s, 3H); 3.75 (m, 1H); 3.88 (m, 2H); 6.75 (m, 4H).

6.3.23: 2-Amino-3-[2-(hydroxymethyl)-1H-1,3-benzodiazol-1-yl]propanoic acid attempt
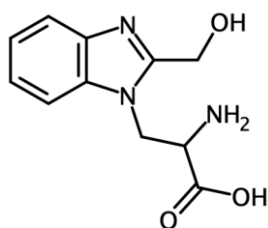
2-Amino-2-[(2-aminophenyl)amino]acetic acid (0.1 g; 0.4 mmol) was solubilized in HCl 2M (10 ml) followed by the addition of a solution of glycolic acid (0.06 g in 10 ml 2 M HCl, 1.5 eq) dropwise. After 3 hours refluxing, the mixture was cooled to room temperature and neutralized with 2 M NaOH, without observing precipitation. The product was extracted with EtOAc, the organic layer was dried over Na_2SO_4 and the solvent evaporated. The desired product was not isolated.

6.3.24: General procedure for the synthesis of propan-x-yl 4-methylbenzene-1-sulfonate

Alcohol (1 ml, 1 eq) was stirred in DCM (20 ml) for 5 minutes. Triethylamine (1.5 eq) was added on ice, dropwise, followed by the addition of DMAP (0.2 eq). The mixture was stirred on ice for 30 minutes and then at room temperature for 8 hours. Water (10 ml) was added and then 1 M HCl. The organic layer was washed with $NaHCO_3$ then brine, and dried over $MgSO_4$. Removal of the solvent gave the desired product.

6.3.24.1: Propyl 4-methylbenzene-1-sulfonate

Yellow oil (84% yield). Rf 0.87 (EtOAc:hexane 50%). ^{1}H-NMR (500 MHz, $CDCl_3$) δ (ppm): 0.87 (t, 3H, H1); 1.63 (m, 2H, H2); 2.42 (s, 3H); 3.98 (t, 2H); 7.35 (d, 2H); 7.77 (d, 2H). ^{13}C-NMR (125 MHz, $CDCl_3$): 10.0; 21.5; 22.4; 72.4; 127.0; 130.0; 133.3; 144.9.

6.3.24.2: Prop-2-yl 4-methylbenzene-1-sulfonate

Yellow oil (52% yield). Rf 0.85 (EtOAc:hexane 50%). ^{1}H NMR (500 MHz, CDCl$_3$) δ 7.65 (dd, J = 6.7, 4.9 Hz, 2H), 7.20 (m, 2H), 2.28 (d, J = 3.9 Hz, 3H), 1.11 (dt, J = 6.3, 3.2 Hz, 6H). ^{13}C NMR (125 MHz, CDCl$_3$) δ 144.4, 134.4, 129.8, 127.4, 77.0, 22.5, 21.3.

6.3.25: General procedure for the synthesis of N-propylbenzene-1,2-diamine

Propyl-p-toluenesulfonate (1.2 g, 1 eq) was stirred in MeOH (10 ml) for 5 minutes. Triethylamine (1 eq) was added dropwise followed by the addition of o-phenylenediamine solution (1 eq, in 5 ml MeOH). After 1 hour of gentle heating, the mixture was refluxed for 7 hours. Water (5 ml) and DCM (10 ml) were added. The organic layer was washed with 1 M HCl (10 ml). The aqueous layer was evaporated and the solid dissolved in MeOH. The solution was filtered and the filtrate was evaporated giving the desired product.

6.3.25.1: N1-propylbenzene-1,2-diamine
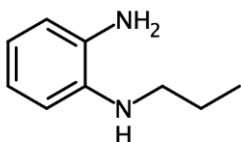
Brown oil (71% yield). Rf 0.8 (EtOAc: hexanes_2:1). ^{1}H-NMR (500 MHz, MeOD) δ (ppm): 1.05 (t, 3H, H1); 1.71 (m, 2H); 3.08 (t, 2H); 6.61 (m, 2H); 6.72 (m, 2H). ^{13}C-NMR (125 MHz, MeOD): 10.7; 22.2; 46.0; 116.0; 119.8; 137.3.

6.3.25.2: N1-(propan-2-yl)benzene-1,2-diamine
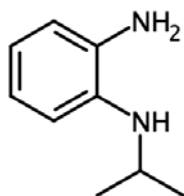
Brown oil (6% yield). Rf 0.8 (EtOAc: hexanes (2:1)). ^{1}H NMR (500 MHz, CDCl$_3$) δ 6.73 (ddd, J = 7.8, 7.1, 1.7 Hz, 1H), 6.69–6.53 (m, 3H), 3.52 (p, J = 6.2 Hz, 1H), 1.16 (d, J = 6.2 Hz, 6H). ^{13}C NMR (125 MHz, CDCl$_3$) δ 136.7, 134.5, 120.7, 118.5, 116.8, 113.0, 44.3, 23.1.

6.3.26: General procedure for the synthesis of (1-alkyl-1H-1,3-benzodiazol-2-yl)methanol

N1-Alkylbenzene-1,2-diamine (0.31 g, 1 eq) was stirred in 2 M HCl (25 ml) and then glycolic acid solution (1.5 eq, in 20 ml 2 M HCl) was added dropwise. The mixture was stirred for 24 hours, cooled down to room temperature and alkalized by adding 2 M NaOH (to pH 8). DCM and 0.5 M HCl were added and the two layers separated. The aqueous layer was washed with DCM and evaporated giving the desired product.

6.3.26.1: (1-Propyl-1H-1,3-benzodiazol-2-yl)methanol
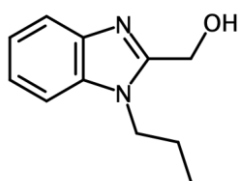
Red powder (95% yield). Rf 0.4 (EtOAc:MeOH; 9:1). Melting point 91-93 ºC. ^{1}H-NMR (500 MHz, MeOD) δ (ppm): 0.90 (t, 3H, H12); 1.87 (m, 2H, H11); 4.29 (t, 2H, H10); 5.15 (s, 2H, H13); 7.55 (m, 2H, H6,7); 7.71 (m, 1H, H5); 7.77 (m, 1H, H8). ^{13}C-NMR (125 MHz, MeOD): 10.3 (C12); 21.9 (C11); 46.7 (C10); 54.7 (C13); 112.7 (C5-8); 114.0 (C6-7); 129.8 (C4-9); 132.3 (C4-9); 152.2 (C2).

6.3.26.2: [1-(Prop-2-yl)-1H-1,3-benzodiazol-2-yl]methanol
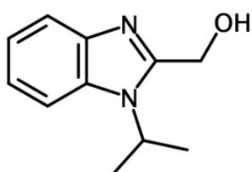
Brown oil (6% yield). Rf= 0.8 (EtOAc: hexanes (2:1)). ^{1}H NMR (500 MHz, CDCl$_3$) δ 6.73 (ddd, J = 7.8, 7.1, 1.7 Hz, 1H), 6.69 – 6.53 (m, 3H), 3.52 (p, J = 6.2 Hz, 1H), 1.16 (d, J = 6.3 Hz, 6H). ^{13}C NMR (125 MHz, CDCl$_3$) δ 136.73, 134.50, 120.67, 118.50, 116.82, 113.01, 44.34, 23.13.

6.3.26.3: (1-Propyl-1H-1,3-benzodiazol-2-yl)methyl acetate
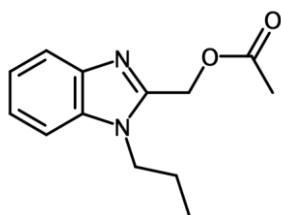
(1-Propyl-1H-1,3-benzodiazol-2-yl)methanol (0.05 g, 0.3 mmol) was stirred in acetic anhydride (5 ml, 176 eq) and sulfuric acid conc. was then added (1 drop per ml of Ac_2O). The mixture was refluxed for 4 hr and then it was cooled down to room temperature. Water (2 ml) was added and the product extracted in DCM. The organic layer was washed with 0.1 M NaOH, dried over $MgSO_4$ and the solvent evaporated giving (1-propyl-1H-1,3-benzodiazol-2-yl)methyl acetate (0.004 g, 6% yield). Rf 0.56 (EtOAc:MeOH; 9:1). ^{1}H-NMR (500 MHz, CDCl$_3$) δ (ppm): 0.92 (t, 3H, H12); 1.82 (m, 2H, H11); 2.07 (s, 3H, H15); 4.10 (t, 3H, H10); 5.31 (s, 2H,. H13); 7.24 (m, 2H, H6,7); 7.31 (d, 1H, H5); 7.72 (d, 1H, H8). ^{13}C-NMR (125 MHz, CDCl$_3$): 11.4 (C12); 20.7 (C11); 23.4 (C10); 45.8 (C13); 58.2 (C15); 109.9 (C5-8); 120.3 (C6-7); 122.5 (C4-9); 123.4 (C4-9); 142.3 (C2); 170.3 (C14).

6.3.27: General procedure for the synthesis of (1H-1,3-benzodiazol-2-yl)methanol

Ortho-phenylenediamine (10.09 g, 1 eq) and glycolic acid (1.5 eq) were dissolved in 2 M aqueous hydrochloric acid (90 ml). The mixture was adjusted to pH 2 and heated under reflux for 4 hours before cooling to room temperature. 2 M aqueous NaOH was added until the pH reached 8-9, with precipitation of the product observed from pH 7. After filtering the suspension, the powder was recrystallised from 50% ethanol:water giving (1H-1,3-benzodiazol-2-yl)methanol.

6.3.27.1: (1H-1,3-Benzodiazol-2-yl)methanol
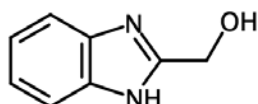
White crystals (83% yield), Rf 0.54 (EtOAc:MeOH 9:1). Melting point: 173-175 ºC. ^{1}H-NMR (500 MHz, DMSO-d$_6$): δ (ppm) 4.72 (s, 2H, H-10); 5.78 (s, 1H, OH); 7.13-7.14 (q, 2H, H5-8); 7.51 (s,

2H,H6-7); 12.36 (s, 1H, HN1). ^{13}C-NMR (125 MHz, DMSO-d$_6$): δ (ppm) 58.2 (C10); 112.1 (C6-7); 118.2 (C6-7); 121.8 (C5-8); 134.9(C4-9); 143.8 (C4-9); 155.5 (C2).

6.3.27.2: (5,6-Dimethyl-1H-1,3-benzodiazol-2-yl)methanol
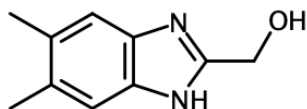
Beige solid (95% yield). Rf 0.26 (EtOAc:MeOH 9:1). Melting point: 253.2-255.2 ºC. ^{1}H NMR (500 MHz, DMSO) δ 12.04 (s, 1H), 7.25 (d, *J* = 49.8 Hz, 1H), 6.30 (s, 1H), 4.73 – 4.54 (m, 1H), 4.13 (s, H), 2.51 (p, *J* = 1.9 Hz, 3H), 1.98 (s, 3H). ^{13}C NMR (126 MHz, DMSO) δ 154.48, 133.08, 130.41, 124.23, 119.01, 117.04, 111.78, 58.22, 20.43, 19.08.

6.3.27.3: (5-Chloro-1H-1,3-benzodiazol-2-yl)methanol
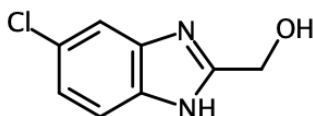
Brown solid (70% yield). Rf 0.45 (EtOAc:MeOH 9:1). Melting point: 206.1-208.1 ºC. ^{1}H NMR (500 MHz, DMSO) δ 12.50 (s, 1H), 7.66 – 7.36 (m, 2H), 7.16 (dd, *J* = 8.5, 2.1 Hz, 1H), 5.75 (t, *J* = 5.7 Hz, 1H), 4.69 (d, *J* = 5.5 Hz, 2H), 3.35 (s, 6H). ^{13}C NMR (126 MHz, DMSO) δ 157.15, 126.12, 122.01, 58.10.

6.3.27.4: (5-Nitro-1H-1,3-benzodiazol-2-yl)methanol
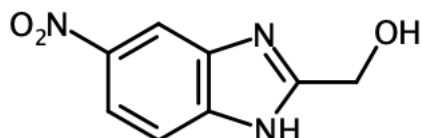
Dark brown solid (95% yield). Rf 0.45 (EtOAc:MeOH 9:1). Melting point: 127.4-129.4 ºC. ^{1}H NMR (500 MHz, DMSO) δ 8.55 – 8.30 (m, 1H), 8.09 (dd, *J* = 8.8, 2.3 Hz, 1H), 7.67 (d, *J* = 8.9 Hz, 1H), 5.94 (t, *J* = 5.8 Hz, 1H), 4.78 (d, *J* = 4.6 Hz, 2H).

6.3.27.5: 2-(Hydroxymethyl)-1H-1,3-benzodiazole-5-carboxylic acid
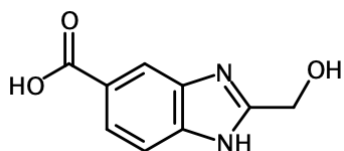
Grey solid (91% yield). Rf 0.10 (EtOAc:MeOH 9:1). Melting point: 317.9-319.9 ºC. ^{1}H NMR (500 MHz, D_2O) δ 8.15 (dd, J = 1.5, 0.7 Hz, 1H), 7.96 (dd, J = 8.7, 1.5 Hz, 1H), 7.63 (dd, J = 8.7, 0.7 Hz, 1H), 5.03 (s, 2H). ^{13}C NMR (125 MHz, D_2O) δ 169.4, 155.9, 133.7, 130.4, 127.9, 127.1, 115.9, 113.9, 55.4.

6.3.27.6: (5-Benzoyl-1H-1,3-benzodiazol-2-yl)methanol
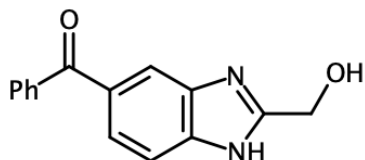
Beige solid (40% yield). Rf 0.39 (EtOAc:MeOH 9:1). Melting point: 249.7-251.7 ºC. ^{1}H NMR (500 MHz, DMSO-d_6) δ 8.06–8.02 (s, 1H), 7.90 (d, J = 8.5 Hz, 1H), 7.86 (dd, J = 8.6, 1.5 Hz, 1H), 7.74 (dd, J = 7.0, 1.3 Hz, 2H), 7.71–7.65 (m, 1H), 7.57 (t, J = 7.7 Hz, 2H), 5.07 (s, 2H). ^{13}C NMR (125 MHz, DMSO-d_6) δ 195.3, 157.8, 137.4, 134.5, 134.2, 133.3, 131.2, 130.1, 129.1, 127.3, 116.4, 114.6, 55.8.

6.3.28: General procedure for the synthesis of (1-acetyl-1H-1,3-benzodiazol-2-yl)methyl acetate

(1H-1,3-Benzodiazol-2-yl)methanol (5.01 g, 1 eq) was added to acetic anhydride (12 eq) and sulfuric acid (2 drops per ml of acetic anhydride) on ice. The mixture was heated under reflux for 4 hours. Product was extracted with ethyl acetate (3x20 ml) and washed with 5% aqueous sodium bicarbonate (2x20 ml). Removal of the solvent gave the desired product.

6.3.28.1: (1-Acetyl-1H-1,3-benzodiazol-2-yl)methyl acetate
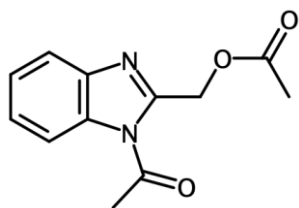
Light yellow crystals (53% yield). Rf 0.85 (EtOAc:MeOH 9:1). Melting point: 87-89 ºC. ^{1}H-NMR (500 MHz, CDCl$_3$): δ (ppm) 2.25 (s, 3H, H12); 2.86 (s, 3H, H14); 5.59 (s, 2H, H10); 7.41 (t, 2H,H6-7); 7.68 (d, 1H,H8); 7.82 (d, 1H,H5). ^{13}C-NMR (125 MHz, CDCl$_3$): δ (ppm) 20.8 (C12); 24.59 (C14); 61.4 (C10); 121.2 (C5); 124.7(C6-7); 132.1(C4-9); 142.2 (C4-9); 151.3 (C2); 168.8 (C13); 170.5 (C11).

6.3.28.2: (1-H-Benzimidazole-2yl)methyl acetate
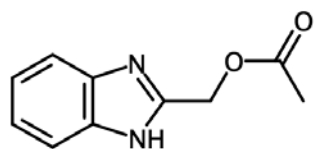
(1-Acetyl-1H-1,3-benzodiazol-2-yl)methyl acetate (0.30 g, 1.3 mmol, 1 eq) was solubilized in a mixture of dried DCM (20.0 ml) and methanol (40 ml) and stirred at room temperature. Sodium bicarbonate (4 g, 48 mmol, 30 eq) was added and the reaction was run for 30 minutes. Reaction was monitored by TLC (EtOAc:MeOH 9:1) and, when completed, the mixture was washed with 1 M HCl (2x20.0ml) and the organic layer evaporated to give the desired product, (1-H-benzimidazole-2yl)methyl acetate, as white crystals (46% yield). Rf 0.76 (EtOAc:MeOH 9:1). Melting point: 153-155 ºC. H-NMR (500 MHz, DMSO-d$_6$): δ (ppm) 2.06 (s, 3H, H-12); 5.42 (s, 2H, H-10); 7.30 (m, 2H, H5-6); 7.63 (m, 2H, H4-7); 9.29 (s, 1H, N1-H). ^{13}C-NMR (125 MHz, DMSO-d$_6$): δ (ppm) 20.6 (C12); 59.8 (C10); 117.5 (C5-8); 121.2 (C6-7); 148.8 (C2); 171.0 (C11).

6.3.29: General procedure for the synthesis of (1H-1,3-benzodiazol-2-yl)methyl acetate

(1H-1,3-Benzodiazol-2-yl)methanol (1 g, 1 eq) was solubilized in DMSO (20 ml). Acetic anhydride (1 eq) was added dropwise and the mixture was stirred at room temperature until complete (5-24 h). The reaction mixture was diluted with water (10 ml) and the product extracted with DCM (3 x 15 ml). The combined organic layers were washed with water (2 x 30 ml), with brine (2 x 20 ml) and dried over $MgSO_4$. The solvent was removed giving the desired product.

6.3.29.1: (1-H-Benzimidazole-2yl)methyl acetate
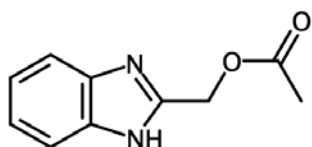
White crystals (60% yield). Rf= 0.76 (EtOAc:MeOH 9:1). Melting point: 153-155ºC. H-NMR (500 MHz, in DMSO-d_6): δ (ppm) 2.06 (s, 3H, H-12); 5.42 (s, 2H, H-10); 7.30 (m, 2H, H5-6); 7.63 (m, 2H, H4-7); 9.29 (s, 1H, N1-H). ^{13}C-NMR (125 MHz, DMSO-d_6): δ (ppm) 20.6 (C12); 59.8 (C10); 117.5 (C5-8); 121.2 (C6-7); 148.8 (C2); 171.0 (C11).

6.3.30: General procedure for esterification of glycolic acid

Glycolic acid (1.0 g, 13 mmol) was dissolved in alcohol (50 ml- methanol or ethanol) followed by the addition of sulfuric acid conc. (2 drops/ ml). The mixture was refluxed and the reaction was monitored by TLC. The reaction was quenched with NaHCO3 and the alcohol evaporated. The product was extracted with DCM (2 x 50 ml), the organic layer was washed with water (2 x 20 ml), brine (2 x 20 ml) and the solvent evaporated giving the desired product.

6.3.30.1: Methyl 2-hydroxyacetate
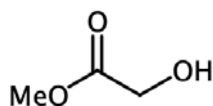
Transparent oil (1.0 g, 85% yield). ^{1}H NMR (500 MHz, CDCl$_3$) δ 4.03 (s, 2H), 3.61 (s, 3H).

6.3.30.2: Ethyl 2-hydroxyacetate
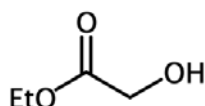
Light yellow oil (0.9 g, 65% yield). ^{1}H NMR (500 MHz, CDCl$_3$) δ 3.85 (q, *J* = 7.2 Hz, 2H), 1.30 (t, *J* = 7.1 Hz, 2H), 1.19 (t, *J* = 7.1 Hz, 3H).

6.3.31: General procedure for the tosylation of methyl/ethyl 2-hydroxyacetate

Esterified 2-hydroxyacetate (1.0 ml) was stirred in DCM (20 ml) for 5 minutes. Triethylamine (3.5 ml, 1.5 eq) was added on ice, dropwise, followed by the addition of DMAP (0.4 g, 0.2 eq). The mixture was stirred on ice for 30 minutes and then at room temperature for 8 hours. Water (10 ml) was added and then 1 M HCl. The product was extracted with DCM and the organic layer was washed with NaHCO$_3$ and brine, then dried over MgSO$_4$. Removal of the solvent gave the desired product.

6.3.31.1: Methyl 2-[(4-methylbenzenesulfonyl)oxy]acetate
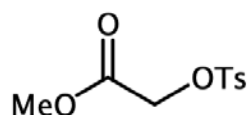
Transparent oil (74% yield). ^{1}H NMR (500 MHz, CDCl$_3$) δ 7.69 (dd, *J* = 8.2, 1.5 Hz, 2H), 7.26 (t, *J* = 6.8 Hz, 2H), 4.47 (d, *J* = 1.3 Hz, 2H), 3.59 (d, *J* = 1.8 Hz, 3H), 2.33 (s, 3H).

6.3.31.2: Ethyl 2-[(4-methylbenzenesulfonyl)oxy]acetate
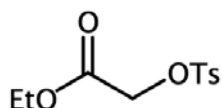
Light yellow oil (1.8 g, 73% yield). ^{1}H NMR (500 MHz, CDCl$_3$) δ 7.69 (d, *J* = 8.3 Hz, 2H), 7.24 (dd, *J* = 8.6, 0.8 Hz, 2H), 4.01 (dd, *J* = 5.8, 5.0 Hz, 2H), 2.35 (s, 3H), 1.91 (s, 3H).

6.3.32: General procedure for the synthesis of quinoxalin-2-ol
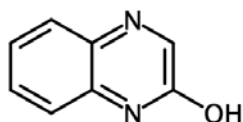
Methyl (or ethyl) 2-[(4-methylbenzenesulfonyl)oxy]acetate (1 g) was stirred in MeOH (10 ml) for 5 minutes. Triethylamine (1 eq) was added dropwise followed by the addition of o-phenylenediamine solution (1 eq, in 5 ml MeOH). After 1 hour of gentle heating, the mixture was refluxed for 7 hours. Water (5 ml) and DCM (10 ml) were added. The organic layer was washed with HCl 1 M (10 ml). The aqueous layer was evaporated and the solid dissolved in MeOH. The solution was filtered and the filtrate was evaporated giving the product (white powder, 0.6 g, 45% yield). Rf 0.7 (EtOAc:PE (1:2)).

6.3.33: N-(2-Hydroxyethyl)acetamide
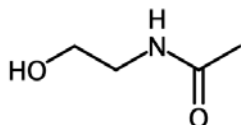
Ethanolamine (1 ml) was dissolved in DMSO (10 ml) and the acetic anhydride (1.2eq) was added. The reaction was stirred at room temperature for 24h. The reaction was monitored by TLC. The mixture was diluted with water and the product extracted with DCM (2 x 20 ml). The organic layer was washed with water (2 x 10 ml), brine (1 x 10 ml) and finally dried over MgSO$_4$. The solvent was removed giving N-(2-hydroxyethyl)acetamide as a yellow solid (1 g, 62% yield). Rf 0.6 (EtOAc:PE (1:2)). ^{1}H NMR (500 MHz, D$_2$O) δ 3.74 (s, 1H), 3.41 (t, J = 5.6 Hz, 2H), 2.12 (s, 3H).

6.3.34: N-{2-[(4-Methylbenzenesulfonyl)oxy]ethyl}acetamide attempt
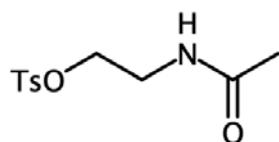
N-(2-Hydroxyethyl)acetamide (1.0 g) was stirred in DCM (20 ml) for 5 minutes. Triethylamine (1.5 eq) was added on ice, dropwise, followed by the addition of DMAP (0.2 eq). The mixture was stirred on ice for 30 minutes and then at room temperature for 8 hours. Water (10 ml) was added and then 1 M HCl. The product was extracted with DCM and the organic layer was washed

with NaHCO$_3$ then brine, and dried over MgSO$_4$. The solvent was removed and the desired product isolated as a yellow solid (1.1 g, 40% yield).

6.3.35: (2,2-Dimethyl-1,3-dioxolan-4-yl)methanol
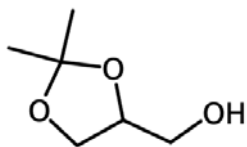
Glycerol (0.5 g) was dissolved in acetone (20 ml) and sulfuric acid conc. (20 drops) was added on ice. The mixture was stirred on ice for 7h and then left at room temperature overnight. The reaction was monitored by TLC. The mixture was diluted with water and neutralized with sodium bicarbonate. The product was extracted with CHCl$_3$ (30 ml) and the organic layer washed with brine (1 x 20 ml). The solvent was removed giving (2,2-dimethyl-1,3-dioxolan-4-yl)methanol, as a transparent oil (0.4 g, 57% yield). Rf 0.7 (EtOAc:PE (1:2)).

6.3.36: (2,2-Dimethyl-1,3-dioxolan-4-yl)methyl 4-methylbenzene-1-sulfonate
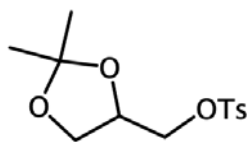
(2,2-Dimethyl-1,3-dioxolan-4-yl)methanol (0.5 g) was stirred in DCM (20 ml) for 5 minutes. Triethylamine (1.5 eq) was added on ice, dropwise, followed by the addition of DMAP (0.2 eq). The mixture was stirred on ice for 30 minutes and then at room temperature for 8 hours. Water (10 ml) was added and then 1 M HCl. The organic layer was washed with NaHCO$_3$ then brine, and dried over MgSO$_4$. Removal of the solvent gave (2,2-dimethyl-1,3-dioxolan-4-yl)methyl 4-methylbenzene-1-sulfonate as a yellow oil (0.6 g, 55% yield). Rf 0.9 (EtOAc:PE (1:2)).

6.3.37: N1-[(2,2-Dimethyl-1,3-dioxolan-4-yl)methyl]benzene-1,2-diamine
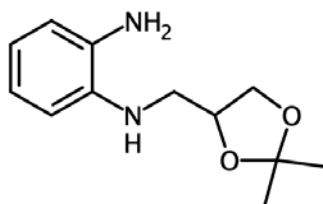
(2,2-Dimethyl-1,3-dioxolan-4-yl)methanol (1.0 ml) was stirred in MeOH (10 ml) for 5 minutes. Triethylamine (0.8 ml, 1 eq) was added dropwise followed by the addition of o-phenylenediamine solution (1 eq, in 5 ml MeOH). After 1 hour of gentle heating, the mixture was refluxed for 7 hours. The mixture was diluted with water (5 ml) and the product extracted with DCM (10 ml). The organic layer was washed with HCl 1 M (10 ml). The aqueous layer was dried over MgSO₄ and the solvent evaporated. Starting material was recovered.

6.3.38: (Chloromethyl)benzene
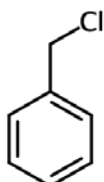
Benzyl-alcohol (1 ml, 1eq) was stirred in DCM (20 ml) for 5 minutes. Triethylamine (1.5 eq) was added on ice, dropwise, followed by the addition of DMAP (0.2 eq). The mixture was stirred on ice for 30 minutes and then at room temperature for 8 hours. Water (10 ml) was added and then HCl 1M. The organic layer was washed with NaHCO3, brine and then dried over MgSO4. Removal of the solvent gave (chloromethyl)benzene as a transparent oil (1.0 g, 85% yield). ^{1}H NMR (500 MHz, CDCl₃) δ 7.23 (ddt, J = 12.7, 5.8, 1.3 Hz, 1H), 4.43 (d, J = 2.2 Hz, 1H). ^{13}C NMR (125 MHz, CDCl₃) δ 137.6, 128.8, 46.4.

6.3.39: N-Benzyl benzene-1,2-diamine
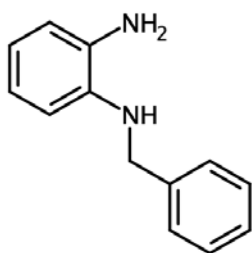
(Chloromethyl)benzene (1 ml) was stirred in MeOH (10 ml) for 5 minutes. Triethylamine (1 eq) was added dropwise followed by the addition of o-phenylenediamine solution (1 eq, in 5 ml MeOH). After 1 hour of gentle heating, the mixture was refluxed for 7 hours. Water (5 ml) and DCM (10 ml) were added. The organic layer was washed with 1 M HCl (10 ml). The aqueous layer was evaporated and the solid dissolved in MeOH. The solution was filtered and the filtrate was evaporated giving N-benzyl benzene-1,2-diamine as a brown oil (0.5 g, 33% yield). ^{1}H NMR (500 MHz, CDCl$_3$) δ 7.38 – 7.04 (m, 9H), 4.19 (s, 2H). ^{13}C NMR (125 MHz, CDCl$_3$) δ 139.2, 137.2, 137.0, 129.1, 128.7, 128.0, 123.0, 119.7, 118.0, 116.5, 112.6, 104.6, 57.1.

6.3.40: (1-Benzyl-1H-1,3-benzodiazol-2-yl)methanol
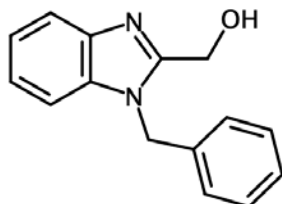
N-Benzyl benzene-1,2-diamine (1 g, 1 eq) was stirred in 2 M HCl (25 ml) and then glycolic acid solution (1.5 eq, in 20 ml 2 M HCl) was added dropwise. The mixture was stirred for 24 hours, cooled down to room temperature and alkalized by adding 2 M NaOH (to pH 8). DCM and 0.5 M HCl were added and the two layers separated. The aqueous layer was washed with DCM (2 x 20 ml), the organic layers combined and washed with brine (1 x 15 ml). The organic phase was dried over MgSO$_4$ and the solvent evaporated giving (1-benzyl-1H-1,3-benzodiazol-2-yl)methanol as a white solid (0.3 g, 25% yield). Rf 0.8 (EtOAc:PE (1:2)). Melting point 178.9-181.9 ºC. ^{1}H NMR (500 MHz, CDCl$_3$) δ 7.76 (d, J = 7.5 Hz, 1H), 7.42–7.23 (m, 6H), 7.14 (dd, J = 7.4, 2.1 Hz, 2H), 5.51 (s, 2H), 4.95 (s, 2H). ^{13}C NMR (125 MHz, CDCl$_3$) δ 135.2, 129.1, 128.2, 126.6, 123.8, 123.2, 118.9, 110.4, 56.9, 47.5.

6.3.41: General procedure for the synthesis of the synthesis of 2-phenyl-1H-1,3-benzodiazole-attempt 1

Ortho-phenylenediamine (1 g, 1 eq) and benzoic acid (1.5 eq) were dissolved in 2 M aqueous hydrochloric acid (90 ml). The mixture was adjusted to pH 2 and heated under reflux for 24 hours before cooling to room temperature. The mixture was neutralized with NaOH (2 M aqueous). In case of no precipitation, the product was extracted with EtOAc, the organic layer was washed with water (2 x 30 ml) and finally with brine (1 x 20 ml). The organic layer was dried over $MgSO_4$ and the solvent removed. Starting materials were recovered.

6.3.42: General procedure for the synthesis of the synthesis of 2-phenyl-1H-1,3-benzodiazole-attempt 2

Ortho-phenylenediamine (1g, 1 eq) and benzoic acids (1.5 eq) were dissolved in water (90 ml). NH_4Cl was then added and the mixture was refluxed for 24 hours. The mixture was diluted with water and the product was extracted with EtOAc. The organic layer was washed with water (2 x 30 ml) and finally with brine (1 x 20 ml). The organic layer was dried over $MgSO_4$ and the solvent removed. Starting materials were recovered.

6.3.43: General procedure for the synthesis of N-(phenylmethylidene)benzene-1,2-diamines

o-Phenylenediamine (5 g, 1 eq) and benzaldehyde (1 eq) were dissolved in ethanol (70 ml). Glacial acetic acid (20 drops) was added dropwise and then the mixture was refluxed for 1 hour. The reaction mixture was cooled down to room temperature and poured into ice-water (70 ml). The precipitated product was filtered out, washed with water (2 x 30 ml) and dried giving the desired product in a complex mixture (20-57% yield). The crude product was used in the subsequent reduction step.

6.3.44: General procedure for the synthesis of N1-benzylbenzene-1,2-diamines

N-(Phenylmethylidene)benzene-1,2-diamine (3.0 g) was dissolved in dry methanol (10% solution) under inert atmosphere and stirred at room temperature for 10 minutes. Sodium borohydride ($NaBH_4$, 1 eq) was added in portions and the reaction mixture was refluxed for 15 minutes. The mixture was cooled down to room temperature and poured into ice-water (100 ml) while stirring. The solid was filtered off and washed with water (2 x 20 ml) giving the desired product in a complex mixture. The crude product was used in subsequent steps of reaction.

6.3.44.1: N1-[(4-Bromophenyl)methyl]benzene-1,2-diamine
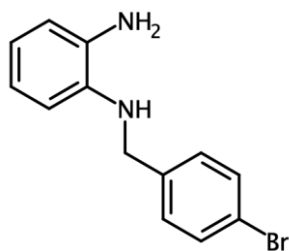
Red solid, complex mixture of products. ^{1}H NMR (500 MHz, CDCl$_3$) δ 7.16–7.06 (m, 2H), 6.98 (d, 2H), 6.87–6.76 (m, 2H), 6.76–6.70 (m, 2H), 5.40 (s, 2H).

6.3.44.2: N1-[(3-Nitrophenyl)methyl]benzene-1,2-diamine
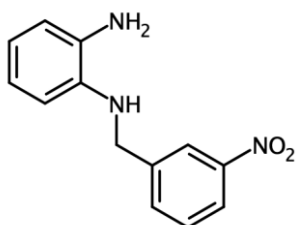
Red solid, complex mixture of products. ^{1}H NMR (500 MHz, CDCl$_3$) δ 8.06 (dd, J = 8.5, 4.8 Hz, 1H), 7.63–7.53 (m, 2H), 7.44 (q, J = 7.0 Hz, 1H), 7.29 (d, J = 5.1 Hz, 1H), 6.84–6.69 (m,2H), 6.54–6.46 (m, 1H), 4.92–4.67 (m, 2H).

6.3.44.3: N1-[(4-Methoxyphenyl)methyl]benzene-1,2-diamine
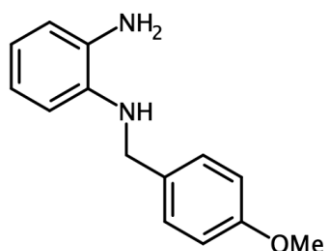
Yellow solid, complex mixture of products. ^{1}H NMR (500 MHz, CDCl$_3$) δ 7.55 (d, J = 8.8 Hz, 1H), 7.23 (d, J = 8.5 Hz, 2H), 6.88 (d, J = 8.8 Hz, 1H), 6.80 (d, J = 8.6 Hz, 2H), 6.66 – 6.58 (m, 2H).

6.3.44.4: N1-[(4-Chlorophenyl)methyl]benzene-1,2-diamine
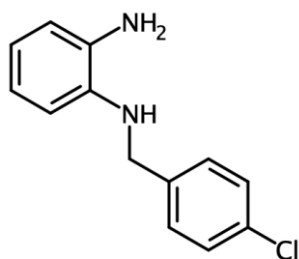
Yellow solid (35% yield)- complex mixture of products.

6.3.44.5: N1-[(4-Fluorophenyl)methyl]benzene-1,2-diamine
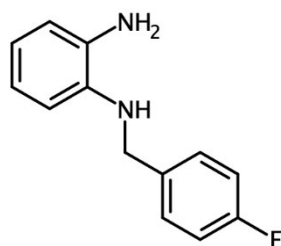
Yellow solid, complex mixture of products.

6.3.44.6: 3-{[(2-Aminophenyl)amino]methyl}phenol
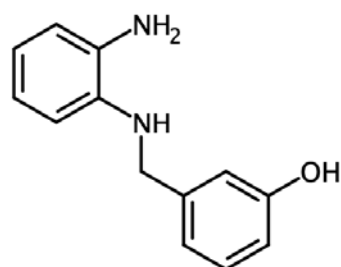
Beige solid, complex mixture of products.

6.3.45: General procedure for the synthesis of (1-benzyl-1H-1,3-benzodiazol-2-yl)methanol and 2-phenyl-1H-1,3-benzodiazole: ''2 products in 1 pot''

N-benzyl benzene-1,2-diamines mixture (1eq) and glycolic acid (1.5 eq) were dissolved in 2 M HCl (30 ml). The mixture was refluxed for 24 h. The formation of a gum was observed. The liquid was decanted when hot giving the (1-benzyl-1H-1,3- benzodiazol-2-yl)methanol derivative as a solid which was filtered and washed with water (1 x 3 ml) then petroleum ether (2 x 10 ml). In case of no precipitation, the solution was cooled down to room temperature and neutralized

with 2 M NaOH. The resulting solid was filtered, washed with water (1 x 3 ml) then petroleum ether (2 x 10 ml) giving the (1-benzyl-1H-1,3-benzodiazol-2-yl)methanol. The gum was triturated in ethyl acetate or acetone (12 hr) and the resulting solid washed with petroleum ether (2 x 30 ml) giving the desired product, 2-phenyl-1H-1,3-benzodiazole. In case of impurities, the solid was refluxed in 2 M HCl (12 hr), the solid filtered and washed with water then petroleum ether giving 2-phenyl-1H-1,3-benzodiazole.

6.3.45.1: (1-Benzyl-1H-1,3-benzodiazol-2-yl)methanol
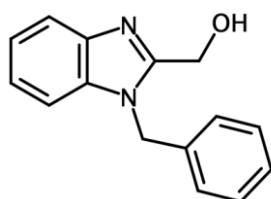
Beige solid (3% yield). Rf 0.8 (EtOAc:PE (1:2)). Melting point 178.9-181.9 ºC. ^{1}H NMR (500 MHz, CDCl$_3$) δ 7.76 (d, J = 7.5 Hz, 1H), 7.42 – 7.23 (m, 6H), 7.14 (dd, J = 7.4, 2.1 Hz, 2H), 5.51 (s, 2H), 4.95 (s, 2H). ^{13}C NMR (125 MHz, CDCl$_3$) δ 135.2, 129.1, 128.2, 126.6, 123.8, 123.2, 118.9, 110.4, 56.9, 47.5.

6.3.45.2: (1-[(4-Bromophenyl)methyl]-1*H*-1,3-benzodiazol-2-yl)methanol
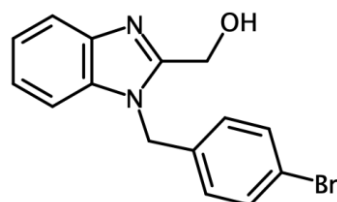
White solid (2% yield). Rf 0.57 (EtOAc:PE (1:2)). Melting point 84.3-86.3 ºC. ^{1}H NMR (500 MHz, DMSO) δ 7.64–7.57 (m, 1H), 7.56–7.45 (m, 2H), 7.40–7.33 (m, 1H), 7.23–7.13 (m, 4H), 5.54 (s, 2H), 4.74 (s, 2H). ^{13}C NMR (125 MHz, DMSO) δ 154.3, 142.4, 136.9, 135.7, 131.9, 129.5, 123.0, 122.2, 119.6, 111.0, 57.0, 46.5.

6.3.45.3: {1-[(4-Chlorophenyl)methyl]-1H-1,3-benzodiazol-2-yl}methanol
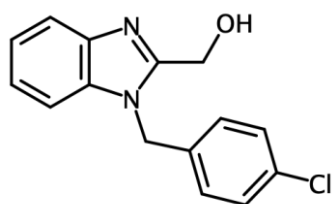
White solid (3% yield). Rf 0.54 (EtOAc:PE (1:2)). Melting point 168.4-170.4 °C. ^{1}H NMR (500 MHz, DMSO) δ 7.70–7.59 (m, 1H), 7.52 (dd, J = 8.4, 2.0 Hz, 2H), 7.38 (dt, J = 7.1, 2.3 Hz, 1H), 7.23 – 7.15 (m, 4H), 5.55 (d, J = 2.0 Hz, 2H), 4.74 (d, J = 2.0 Hz, 2H). ^{13}C NMR (126 MHz, DMSO) δ 154.34, 142.49, 137.0, 135.8, 132.0, 129.7, 122.9, 122.2, 121.0, 119.6, 111.0, 57.0, 46.5.

6.3.45.4: 4-{[2-(Hydroxymethyl)-1H-1,3-benzodiazol-1-yl]methyl}phenol
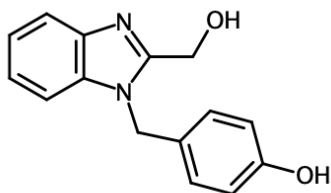
White solid (5% yield). Rf 0.26 (EtOAc:PE (1:2)). Melting point 195.7-197.7 °C. ^{1}H NMR (500 MHz, DMSO-d$_6$) δ 12.25 (s, 1H), 9.22 (s, 1H), 7.52–7.46 (m, 0H), 7.37 (d, J = 8.2 Hz, 1H), 7.26 (s, 1H), 7.13 (dd, J = 6.0, 3.2 Hz, 2H), 7.04–6.99 (m, 2H), 6.97 (dd, J = 8.3, 1.6 Hz, 1H), 6.70–6.62 (m, 2H), 4.65 (s, 2H), 3.89 (s, 2H). ^{13}C NMR (125 MHz, DMSO-d$_6$) δ 155.9, 130.0, 115.6, 58.2.

6.3.45.5: {1-[(4-Fluorophenyl)methyl]-1H-1,3-benzodiazol-2-yl}methanol
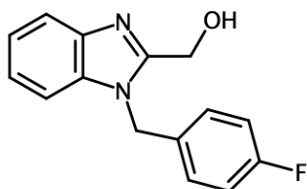
White solid (14% yield). Rf 0.91 (EtOAc:PE (1:2)). Melting point 96.7-98.7 °C

6.3.45.6: 3-{[2-(Hydroxymethyl)-1H-1,3-benzodiazol-1-yl]methyl}phenol
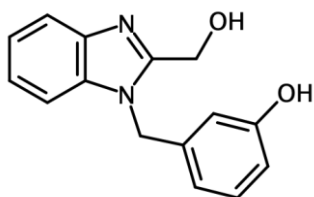
White solid (5% yield). Rf 0.82 (EtOAc:PE (1:2). Melting point 186.2-188.2 ºC. ^{1}H NMR (500 MHz, DMSO-d$_6$) δ 9.48 (s, 1H), 7.67–7.58 (m, 1H), 7.44–7.28 (m, 1H), 7.27–7.15 (m, 2H), 7.11 (t, J = 7.8 Hz, 1H), 6.65 (td, J = 8.1, 1.9 Hz, 2H), 6.53 (t, J = 2.0 Hz, 1H), 5.49 (s, 2H), 4.71 (s, 2H). ^{13}C NMR (125 MHz, DMSO-d$_6$) δ 158.1, 154.4, 142.5, 138.9, 136.0, 130.1, 122.8, 122.0, 119.6, 117.8, 114.9, 114.0, 111.0, 57.1, 46.9.

6.3.45.7: 2-Ethoxy-4-{[2-(hydroxymethyl)-1H-1,3-benzodiazol-1-yl]methyl}phenol
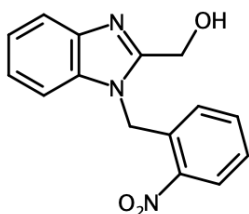
Brown solid (3% yield). Rf 0.35 (EtOAc:PE (1:2). Melting point 162.1-164.1 ºC. ^{1}H NMR (500 MHz, DMSO-d$_6$) δ 8.24–8.18 (m, 1H), 7.68 (d, J = 7.8 Hz, 1H), 7.63–7.49 (m, 2H), 7.43–7.38 (m, 1H), 7.26–7.14 (m, 2H), 6.44–6.37 (m, 1H), 5.97 (s, 2H), 4.71–4.67 (m, 2H). ^{13}C NMR (125 MHz, DMSO-d$_6$) δ 154.7, 147.6, 142.4, 135.9, 134.8, 133.4, 129.0, 127.6, 125.6, 123.2, 122.5, 119.7, 111.0, 57.2, 44.9.

6.3.45.8:{1-[(4-Methoxyphenyl)methyl]-1H-1,3-benzodiazol-2-yl}methanol
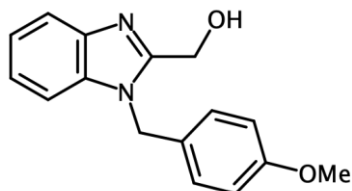
Beige solid (15% yield). Rf 0.97 (EtOAc:PE (1:2). Melting point 90.1-92.1 ºC. ^{1}H NMR (500 MHz, CDCl$_3$) δ 7.76 (s, 1H), 7.56 (d, J = 8.2 Hz, 2H), 7.16–7.11 (m, 2H), 7.00 (s, 1H), 6.93 (s, 2H), 5.29 (t, J = 4.8 Hz, 2H), 5.19 (d, J = 3.8 Hz, 2H), 3.75 (d, J = 5.1 Hz, 3H).

6.3.46: General procedure for the synthesis of 2-phenyl-1H-1,3-benzodiazole- attempt-1

Ortho-phenylenediamine (1 g, 1 eq) and benzoic acid (1.5 eq) were dissolved in 2 M aqueous hydrochloric acid (90 ml). The mixture was adjusted to pH 2 and heated under reflux for 4-7 hours before cooling to room temperature. The mixture was neutralized without observing any product precipitation. Ethyl acetate was then added and the organic phase washed with water (2 x 30 ml) and then brine (1 x 30 ml). The organic layer was dried over $MgSO_4$ and the solvent removed. The desired product was not isolated. Starting materials were recovered.

6.3.47: General procedure for the synthesis of 2-phenyl-1H-1,3-benzodiazole- attempt-2

Ortho-phenylenediamine (1 g, 1 e q) and benzoic acid (1.5 eq) were dissolved in ethanol (50 ml). NH_4Cl (1.5eq) was added and the mixture was refluxed for 4 hours. The reaction mixture was cooled down to room temperature and diluted with water. Ethyl acetate was added and the phases separated. The organic layer was washed with water (2 x 35 ml), brine (1 x 30 ml) and then dried over $MgSO_4$. The solvent was removed without isolating the desired product. Starting materials were recovered.

6.3.48: General procedure for the selective synthesis of 2-substituted-1H-1,3-benzodiazole

Ortho-phenylenediamine (1 g, 1 eq) and benzoic acid (1 eq) were dissolved in ethanol (70 ml). Sodium metabisulfite (1 eq) was added in portions and the mixture refluxed for 24 hours. The reaction mixture was cooled down to room temperature and poured into stirring water (200 ml). The solid product was filtered off and washed with water (2 x 50 ml) and then with petroleum ether (3 x 50 ml) giving the desired product as solid. Where product formed as a gum, the water was decanted and the gum triturated in acetone or petroleum ether. Where the product was isolated as complex mixture, the solid was refluxed in 2 M HCl for 24 hr. The mixture was cooled, the HCl decanted and the solid triturated in petroleum ether giving the desired product as a solid.

6.3.48.1: 2-Phenyl-1H-1,3-benzodiazole
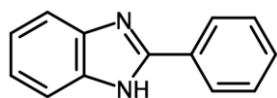
White solid (55% yield). Rf 0.85 (EtOAc:PE (1:2)).Melting point 290.1-292.1 ºC. ^{1}H NMR (500 MHz, DMSO-d$_6$) δ 8.42 (dd, J = 7.9, 1.8 Hz, 1H), 7.87 (dd, J = 6.1, 3.1 Hz, 1H), 7.78–7.69 (m, 1H), 7.57 (dd, J = 6.1, 3.1 Hz, 1H). ^{13}C NMR (125 MHz, DMSO-d$_6$) δ 149.2, 133.8, 132.5, 132.4, 130.1, 128.6, 126.4, 123.8, 114.5.

6.3.48.2: 2-(4-Bromophenyl)-1H-1,3-benzodiazole
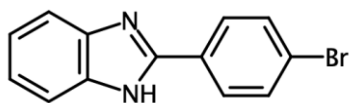
Beige solid (75% yield). Rf 0.77 (EtOAc:PE (1:2)). Melting point= 308.6-310.6 ºC. ^{1}H NMR (500 MHz, DMSO-d$_6$) δ 8.31 (d, J = 8.6 Hz, 1H), 7.97 (d, J = 8.6 Hz, 1H), 7.85 (dd, J = 6.1, 3.1 Hz, 1H), 7.56 (dd, J = 6.2, 3.1 Hz, 1H). ^{13}C NMR (125 MHz, DMSO-d$_6$) δ 148.55, 133.14, 133.06, 130.29, 127.36, 126.22, 123.68, 114.64.

6.3.48.3: 2-(4-Chlorophenyl)-1H-1,3-benzodiazole
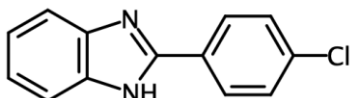
Pink solid (65% yield). Rf 0.87 (EtOAc:PE (1:2)). Melting point 327.5-329.5 ºC. ^{1}H NMR (500 MHz, DMSO-d$_6$) δ 8.38–8.29 (m, 1H), 8.00–7.94 (m, 1H), 7.86–7.83 (m, 1H), 7.56 (ddd, J = 6.1, 3.1, 1.4 Hz, 1H). ^{13}C NMR (125 MHz, DMSO-d$_6$) δ 148.5, 133.1, 133.0, 130.3, 127.4, 126.2, 123.6, 114.6.

6.3.48.4: 4-(1H-1,3-Benzodiazol-2-yl)phenol
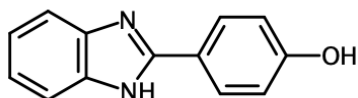
Pink solid (45% yield). Rf 0.71 (EtOAc:PE (1:2)). Melting point 327.5-329.5 ºC. ^{1}H NMR (500 MHz, DMSO-d$_6$) δ 8.34 (d, J = 8.8 Hz, 1H), 7.88 – 7.77 (m, 2H), 7.50 (dd, J = 6.1, 3.2 Hz, 1H), 7.11 (dd, J = 8.8, 3.1 Hz, 2H), 7.00 (d, J = 8.6 Hz, 1H), 6.73 (d, J = 8.6 Hz, 1H), 5.65 (s, 1H). ^{13}C NMR (125 MHz, DMSO-d$_6$) δ 163.0, 162.3, 157.8, 151.1, 149.4, 132.4, 131.9, 130.8, 128.6, 126.0, 117.0, 116.9, 116.2, 114.0.

6.3.48.5: 2-(4-Fluorophenyl)-1H-1,3-benzodiazole
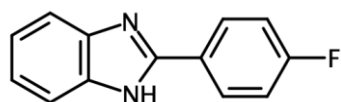
Yellow solid (55% yield). Rf 0.87 (EtOAc:PE (1:2)). Melting point 249.1-251.7 ºC. ^{1}H NMR (500 MHz, DMSO) δ 12.93 (s, 1H), 8.24 (ddd, J = 8.9, 5.4, 1.7 Hz, 2H), 7.61 (s, 2H), 7.45 – 7.34 (m, 2H), 7.21 (dd, J = 6.1, 3.1 Hz, 2H). ^{13}C NMR (125 MHz, DMSO-d$_6$) δ 164.5, 162.6, 150.9, 129.2, 129.2, 127.3, 127.3, 116.6, 116.4

6.3.48.6: 3-(1H-1,3-Benzodiazol-2-yl)phenol
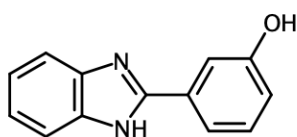
White solid (57% yield). Rf 0.65 (EtOAc:PE (1:2)). Melting point 249.1-251.7 ºC.

6.3.48.7: 4-(1H-1,3-Benzodiazol-2-yl)-2-ethoxyphenol
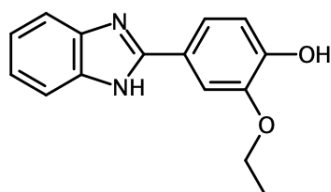
Beige solid (25% yield). Rf 0.87 (EtOAc:PE (1:2)). Melting point 249.1-251.7 ºC.

6.3.48.8: 2-(2-Nitrophenyl)-1H-1,3-benzodiazole
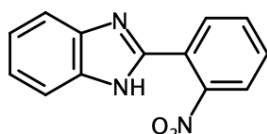
Beige solid (40% yield). Rf 0.77 (EtOAc:PE (1:2)). Melting point 307.2-309.2 ºC. ^{1}H NMR (500 MHz, DMSO-d$_6$) δ 8.38 (dd, J = 8.2, 1.3 Hz, 1H), 8.17 – 8.10 (m, 1H), 8.10 – 8.05 (m, 1H), 8.04 – 7.96 (m, 1H), 7.88 (dd, J = 6.2, 3.2 Hz, 2H), 7.57 (dd, J = 6.1, 3.2 Hz, 2H). ^{13}C NMR (126 MHz, DMSO-d$_6$) δ 148.06, 146.93, 134.82, 133.98, 133.43, 133.37, 126.04, 126.01, 120.26, 115.09.

6.3.48.9: 2-(3-Nitrophenyl)-1H-1,3-benzodiazole
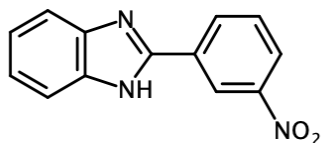
Yellow solid (40% yield). Rf 0.87 (EtOAc:PE (1:2)). Melting point 249.1-251.7 ºC.

6.3.48.10: 2-(Thiophen-2-yl)-1H-1,3-benzodiazole
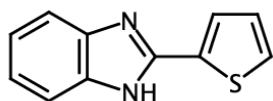
Light green solid (81% yield). Rf 0.85 (EtOAc:PE (1:2)). Melting point 307.2-309.2 ºC ^{1}H NMR (500 MHz, DMSO) δ 8.48 (dd, J = 3.8, 1.2 Hz, 1H), 8.15 (dd, J = 4.9, 1.2 Hz, 1H), 7.77 (dd, J = 6.1, 3.2 Hz, 2H), 7.50 (dd, J = 6.1, 3.2 Hz, 2H), 7.41 (dd, J = 5.0, 3.8 Hz, 1H). ^{13}C NMR (126 MHz, DMSO) δ 144.32, 134.83, 134.02, 132.39, 129.60, 126.11, 125.37, 114.21.

6.3.48.11: 2-(1H-Pyrrol-2-yl)-1H-1,3-benzodiazole
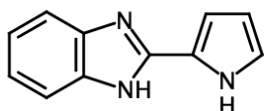
Beige solid (80% yield).). Rf= 0.85 (EtOAc: petroleum ether (1:2)). Melting point= 151.1-153.1 ºC. ^{1}H NMR (500 MHz, DMSO) δ 11.78 (s, 1H), 7.52 (dd, J = 5.9, 3.2 Hz, 2H), 7.17 (dd, J = 6.0, 3.2 Hz, 2H), 6.99 (t, J = 2.0 Hz, 1H), 6.92 – 6.87 (m, 1H), 6.25 – 6.20 (m, 1H).

6.3.48.12: 5-chloro-2-phenyl-1H-1,3-benzodiazole
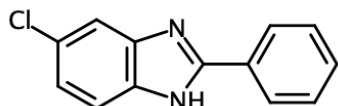
Light grey solid (56% yield). Rf= 0.89 (EtOAc: petroleum ether (1:2)). Melting point= 307.0-309.0 ºC.

6.3.48.13: 2-(4-bromophenyl)-5-chloro-1H-1,3-benzodiazole
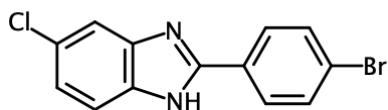
Light grey solid (67% yield). Rf= 0.93 (EtOAc: petroleum ether (1:2)). Melting point= 322.9-325.9 ºC.

6.3.48.14: 5-chloro-2-(4-chlorophenyl)-1H-1,3-benzodiazole
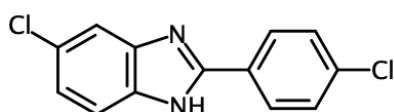
Light pink solid (59% yield). Rf= 0.92 (EtOAc: petroleum ether (1:2)). Melting point= 334.1-336.1 ºC. ^{1}H NMR (500 MHz, DMSO) δ 8.32 (d, J = 8.6 Hz, 2H), 7.83 (d, J = 2.0 Hz, 1H), 7.81 – 7.74 (m, 3H), 7.49 (dd, J = 8.7, 2.0 Hz, 1H). ^{13}C NMR (126 MHz, DMSO) δ 150.25, 137.78, 135.74, 133.59, 130.08, 129.93, 129.60, 125.65, 124.58, 116.28, 114.59.

### 6.3.48.15: 4-(5-chloro-1H-1,3-benzodiazol-2-yl)phenol
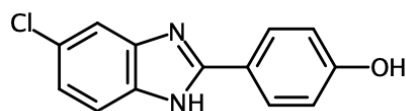
Pail green solid (41% yield). Rf= 0.88 (EtOAc: petroleum ether (1:2)). Melting point= 221.6-223.6 ºC. ^{1}H NMR (500 MHz, DMSO) δ 10.91 (s, 1H), 8.52 – 8.03 (m, 2H), 7.96 – 7.61 (m, 2H), 7.47 (dd, J = 8.6, 2.0 Hz, 1H), 7.21 – 6.93 (m, 2H). ^{13}C NMR (126 MHz, DMSO) δ 163.12, 150.56, 132.99, 131.07, 130.86, 130.08, 126.12, 116.96, 115.44, 113.59, 113.41.

6.3.48.16: 5-chloro-2-(4-fluorophenyl)-1H-1,3-benzodiazole
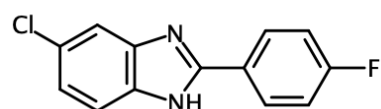
Yellow solid (62% yield). Rf= 0.91 (EtOAc: petroleum ether (1:2)). Melting point= 77.5-79.5 ºC.

^{1}H NMR (500 MHz, DMSO) δ 8.34 (ddd, *J* = 8.4, 5.0, 2.2 Hz, 2H), 7.84 – 7.74 (m, 3H), 7.66 – 7.59 (m, 1H), 7.38 (ddd, *J* = 9.6, 4.7, 2.5 Hz, 1H). ^{13}C NMR (126 MHz, DMSO) δ 130.10, 129.92, 116.15.

### 6.3.48.17: 5-chloro-2-(4-methoxyphenyl)-1H-1,3-benzodiazole
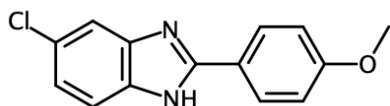
Grey solid (21% yield). Rf= 0.79 (EtOAc: petroleum ether (1:2)). Melting point= 285.7-287.7 ºC. ^{1}H NMR (500 MHz, DMSO) δ 8.42 – 8.23 (m, 2H), 7.97 – 7.67 (m, 2H), 7.53 (dd, *J* = 8.6, 2.0 Hz, 1H), 7.33 – 7.19 (m, 2H), 3.90 (d, *J* = 1.4 Hz, 3H). ^{13}C NMR (126 MHz, DMSO) δ 163.71, 150.56, 130.62 (d, *J* = 5.0 Hz), 129.98, 126.05, 115.67 (d, *J* = 10.0 Hz), 113.90, 56.29.

6.3.48.18: 3-(5-chloro-1H-1,3-benzodiazol-2-yl)phenol
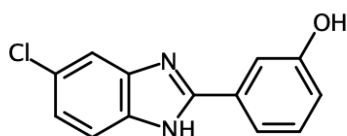
White solid (47% yield). Rf= 0.87 (EtOAc: petroleum ether (1:2)). Melting point= 290.9-292.9 ºC. ^{1}H NMR (500 MHz, DMSO) δ 13.02 (s, 1H), 9.77 (d, *J* = 2.3 Hz, 1H), 7.65 – 7.56 (m, 4H), 7.36 (s, 1H), 7.22 (dd, *J* = 8.5, 2.1 Hz, 1H), 6.93 – 6.90 (m, 1H). ^{13}C NMR (126 MHz, DMSO) δ 158.27, 153.24, 131.39, 130.53, 126.79, 122.75, 117.79, 113.89.

6.3.48.19: 4-(5-chloro-1H-1,3-benzodiazol-2-yl)-2-ethoxyphenol
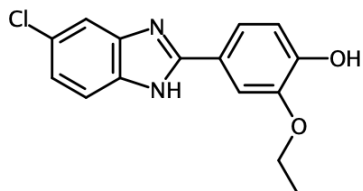
Brown solid (31% yield). Rf= 0.87 (EtOAc: petroleum ether (1:2)). Melting point= 280.3-282.3 ºC. ^{1}H NMR (500 MHz, DMSO) δ 8.02 (d, *J* = 2.2 Hz, 1H), 7.84 (dd, *J* = 8.4, 2.2 Hz, 1H), 7.81 (d, *J* = 2.0 Hz, 1H), 7.78 (d, *J* = 8.6 Hz, 1H), 7.53 (dd, *J* = 8.7, 2.0 Hz, 1H), 7.09 (d, *J* = 8.3 Hz, 1H), 4.20 (q, *J* =

7.0 Hz, 2H), 1.42 (t, *J* = 6.9 Hz, 3H). ^{13}C NMR (126 MHz, DMSO) δ 152.60, 151.02, 147.89, 133.61, 131.62, 129.92, 125.98, 122.65, 116.73, 115.52, 114.09, 113.73, 113.29, 64.86, 31.16, 15.10.

6.3.48.20: 5-chloro-2-(2-nitrophenyl)-1H-1,3-benzodiazole
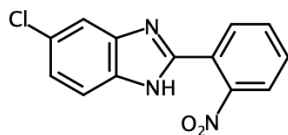
Light grey solid (20% yield). Rf= 0.75 (EtOAc: petroleum ether (1:2)). Melting point= 278.7-280.7 ºC. ^{1}H NMR (500 MHz, DMSO) δ 8.30 (dd, *J* = 8.1, 1.3 Hz, 1H), 8.10 (dd, *J* = 7.6, 1.5 Hz, 1H), 8.02 (td, *J* = 7.6, 1.3 Hz, 1H), 7.95 (td, *J* = 7.7, 1.5 Hz, 1H), 7.92 (d, *J* = 2.0 Hz, 1H), 7.84 (d, *J* = 8.7 Hz, 1H), 7.53 (dd, *J* = 8.8, 2.0 Hz, 1H). ^{13}C NMR (126 MHz, DMSO) δ 148.33 (d, *J* = 12.8 Hz), 135.54, 134.46, 133.54 (d, *J* = 13.1 Hz), 133.05, 129.72, 125.73 (d, *J* = 3.8 Hz), 120.86 (d, *J* = 4.0 Hz), 116.72.

6.3.48.21: 5-chloro-2-(3-nitrophenyl)-1H-1,3-benzodiazole
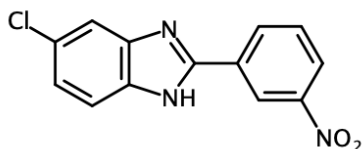
Grey solid (37% yield). Rf= 0.88 (EtOAc: petroleum ether (1:2)). Melting point= 223.1-225.1 ºC. ^{1}H NMR (500 MHz, DMSO) δ 9.03 (dt, *J* = 2.9, 1.9 Hz, 1H), 8.64 (dq, *J* = 8.0, 1.9 Hz, 1H), 8.40 (td, *J* = 2.5, 1.0 Hz, 1H), 7.90 (t, *J* = 8.0 Hz, 1H), 7.78 – 7.74 (m, 1H), 7.74 – 7.68 (m, 1H), 7.34 (dt, *J* = 8.4, 2.1 Hz, 1H). ^{13}C NMR (126 MHz, DMSO) δ 148.82, 133.37, 131.36, 121.82.

6.3.48.22: 5-chloro-2-(thiophen-2-yl)-1H-1,3-benzodiazole
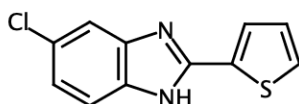
Grey solid (53% yield).). Rf= 0.89 (EtOAc: petroleum ether (1:2)). Melting point= 345.1-347.1 ºC. ^{1}H NMR (500 MHz, DMSO) δ 8.22 (dd, *J* = 3.8, 1.2 Hz, 1H), 8.03 (dd, *J* = 5.0, 1.2 Hz, 1H), 7.75 (d, *J* = 2.0 Hz, 1H), 7.71 (d, *J* = 8.7 Hz, 1H), 7.43 (dd, *J* = 8.6, 2.0 Hz, 1H), 7.36 (dd, *J* = 5.0, 3.7 Hz, 1H).

^{13}C NMR (126 MHz, DMSO) δ 146.84, 136.18, 133.93, 133.26, 131.90, 129.41, 129.07, 128.29, 125.10, 115.93, 114.37.

6.3.48.23: 5-chloro-2-(1H-pyrrol-2-yl)-1H-1,3-benzodiazole
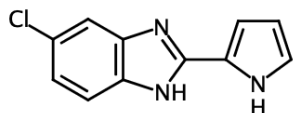
Beige solid (71% yield). Rf= 0.89 (EtOAc: petroleum ether (1:2)). Melting point= 160.4-162.4 ºC. ^{1}H NMR (500 MHz, DMSO) δ 11.81 (s, 1H), 7.54 (d, J = 2.1 Hz, 1H), 7.49 (d, J = 8.4 Hz, 1H), 7.16 (dd, J = 8.5, 2.1 Hz, 1H), 6.97 (d, J = 1.6 Hz, 1H), 6.88 (m, 1H), 6.22 (m, J = 3.6 Hz, 1H). ^{13}C NMR (126 MHz, DMSO) δ 148.51, 126.22, 122.49 – 121.61 (m), 114.57, 110.02 (d, J = 41.8 Hz).

6.3.48.24: 5-nitro-2-phenyl-1H-1,3-benzodiazole
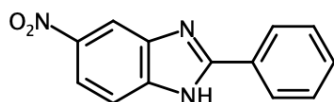
Yellow solid (40% yield). Rf= 0.89 (EtOAc: petroleum ether (1:2)). Melting point= 145.8-147.8 ºC. ^{1}H NMR (500 MHz, DMSO) δ 13.58 (s, 1H), 8.48 (s, 1H), 8.27 – 8.18 (m, 2H), 8.15 – 8.07 (m, 1H), 7.73 (s, 1H), 7.65 – 7.51 (m, 3H). ^{13}C NMR (126 MHz, DMSO) δ 143.14, 131.41, 129.58, 129.46, 127.59, 127.43.

6.3.48.25: 2-(4-bromophenyl)-5-nitro-1H-1,3-benzodiazole
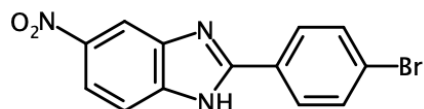
Green solid (43% yield). Rf= 0.92 (EtOAc: petroleum ether (1:2)). Melting point= 251.2-253.2 ºC. ^{1}H NMR (500 MHz, DMSO) δ 8.50 (d, J = 2.1 Hz, 1H), 8.23 – 8.19 (m, 2H), 8.18 (dd, J = 8.9, 2.1 Hz, 1H), 7.86 – 7.80 (m, 3H). ^{13}C NMR (126 MHz, DMSO) δ 154.80, 143.62, 132.77, 129.63, 127.73, 125.61, 119.09, 115.30, 112.37.

6.3.48.26: 2-(4-chlorophenyl)-5-nitro-1H-1,3-benzodiazole
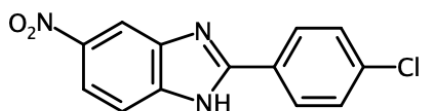
Pail orange solid (56% yield). Rf= 0.90 (EtOAc: petroleum ether (1:2)). Melting point= 294.5-296.5 ºC. ^{1}H NMR (500 MHz, DMSO) δ 8.44 (s, 1H), 8.16 (d, J = 8.6 Hz, 2H), 8.10 (dd, J = 8.9, 2.3 Hz, 1H), 7.76 – 7.70 (s, 1H), 7.63 (d, J = 8.6 Hz, 2H). ^{13}C NMR (126 MHz, DMSO) δ 143.25, 136.20, 129.70, 129.37, 129.09, 128.67, 128.18, 127.88, 118.67.

6.3.48.27: 4-(5-nitro-1H-1,3-benzodiazol-2-yl)phenol
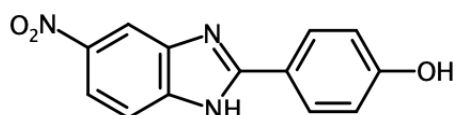
Orange solid (36% yield). Rf= 0.77 (EtOAc: petroleum ether (1:2)). Melting point= 314.9-316.9 ºC. ^{1}H NMR (500 MHz, DMSO) δ 13.41 (s, 1H), 10.30 (s, 1H), 8.41 (s, 1H), 8.26 – 7.88 (m, 3H), 7.69 (s, 1H), 6.99 – 6.92 (m, 2H). ^{13}C NMR (126 MHz, DMSO) δ 160.60, 131.39, 129.33, 128.00, 120.33, 118.15, 116.38, 116.20, 116.09.

6.3.48.28: 2-(4-fluorophenyl)-5-nitro-1H-1,3-benzodiazole
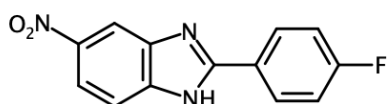
Yellow solid (57% yield). Rf= 0.77 (EtOAc: petroleum ether (1:2)). Melting point= 249.7-251.7 ºC. ^{1}H NMR (500 MHz, DMSO) δ 13.56 (s, 1H), 8.48 (s, 1H), 8.27 – 8.18 (m, 2H), 8.14 – 7.97 (m, 1H), 7.69 (s, 1H), 7.47 – 7.38 (m, 2H). ^{13}C NMR (126 MHz, DMSO) δ 165.11, 163.13, 143.14, 129.84, 126.10, 126.07, 118.63, 116.77, 116.59, 115.35, 112.18.

6.3.48.29: 2-(4-methoxyphenyl)-5-nitro-1H-1,3-benzodiazole
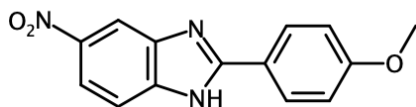
Orange solid (21% yield). Rf= 0.77 (EtOAc: petroleum ether (1:2)). Melting point= 307.2-309.2 ºC. ^{1}H NMR (500 MHz, DMSO) δ 8.34 (d, J = 2.3 Hz, 1H), 8.07 – 7.99 (m, 3H), 7.63 (d, J = 8.9 Hz, 1H), 7.10 – 7.00 (m, 2H), 3.79 (s, 3H). ^{13}C NMR (126 MHz, DMSO) δ 161.88, 156.30, 142.85, 129.07, 128.85, 128.73, 128.65, 121.42, 118.28, 115.10, 114.93, 114.14, 55.85, 55.78, 55.42.

6.3.48.30: 3-(5-nitro-1H-1,3-benzodiazol-2-yl)phenol
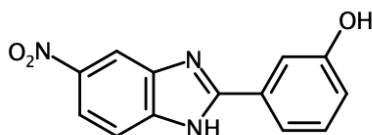
Yellow solid (37% yield). Rf= 0.82 (EtOAc: petroleum ether (1:2)). Melting point= 301.9-303.9 ºC. ^{1}H NMR (500 MHz, DMSO) δ 13.55 (s, 1H), 9.96 (s, 1H), 8.46 (s, 1H), 8.10 (d, J = 2.3 Hz, 1H), 7.73 (s, 1H), 7.64 – 7.59 (m, 2H), 7.39 (t, J = 7.9 Hz, 1H), 7.01 – 6.94 (m, 1H). ^{13}C NMR (126 MHz, DMSO) δ 158.30, 143.13, 130.76, 130.59, 118.60, 118.19, 114.17.

6.3.48.31: 2-ethoxy-4-(5-nitro-1H-1,3-benzodiazol-2-yl)phenol
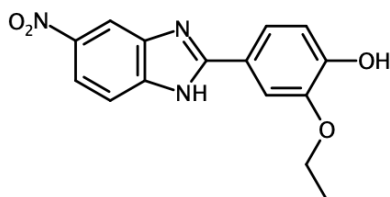
Beige solid (23% yield). Rf= 0.77 (EtOAc: petroleum ether (1:2)). Melting point= 307.2-309.2 ºC. ^{1}H NMR (500 MHz, DMSO) δ 13.33 (s, 1H), 9.70 – 9.67 (m, 1H), 8.10 (d, J = 8.8 Hz, 1H), 7.76 (d, J = 2.0 Hz, 1H), 7.68 (dd, J = 8.2, 2.1 Hz, 2H), 6.98 (d, J = 8.3 Hz, 1H), 4.16 (q, J = 6.9 Hz, 2H), 1.42 (d, J = 7.0 Hz, 3H). ^{13}C NMR (126 MHz, DMSO) δ 147.58, 120.54, 116.40, 112.34, 64.50, 15.21.

6.3.48.32: 5-nitro-2-(2-nitrophenyl)-1H-1,3-benzodiazole
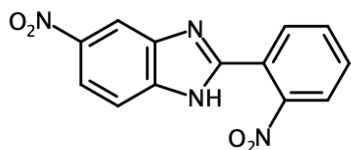
Brown solid (20% yield). Rf= 0.76 (EtOAc: petroleum ether (1:2)). Melting point= 249.6-251.6 ºC.
^{1}H NMR (500 MHz, DMSO) δ 9.06 (s, 1H), 8.46 (dd, J = 7.9, 1.5 Hz, 1H), 8.11 (dd, J = 8.1, 1.2 Hz, 1H), 8.01 (d, J = 2.5 Hz, 1H), 7.97 (dd, J = 9.0, 2.5 Hz, 1H), 7.87 (td, J = 7.5, 1.2 Hz, 1H), 7.78 (td, J = 7.7, 1.5 Hz, 1H). ^{13}C NMR (126 MHz, DMSO) δ 156.50, 151.46, 149.78, 136.42, 133.97, 133.91, 132.41, 130.86, 130.33, 125.40, 124.83, 114.06, 113.60.

6.3.48.33: 5-nitro-2-(3-nitrophenyl)-1H-1,3-benzodiazole
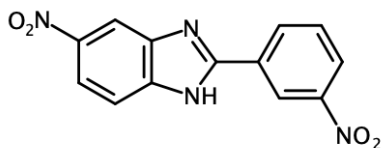
Orange solid (15% yield)/). Rf= 0.88 (EtOAc: petroleum ether (1:2)). Melting point= 189.9-291.9 ºC. ^{1}H NMR (500 MHz, DMSO) δ 9.00 (s, 1H), 8.87 (s, 1H), 8.52 (s, 1H), 8.35 (dd, J = 7.9, 2.6 Hz, 1H), 8.10 (d, J = 2.6 Hz, 1H), 7.95 (d, J = 2.0 Hz, 1H), 7.84 − 7.76 (m, 1H). ^{13}C NMR (126 MHz, DMSO) δ 158.30, 151.67, 148.69, 138.11, 136.35, 135.54, 133.55, 130.68, 126.11, 125.27, 123.90, 123.88, 113.91, 113.53.

6.3.48.34: 5-nitro-2-(1H-pyrrol-2-yl)-1H-1,3-benzodiazole
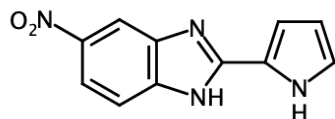
Brown solid (59% yield). Rf= 0.88 (EtOAc: petroleum ether (1:2)). Melting point= 307.2-309.2 ºC.
^{1}H NMR (500 MHz, DMSO) δ 12.47 − 12.43 (s, 1H), 8.42 (d, J = 2.2 Hz, 1H), 8.24 (dt, J = 8.9, 1.9 Hz, 1H), 7.82 (dd, J = 8.9, 1.9 Hz, 1H), 7.44 − 7.34 (m, 2H), 6.41 (dd, J = 4.0, 2.1 Hz, 1H). ^{13}C NMR (126 MHz, DMSO) δ 144.11, 126.80, 120.16, 116.15, 114.18, 111.69, 110.12.

6.3.48.35: 2-phenyl-1H-1,3-benzodiazole-5-carboxylic acid
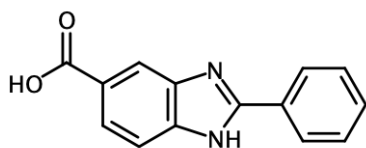
Light purple solid (35% yield). Rf= 0.38 (EtOAc: petroleum ether (1:2)). Melting point= 323.2-325.2 ºC.

6.3.48.36: 2-(4-bromophenyl)-1H-1,3-benzodiazole-5-carboxylic acid
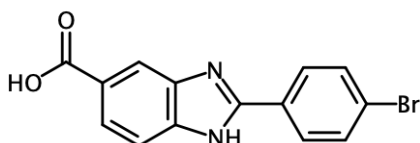
White solid (45% yield). Rf= 0.44 (EtOAc: petroleum ether (1:2)). Melting point= 332.5-335.2 ºC. ^{1}H NMR (500 MHz, DMSO) δ 8.36 – 8.29 (m, 2H), 8.09 – 8.03 (m, 1H), 7.94 (d, J = 8.2 Hz, 2H), 7.87 (d, J = 8.5 Hz, 1H). ^{13}C NMR (126 MHz, DMSO) δ 167.24, 150.80, 136.69, 133.69, 133.09, 130.35, 128.12, 127.46, 126.69, 123.99, 116.23, 114.70.

6.3.48.37: 2-(4-chlorophenyl)-1H-1,3-benzodiazole-5-carboxylic acid
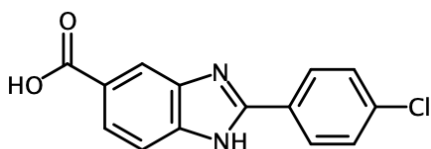
White solid (42% yield). Rf= 0.48 (EtOAc: petroleum ether (1:2)). Melting point= 352.7-354.7 ºC. ^{1}H NMR (500 MHz, DMSO) δ 12.90 (s, 1H), 8.42 (d, J = 8.2 Hz, 2H), 8.31 (s, 1H), 8.06 (d, J = 8.5 Hz, 1H), 7.88 (d, J = 8.5 Hz, 1H), 7.80 (d, J = 8.2 Hz, 2H).

6.3.48.38: 2-(4-hydroxyphenyl)-1H-1,3-benzodiazole-5-carboxylic acid
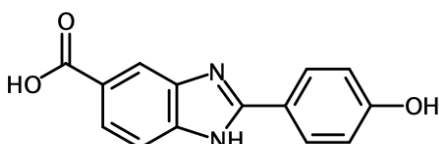
White solid (40% yield). Rf= 0.64 (EtOAc: petroleum ether (1:2)). Melting point= 350.0-352.0 ºC. ^{1}H NMR (500 MHz, DMSO) δ 10.93 (s, 1H), 8.27 (d, J = 8.8 Hz, 2H), 8.24 (d, J = 1.5 Hz, 1H), 8.03 (dd, J = 8.5, 1.5 Hz, 1H), 7.82 (d, J = 8.5 Hz, 1H), 7.08 (d, J = 8.8 Hz, 2H). ^{13}C NMR (126 MHz, DMSO)

δ 167.06, 163.23, 151.41, 135.14, 132.09, 131.03, 128.20, 126.84, 117.00, 115.31, 113.96, 113.45.

6.3.48.39: 2-(4-fluorophenyl)-1H-1,3-benzodiazole-5-carboxylic acid
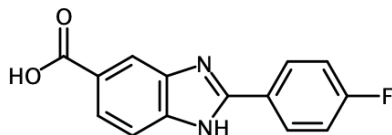
White solid (45% yield). Rf= 0.31 (EtOAc: petroleum ether (1:2)). Melting point= 352.9-354.9 ºC.^{1}H NMR (500 MHz, DMSO) δ 8.33 (dd, J = 8.6, 5.4 Hz, 2H), 8.25 (s, 1H), 8.06 – 7.93 (m, 1H), 7.79 (d, J = 8.4 Hz, 1H), 7.54 (t, J = 8.6 Hz, 2H). ^{13}C NMR (126 MHz, DMSO) δ 130.27,126.16, 116.98.

6.3.48.40: 2-(4-methoxyphenyl)-1H-1,3-benzodiazole-5-carboxylic acid
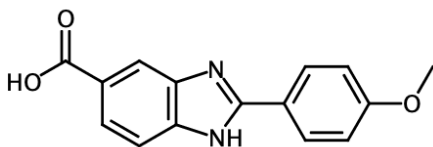
White solid (30% yield). Rf= 0.38 (EtOAc: petroleum ether (1:2)). Melting point= 332.5-335.2 ºC.^{1}H NMR (500 MHz, DMSO) δ 8.26 – 8.23 (m, 2H), 8.02 (d, J = 8.5 Hz, 1H), 7.81 (d, J = 8.6 Hz, 1H), 7.27 (d, J = 8.9 Hz, 2H), 3.91 (s, 3H). ^{13}C NMR (126 MHz, DMSO) δ 130.62, 126.78, 116.12, 56.39.

6.3.48.41: 2-(3-hydroxyphenyl)-1H-1,3-benzodiazole-5-carboxylic acid
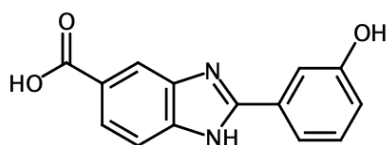
Beige solid (55% yield). Rf= 0.40 (EtOAc: petroleum ether (1:2)). Melting point= 311.5-313.5 ºC.^{1}H NMR (500 MHz, DMSO) δ 10.32 (s, 1H), 8.33 (d, J = 1.5 Hz, 1H), 8.08 (dd, J = 8.6, 1.5 Hz, 1H), 7.89 (d, J = 8.5 Hz, 1H), 7.82 (dd, J = 7.6, 1.8 Hz, 1H), 7.73 (t, J = 2.1 Hz, 1H), 7.52 (t, J = 8.0 Hz, 1H), 7.18 (s, 1H).

6.3.48.42: 2-(3-ethoxy-4-hydroxyphenyl)-1H-1,3-benzodiazole-5-carboxylic acid
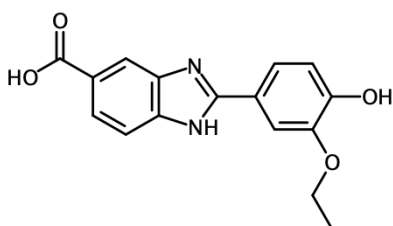
White solid (31% yield). Rf= 0.30 (EtOAc: petroleum ether (1:2)). Melting point= 279.1-281.1 ºC.^{1}H NMR (500 MHz, DMSO) δ 10.41 (s, 1H), 8.27 (d, J = 1.4 Hz, 1H), 8.10 – 8.04 (m, 2H), 7.89 (dd, J = 8.4, 2.2 Hz, 1H), 7.85 (d, J = 8.5 Hz, 1H), 7.10 (d, J = 8.4 Hz, 1H), 4.22 (q, J = 7.0 Hz, 2H), 1.42 (t, J = 6.9 Hz, 3H). ^{13}C NMR (126 MHz, DMSO) δ 167.18, 152.78, 151.79, 147.93, 135.64, 132.57, 128.06, 126.73, 122.85, 116.76, 115.36, 114.03, 113.43, 64.90, 15.11.

6.3.48.43: 2-(2-nitrophenyl)-1H-1,3-benzodiazole-5-carboxylic acid
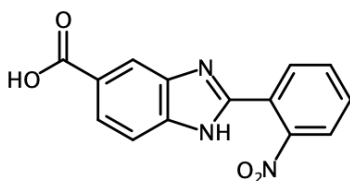
White solid (37% yield). Rf= 0.38 (EtOAc: petroleum ether (1:2)). Melting point= 277.5-279.5 ºC. ^{1}H NMR (500 MHz, DMSO) δ 8.36 (d, J = 1.5 Hz, 1H), 8.32 (dd, J = 8.2, 1.2 Hz, 1H), 8.12 (dd, J = 7.6, 1.5 Hz, 1H), 8.09 – 8.00 (m, 2H), 7.97 (td, J = 7.8, 1.5 Hz, 1H), 7.90 (d, J = 8.6 Hz, 1H). ^{13}C NMR (126 MHz, DMSO) δ 167.37, 149.31, 148.24, 134.56, 134.51, 133.73, 133.11, 127.83, 126.31, 125.81, 120.84, 116.95, 115.22.

6.3.48.44: 2-(3-nitrophenyl)-1H-1,3-benzodiazole-5-carboxylic acid
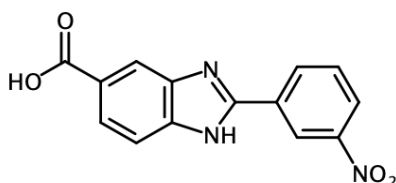
White solid (41% yield). Rf= 0.79 (EtOAc: petroleum ether (1:2)). Melting point= >360 ºC. ^{1}H NMR (500 MHz, DMSO) δ 9.01 (s, 1H), 8.61 (d, J = 8.1 Hz, 1H), 8.36 (d, J = 8.1 Hz, 1H), 8.25 (s, 1H), 7.88 (q, J = 8.7 Hz, 2H), 7.73 (d, J = 8.8 Hz, 1H). ^{13}C NMR (126 MHz, DMSO) δ 168.23, 151.79, 149.57, 148.74, 133.17, 131.50, 131.23, 130.48, 129.97, 125.18, 121.55, 114.70, 112.46.

6.3.48.45: 2-(thiophen-2-yl)-1H-1,3-benzodiazole-5-carboxylic acid
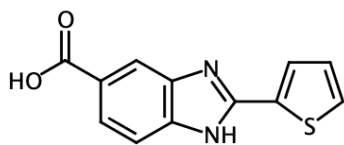
Brown solid 55% yield). Rf= 0.38 (EtOAc: petroleum ether (1:2)). Melting point= 292.5-294.5 ºC.^{1}H NMR (500 MHz, DMSO) δ 8.37 (d, J = 3.8 Hz, 1H), 8.23 (s, 1H), 8.10 (d, J = 5.0 Hz, 1H), 8.02 (s, 0H), 7.79 (d, J = 8.5 Hz, 1H), 7.40 (t, J = 4.5 Hz, 1H). ^{13}C NMR (126 MHz, DMSO) δ 167.35, 147.11, 137.13, 134.34, 134.01, 133.17, 129.57, 127.66, 127.04, 126.36, 115.91, 114.38.

6.3.48.46: 2-(1H-pyrrol-2-yl)-1H-1,3-benzodiazole-5-carboxylic acid
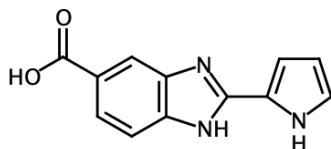
Brown solid solid (59% yield). Rf= 0.38 (EtOAc: petroleum ether (1:2)). Melting point= 345.0-347.0 ºC. ^{1}H NMR (500 MHz, DMSO) δ 12.86 (s, 1H), 11.98 (q, J = 2.5 Hz, 1H), 8.16 (s, 1H), 7.87 (dd, J = 8.4, 1.6 Hz, 1H), 7.61 (d, J = 8.4 Hz, 1H), 7.00 (ddt, J = 31.3, 3.8, 1.6 Hz, 2H), 6.28 (q, J = 2.6 Hz, 1H). ^{13}C NMR (126 MHz, DMSO) δ 168.47, 149.39, 124.38, 123.69, 122.61, 122.52, 110.51, 109.96.

6.3.48.47: 5-benzoyl-2-phenyl-1H-1,3-benzodiazole
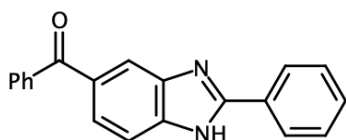
Yellow solid (47% yield). Rf= 0.87 (EtOAc: petroleum ether (1:2)). Melting point= 223.5-225.5 ºC.^{1}H NMR (500 MHz, DMSO) δ 13.31 (s, 1H), 8.25 – 8.19 (d, 2H), 7.98 (s, 1H), 7.80 – 7.74 (m, 3H), 7.69 (ddd, J = 17.3, 7.8, 1.5 Hz, 2H), 7.58 (dtt, J = 11.5, 7.3, 3.7 Hz, 5H).

6.3.48.48: 5-benzoyl-2-(4-bromophenyl)-1H-1,3-benzodiazole
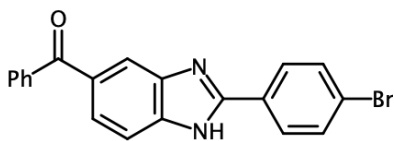
White solid (51% yield). Rf= 0.91 (EtOAc: petroleum ether (1:2)). Melting point= 292.5-294.5 ºC.^{1}H NMR (500 MHz, DMSO) δ 8.35 (d, J = 8.6 Hz, 1H), 8.13 – 8.01 (m, 1H), 8.01 – 7.89 (m, 2H), 7.86 (dd, J = 8.5, 1.5 Hz, 1H), 7.82 – 7.75 (m, 2H), 7.74 – 7.68 (m, 1H), 7.60 (t, J = 7.7 Hz, 1H). ^{13}C NMR (126 MHz, DMSO) δ 195.33, 151.05, 137.63, 136.79, 134.15, 133.73, 133.20, 133.10, 130.34, 130.10, 129.08, 127.46, 127.15, 124.11, 116.91, 114.87.

6.3.48.49: 5-benzoyl-2-(4-chlorophenyl)-1H-1,3-benzodiazole
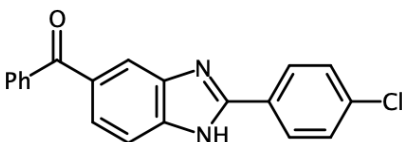
Yellow solid (51% yield). Rf= 0.93 (EtOAc: petroleum ether (1:2)). Melting point= 228.9-230.9 ºC.

6.3.48.50: 4-(5-benzoyl-1H-1,3-benzodiazol-2-yl)phenol
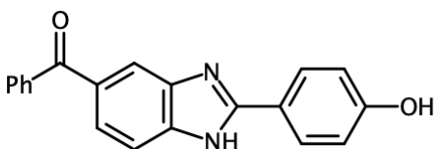
Beige solid (49% yield). Rf= 0.44 (EtOAc: petroleum ether (1:2)). Melting point= 332.5-335.2 ºC.^{1}H NMR (500 MHz, DMSO) δ 13.06 (s, 1H), 10.12 (s, 1H), 8.06 (d, J = 8.7 Hz, 2H), 7.92 (s, 1H), 7.80 – 7.73 (m, 2H), 7.71 – 7.61 (m, 2H), 7.57 (t, J = 7.6 Hz, 2H), 6.96 (d, J = 8.8 Hz, 2H). ^{13}C NMR (126 MHz, DMSO) δ 196.08, 160.20, 138.71, 132.43, 131.03, 129.87, 129.04, 128.85, 124.43, 120.88, 116.32, 116.08.

6.3.48.51: 5-benzoyl-2-(4-fluorophenyl)-1H-1,3-benzodiazole
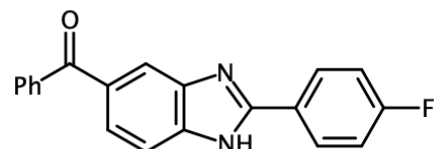
White solid (45% yield). Rf= 0.90 (EtOAc: petroleum ether (1:2)). Melting point= 239.1-241.1 ºC.^{1}H NMR (500 MHz, DMSO) δ 13.31 (s, 1H), 8.30 – 8.22 (m, 2H), 7.96 (s, 1H), 7.77 (d, J = 8.1, 1.4 Hz, 2H), 7.74 (d, 1H), 7.72 – 7.64 (m, 2H), 7.58 (t, J = 7.6 Hz, 2H), 7.44 (t, J = 8.8 Hz, 2H). ^{13}C

NMR (126 MHz, DMSO) δ 196.05, 164.89, 162.91, 138.56, 132.55, 131.52, 129.91, 129.63, 129.56, 128.88, 126.63, 126.61, 124.72, 116.74, 116.57.

6.3.48.52: 3-(5-benzoyl-1H-1,3-benzodiazol-2-yl)phenol
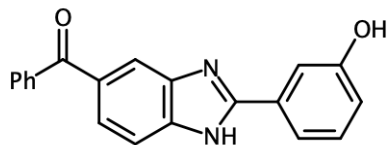
Yellow solid (39% yield). Rf= 0.86 (EtOAc: petroleum ether (1:2)). Melting point= 207.1-209.1 ºC.

6.3.48.53: 4-(5-benzoyl-1H-1,3-benzodiazol-2-yl)-2-ethoxyphenol
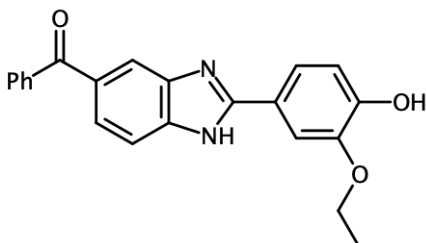
Yellow solid (35% yield). Rf= 0.87 (EtOAc: petroleum ether (1:2)). Melting point= 215.0-217.0 ºC. ^{1}H NMR (500 MHz, DMSO) δ 13.05 (s, 1H), 9.62 (s, 1H), 7.92 (s, 1H), 7.80 – 7.74 (m, 3H), 7.67 (td, J = 6.4, 3.0 Hz, 3H), 7.58 (t, J = 7.6 Hz, 2H), 6.97 (d, J = 8.3 Hz, 1H), 4.16 (q, J = 6.9 Hz, 2H), 1.41 (t, J = 7.0 Hz, 3H). ^{13}C NMR (126 MHz, DMSO) δ 196.03, 149.82, 147.54, 138.70, 132.43, 131.03, 129.88, 128.85, 121.12, 120.64, 116.36, 112.20, 64.46, 15.22.

6.3.48.55: 5-benzoyl-2-(4-methoxyphenyl)-1H-1,3-benzodiazole
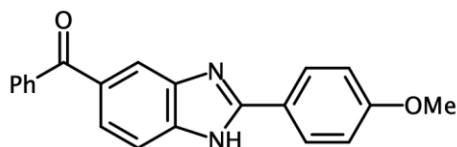
White solid (30% yield). Rf= 0.80 (EtOAc: petroleum ether (1:2)). Melting point= 258.1-260.1 ºC. ^{1}H NMR (500 MHz, DMSO) δ 8.43 – 8.35 (d, 2H), 8.06 (s, J = 1.4 Hz, 1H), 7.94 – 7.85 (m, 2H), 7.83 – 7.77 (m, 2H), 7.77 – 7.69 (m, 1H), 7.61 (t, J = 7.7 Hz, 2H), 7.33 – 7.25 (m, 2H), 3.92 (s, 3H). ^{13}C NMR (126 MHz, DMSO) δ 195.36, 163.71, 151.91, 137.69, 134.00, 133.21, 130.64, 130.11, 129.10, 127.07, 116.36, 115.67, 114.45, 56.30.

6.3.48.56: 5-benzoyl-2-(3-nitrophenyl)-1H-1,3-benzodiazole
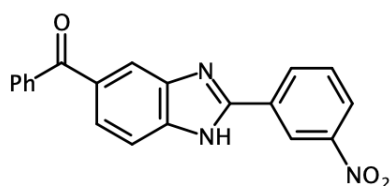
Orange solid (41% yield). Rf= 0.85 (EtOAc: petroleum ether (1:2)). Melting point= 215.0-217.0 ºC.

6.3.48.57: 5-benzoyl-2-(thiophen-2-yl)-1H-1,3-benzodiazole
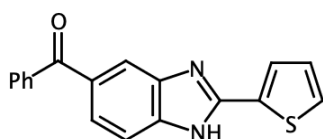
White solid (51% yield). Rf= 0.81 (EtOAc: petroleum ether (1:2)). Melting point= 190.5-192.5 ºC. ^{1}H NMR (500 MHz, DMSO) δ 7.99 (dd, *J* = 3.8, 1.3 Hz, 1H), 7.96 (d, *J* = 1.6 Hz, 1H), 7.91 (dd, *J* = 5.0, 1.2 Hz, 1H), 7.80 – 7.75 (m, 3H), 7.74 (d, *J* = 1.6 Hz, 1H), 7.73 – 7.67 (m, 1H), 7.59 (t, *J* = 7.7 Hz, 2H), 7.32 (ddd, *J* = 5.0, 3.7, 1.5 Hz, 1H). ^{13}C NMR (126 MHz, DMSO) δ 195.79, 149.40, 138.27, 132.77, 132.26, 131.55, 130.00, 129.22, 128.95, 125.46.

6.3.48.58: 5-benzoyl-2-(1H-pyrrol-2-yl)-1H-1,3-benzodiazole
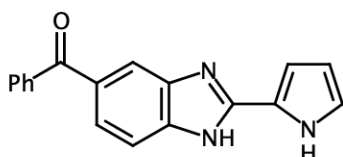
White solid (65% yield). Rf= 0.81 (EtOAc: petroleum ether (1:2)). Melting point= 216.7-218.7ºC. ^{1}H NMR (500 MHz, DMSO) δ 13.00 (m, *J* = 3.8, 1.3 Hz, 1H), 7.96 (d, *J* = 1.6 Hz, 1H), 7.91 (dd, *J* = 5.0, 1.2 Hz, 1H), 7.80 – 7.75 (m, 3H), 7.74 (d, *J* = 1.6 Hz, 1H), 7.73 – 7.67 (m, 1H), 7.59 (t, *J* = 7.7 Hz, 2H), 7.32 (ddd, *J* = 5.0, 3.7, 1.5 Hz, 1H). ^{13}C NMR (126 MHz, DMSO) δ 195.79, 149.40, 138.27, 132.77, 132.26, 131.55, 130.00, 129.22, 128.95, 125.46.

6.3.48.59: 5,6-dimethyl-2-(3-nitrophenyl)-1H-1,3-benzodiazole
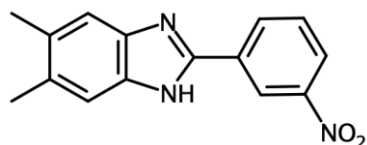
Beige solid (47% yield). Rf= 0.85 (EtOAc: petroleum ether (1:2)). Melting point= 254.9-256.9 ºC.

6.3.48.60: 2-(4-bromophenyl)-5,6-dimethyl-1H-1,3-benzodiazole
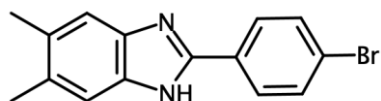
White solid (35% yield). Rf= 0.88 (EtOAc: petroleum ether (1:2)). Melting point= 341.2-343.2 ºC.

6.3.48.61: 2-(4-chlorophenyl)-5,6-dimethyl-1H-1,3-benzodiazole
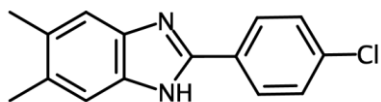
White solid (60% yield). Rf= 0.87 (EtOAc: petroleum ether (1:2)). Melting point= 335.9-339.9 ºC. ^{1}H NMR (500 MHz, DMSO) δ 8.38 (d, *J* = 8.3 Hz, 1H), 7.82 (d, *J* = 8.3 Hz, 1H), 7.60 (s, 1H), 2.40 (s, 3H). ^{13}C NMR (126 MHz, DMSO) δ 146.97, 138.22, 136.00, 130.99, 130.18, 130.08, 122.94, 114.04, 20.43.

6.3.48.62: 4-(5,6-dimethyl-1H-1,3-benzodiazol-2-yl)phenol
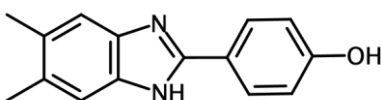
Light grey solid (52% yield). Rf= 0.80 (EtOAc: petroleum ether (1:2)). Melting point= >360 ºC. ^{1}H NMR (500 MHz, DMSO) δ 15.22 (s, 1H), 10.82 (d, *J* = 34.7 Hz, 1H), 8.28 – 8.21 (m, 1H), 7.73 (d, *J* = 8.7 Hz, 1H), 7.55 (s, 1H), 2.38 (s, 3H). ^{13}C NMR (126 MHz, DMSO) δ 135.38, 132.24, 130.54, 130.37, 128.45, 116.91, 116.84, 116.16, 113.65, 20.37.

6.3.48.63: 5,6-dimethyl-2-(1H-pyrrol-2-yl)-1H-1,3-benzodiazole
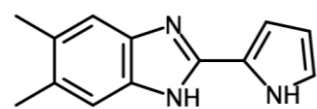
White solid (71% yield). Rf= 0.79 (EtOAc: petroleum ether (1:2)). Melting point= 145.9-147.9 ºC. ^{1}H NMR (500 MHz, DMSO) δ 11.85 – 11.64 (s, 1H), 7.28 (s, 2H), 6.91 (td, *J* = 2.6, 1.4 Hz, 1H), 6.81 (dt, *J* = 3.7, 1.7 Hz, 1H), 6.19 (q, *J* = 2.5 Hz, 1H).

6.3.48.64: 2-(4-fluorophenyl)-5,6-dimethyl-1H-1,3-benzodiazole
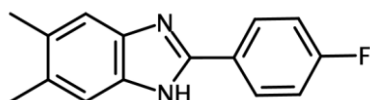
Beige solid (45% yield). Rf= 0.85 (EtOAc: petroleum ether (1:2)). Melting point= 319.5-321.5 ºC. ^{1}H NMR (500 MHz, DMSO) δ 8.52 – 8.45 (m, 1H), 7.60 (d, J = 8.8 Hz, 1H), 7.57 (s, 1H), 2.38 (s, 3H).

6.3.48.65: 3-(5,6-dimethyl-1H-1,3-benzodiazol-2-yl)phenol
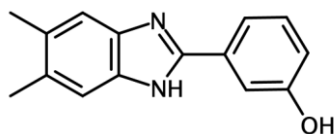
White solid (55% yield). Rf= 0.78 (EtOAc: petroleum ether (1:2)). Melting point= 322.1-324.1 ºC. ^{1}H NMR (500 MHz, DMSO) δ 10.34 (s, 1H), 7.80 (dd, J = 7.7, 1.7 Hz, 1H), 7.70 (t, J = 2.1 Hz, 1H), 7.54 (s, 2H), 7.48 (t, J = 8.0 Hz, 1H), 7.18 (dd, J = 8.2, 2.3 Hz, 1H), 2.35 (s, 6H).

6.3.48.66: 5-fluoro-2-phenyl-1H-1,3-benzodiazole
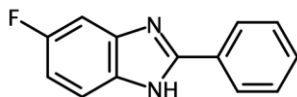
Beige solid (40% yield). Rf= 0.87 (EtOAc: petroleum ether (1:2)). Melting point= 281.6-283.6 ºC. ^{1}H NMR (500 MHz, DMSO) δ 8.40 – 8.23 (m, 2H), 7.85 (dd, J = 8.9, 4.6 Hz, 1H), 7.74 – 7.71 (m, 2H), 7.71 (s, 1H), 7.65 (dd, J = 8.7, 2.4 Hz, 1H), 7.40 (td, J = 9.3, 2.5 Hz, 1H). ^{13}C NMR (126 MHz, DMSO) δ 161.28, 159.37, 150.95, 133.31, 130.02, 128.28, 116.16, 116.07, 114.27, 114.07, 101.30, 101.08.

6.3.48.67: 2-(4-bromophenyl)-5-fluoro-1H-1,3-benzodiazole
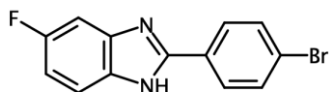
Light brown solid (57% yield). Rf= 0.91 (EtOAc: petroleum ether (1:2)). Melting point= 323.0-325.0 ºC. ^{1}H NMR (500 MHz, DMSO) δ 8.33 – 8.25 (m, 2H), 7.93 (dd, J = 8.7, 1.9 Hz, 2H), 7.83 (dd, J = 9.0, 4.5 Hz, 1H), 7.63 (dd, J = 8.6, 2.4 Hz, 1H), 7.39 (td, J = 9.3, 2.5 Hz, 1H). ^{13}C NMR (126 MHz, DMSO) δ 133.06, 130.15, 116.20, 116.13, 101.25, 101.04, 31.17.

6.3.48.68: 2-(4-chlorophenyl)-5-fluoro-1H-1,3-benzodiazole
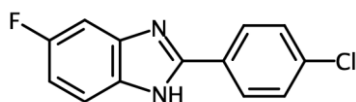
White solid (50% yield). Rf= 0.91 (EtOAc: petroleum ether (1:2)). Melting point= 329.7-331.7 ºC.
^{1}H NMR (500 MHz, DMSO) δ 8.43 – 8.29 (m, 2H), 7.83 (qd, J = 4.9, 3.3 Hz, 1H), 7.81 – 7.78 (m, 2H), 7.63 (dq, J = 8.4, 2.5 Hz, 1H), 7.38 (dtt, J = 14.1, 9.1, 2.5 Hz, 1H). ^{13}C NMR (126 MHz, DMSO) δ 130.10, 129.92, 116.15, 101.59.

6.3.48.69: 4-(5-fluoro-1H-1,3-benzodiazol-2-yl)phenol
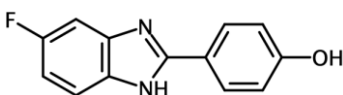
White solid (59% yield). Rf= 0.73 (EtOAc: petroleum ether (1:2)). Melting point= >360 ºC. ^{1}H NMR (500 MHz, DMSO) δ 10.85 (s, 1H), 8.31 – 8.12 (m, 2H), 7.80 (dd, J = 8.9, 4.5 Hz, 1H), 7.61 (dd, J = 8.5, 2.5 Hz, 1H), 7.39 (td, J = 9.4, 2.5 Hz, 1H), 7.19 – 7.05 (m, 2H). ^{13}C NMR (126 MHz, DMSO) δ 162.84, 161.24, 159.33, 150.98, 130.67, 116.96, 115.55, 115.47, 100.90, 100.67.

6.3.48.70: 5-fluoro-2-(4-fluorophenyl)-1H-1,3-benzodiazole
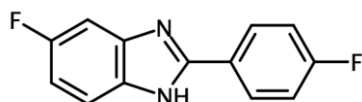
Light grey solid (35% yield). Rf 0.90 (EtOAc:PE (1:2)). Melting point 336.5-338.5 ºC.

6.3.48.71: 3-(5-fluoro-1H-1,3-benzodiazol-2-yl)phenol
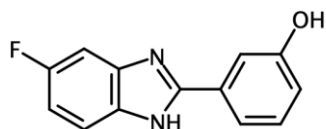
White solid (46% yield). Rf 0.70 (EtOAc:PE (1:2)). Melting point 307.5-309.5 ºC. ^{1}H NMR (500 MHz, DMSO-d$_6$) δ 10.27 (s, 1H), 7.84 (dd, J = 8.8, 4.4 Hz, 1H), 7.78–7.72 (m, 1H), 7.70–7.63 (m, 2H), 7.50 (t, J = 8.0 Hz, 1H), 7.46–7.36 (m, 1H), 7.19–7.11 (m, 1H). ^{13}C NMR (125 MHz, DMSO-d$_6$) δ 159.4, 158.7, 150.9, 131.2, 120.6, 119.0, 116.1, 116.0, 114.9, 101.2, 101.0.

6.3.48.72: 5-fluoro-2-(1H-pyrrol-2-yl)-1H-1,3-benzodiazole
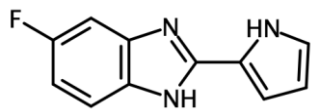
White solid (58% yield). Rf 0.30 (EtOAc:PE (1:2)). Melting point 210.5-212.5 ºC. ^{1}H NMR (500 MHz, DMSO-d_6) δ 12.60 (s, 1H), 11.81 (s, 1H), 7.47 (dd, J = 9.0, 4.9 Hz, 1H), 7.41 − 7.23 (m, 1H), 6.99 (ddd, J = 9.9, 8.6, 2.6 Hz, 1H), 6.95 (q, J = 2.4 Hz, 1H), 6.86 (p, J = 1.8 Hz, 1H), 6.20 (q, J = 2.6 Hz, 1H). ^{13}C NMR (125 MHz, DMSO-d_6) δ 159.8, 157.9, 148.6, 122.8, 122.0, 109.7, 109.7, 109.5.

6.3.48.73: 2-(1H-1,3-benzodiazol-6-yl)-5-chloro-1H-1,3-benzodiazole
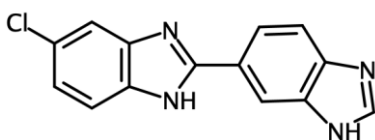
White solid (45% yield). Rf 0.45 (EtOAc:PE (1:2)). Melting point 321.0-323.0 ºC. ^{1}H NMR (500 MHz, DMSO-d_6) δ 8.41 (d, J = 1.6 Hz, 1H), 8.36 (s, 1H), 8.06 (dd, J = 8.4, 1.6 Hz, 1H), 7.75 (d, J = 8.5 Hz, 1H), 7.63 (d, J = 2.1 Hz, 1H), 7.59 (d, J = 8.5 Hz, 1H), 7.22 (dd, J = 8.5, 2.0 Hz, 1H). ^{13}C NMR (125 MHz, DMSO-d_6) δ 154.2, 144.3, 126.6, 124.0, 122.6, 121.5, 31.1.

6.3.48.74: 2-(1H-1,3-Benzodiazol-6-yl)-1H-1,3-benzodiazole-5-carboxylic acid
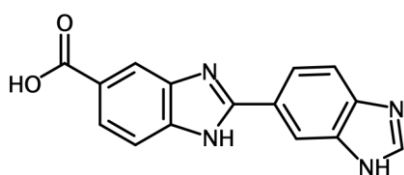
White solid (37% yield). Rf 0.17 (EtOAc: petroleum ether (1:2)). Melting point >360 ºC. ^{1}H NMR (500 MHz, DMSO-d_6) δ 13.14 (s, 1H), 12.86 (s, 1H), 8.46 (s, 1H), 8.38 (d, J = 1.9 Hz, 1H), 8.24 − 8.15 (m, 1H), 8.12 (d, J = 8.5 Hz, 1H), 7.85 (d, J = 8.4 Hz, 1H), 7.77 (d, J = 8.5 Hz, 1H), 7.66 (d, J = 8.3 Hz, 1H). ^{13}C NMR (125 MHz, DMSO-d_6) δ 168.4, 144.3, 124.8, 123.9.

6.3.48.75: 2-(4-Nitrophenyl)-1H-1,3-benzodiazole
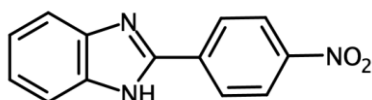
Dark beige solid (40% yield). Rf 0.89 (EtOAc:PE (1:2)). Melting point 307.7-309.7 ºC. ^{1}H NMR (500 MHz, DMSO-d_6) δ 13.29 (s, 1H), 8.42 (dt, J = 6.4, 2.8 Hz, 2H), 7.67 (s, 1H), 7.28 (dq, J = 6.4, 3.4 Hz, 1H). ^{13}C NMR (125 MHz, DMSO-d_6) δ 149.5, 148.3, 136.5, 127.9, 127.9, 124.8, 114.5, 114.1.

6.3.48.76: 5-Chloro-2-(4-nitrophenyl)-1H-1,3-benzodiazole
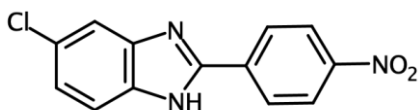
Light brown solid (30% yield). Rf 0.31 (EtOAc:PE (1:2)). Melting point 340.9-342.9 ºC. ^{1}H NMR (500 MHz, DMSO-d_6) δ 8.52–8.43 (m, 3H), 8.27 (d, J = 1.7 Hz, 1H), 7.93 (dd, J = 8.6, 1.7 Hz, 1H), 7.82–7.73 (m, 1H), 6.80 (d, J = 8.8 Hz, 1H). ^{13}C NMR (125 MHz, DMSO-d_6) δ 128.7, 124.9.

6.3.48.77: 2-(4-Nitrophenyl)-5-phenyl-1H-1,3-benzodiazole
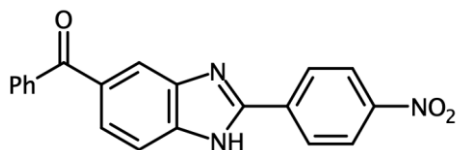
Beige solid (41% yield). Rf 0.89 (EtOAc:PE (1:2)). Melting point 273.5-275.5 ºC. ^{1}H NMR (500 MHz, DMSO-d_6) δ 8.58–8.50 (m, 2H), 8.47 (d, J = 8.8 Hz, 2H), 8.08–8.03 (s, 1H), 7.90–7.83 (m, 1H), 7.79 (ddd, J = 8.3, 6.6, 1.6 Hz, 3H), 7.74 – 7.66 (m, 1H), 7.60 (t, J = 7.6 Hz, 2H). ^{13}C NMR (125 MHz, DMSO-d_6) δ 195.8, 149.1, 138.1, 132.9, 130.1, 130.0, 129.1, 129.0, 128.9, 126.0, 124.9, 115.6.

6.3.48.78: 2-(4-Nitrophenyl)-1H-1,3-benzodiazole-5-carboxylic acid
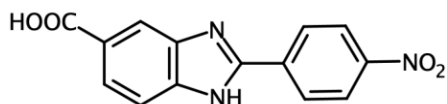
Beige solid (30% yield). Rf 0.89 (EtOAc:PE (1:2)). Melting point 222.9-226.1 ºC. ^{1}H NMR (500 MHz, DMSO-d_6) δ 13.58 (s, 1H), 8.68 – 8.29 (m, 4H), 7.95 – 7.61 (m, 2H), 7.53 – 7.28 (m, 1H). ^{13}C NMR (125 MHz, DMSO-d_6) δ 149.8, 149.2, 129.0, 125.2, 124.9, 116.9, 115.2, 40.3, 39.5.

6.3.48.79: 2-(4-Methylphenyl)-1H-1,3-benzodiazole
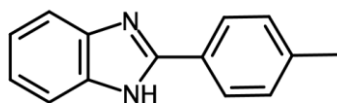
Beige solid (41% yield). Rf 0.80 (EtOAc: petroleum ether (1:2)). Melting point 273.9-275.9 ºC. ^{1}H NMR (500 MHz, DMSO-d$_6$) δ 12.82 (s, 1H), 8.18–7.94 (m, 2H), 7.58 (s, 2H), 7.36 (d, J = 8.0 Hz, 2H), 7.28–6.92 (m, 2H), 2.39 (s, 3H). ^{13}C NMR (125 MHz, DMSO-d$_6$) δ 151.8, 140.0, 130.0, 127.9, 126.9, 21.4.

6.3.48.80: 5-Chloro-2-(4-methylphenyl)-1H-1,3-benzodiazole
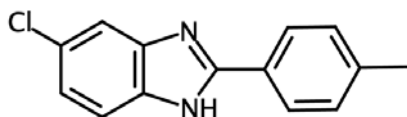
Light beige solid (47% yield). Rf 0.90 (EtOAc:PE (1:2)). Melting point 296.1-298.1 ºC. ^{1}H NMR (500 MHz, DMSO-d$_6$) δ 8.25–8.18 (m, 2H), 7.83 (d, J = 2.0 Hz, 1H), 7.79 (d, J = 8.6 Hz, 1H), 7.51 (dt, J = 8.7, 1.7 Hz, 3H), 2.44 (s, 3H). ^{13}C NMR (125 MHz, DMSO-d$_6$) δ 151.2, 143.8, 130.6, 129.6, 128.3, 125.7, 116.0, 114.3, 21.7.

6.3.48.81: 5-Fluoro-2-(thiophen-2-yl)-1H-1,3-benzodiazole
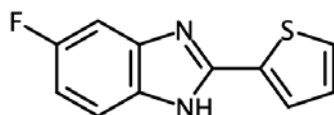
Grey solid (49% yield). Rf 0.83 (EtOAc:PE (1:2)). Melting point >300 ºC. ^{1}H NMR (500 MHz, DMSO) δ 8.21 – 8.07 (m, 1H), 7.98 (dd, J = 5.0, 1.2 Hz, 1H), 7.69 (dd, J = 8.9, 4.7 Hz, 1H), 7.52 (dd, J = 9.0, 2.5 Hz, 1H), 7.34 (dd, J = 5.0, 3.7 Hz, 1H), 7.25 (td, J = 9.4, 2.5 Hz, 1H). ^{13}C NMR (125 MHz, DMSO-d$_6$) δ 132.8, 129.3, 117.0, 112.0, 100.9.

6.3.48.82: 5-Nitro-2-(thiophen-2-yl)-1H-1,3-benzodiazole
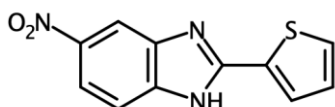
Beige solid (35% yield). Rf 0.80 (EtOAc:PE (1:2)). Melting point 277.2-279.2 ºC. ^{1}H NMR (500 MHz, DMSO-d$_6$) δ 8.45 (d, J = 2.2 Hz, 1H), 8.15 (dd, J = 8.9, 2.2 Hz, 1H), 8.09 (dd, J = 3.7, 1.2 Hz,

1H), 7.91 (dd, J = 4.9, 1.2 Hz, 1H), 7.76 (d, J = 8.8 Hz, 1H), 7.31 (dd, J = 5.0, 3.7 Hz, 1H). ^{13}C NMR (125 MHz, DMSO-d_6) δ 151.5, 143.4, 131.9, 131.7, 129.9, 129.2, 118.9, 114.9, 111.9.

6.4: <u>Disk diffusion assay</u>

Disk diffusion assays with *E. coli* JM109 were performed in-house as part of this work. Disk diffusion assays with *E. coli* ATCC 35218, *S. aureus* and *P. aeruginosa* were performed by collaborators at Kingston University.

6.4.1: Liquid media

Mueller Hinton (MH) broth powder was solubilized in water (25 g/L) and autoclaved at 121 ºC for 15 minutes.

6.4.2: Solid media

Agar (2 g /100 ml of liquid medium) was added to the liquid medium and autoclaved at 121 ºC for 15 minutes. When the autoclaved media had cooled to 50 ºC, It was poured into petri dishes (20 ml/plate) and allowed to set.

6.4.3: Susceptibility testing

Cultures were grown on Mueller Hinton agar (Oxoid) plates at 37 ºC overnight. A single colony was picked and suspended in 5 ml PBS until 0.5 McFarland standard of turbidity was achieved. A sterile cotton bud was used to inoculate the entire surface of MH agar plates. Sterile filter paper discs were added into the plate with 10 ul of 10 mg/ml test compound applied. Plates were incubated at 37 ºC (for 16 hours) and the zones of inhibition were measured. DMSO was used as negative control (all negative, with no zone of inhibition). The inhibition zones of the positive controls (chosen based on standards and clinical practice used for all strains) were also measured.

6.5: MIC

Minimum Inhibitory Concentration (MIC) assays with *E. coli* JM109 were performed in-house as part of this work.

6.5.1: Liquid media

Liquid media was prepared following 6.4.1.

6.5.2: Solid media

Solid media was prepared following 6.4.2.

6.5.3: MIC testing

Cultures were grown on Mueller Hinton agar (Oxoid) plates at 37 ºC overnight. A single colony was picked and suspended in 5 ml PBS until 0.5 McFarland standard of turbidity was achieved. The cultures were loaded using multichannel pipette into a sterile reservoir. Compounds were tested at 256, 128, 64, 32, 16, 8, 4, 2, 1, 0.5 and 0.25 µg/ml while the positive control (ampicillin) was tested at 64, 32, 16, 8, 4, 2, 1, 0.5, 0.25, 0.125 and 0.0625 µg/ml. Media and untreated control were also included in the plate. Plates were incubated at 37 ºC (for 16 hours) and the turbidity observed.

6.6: <u>Anti-schistosomal testing using the Roboworm platform</u>

All anti-schistosomal testing was performed by collaborators at Aberystwyth University.

S. mansoni schistosomula were obtained by mechanical transformation from cercarie as previously described,[241,237] distributed in 384-well tissue culture plates at 120 parasites/well containing selected compounds. Each compound (provided to our collaborators as 10 mM DMSO stock solutions) was screened at both 10 and 50 µM (in 0.625% DMSO) in duplicate (Z' scores above 0.35).

Each screen contained both positive (10 µM auranofin (AUR) and praziquantel (PZQ)) and negative (0.625% DMSO) controls. Following 72 hr schistosomula/compound co-incubation, the plate was imaged and analysed by the Roboworm platform .[254]

Compound HY-22 was further screened as detailed above as a dose-titration (50, 25, 10, 5, 2.5, 1.25 and 0.625 µM). EC_{50} values were calculated from the titrated concentrations by non-linear regression, after log transformation of concentrations and data normalization using GraphPad Prism 8.0.

S. mansoni adult worms were recovered by hepatic portal vein perfusion from TO mice (*Mus musculus* HsdOLa:TO - Tuck Ordinary; Envigo, UK) that were percutaneously infected seven weeks earlier with 180 cercariae. Following perfusion, schistosomes were washed and processed as previously described.Click or tap here to enter text.Subsequently, schistosome pairs were seeded into 48 well tissue culture plates (1 worm pair/well, in triplicate) and dosed with HY-22 (20, 10, 5, 2.5 and 1.25 µM in 0.2% DMSO). DMSO (0.2%) was also included as a negative control. Parasite motility was assessed and scored by eye using the WHO-TDR scoring metric at 24, 48 and 72h.

6.7: Cytotoxicity assay

Cytotoxicity of compound HY-22 was assessed on the human hepatoma HepG2 cell line using the MTT (3-(4,5-dimethylthiazol-2-yl)-2,5-diphenyltetrazolium bromide) reagent, on two separate occasions, as previously described.[11,13,242] Briefly, HepG2 cells (ATCC) were grown to 80% confluency in Minimum Essential Medium Eagle (Sigma Aldrich, UK) supplemented with 2 mM L-glutamine (Sigma Aldrich, UK), 1% v/v non-essential amino acids (Sigma Aldrich, UK), 1% v/v antibiotic/antimycotic (Fisher Scientific, Loughborough, UK) and 10% FBS (Fisher Scientific) before being seeded at a density of 2×10^5 cells/mL (50 µl/well) into 96-well black-sided, clear bottom tissue culture plates and incubated for 24 hours at 37 °C in a humidified environment containing 5% CO_2. To each well, compound was added (in triplicate) to obtain final concentrations (in 1% DMSO) of 100 µM, 75 µM, 50 µM, 25 µM, 12.5 µM, 6.25 µM and 3.125 µM. During each cytotoxicity assay, both negative (1% v/v Triton X-100, Sigma-Aldrich, UK) and positive (1% v/v DMSO or media only) controls were also included in triplicate. After compound addition, the plates were incubated for a further 20 hr before addition of the MTT reagent. After 4 hr, the developed purple formazan crystals were dissolved by treatment with a (1:1) DMSO : isopropanol mixture and absorbance measured at 570 nm using a POLARstar Omega (BMG Labtech, UK) microtiter plate reader. Absolute EC_{50} values were calculated from the corrected absorbance of replicates by non-linear regression, after log transformation of concentrations and data normalization (where DMSO values represents 0% inhibition and TX-100 values represent 100% inhibition) using GrapPad Prism 8.

Dose-response curves were generated using the corrected average absorbance of the replicates in GraphPad Prism 8 software by non-linear regression and the CC_{50} (the concentration of compound that reduced cell viability by 50%) value was estimated.

6.8: Protein stability assay

Enzyme (50 μM of HEWL or HSA) was added to potassium phosphate (50 mM) containing 10% D_2O in a NMR tube. DMSO (at 0, 10, 25, 50, 60 and 75%) was then added (500 μL final sample volume). 1D NMR spectra were acquired using excitation sculpting for solvent suppression (pulse sequence zgesgp. The spectra at different DMSO % were superimposed and changes in the protein peaks visually observed.

6.9: Protein binding assay

Enzyme (50 μM of HEWL or HSA) in potassium phosphate (50 mM) containing 10% D_2O was added to a NMR tube. Test compounds (5 mM dissolved in DMSO) were then added (DMSO 50%). Solvent-suppressed saturation transfer difference NMR was performed using the stddiffesgp pulse sequence, with a train of 50 millisecond E-Burp shaped pulses at 0.5 ppm (on-resonance) or 20 ppm (off resonance) for 5.9 seconds. For each sample run, a control spectrum was collected. The STD amplification factors were calculated for the integrated protons following Equation1 in order to identify the protein binding sites.

$$STD_{amp} \text{ of resonance} = (STD_{diff} / STD_{off}) \times \text{ligand excess}$$

Chapter 7

Appendix

7. Appendix

NMR:

2-acetamidobutanedioic acid:

¹H-NMR
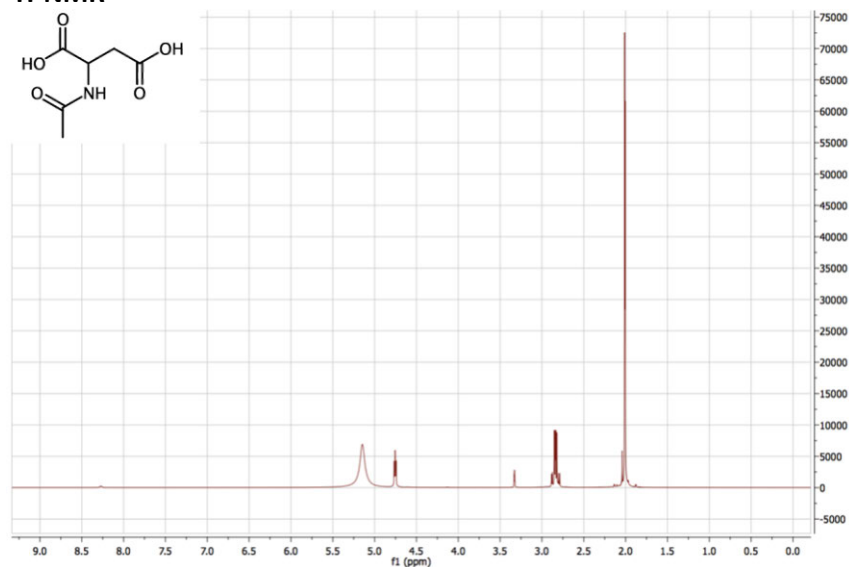
3-(acetyloxy)-2-acetamidopropanoic acid:

¹H-NMR
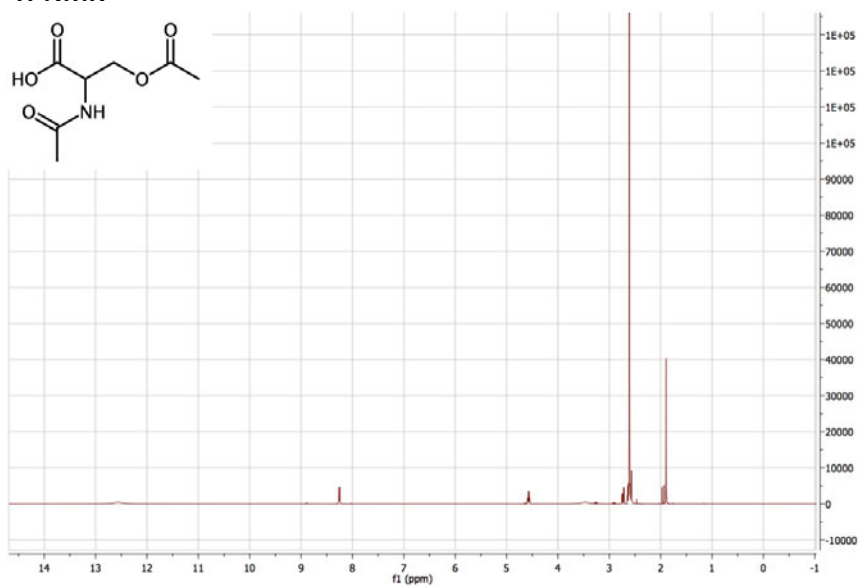
2-acetamido-3-hydroxypropanoic acid:

¹H-NMR
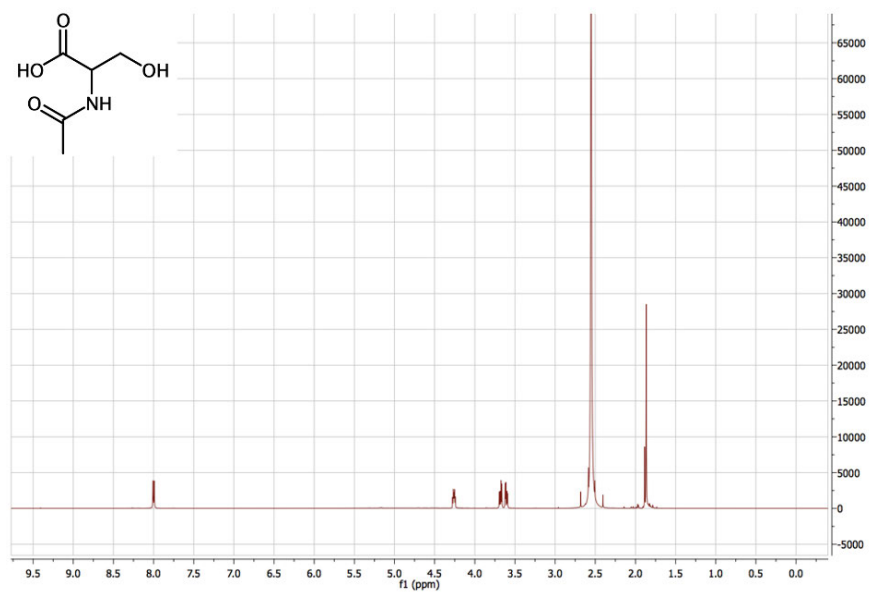
N-(2,5-dioxooxolan-3-yl)acetamide:

¹H-NMR
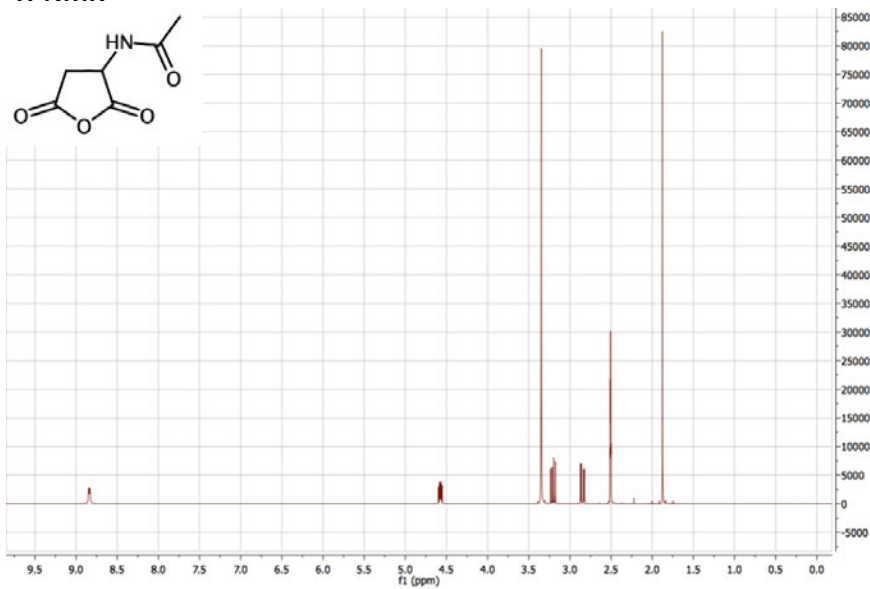
4'-(hydroxymethyl)-5'-oxospiro[bicyclo[3.3.1]nonane-9,2'-[1,3]oxazolidin]-3'-ium:
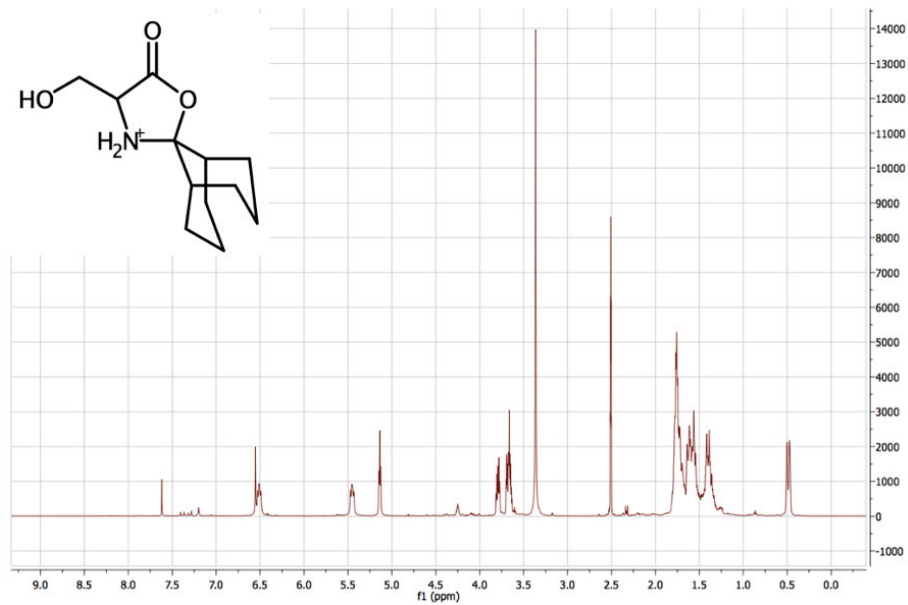
^{1}H-NMR

4'-{[(4-methylbenzenesulfonyl)oxy]methyl}-5'-oxospiro[bicyclo[3.3.1]nonane-9,2'-[1,3]oxazolidin]-3'-ium:
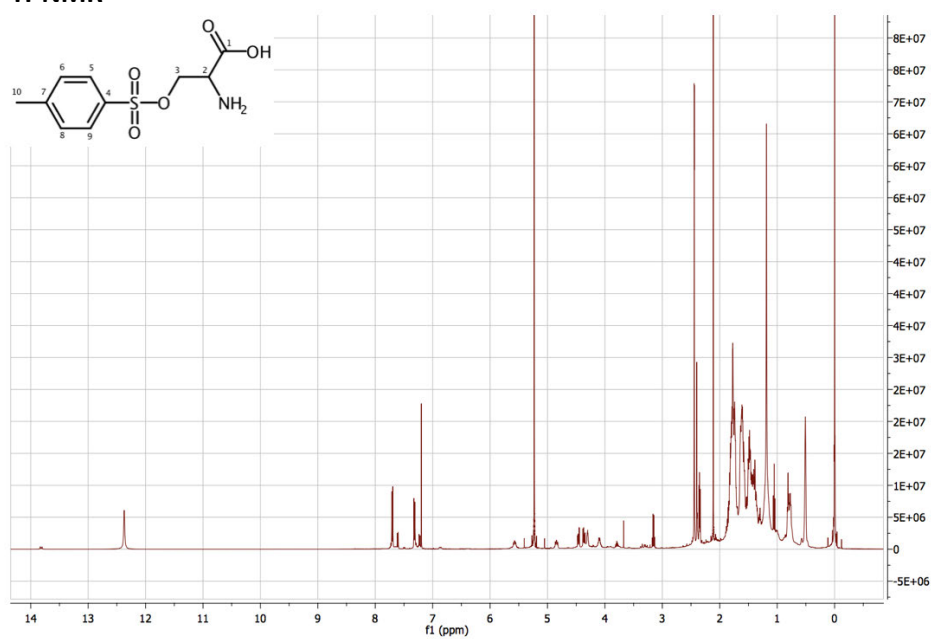
^{1}H-NMR

4'-[(2-aminophenyl)amino]-5'-oxospiro[bicyclo[3.3.1]nonane-9,2'-[1,3]oxazolidin]-3'-ium:
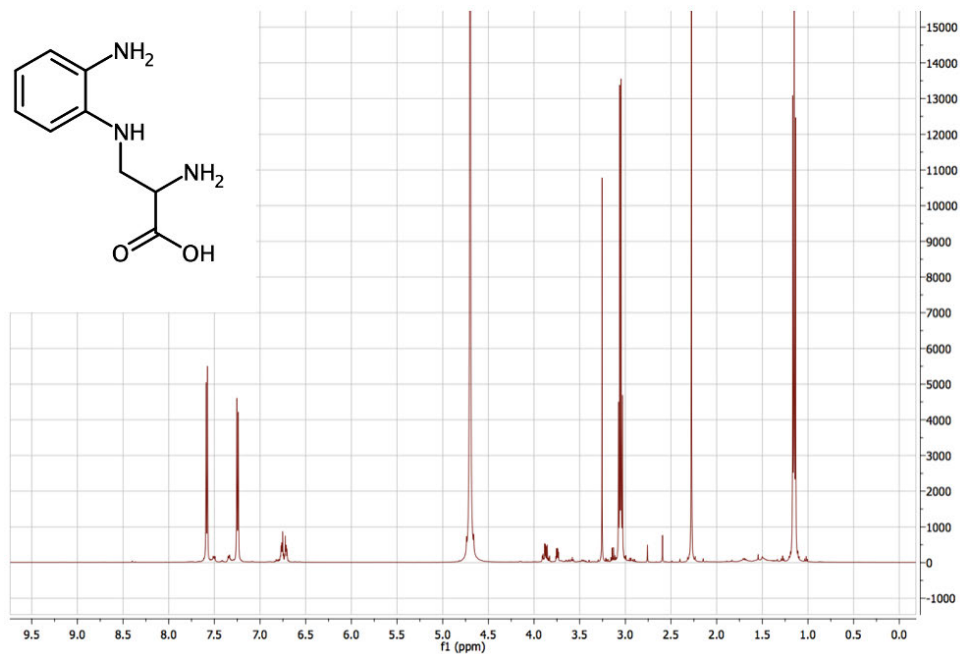
¹H-NMR

Propyl 4-methylbenzene-1-sulfonate:
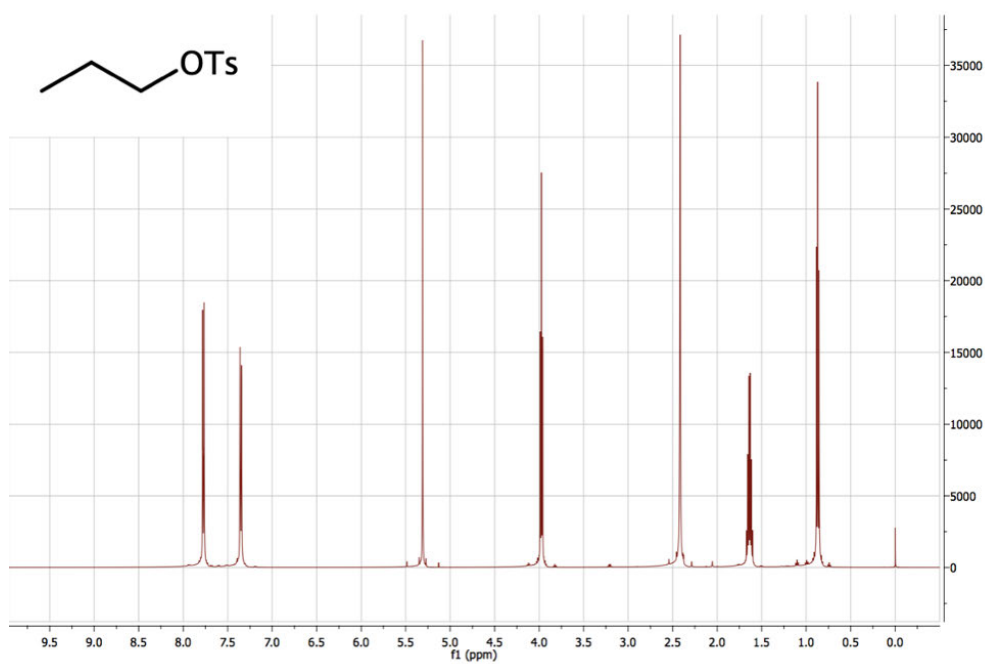
¹H-NMR

Propan-2-yl 4-methylbenzene-1-sulfonate:
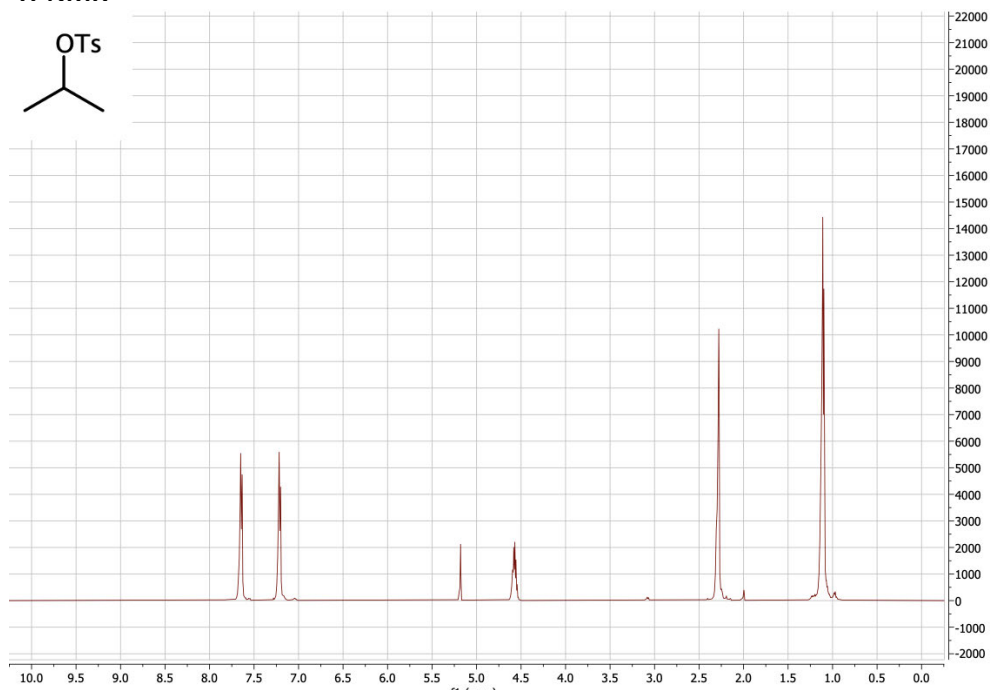
¹H-NMR

N1-propylbenzene-1,2-diamine:
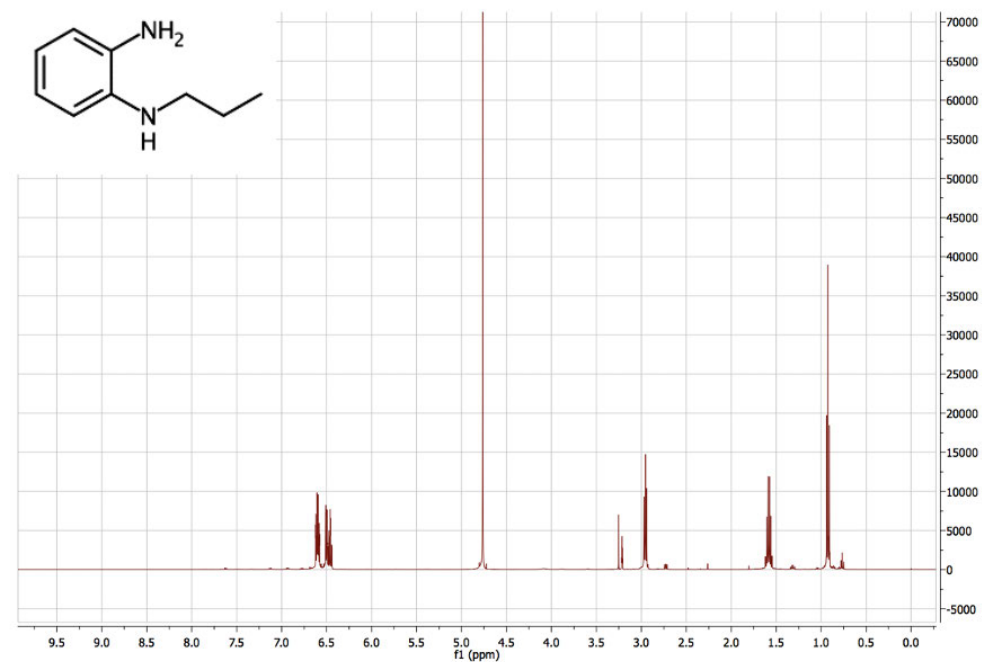
¹H-NMR

N1-(propan-2-yl)benzene-1,2-diamine
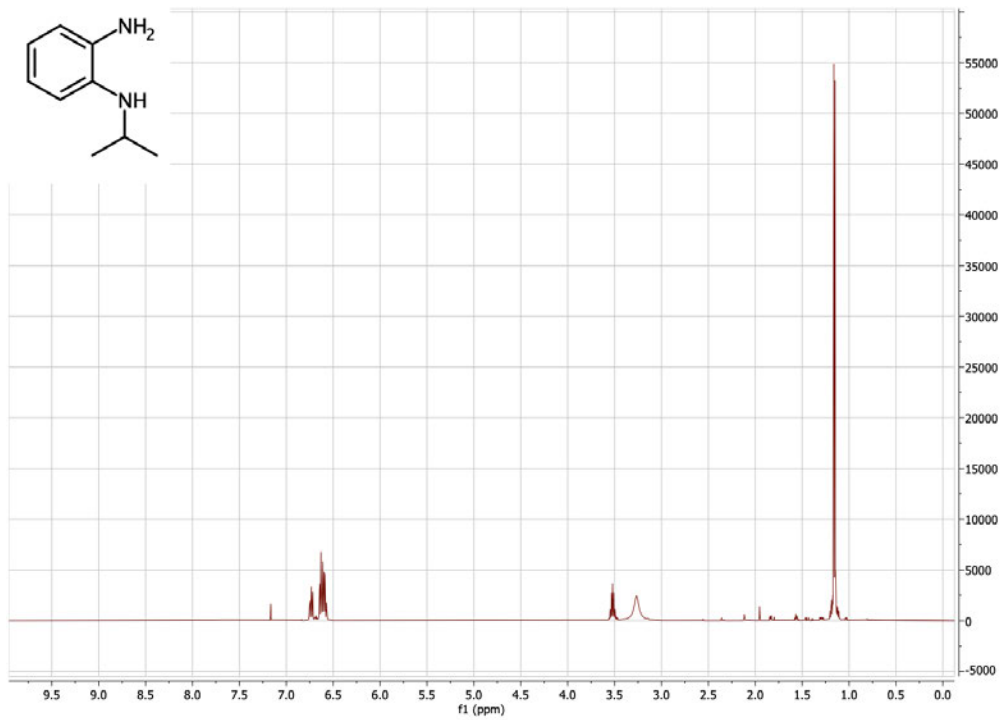
^{1}H-NMR

(1-propyl-1H-1,3-benzodiazol-2-yl)methanol:
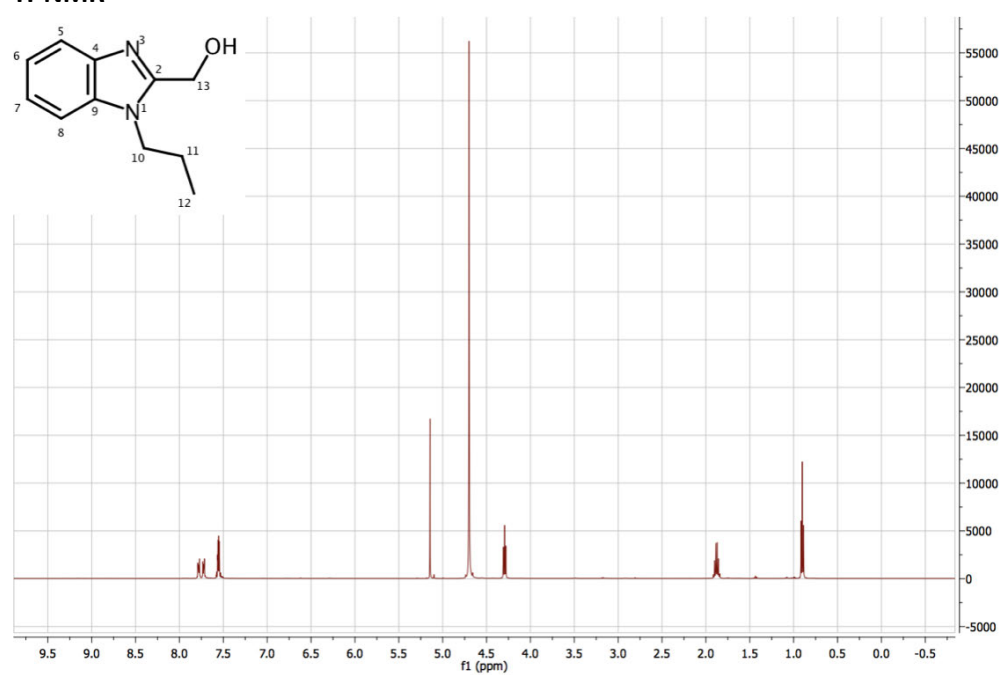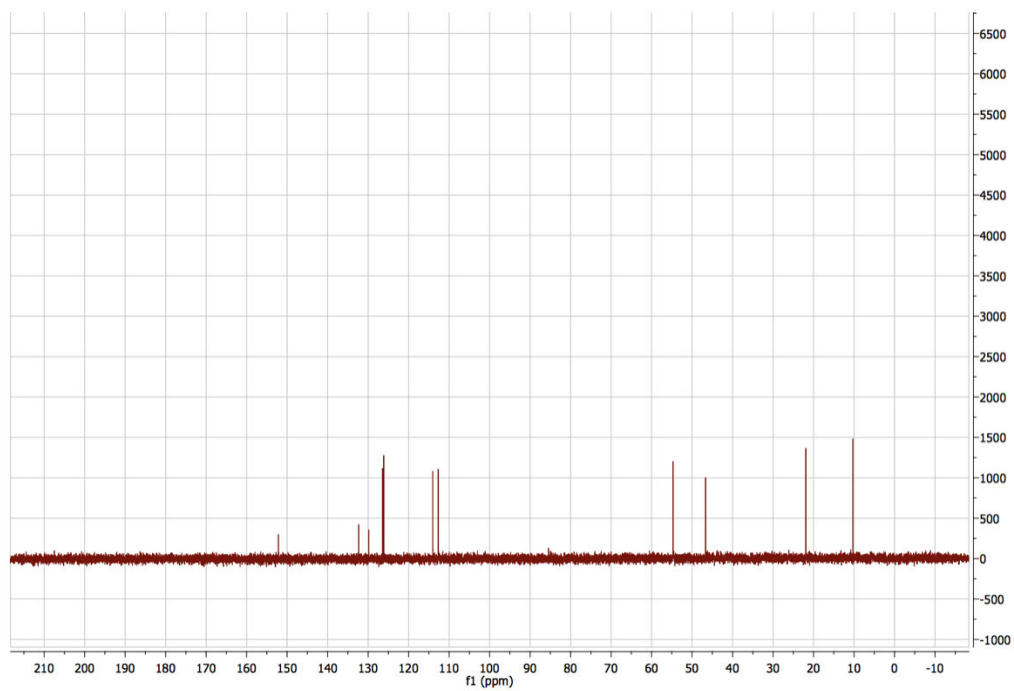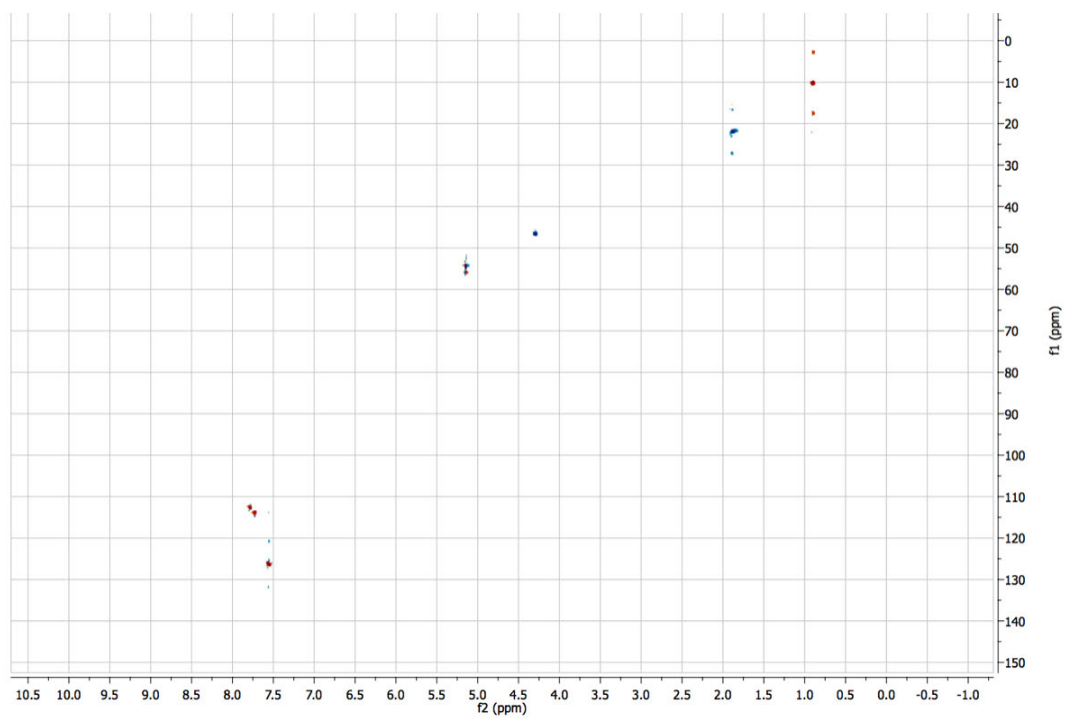
^{1}H-NMR

¹³C-NMR

HSQC

(1-propyl-1H-1,3-benzodiazol-2-yl)methyl acetate:

¹H-NMR
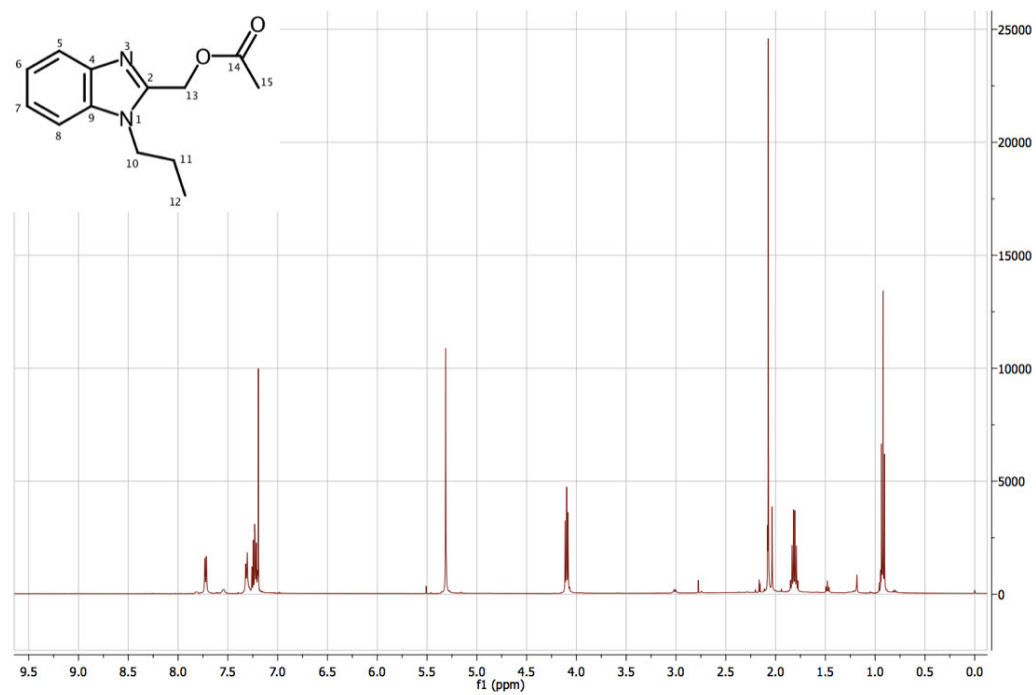
¹³C-NMR
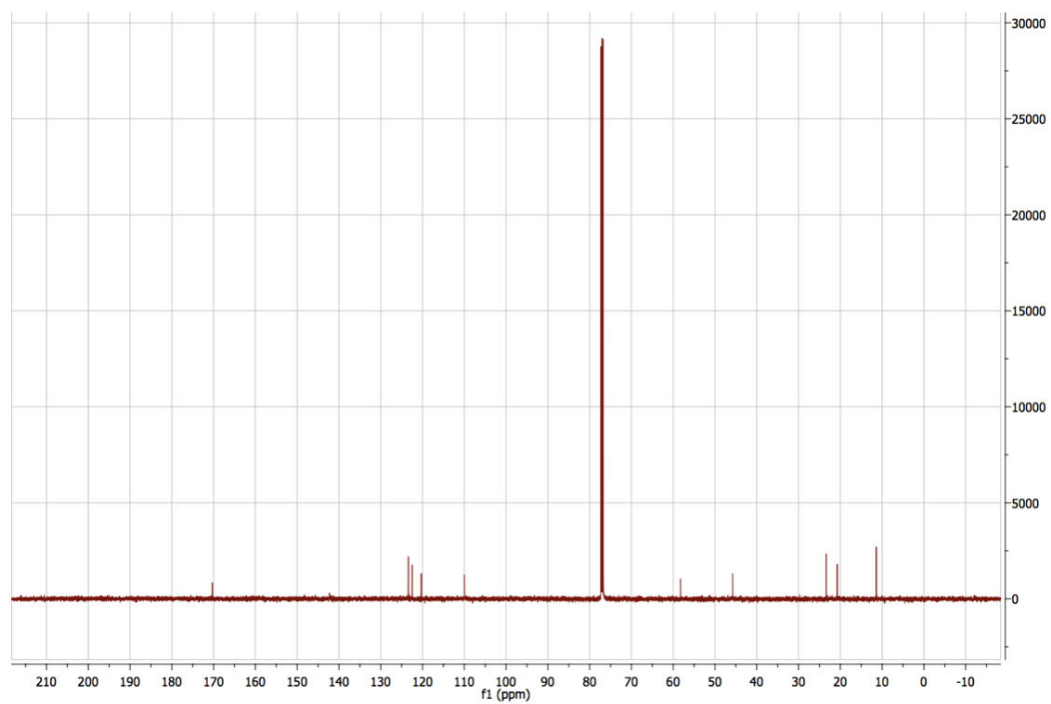
(1H-1,3-benzodiazol-2-yl)methanol
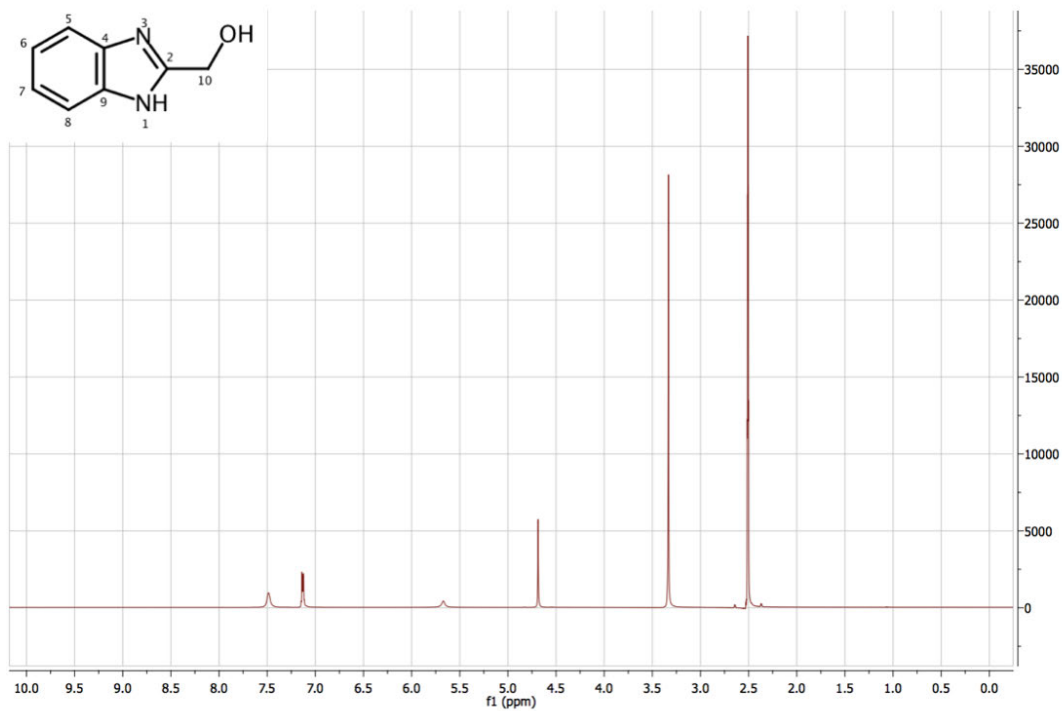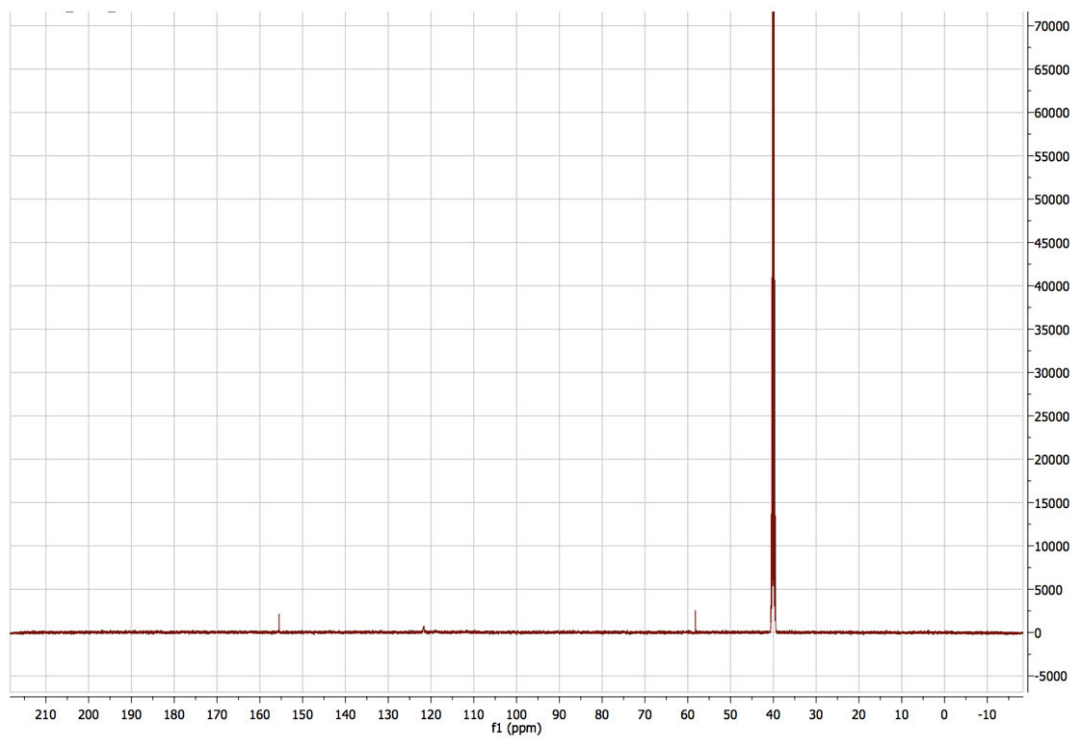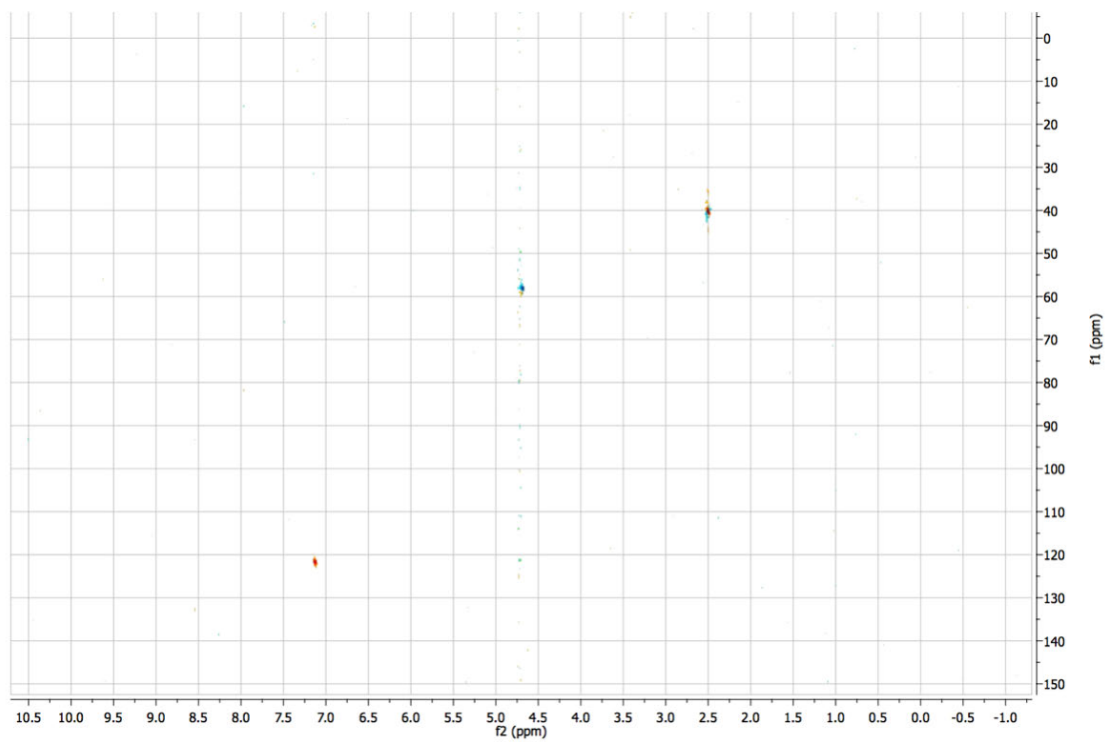
¹H-NMR
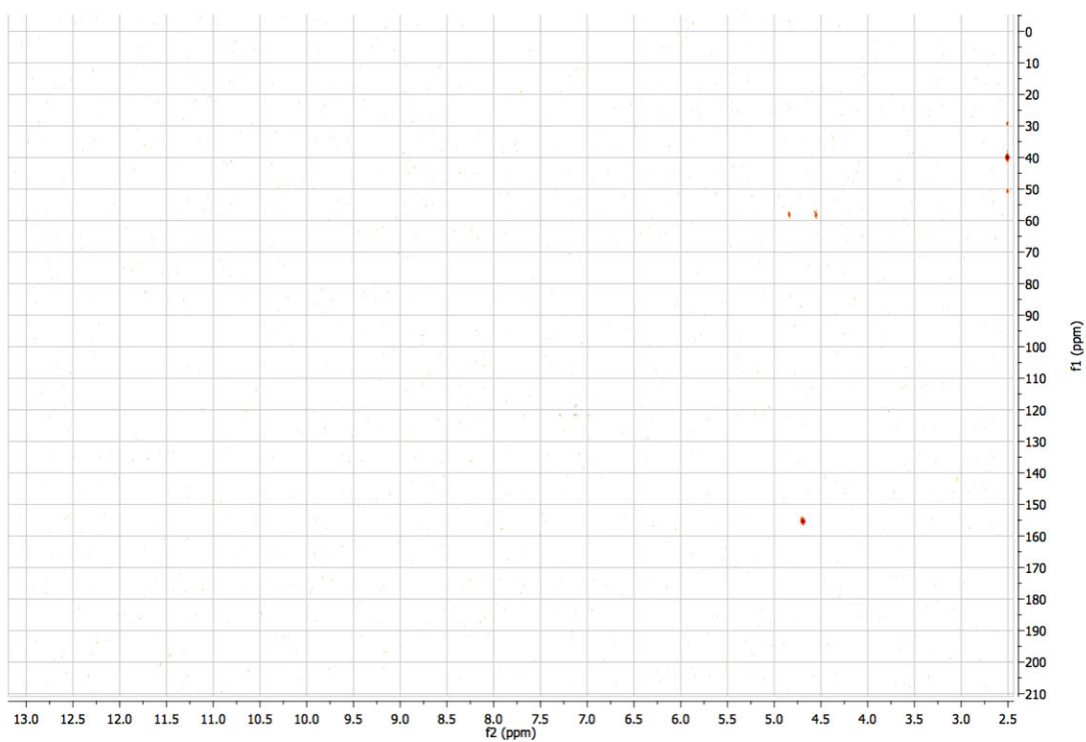
¹³C-NMR

HSQC

HMBC

(5,6-dimethyl-1H-1,3-benzodiazol-2-yl)methanol:
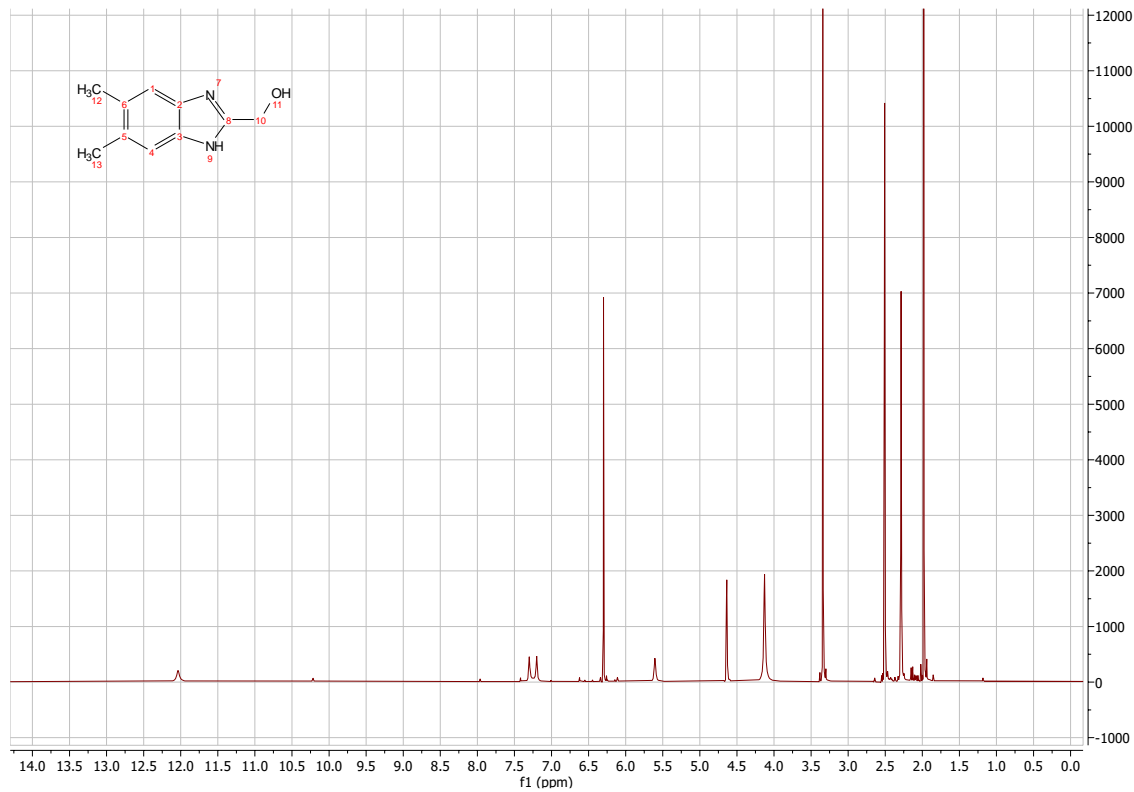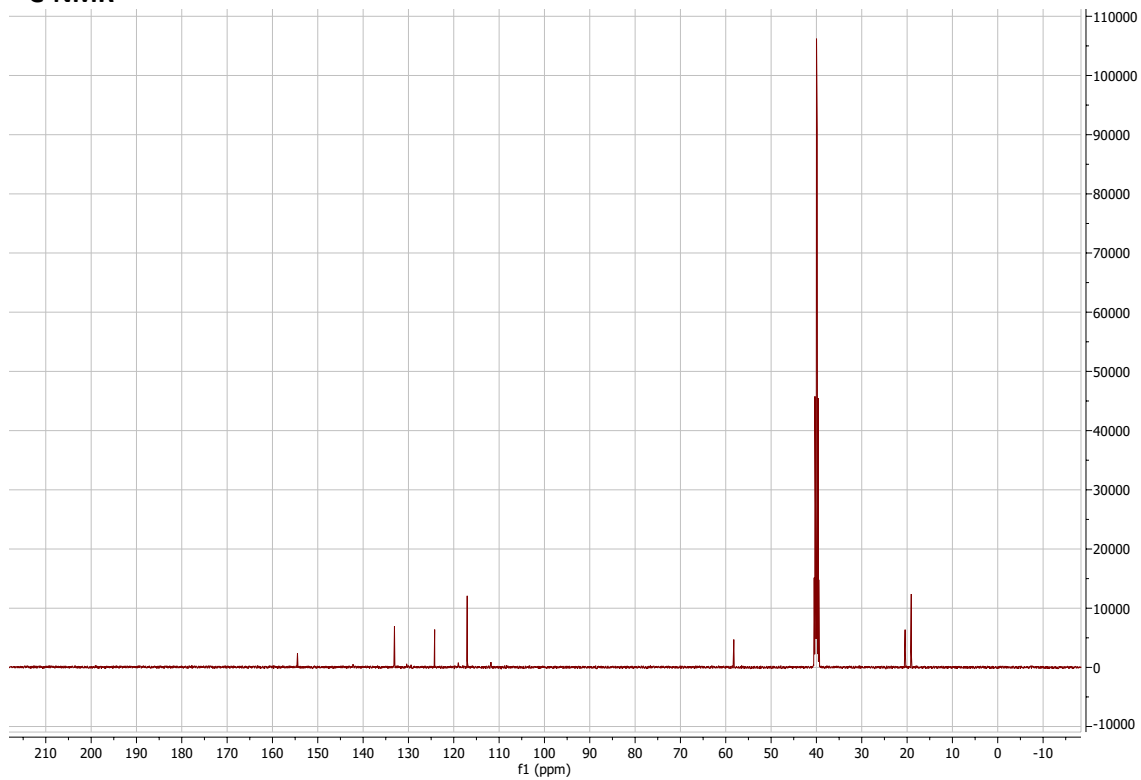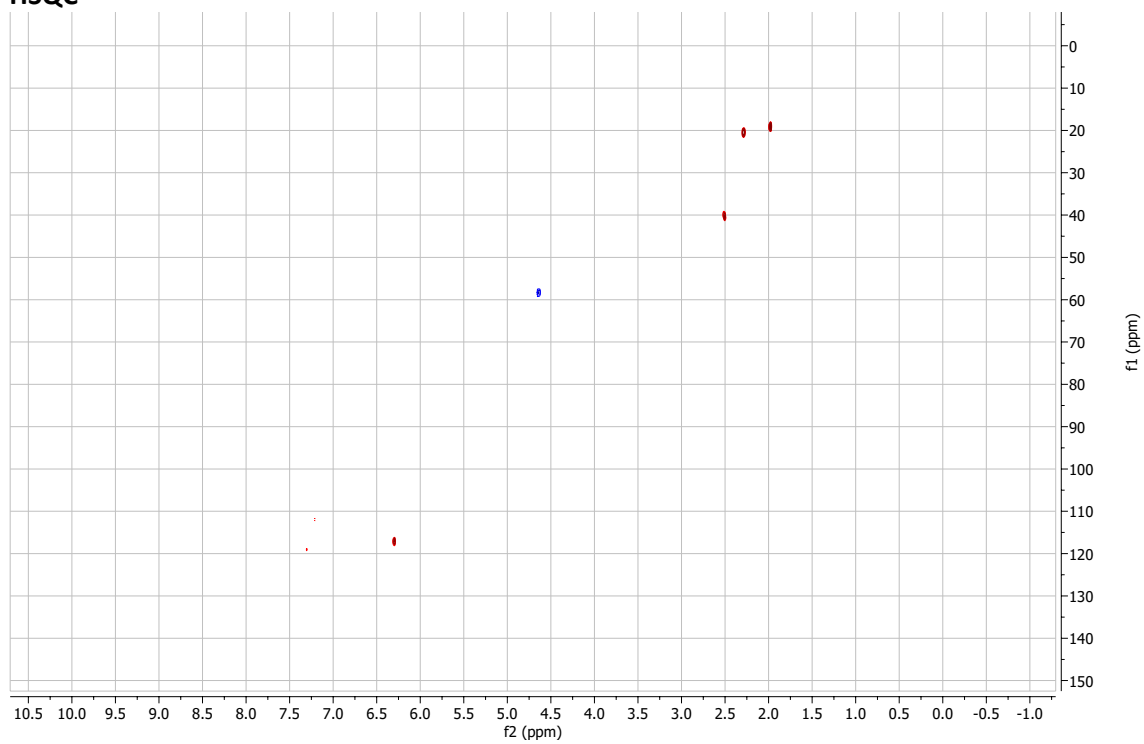
¹H-NMR

¹³C-NMR

HSQC

HMBC

(5-chloro-1H-1,3-benzodiazol-2-yl)methanol

^{1}H-NMR

^{13}C-NMR

264
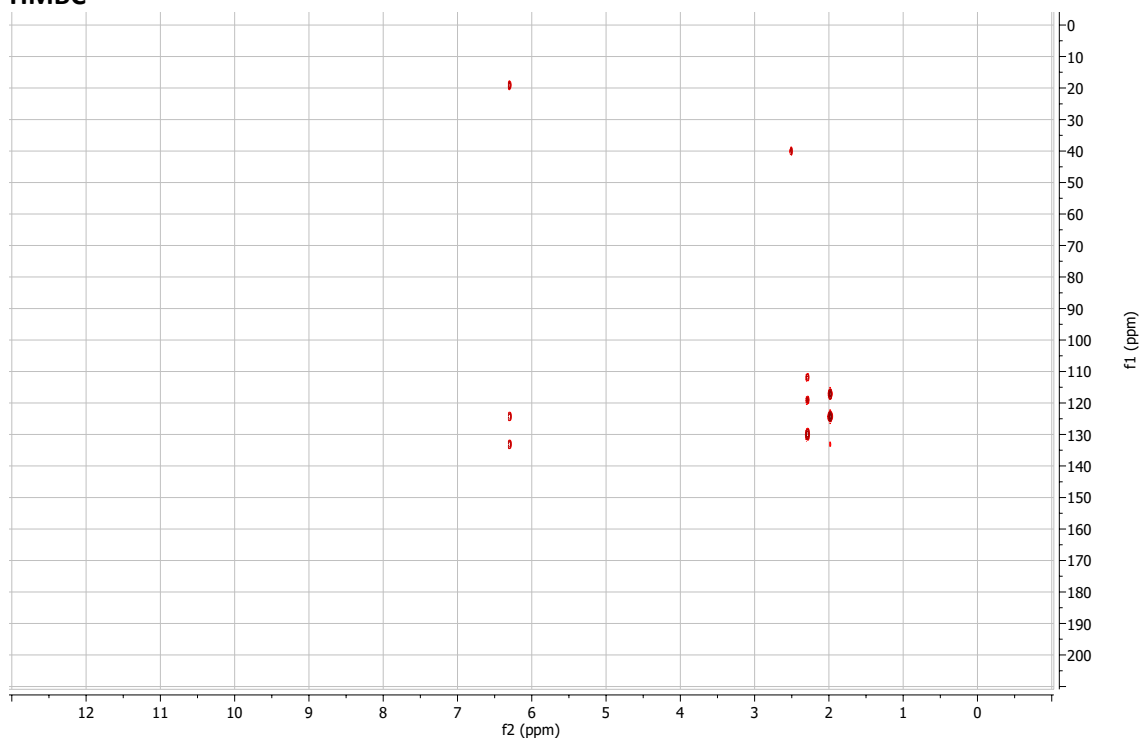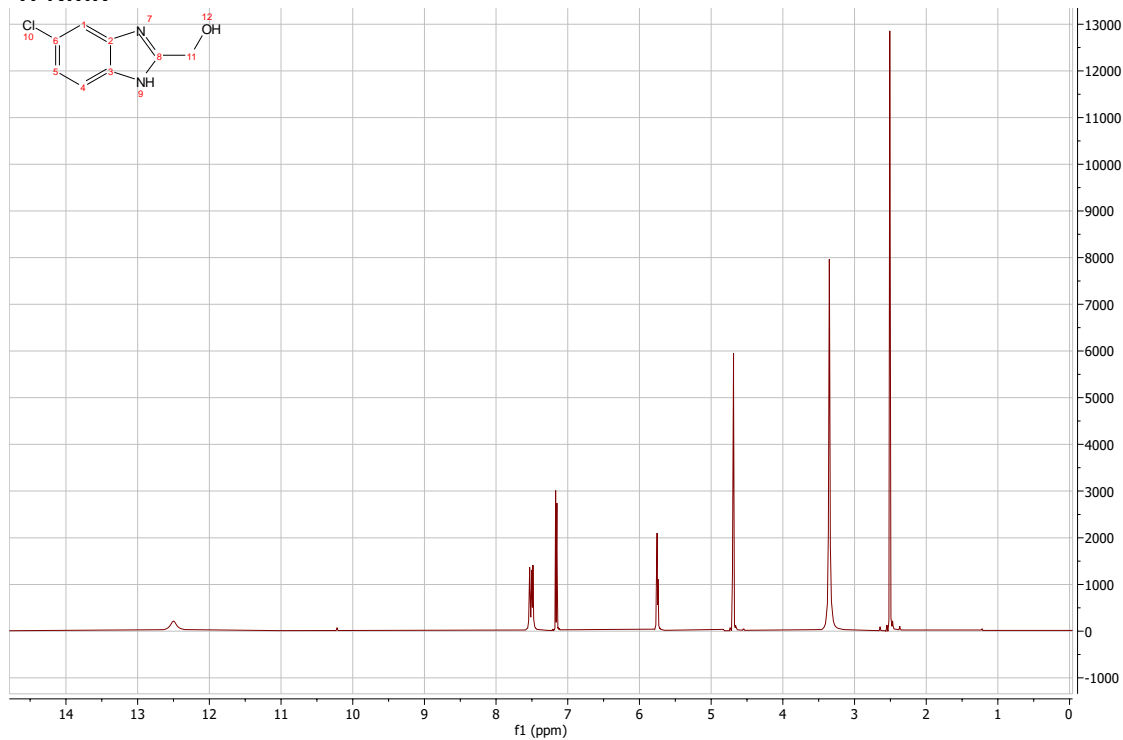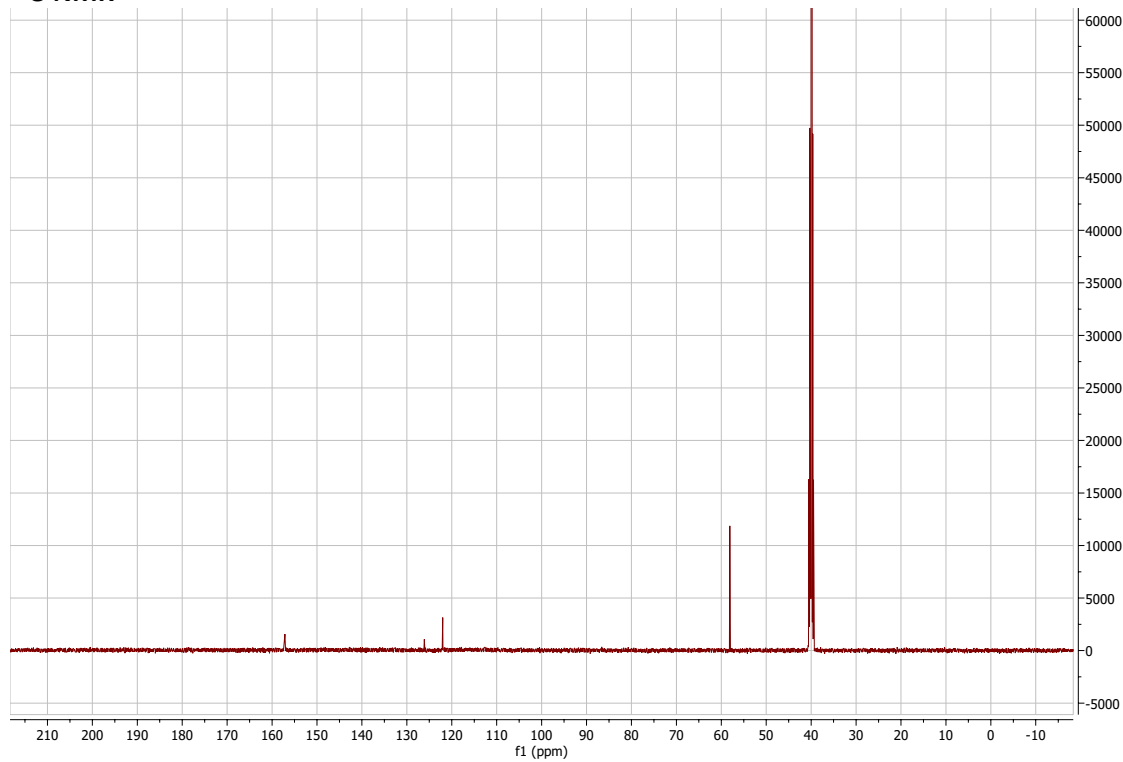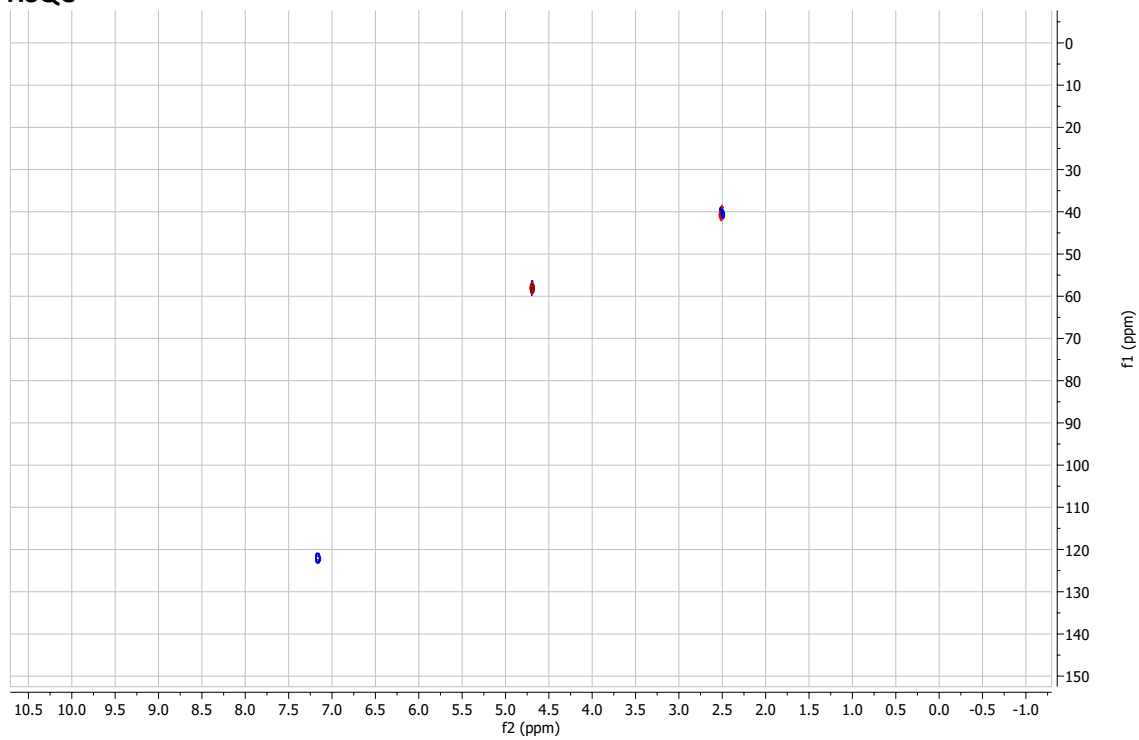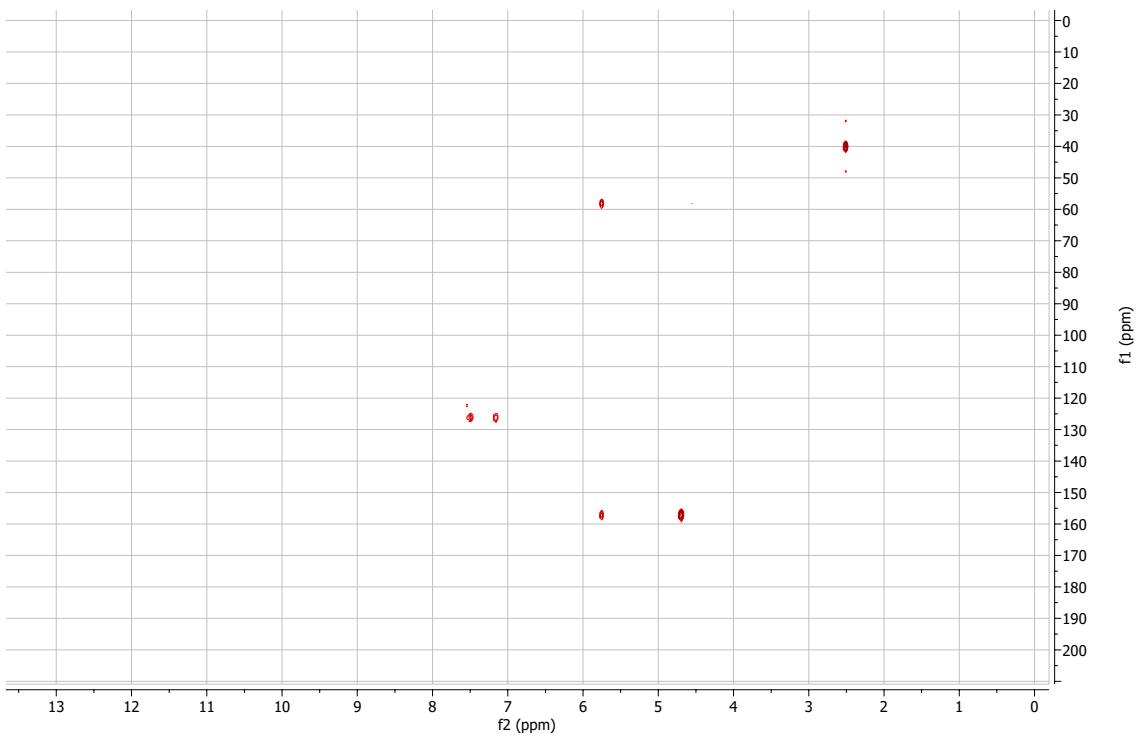
HSQC

HMBC

(5-nitro-1H-1,3-benzodiazol-2-yl)methanol:
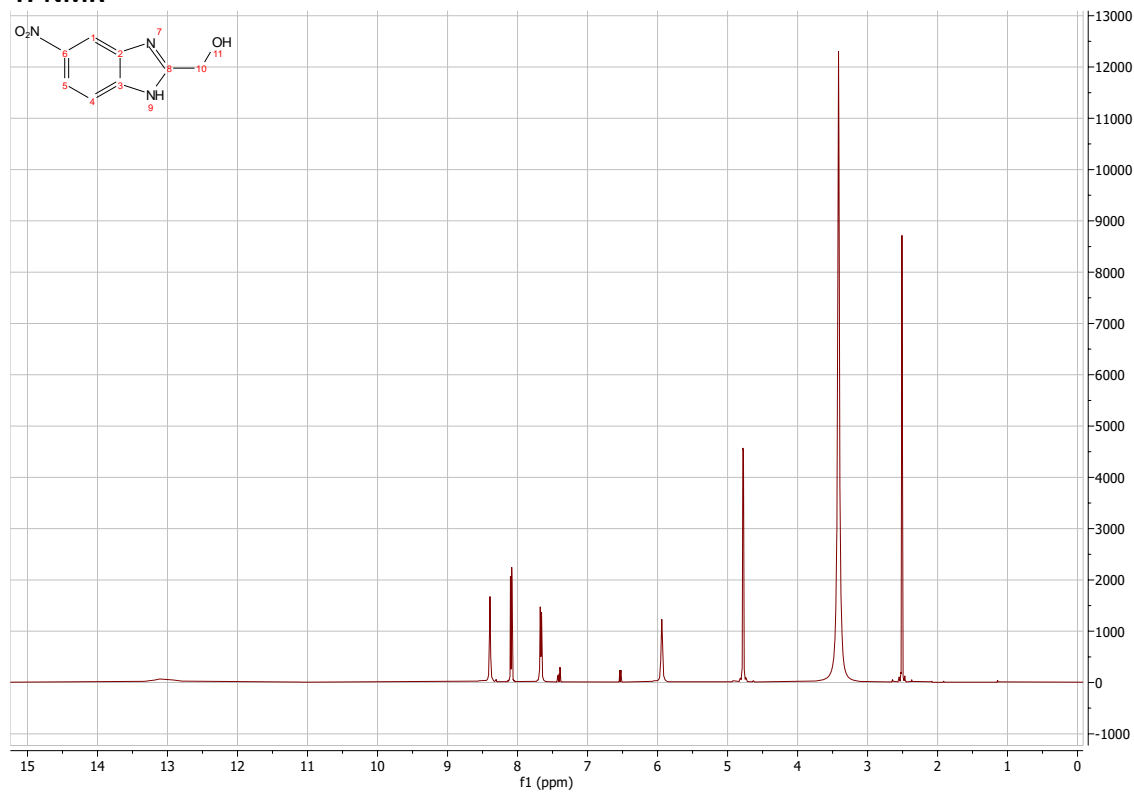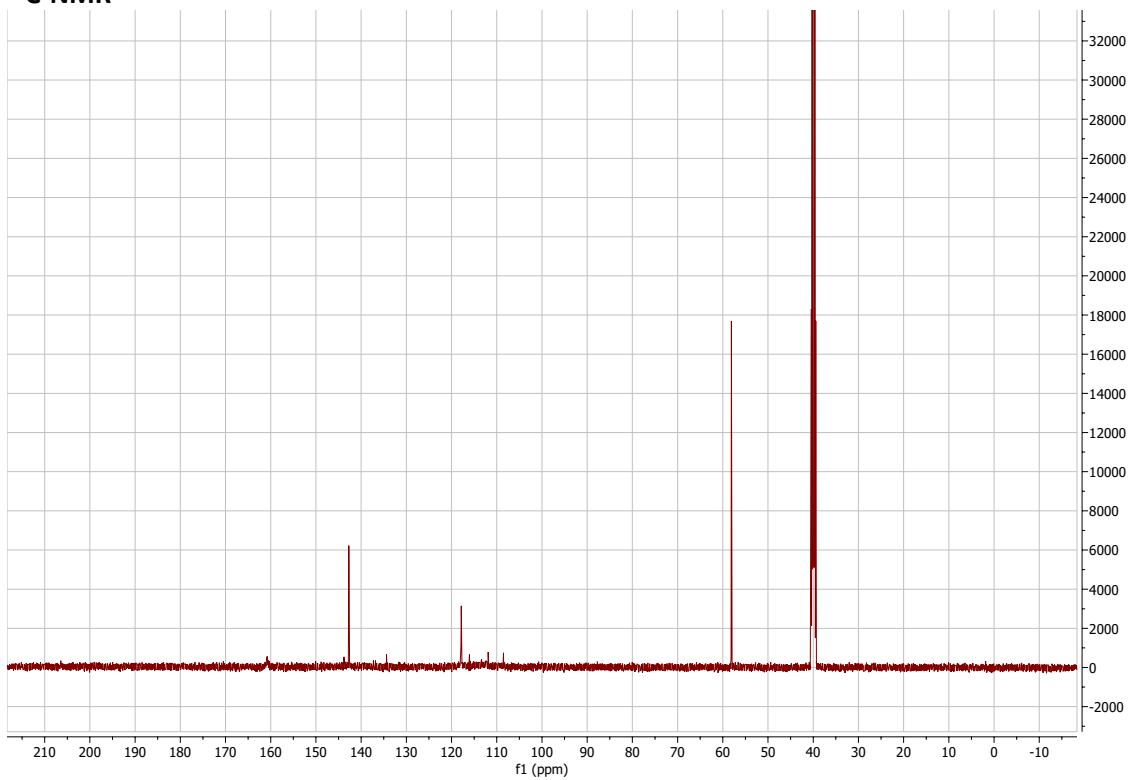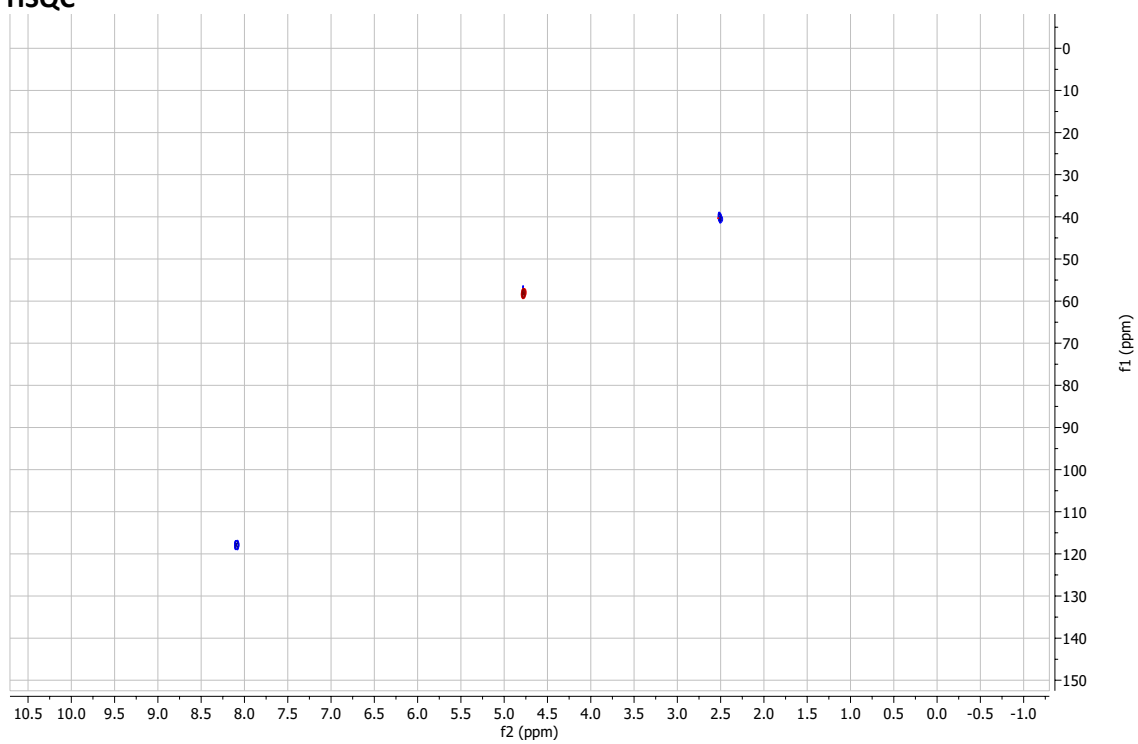
¹H-NMR
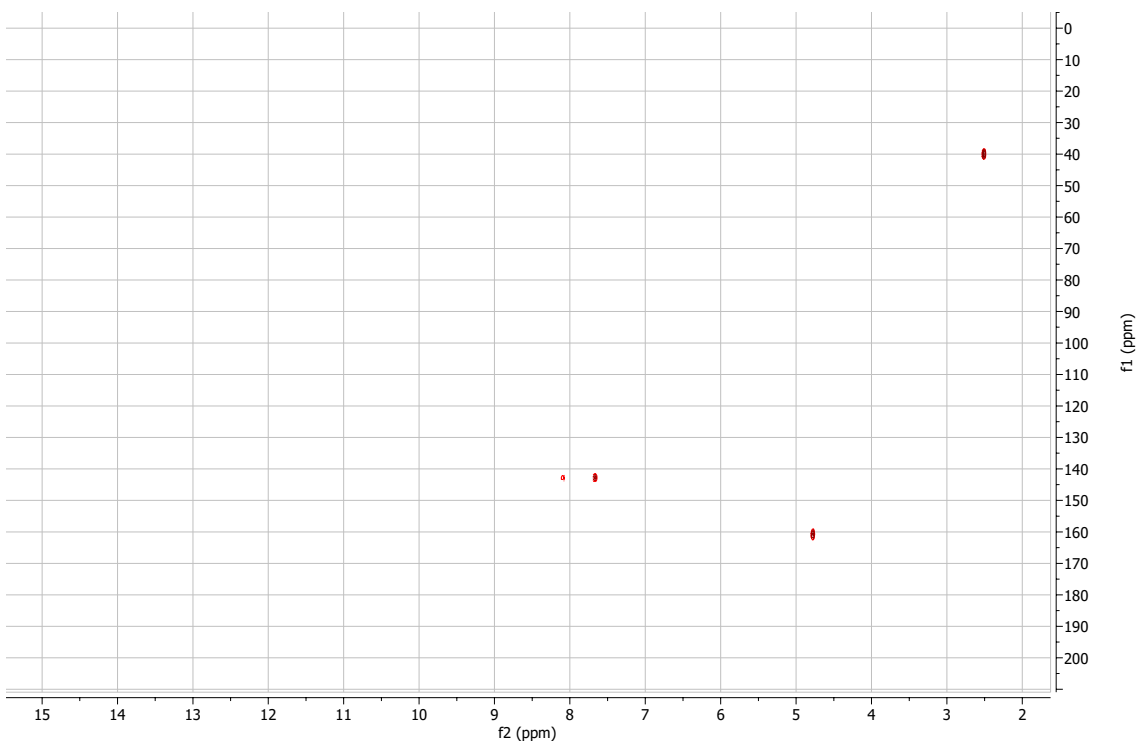
¹³C-NMR

HSQC

HMBC

2-(hydroxymethyl)-1H-1,3-benzodiazole-5-carboxylic acid:
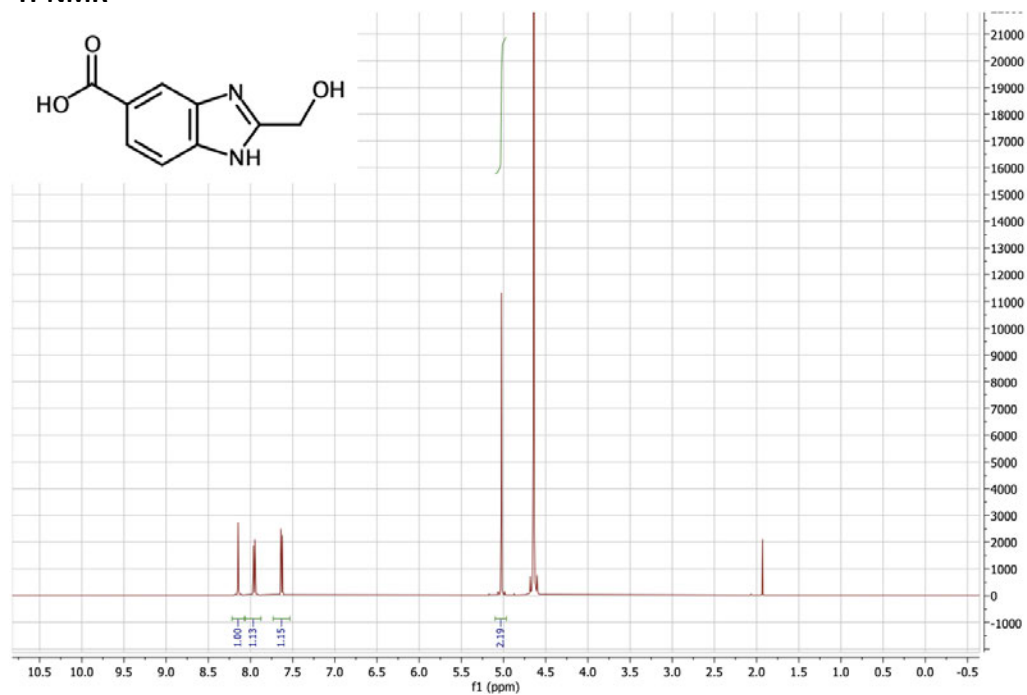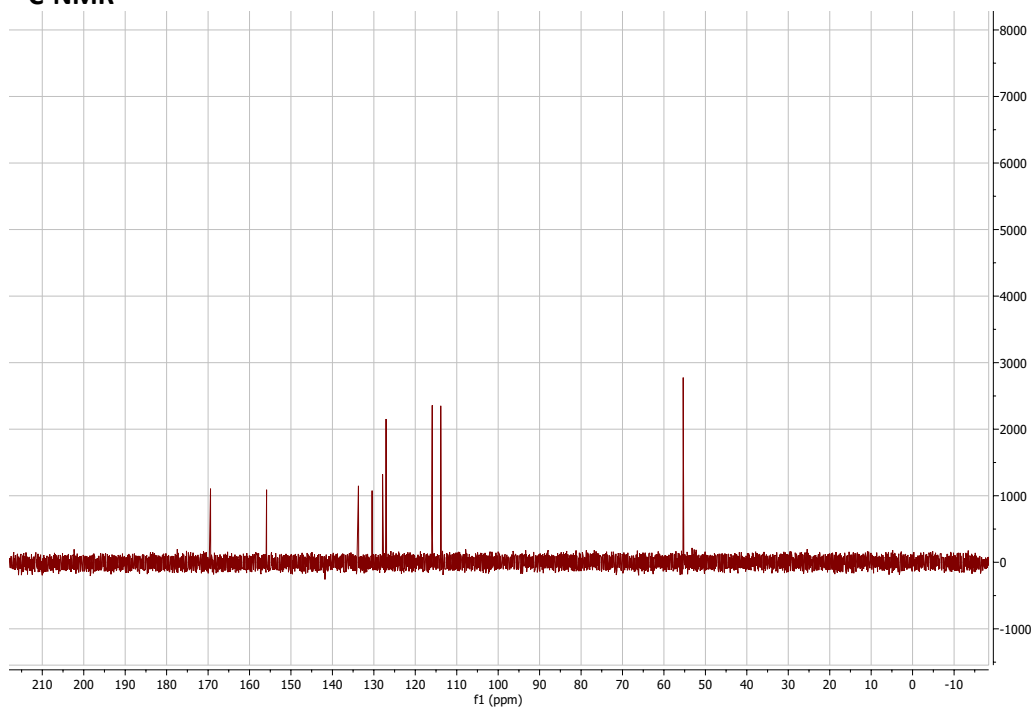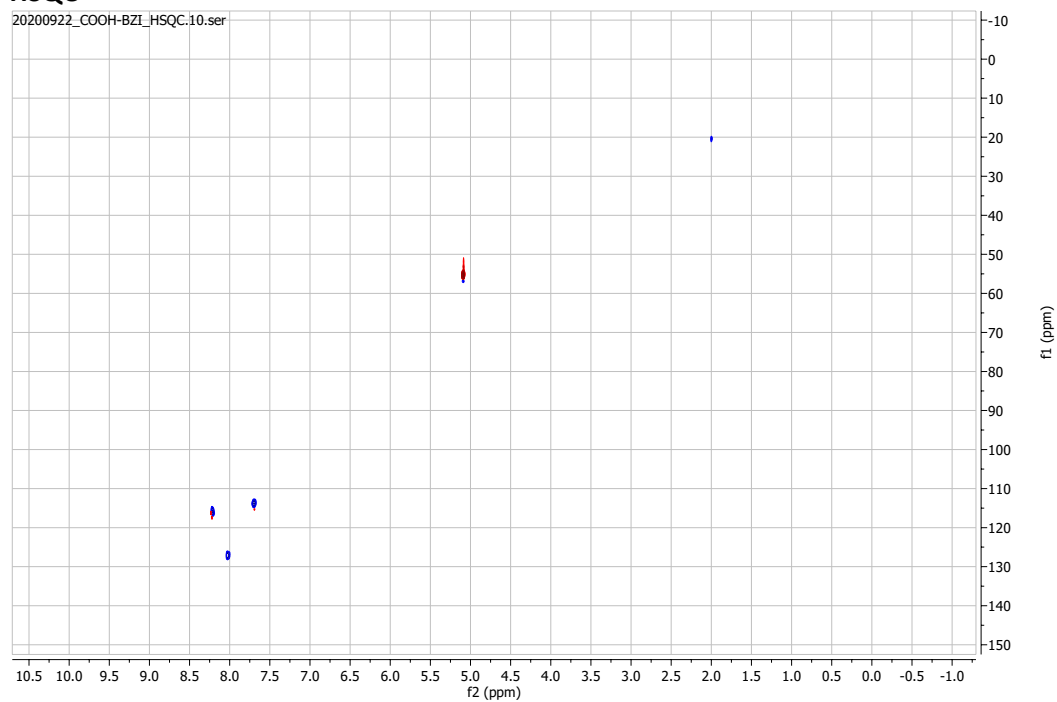
¹H-NMR
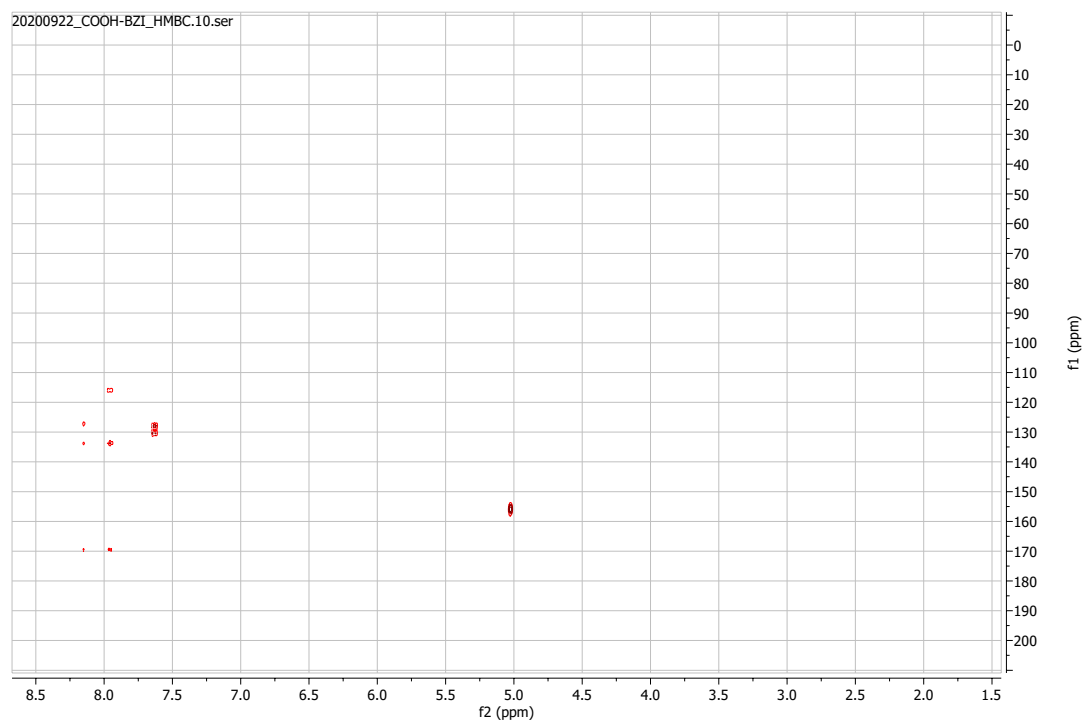
¹³C-NMR

HSQC

HMBC

Example of imines in mixture

¹H-NMR

(5-benzoyl-1H-1,3-benzodiazol-2-yl)methanol:

¹H-NMR

¹³C-NMR

HSQC

20210804_benzopheno-BZI.clean_HSQC.10.ser
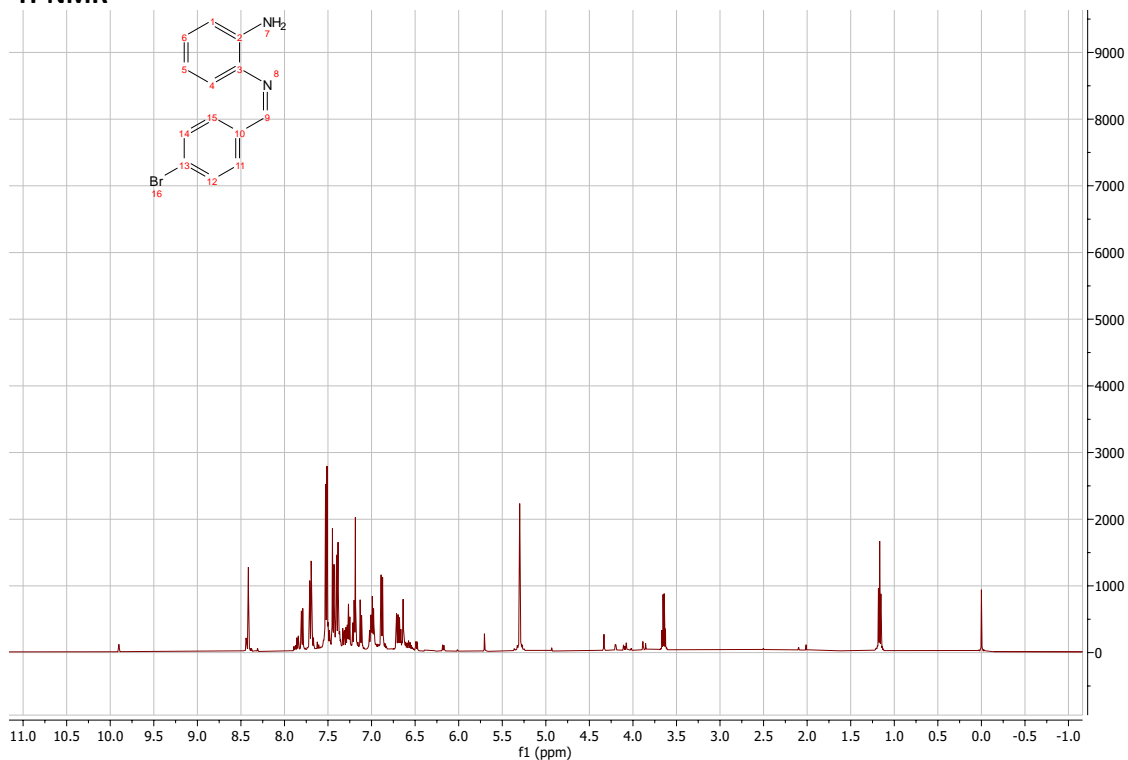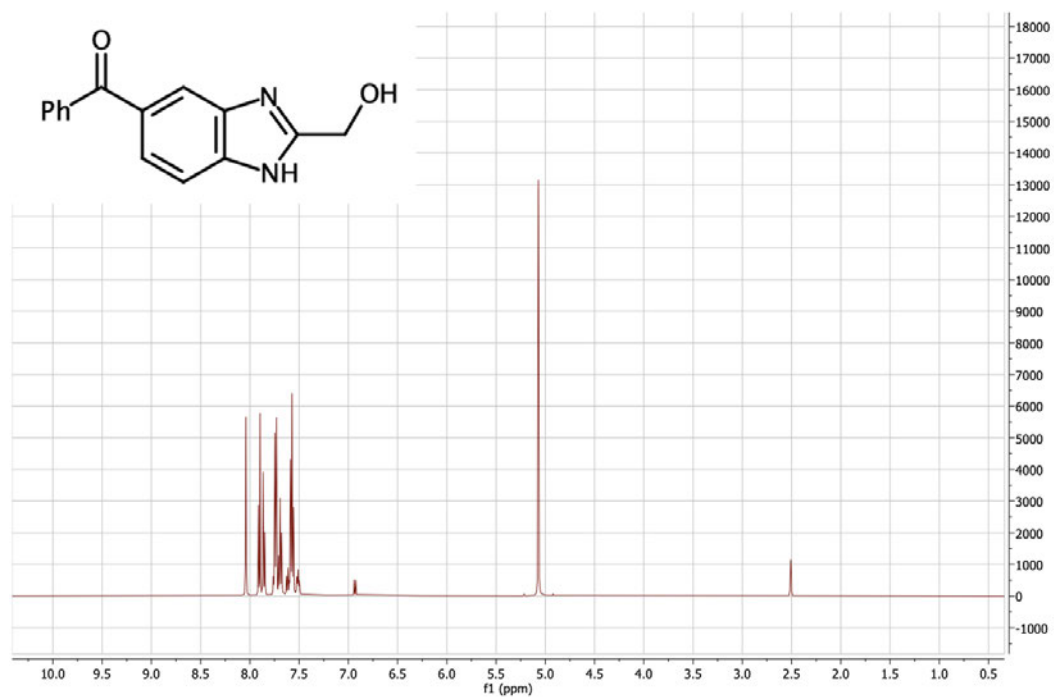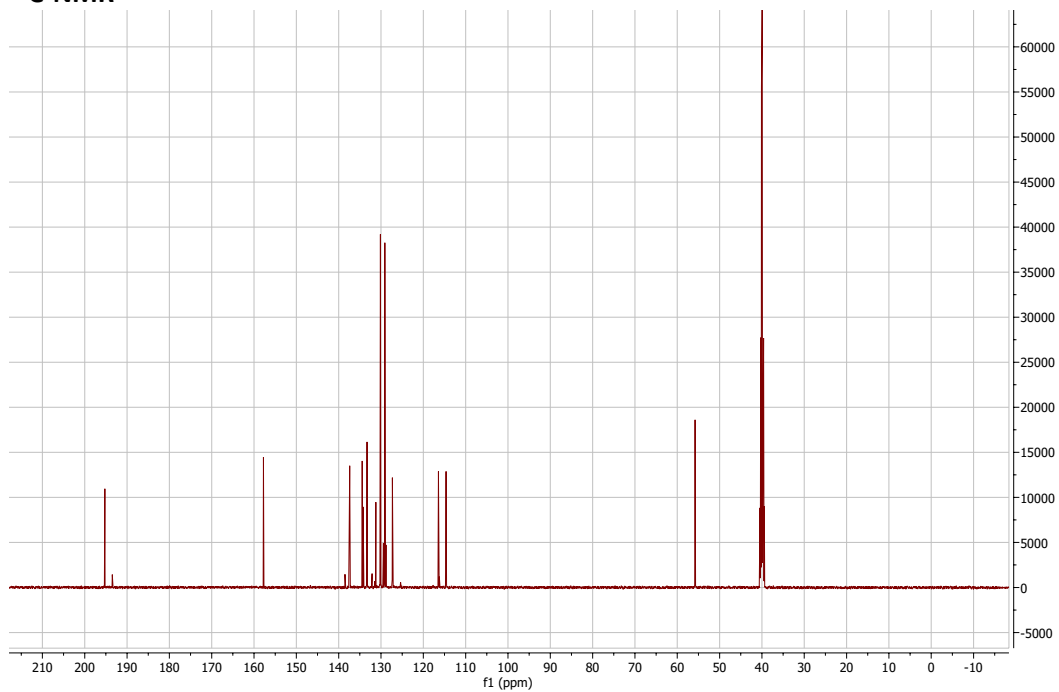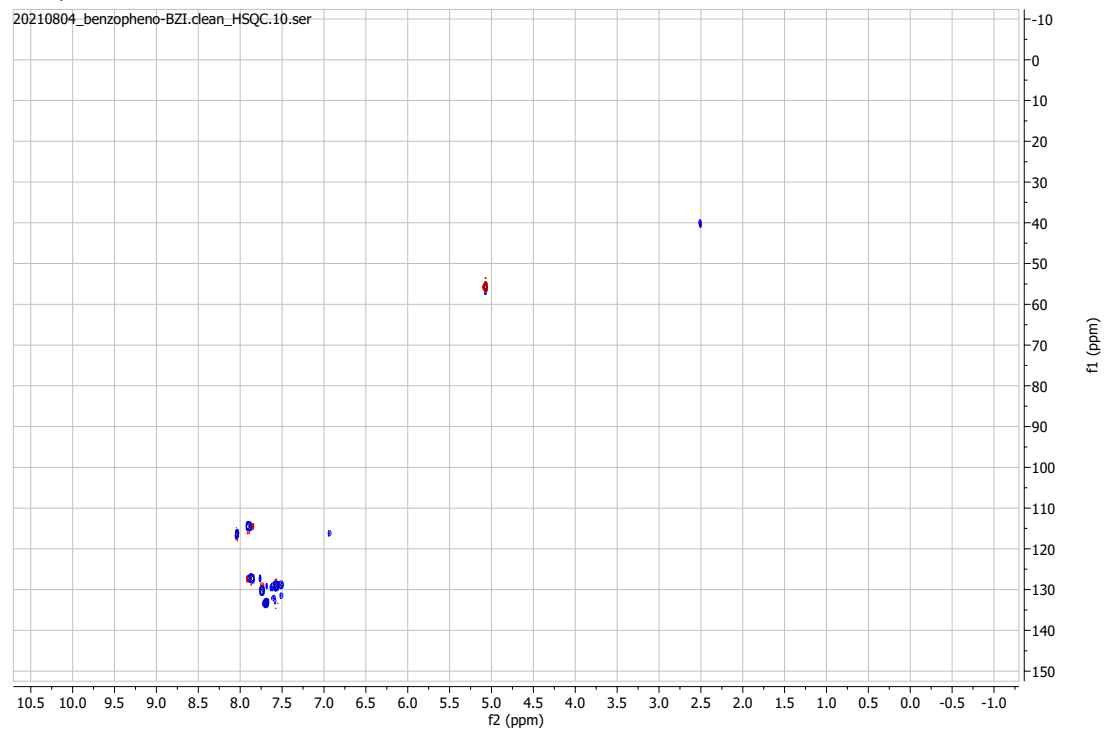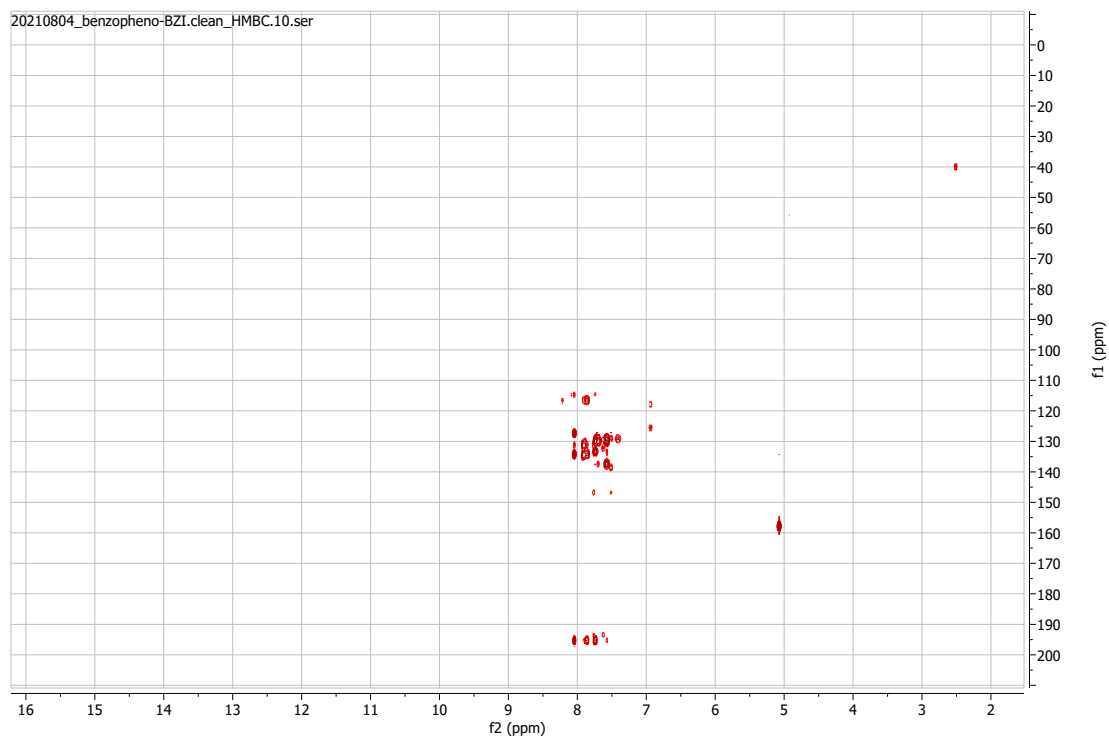
HMBC

(1-benzyl-1H-1,3-benzodiazol-2-yl)methanol:
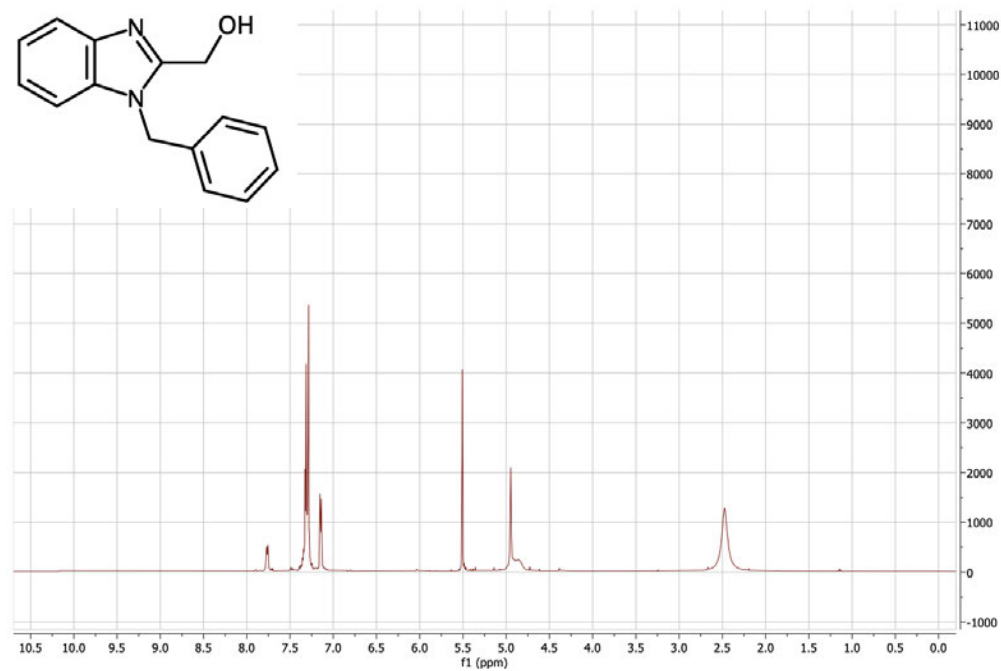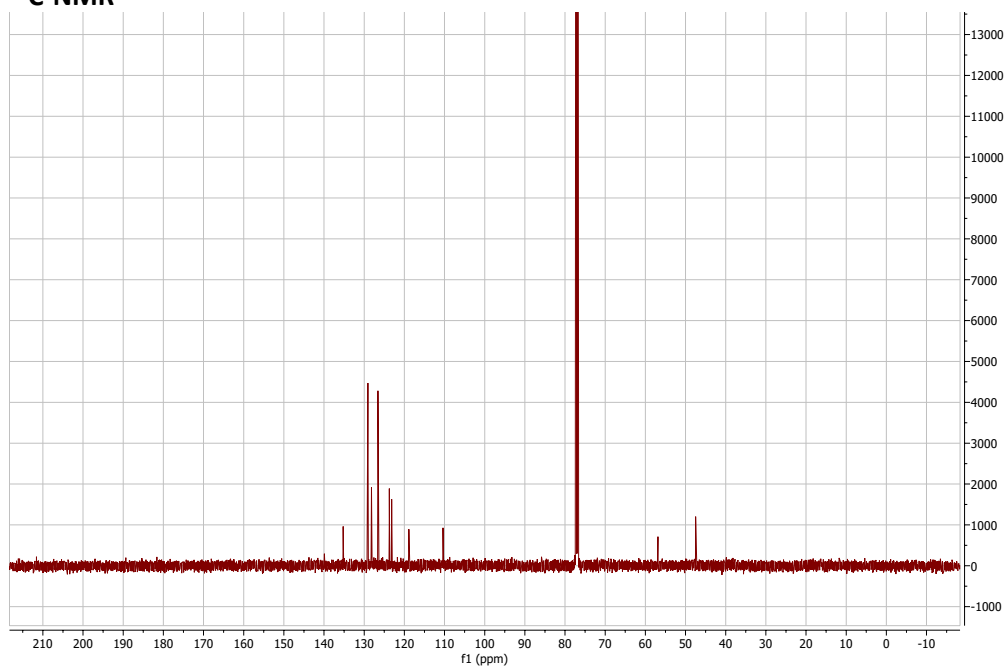
¹H-NMR

^{13}C-NMR

HSQC

20200916_CH176_bz-BZI_HSQC.10.ser

HMBC

20200916_CH176_bz-BZI_HMBC.10.ser

N-HMBC

20200922_CH176_N-HMBC.11.ser
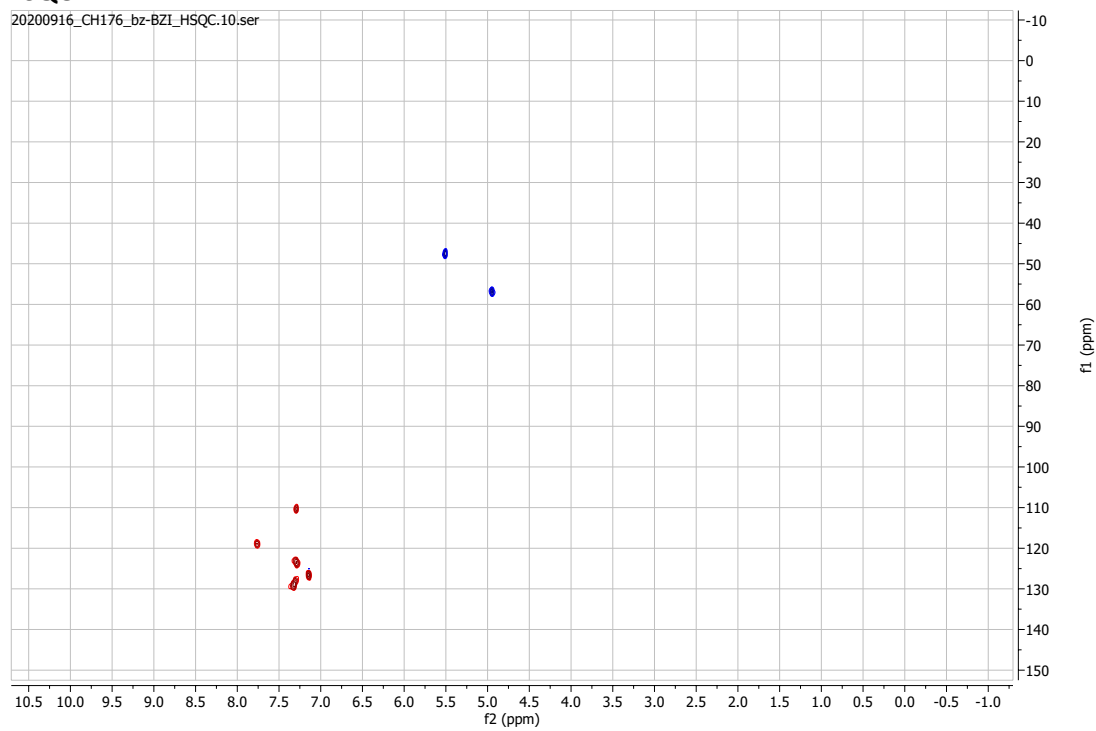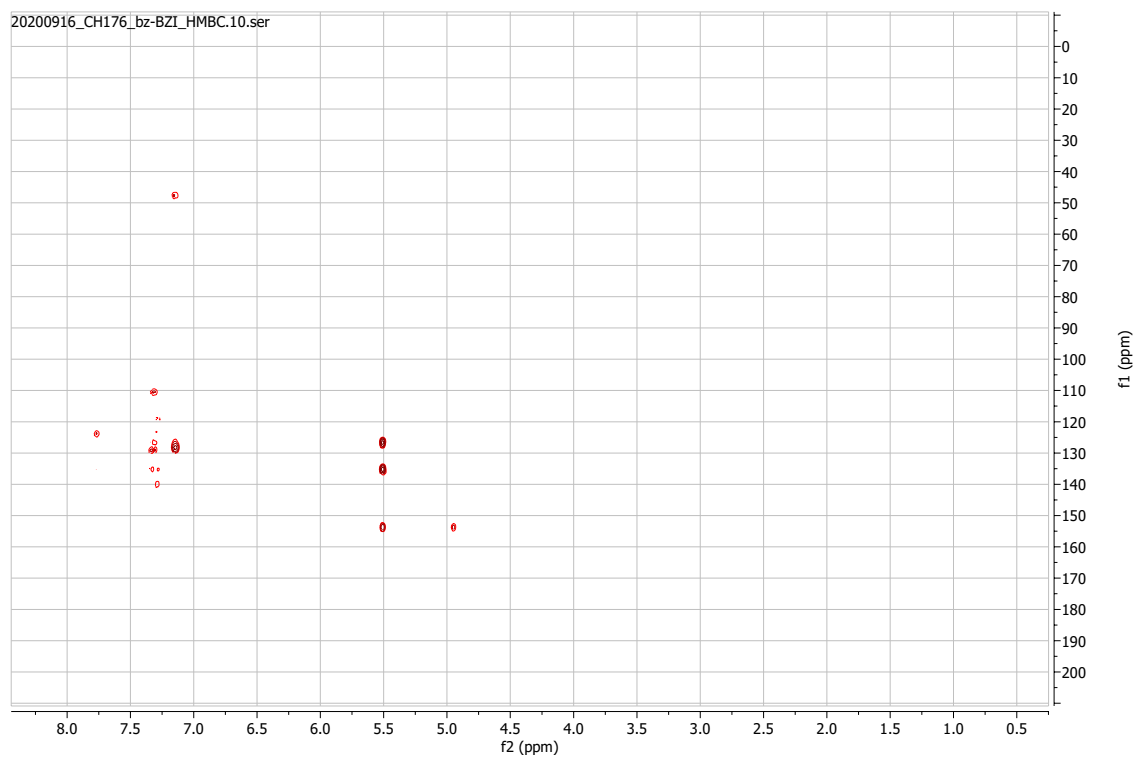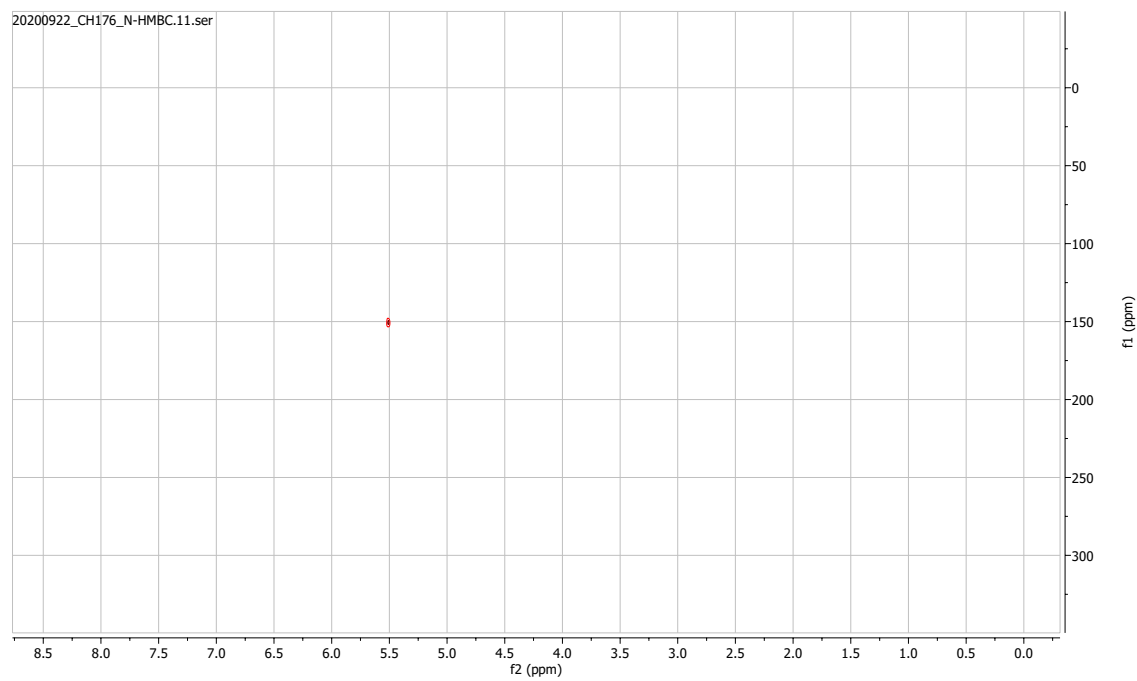
(1-[(4-Bromophenyl)methyl]-1*H*-1,3-benzodiazol-2-yl)methanol:
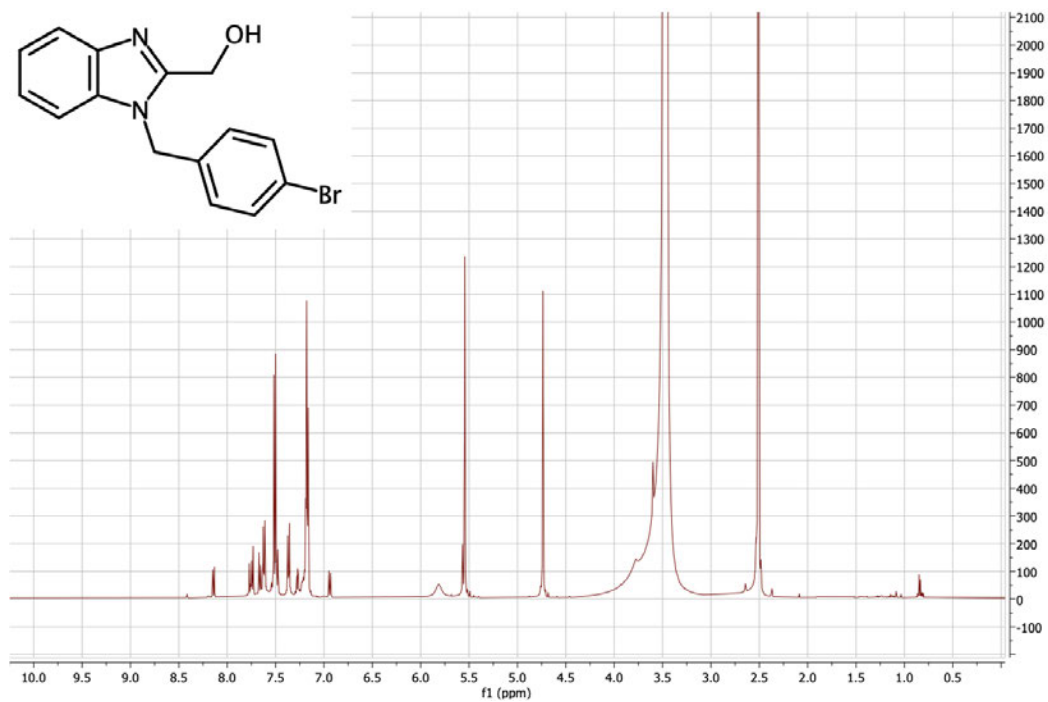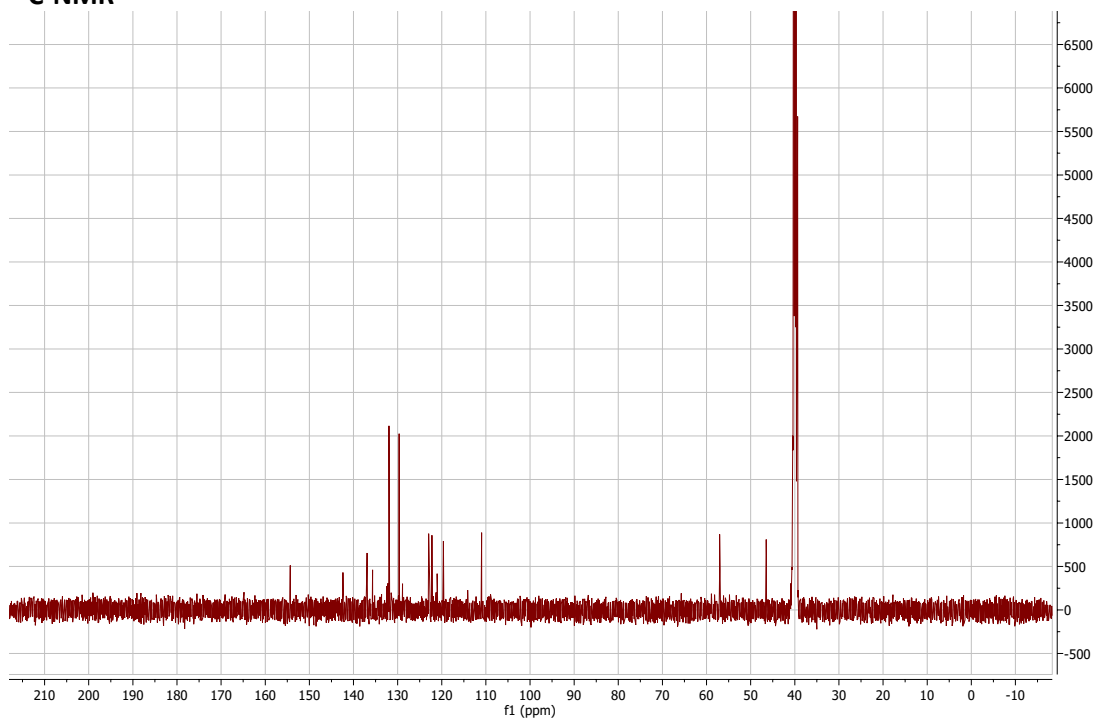
¹H-NMR

¹³C-NMR

HSQC

20210308_Ch271_phe-Br-BZI_DMSO_HSQC.10.ser
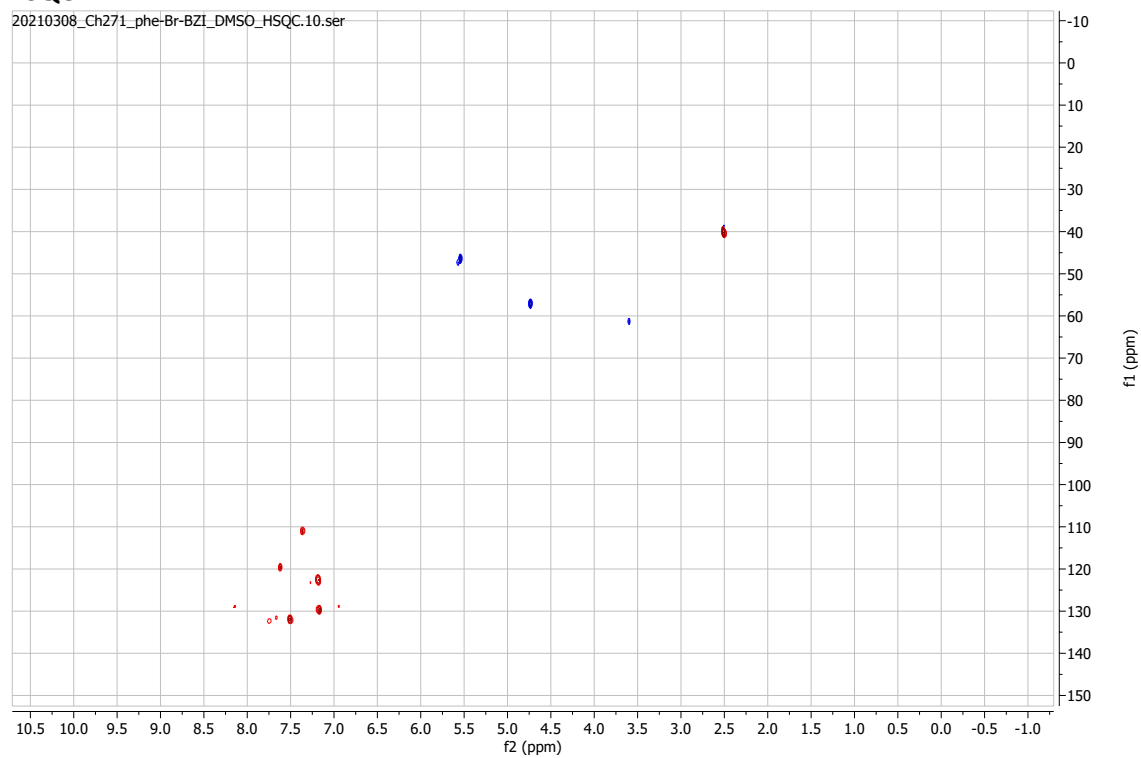
HMBC

20210308_Ch271_phe-Br-BZI_DMSO_HMBC.10.ser
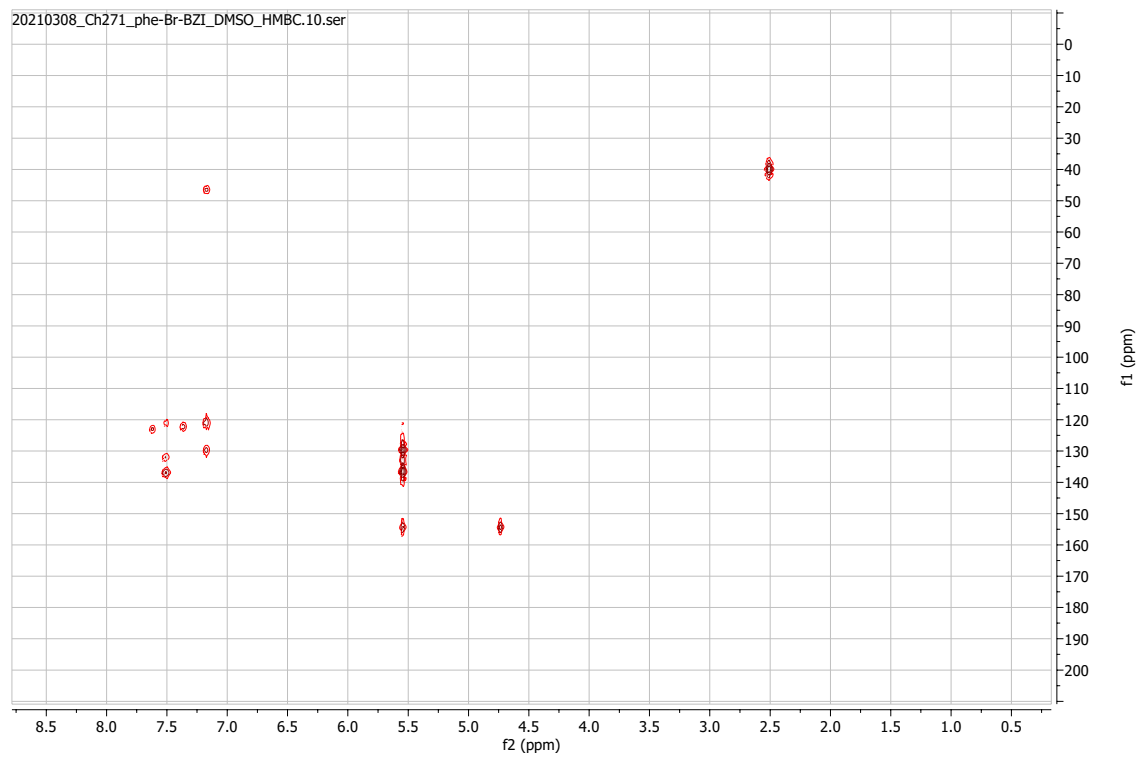
{1-[(4-methoxyphenyl)methyl]-1H-1,3-benzodiazol-2-yl}methanol:
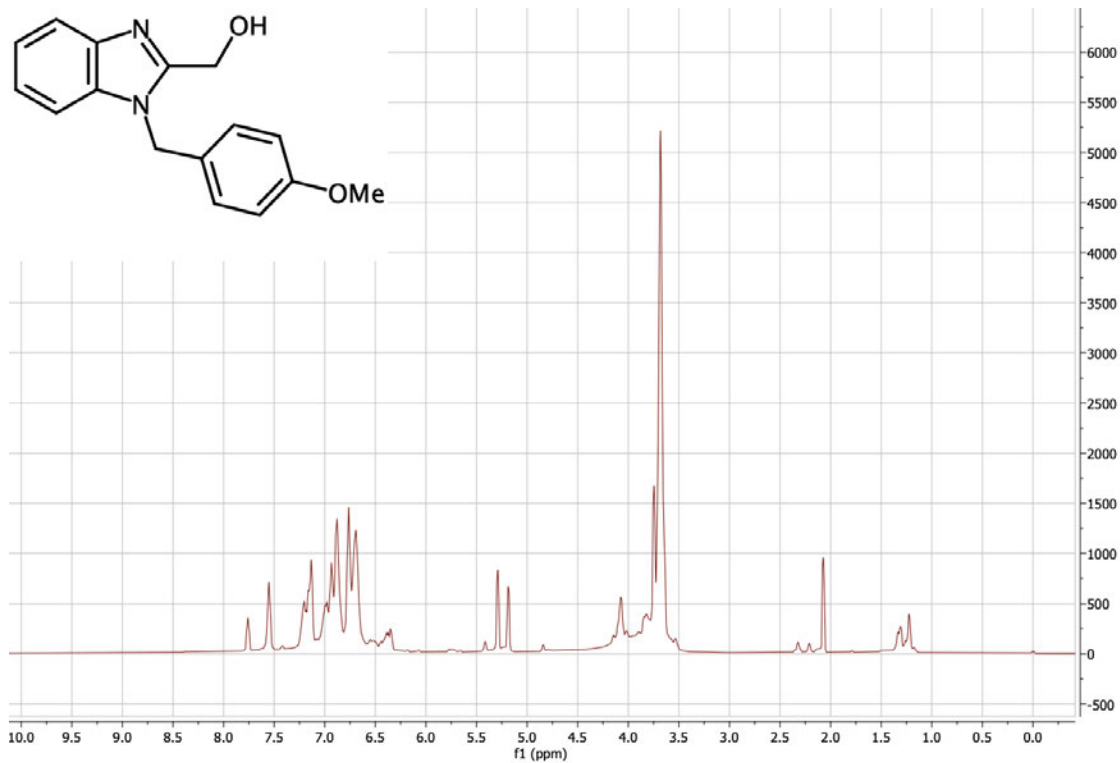
¹H-NMR

{1-[(4-chlorophenyl)methyl]-1H-1,3-benzodiazol-2-yl}methanol:
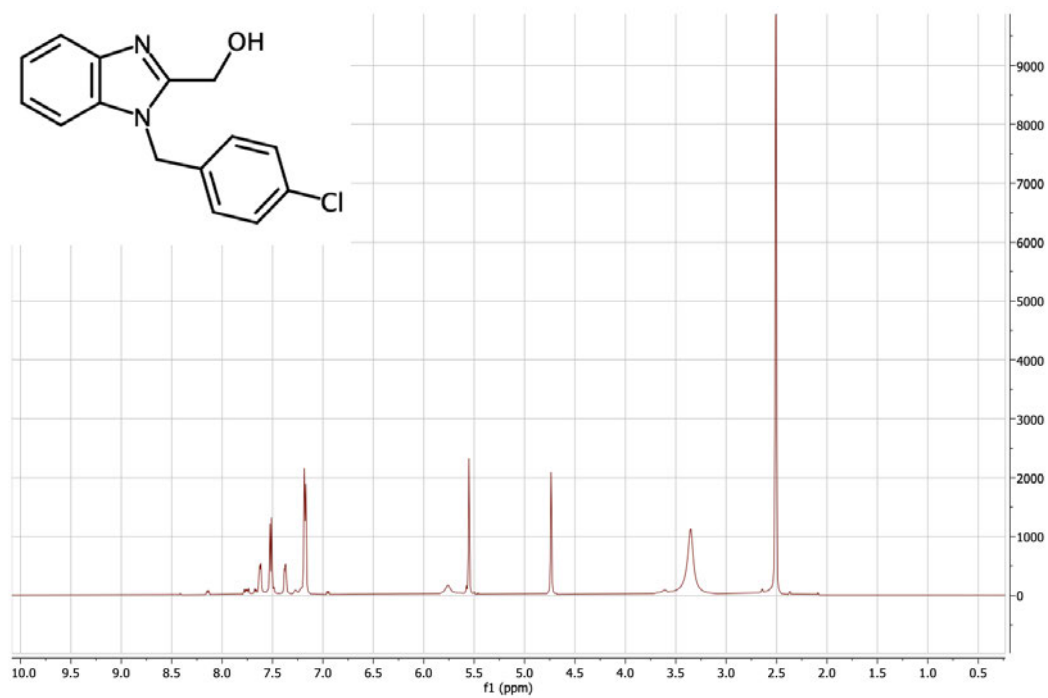
¹H-NMR

¹³C-NMR

HSQC

20210413_CH312_p2_DMSO_HSQC.10.ser

HMBC

20210413_CH312_p2_DMSO_HMBC.10.ser
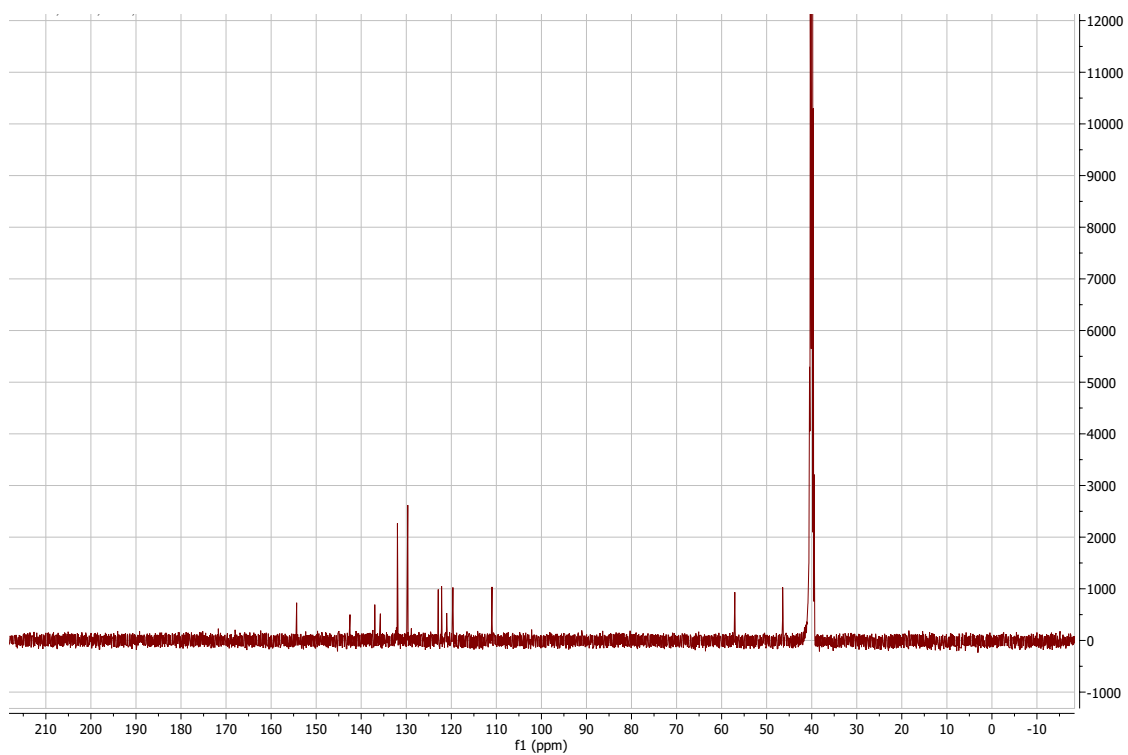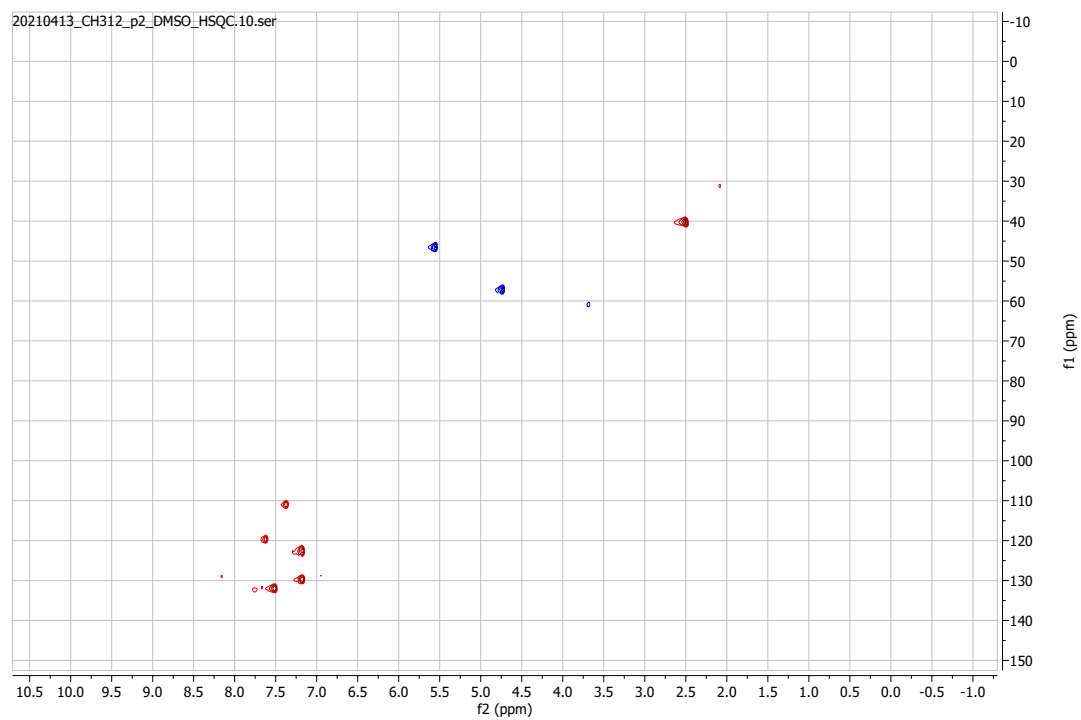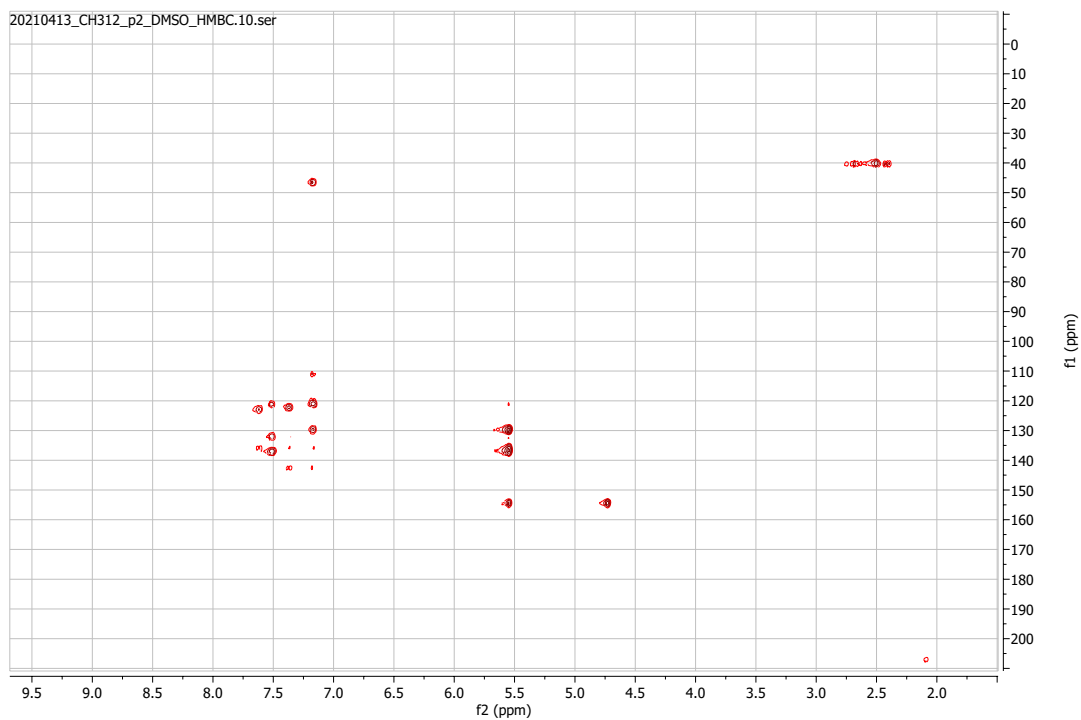
3-{[2-(hydroxymethyl)-1H-1,3-benzodiazol-1-yl]methyl}phenol:
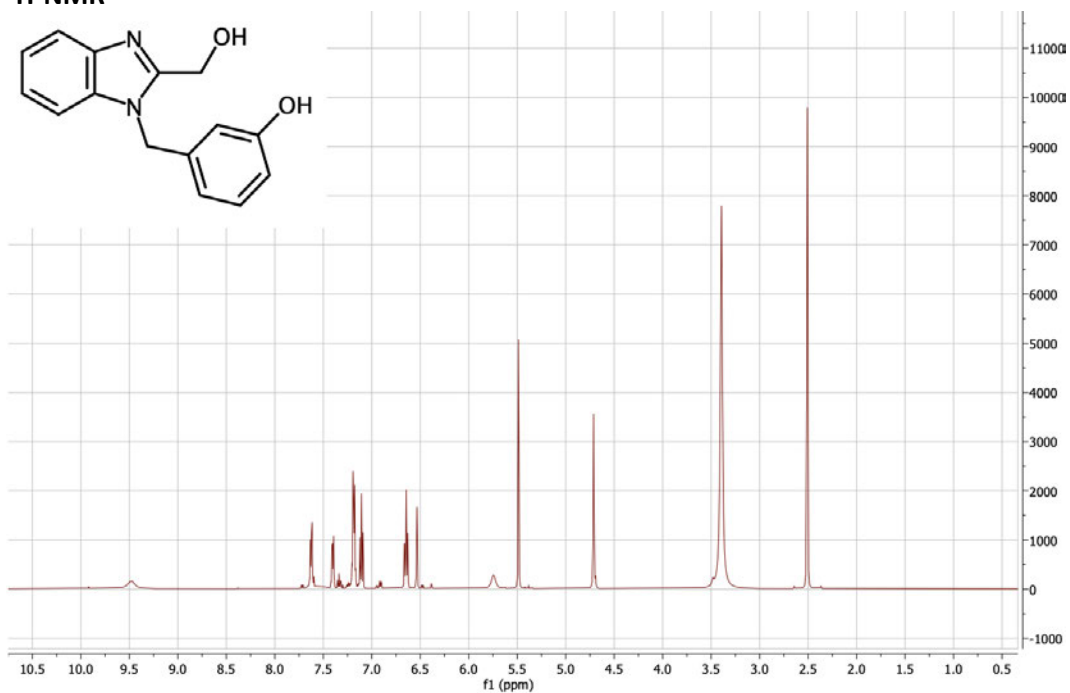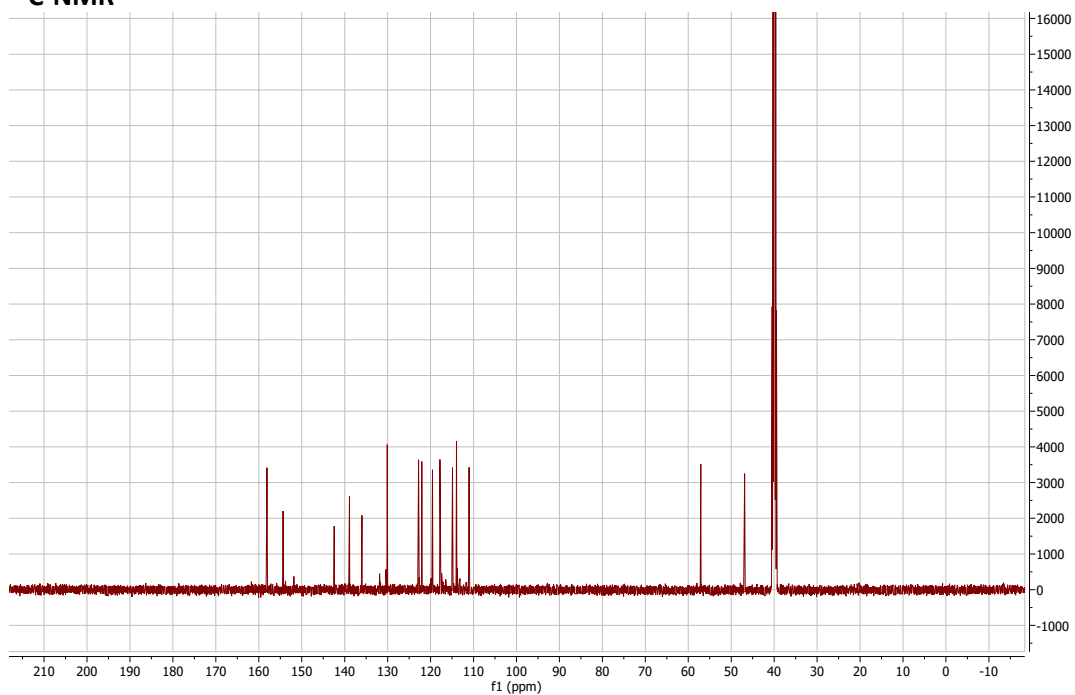
^{1}H-NMR

¹³C-NMR

HSQC

20210420_CH323_mix_DMSO_HSQC.10.ser
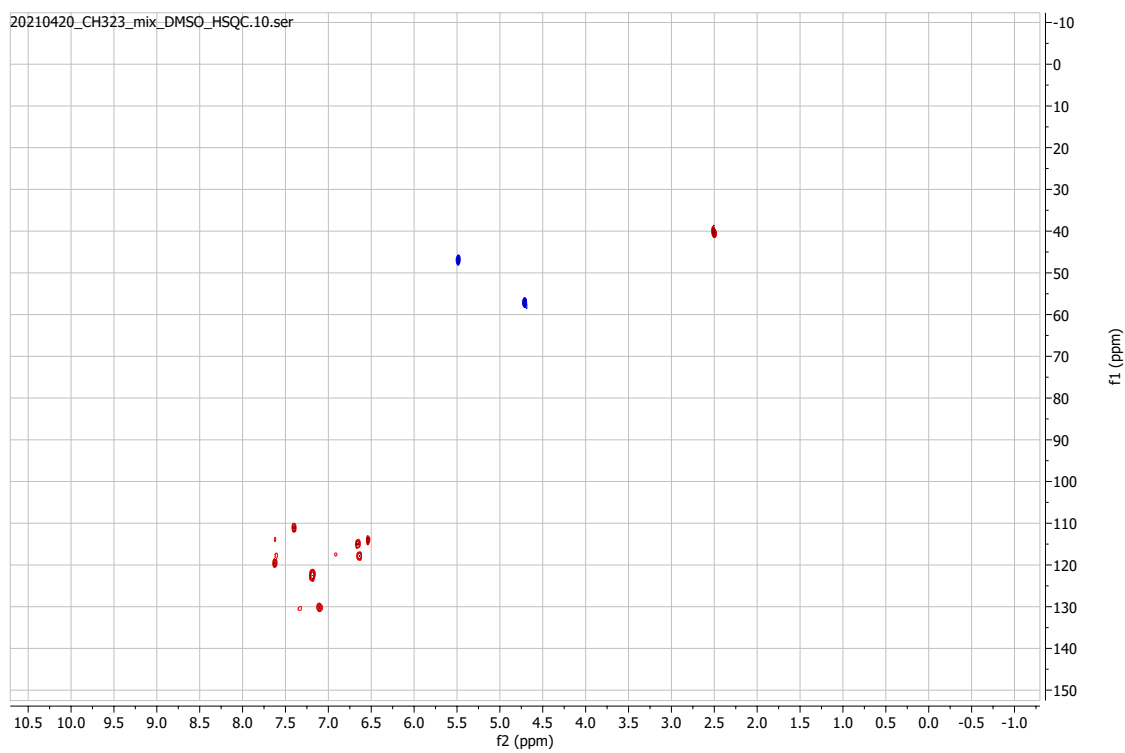
HMBC

20210420_CH323_mix_DMSO_HMBC.10.ser

4-{[2-(hydroxymethyl)-1H-1,3-benzodiazol-1-yl]methyl}phenol:

¹H-NMR

^{13}C-NMR

HMBC

20210428_CH322_mix_DMSO_HMBC.10.ser
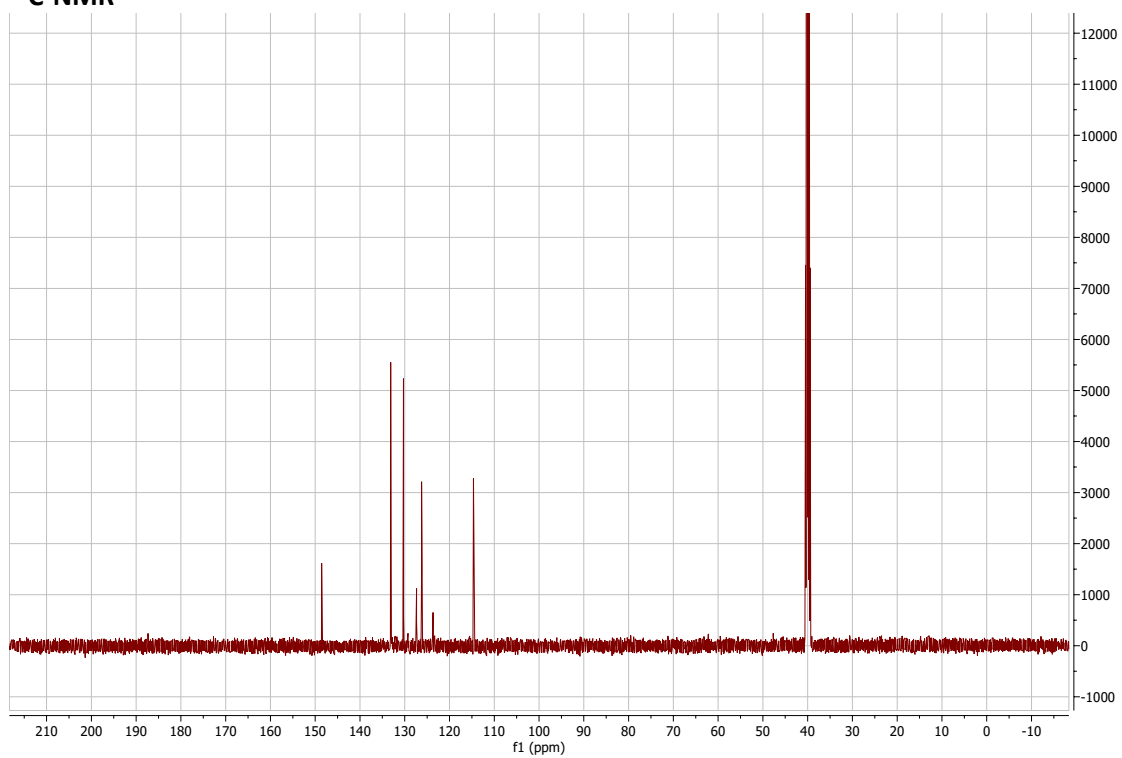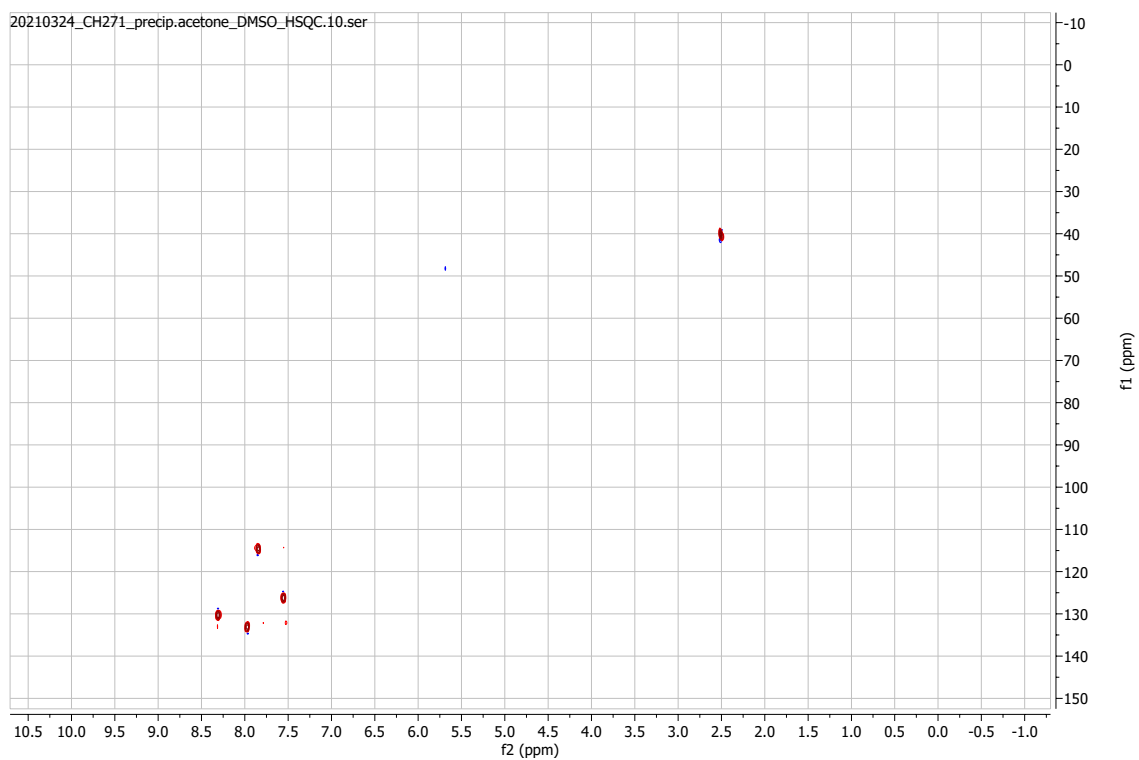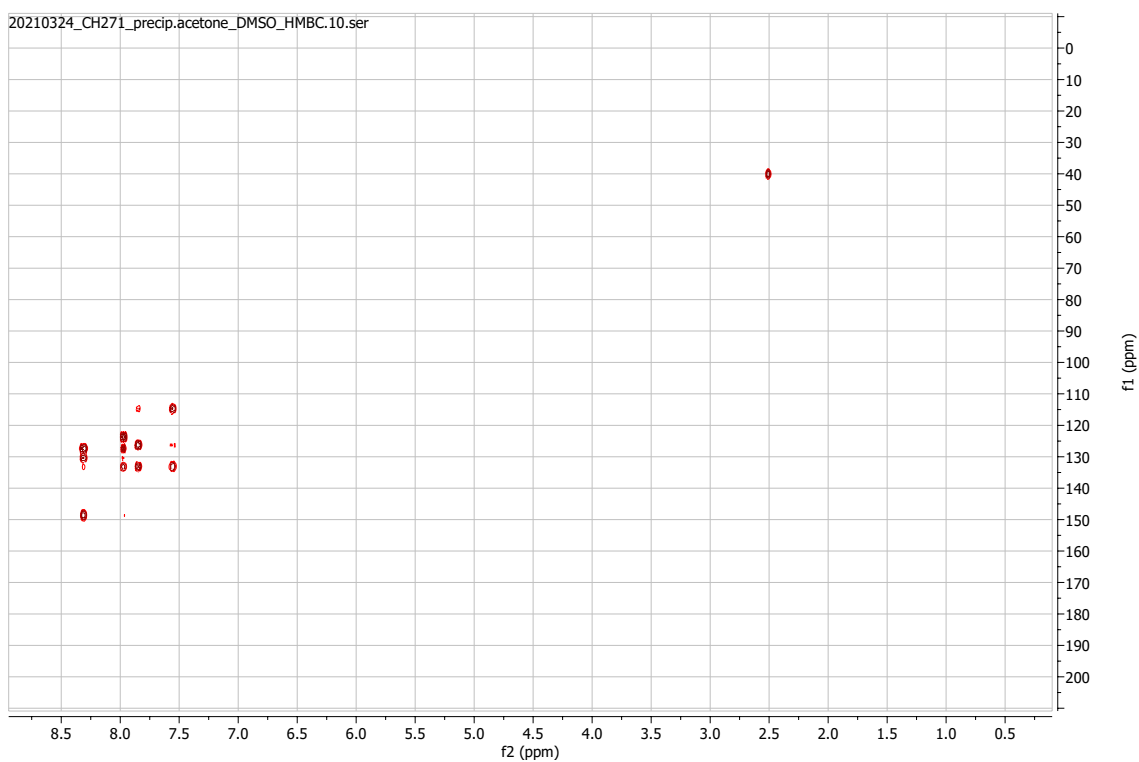
2-(4-bromophenyl)-1H-1,3-benzodiazole:

¹H-NMR

¹³C-NMR

HSQC

HMBC

284

2-(4-chlorophenyl)-1H-1,3-benzodiazole:

¹H-NMR

¹³C-NMR

285

HSQC

HMBC

286

4-(1H-1,3-benzodiazol-2-yl)phenol:

¹H-NMR

¹³C-NMR

HSQC

20210804_CH405_clean_HSQC.10.ser

HMBC

20210804_CH405_clean_HMBC.10.ser

2-(4-fluorophenyl)-1H-1,3-benzodiazole:

¹H-NMR

¹³C-NMR

HSQC

20210416_CH321_DMSO_HSQC.10.ser

HMBC

20210416_CH321_DMSO_HMBC.10.ser

2-(2-nitrophenyl)-1H-1,3-benzodiazole:

¹H-NMR

¹³C-NMR

HSQC

20210514_CH326_gum_HSQC.10.ser

HMBC

20210514_CH326_gum_HMBC.10.ser

2-(thiophen-2-yl)-1H-1,3-benzodiazole:

¹H-NMR

¹³C-NMR

HSQC

20210804_CH389_clean_HSQC.10.ser

HMBC

20210804_CH389_clean_HMBC.10.ser
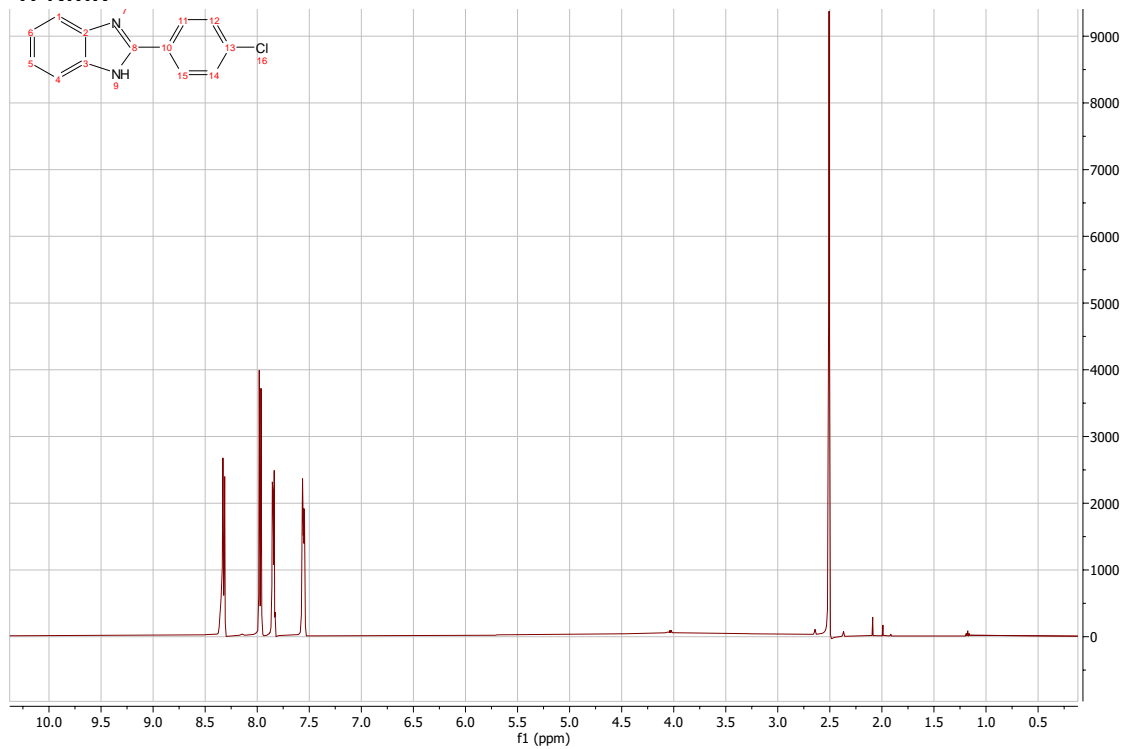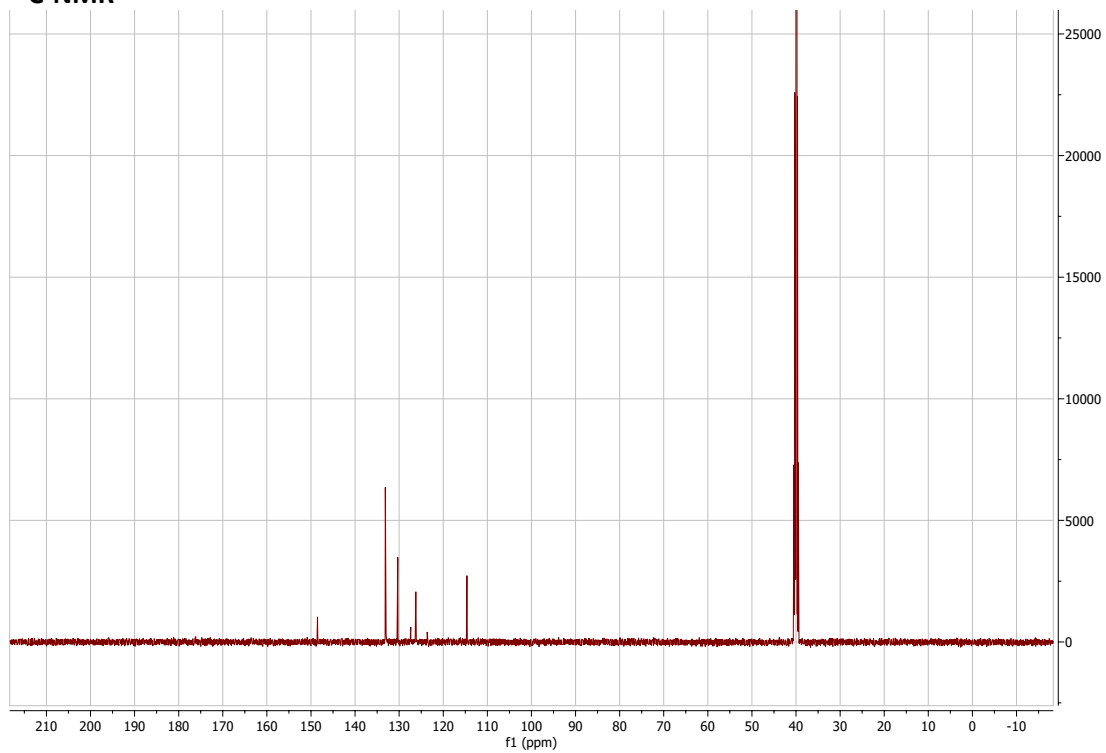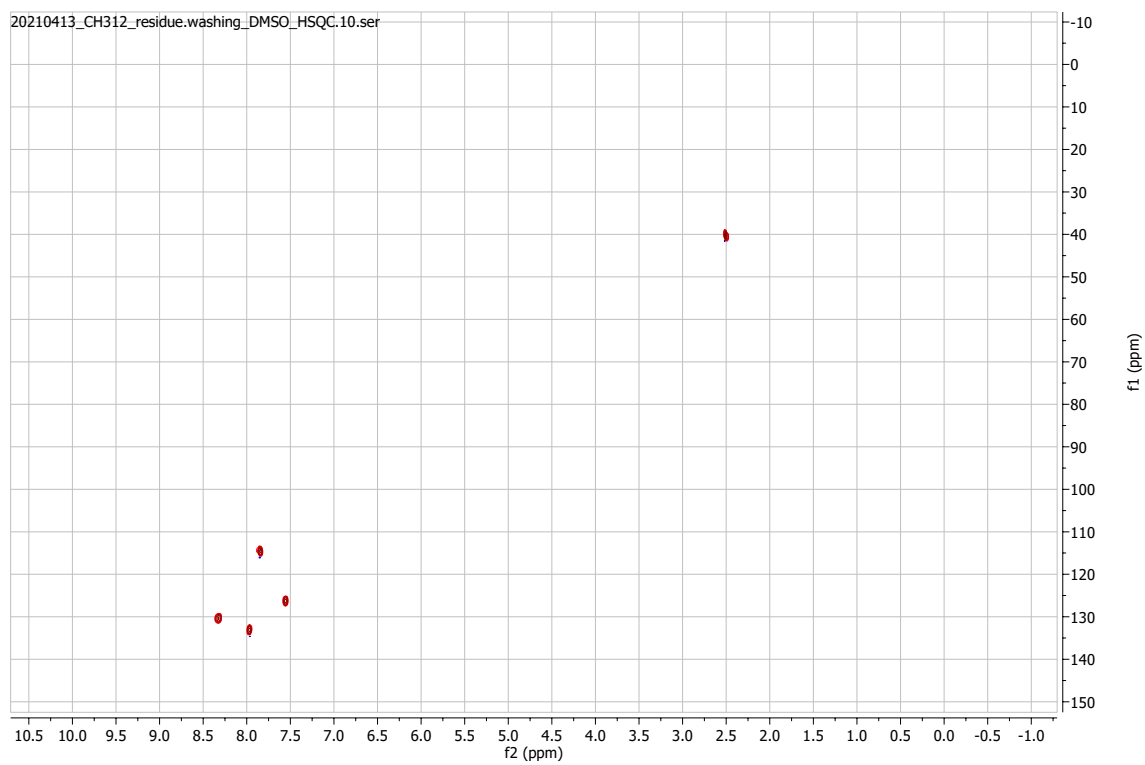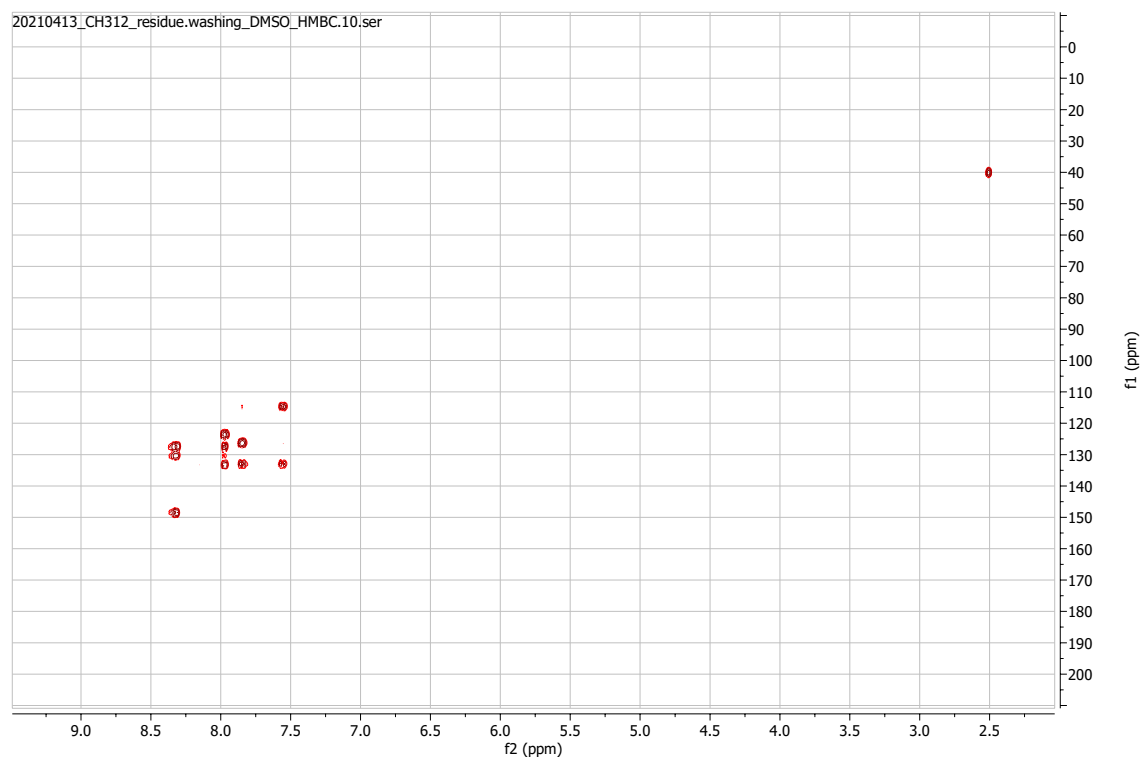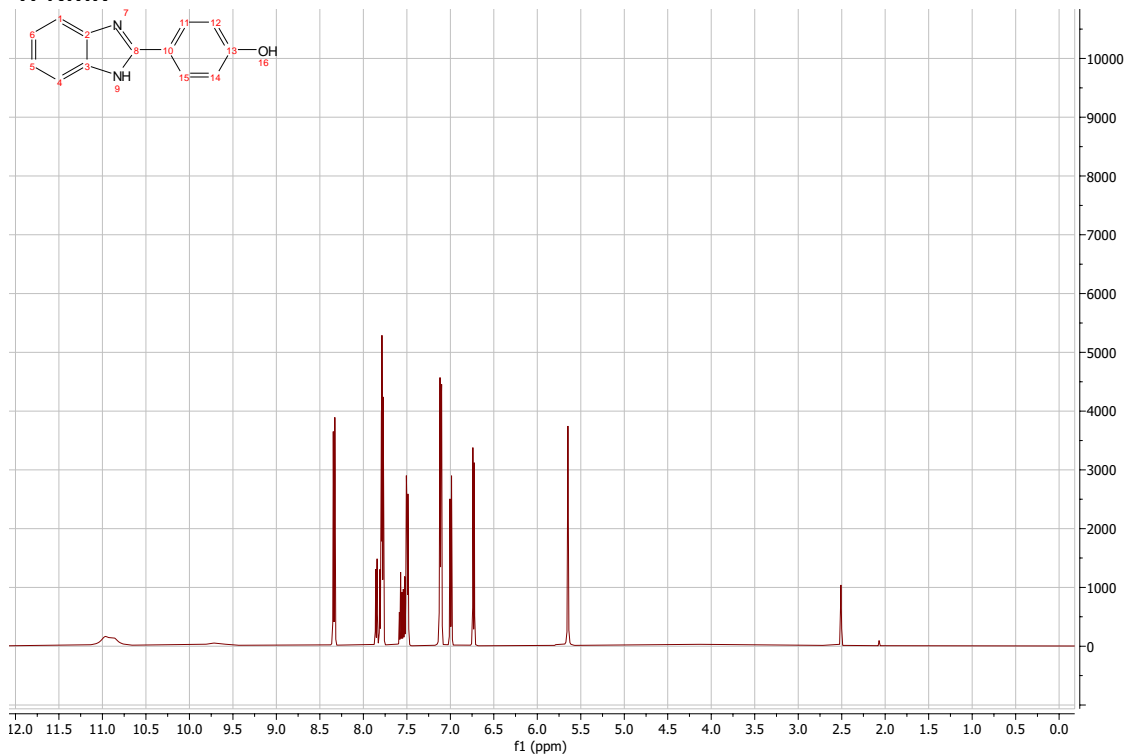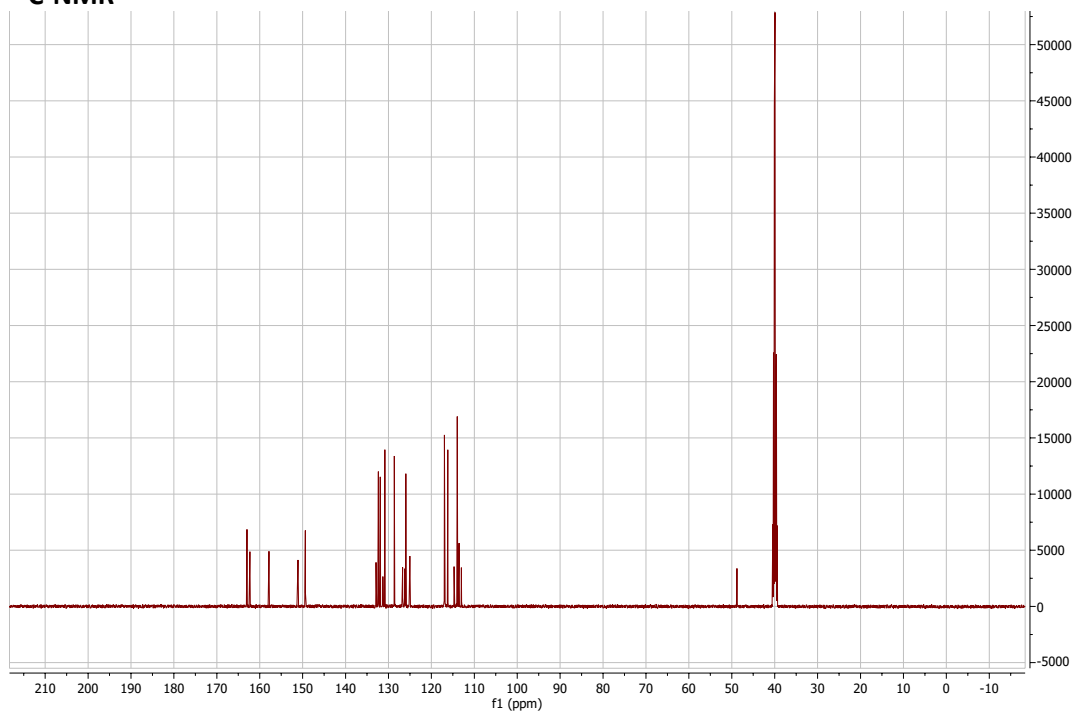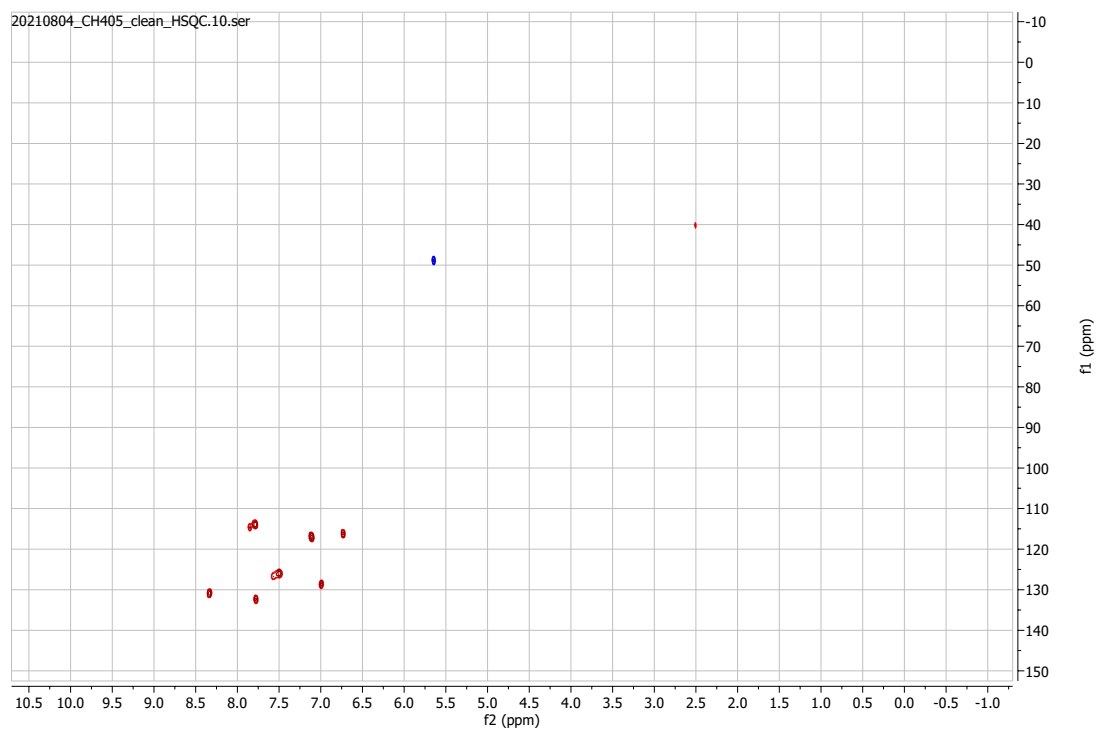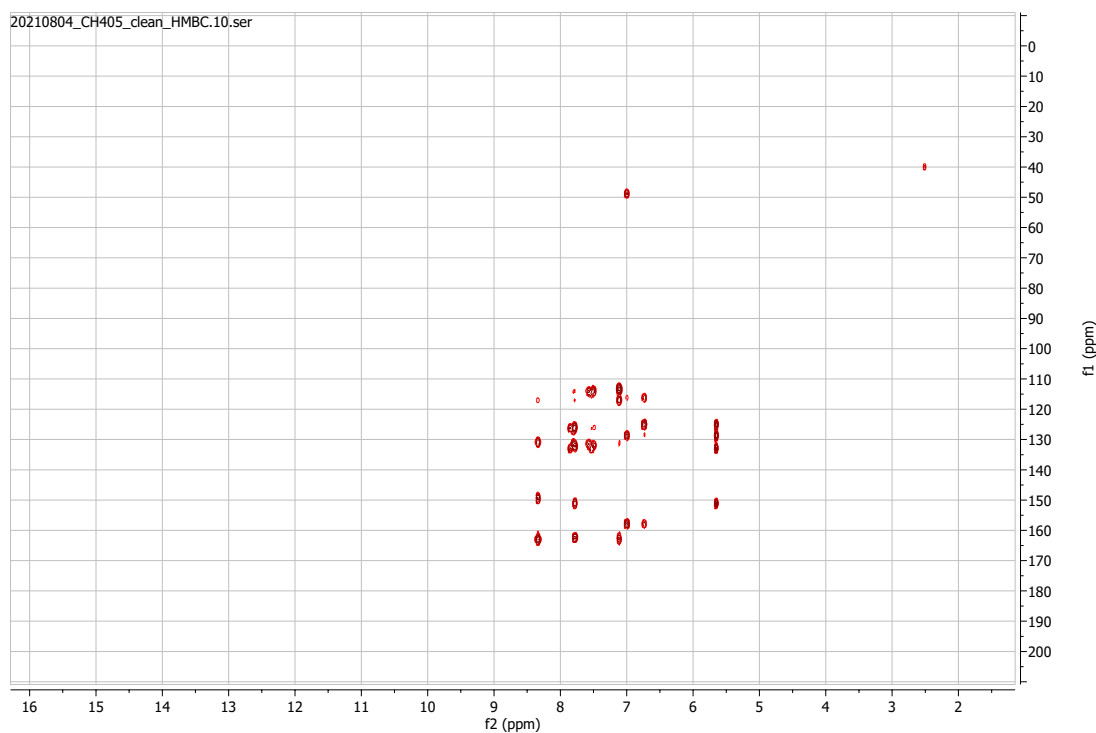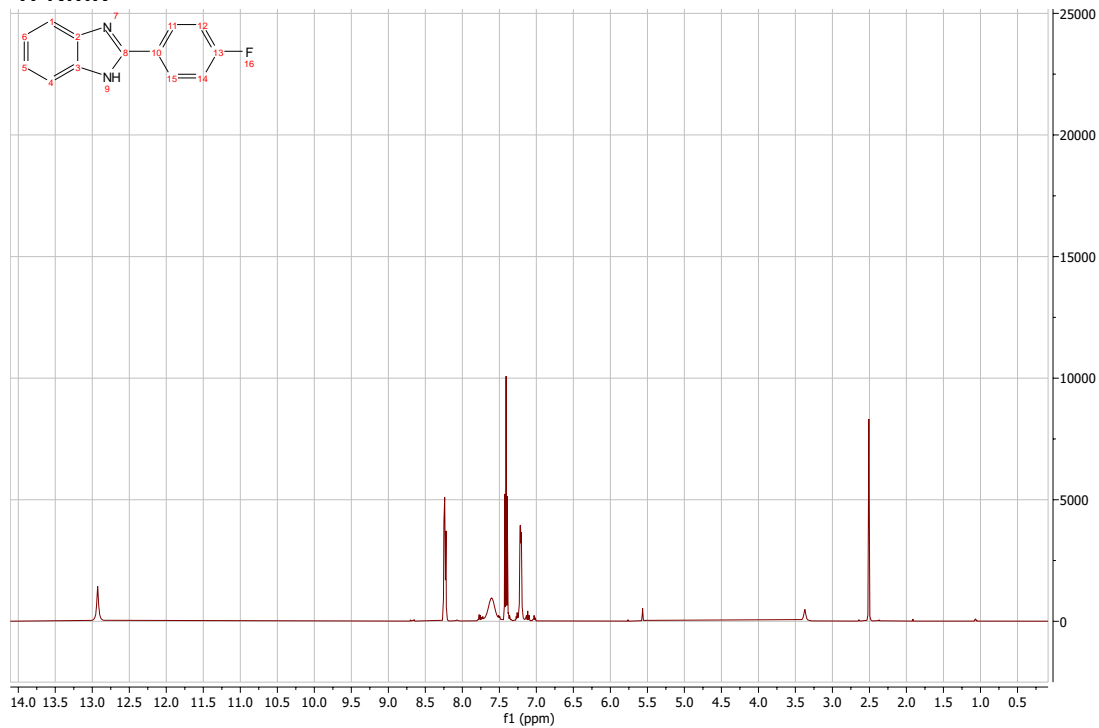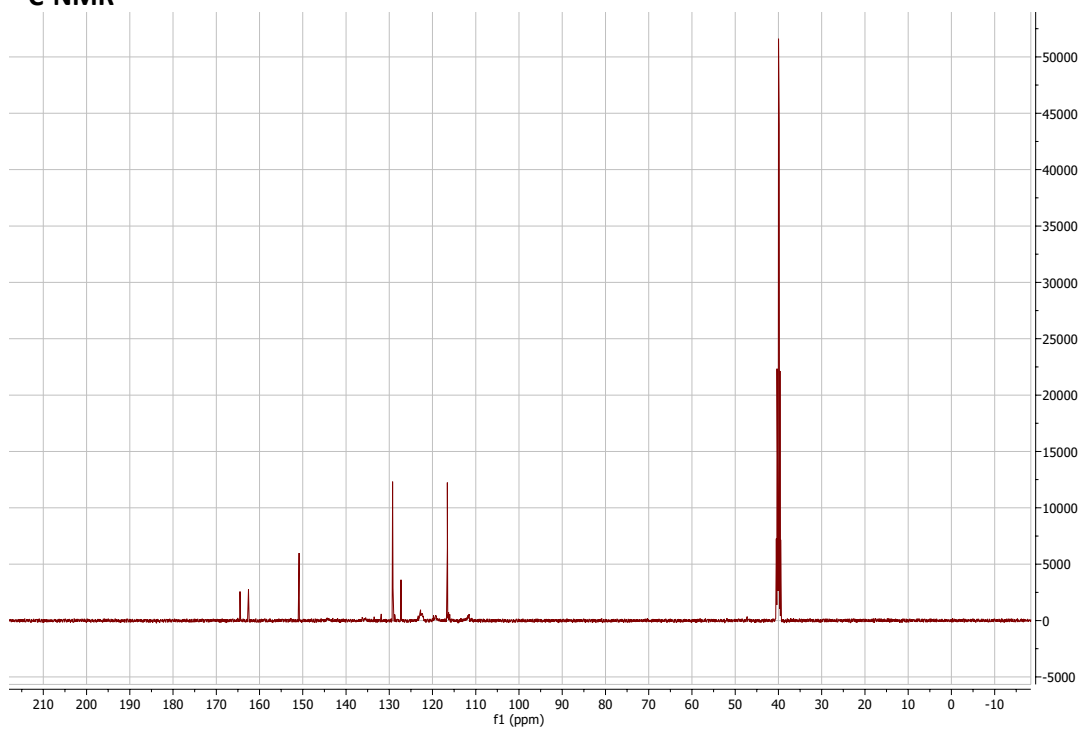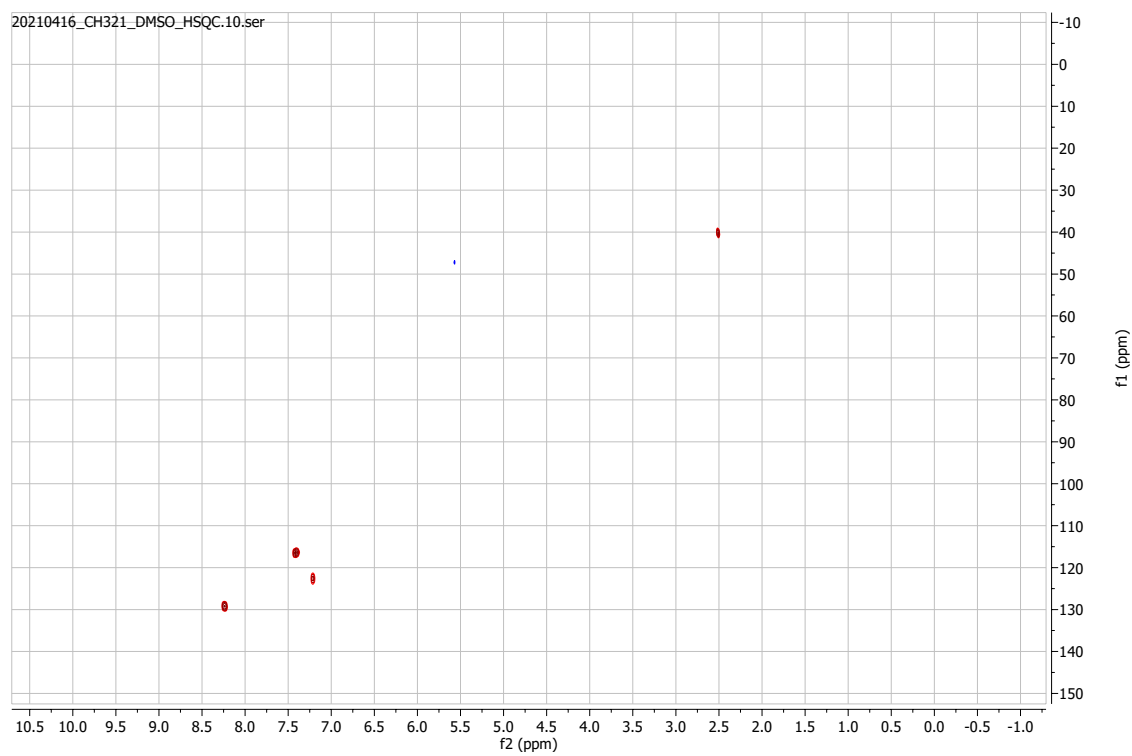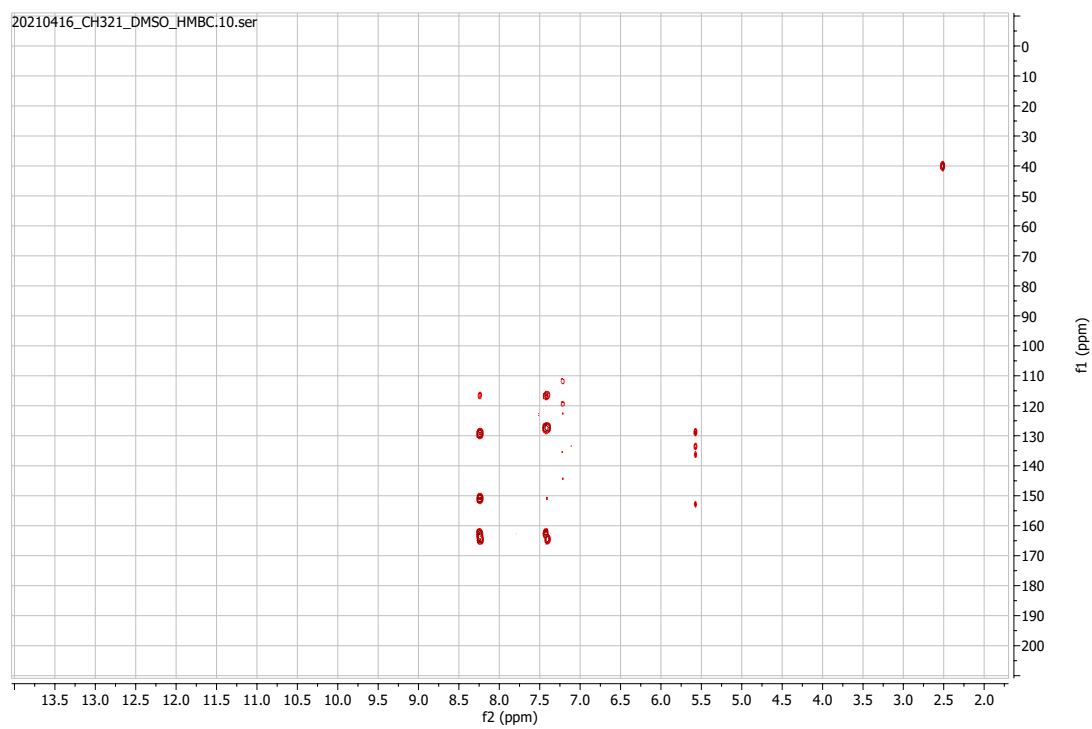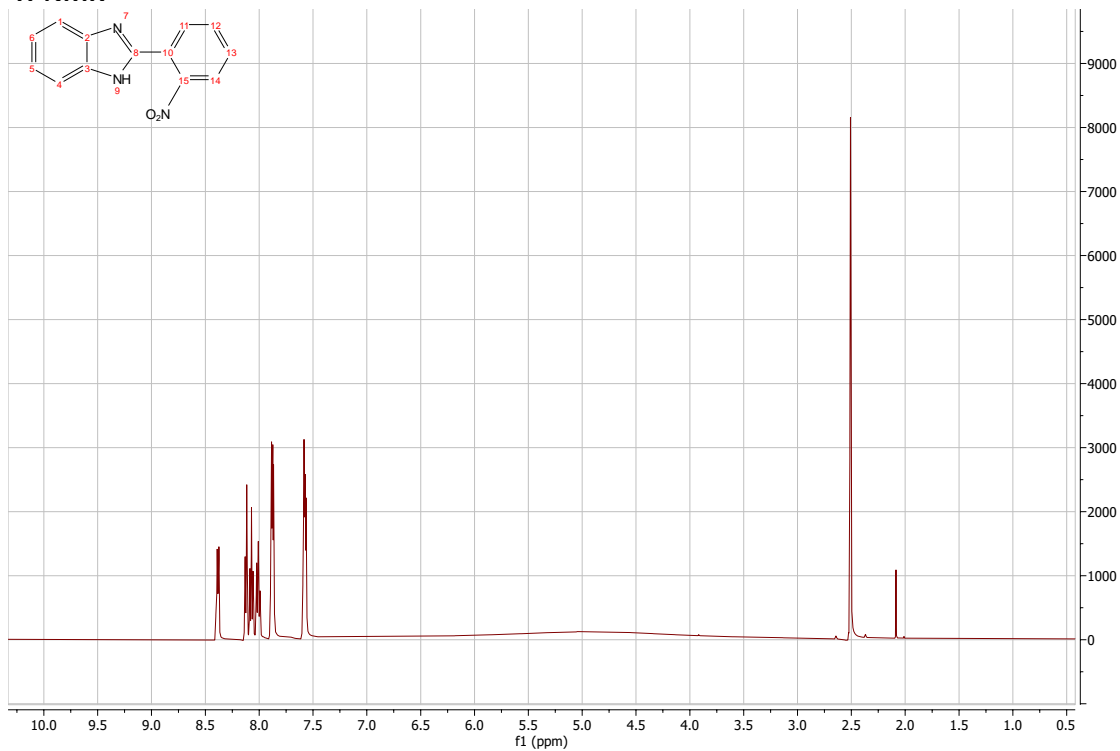
2-(1H-pyrrol-2-yl)-1H-1,3-benzodiazole:

¹H-NMR

5-chloro-2-phenyl-1H-1,3-benzodiazole:

¹H-NMR

295

¹³C-NMR

HSQC

20210603_CH340_DMSO_HSQC.10.ser

HMBC

20210603_CH340_DMSO_HMBC.10.ser
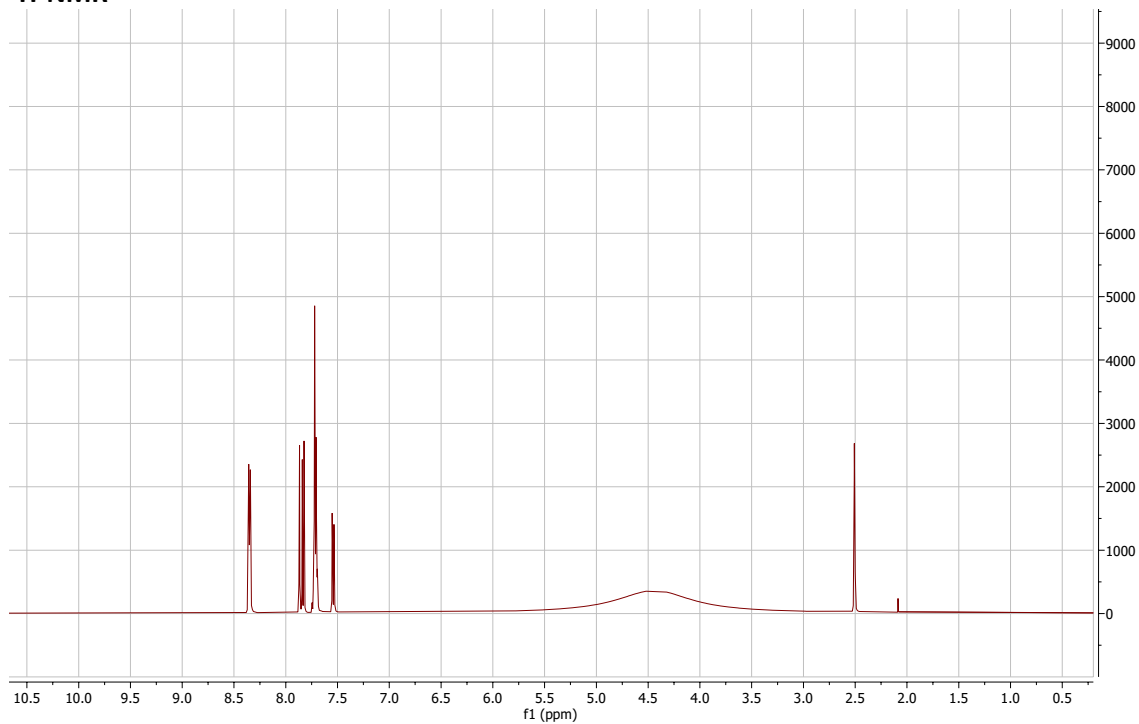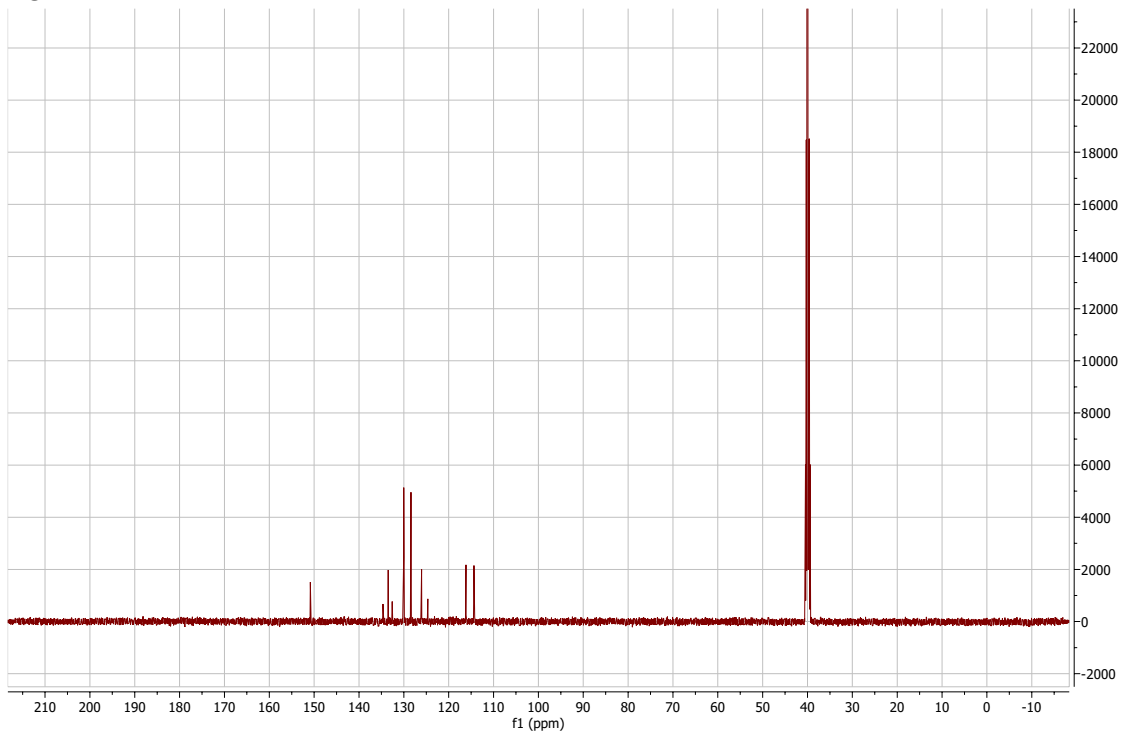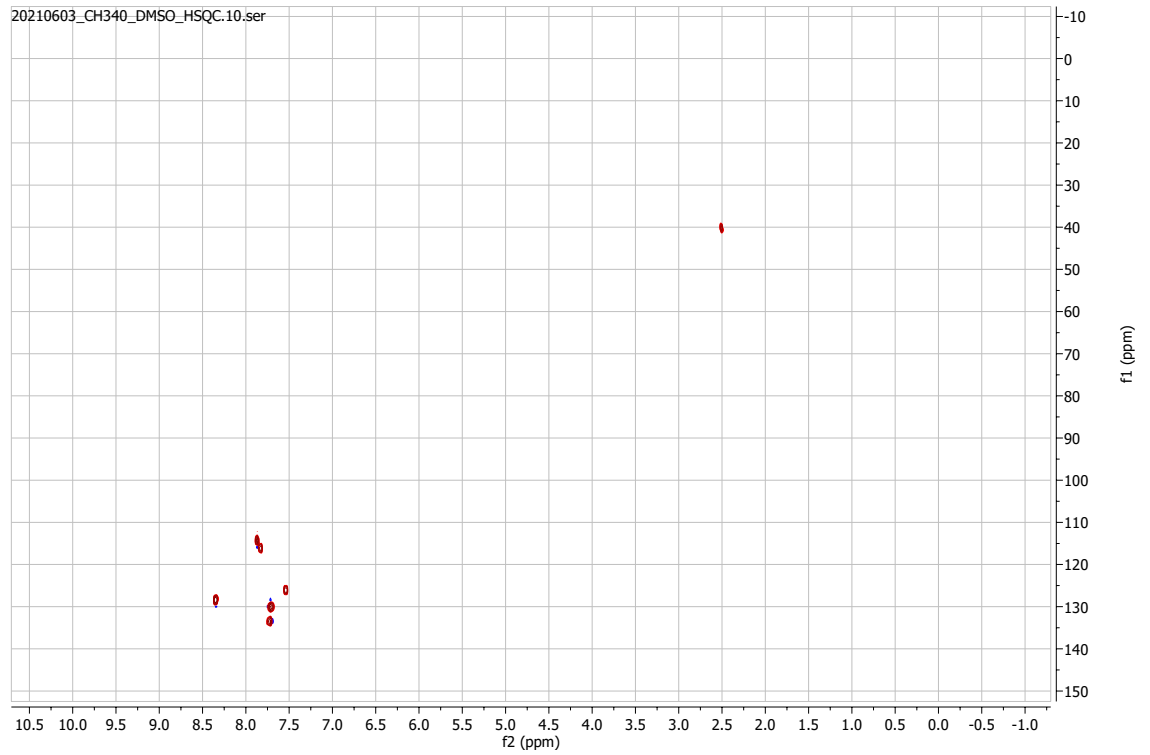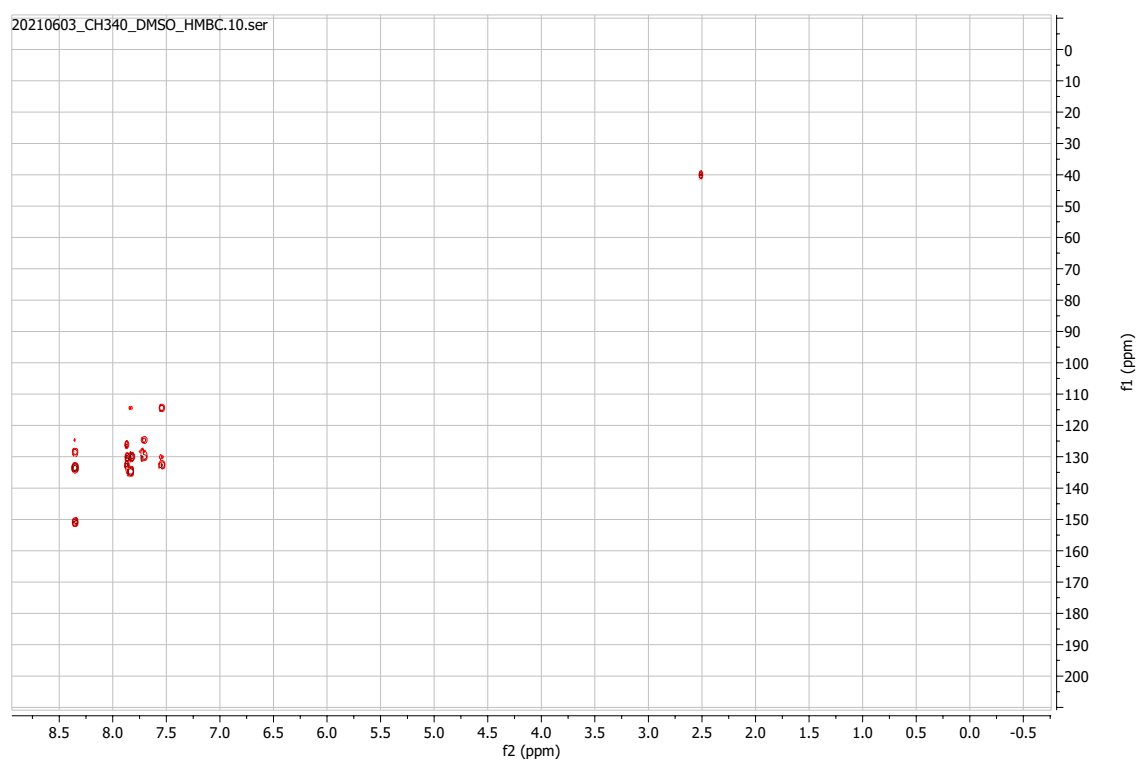
5-chloro-2-(4-chlorophenyl)-1H-1,3-benzodiazole:
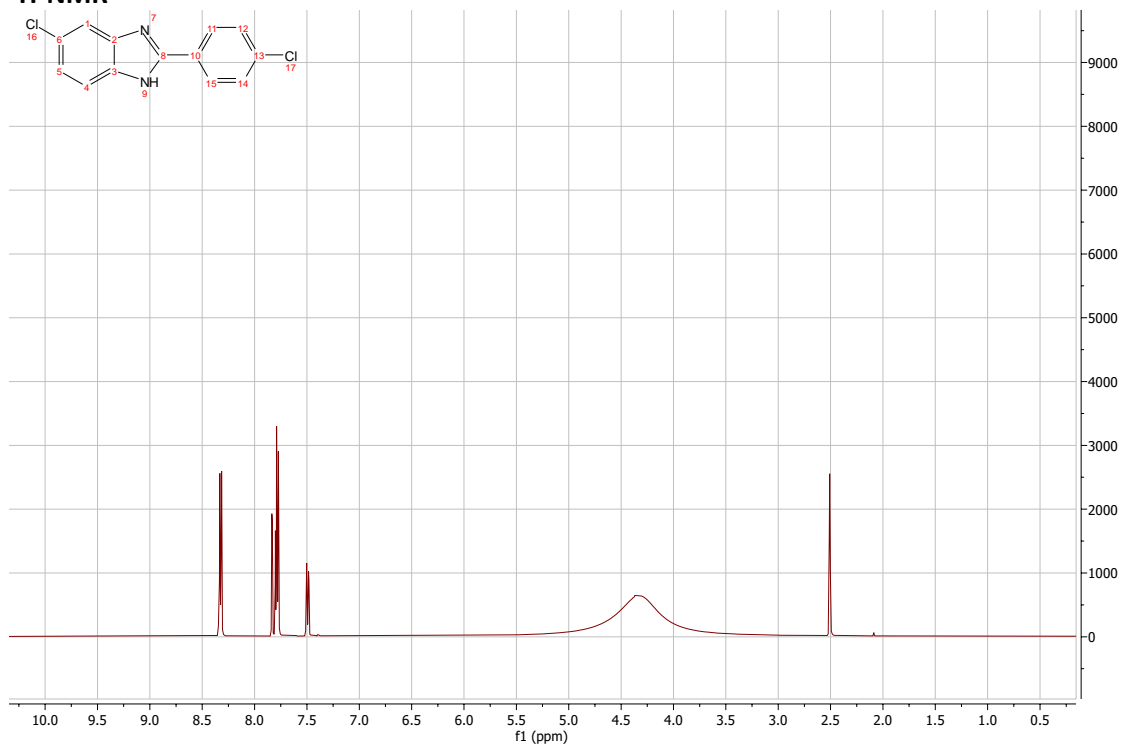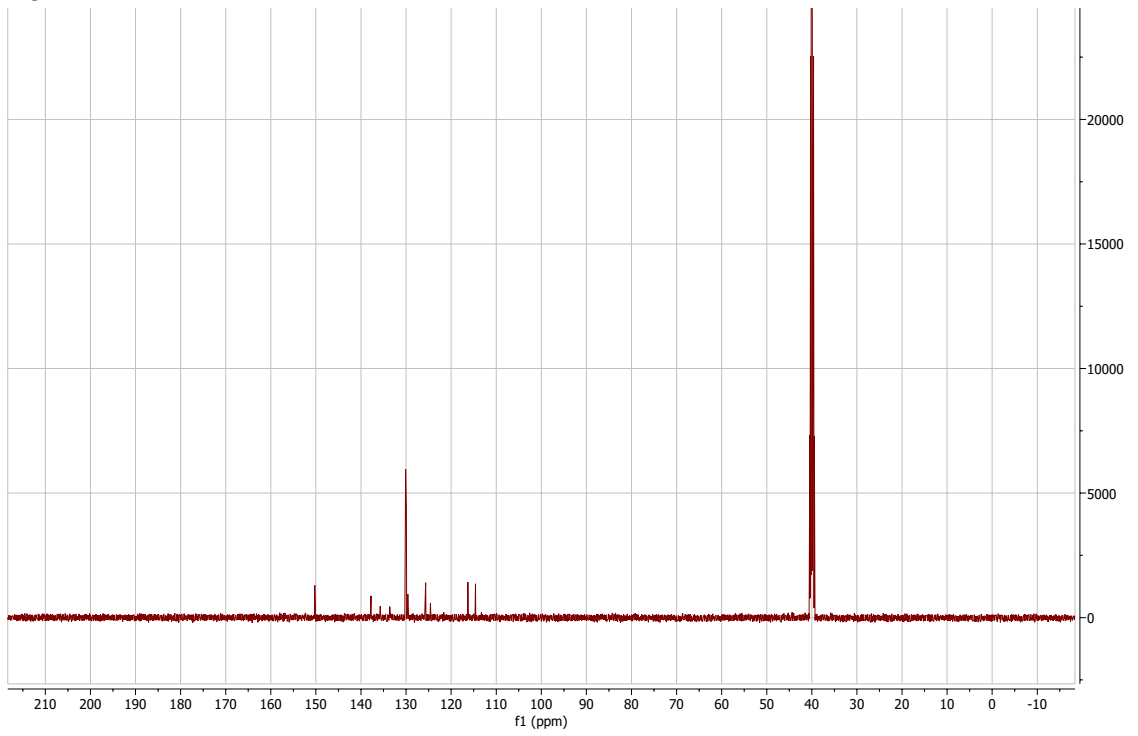
¹H-NMR

¹³C-NMR

4-(5-chloro-1H-1,3-benzodiazol-2-yl)phenol:
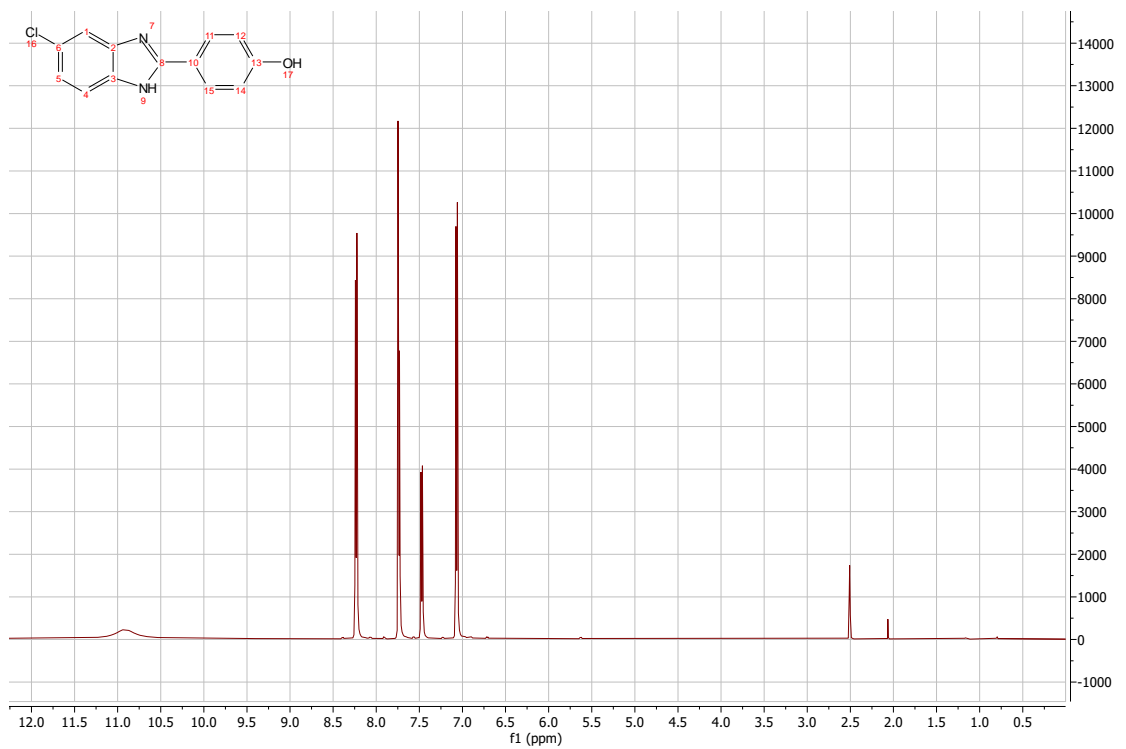
¹H-NMR

^{13}C-NMR

20210804_CH368_clean_C.10.fid
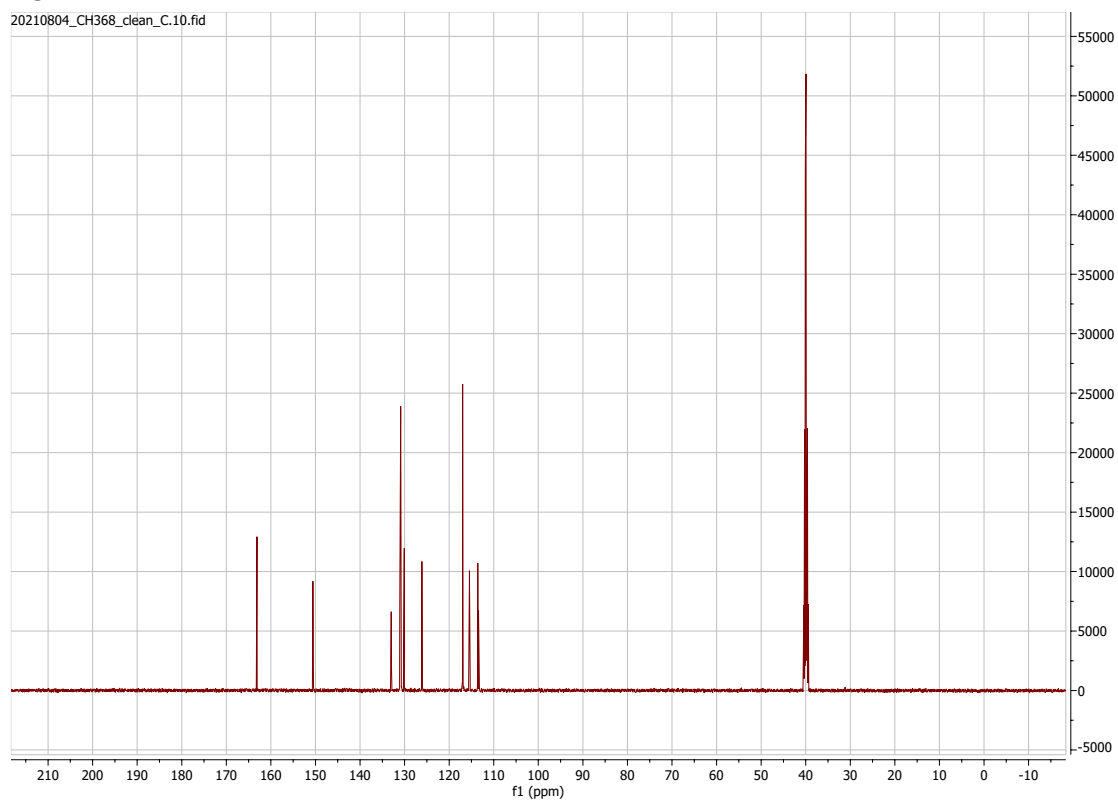
HSQC

20210804_CH368_clean_HSQC.10.ser
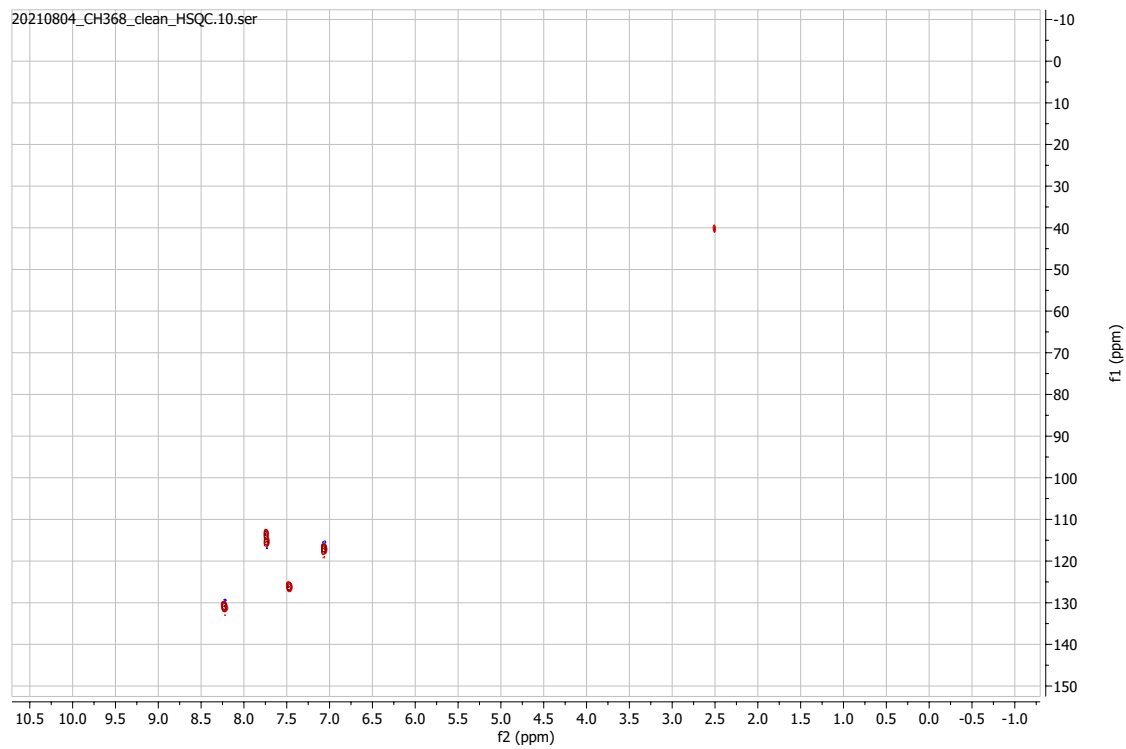
HMBC

20210804_CH368_clean_HMBC.10.ser
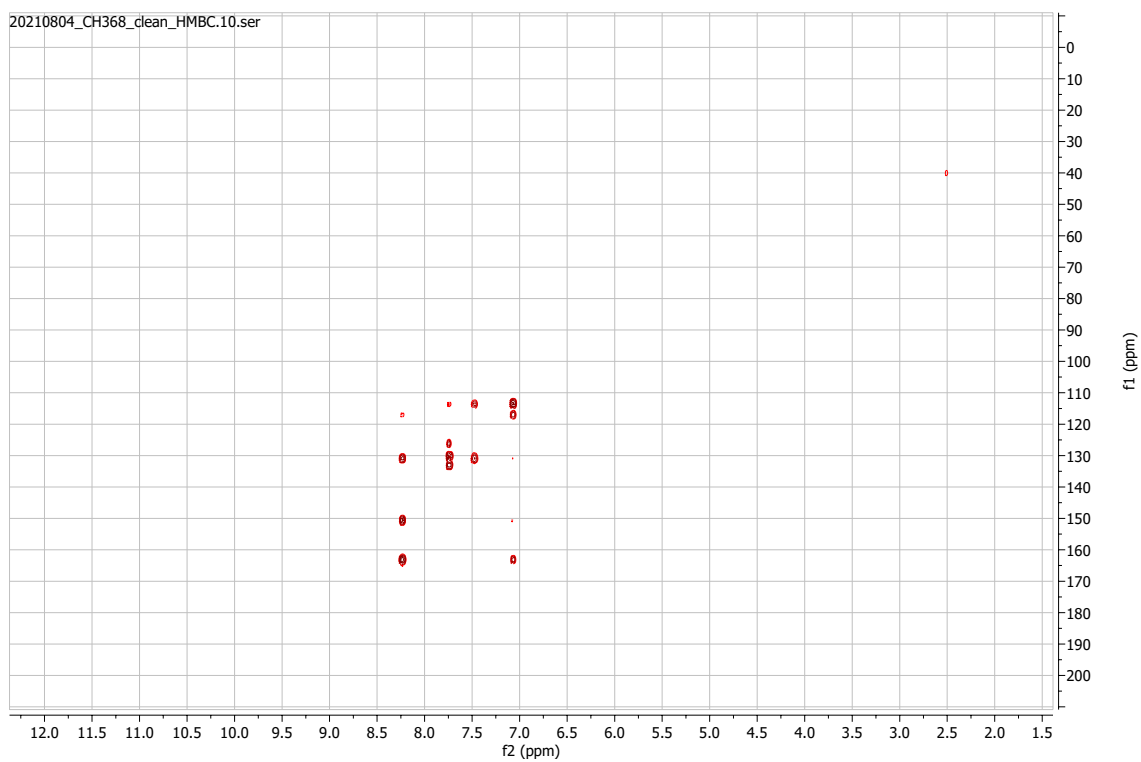
5-chloro-2-(4-fluorophenyl)-1H-1,3-benzodiazole:

¹H-NMR

^{13}C-NMR

HSQC

20220509_CH432_clean_HSQC.10.ser

301

HMBC

20220509_CH432_clean_HMBC.10.ser

5-chloro-2-(4-methoxyphenyl)-1H-1,3-benzodiazole:

¹H-NMR

302
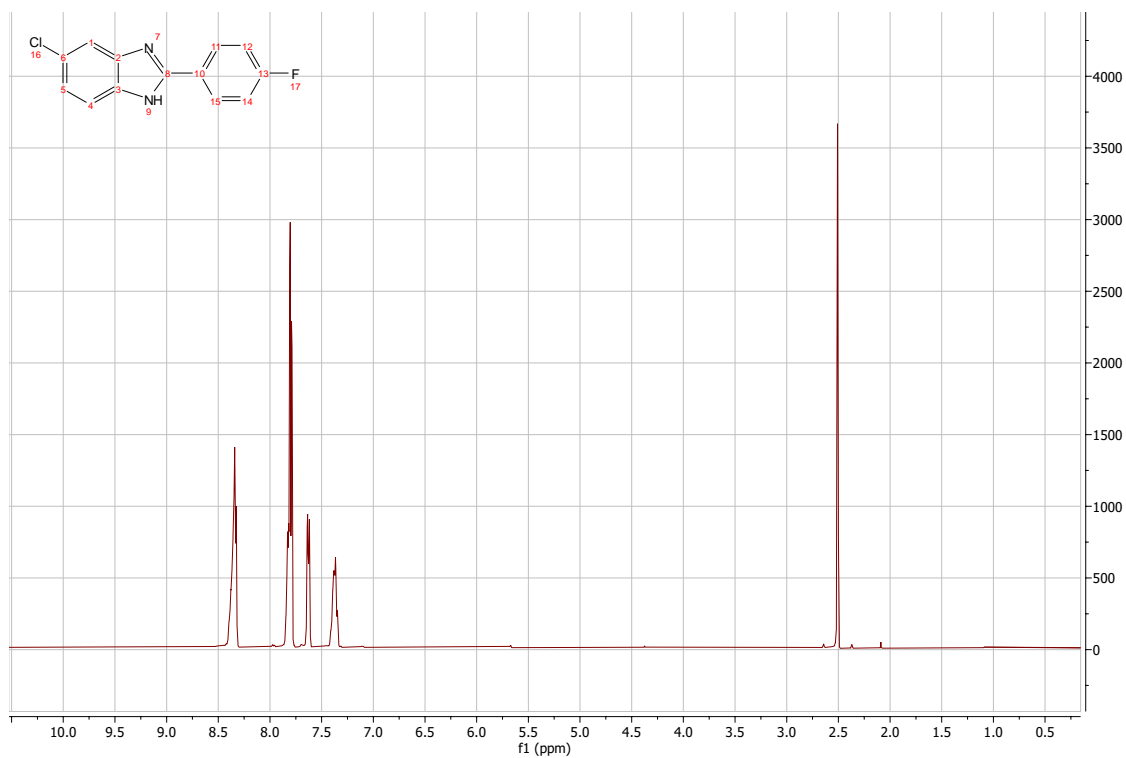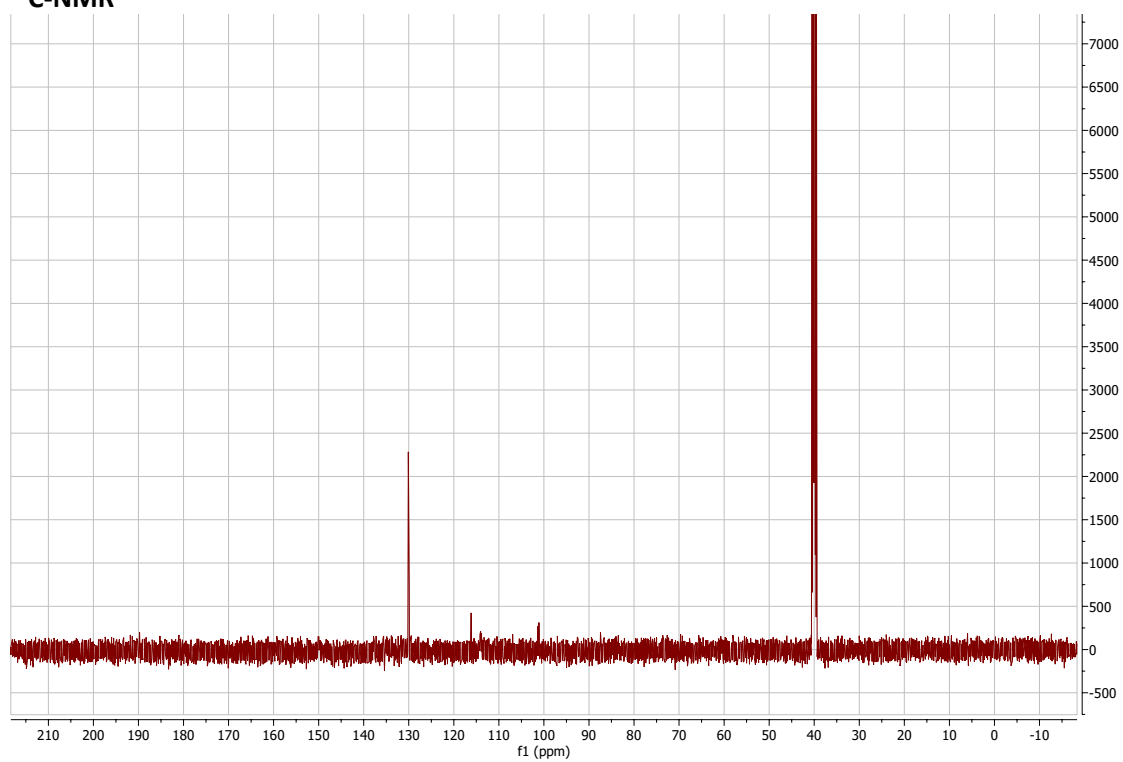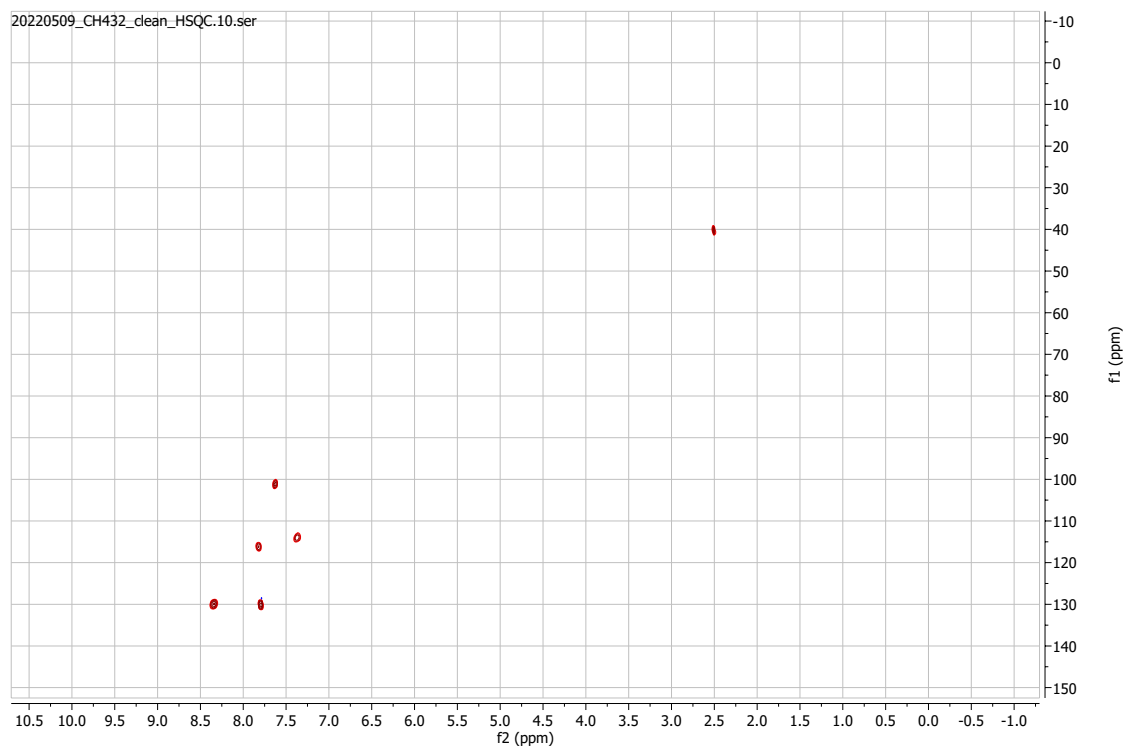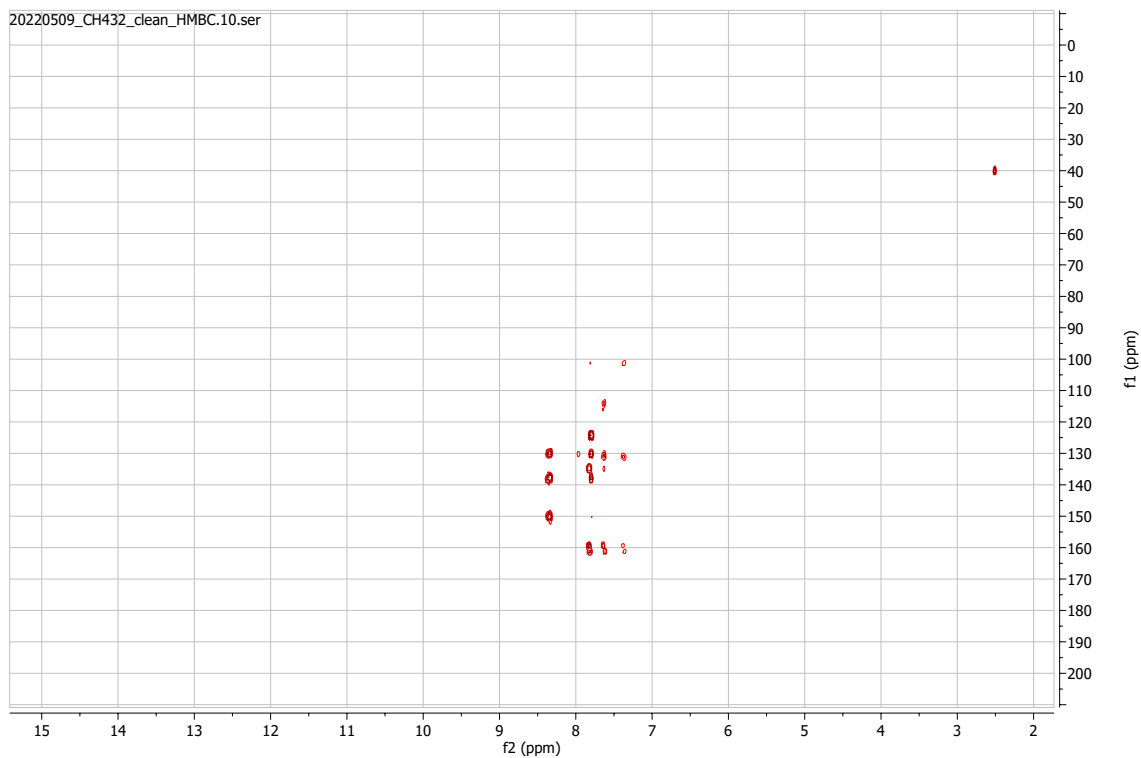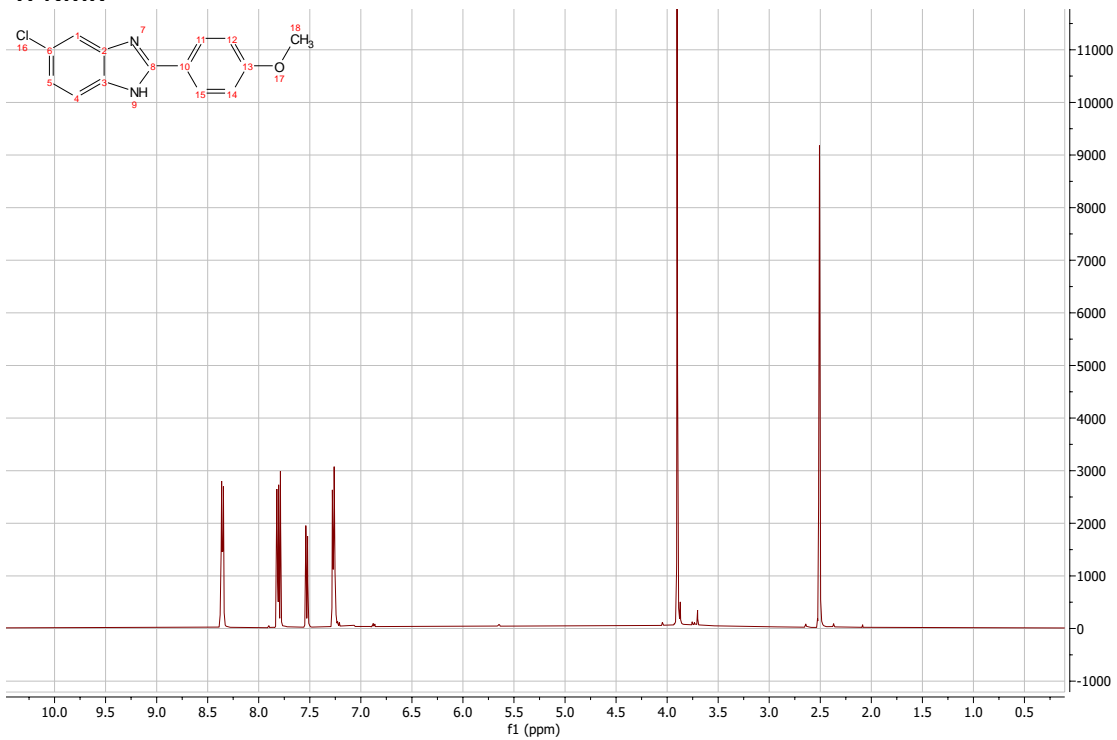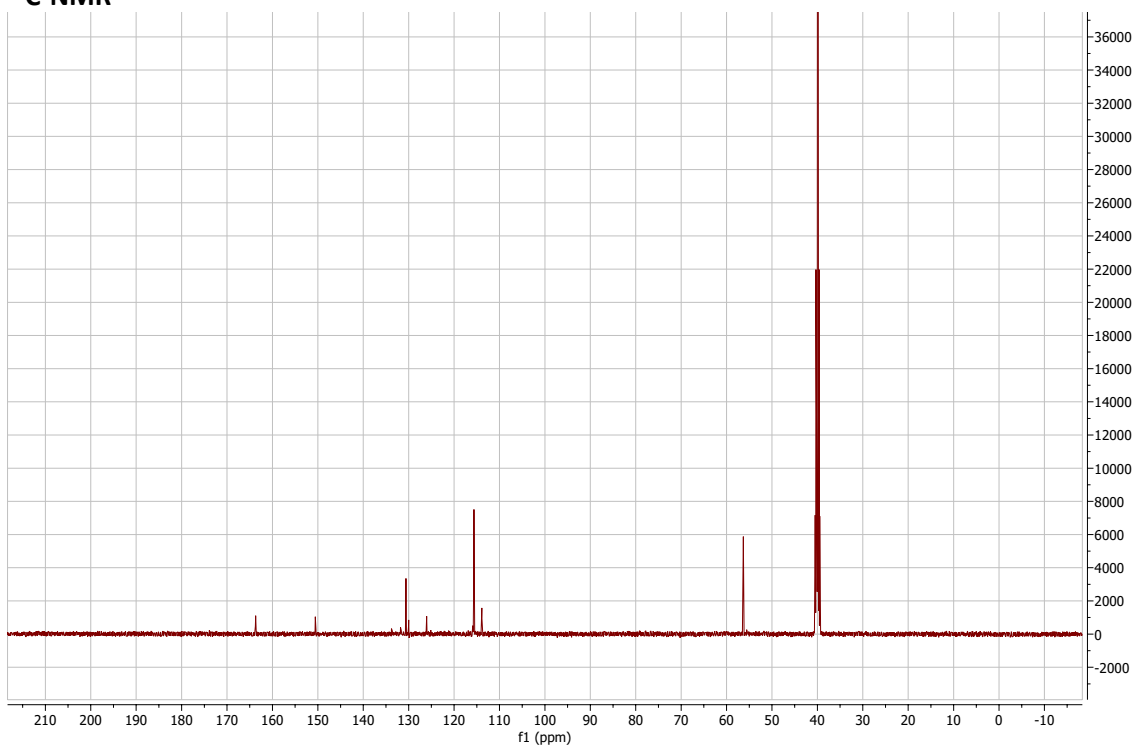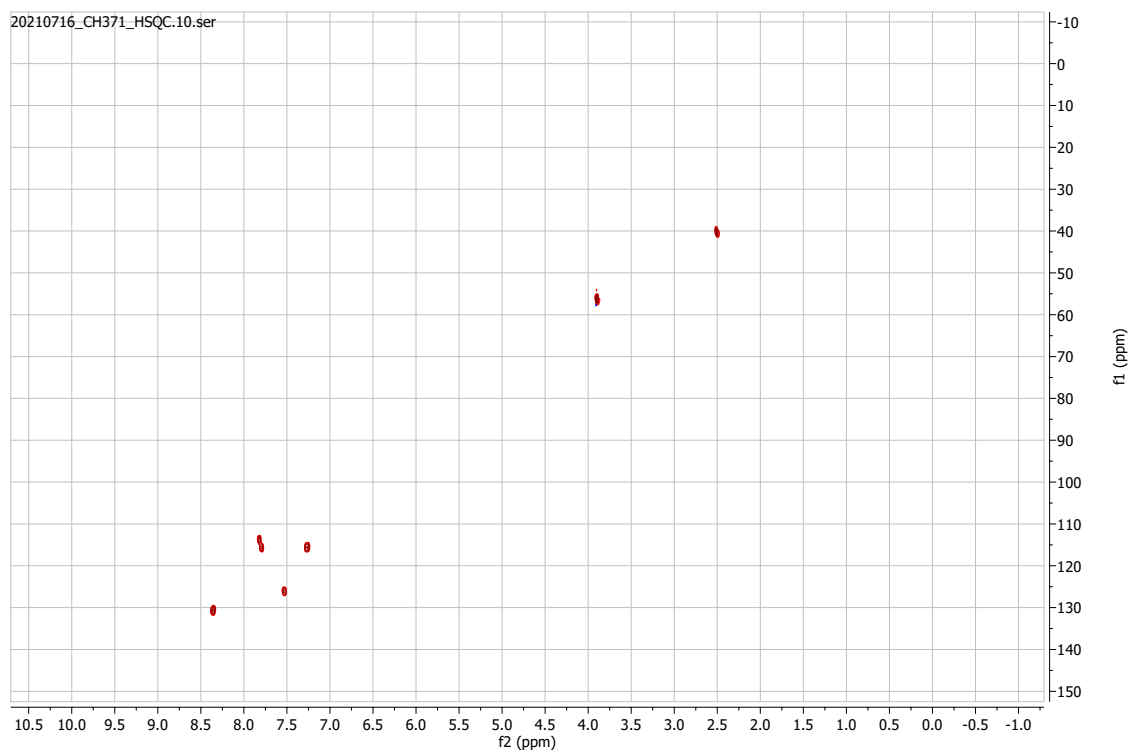
¹³C-NMR

HSQC

HMBC

20210716_CH371_HMBC.10.ser

3-(5-chloro-1H-1,3-benzodiazol-2-yl)phenol:
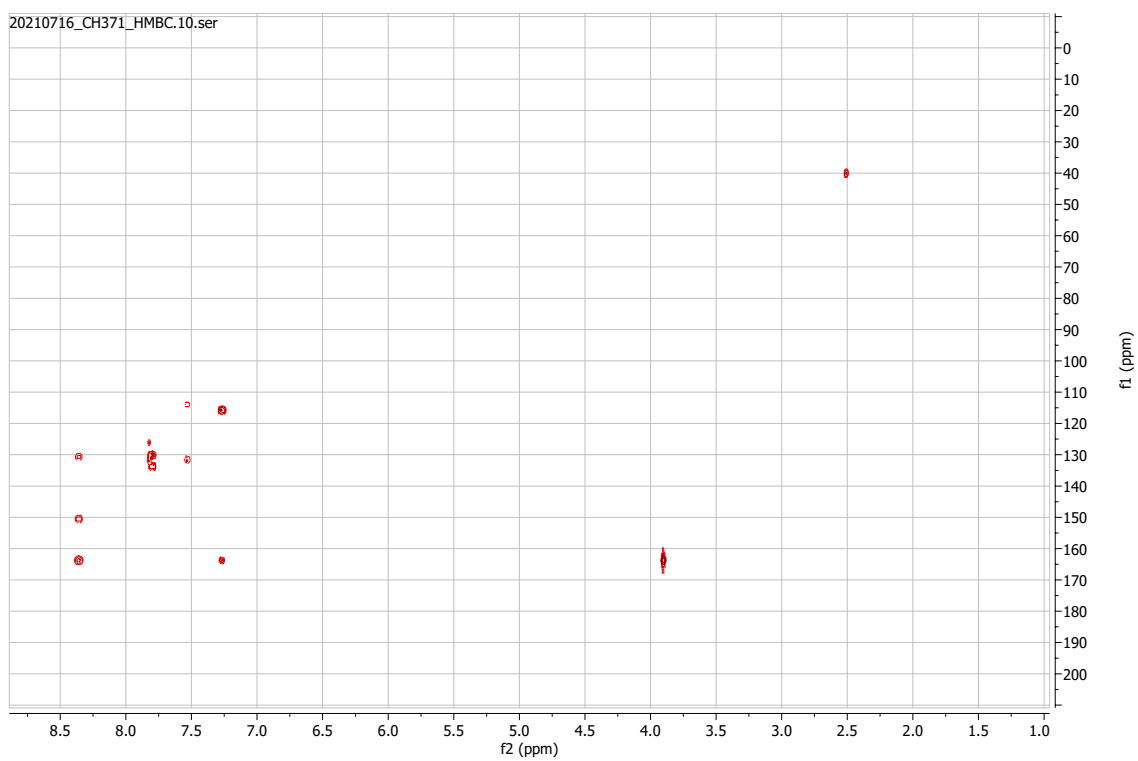
¹H-NMR

^{13}C-NMR
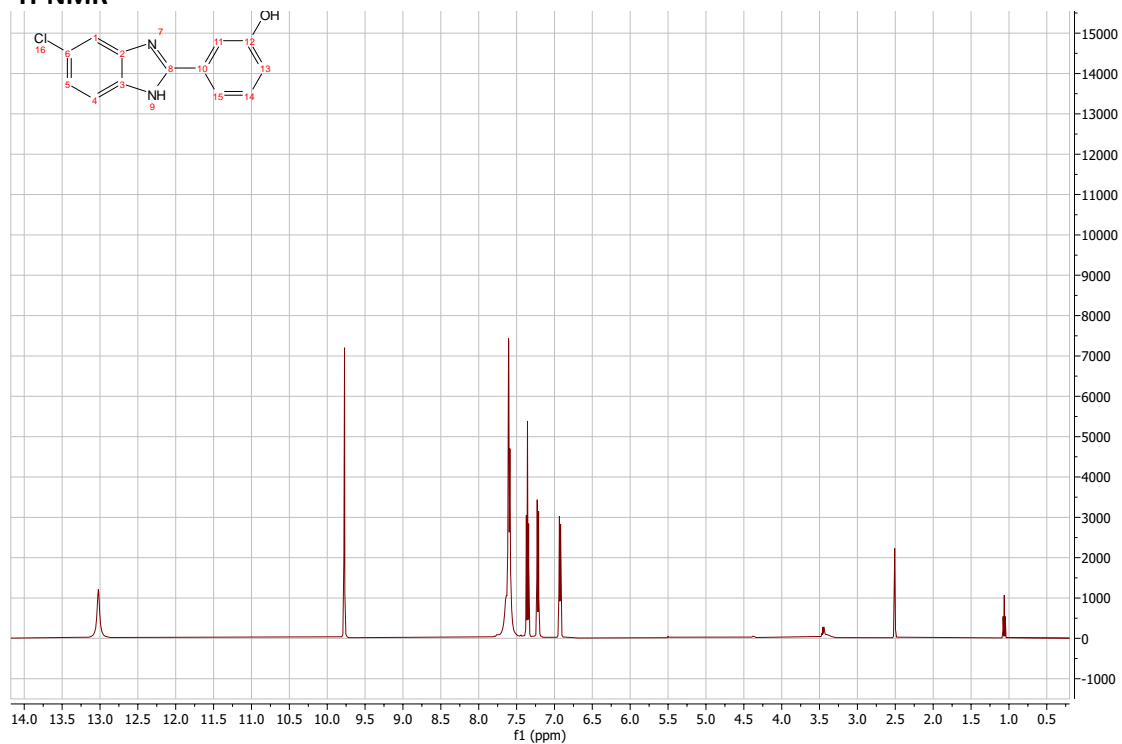
HSQC

20220504_CH434_HSQC.10.ser
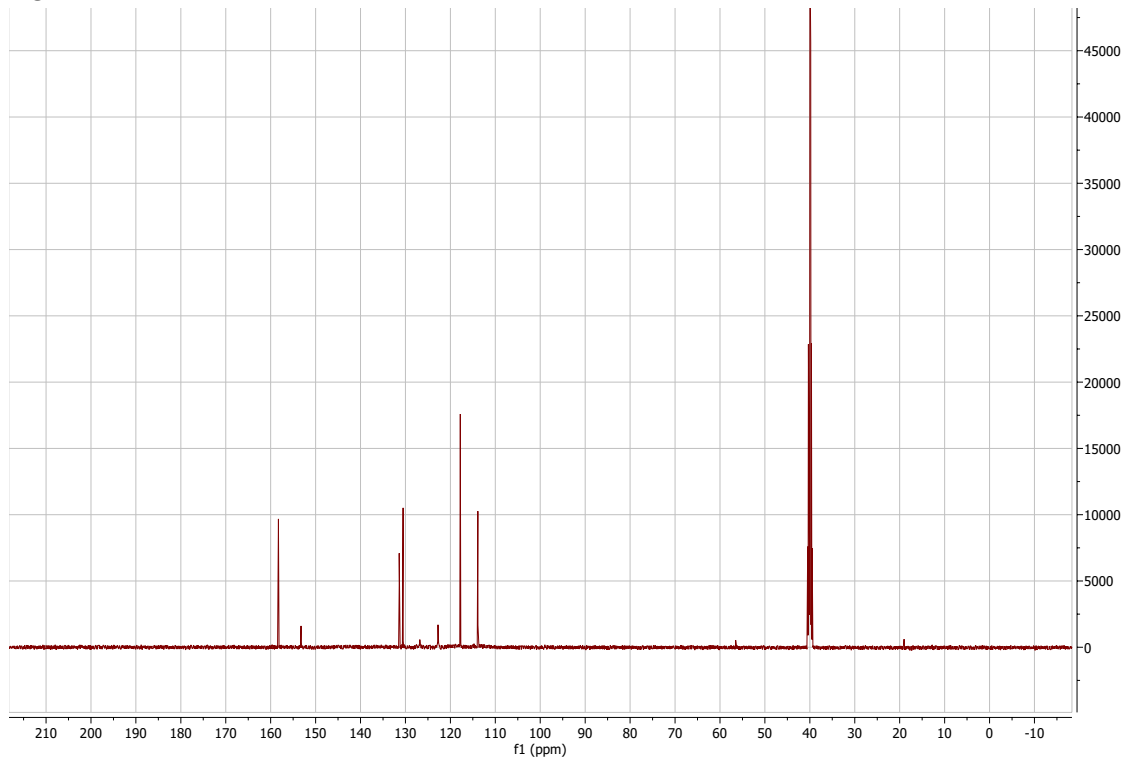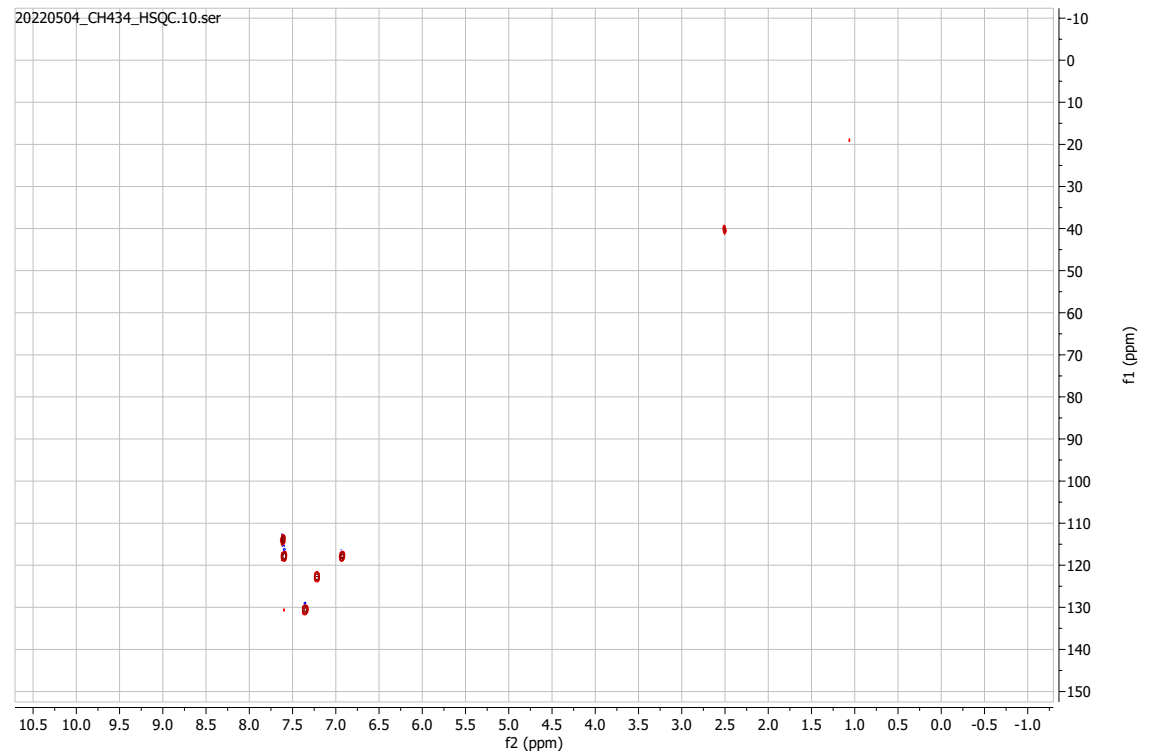
HMBC

20220504_CH434_HMBC.10.ser
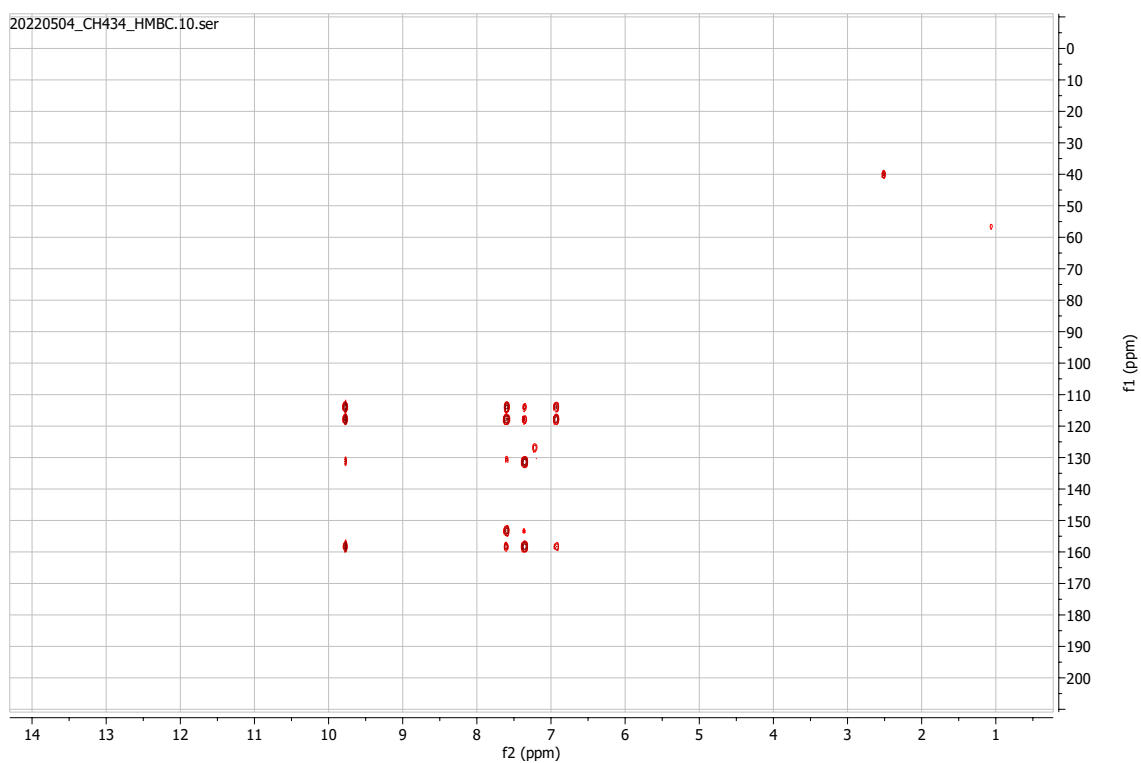
4-(5-chloro-1H-1,3-benzodiazol-2-yl)-2-ethoxyphenol:

¹H-NMR

¹³C-NMR

HSQC

20210716_CH365_HSQC.10.ser

HMBC

20210716_CH365_HMBC.10.ser
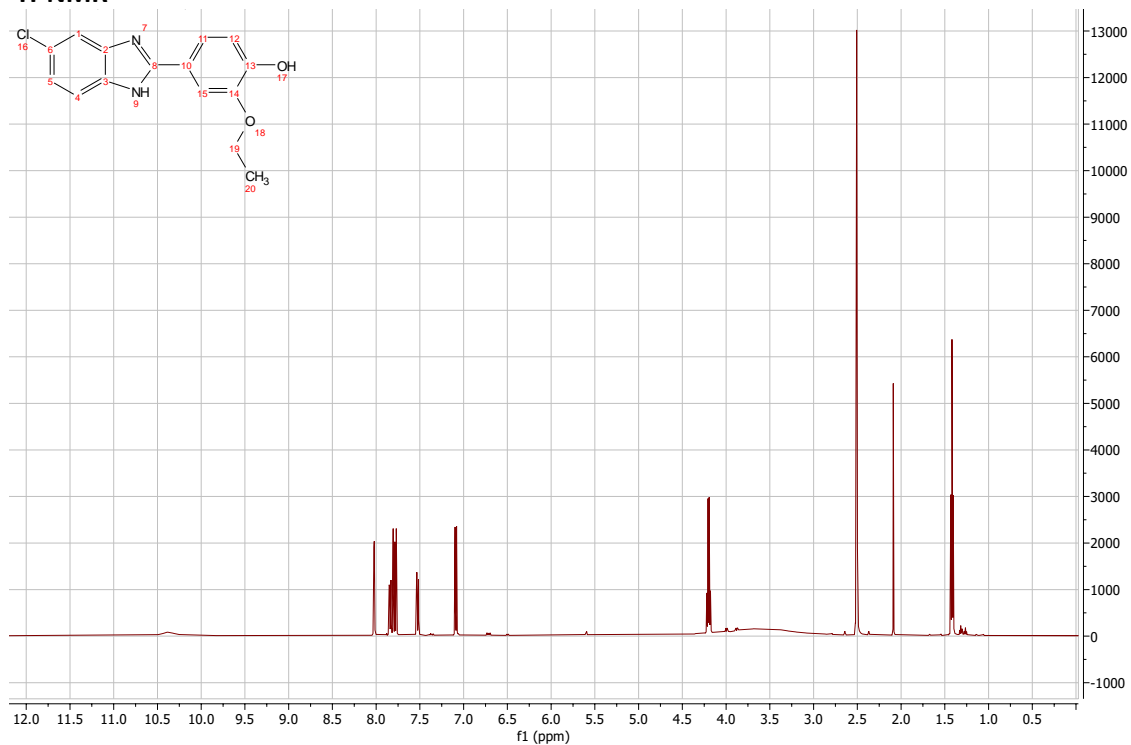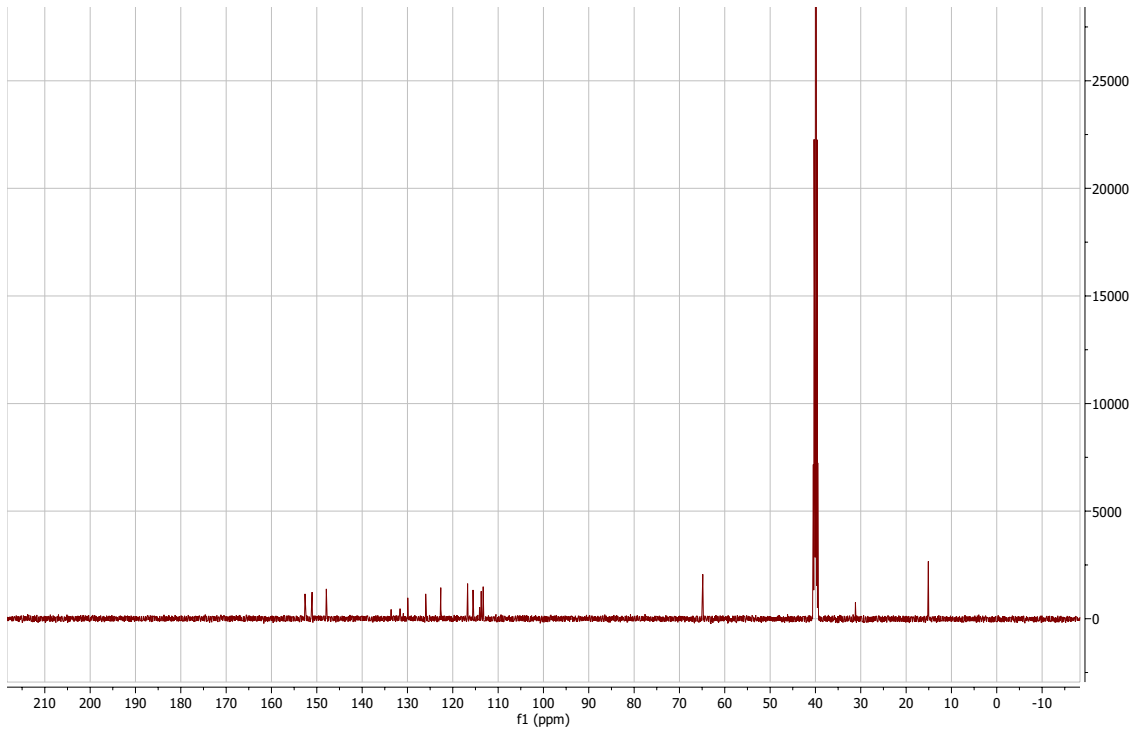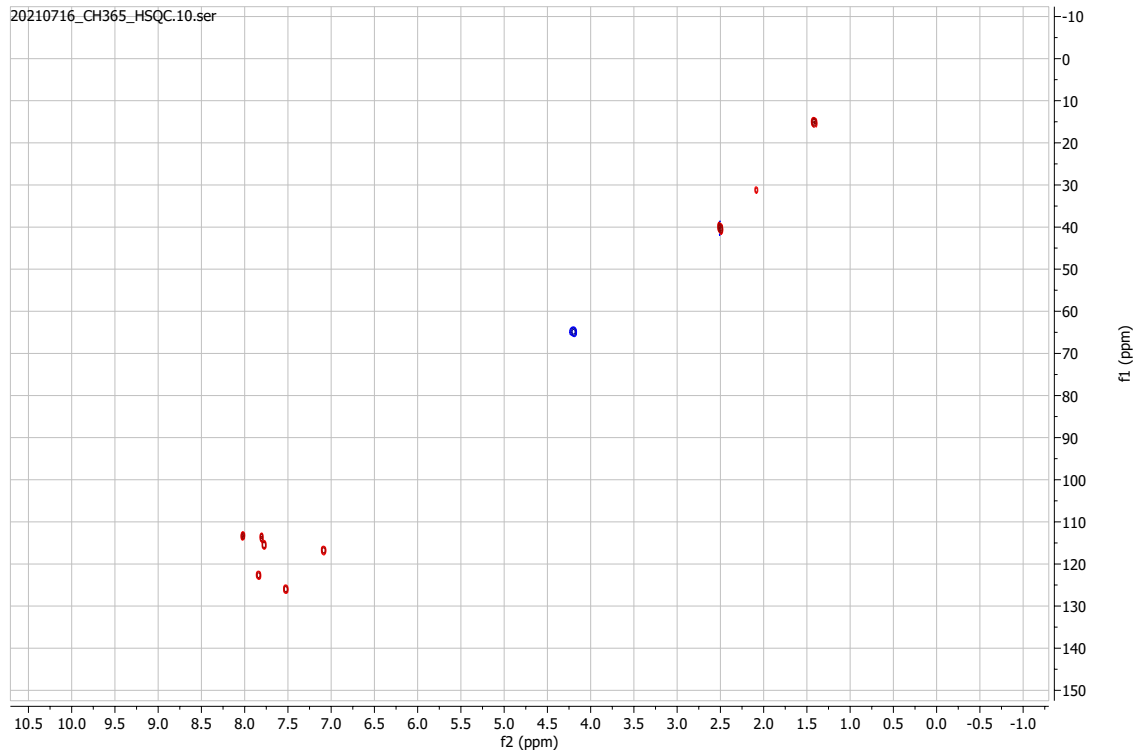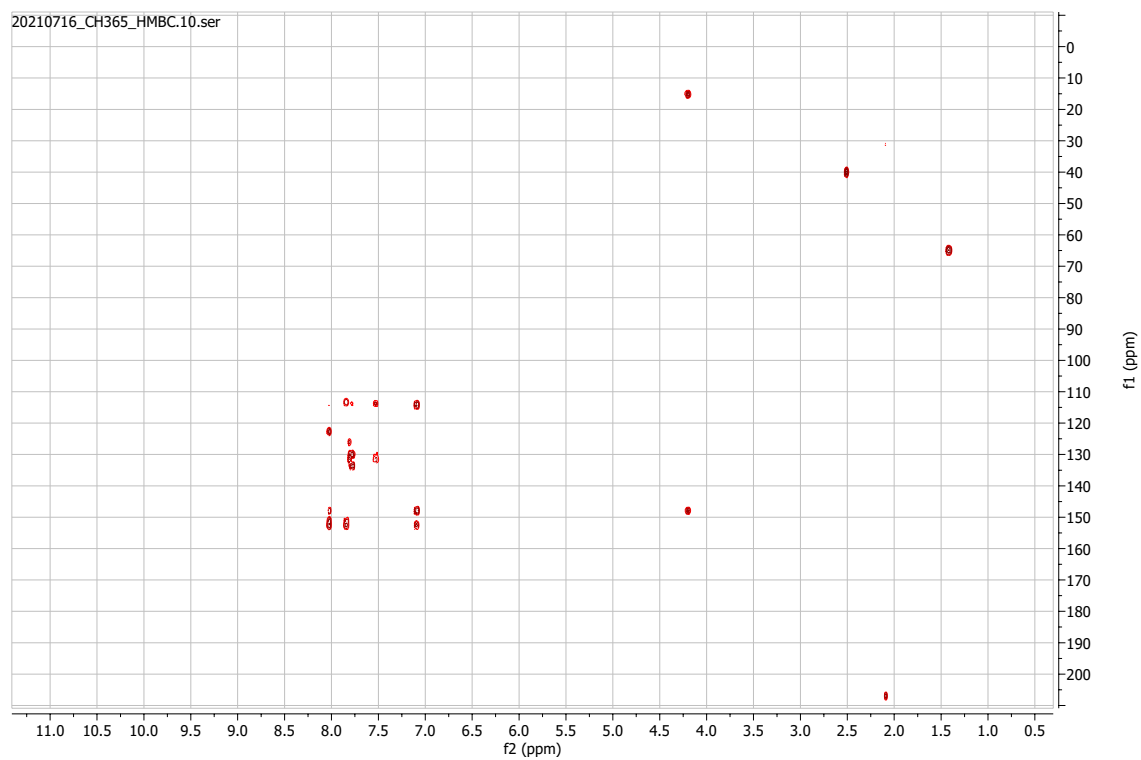
5-chloro-2-(2-nitrophenyl)-1H-1,3-benzodiazole:
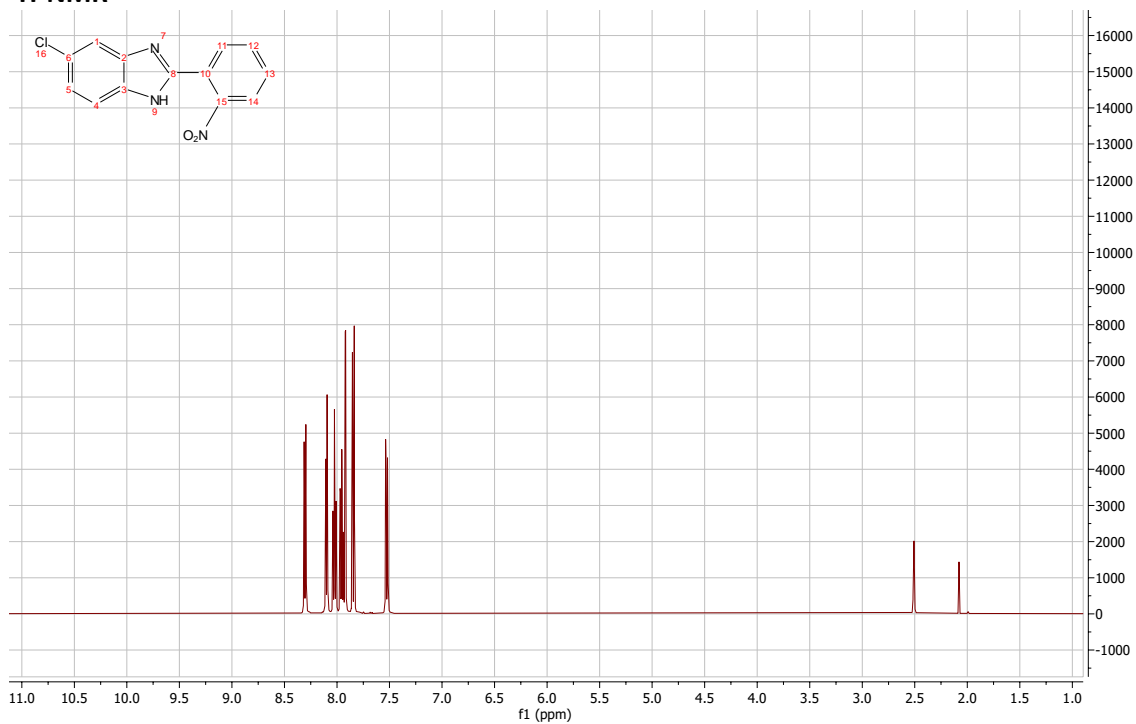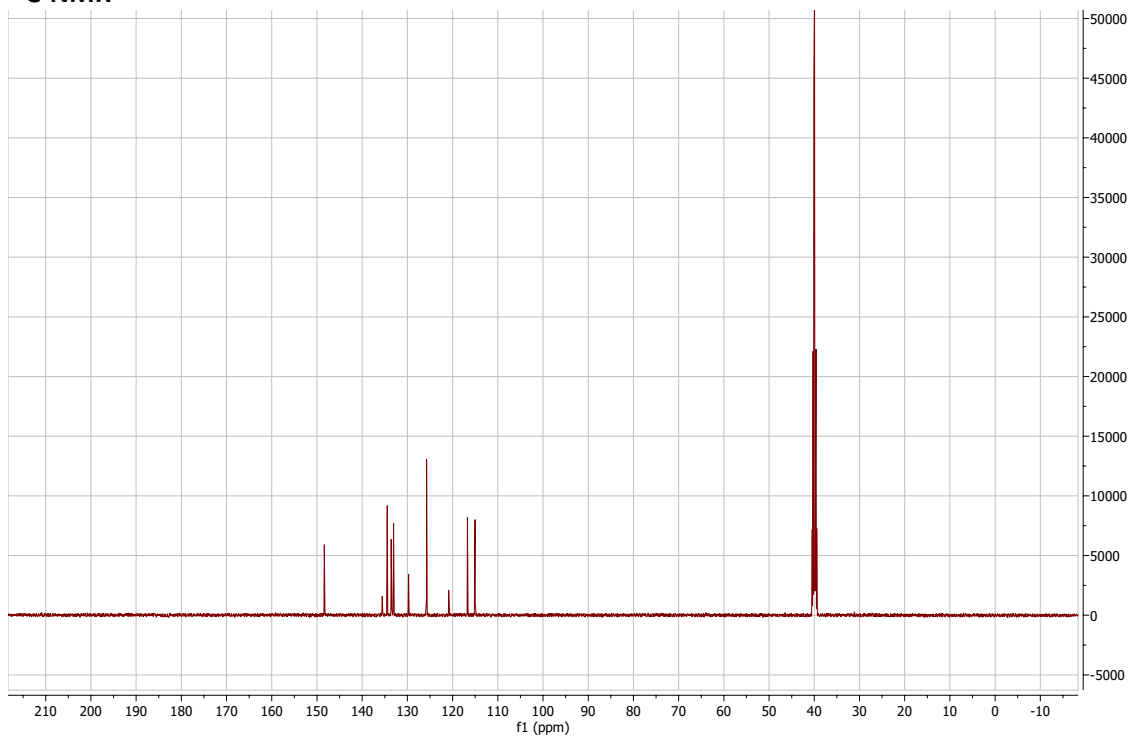
¹H-NMR

^{13}C-NMR

HSQC

20210806_CH367_clean_HSQC.10.ser

HMBC

20210806_CH367_clean_HMBC.10.ser

5-chloro-2-(3-nitrophenyl)-1H-1,3-benzodiazole:
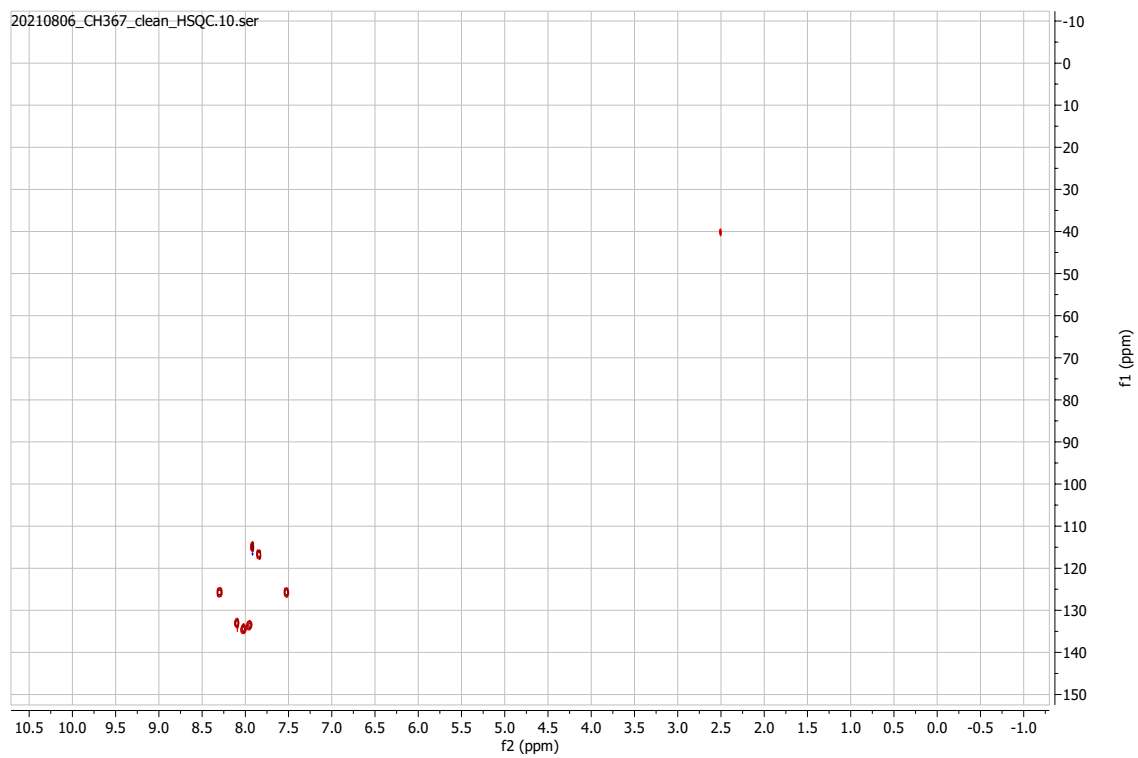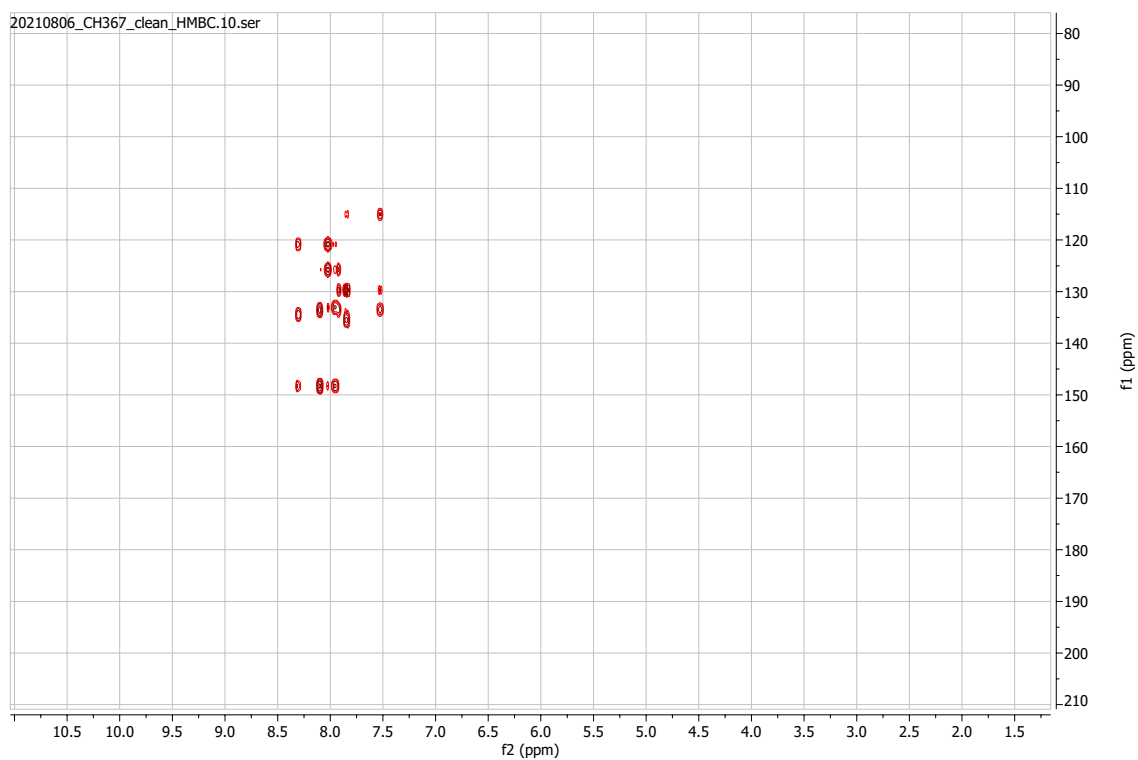
¹H-NMR

^{13}C-NMR

HSQC

20210514_CH327_gum_HSQC.10.ser

HMBC

20210514_CH327_gum_HMBC.10.ser

5-chloro-2-(thiophen-2-yl)-1H-1,3-benzodiazole:

¹H-NMR

¹³C-NMR

HSQC

202108-6_CH390_clean_HSQC.10.ser
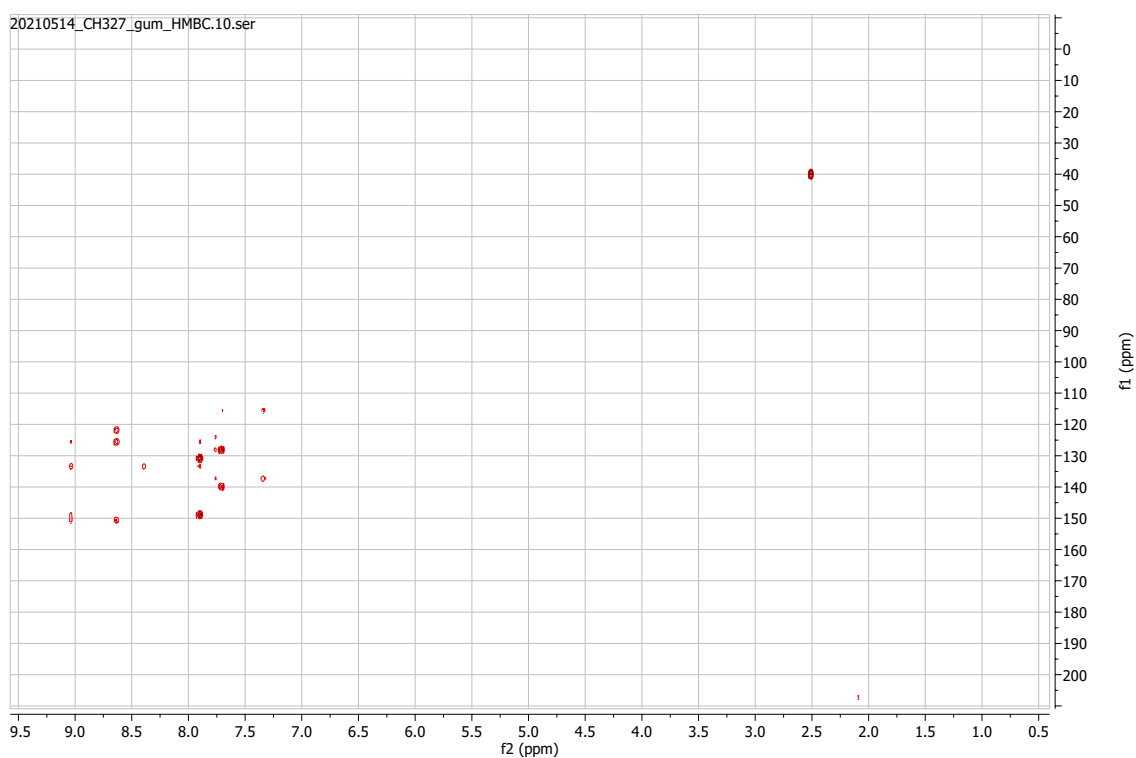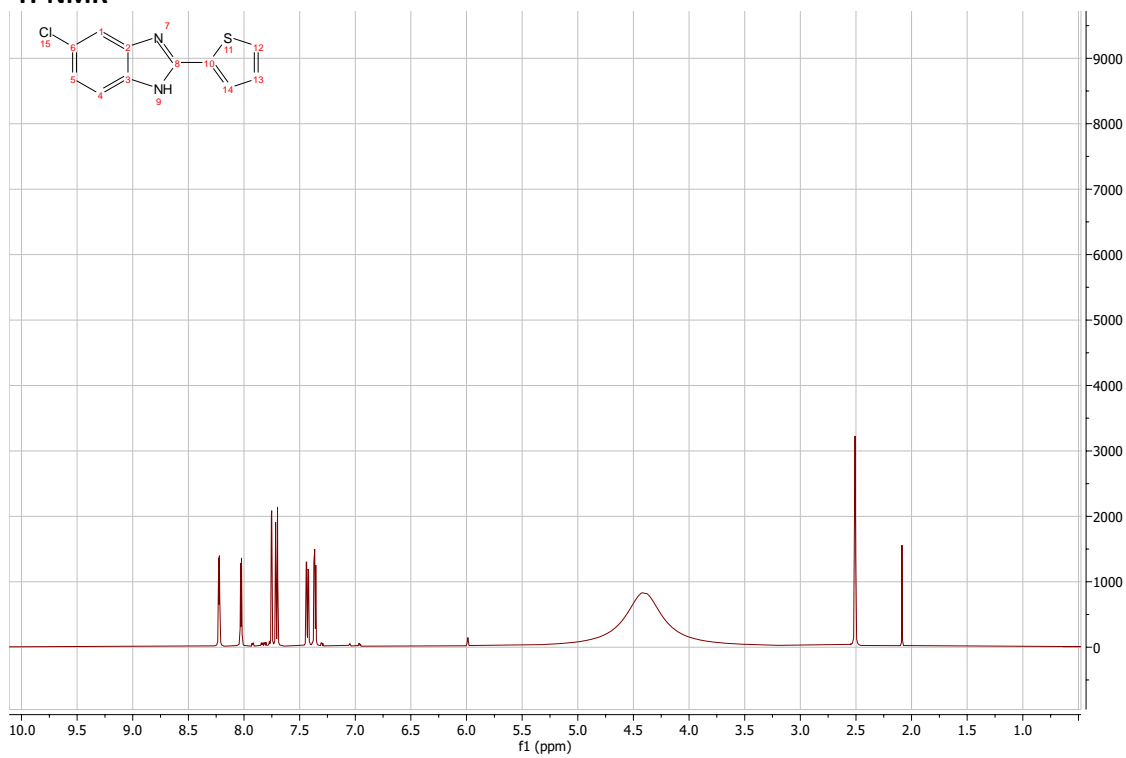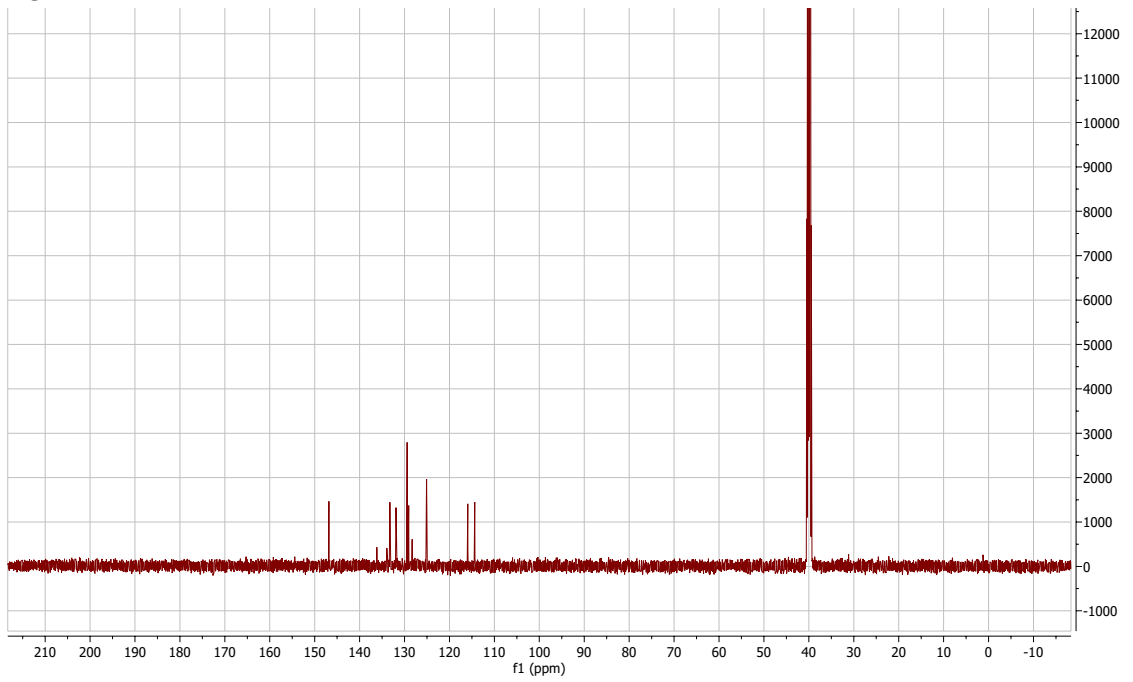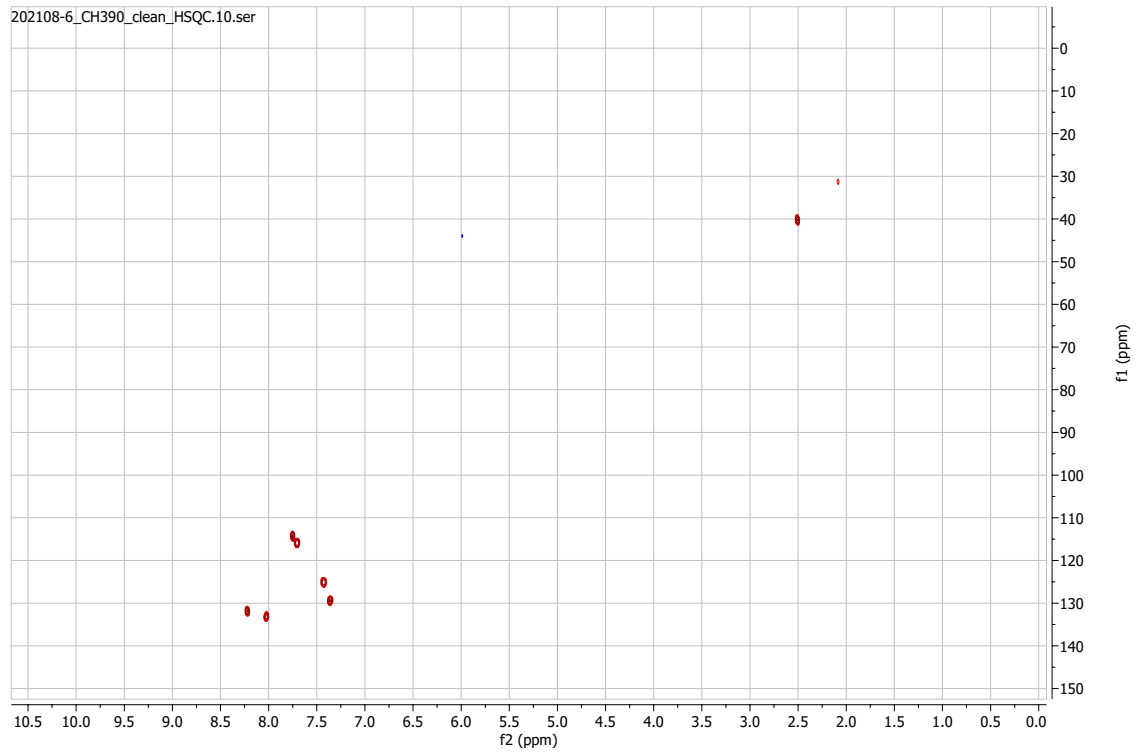
HMBC

5-chloro-2-(1H-pyrrol-2-yl)-1H-1,3-benzodiazole:

¹H-NMR

314
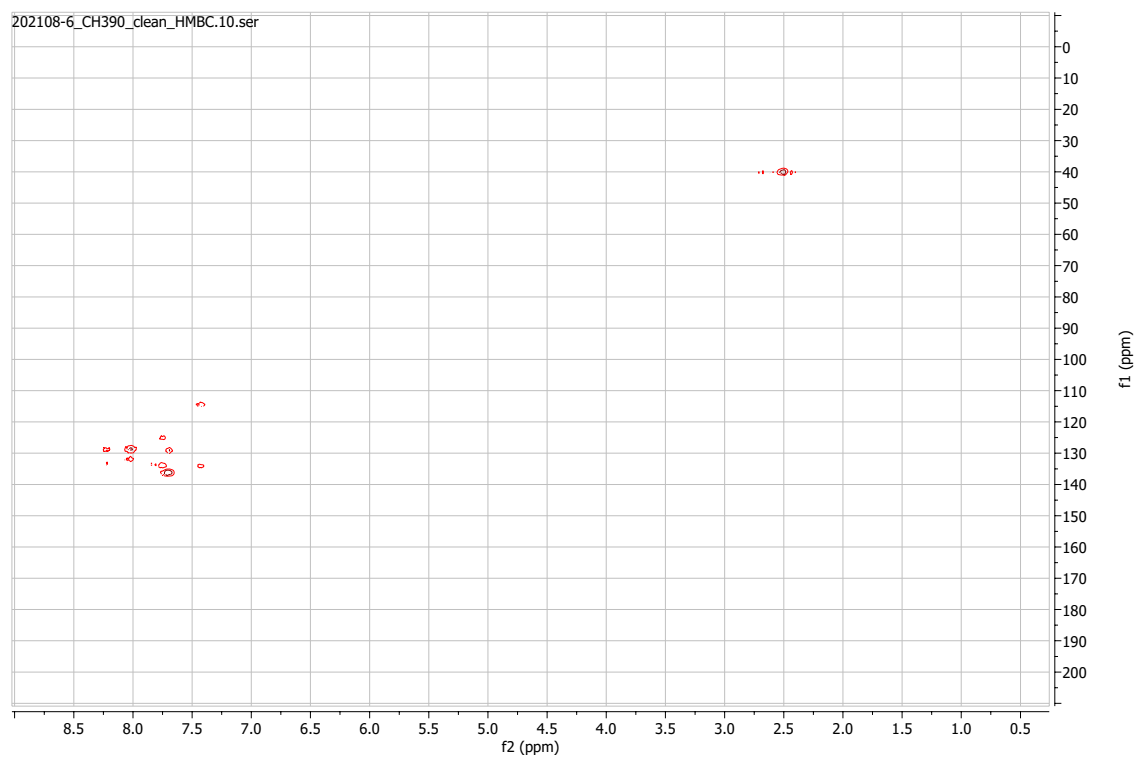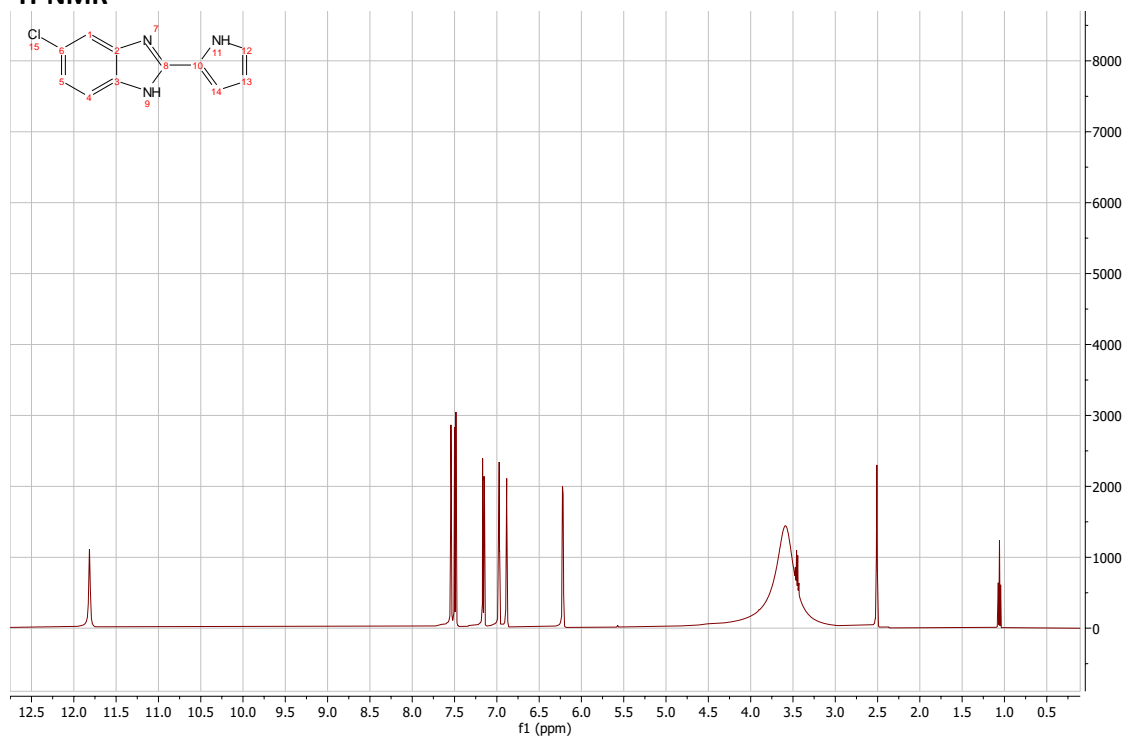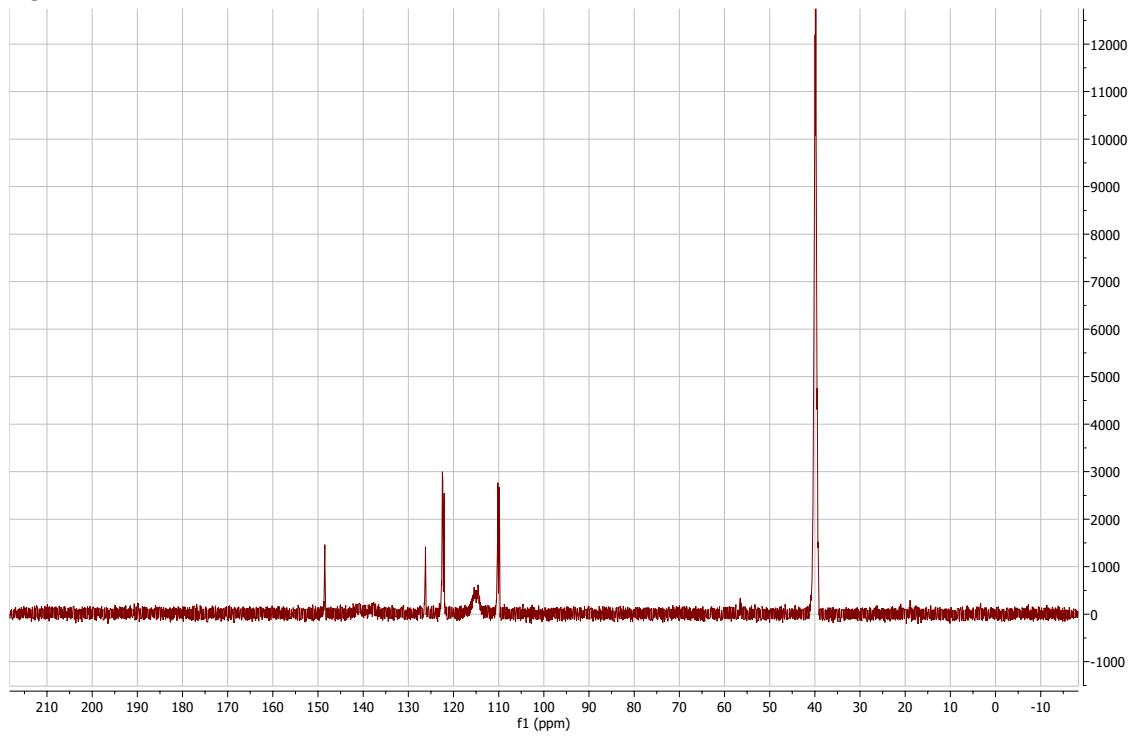
^{13}C-NMR

5-nitro-2-phenyl-1H-1,3-benzodiazole:
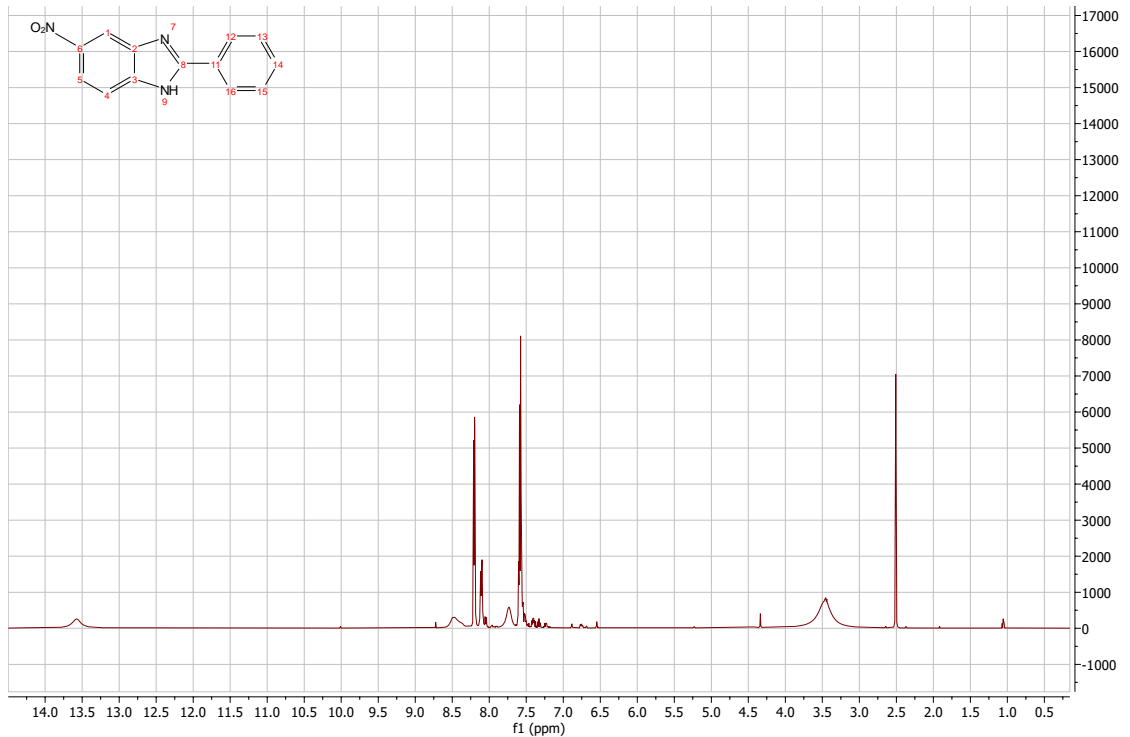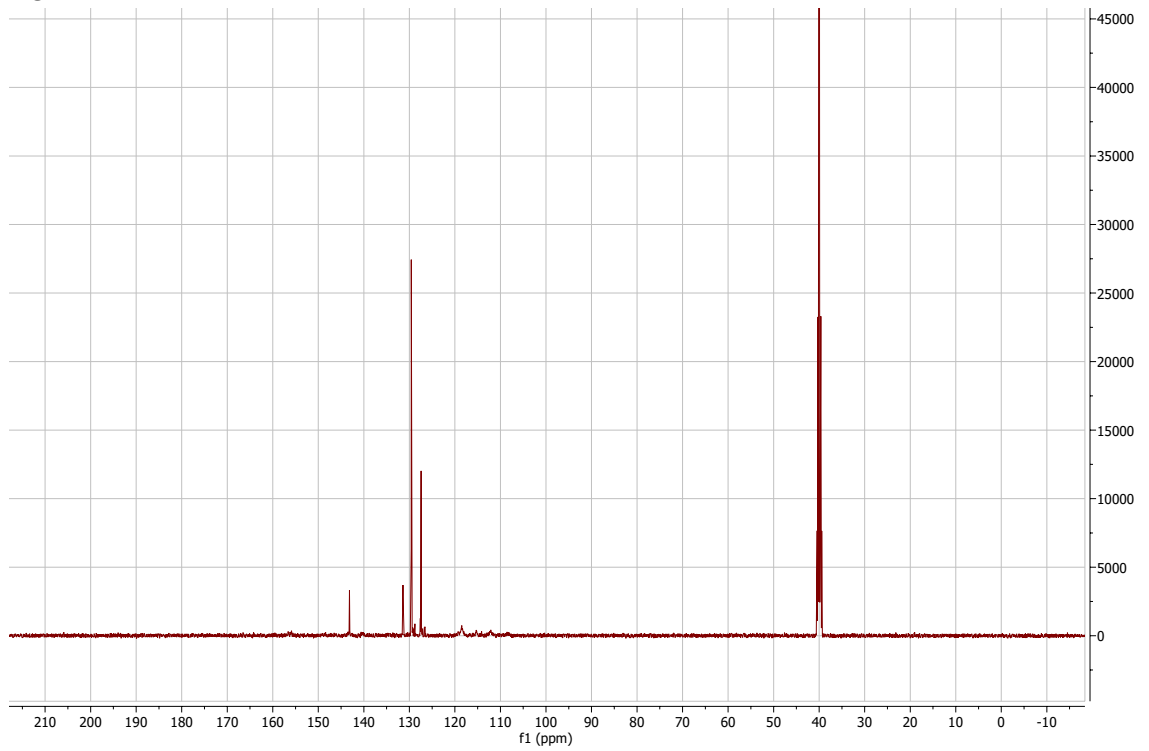
^{1}H-NMR

¹³C-NMR

HSQC

20210728_CH401_HSQC.10.ser

HMBC

20210728_CH401_HMBC.10.ser
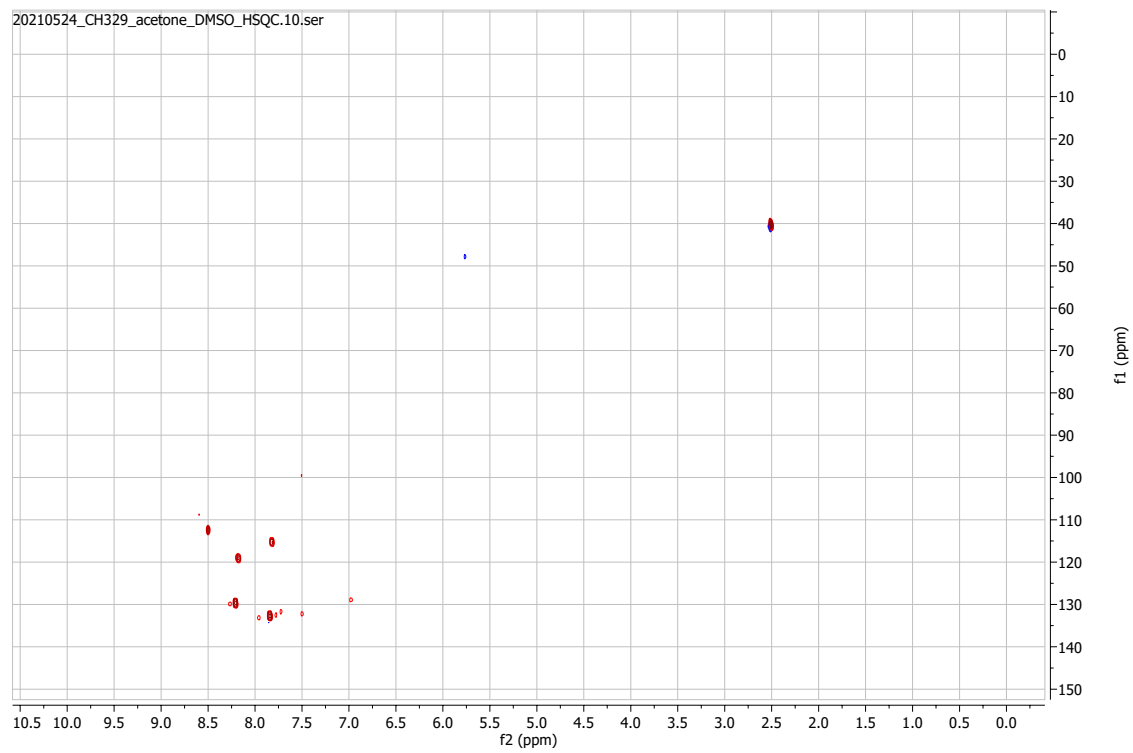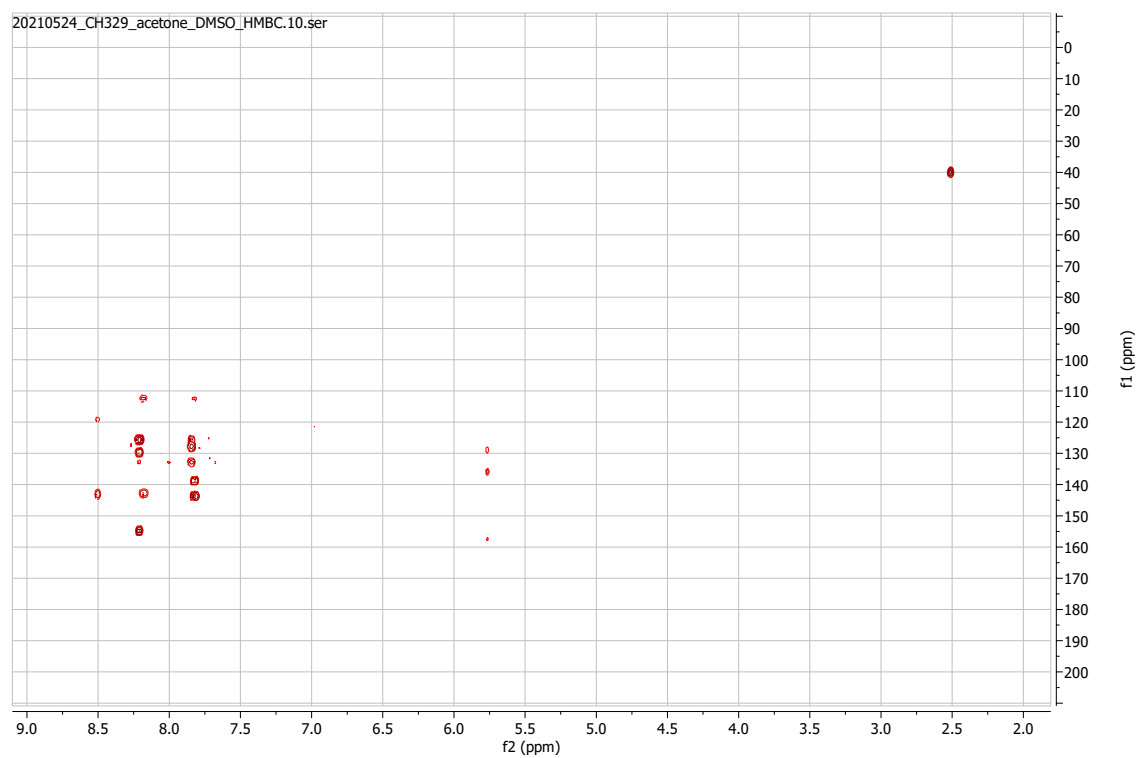
2-(4-bromophenyl)-5-nitro-1H-1,3-benzodiazole:

¹H-NMR

¹³C-NMR

^{13}C-NMR

HSQC

20210524_CH329_acetone_DMSO_HSQC.10.ser

318

HMBC

20210524_CH329_acetone_DMSO_HMBC.10.ser

2-(4-chlorophenyl)-5-nitro-1H-1,3-benzodiazole:

¹H-NMR

^{13}C-NMR

HSQC

20210615_CH359_DMSO_HSQC.10.ser

HMBC

20210615_CH359_DMSO_HMBC.10.ser

4-(5-nitro-1H-1,3-benzodiazol-2-yl)phenol:

¹H-NMR

¹³C-NMR

HSQC

20210608_CH349_DMSO_HSQC.10.ser
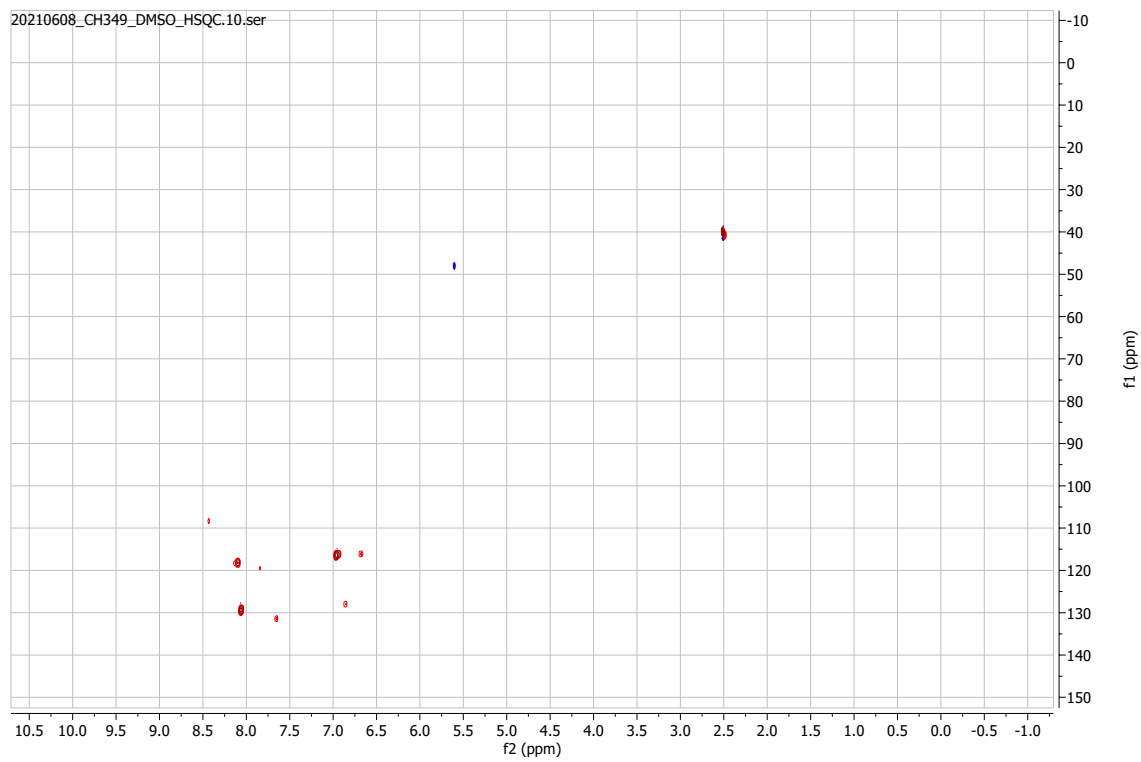
HMBC
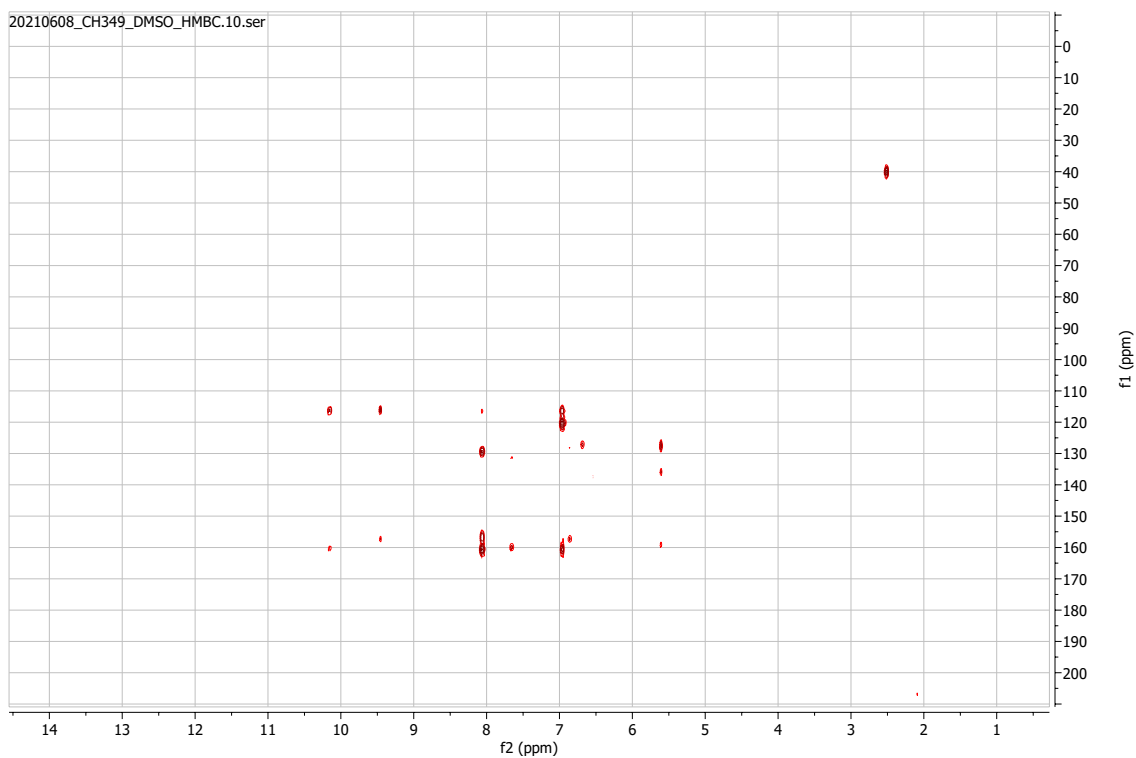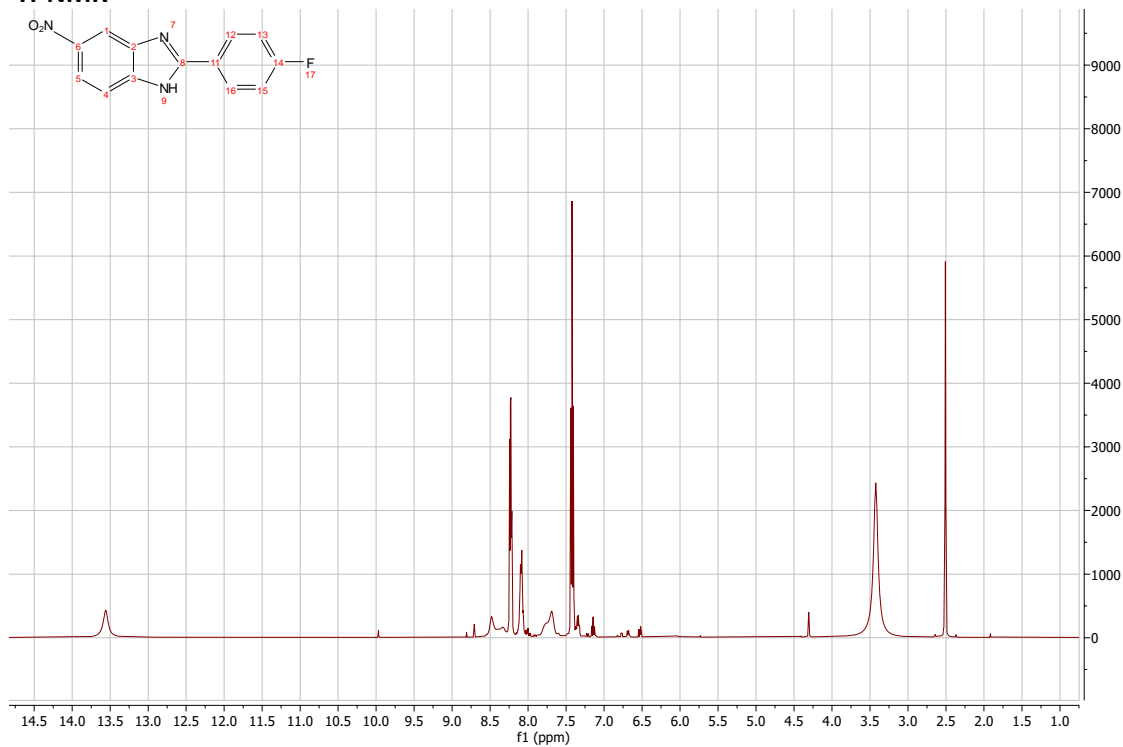
20210608_CH349_DMSO_HMBC.10.ser

2-(4-fluorophenyl)-5-nitro-1H-1,3-benzodiazole:

^{1}H-NMR

¹³C-NMR

HSQC

20210728_CH397_HSQC.10.ser

HMBC
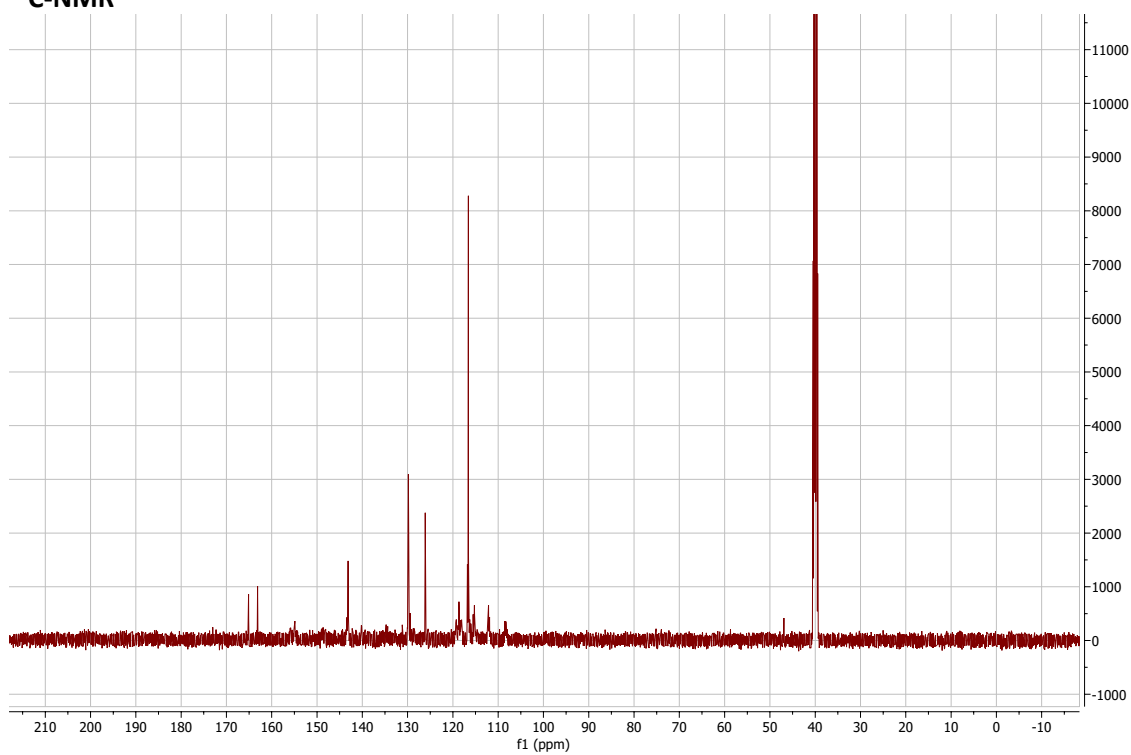
20210728_CH397_HMBC.10.ser
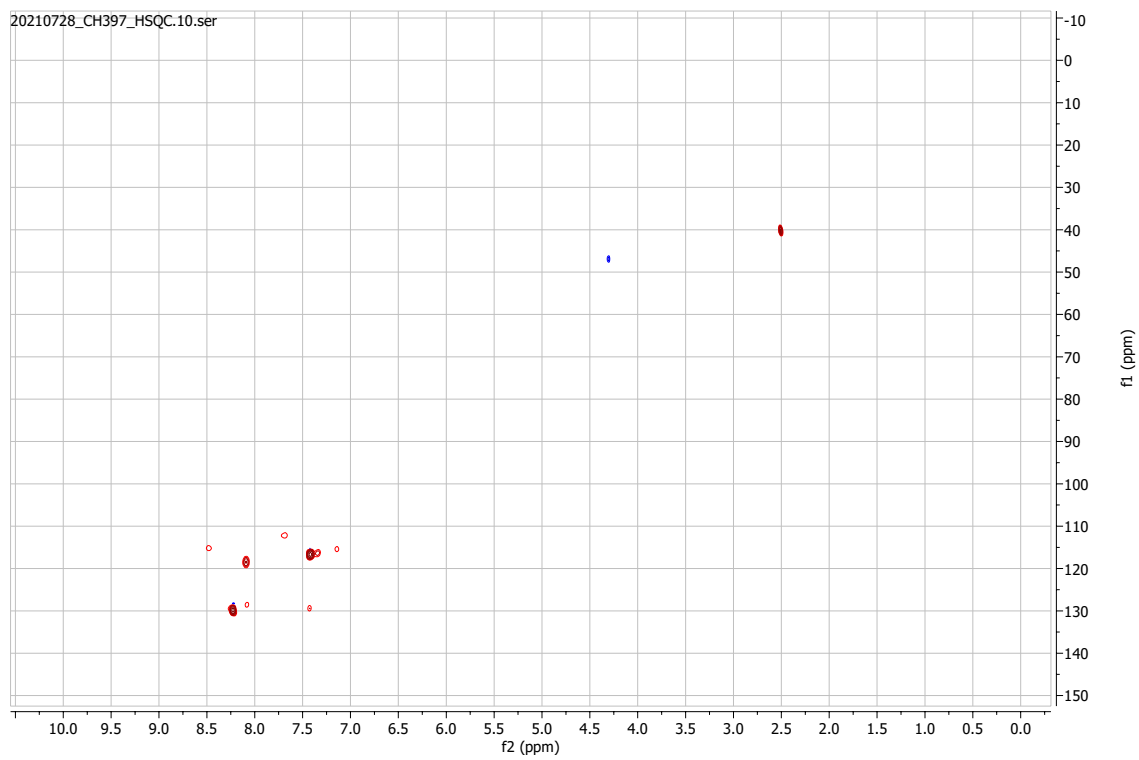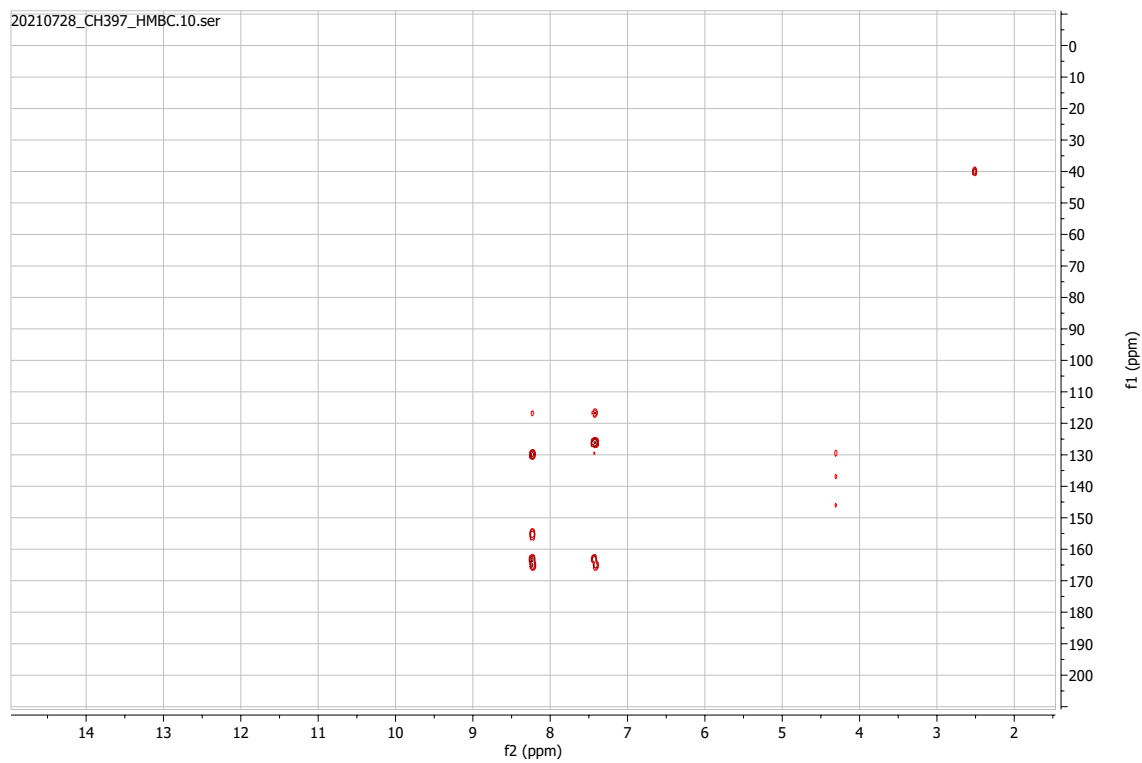
2-(4-methoxyphenyl)-5-nitro-1H-1,3-benzodiazole:
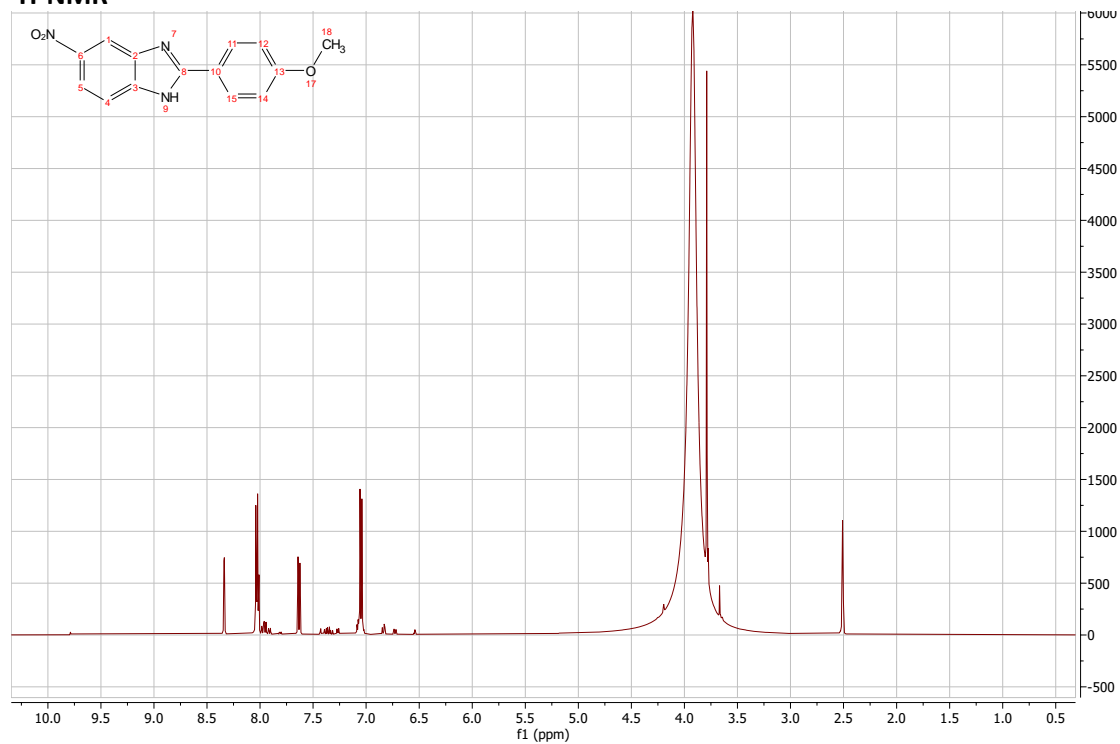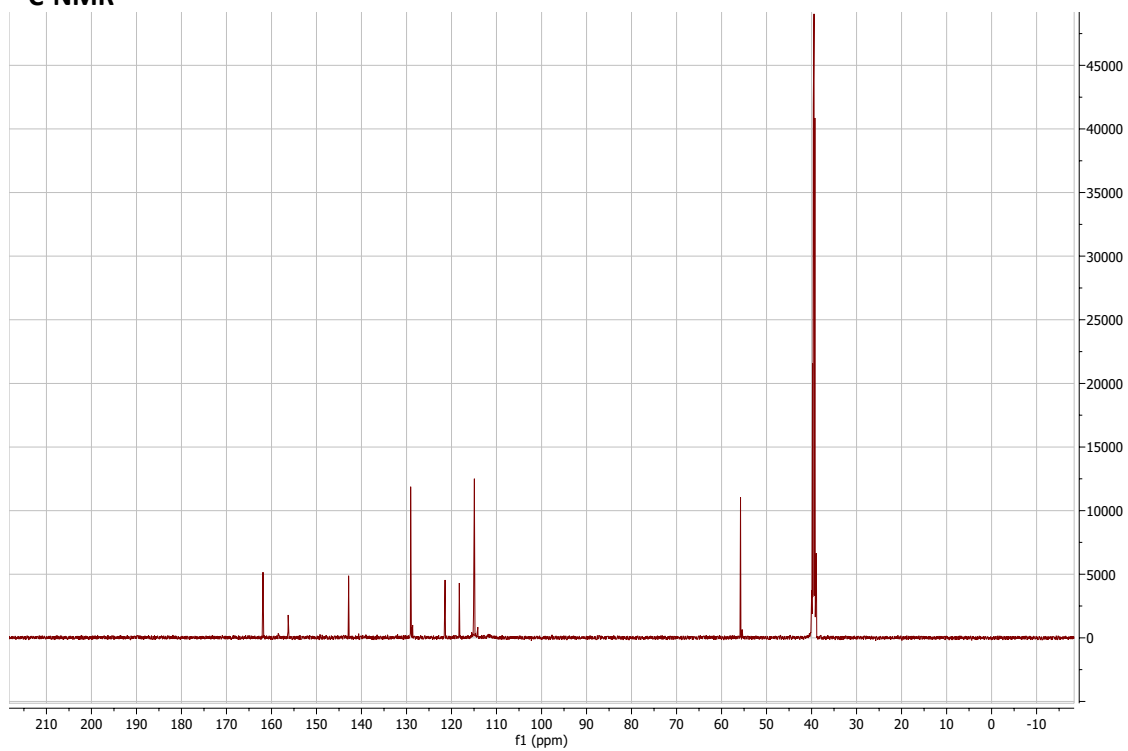
¹H-NMR

¹³C-NMR

HSQC

20210728_CH398_HSQC.10.ser

HMBC

20210728_CH398_HMBC.10.ser

3-(5-nitro-1H-1,3-benzodiazol-2-yl)phenol:
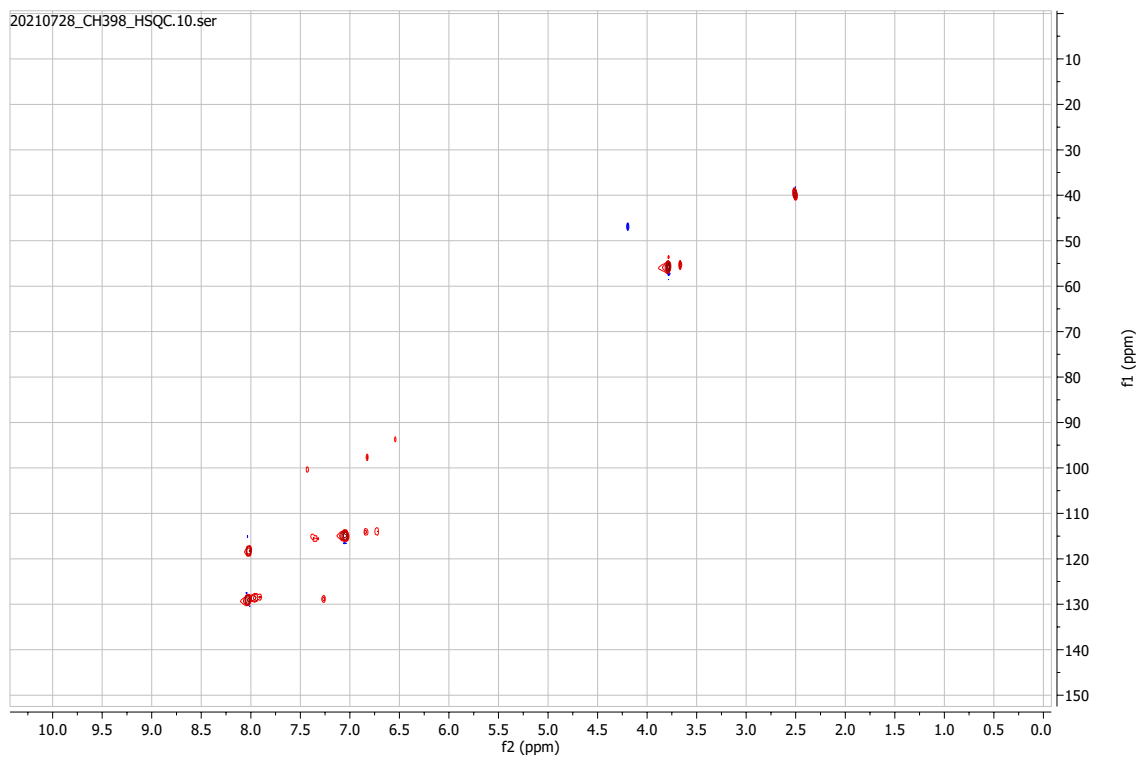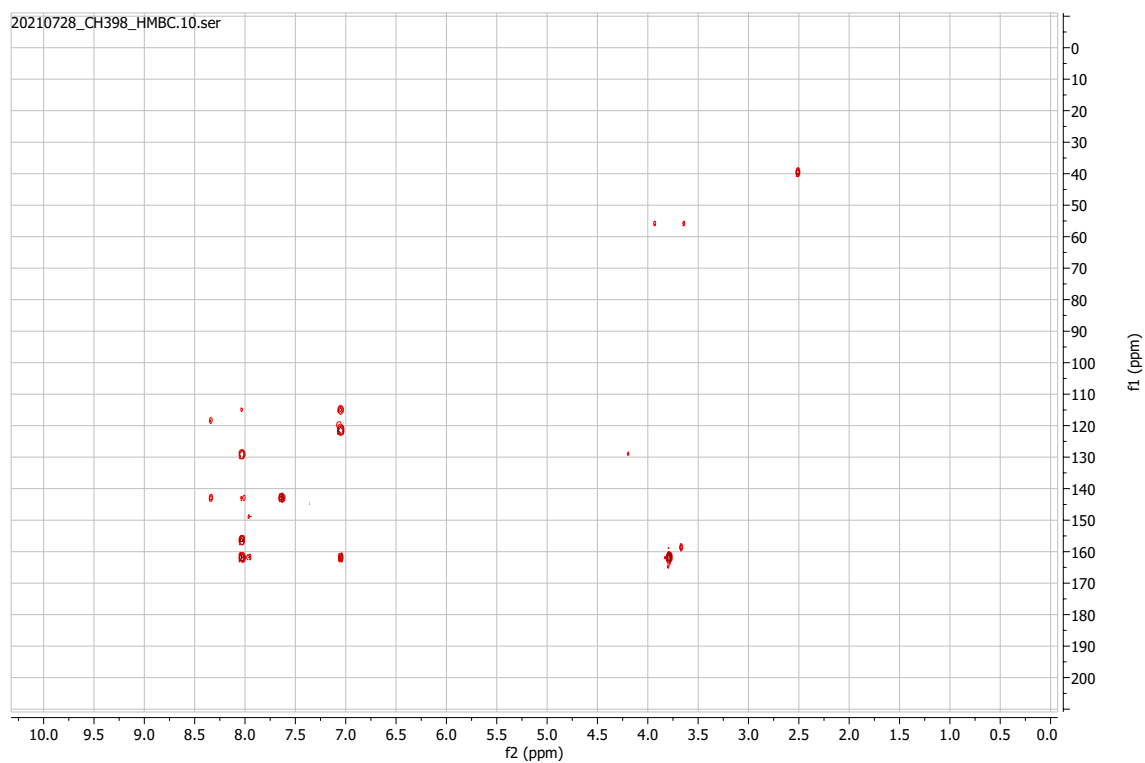
¹H-NMR

¹³C-NMR

HSQC

20210611_CH355_extr_DMSO_HSQC.10.ser
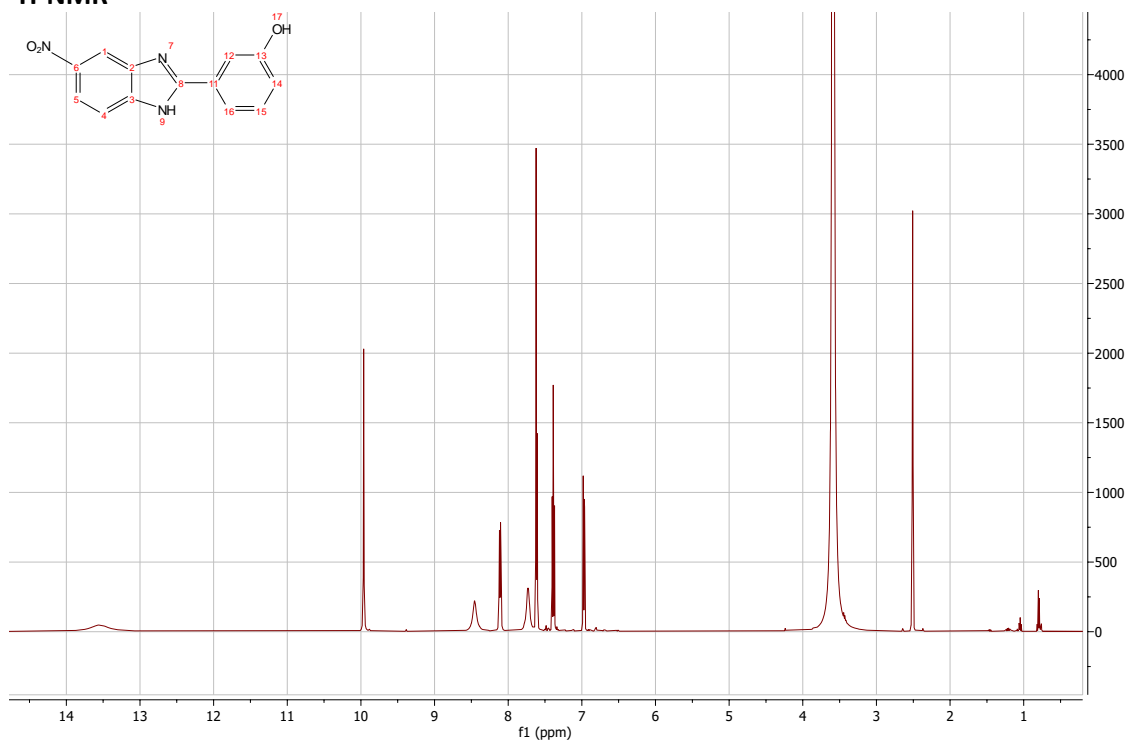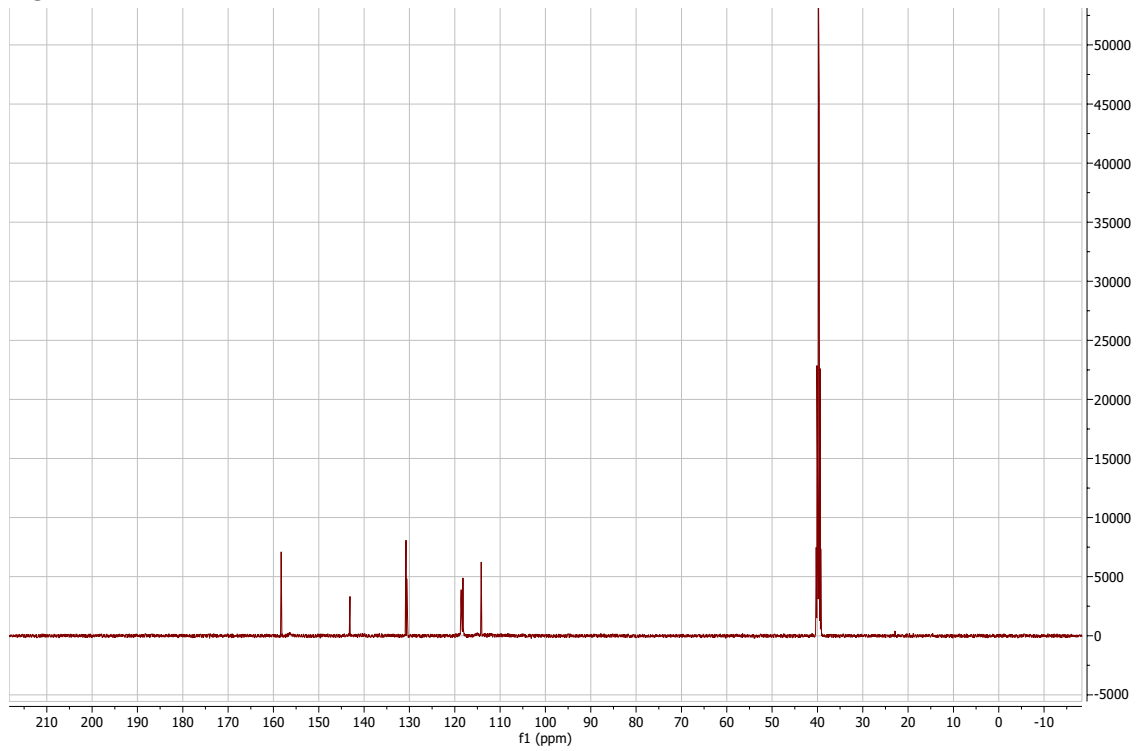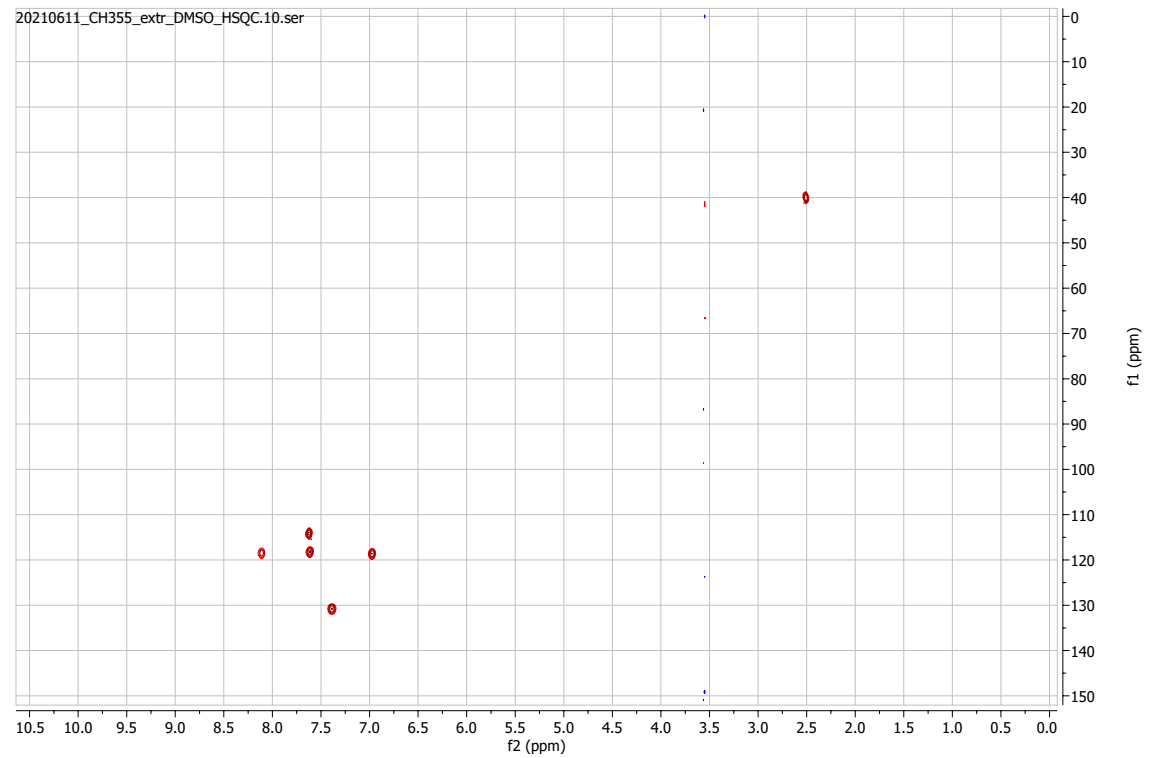
HMBC

20210611_CH355_extr_DMSO_HMBC.10.ser
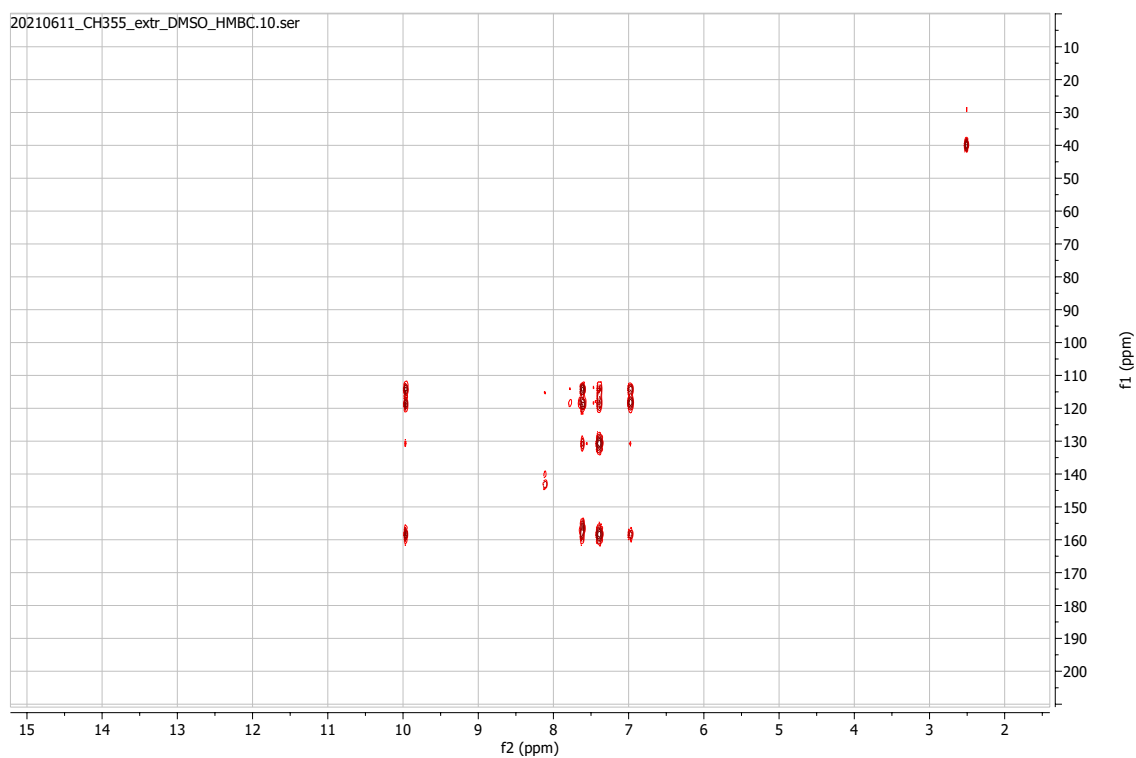
2-ethoxy-4-(5-nitro-1H-1,3-benzodiazol-2-yl)phenol:
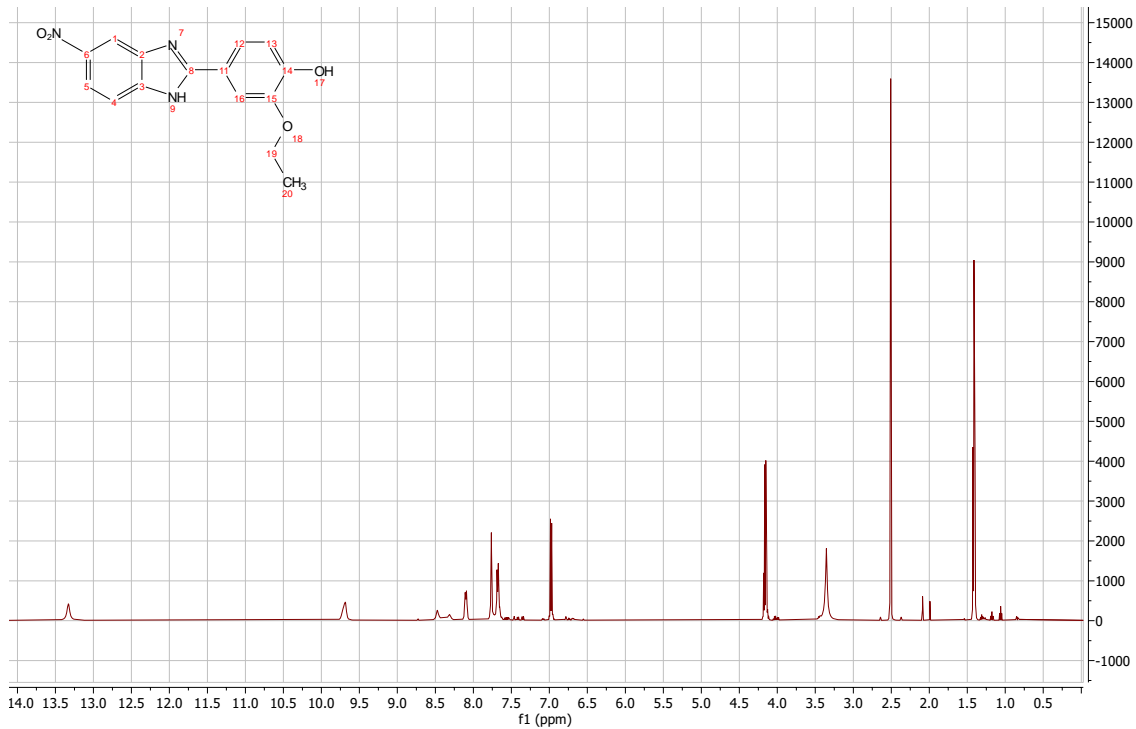
¹H-NMR

¹³C-NMR

HSQC

20210614_CH356_gum+acetone_DMSO_HSQC.10.ser

HMBC

20210614_CH356_gum+acetone_DMSO_HMBC.10.ser

5-nitro-2-(2-nitrophenyl)-1H-1,3-benzodiazole:
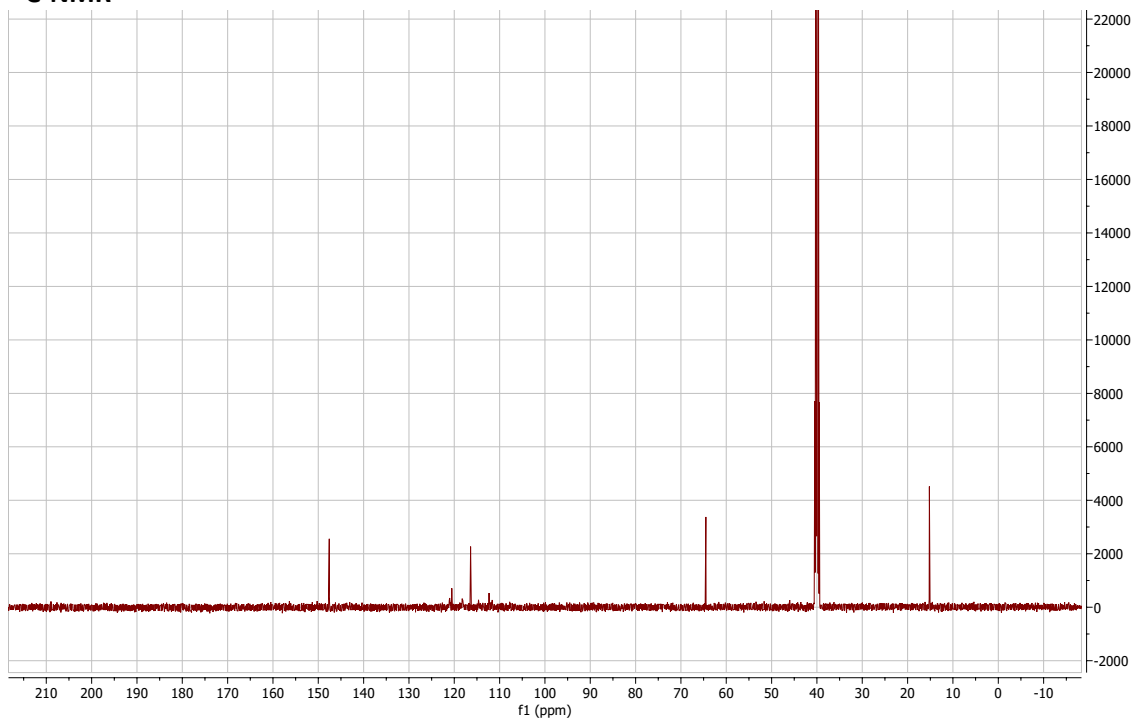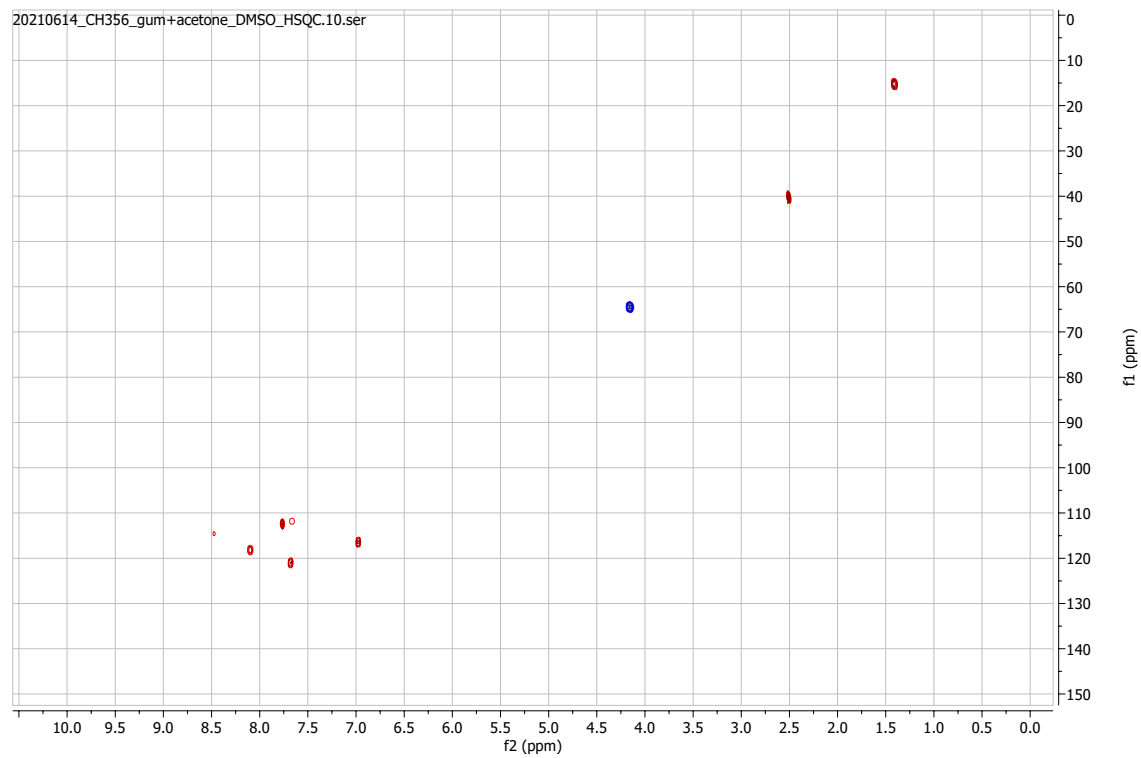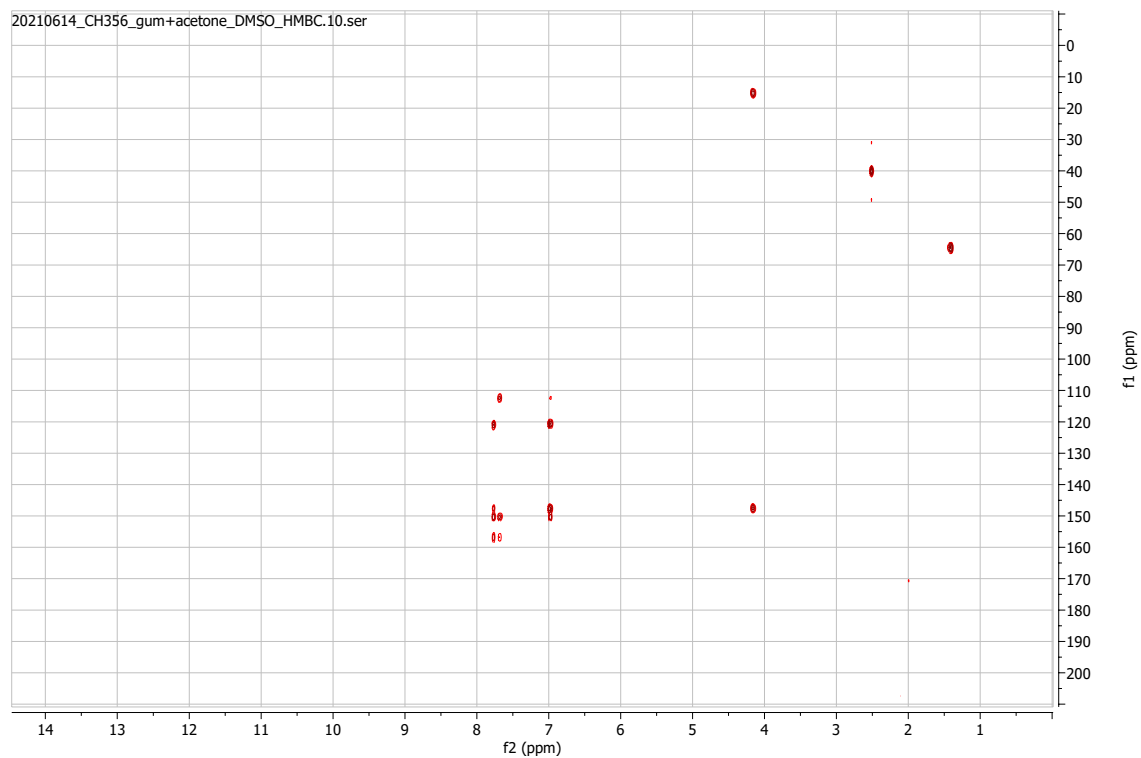
¹H-NMR

¹³C-NMR

HSQC
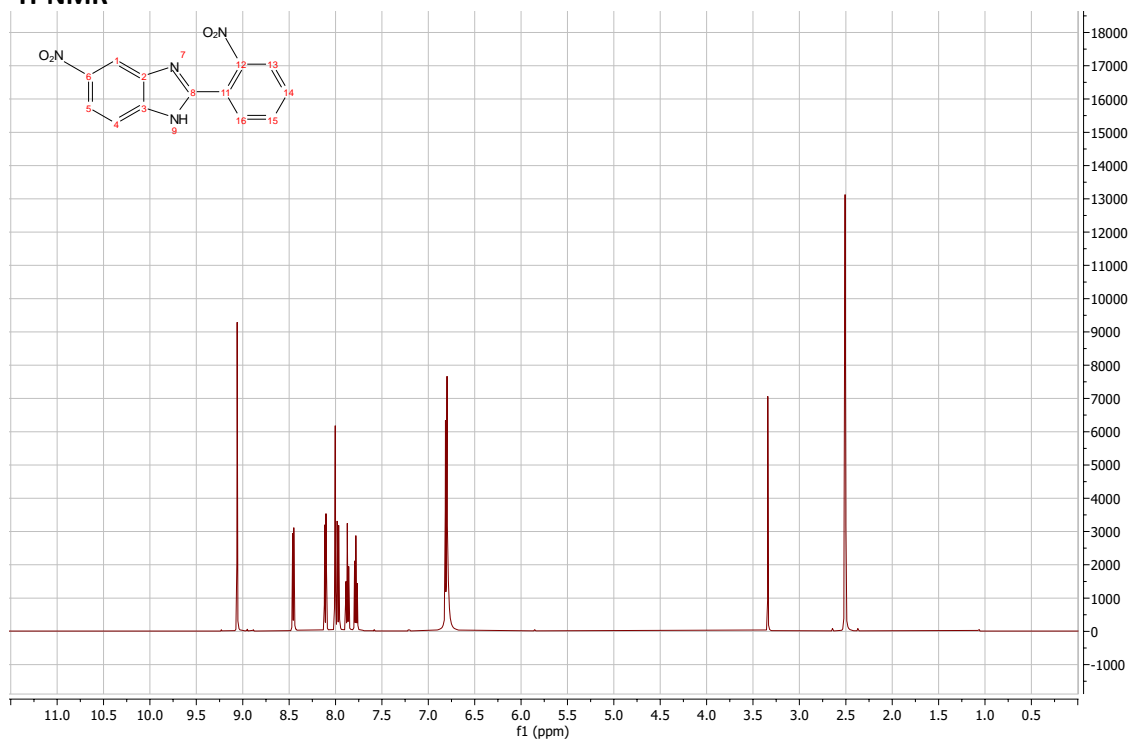
20210611_CH353_DMSO_HSQC.10.ser
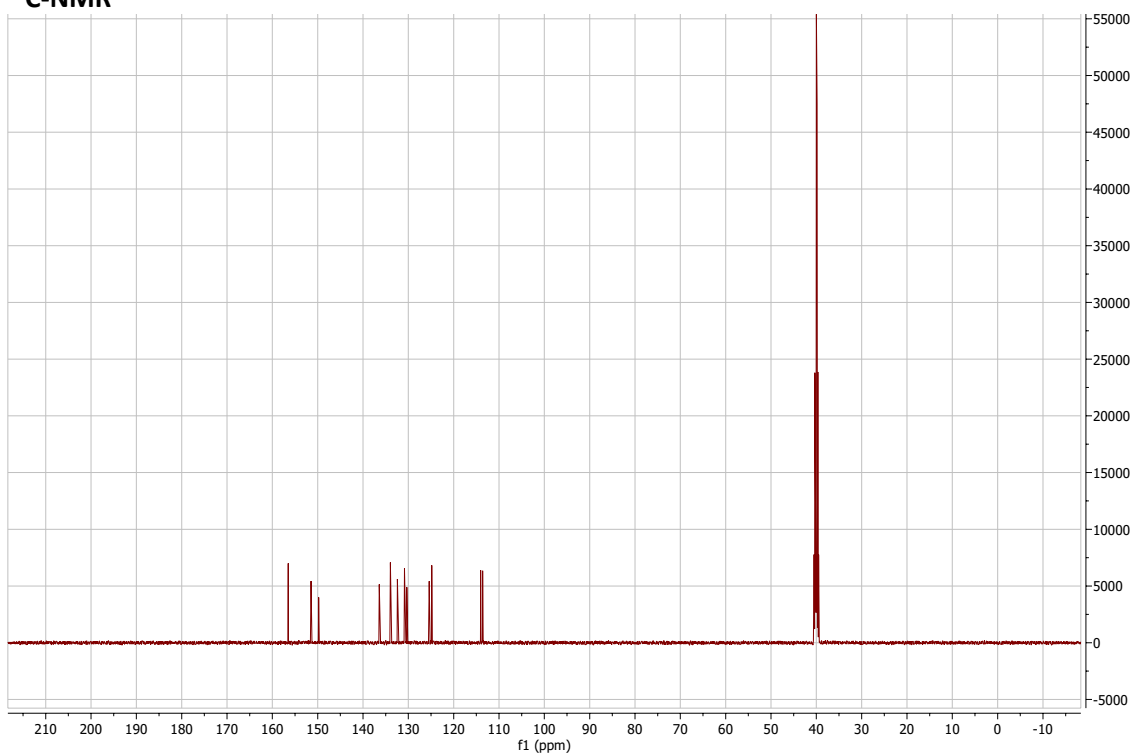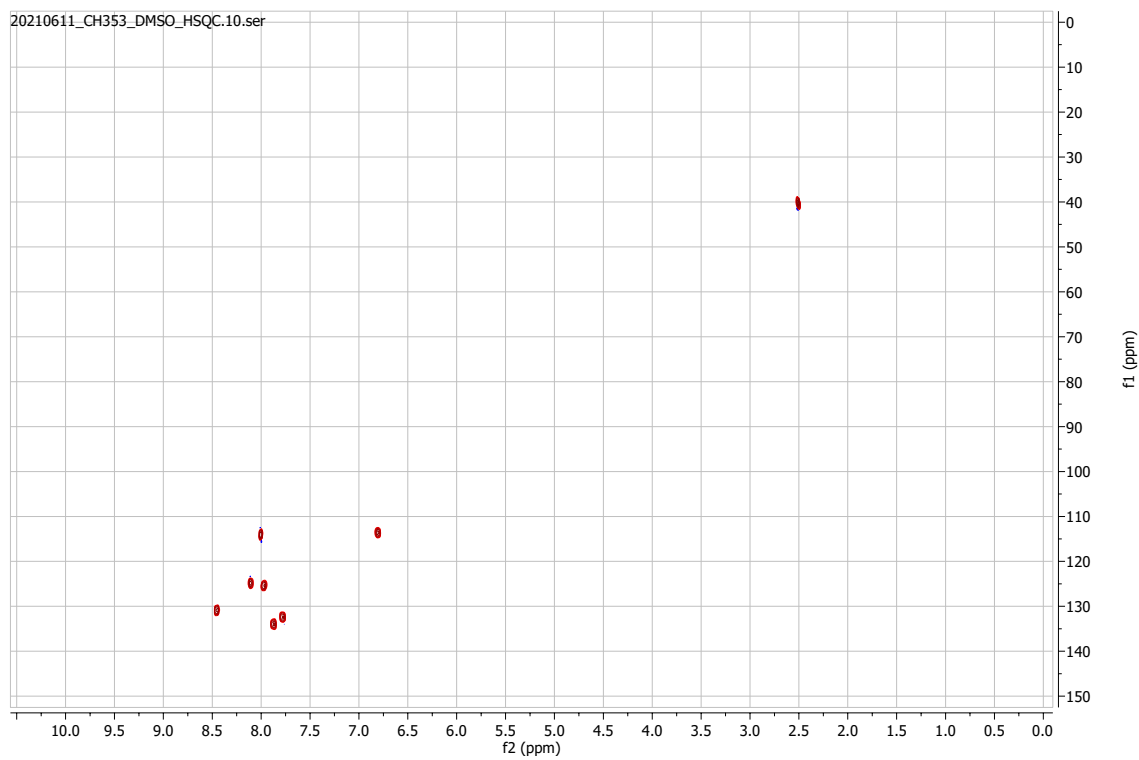
HMBC

20210611_CH353_DMSO_HMBC.20.ser
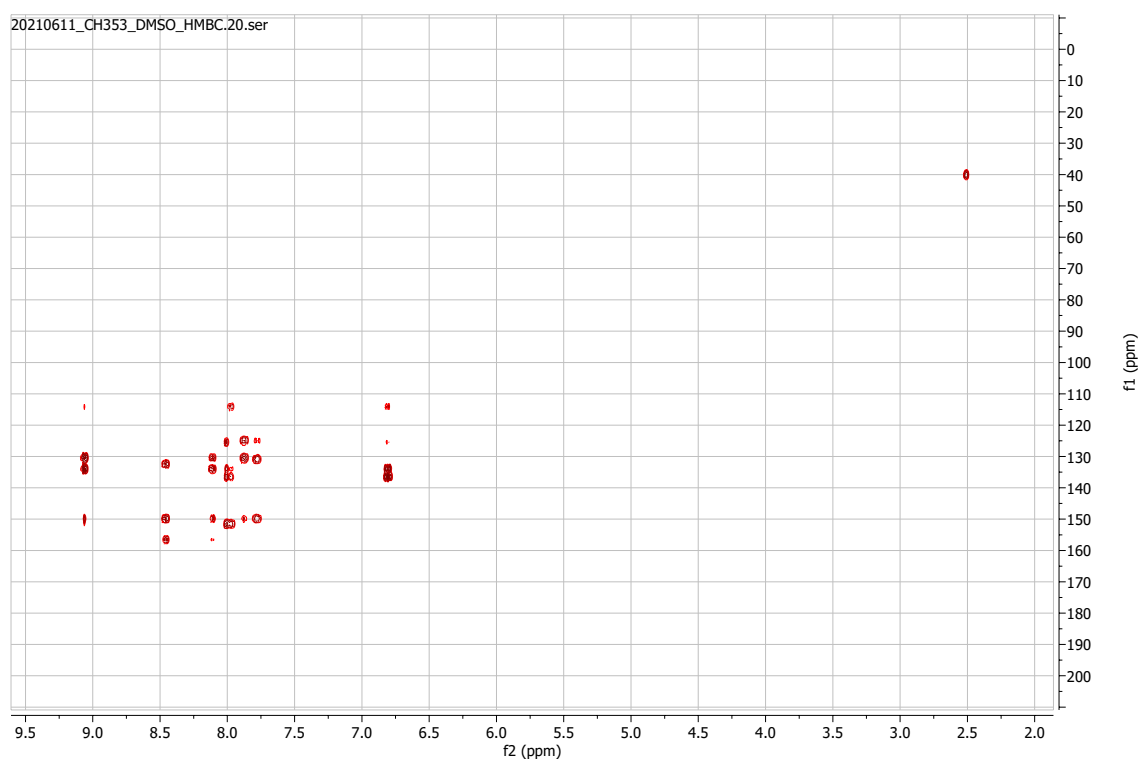
5-nitro-2-(3-nitrophenyl)-1H-1,3-benzodiazole:

^{1}H-NMR

¹³C-NMR

¹³C-NMR

HSQC

20210615_CH360_DMSO_HSQC.10.ser

HMBC

20210615_CH360_DMSO_HMBC.10.ser
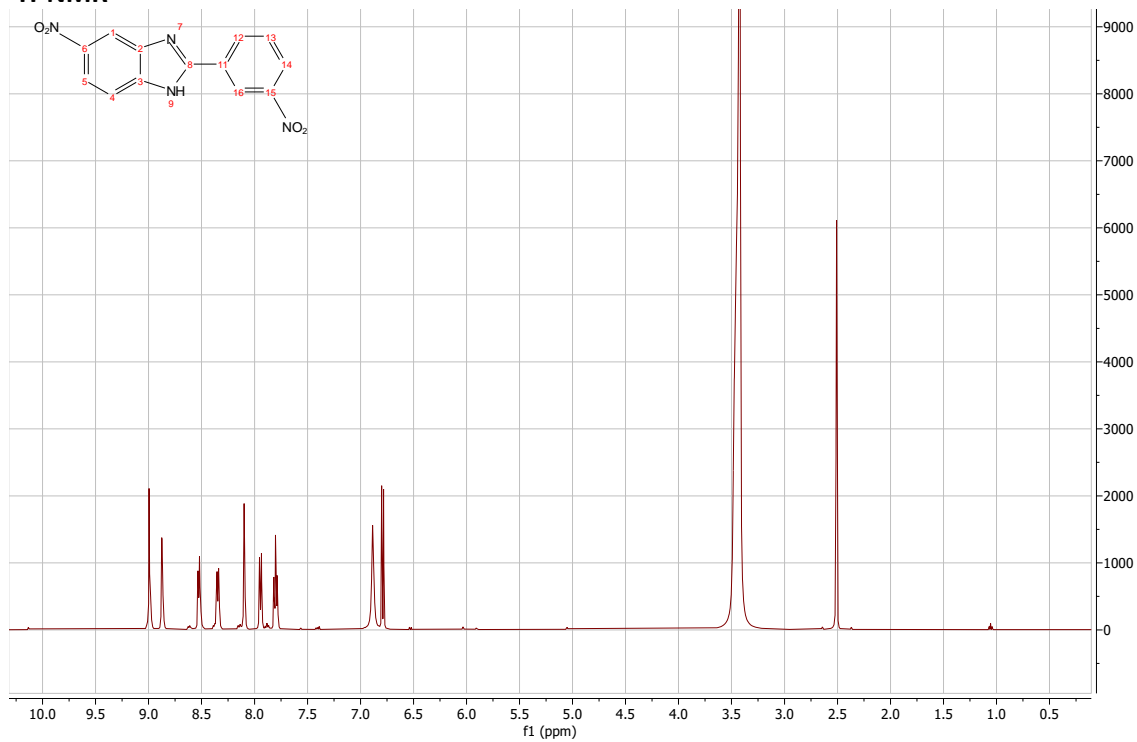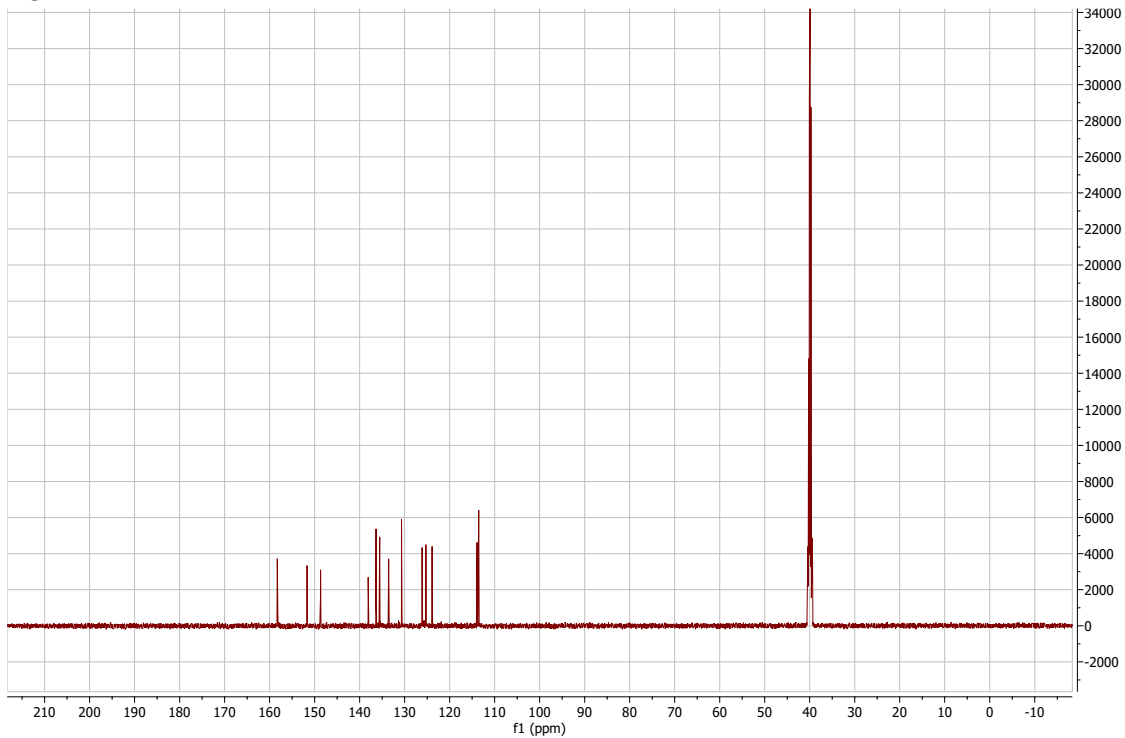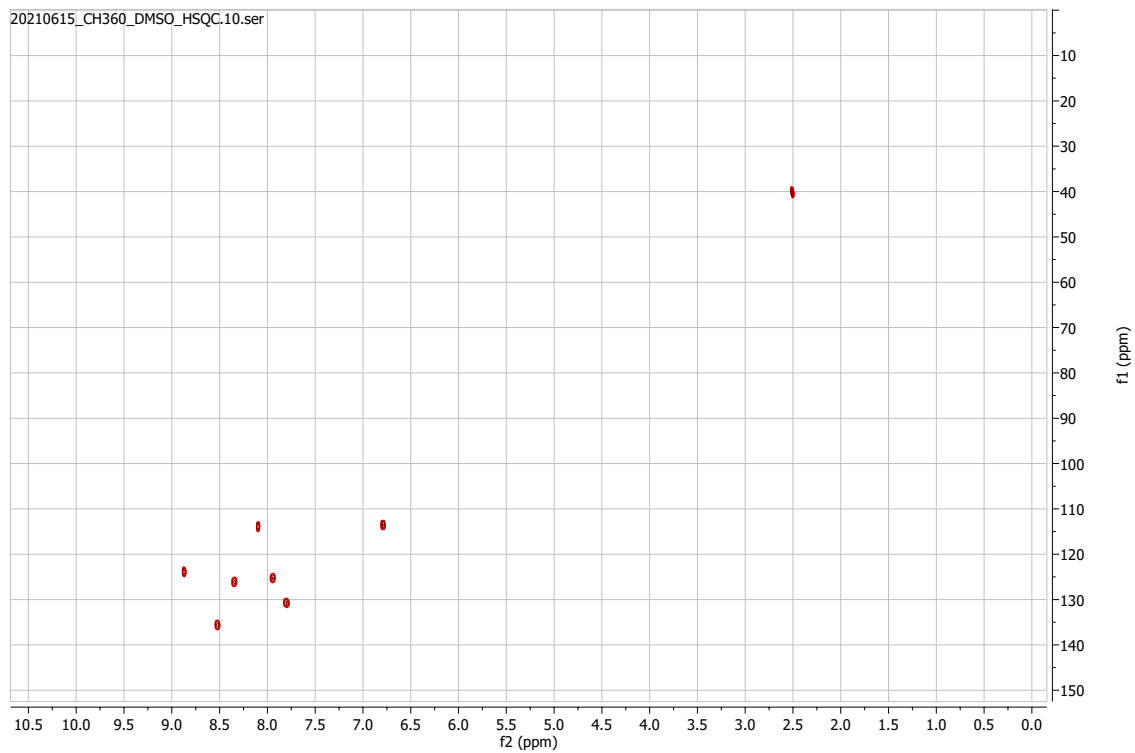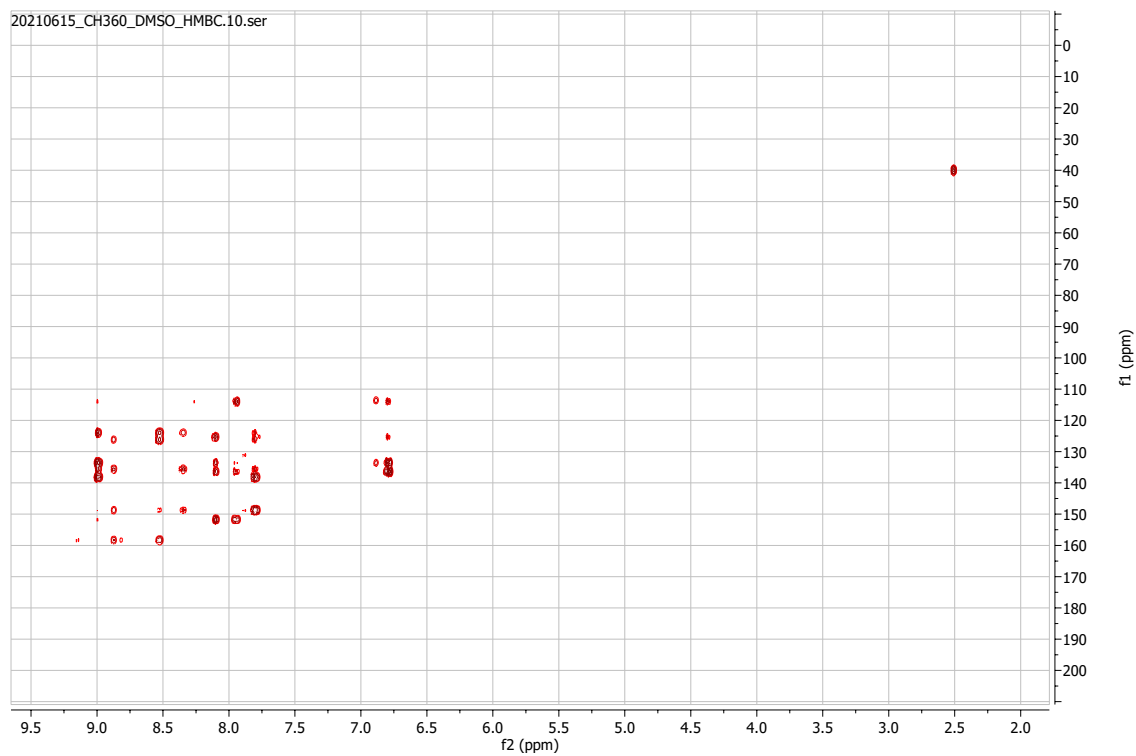
5-nitro-2-(1H-pyrrol-2-yl)-1H-1,3-benzodiazole:
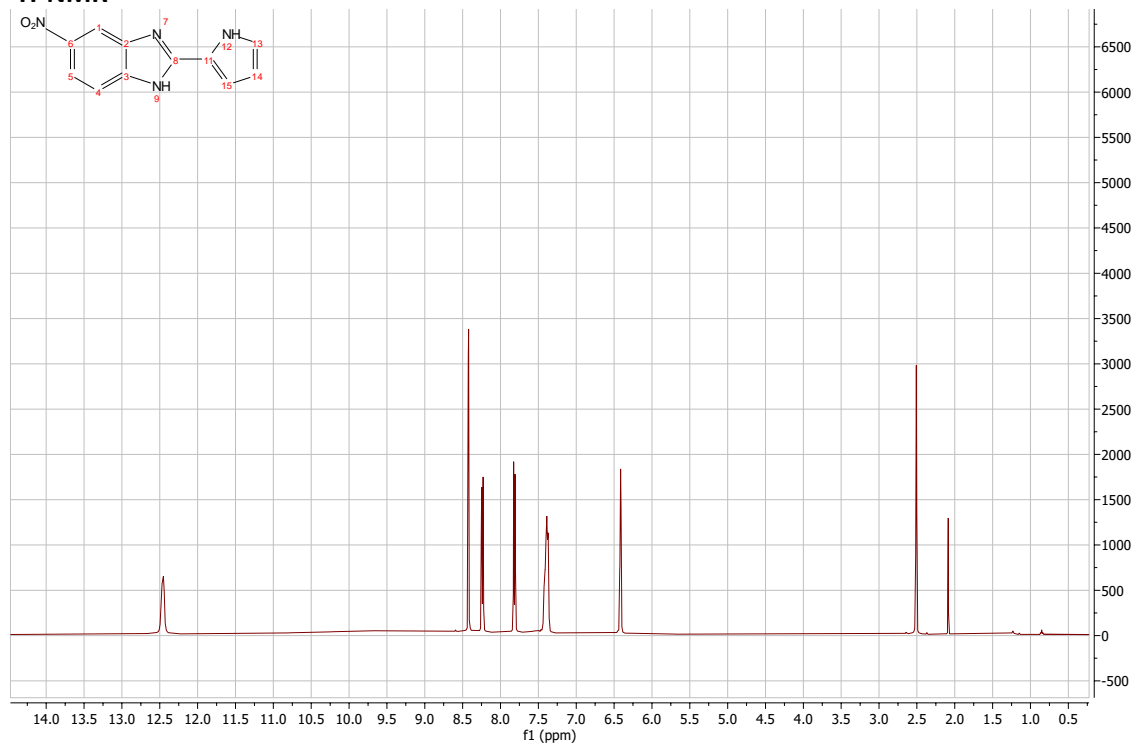
¹H-NMR
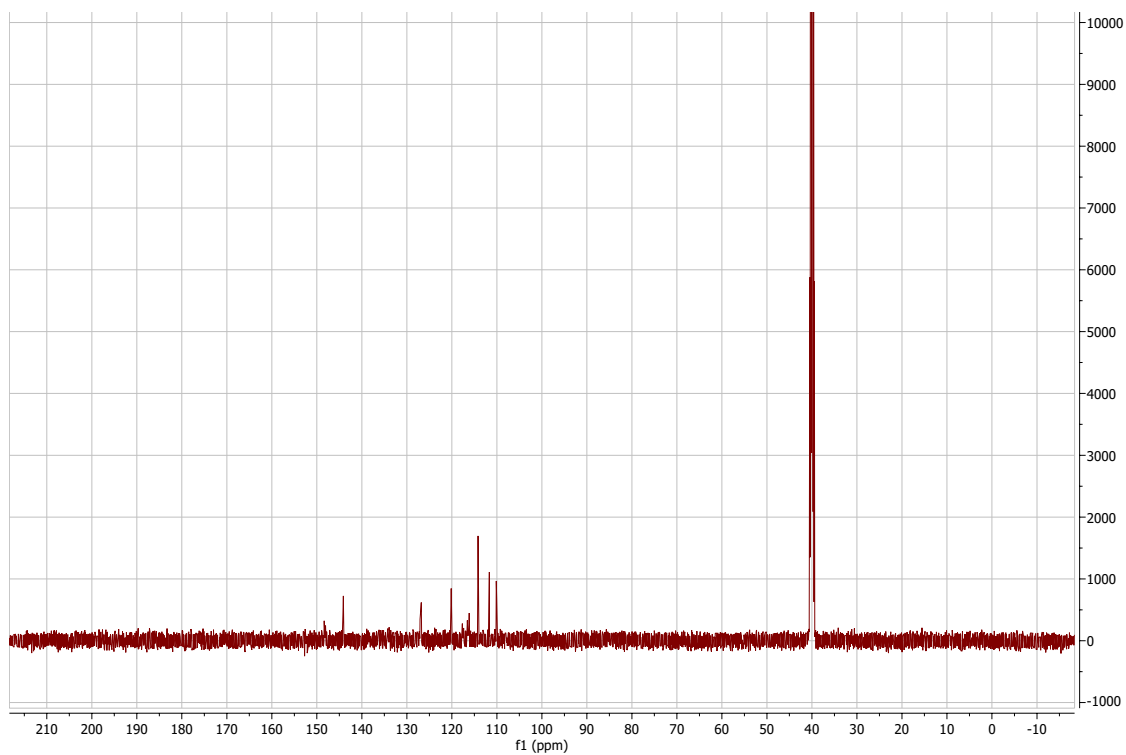
¹³C-NMR

¹³C-NMR

2-(4-bromophenyl)-1H-1,3-benzodiazole-5-carboxylic acid:
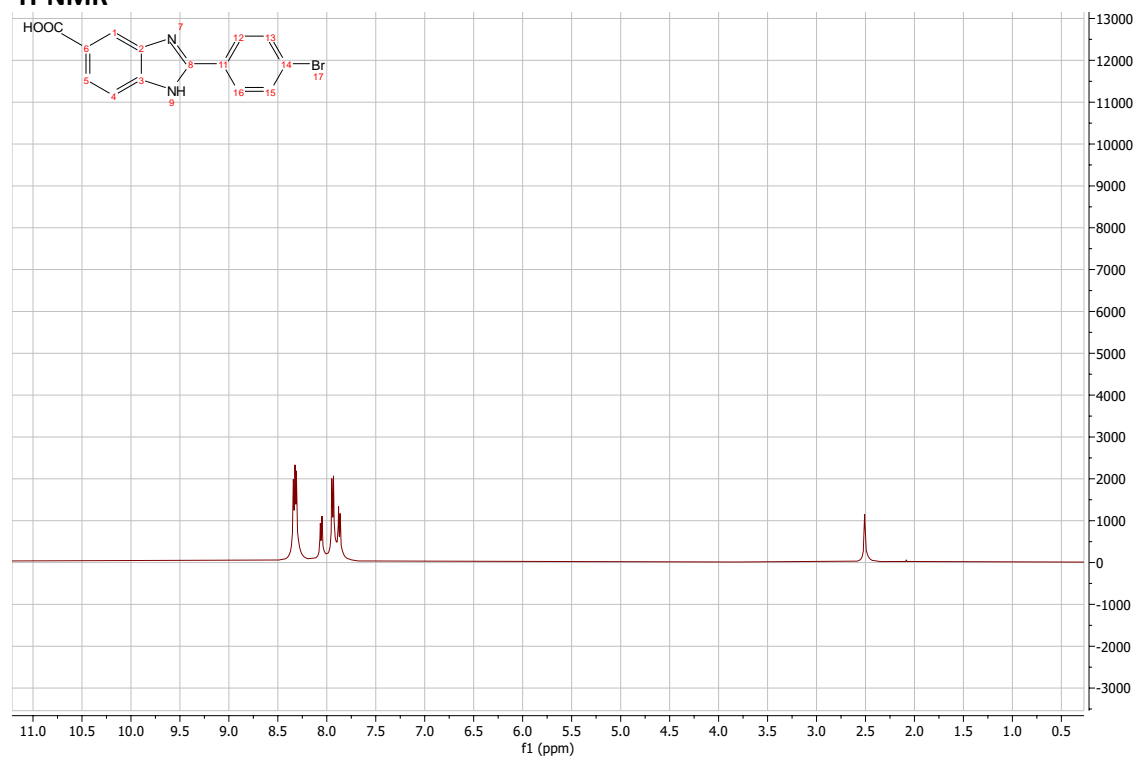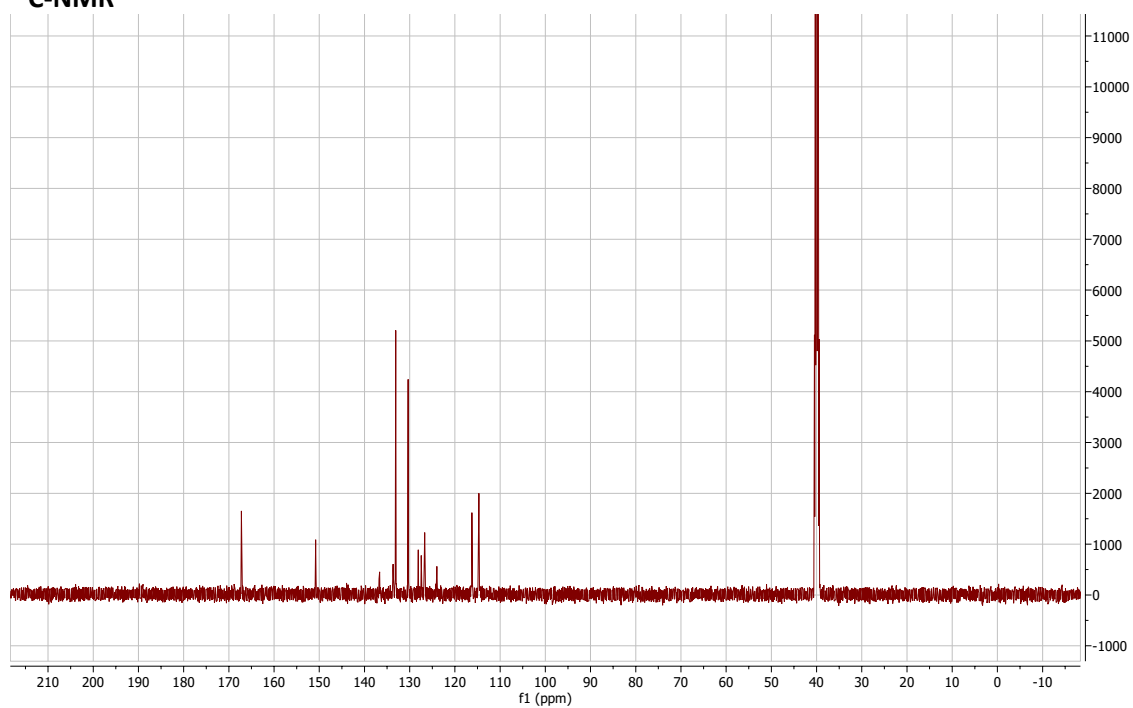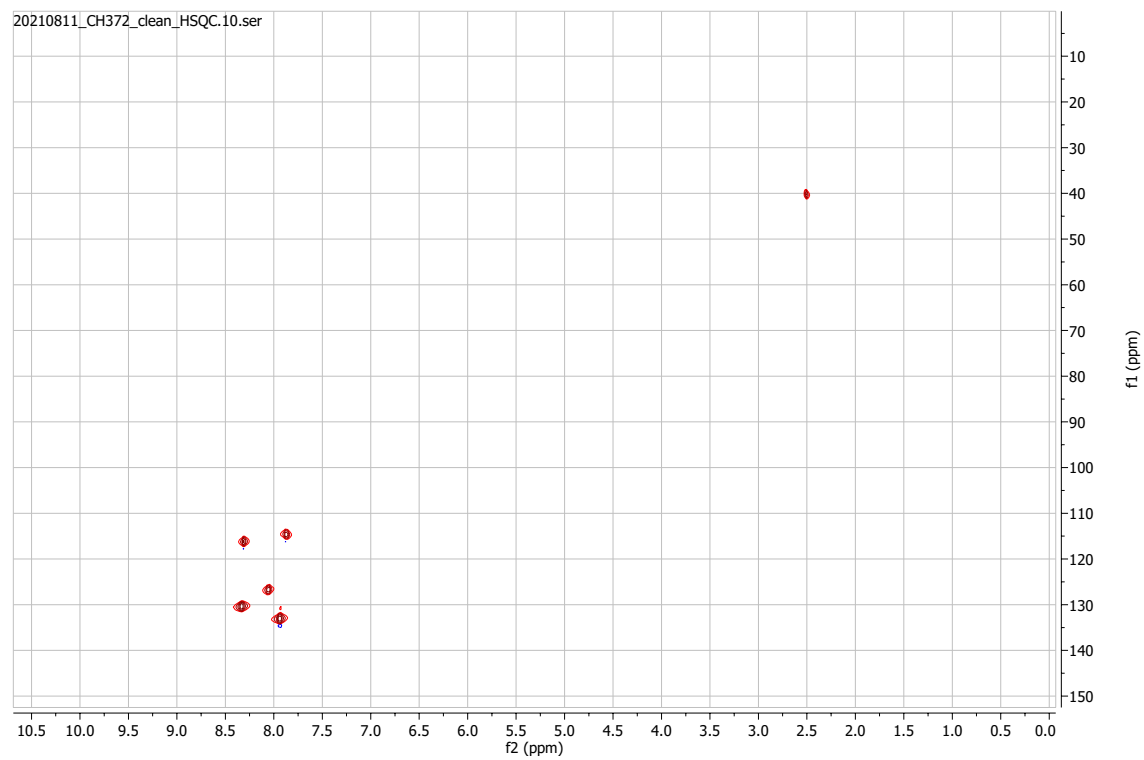
¹H-NMR
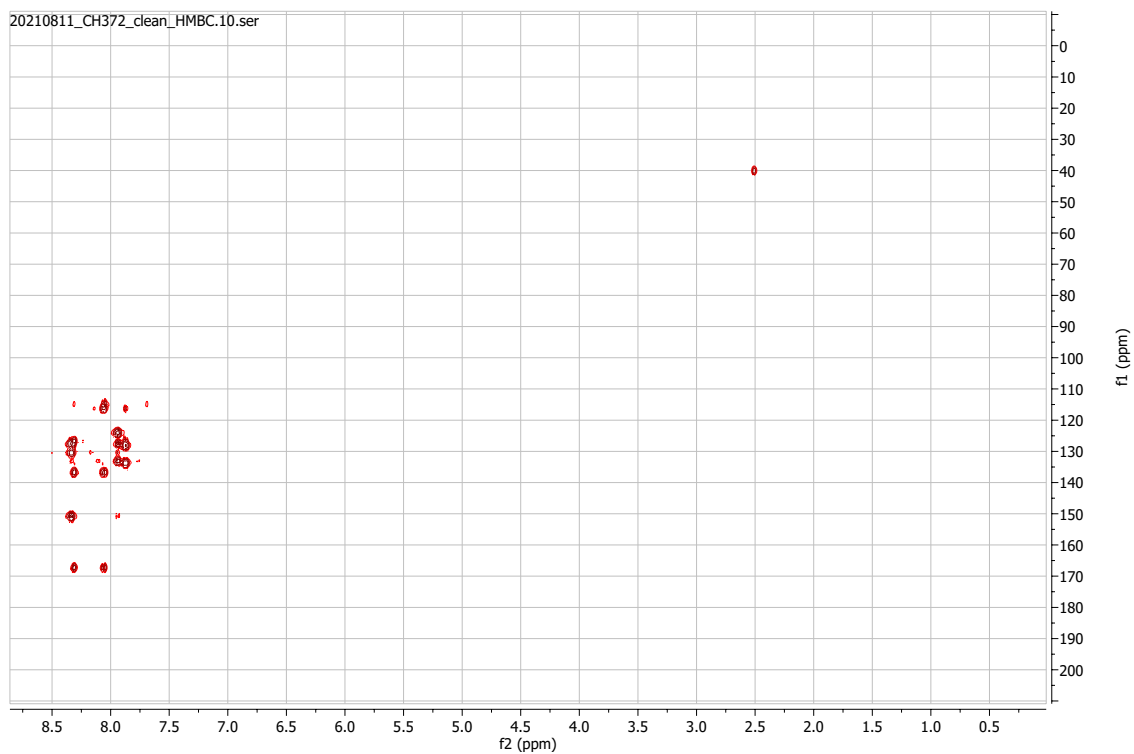
¹³C-NMR

HSQC

HMBC

2-(4-chlorophenyl)-1H-1,3-benzodiazole-5-carboxylic acid:
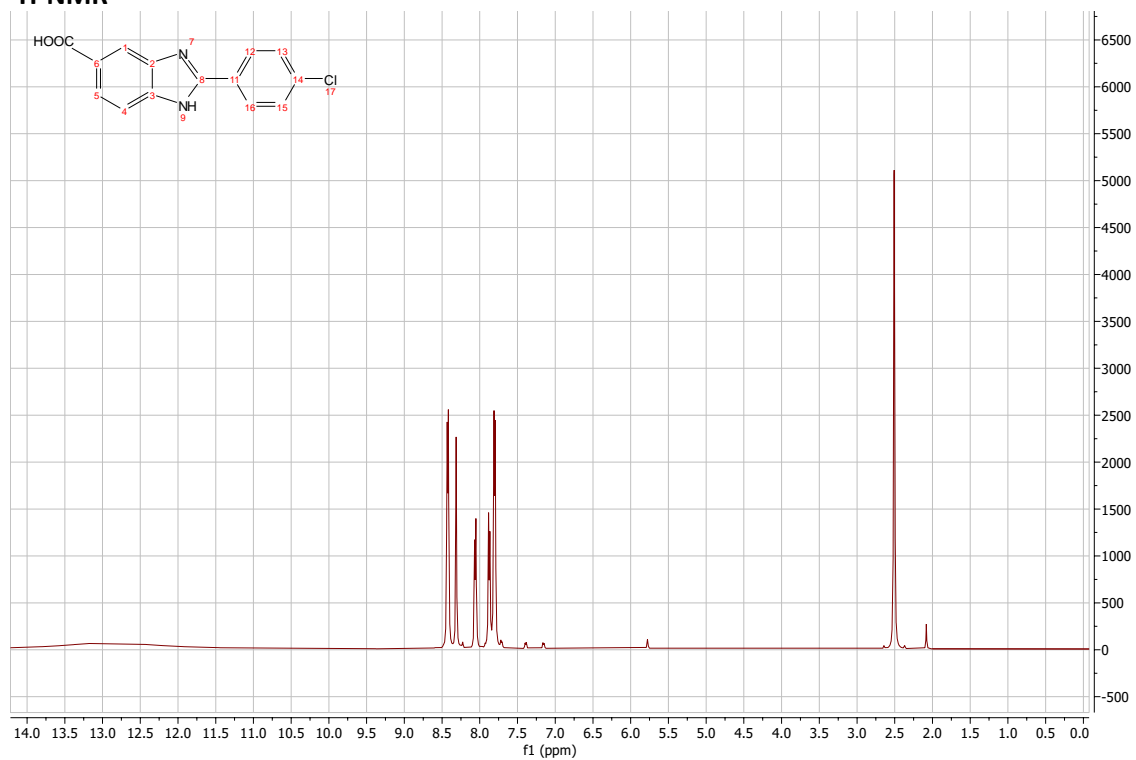
¹H-NMR

2-(4-hydroxyphenyl)-1H-1,3-benzodiazole-5-carboxylic acid:

^{1}H-NMR

^{13}C-NMR

HSQC

20210811_CH374_clean_HSQC.10.ser

HMBC

20210811_CH374_clean_HMBC.10.ser

340
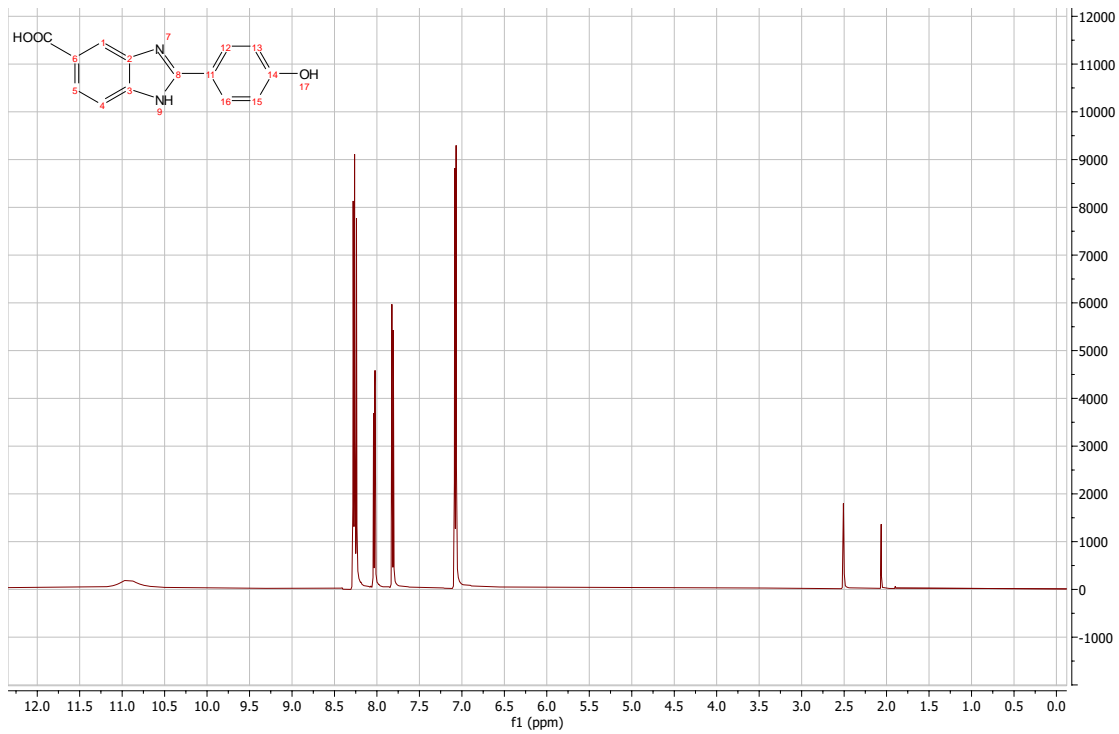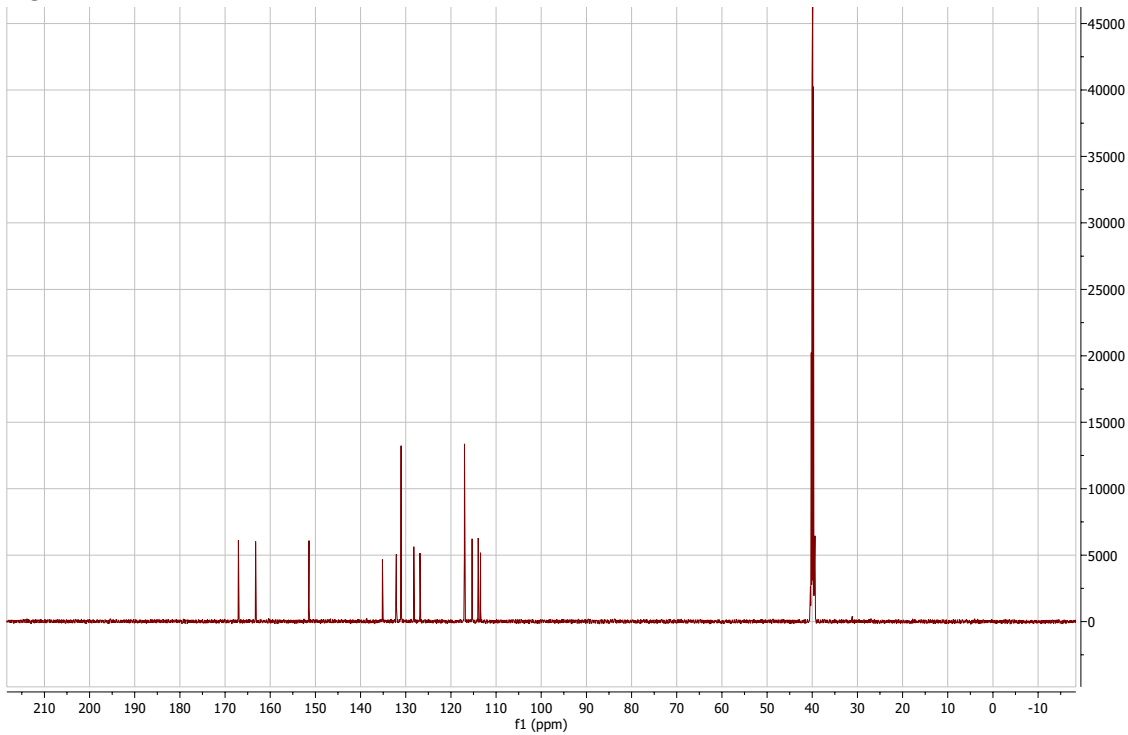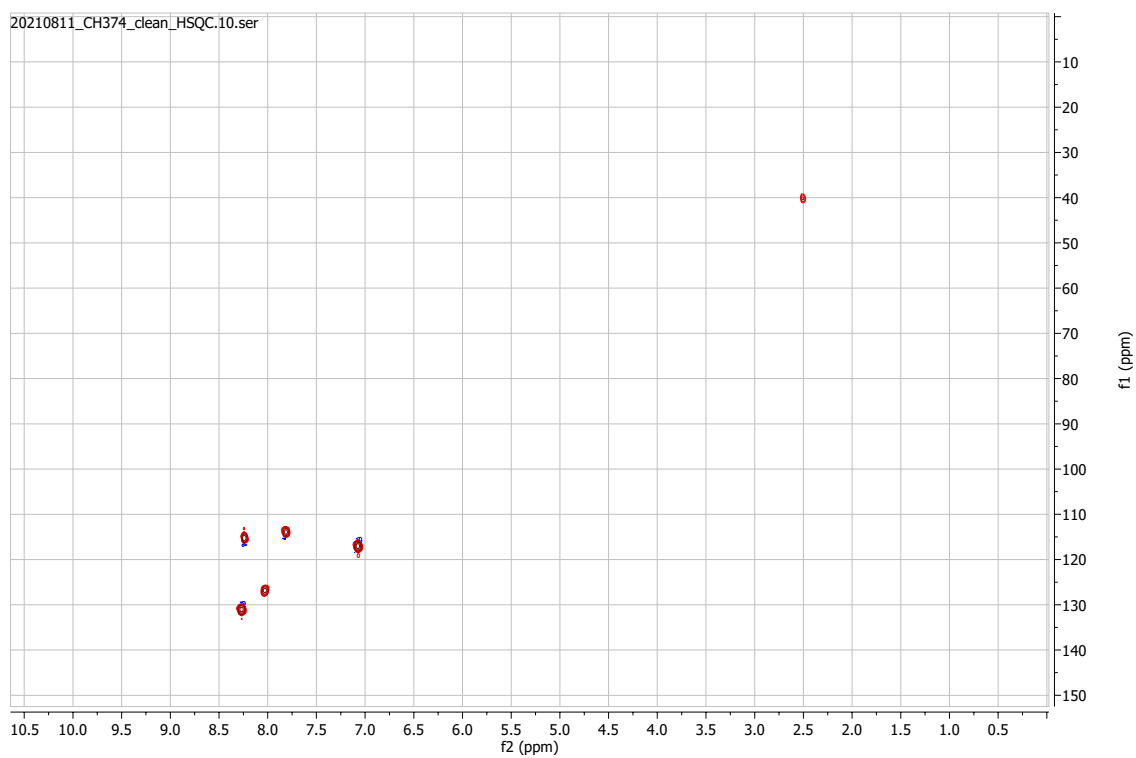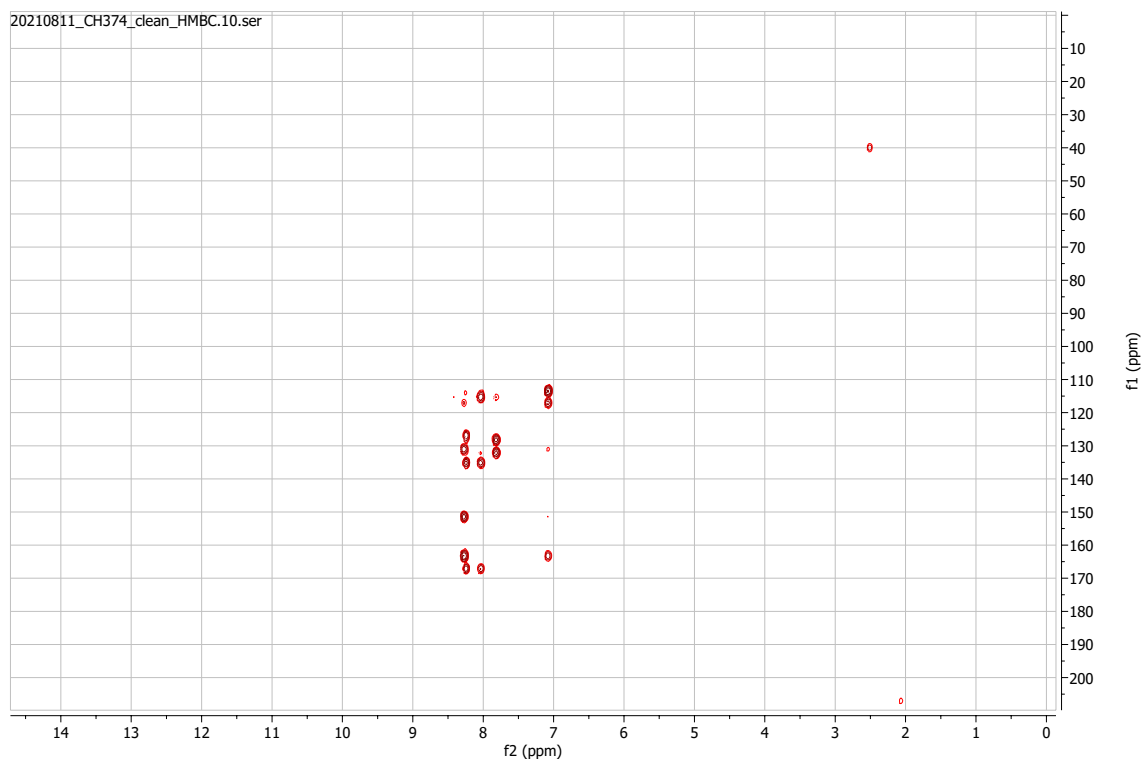
2-(4-fluorophenyl)-1H-1,3-benzodiazole-5-carboxylic acid:
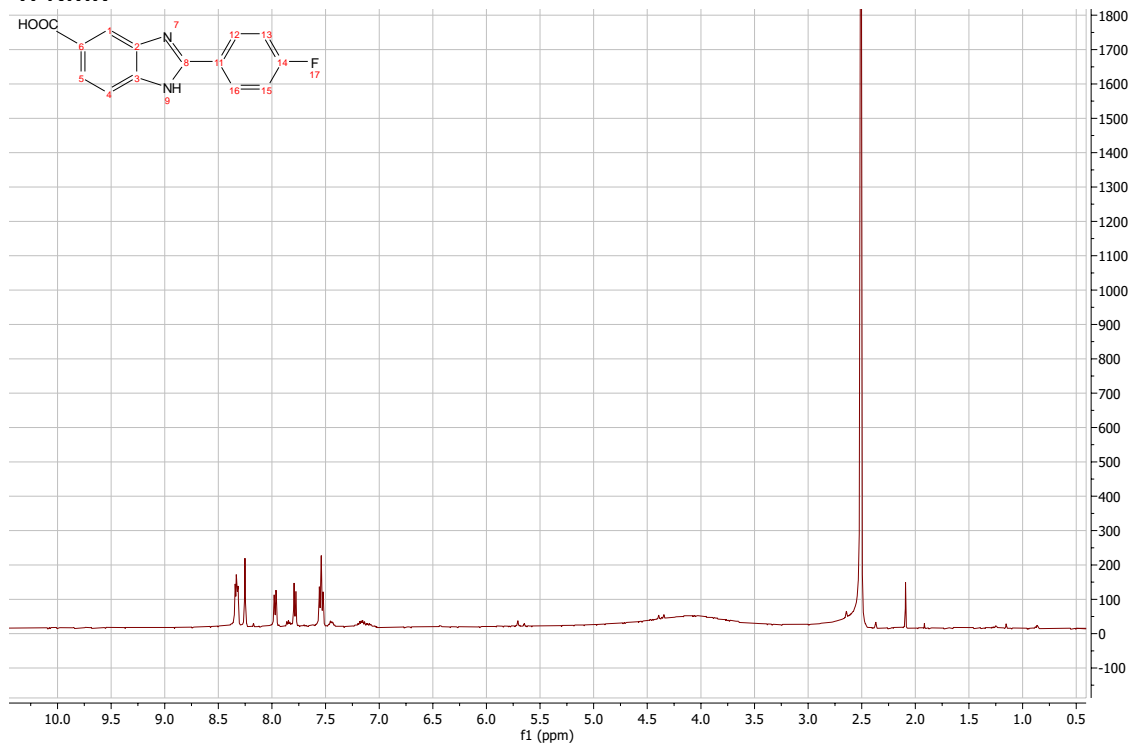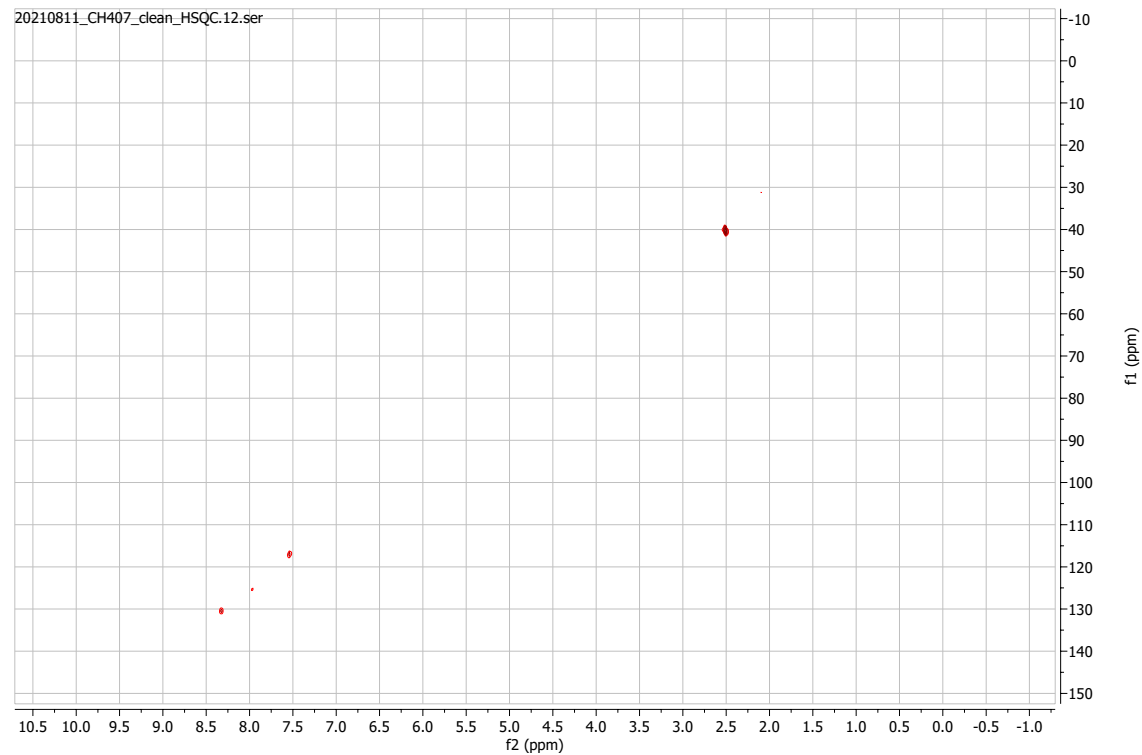
¹H-NMR

HSQC

2-(4-methoxyphenyl)-1H-1,3-benzodiazole-5-carboxylic acid:
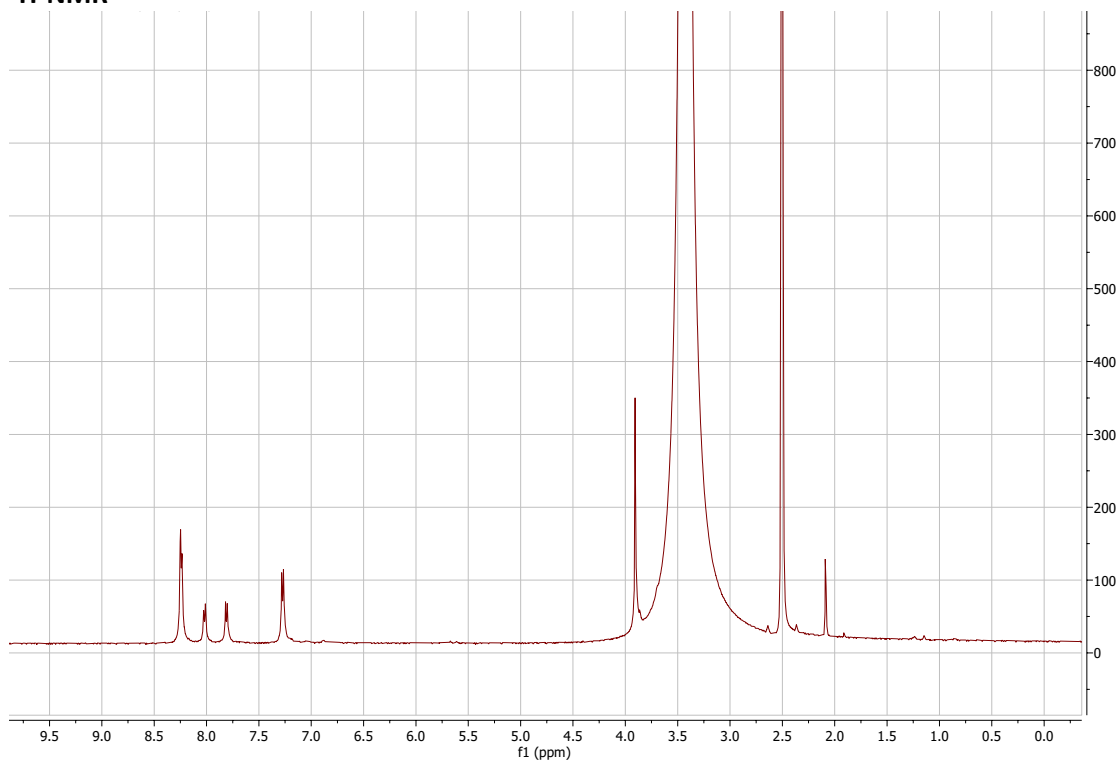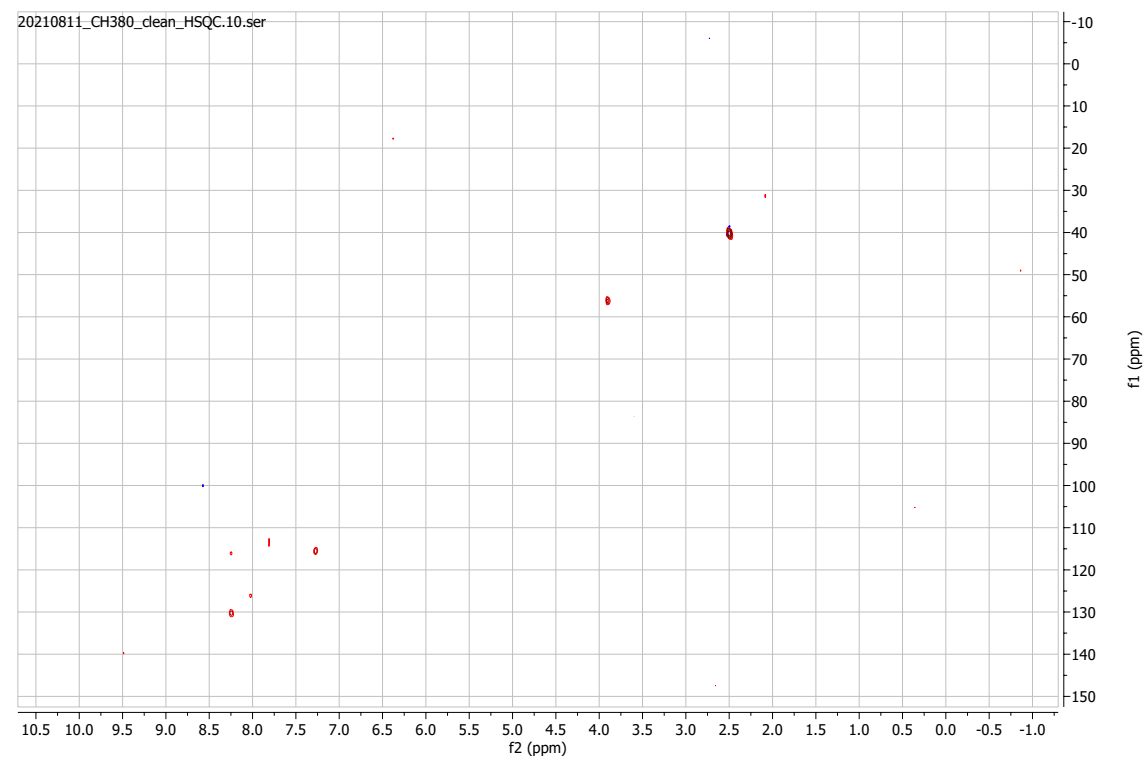
¹H-NMR

HSQC

2-(3-hydroxyphenyl)-1H-1,3-benzodiazole-5-carboxylic acid:
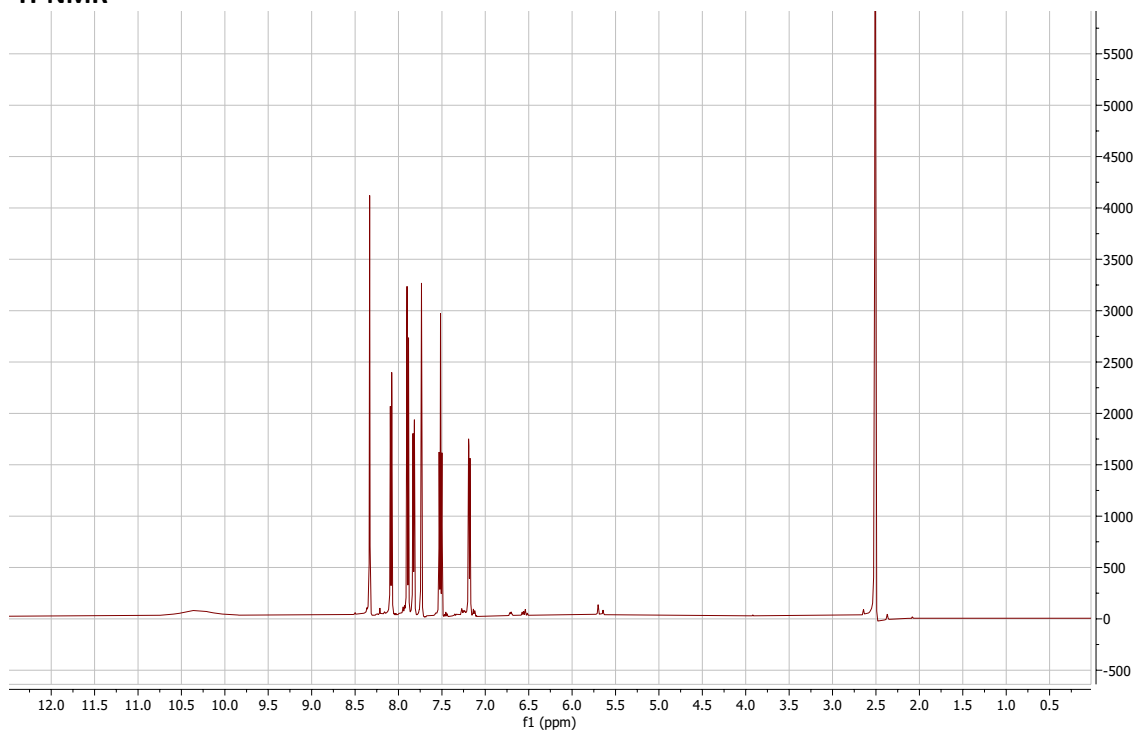
¹H-NMR

2-(3-ethoxy-4-hydroxyphenyl)-1H-1,3-benzodiazole-5-carboxylic acid:

¹H-NMR

¹³C-NMR

¹³C-NMR

HSQC

20211020_CH408_clean2_HSQC.10.ser
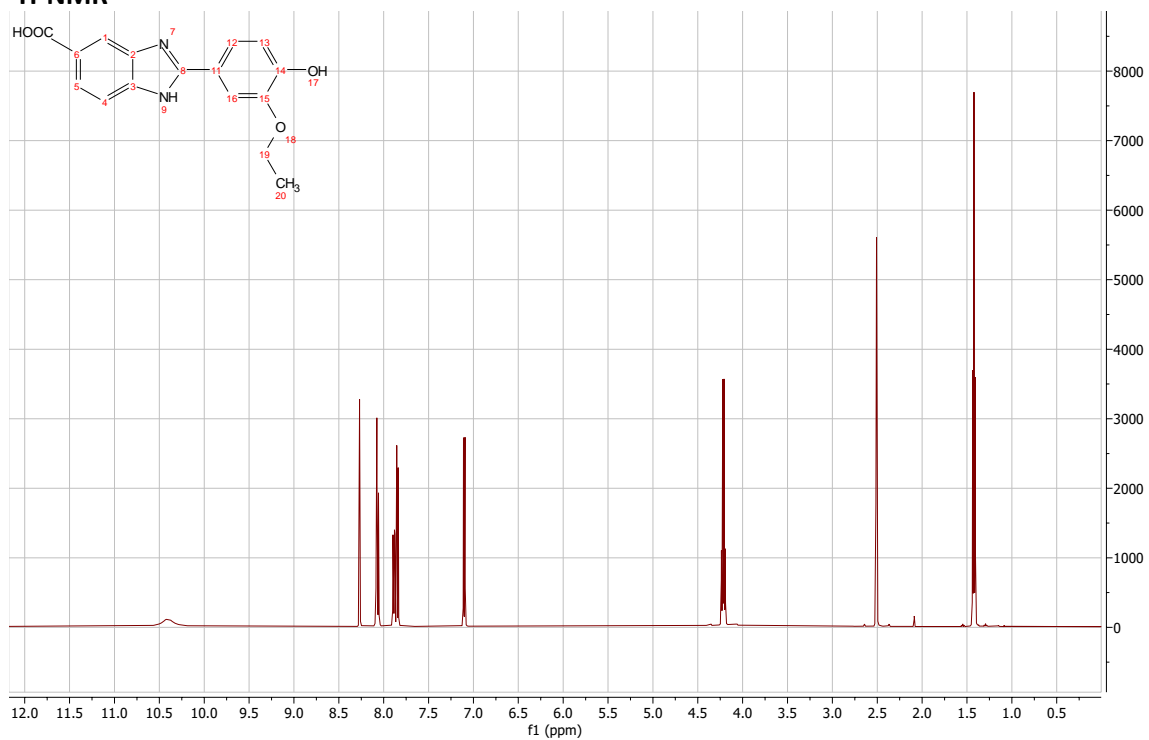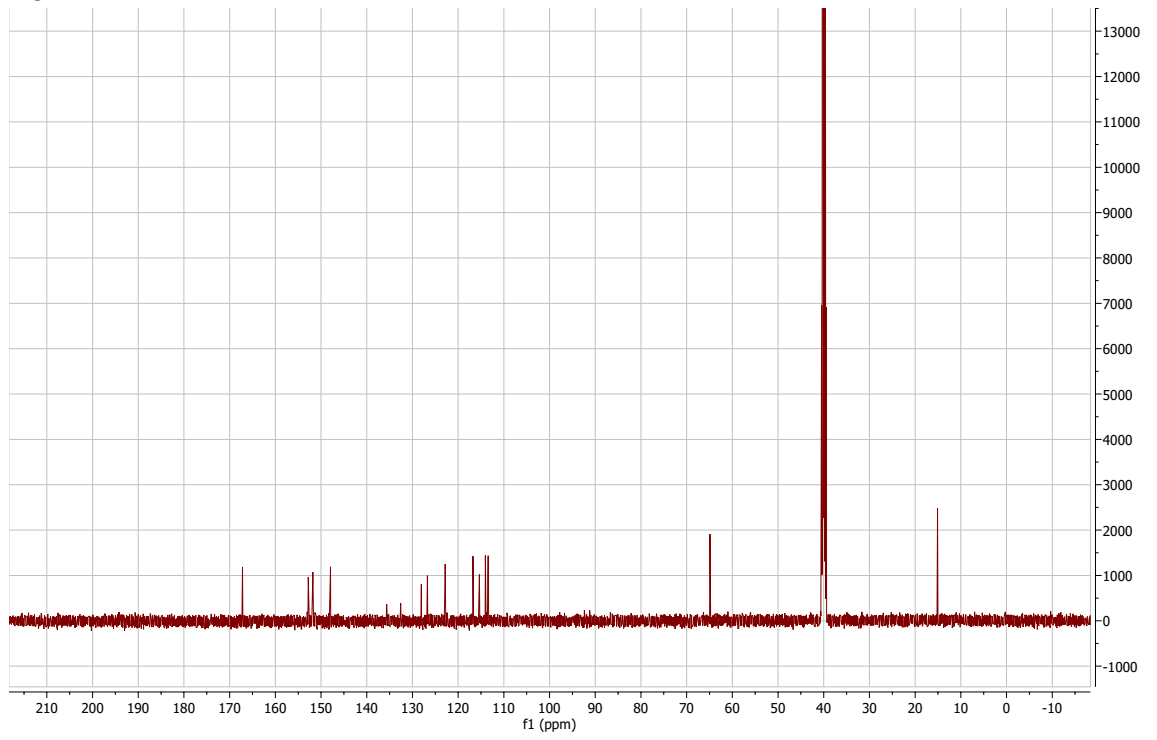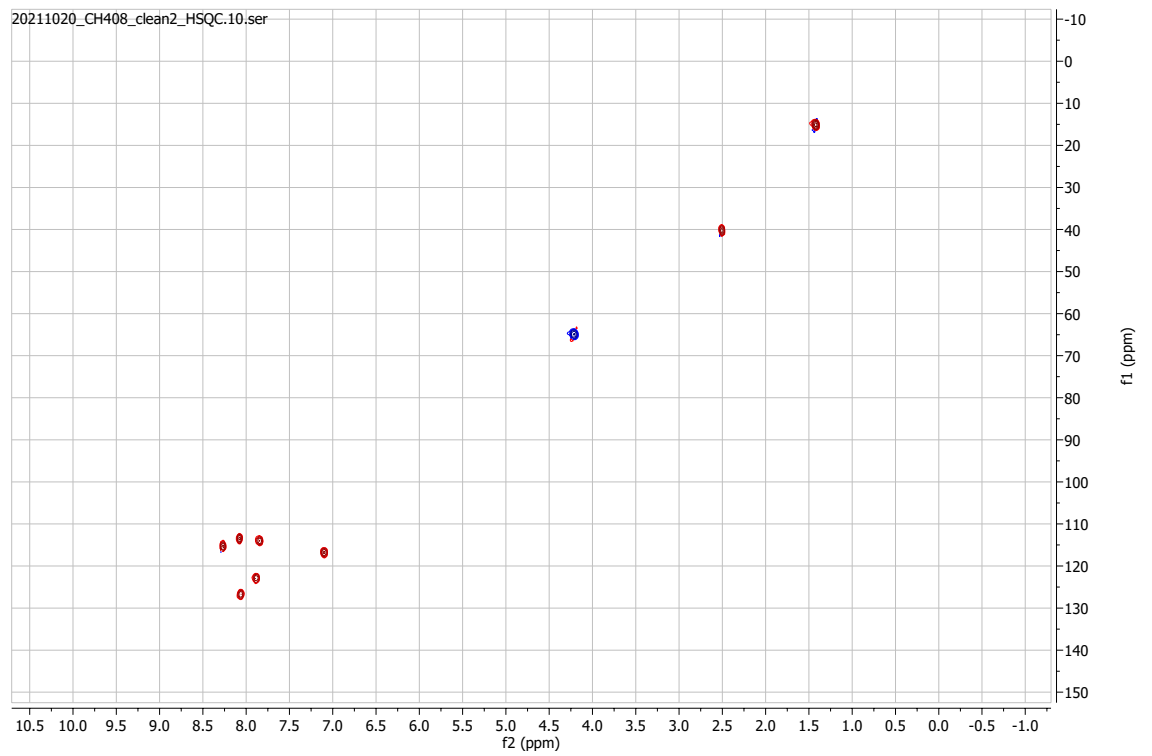
HMBC

20211020_CH408_clean2_HMBC.10.ser
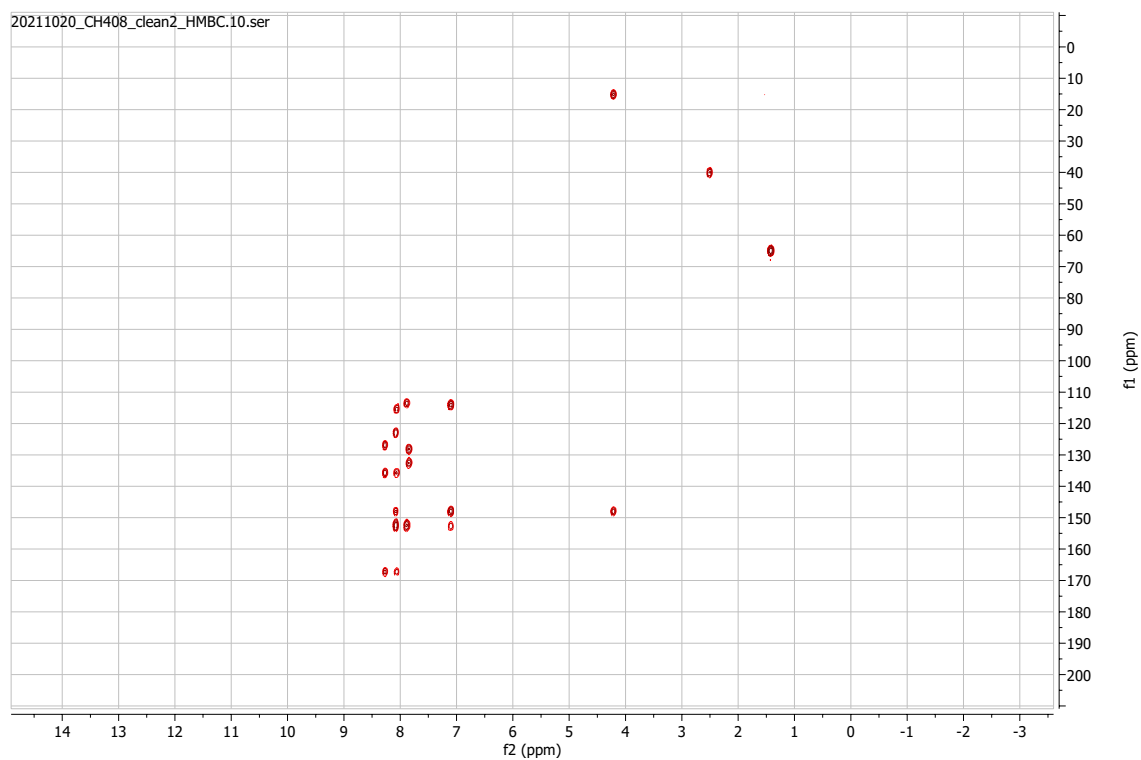
2-(2-nitrophenyl)-1H-1,3-benzodiazole-5-carboxylic acid:
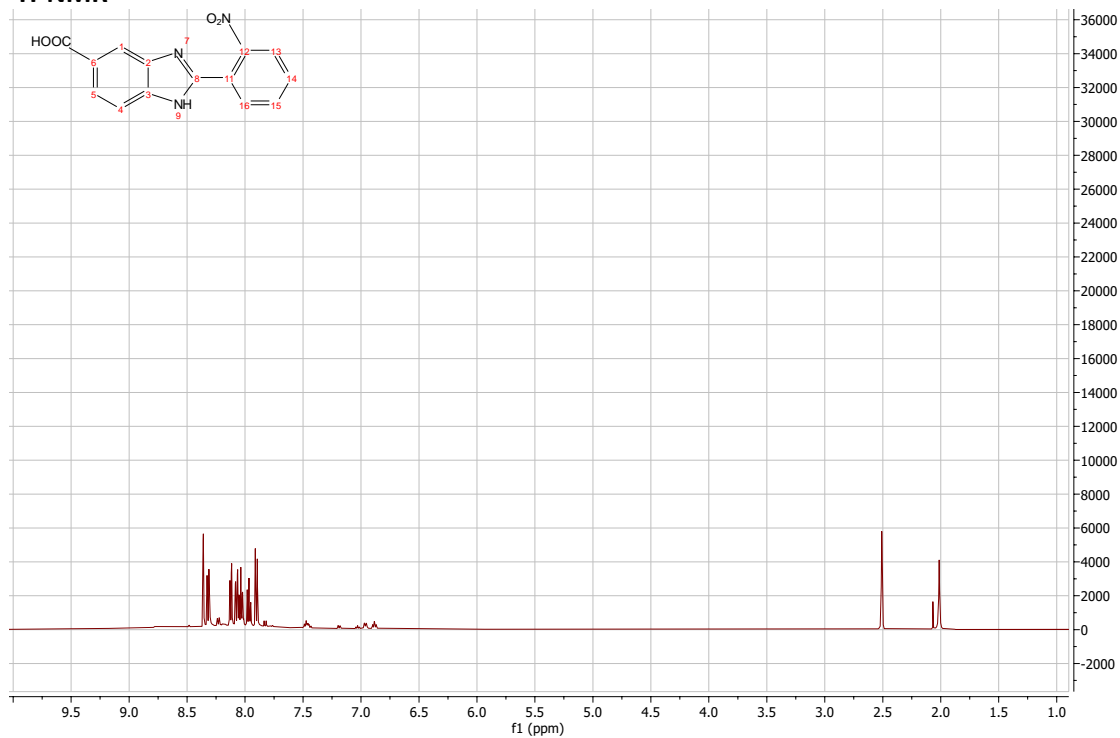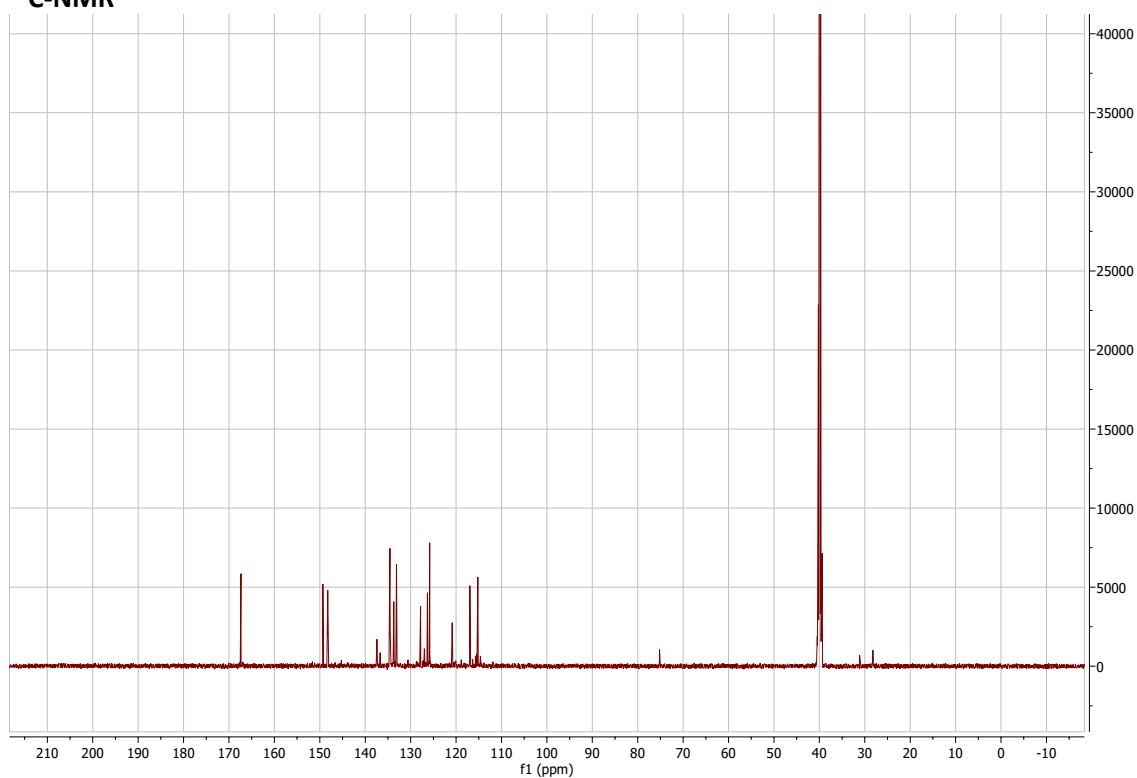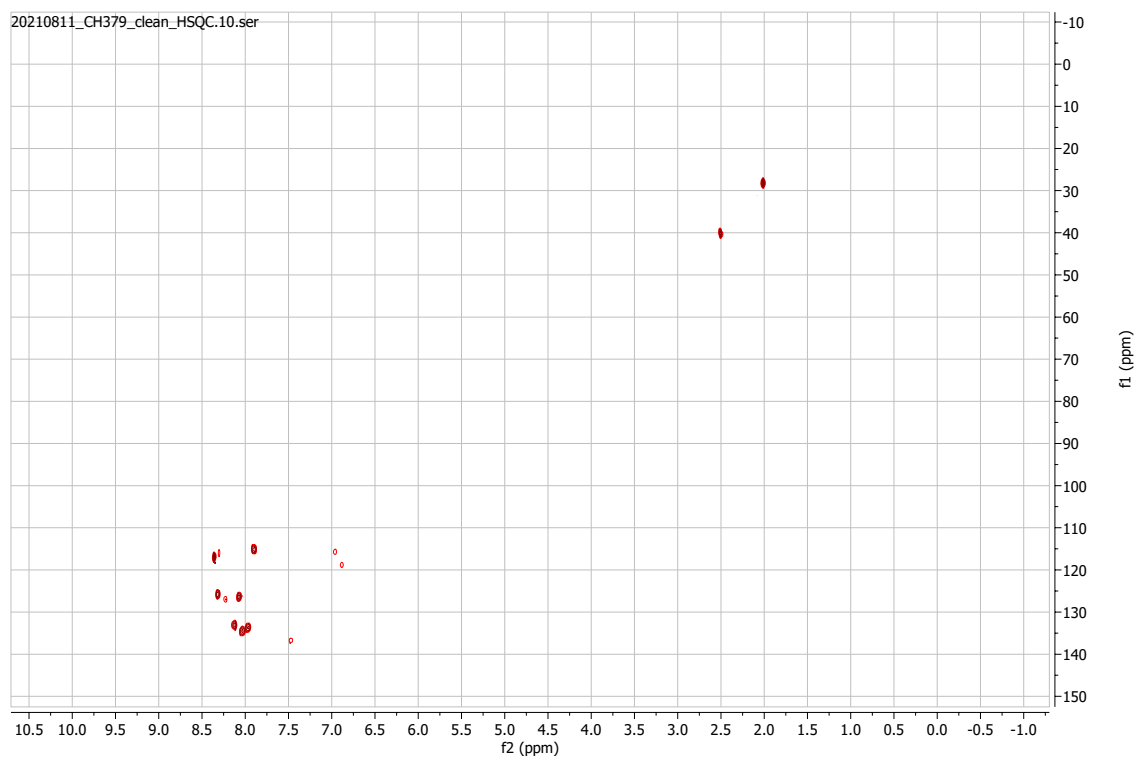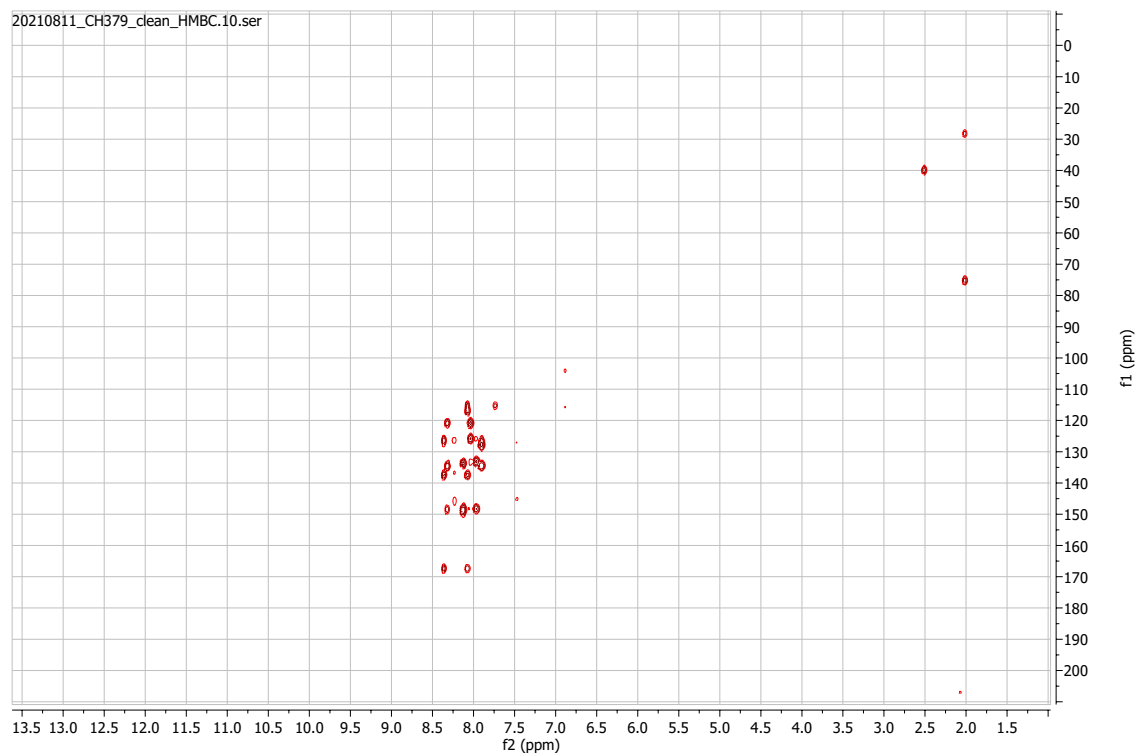
¹H-NMR

^{13}C-NMR

HSQC

20210811_CH379_clean_HSQC.10.ser

HMBC

20210811_CH379_clean_HMBC.10.ser

2-(3-nitrophenyl)-1H-1,3-benzodiazole-5-carboxylic acid:

¹H-NMR

¹³C-NMR

HSQC

20211004_CH413_HSCQ.10.ser

HMBC

20211004_CH413_HMBC.10.ser

2-(thiophen-2-yl)-1H-1,3-benzodiazole-5-carboxylic acid:

¹H-NMR

13C-NMR

HSQC

20210811_CH392_clean_HSQC.10.ser

HMBC

20210811_CH392_clean_HMBC.10.ser
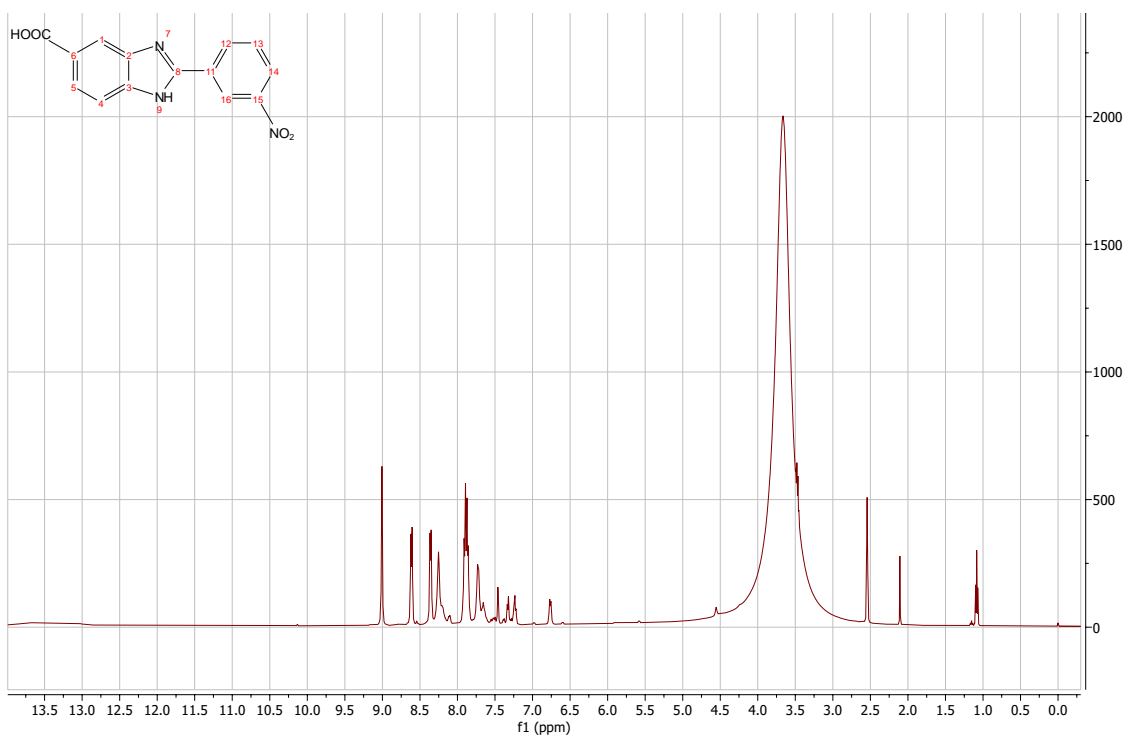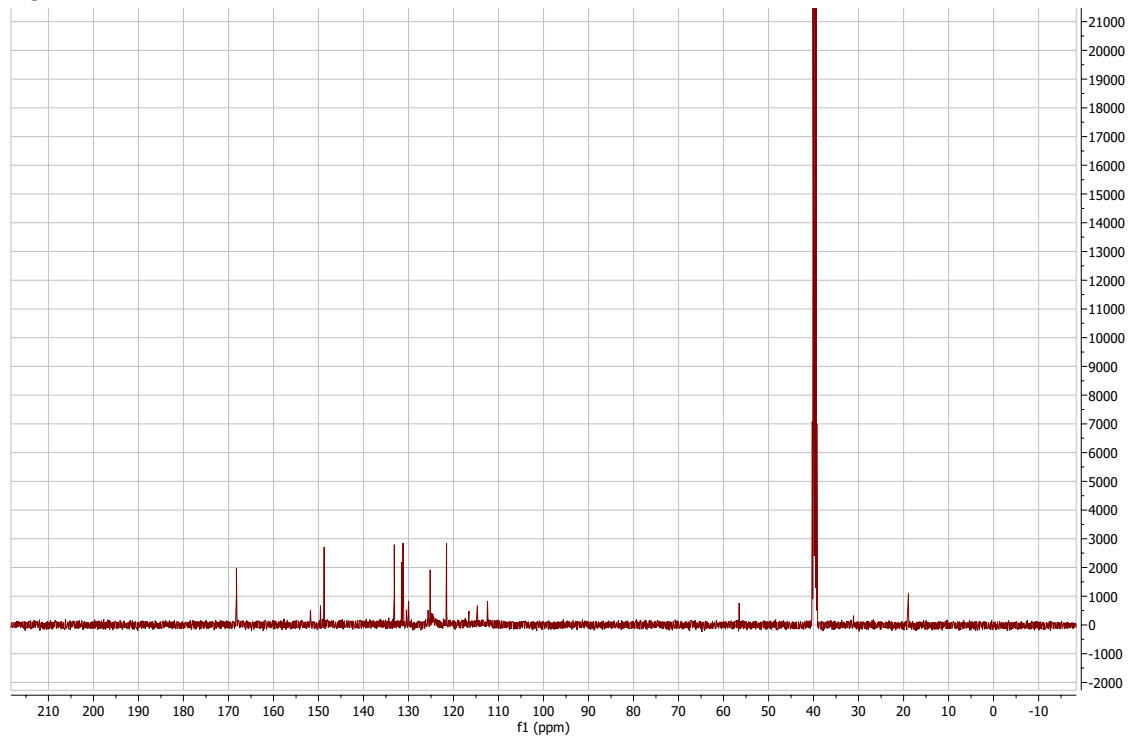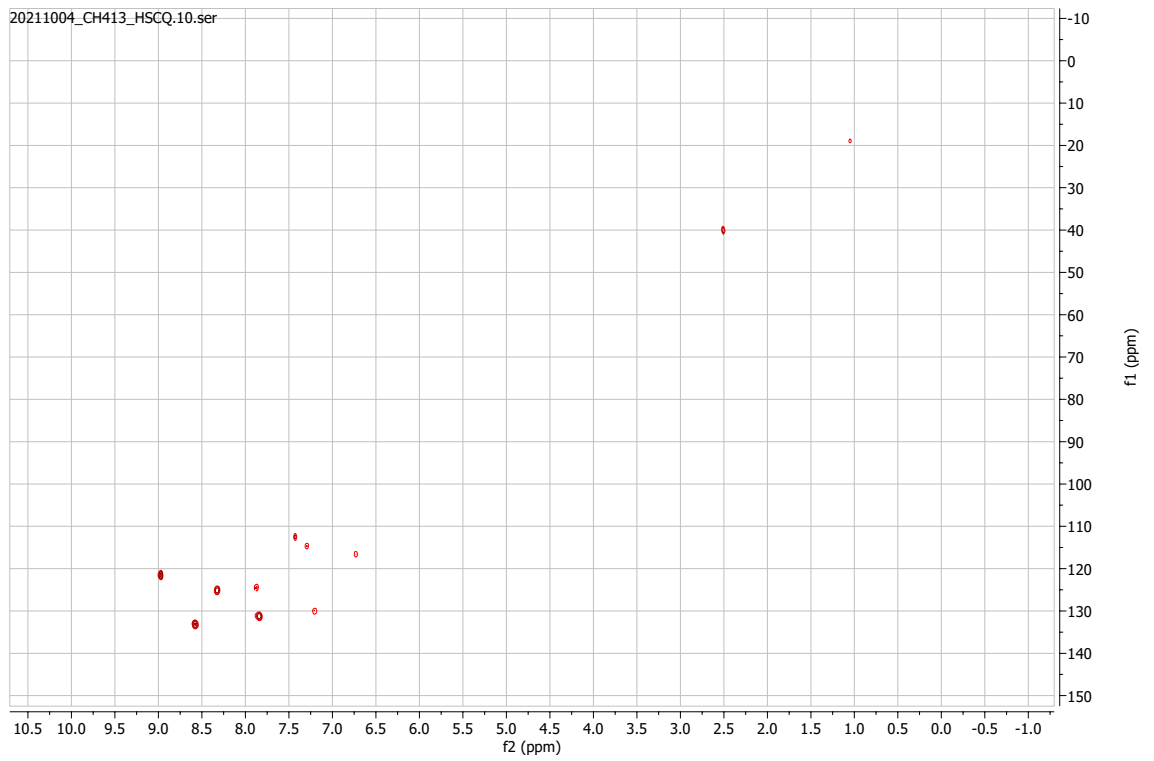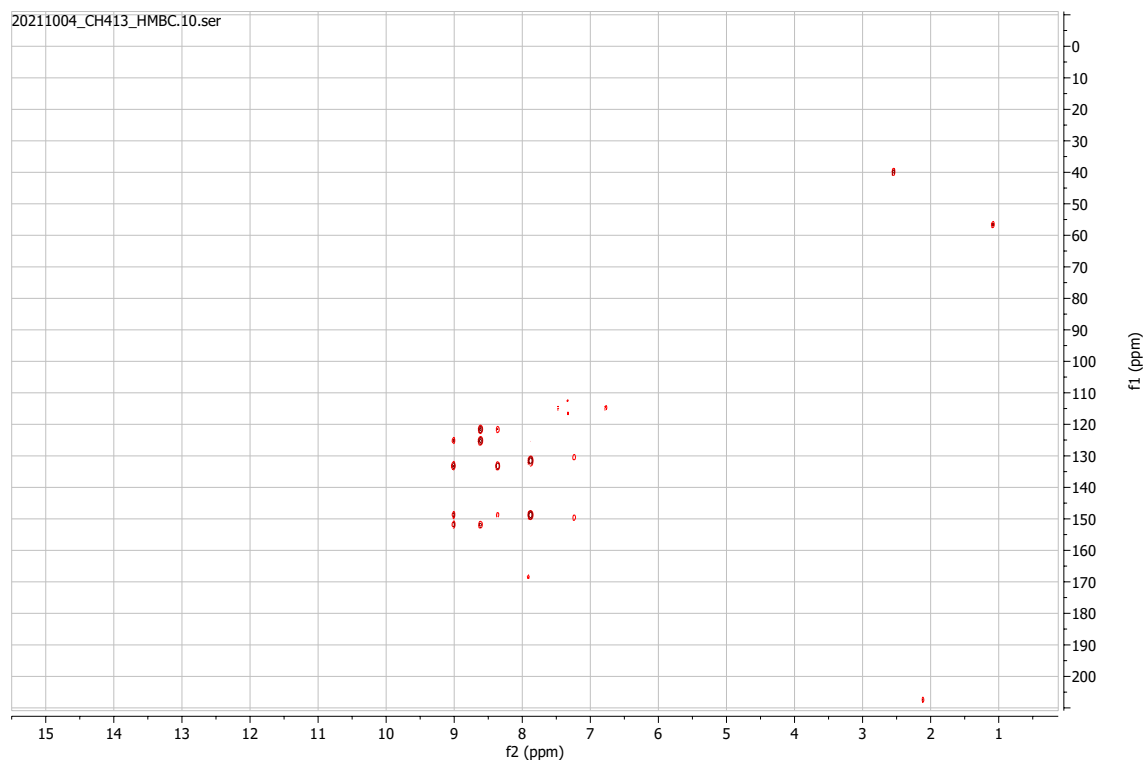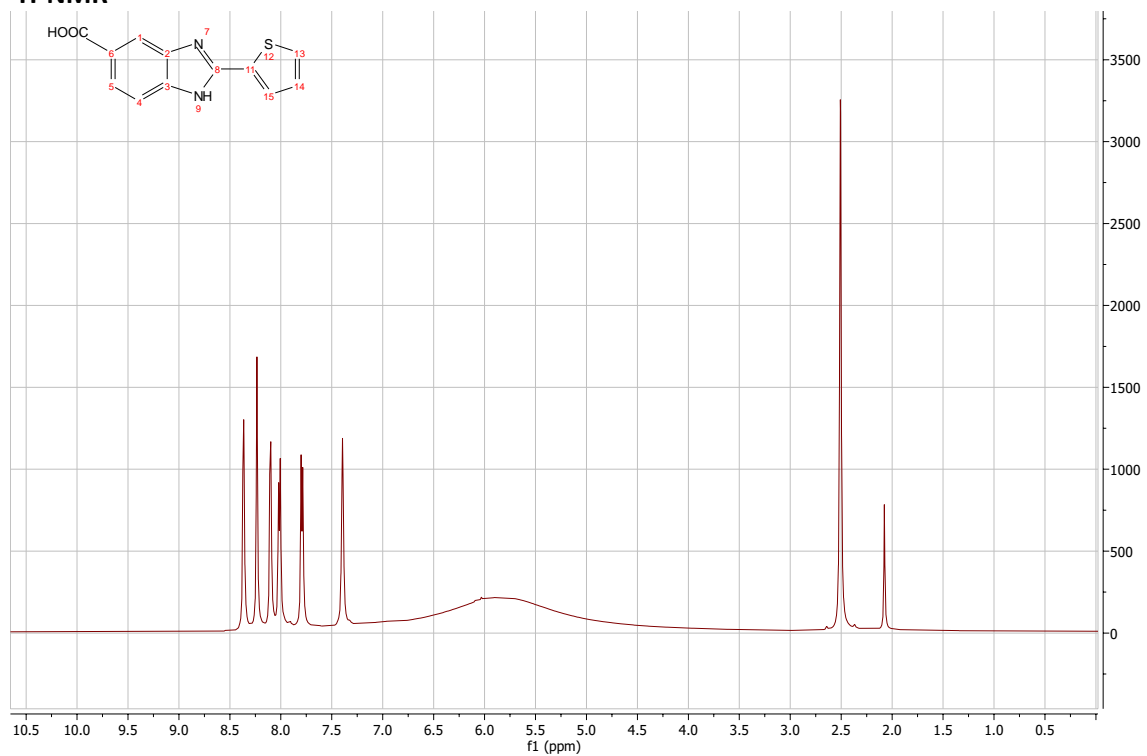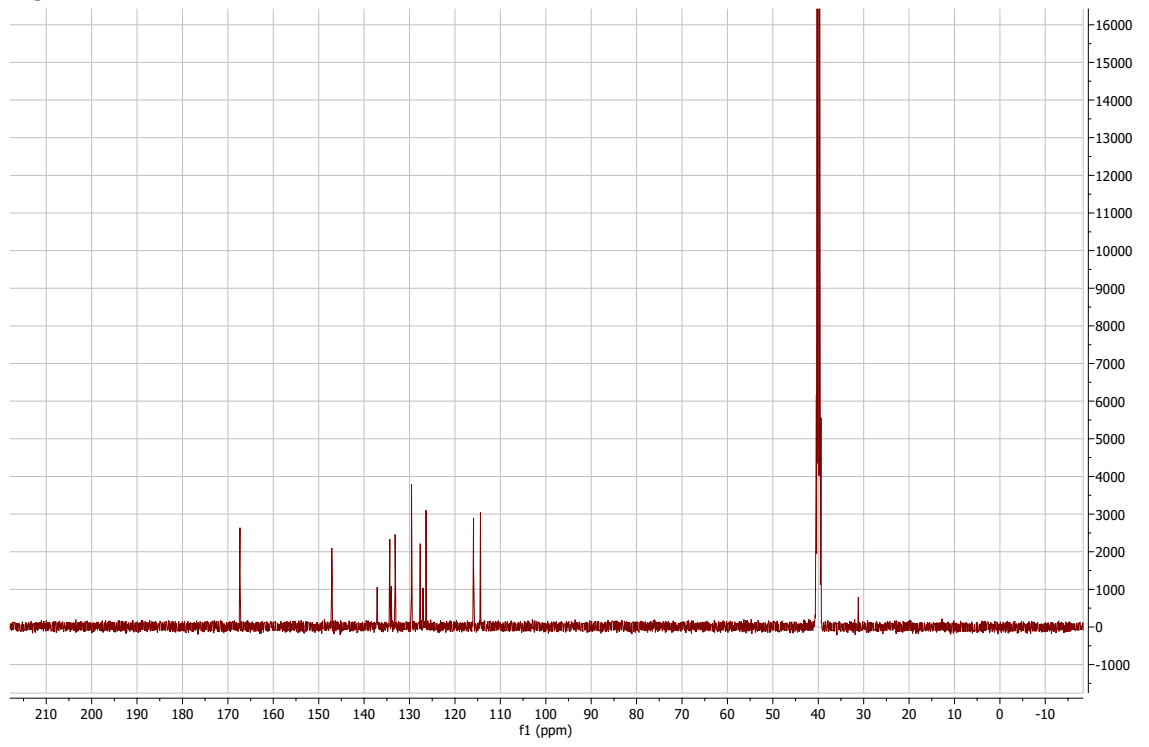
2-(1H-pyrrol-2-yl)-1H-1,3-benzodiazole-5-carboxylic acid:
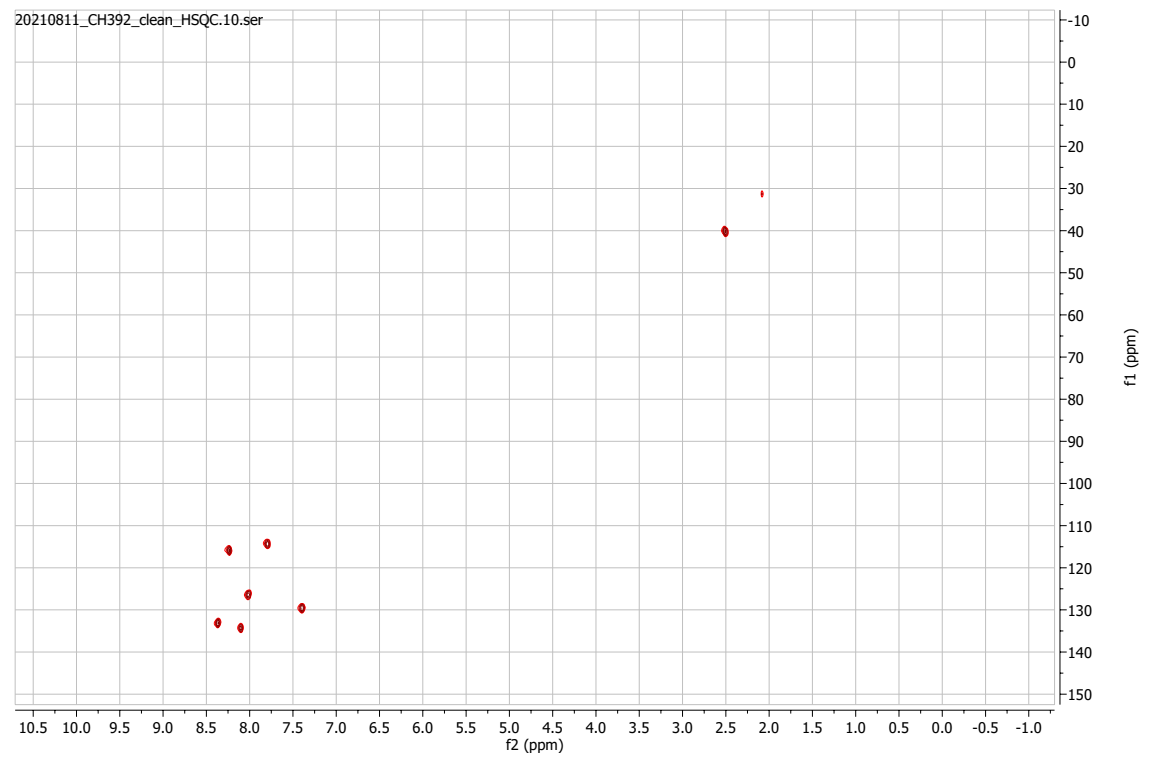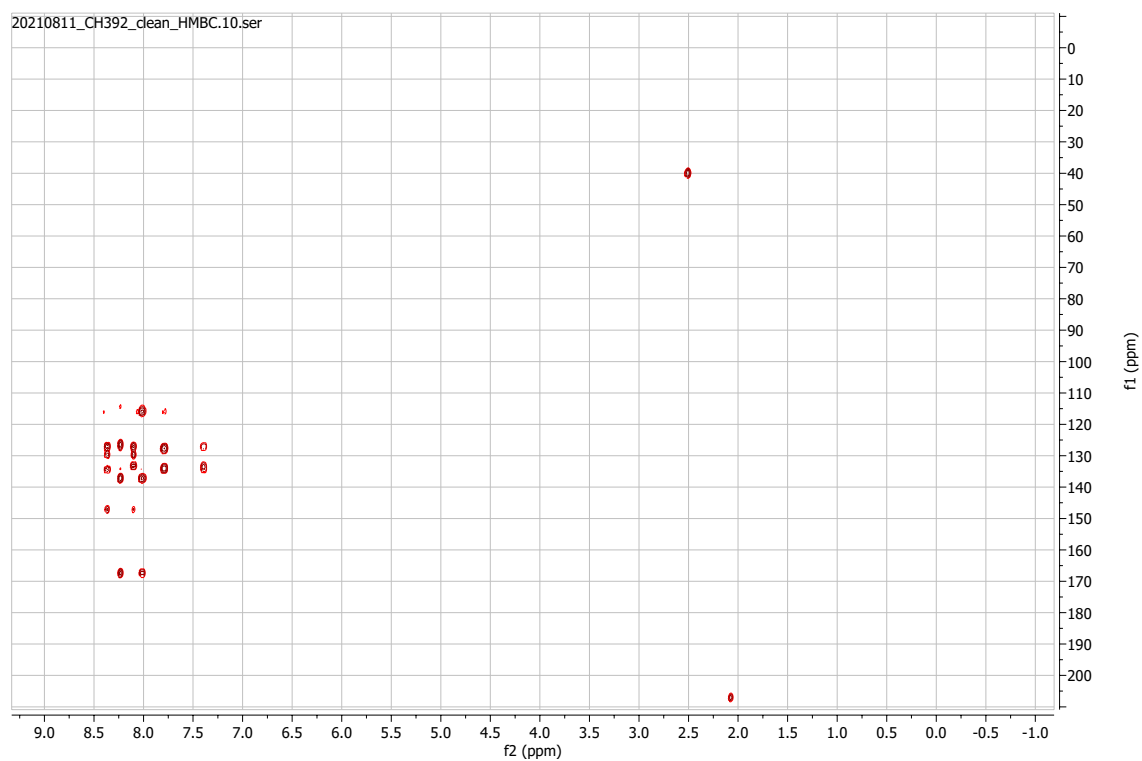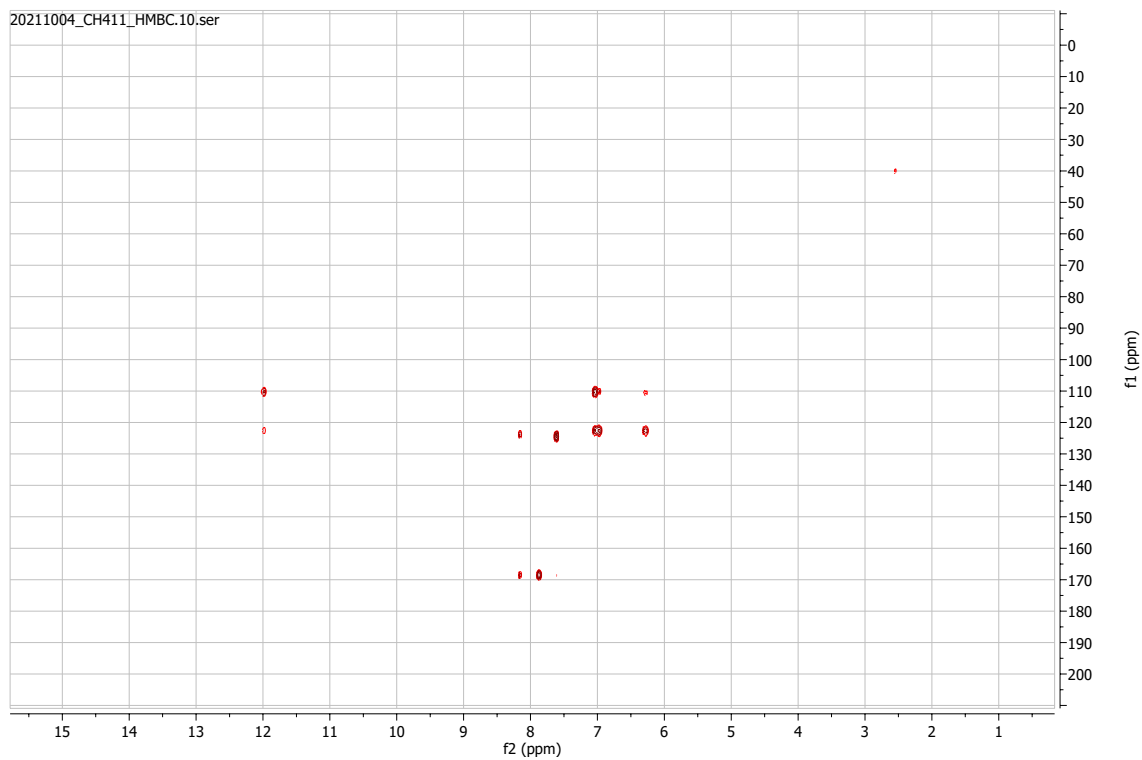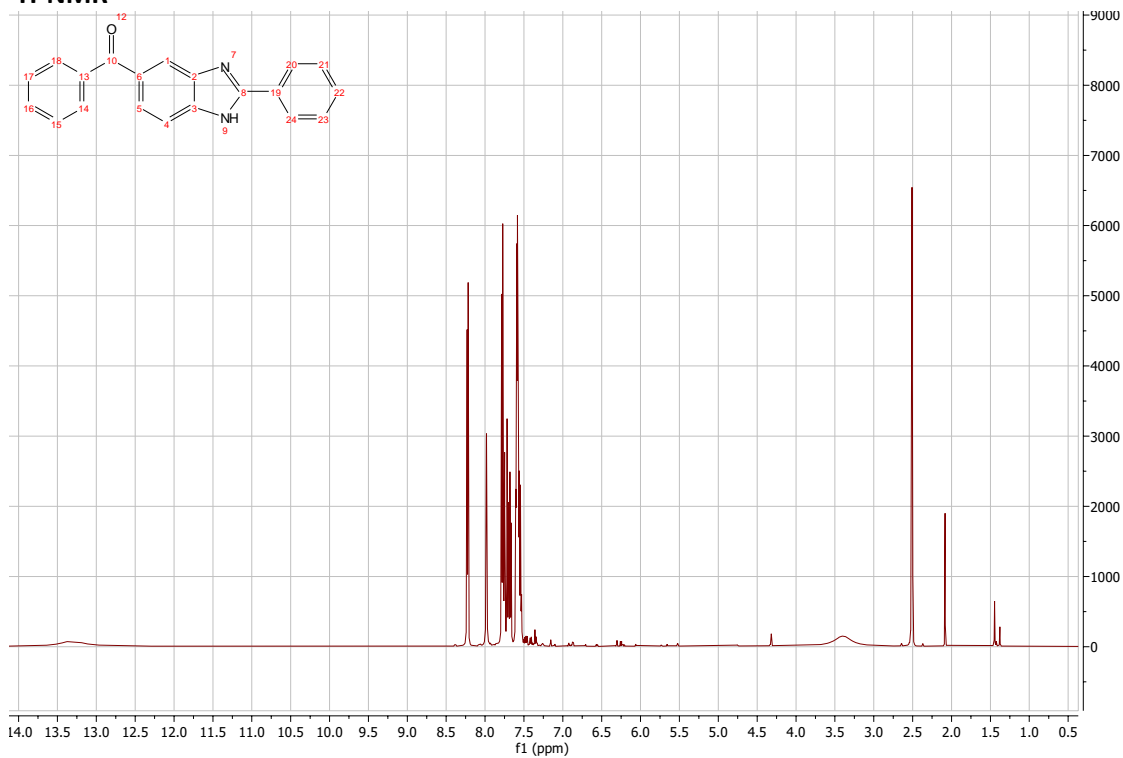
¹H-NMR

¹³C-NMR
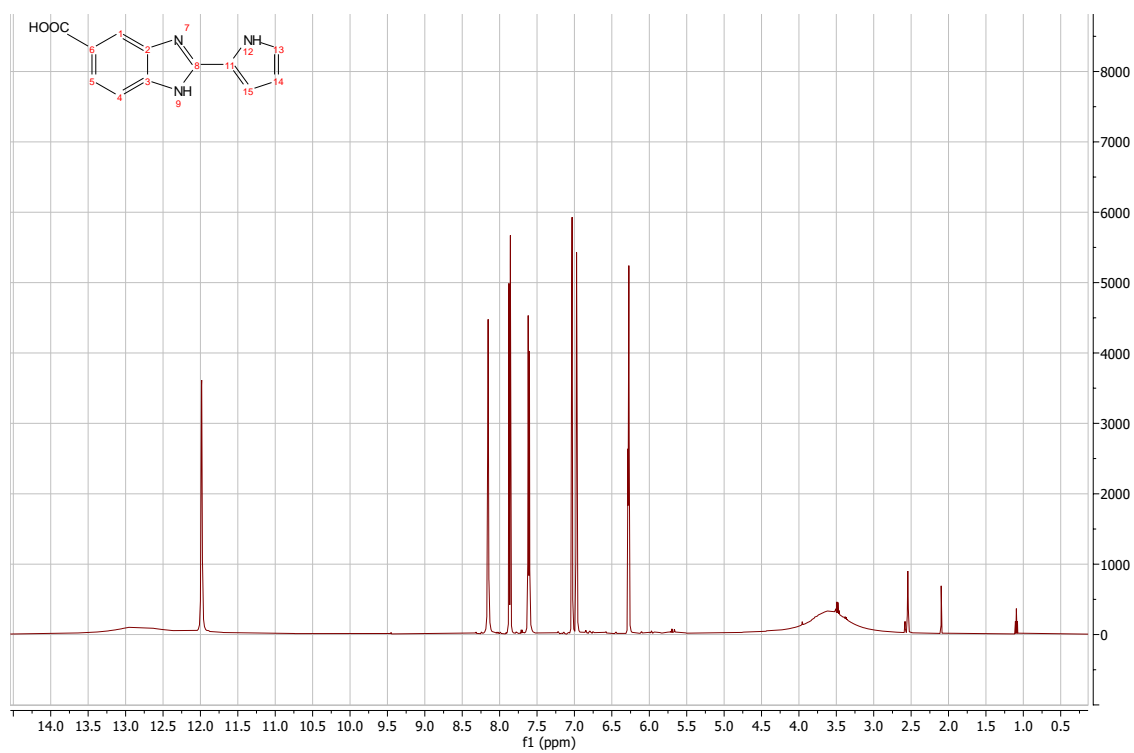
HSQC

20211004_CH411_HSQC.10.ser
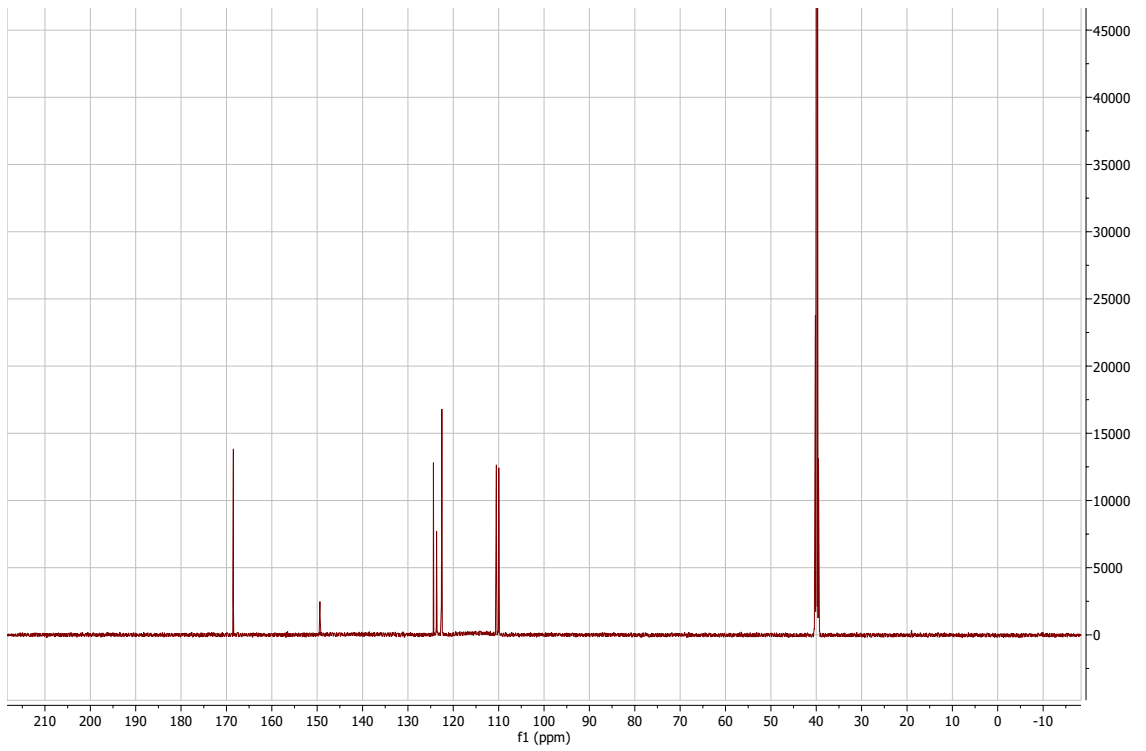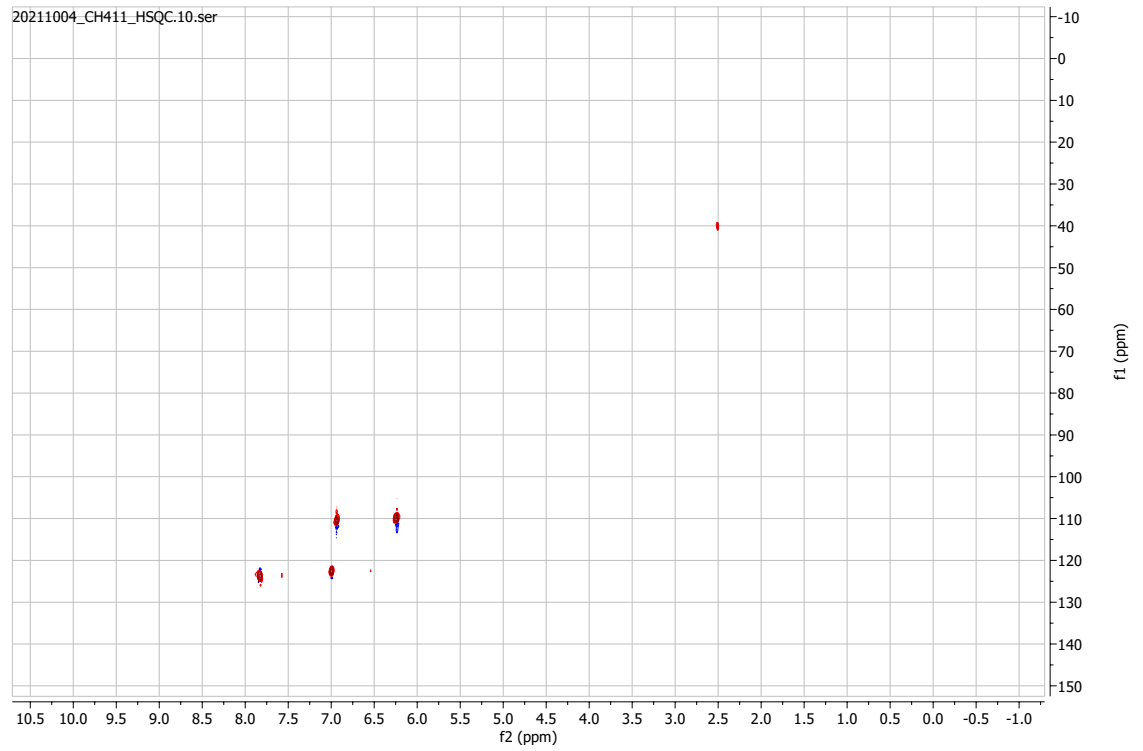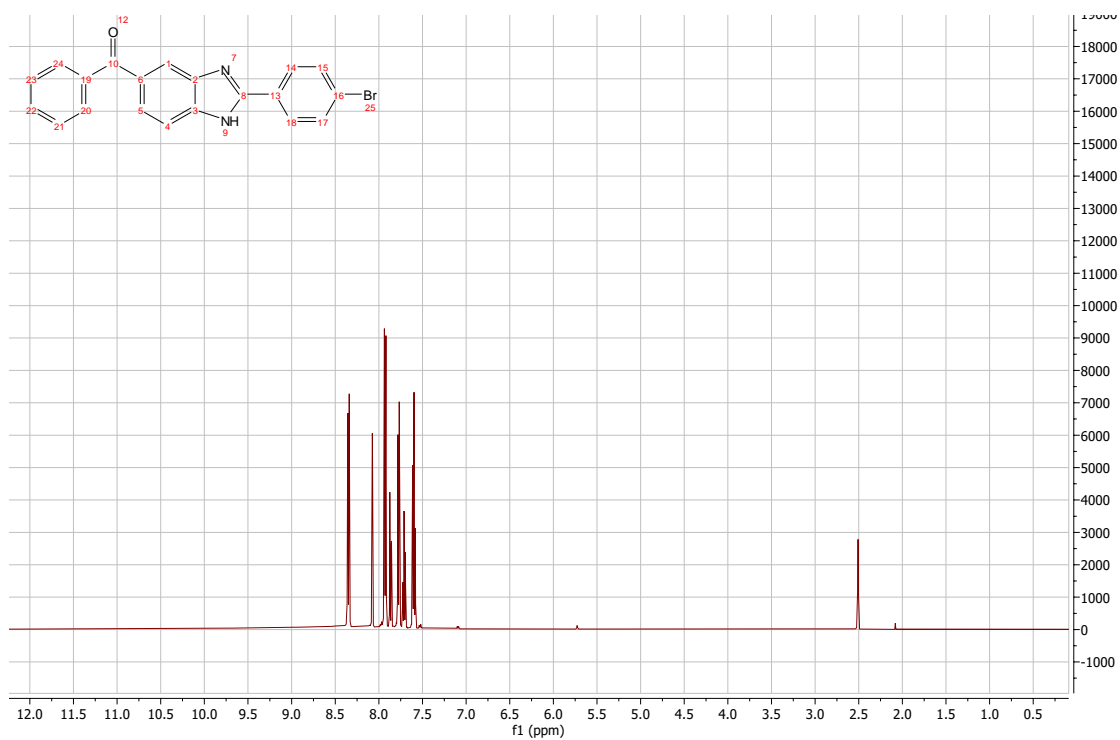
HMBC

20211004_CH411_HMBC.10.ser
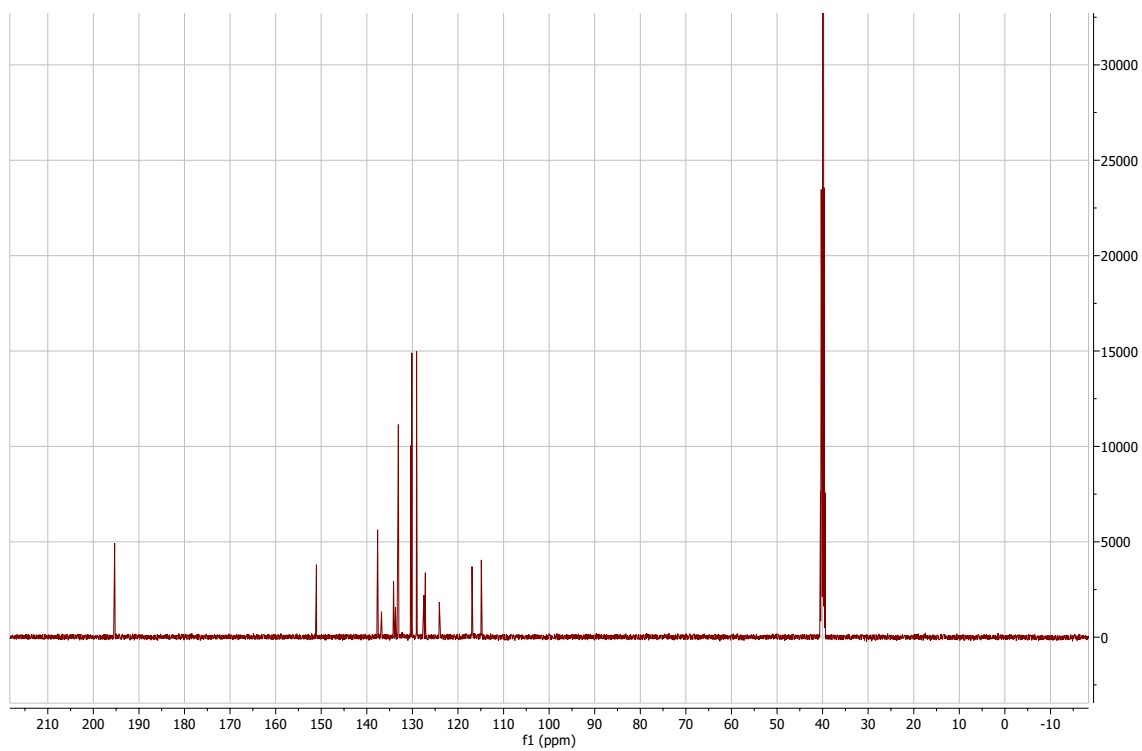

5-benzoyl-2-phenyl-1H-1,3-benzodiazole:

¹H-NMR

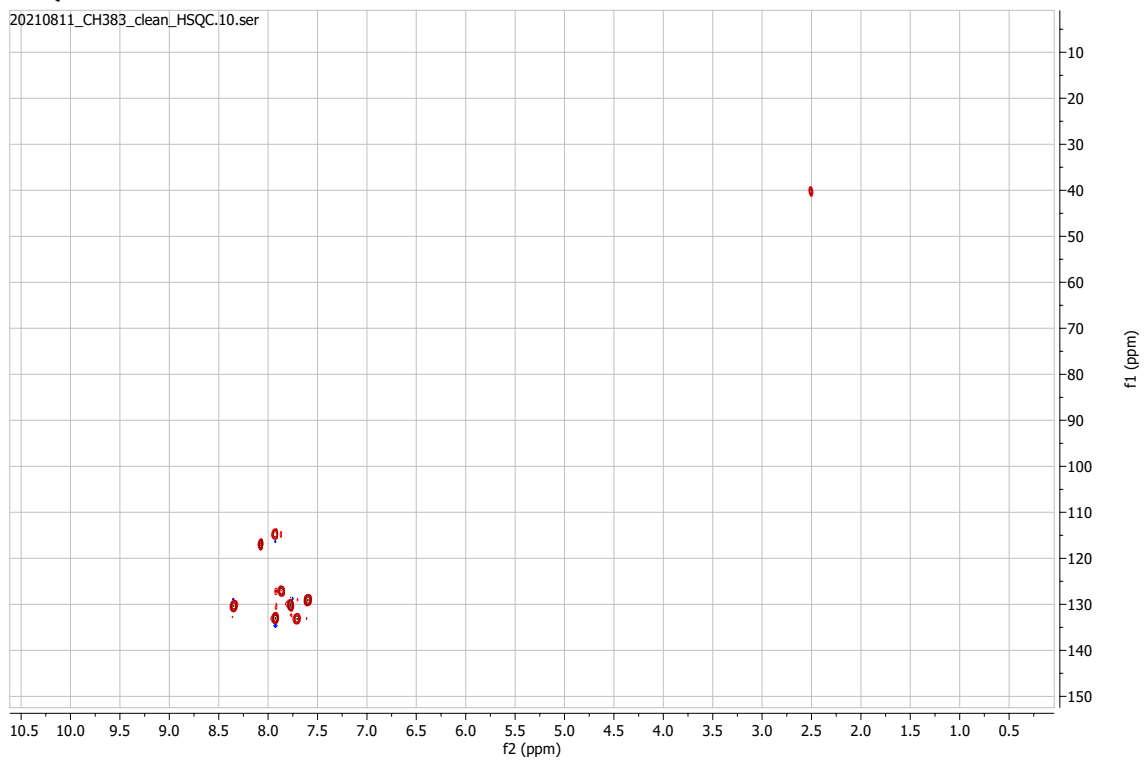## 5-benzoyl-2-(4-bromophenyl)-1H-1,3-benzodiazole:
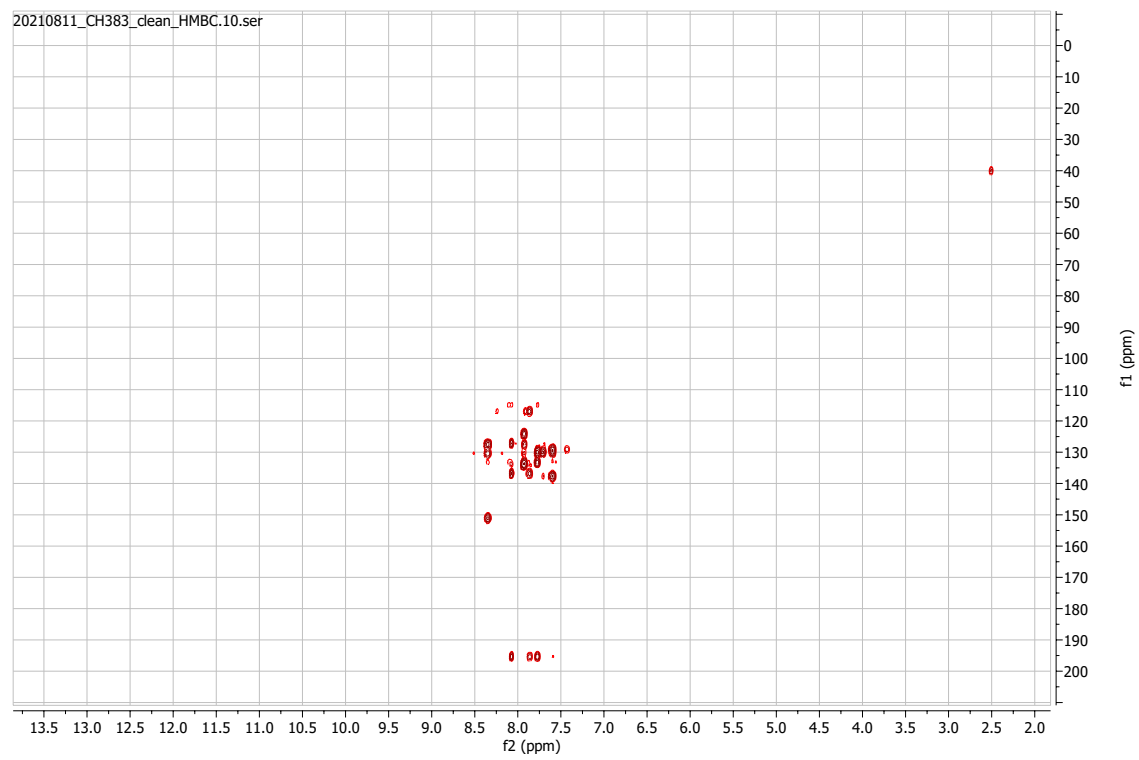
¹H-NMR

¹³C-NMR

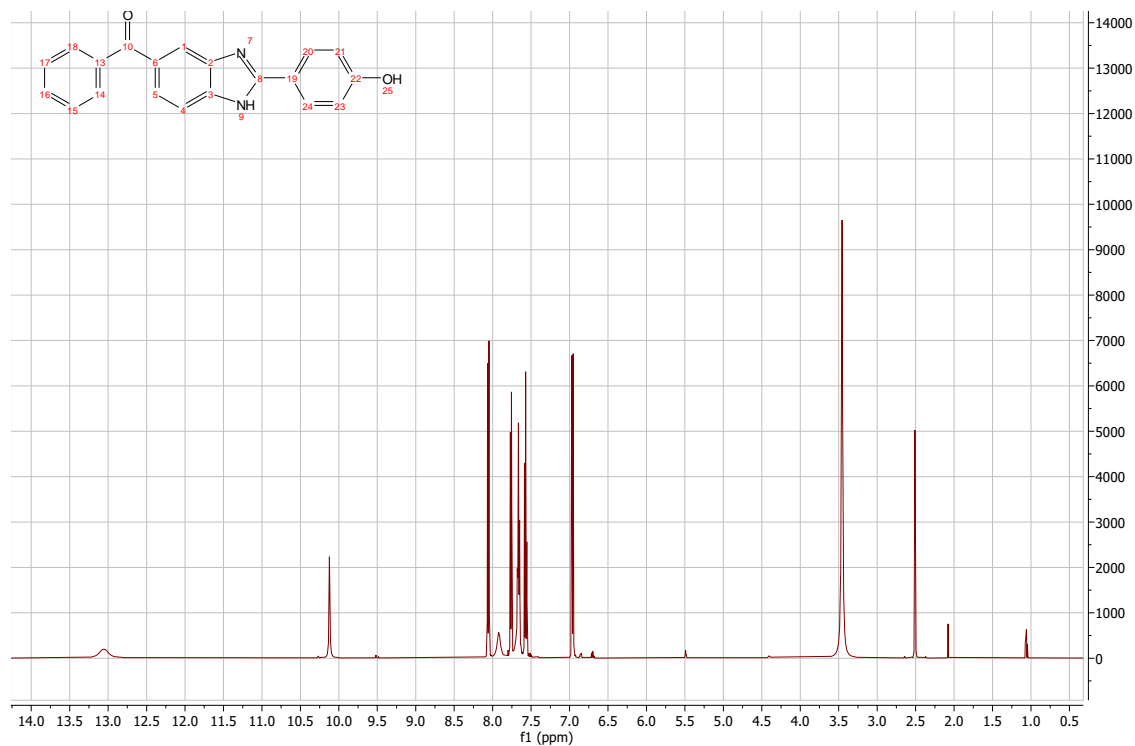354

HSQC

20210811_CH383_clean_HSQC.10.ser
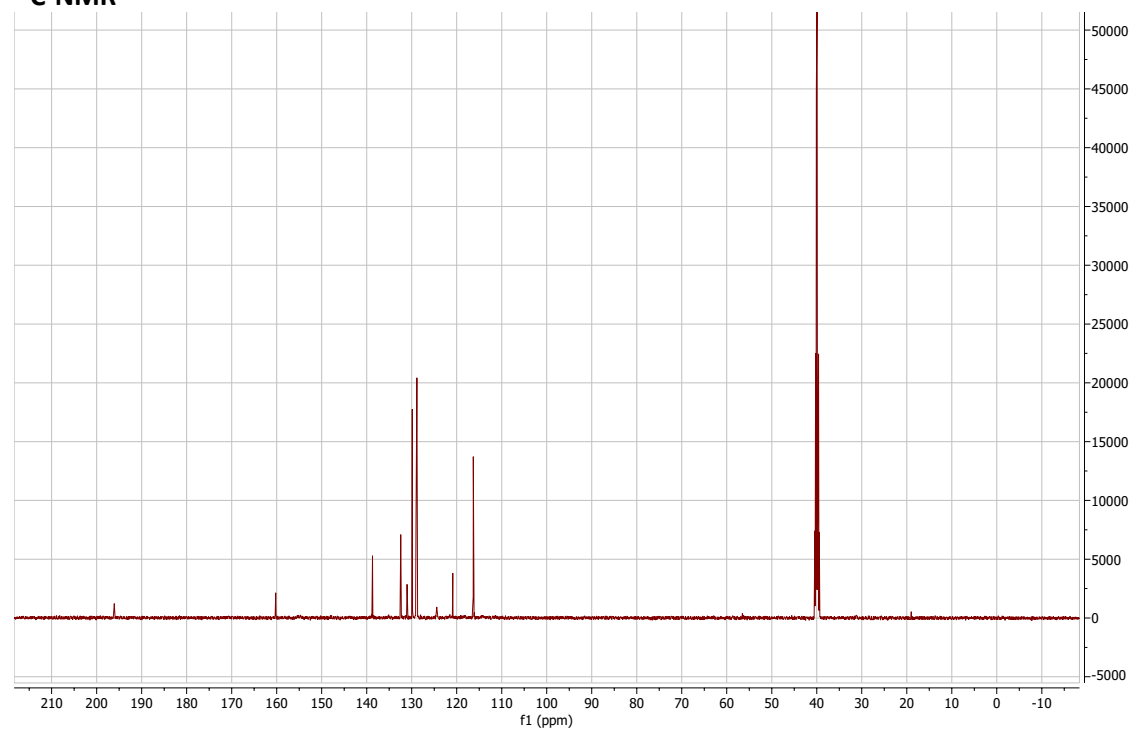

HMBC

20210811_CH383_clean_HMBC.10.ser

355

4-(5-benzoyl-1H-1,3-benzodiazol-2-yl)phenol:

¹H-NMR

¹³C-NMR

HSQC

20210716_CH381_HSQC.10.ser

HMBC

20210716_CH381_HMBC.10.ser
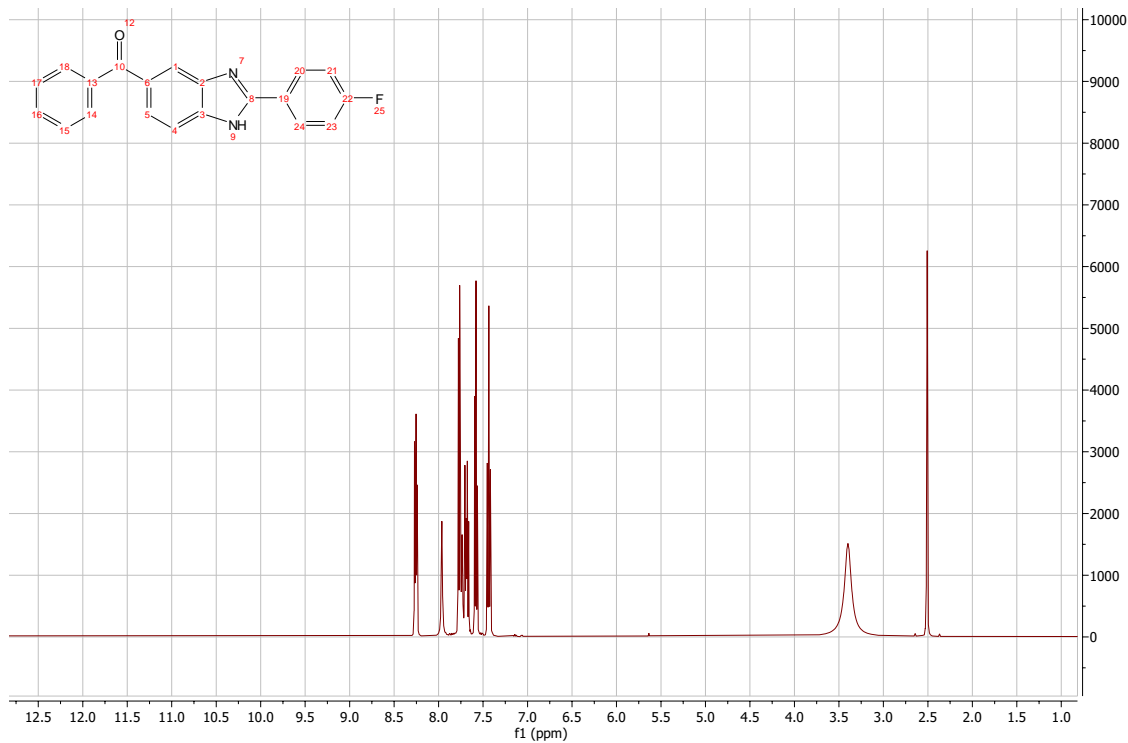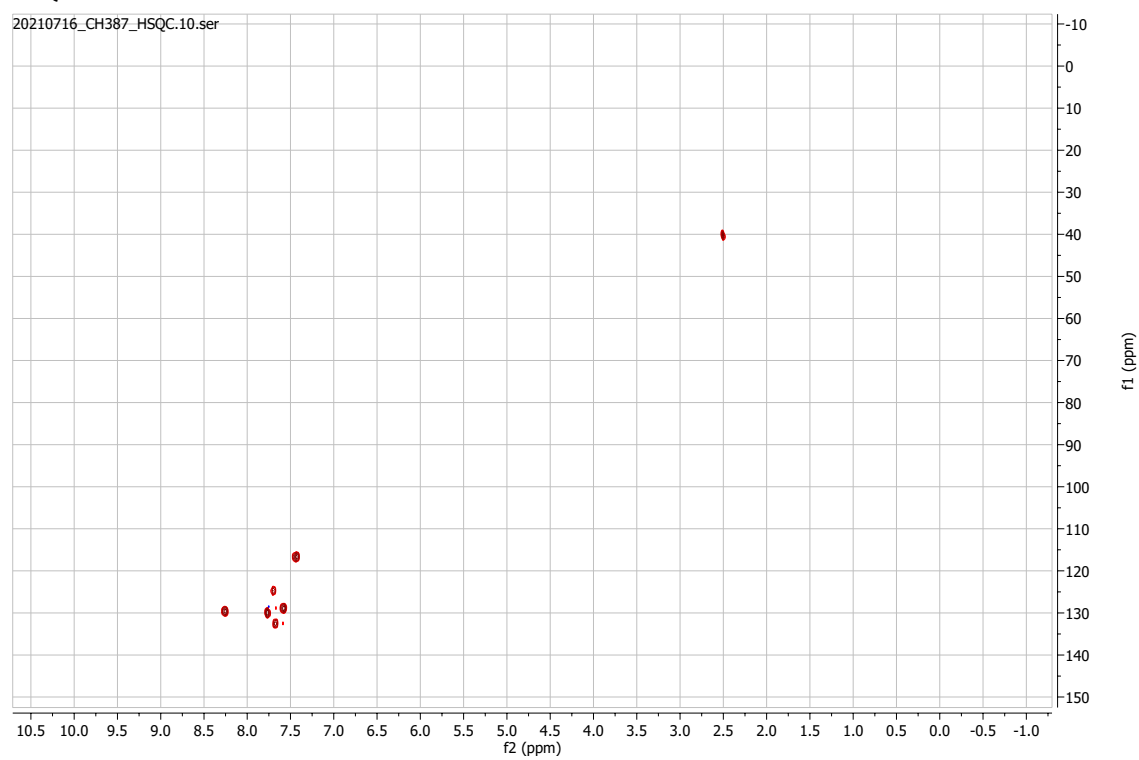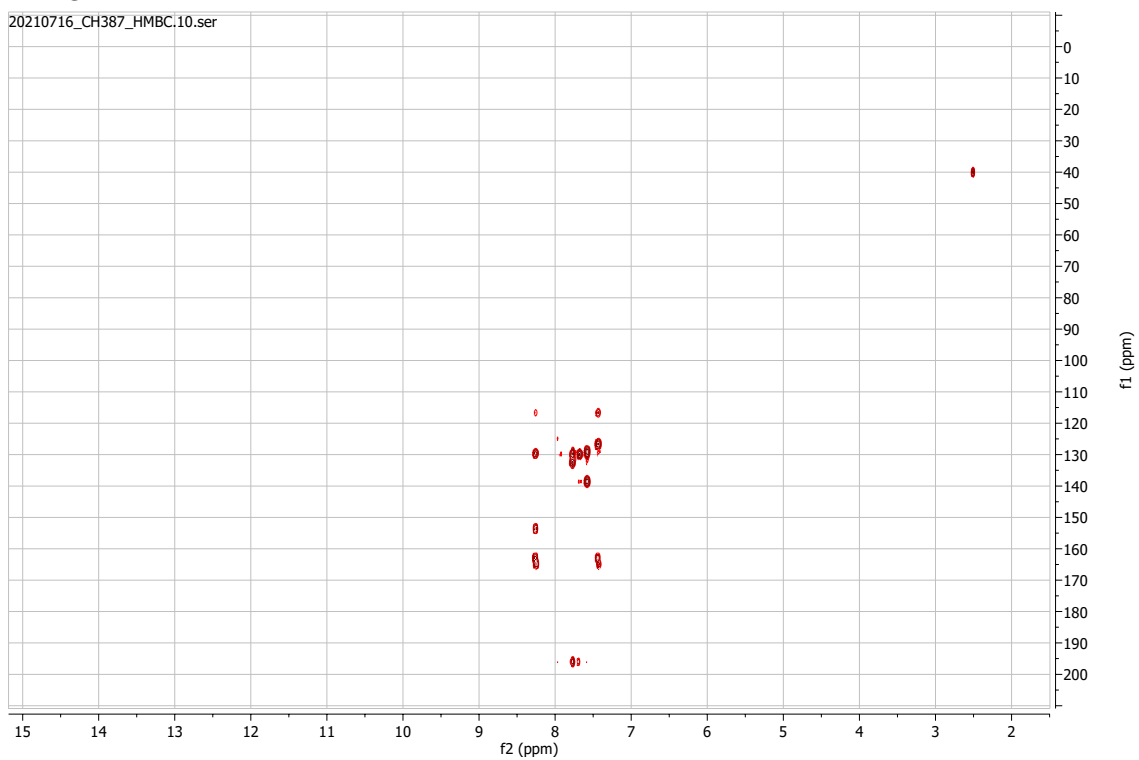
357

5-benzoyl-2-(4-fluorophenyl)-1H-1,3-benzodiazole:

¹H-NMR

¹³C-NMR

HSQC

20210716_CH387_HSQC.10.ser

HMBC

20210716_CH387_HMBC.10.ser

4-(5-benzoyl-1H-1,3-benzodiazol-2-yl)-2-ethoxyphenol:
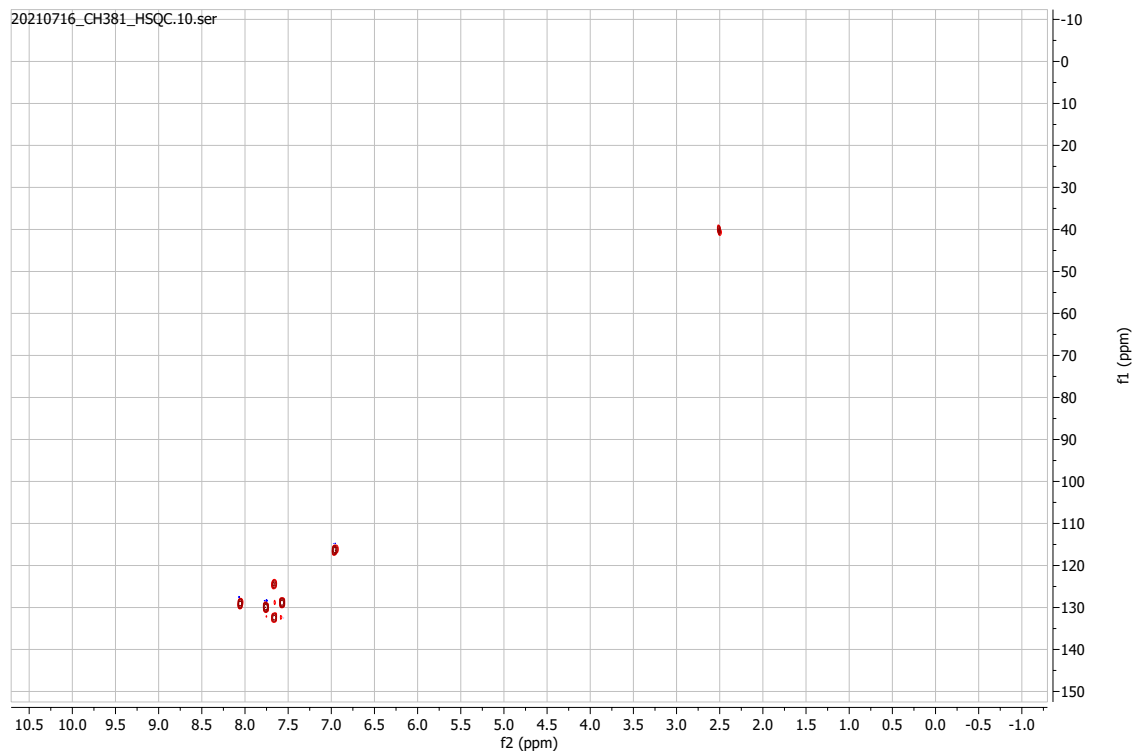
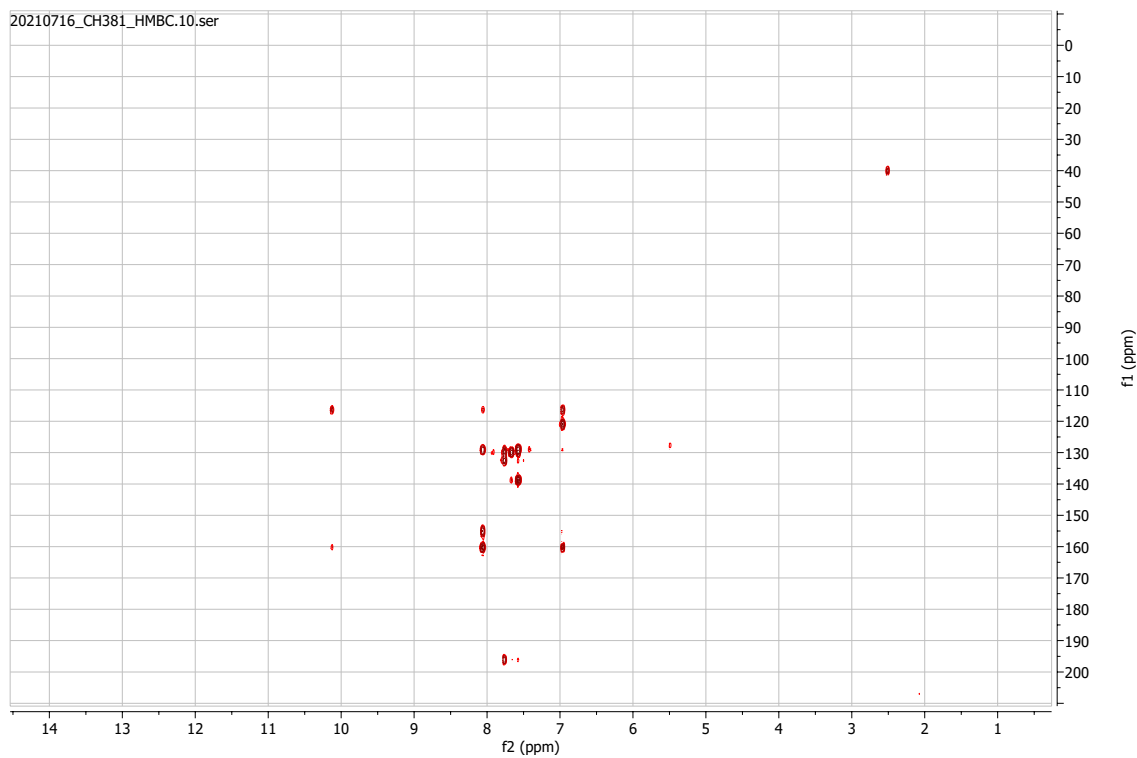**¹H-NMR**

¹³C-NMR

HSQC

20210716_CH386_HSQC.10.ser
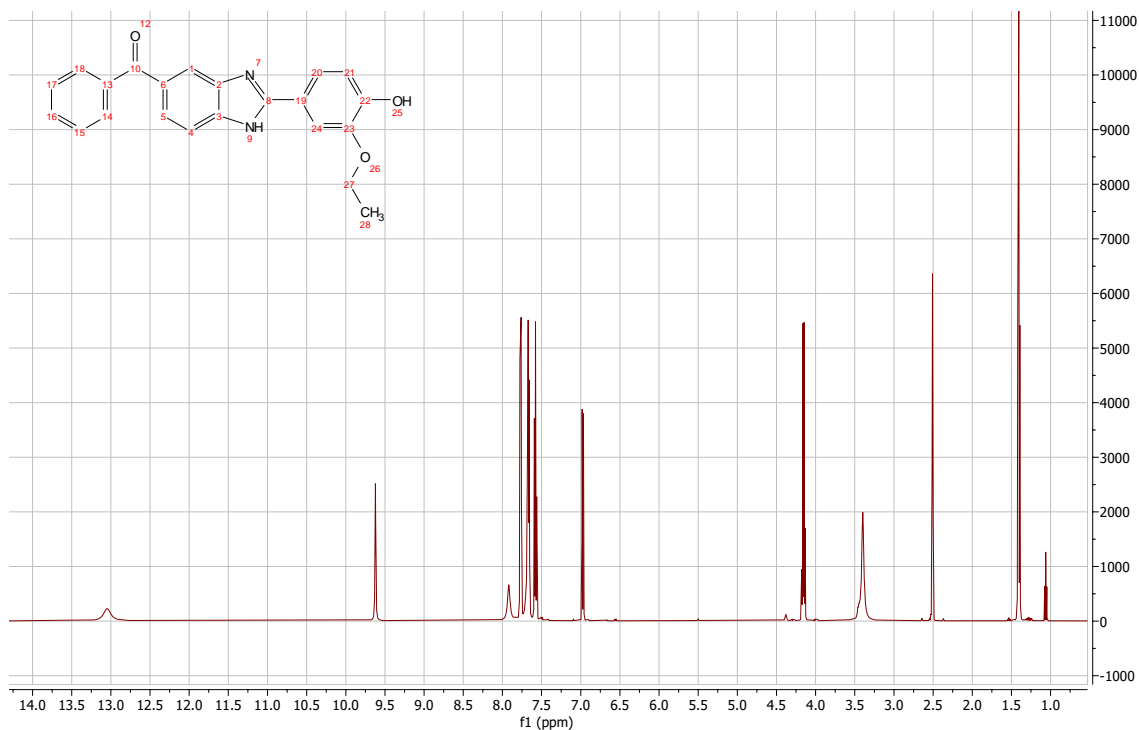
HMBC
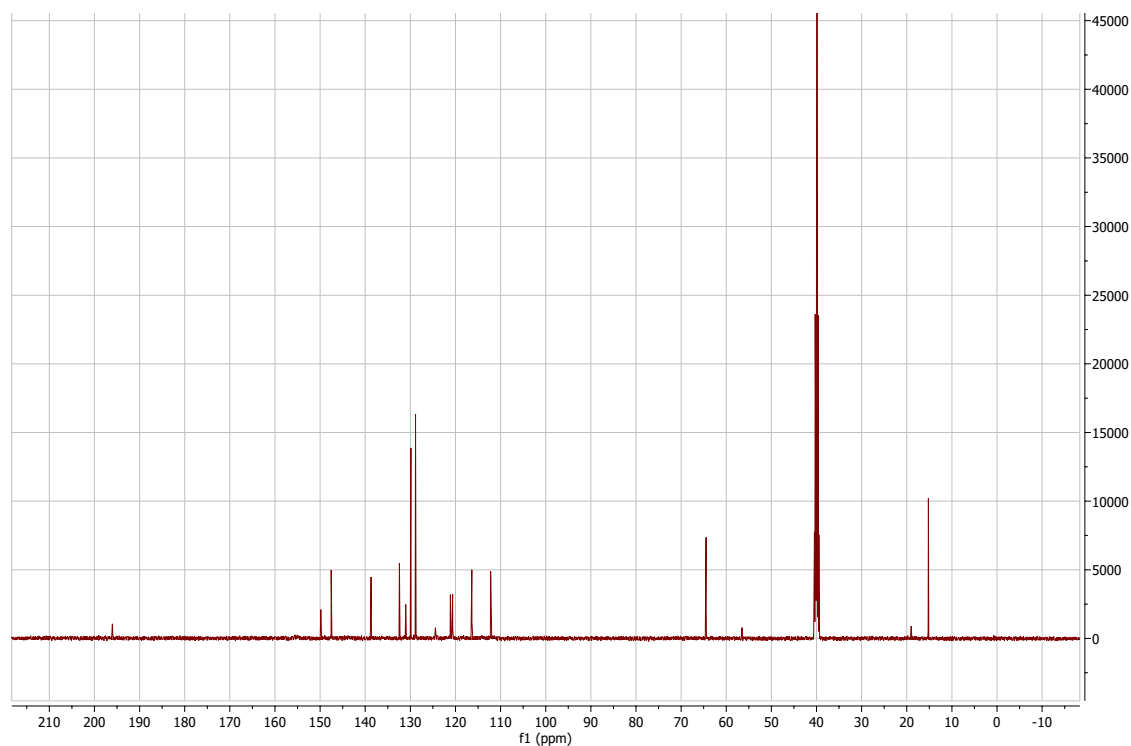
20210716_CH386_HMBC.10.ser
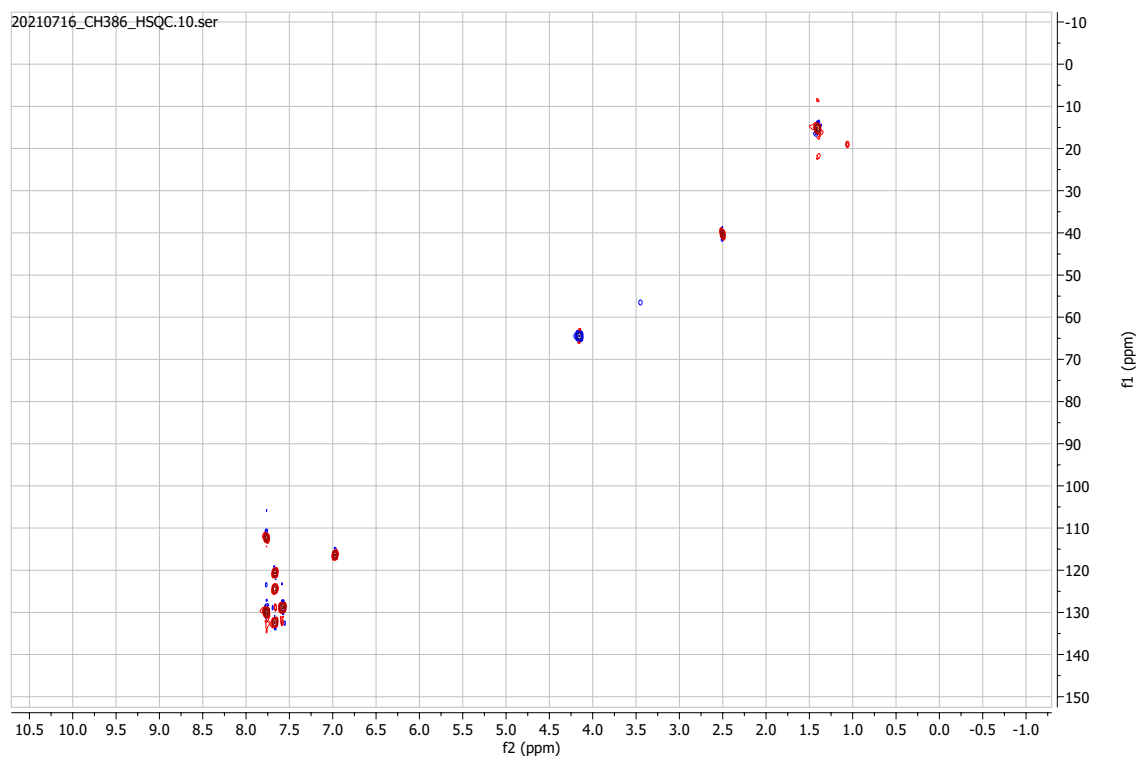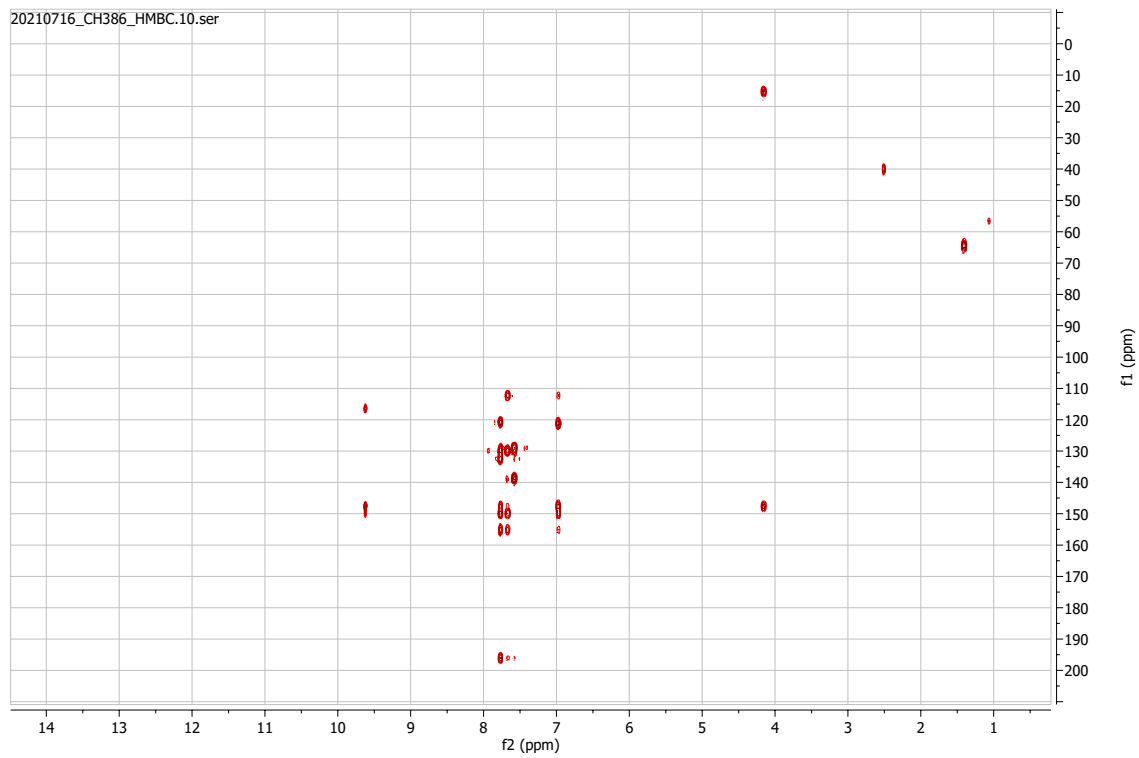
5-benzoyl-2-(thiophen-2-yl)-1H-1,3-benzodiazole:
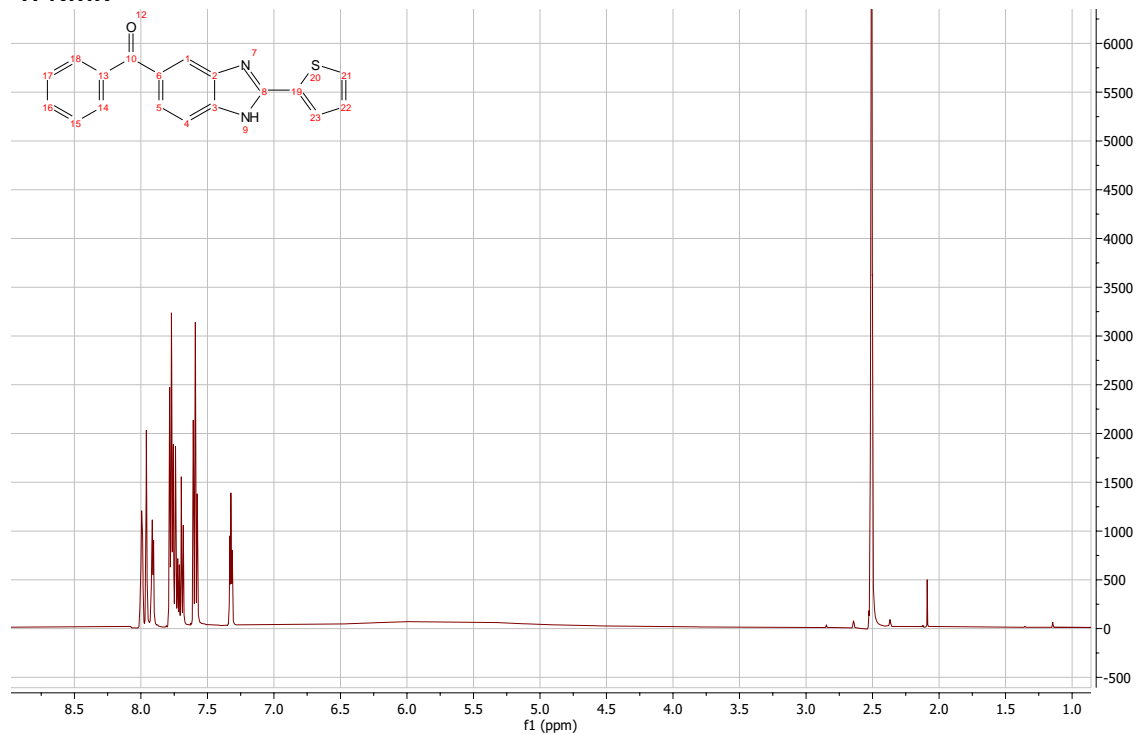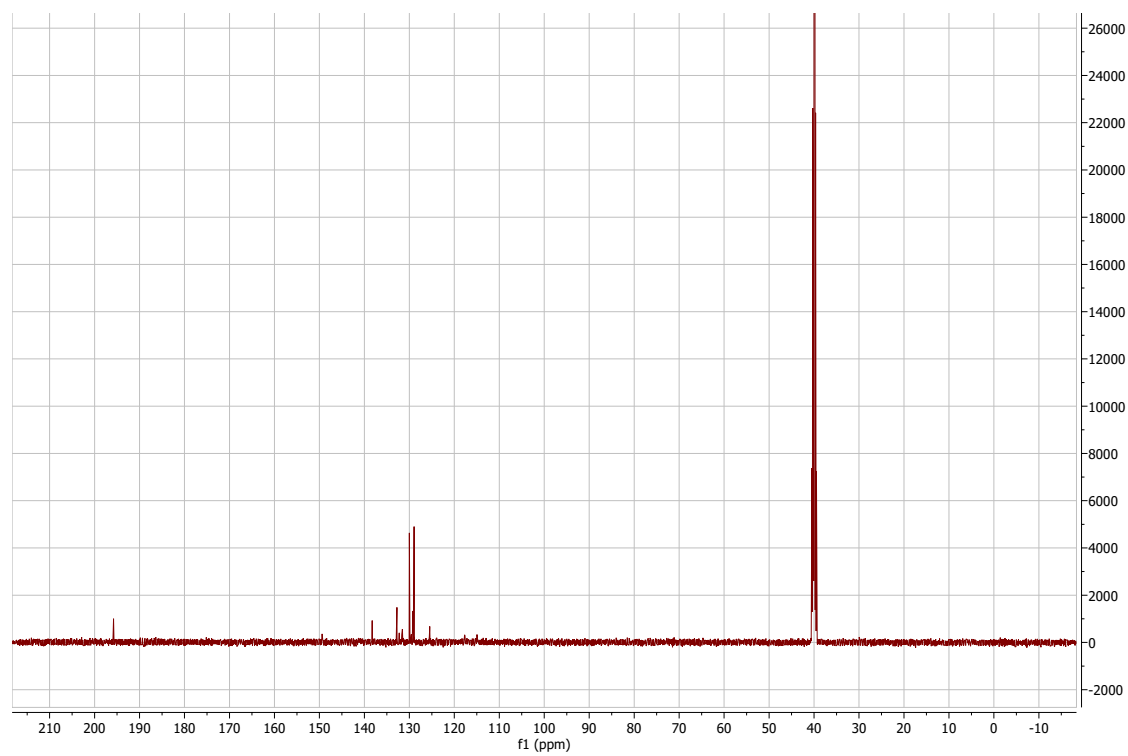
¹H-NMR

¹³C-NMR

HSQC

20210716_CH391_HSQC.10.ser

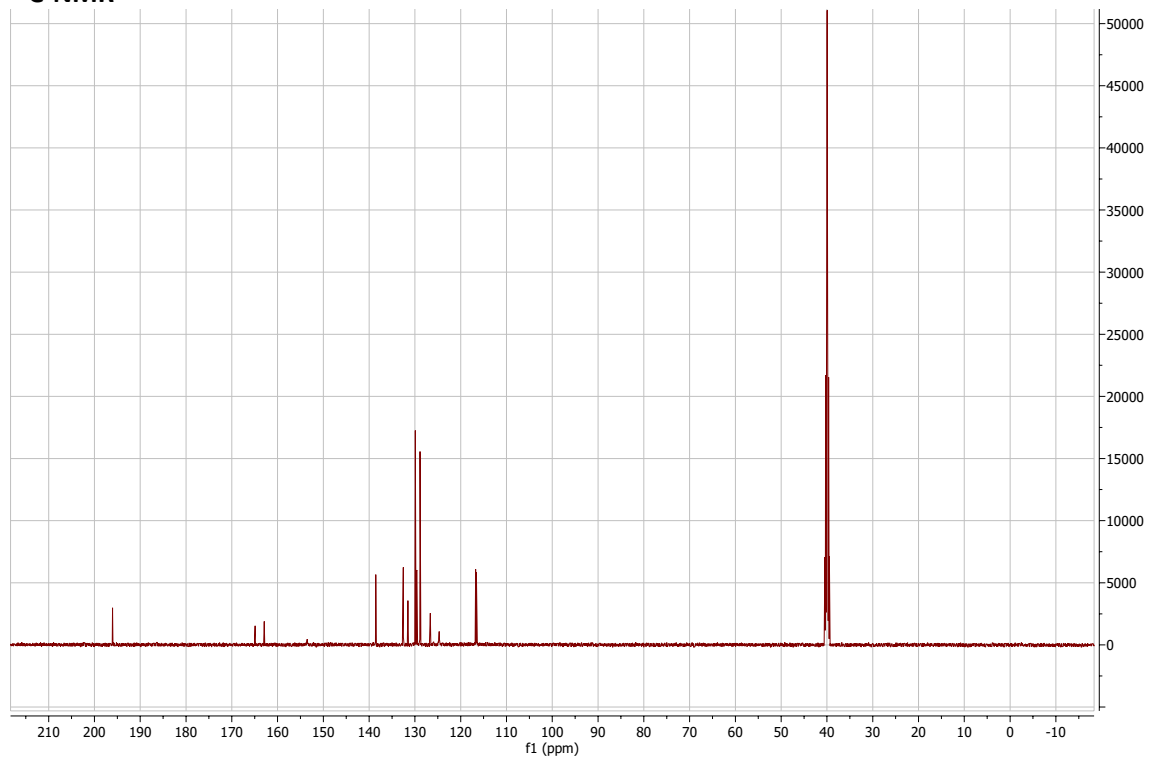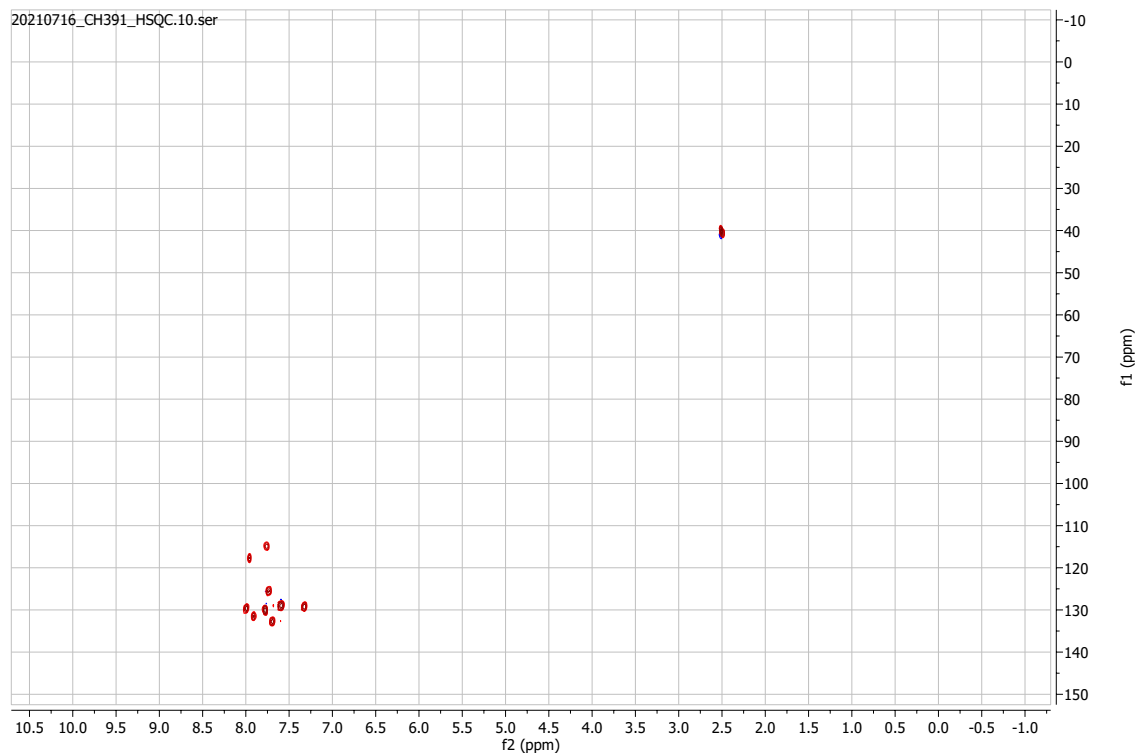## HMBC

20210716_CH391_HMBC.10.ser
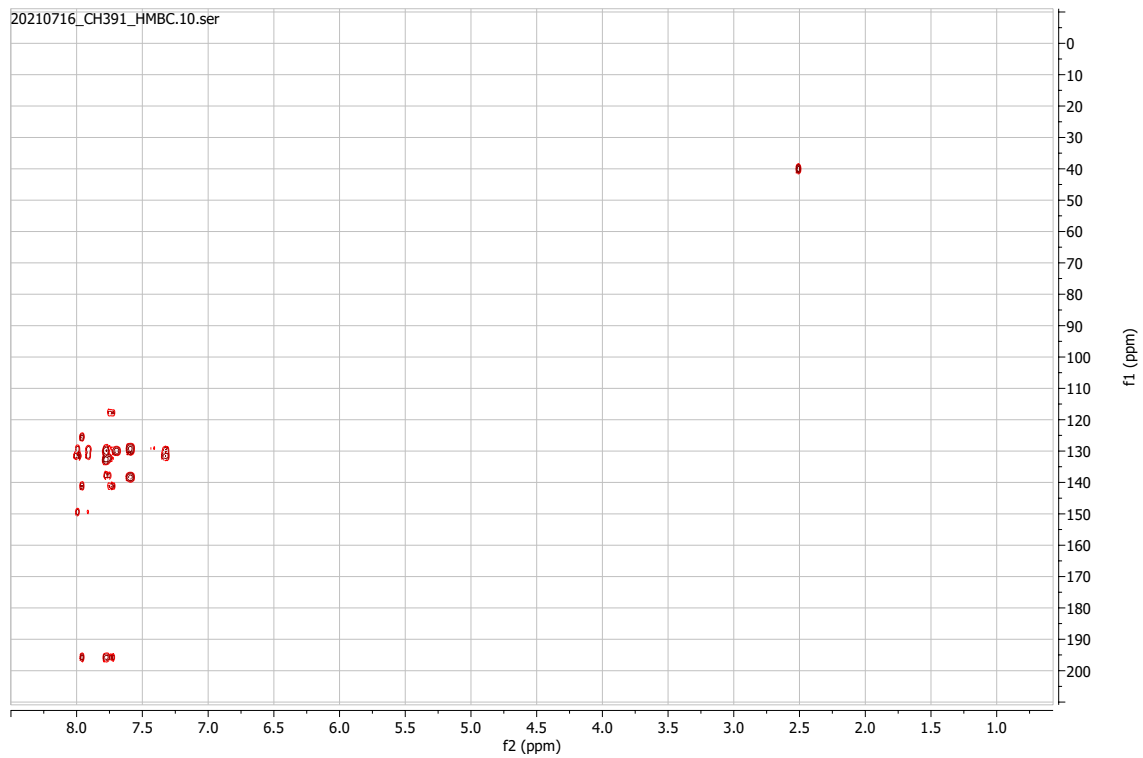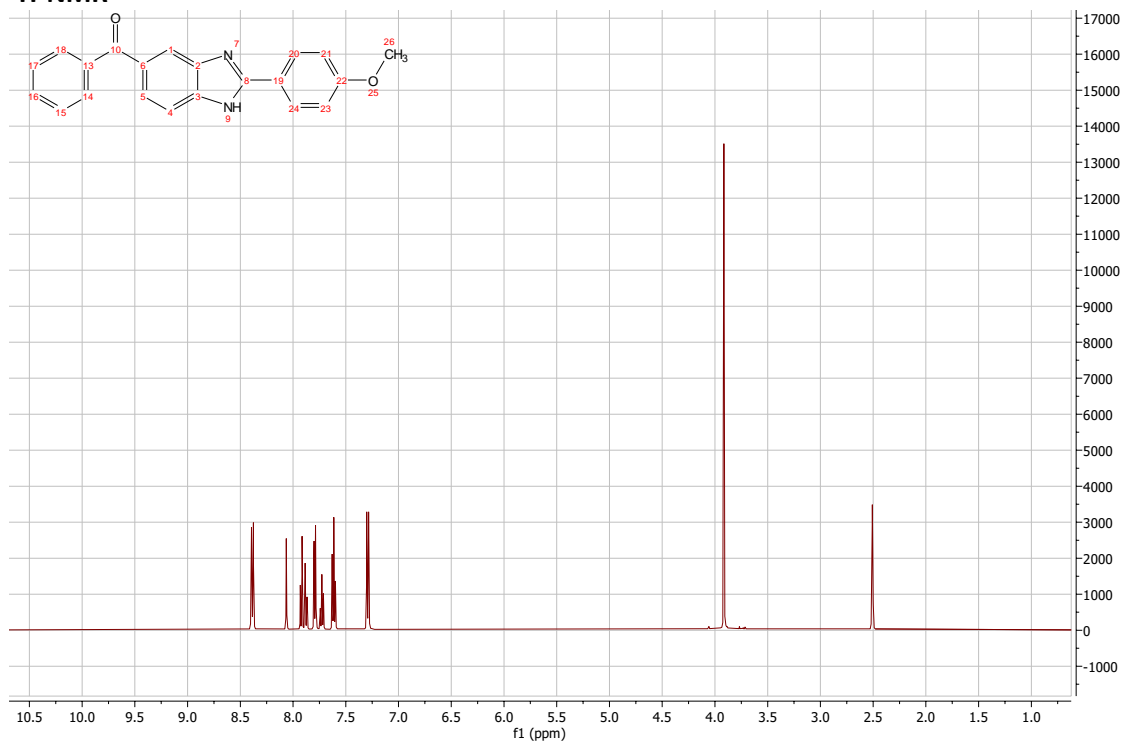
363

5-benzoyl-2-(4-methoxyphenyl)-1H-1,3-benzodiazole

¹H-NMR

¹³C-NMR

HSQC

20220509_CH435_clean_HSQC.10.ser

HMBC

20220509_CH435_clean_HMBC.10.ser

365
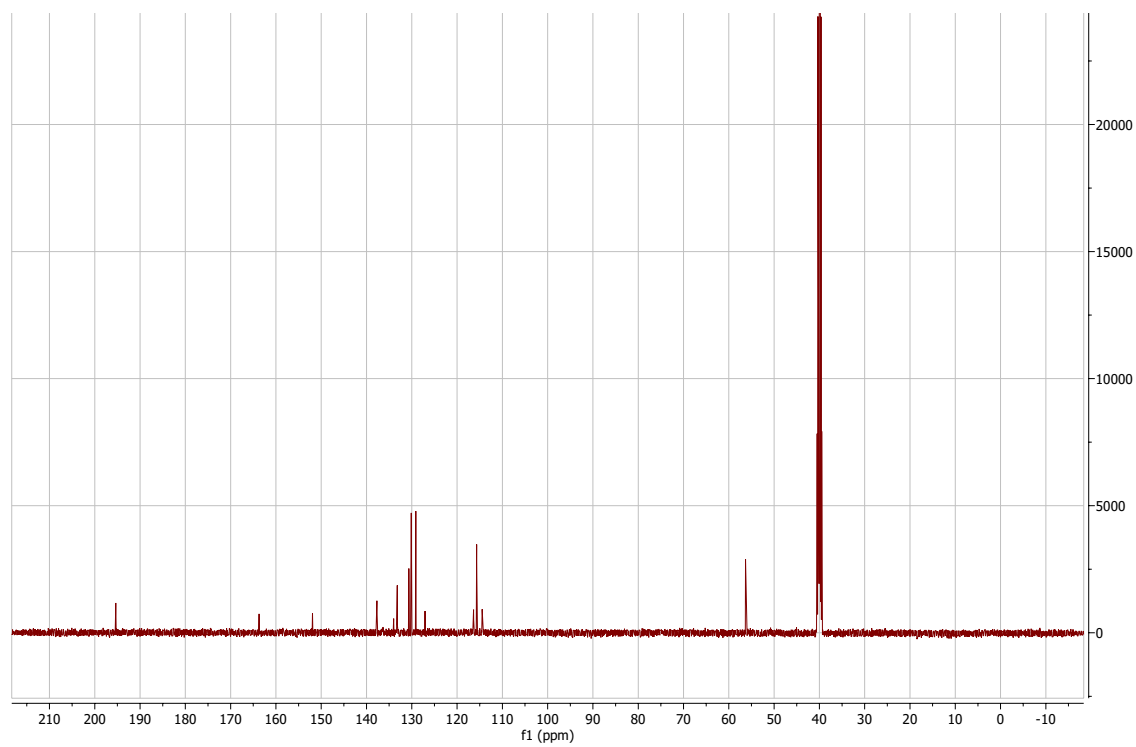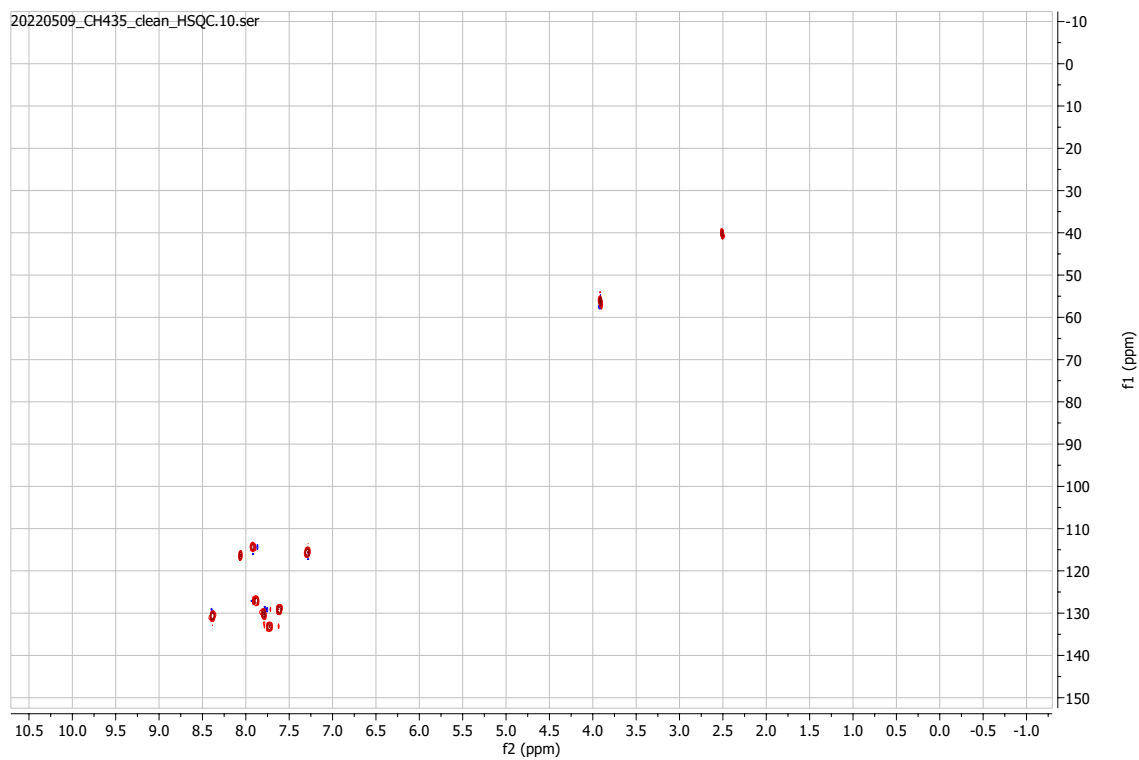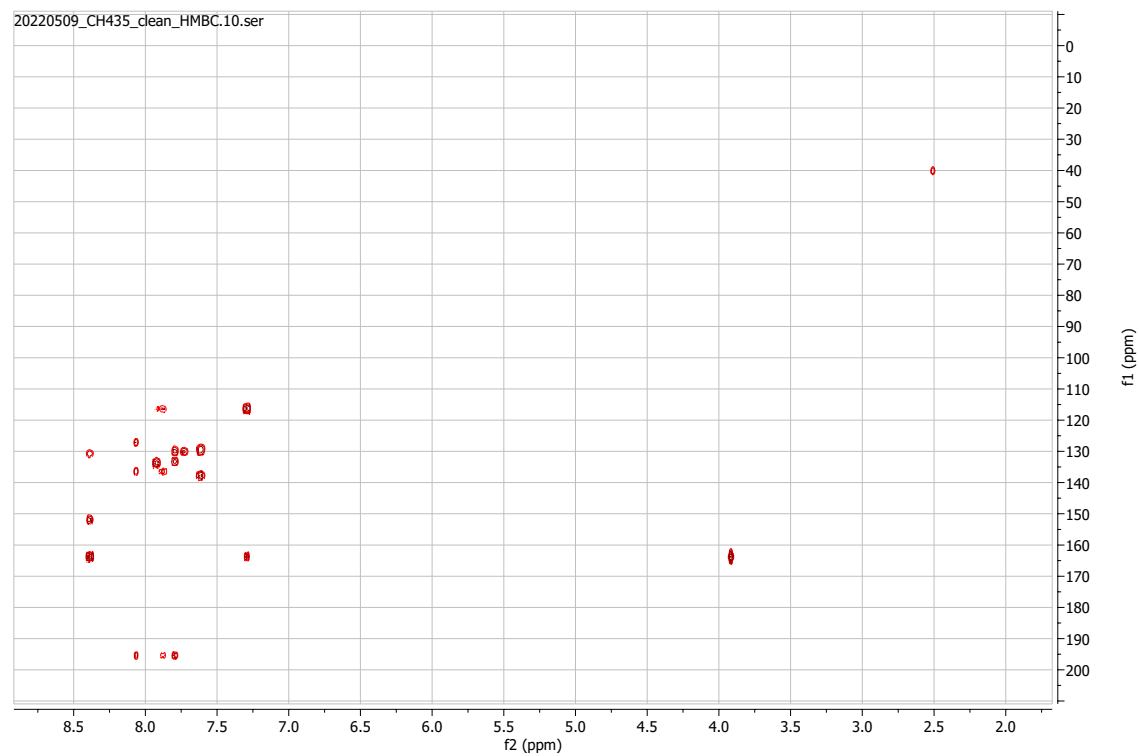
2-(4-chlorophenyl)-5,6-dimethyl-1H-1,3-benzodiazole:
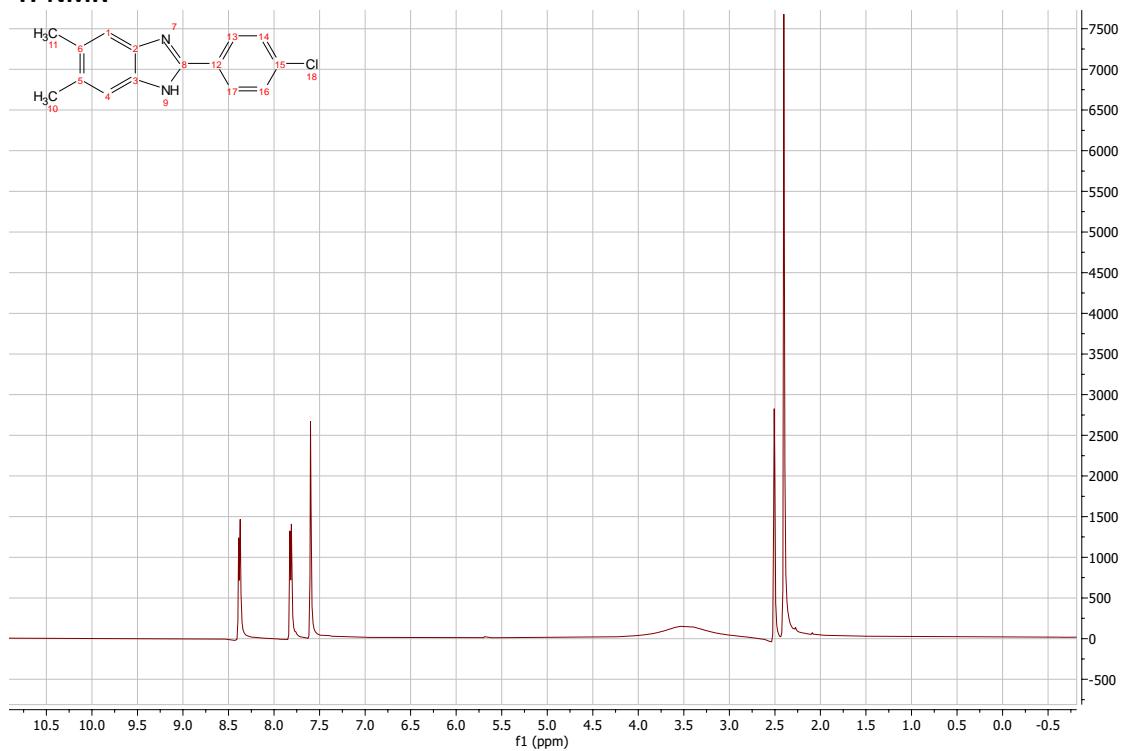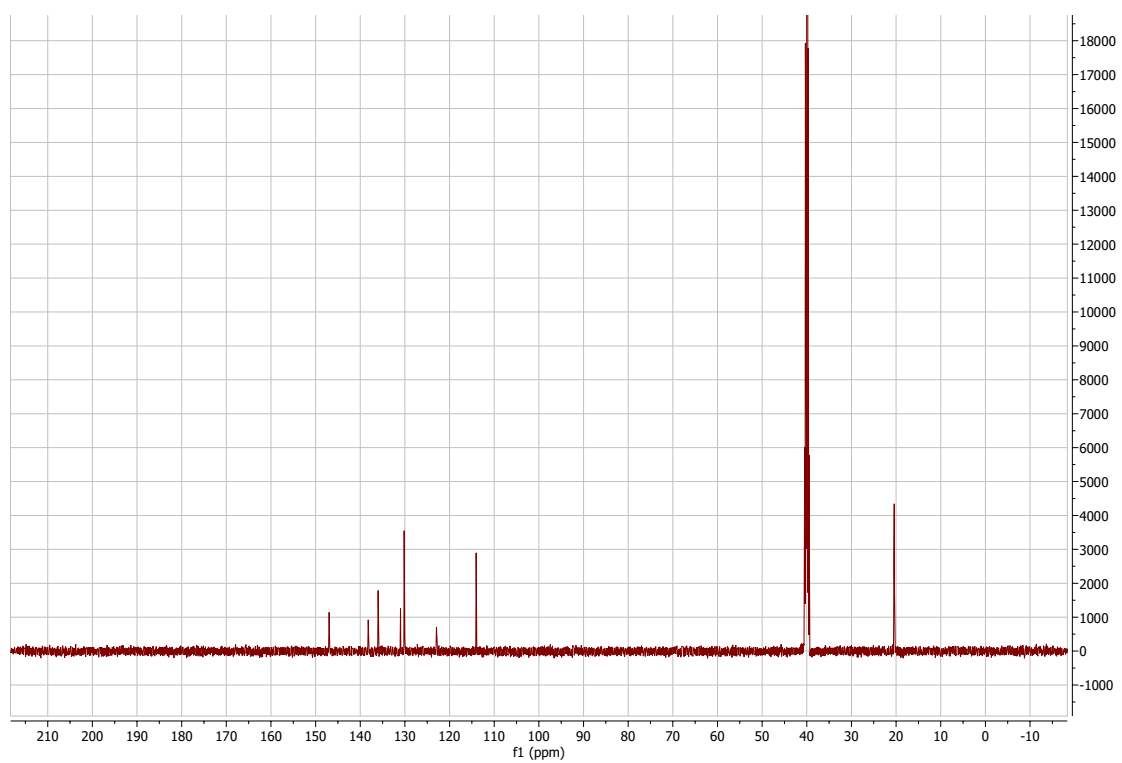
¹H-NMR

¹³C-NMR

HSQC

20211020_CH417_clean_HSQC.10.ser
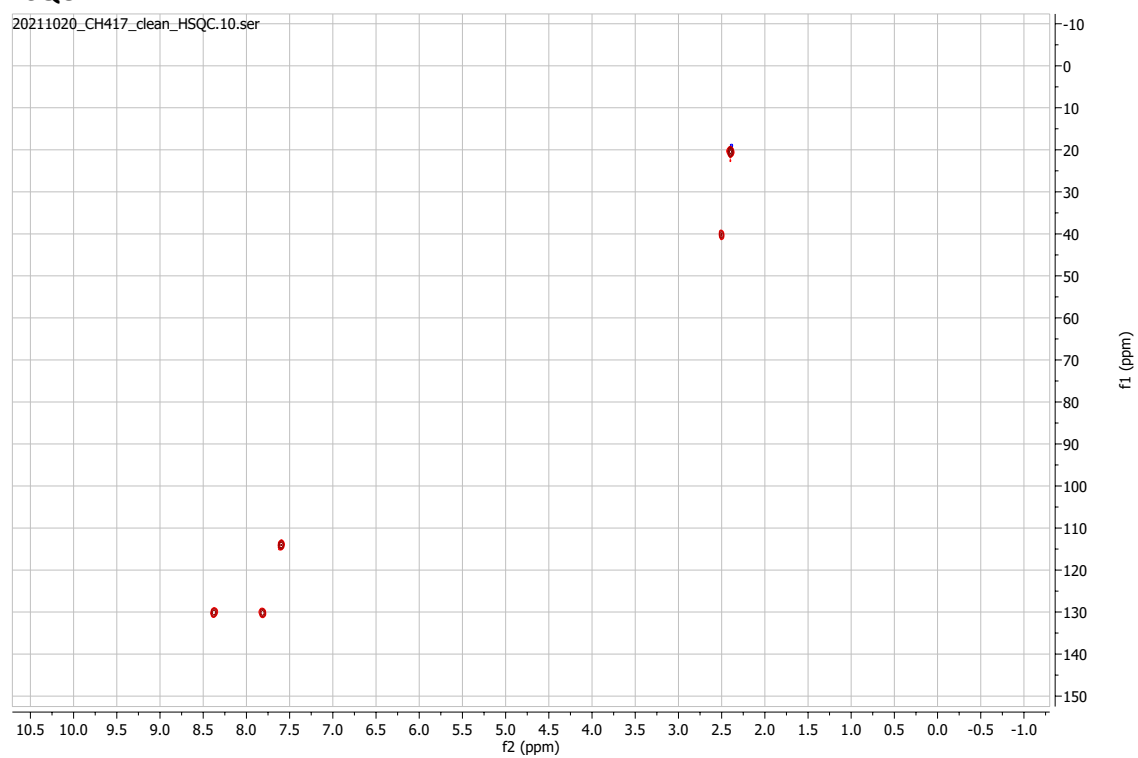
HMBC

20211020_CH417_clean_HMBC.10.ser
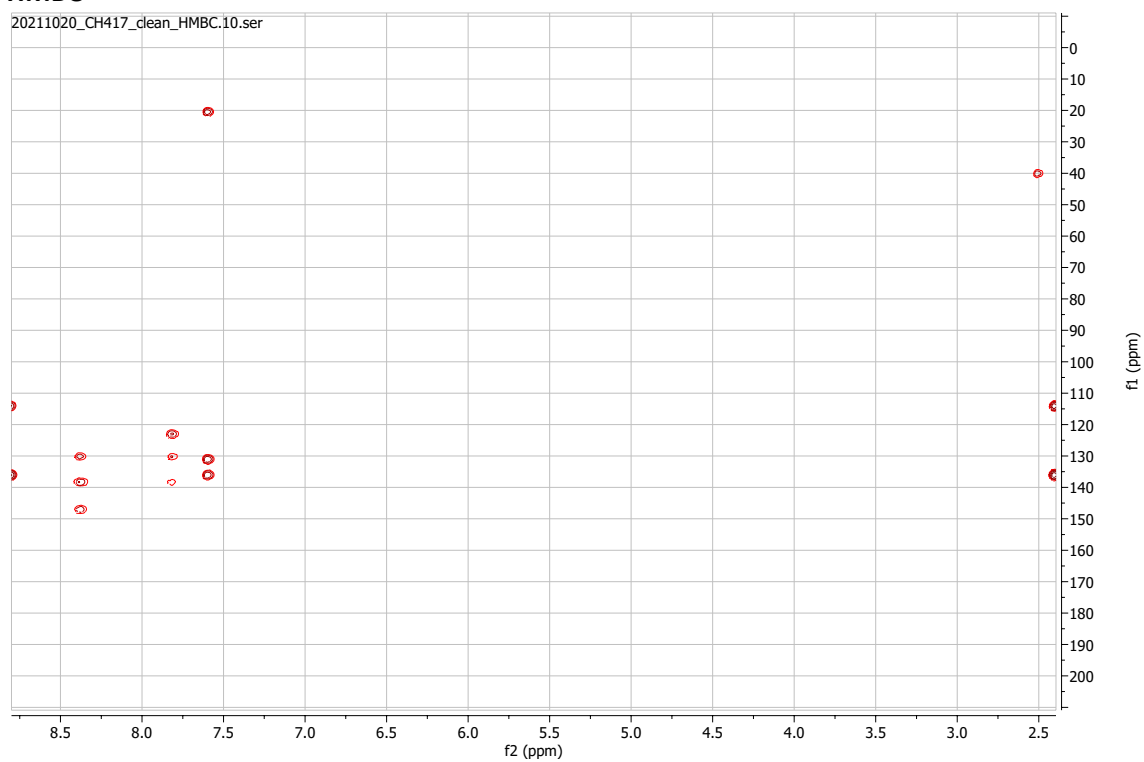
4-(5,6-dimethyl-1H-1,3-benzodiazol-2-yl)phenol:

¹H-NMR

¹³C-NMR

HSQC

20211020_CH418_clean_HSQC.10.ser

HMBC

20211020_CH418_clean_HMBC.10.ser
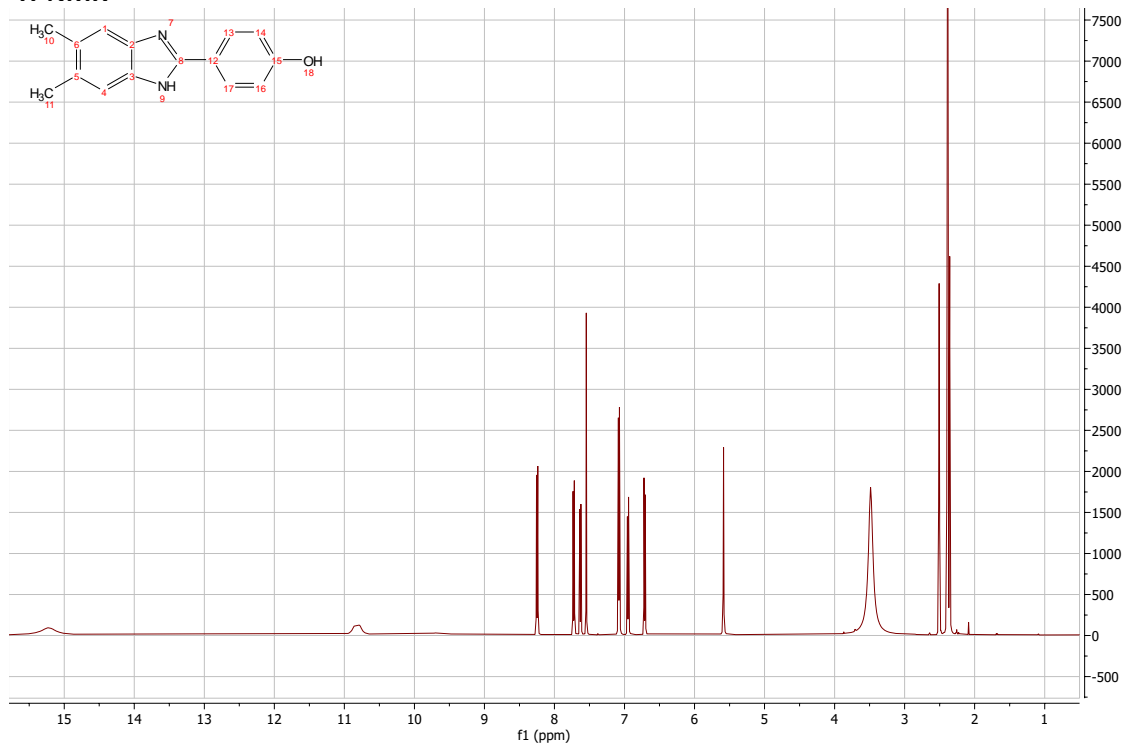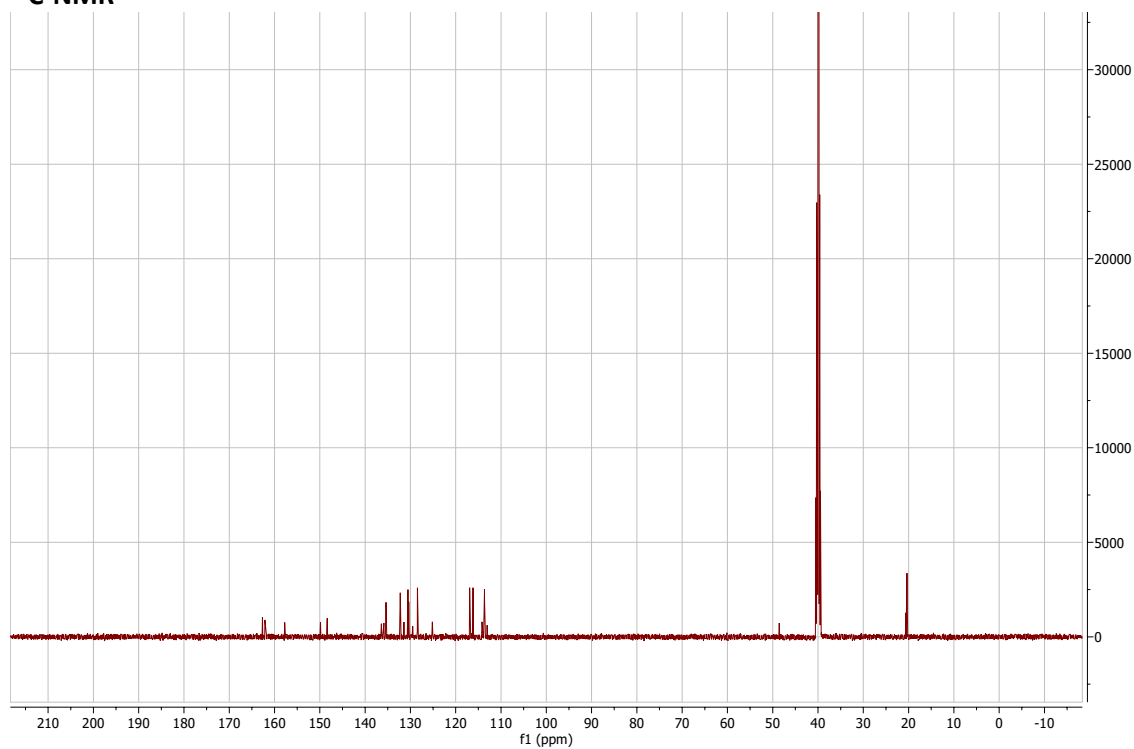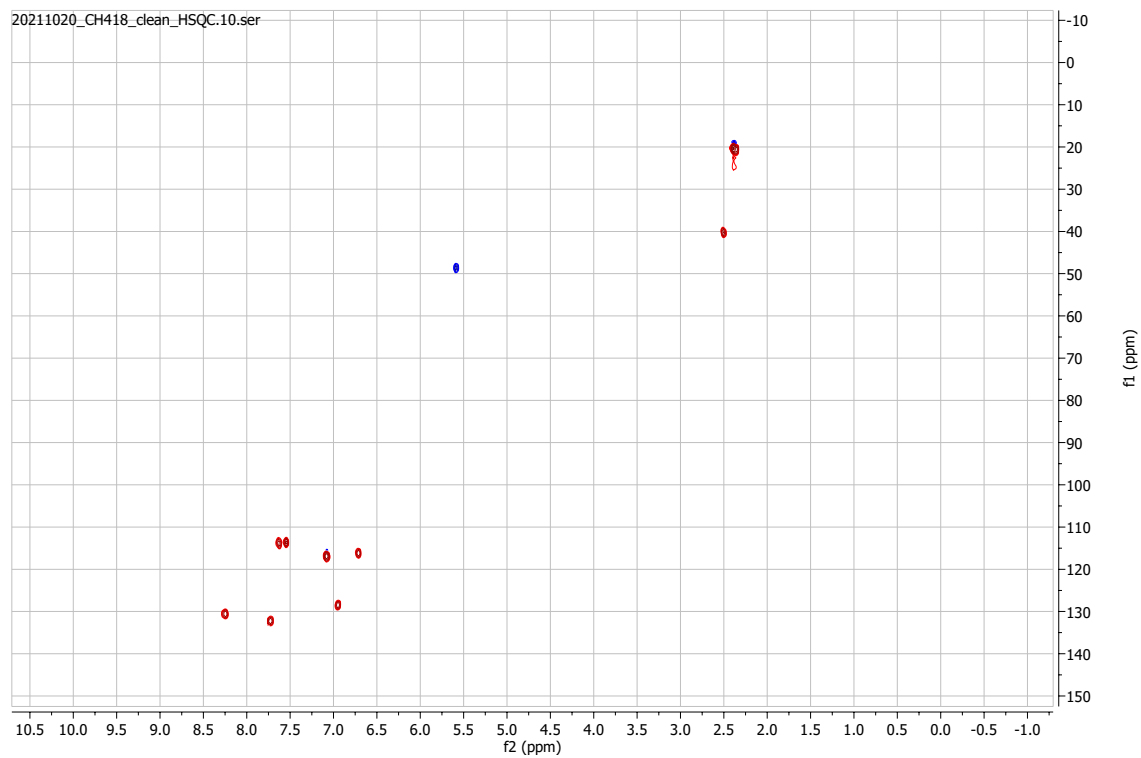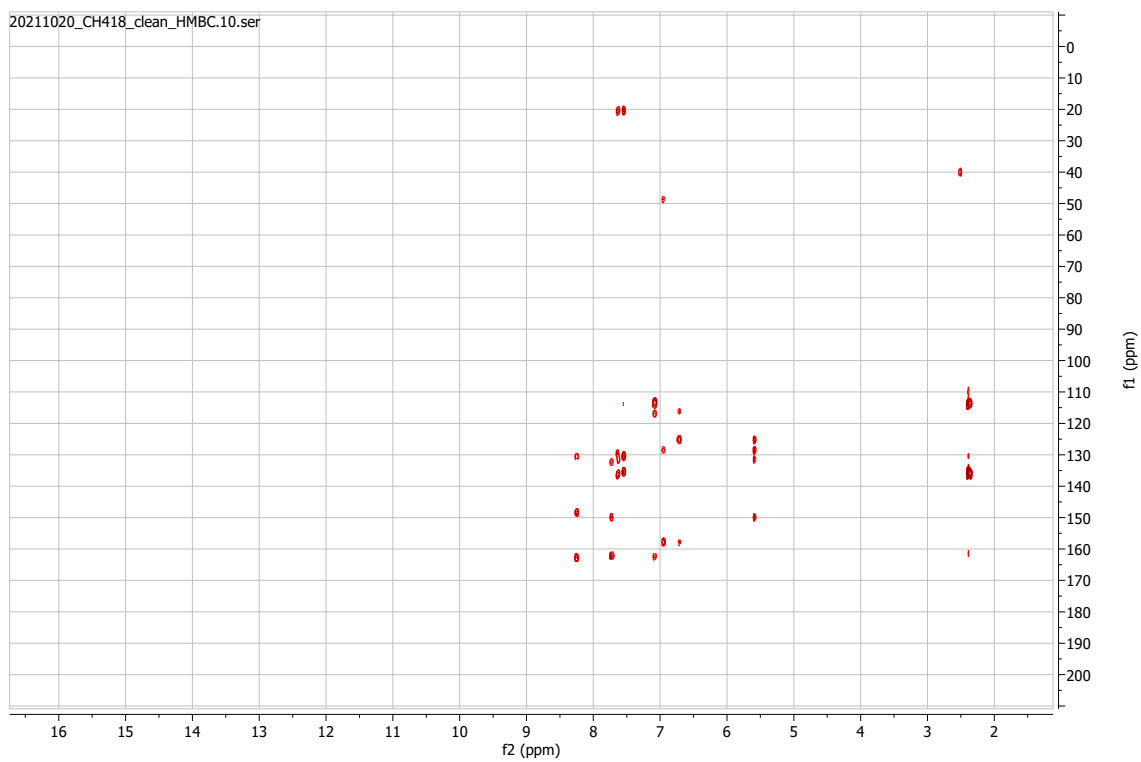
5,6-dimethyl-2-(1H-pyrrol-2-yl)-1H-1,3-benzodiazole:
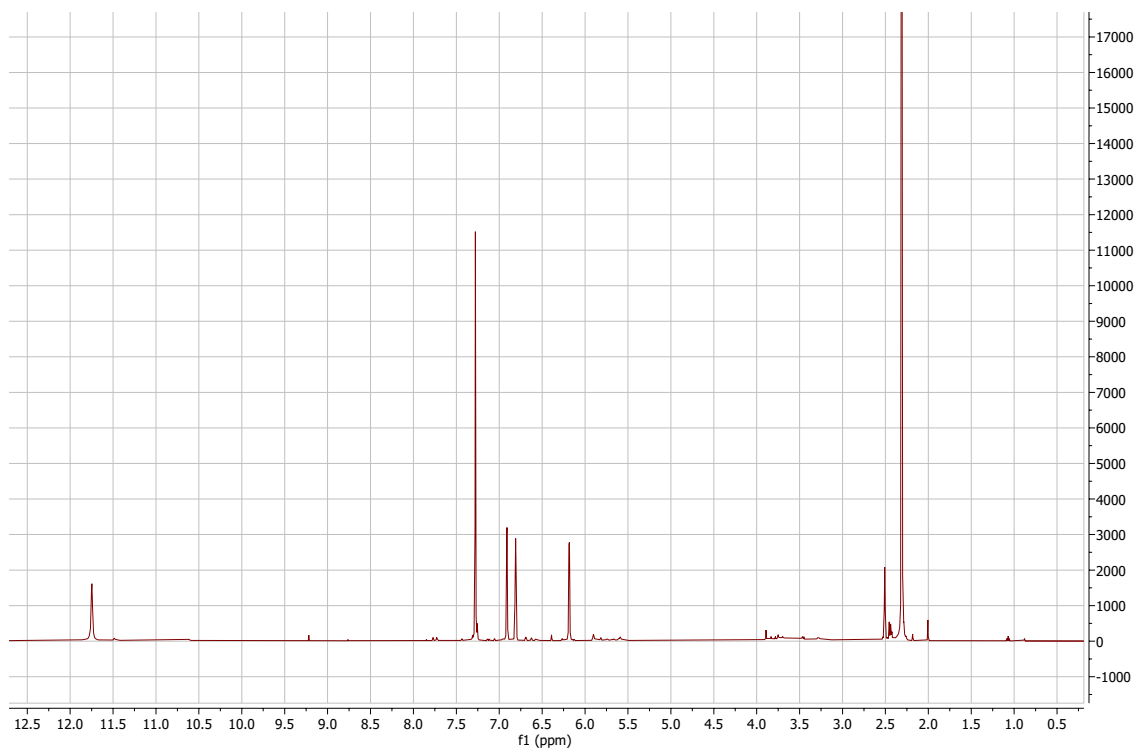
¹H-NMR

2-(4-fluorophenyl)-5,6-dimethyl-1H-1,3-benzodiazole:
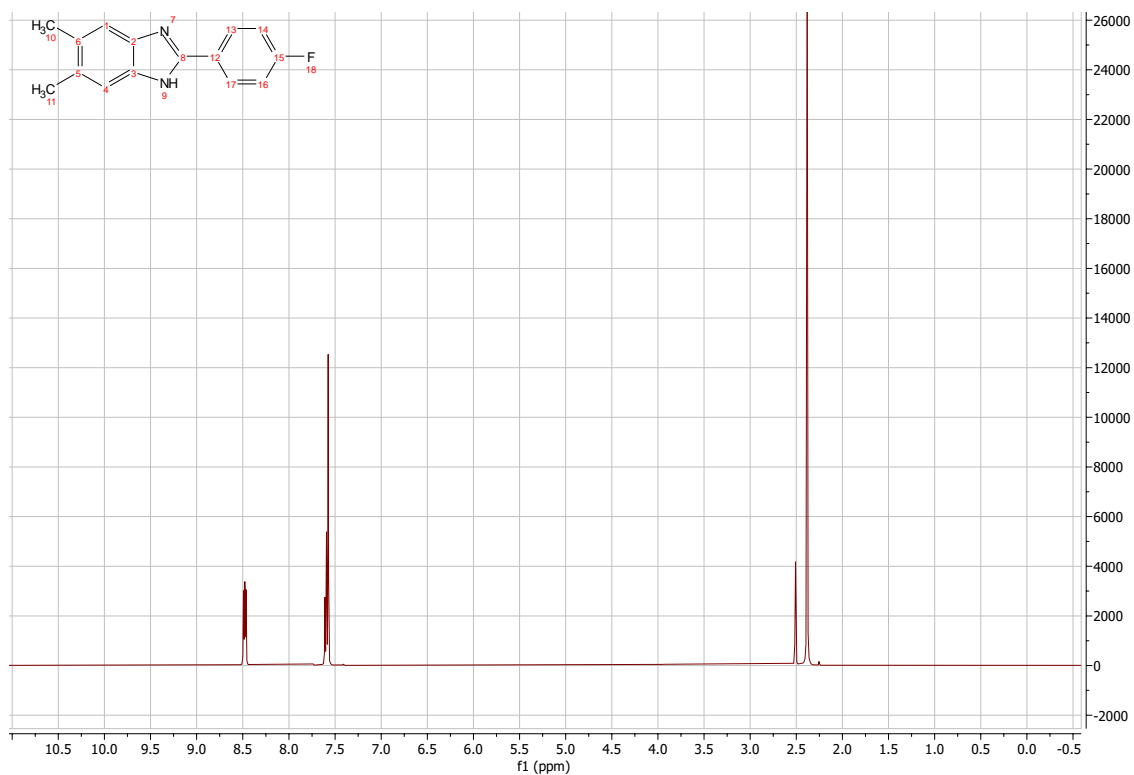
¹H-NMR

3-(5,6-dimethyl-1H-1,3-benzodiazol-2-yl)phenol:
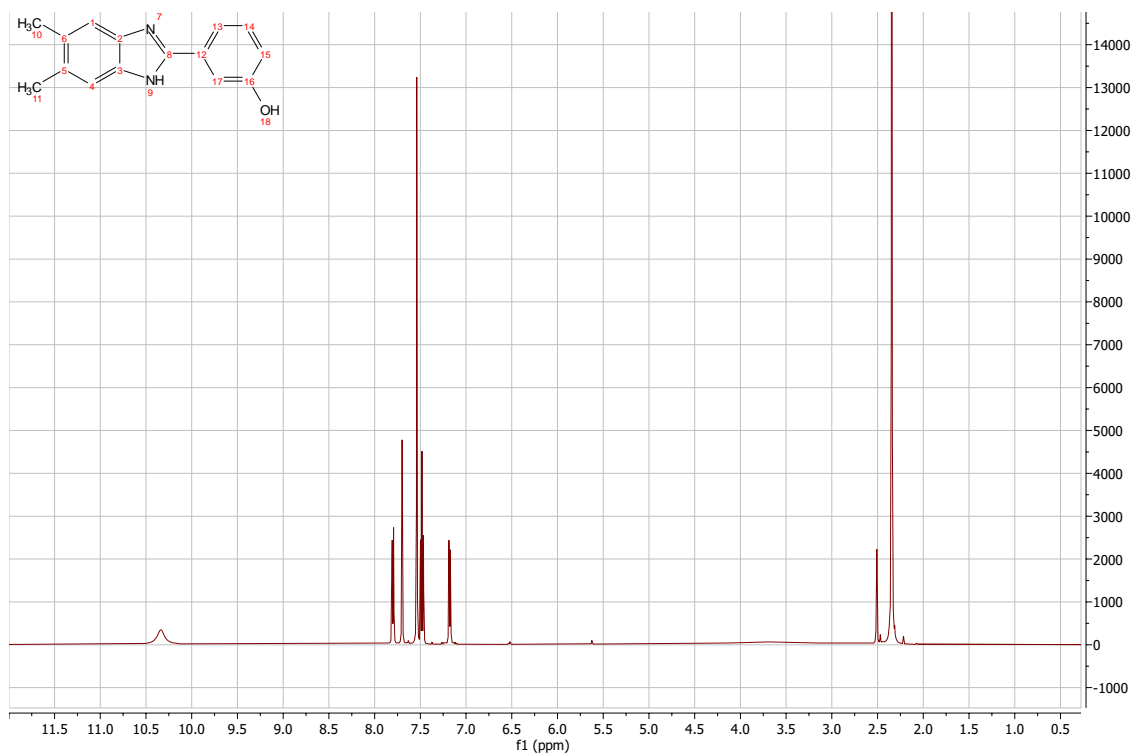
¹H-NMR

5-fluoro-2-phenyl-1H-1,3-benzodiazole:
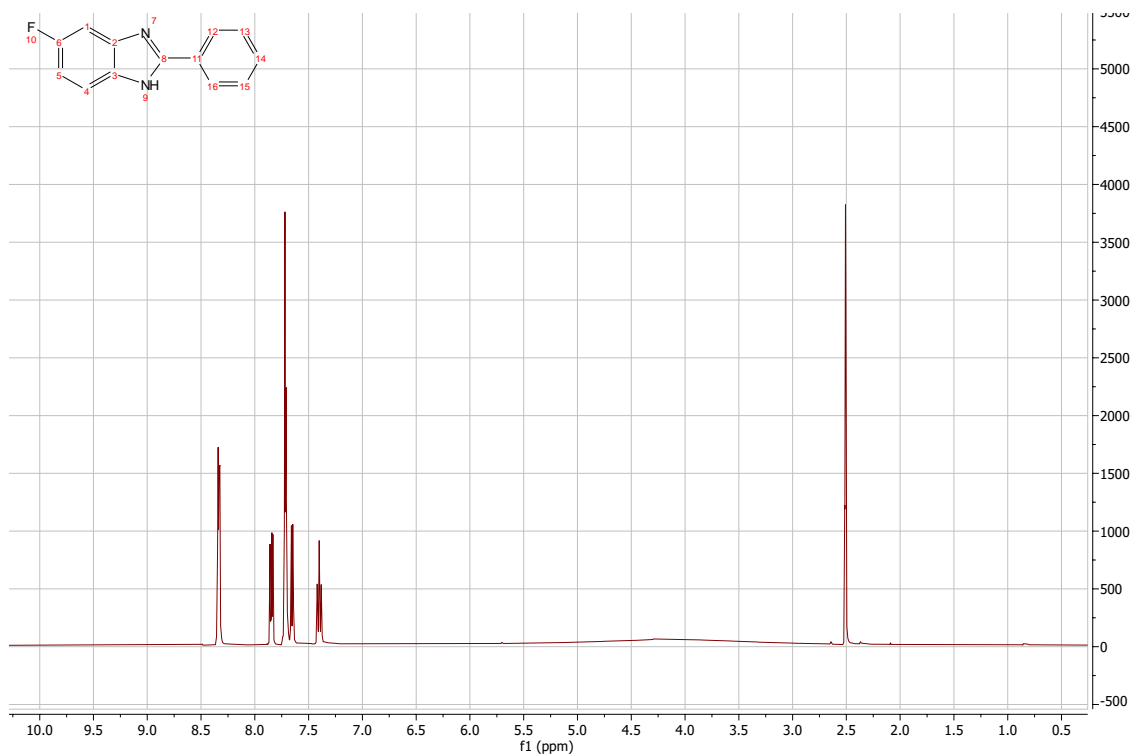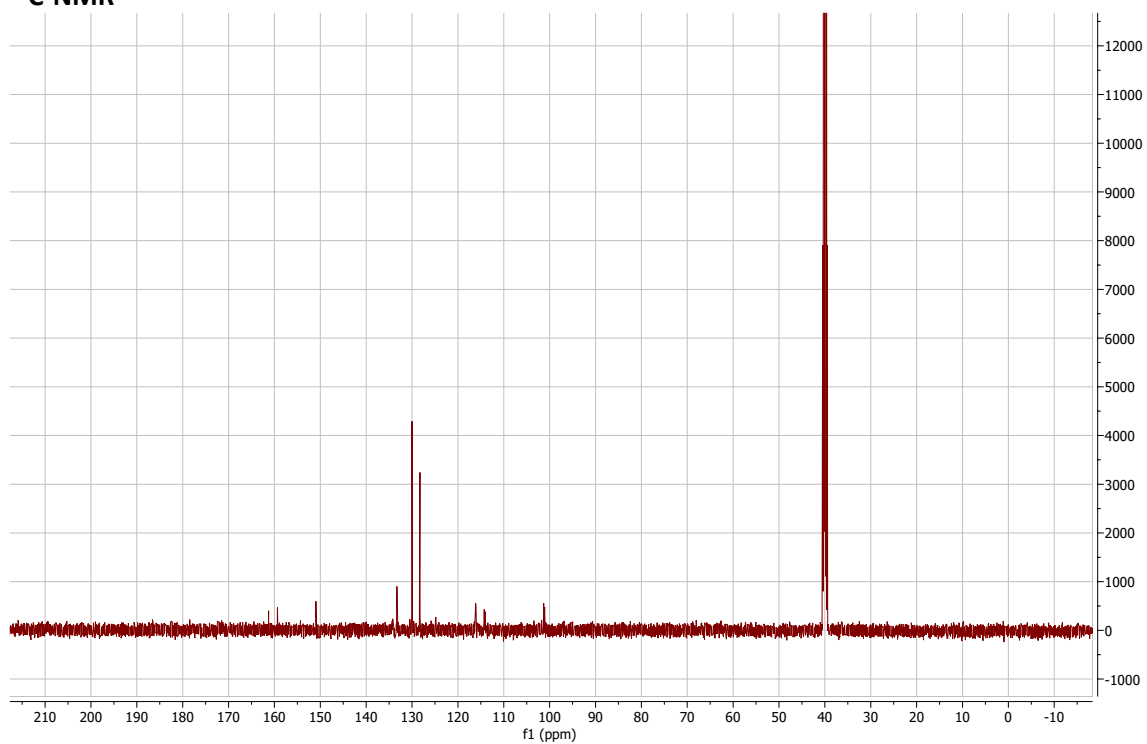
¹H-NMR

¹³C-NMR

HSQC

20220531_CH-442_clean_HSQC.10.ser

HMBC

20220531_CH-442_clean_HMBC.10.ser

2-(4-chlorophenyl)-5-fluoro-1H-1,3-benzodiazole:
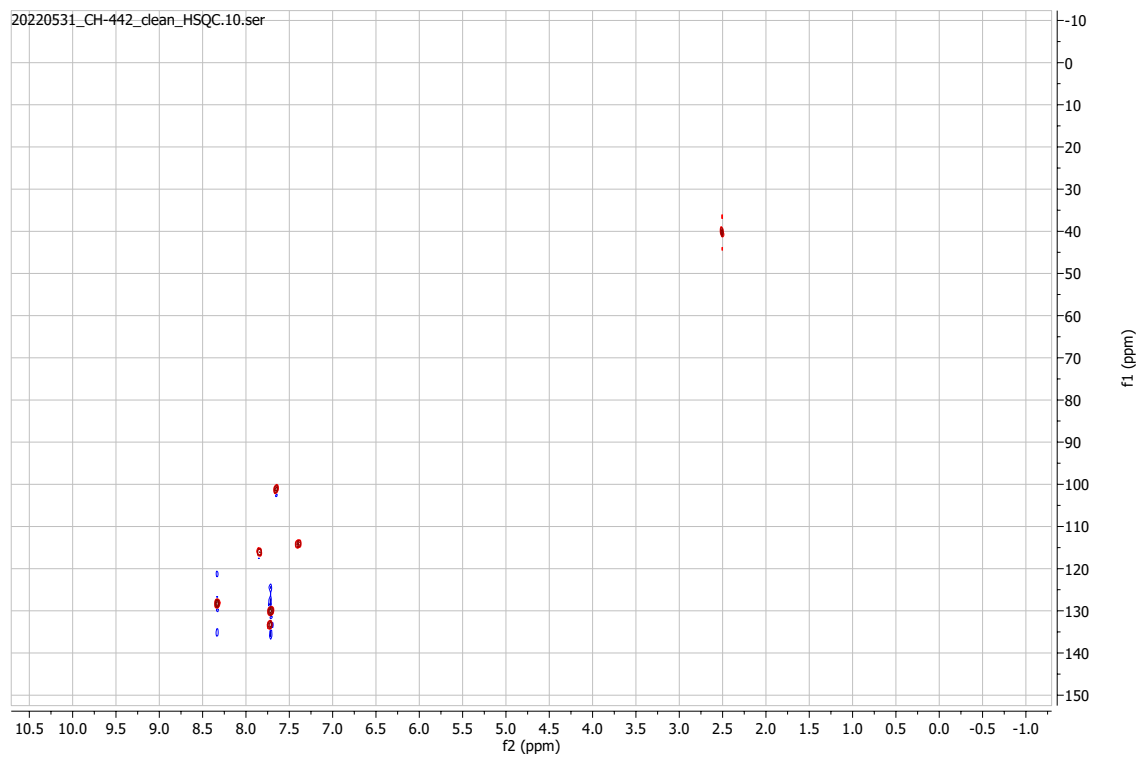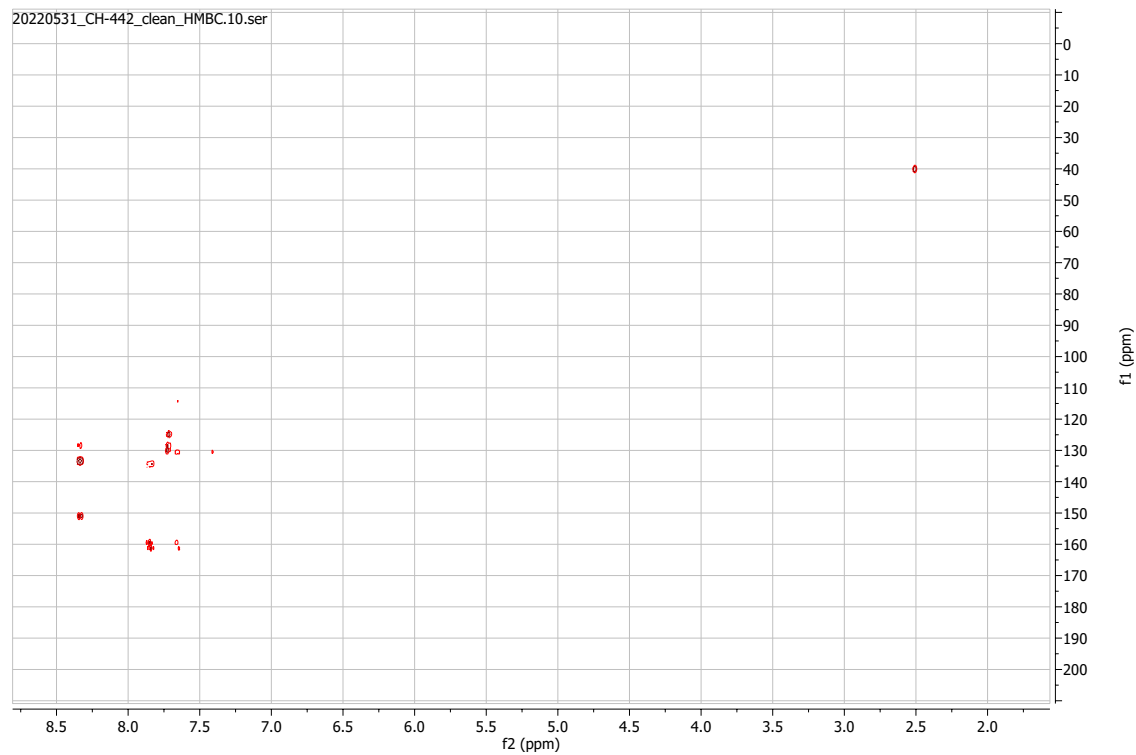
^{1}H-NMR

¹³C-NMR

¹³C-NMR

HSQC

20220504_CH-426-clean_HSQC.10.ser
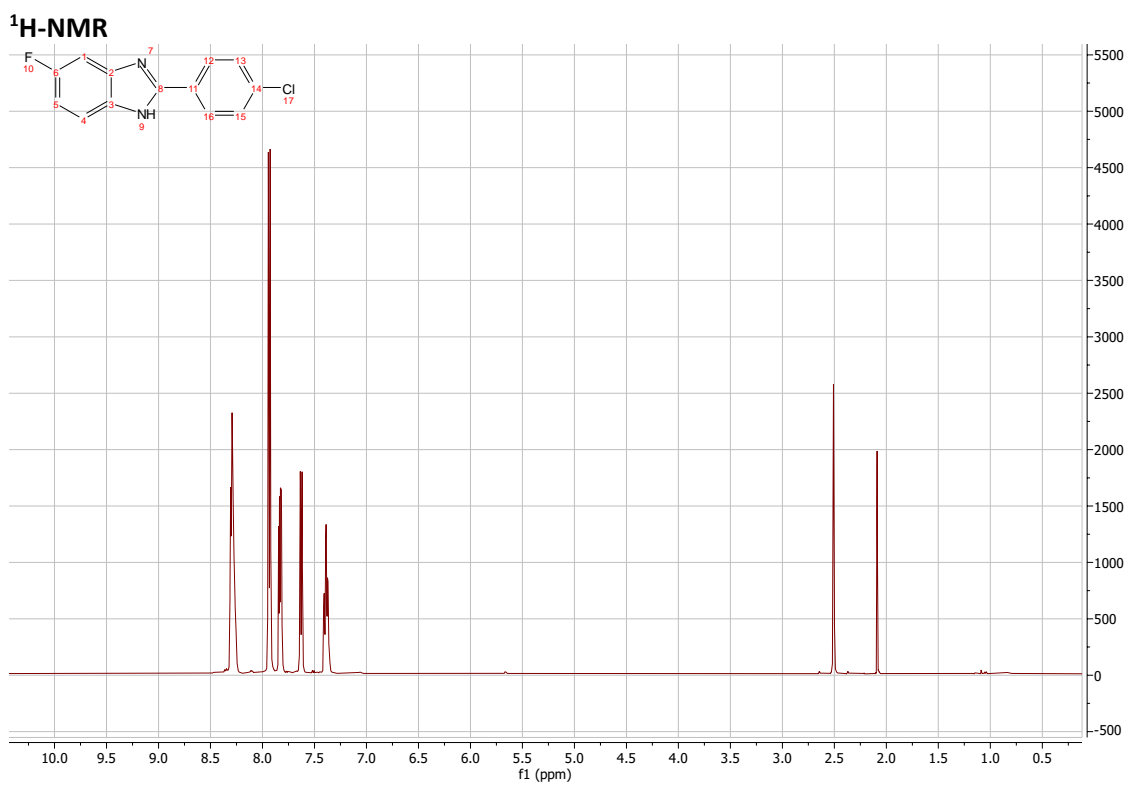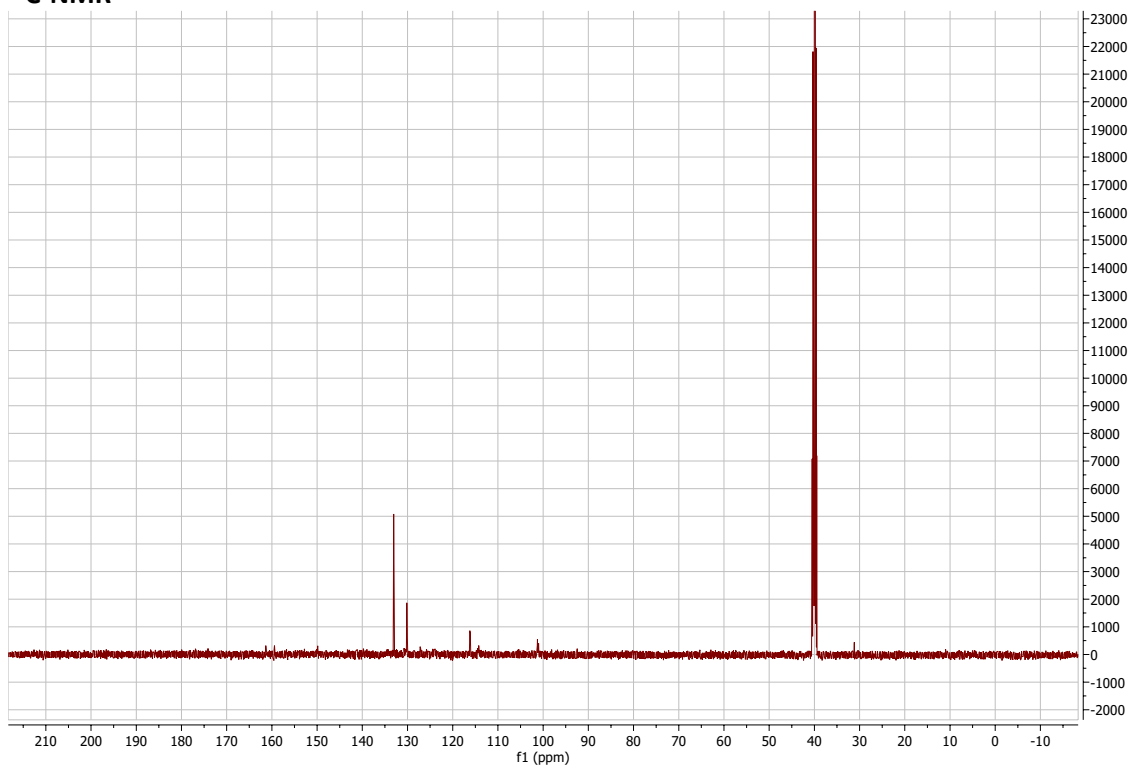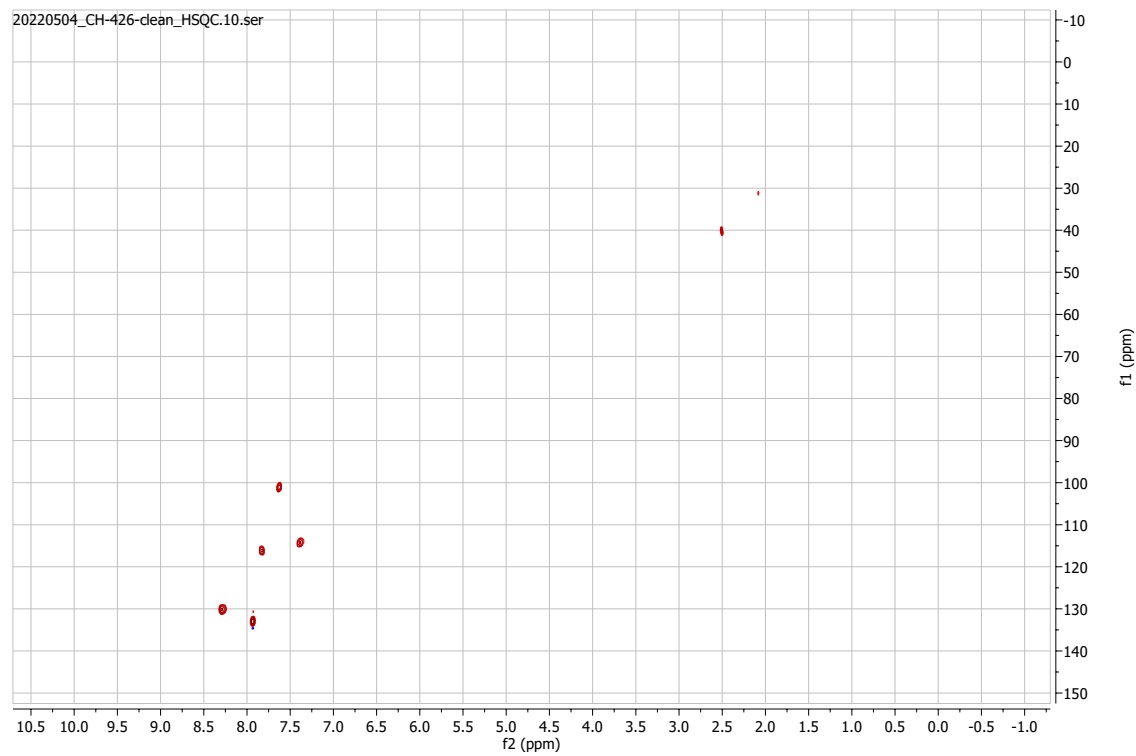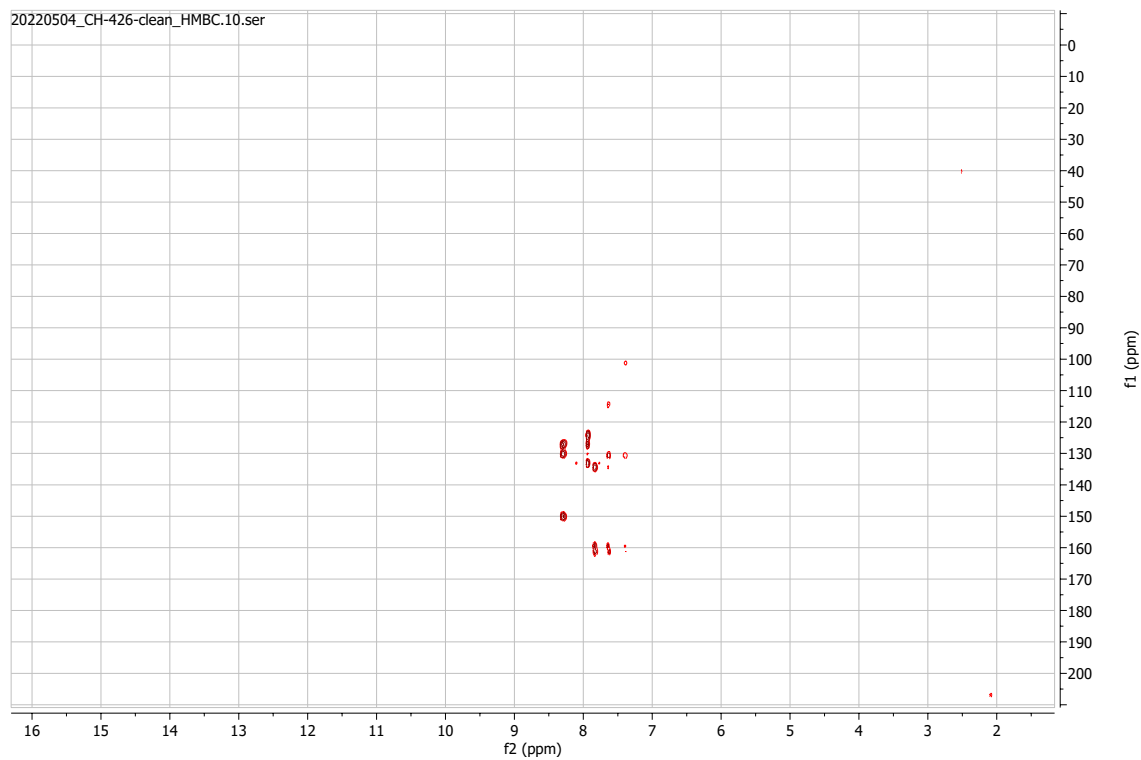
HMBC

4-(5-fluoro-1H-1,3-benzodiazol-2-yl)phenol:
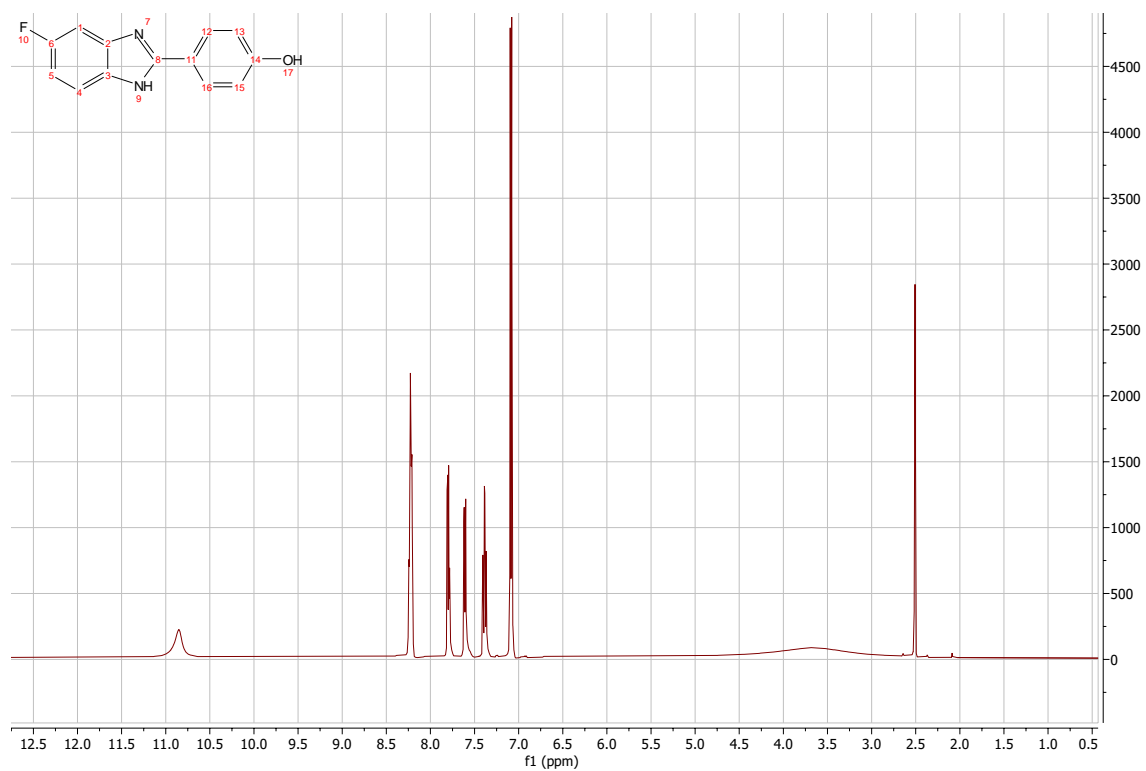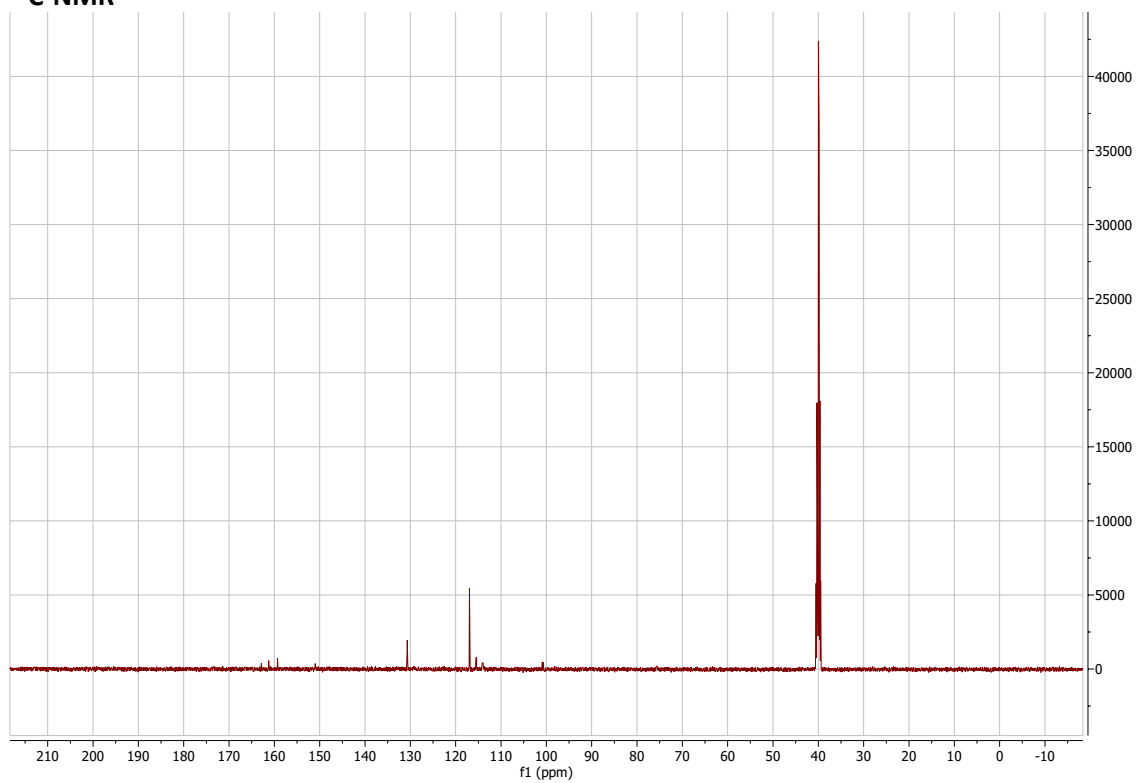
^{1}H-NMR

^{13}C-NMR

HSQC

20220509_CH428_clean_HSQC.10.ser
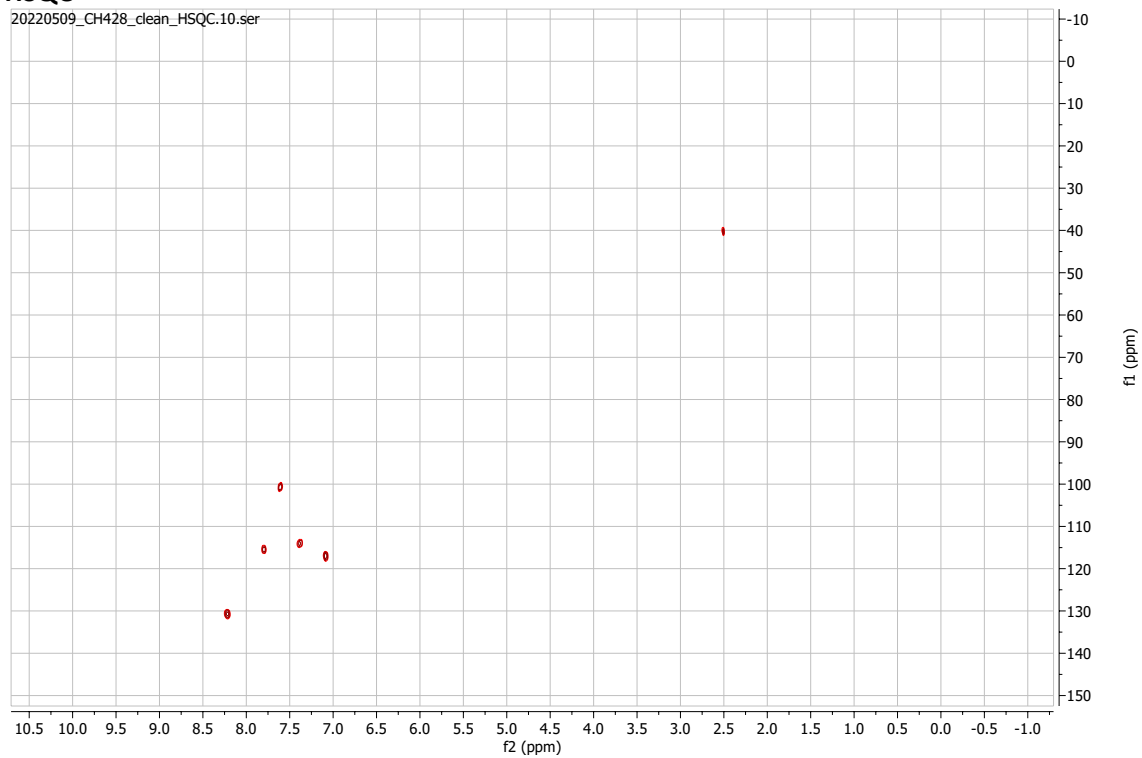
HMBC

20220509_CH428_clean_HMBC.10.ser
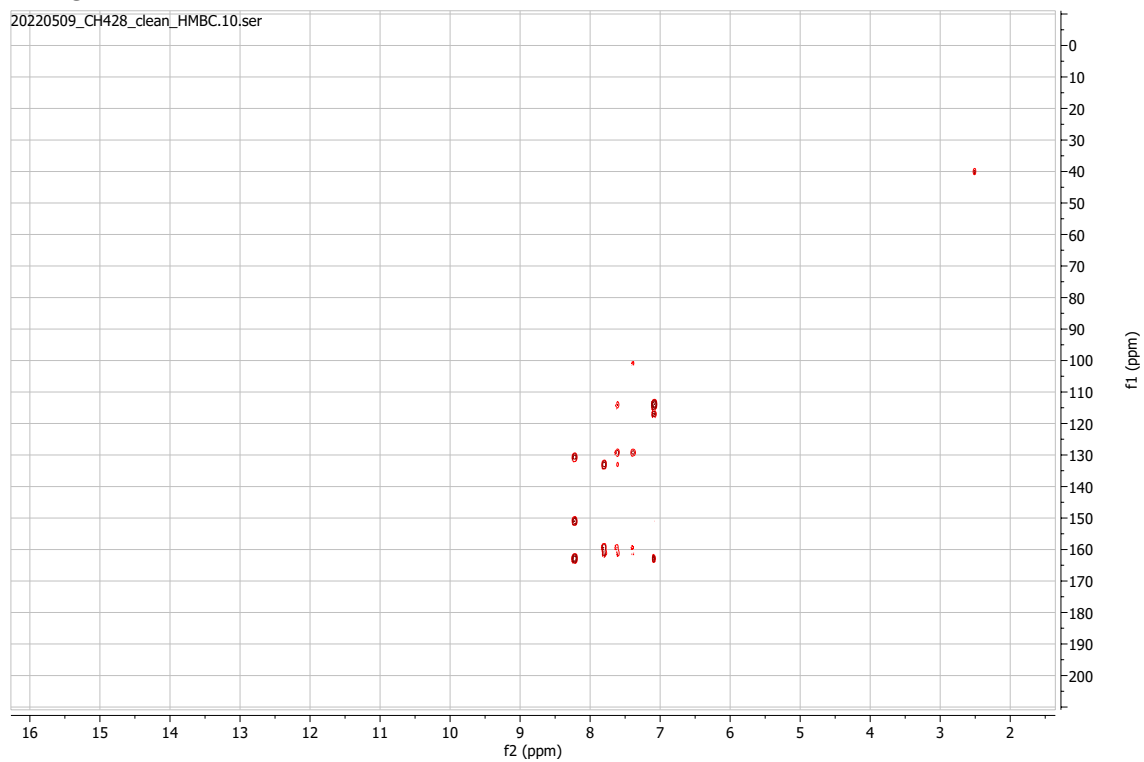
3-(5-fluoro-1H-1,3-benzodiazol-2-yl)phenol:
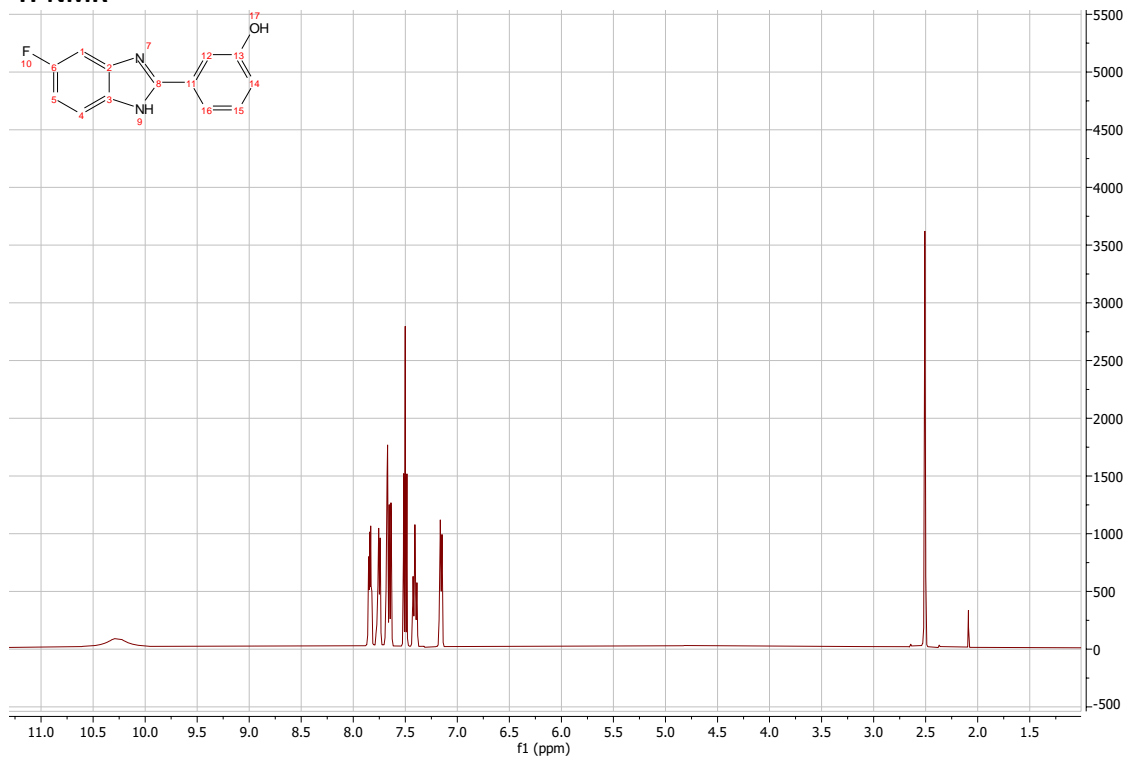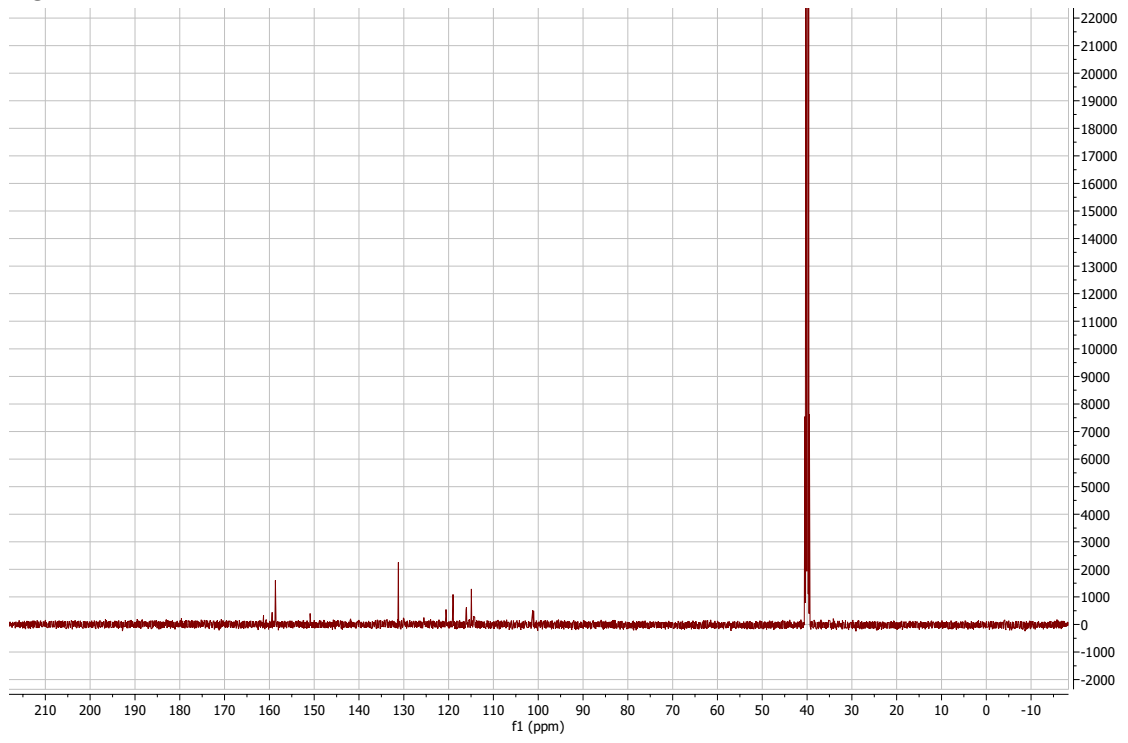
¹H-NMR

^{13}C-NMR

HSQC

20220512_CH429_HSQC.10.ser

HMBC

20220512_CH429_HMBC.10.ser
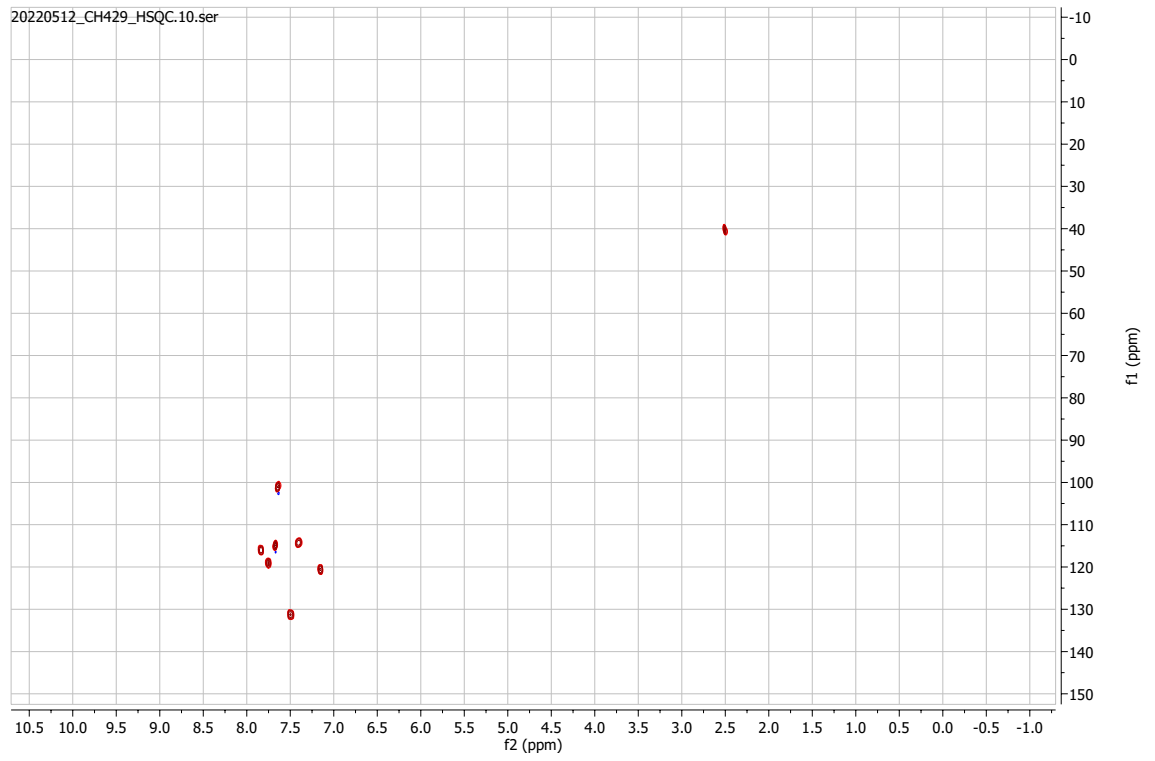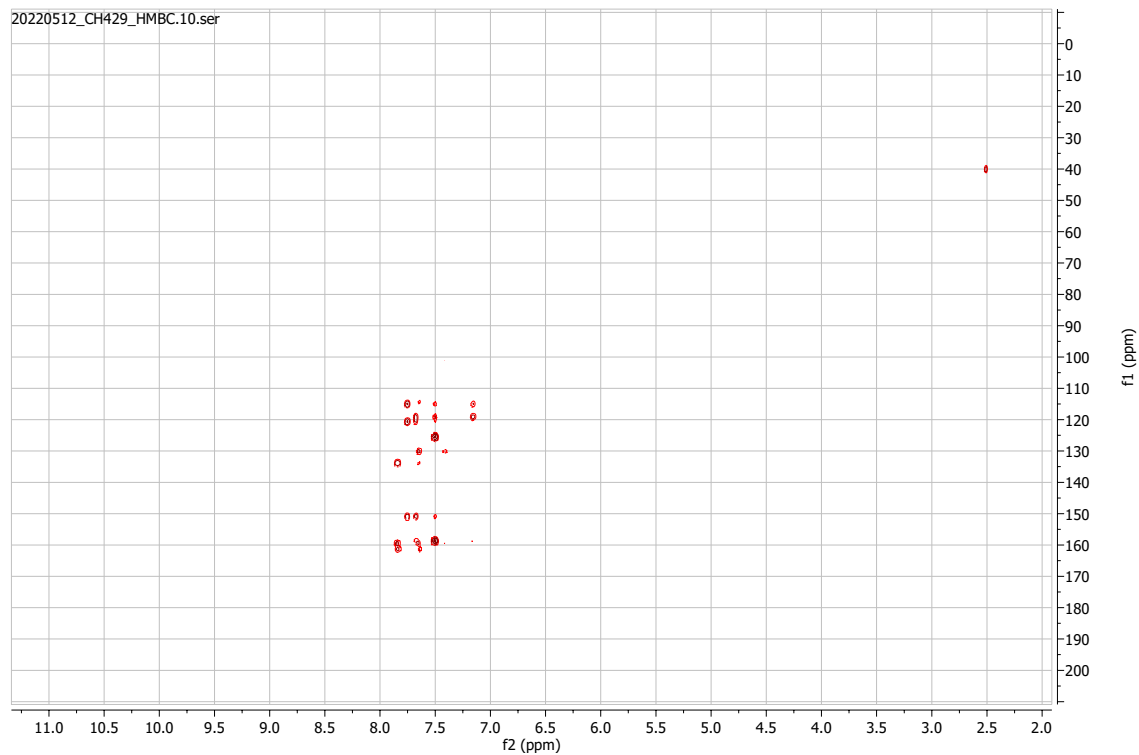
5-fluoro-2-(1H-pyrrol-2-yl)-1H-1,3-benzodiazole:
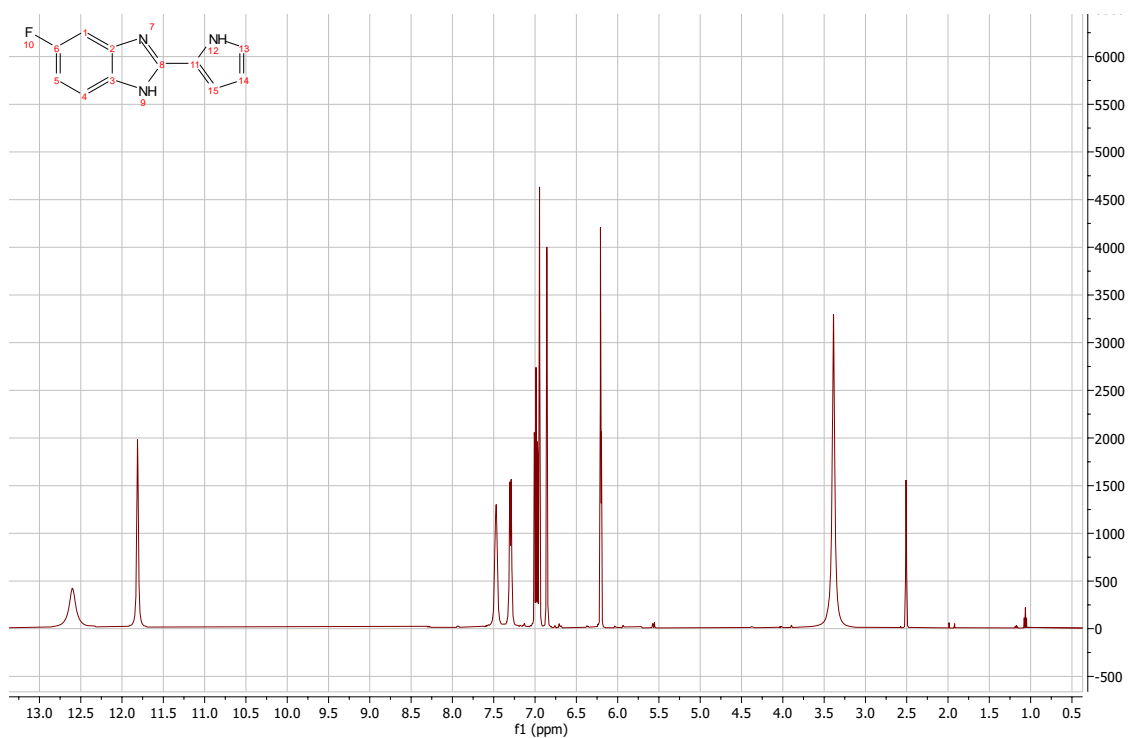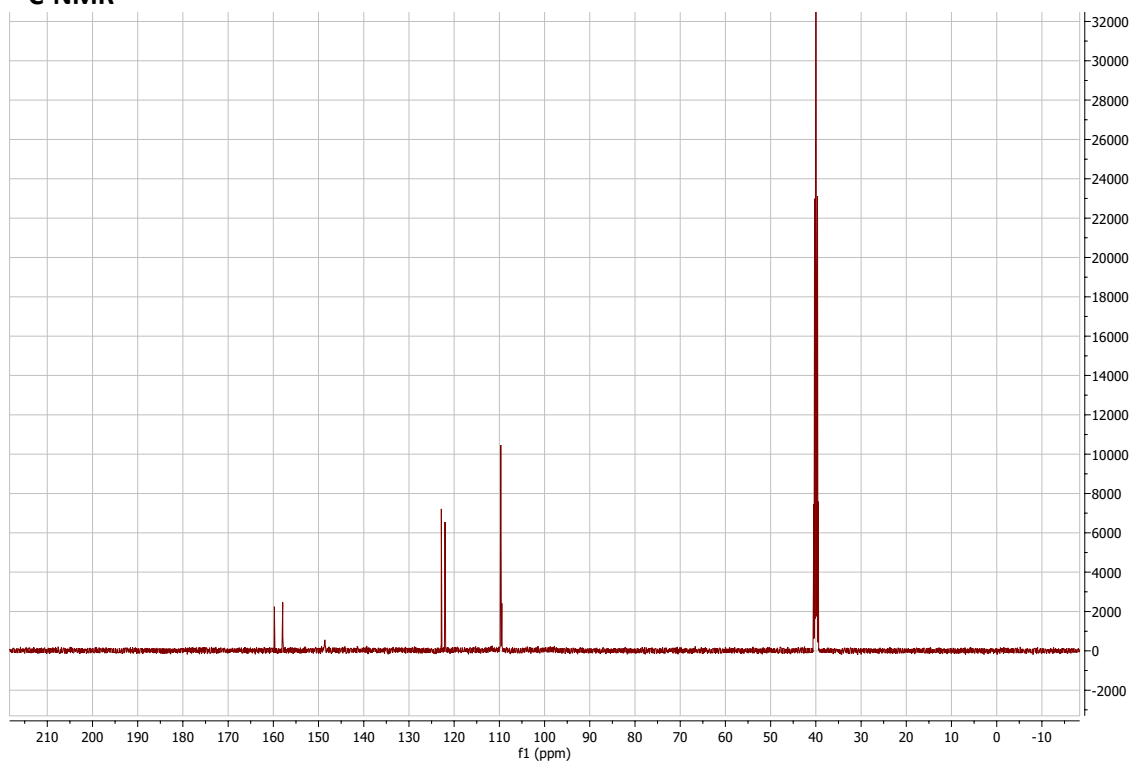
¹H-NMR

¹³C-NMR

HSQC

20220427_CH-424_HSQC.10.ser

HMBC

20220427_CH-424_HMBC.10.ser
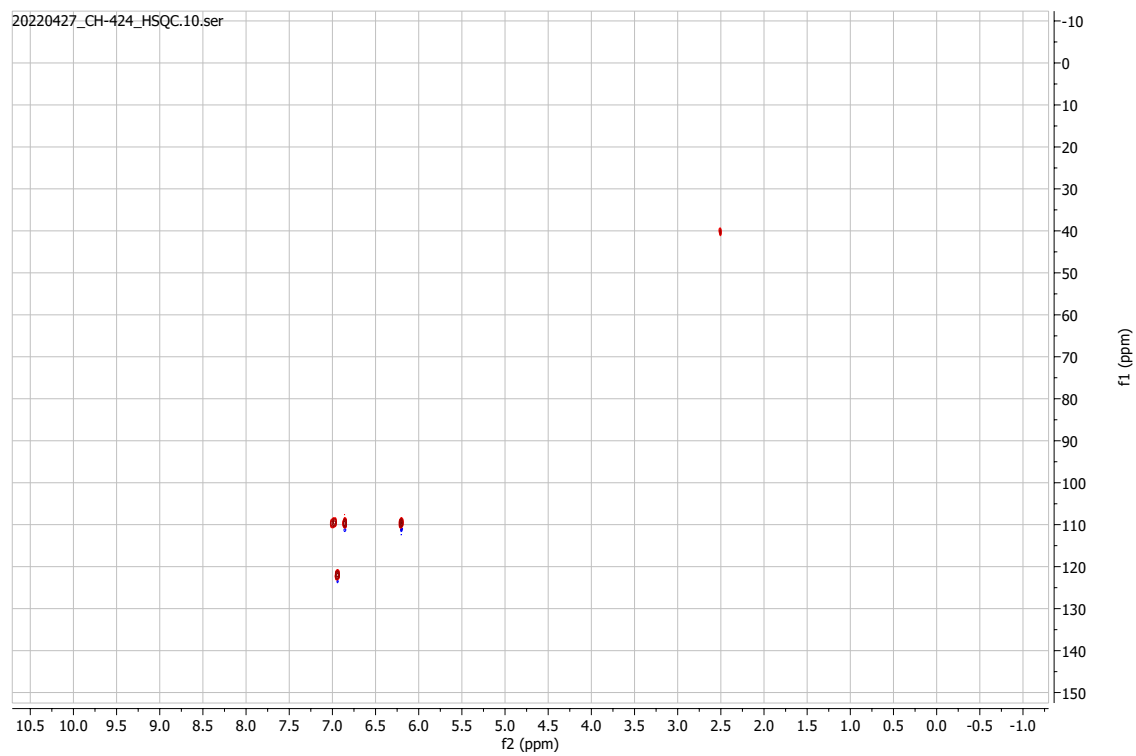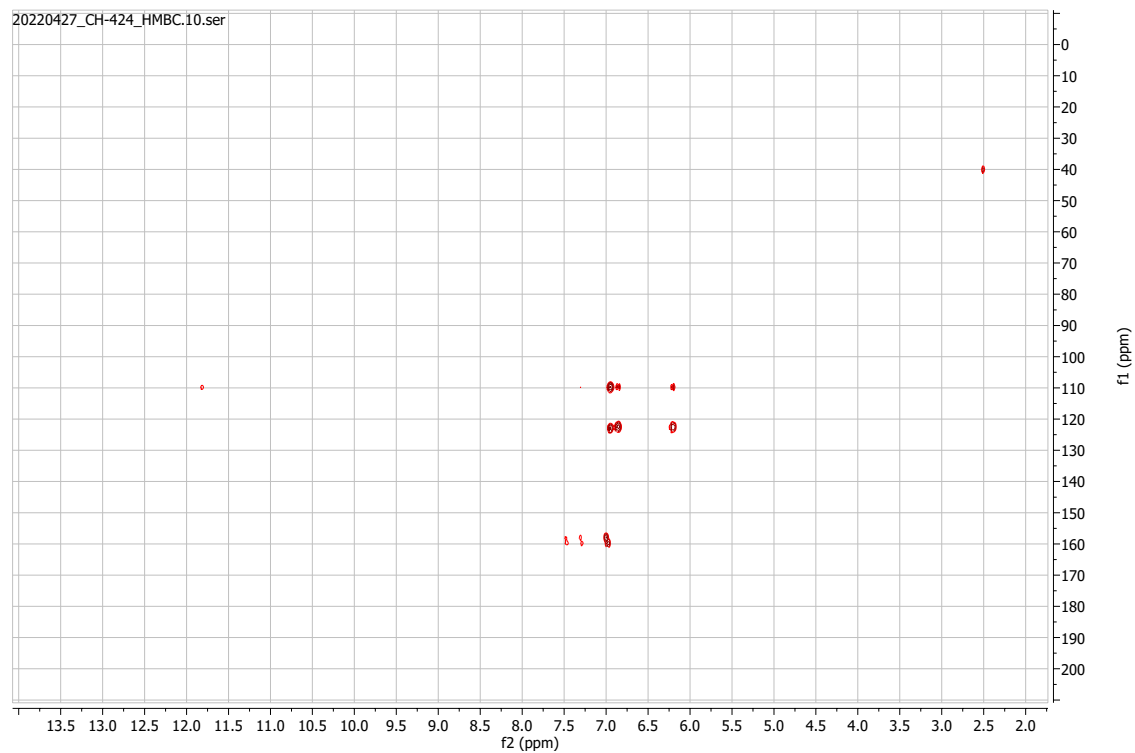
2-(1H-1,3-benzodiazol-6-yl)-5-chloro-1H-1,3-benzodiazole:

¹H-NMR

¹³C-NMR

HSQC

20220504_CH-430_HSQC.10.ser

HMBC

2-(1H-1,3-benzodiazol-6-yl)-1H-1,3-benzodiazole-5-carboxylic acid:
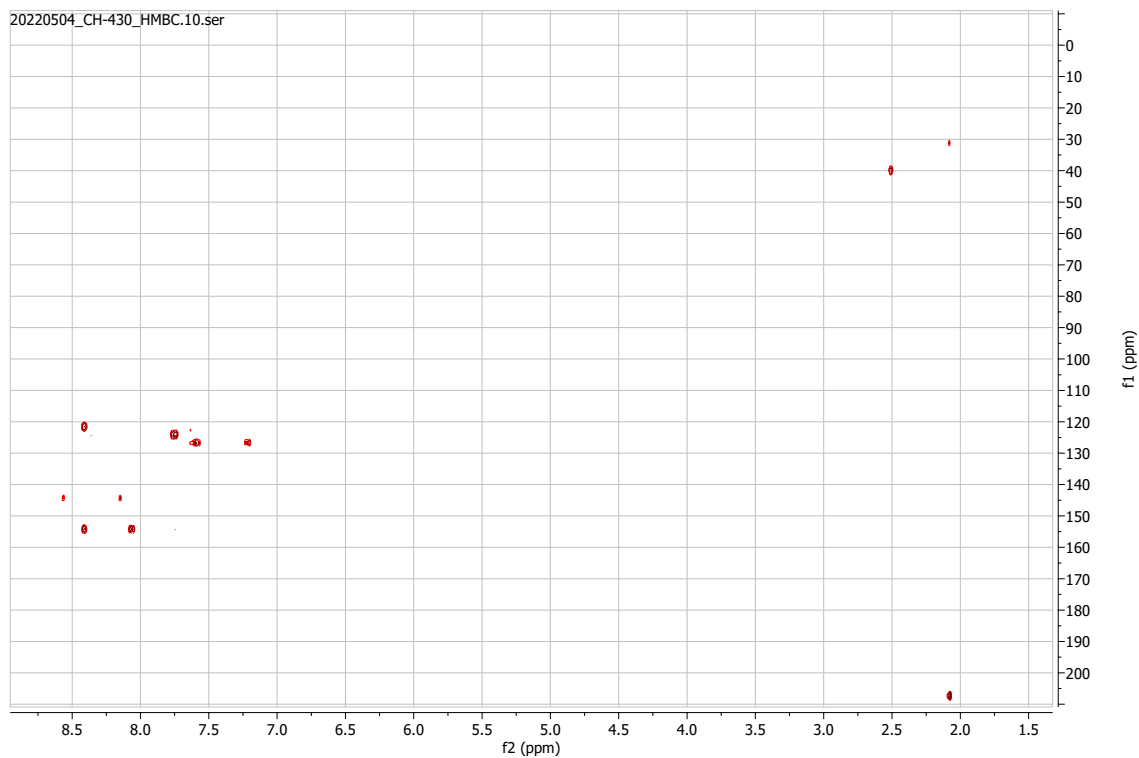
^{1}H-NMR

HSQC

20220504_CH-431_HSQC.10.ser

HMBC

20220504_CH-431_HMBC.10.ser
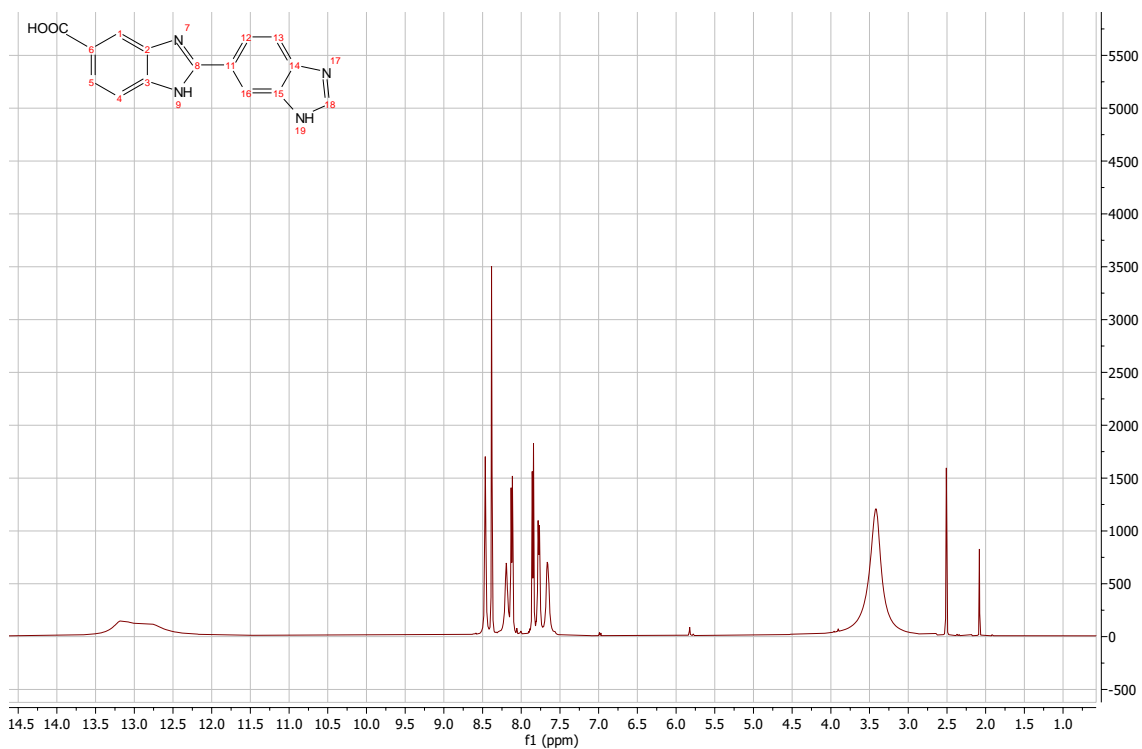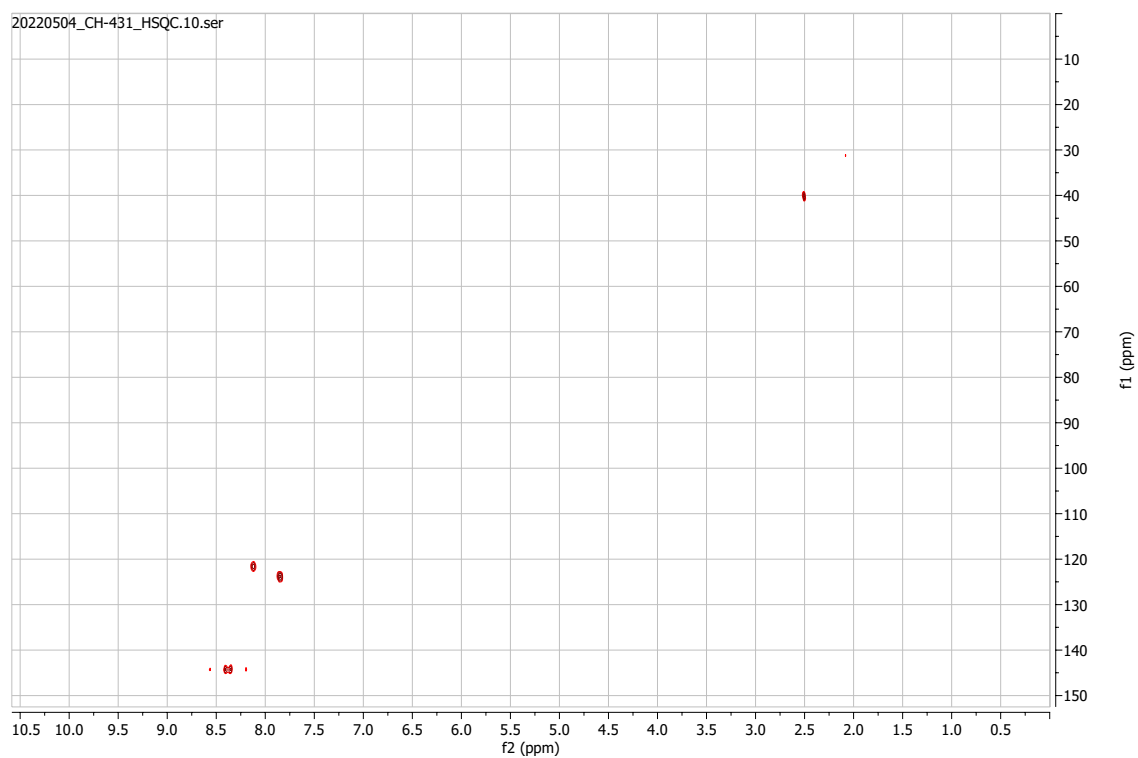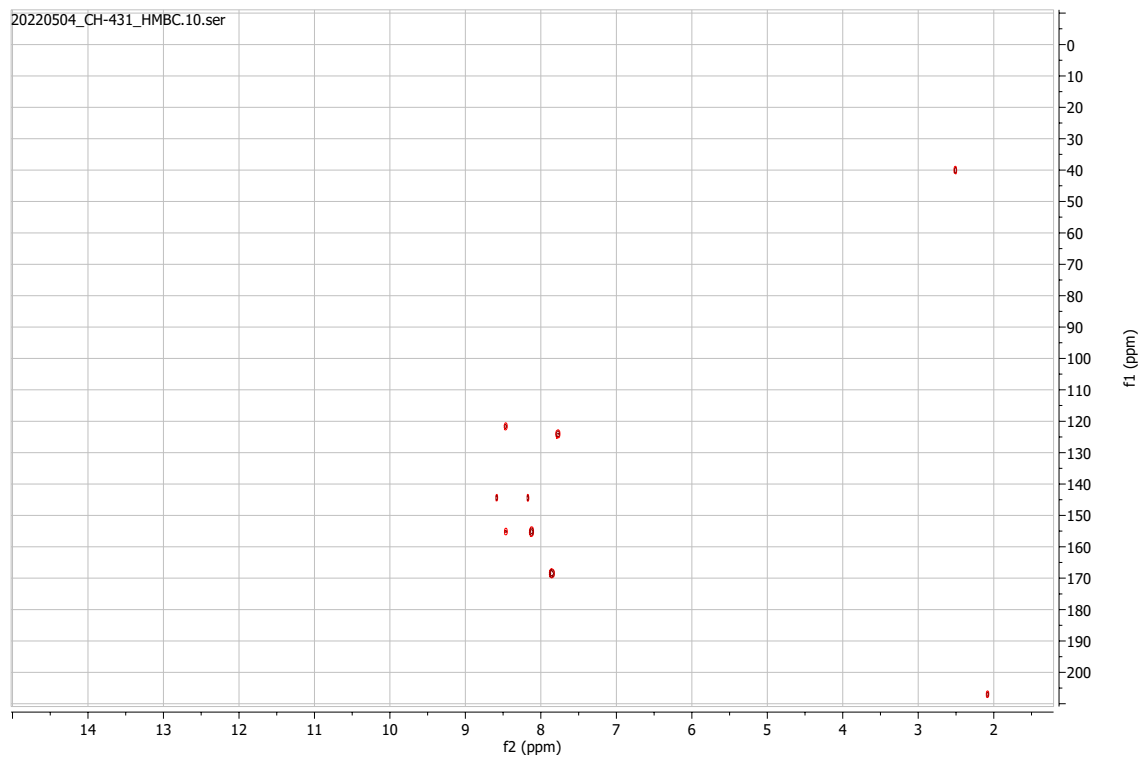
2-(4-nitrophenyl)-1H-1,3-benzodiazole:
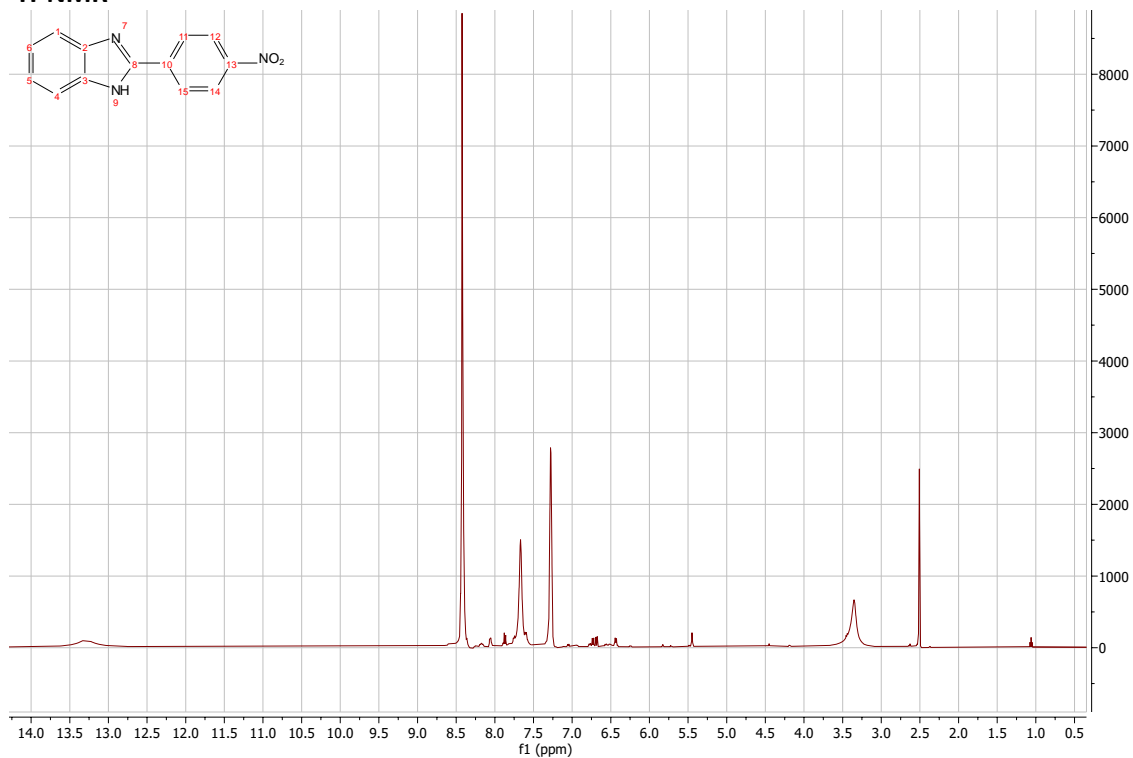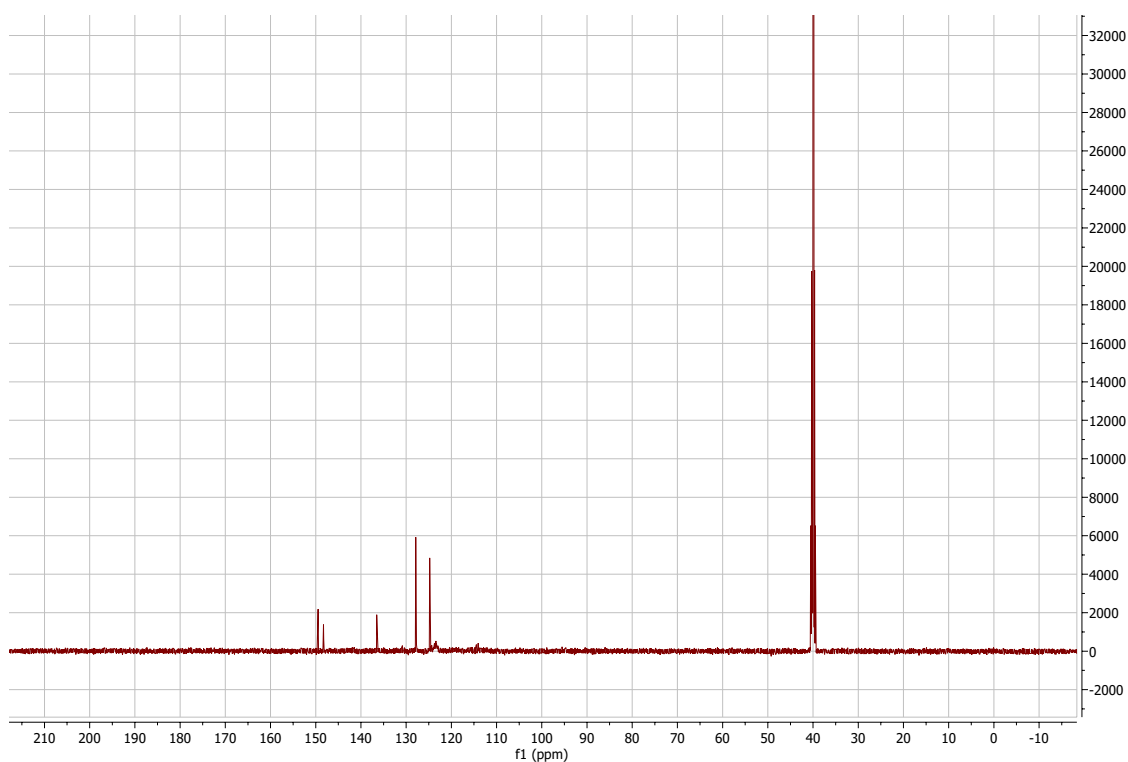
^{1}H-NMR

^{13}C-NMR

HSQC

20220509_CH436_HSQC.10.ser
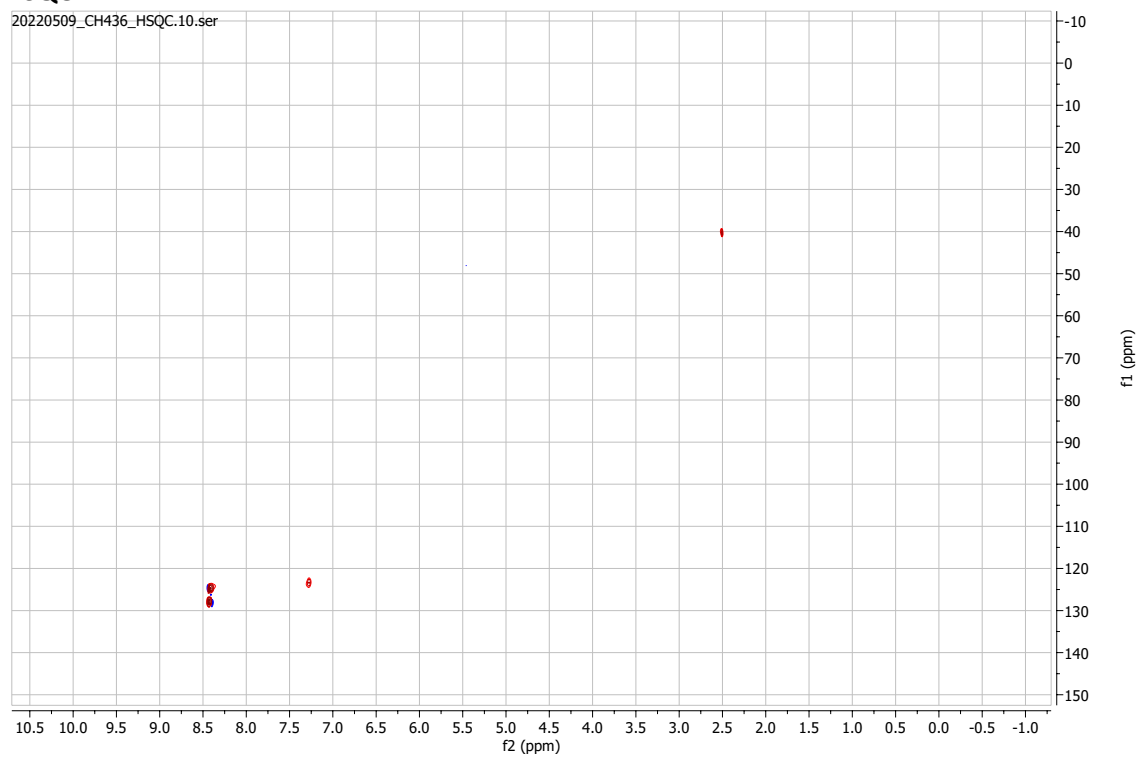
HMBC

20220509_CH436_HMBC.10.ser
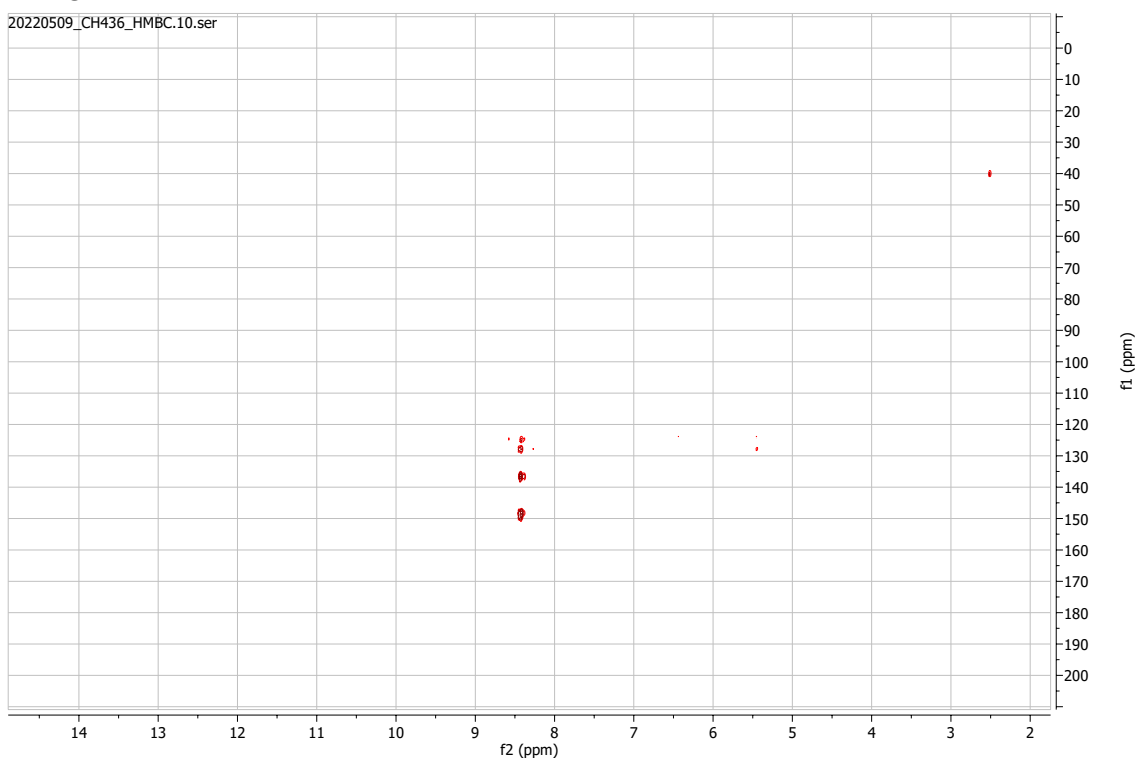
5-chloro-2-(4-nitrophenyl)-1H-1,3-benzodiazole:

¹H-NMR

HSQC

HMBC

20220509_CH437_HMBC.10.ser
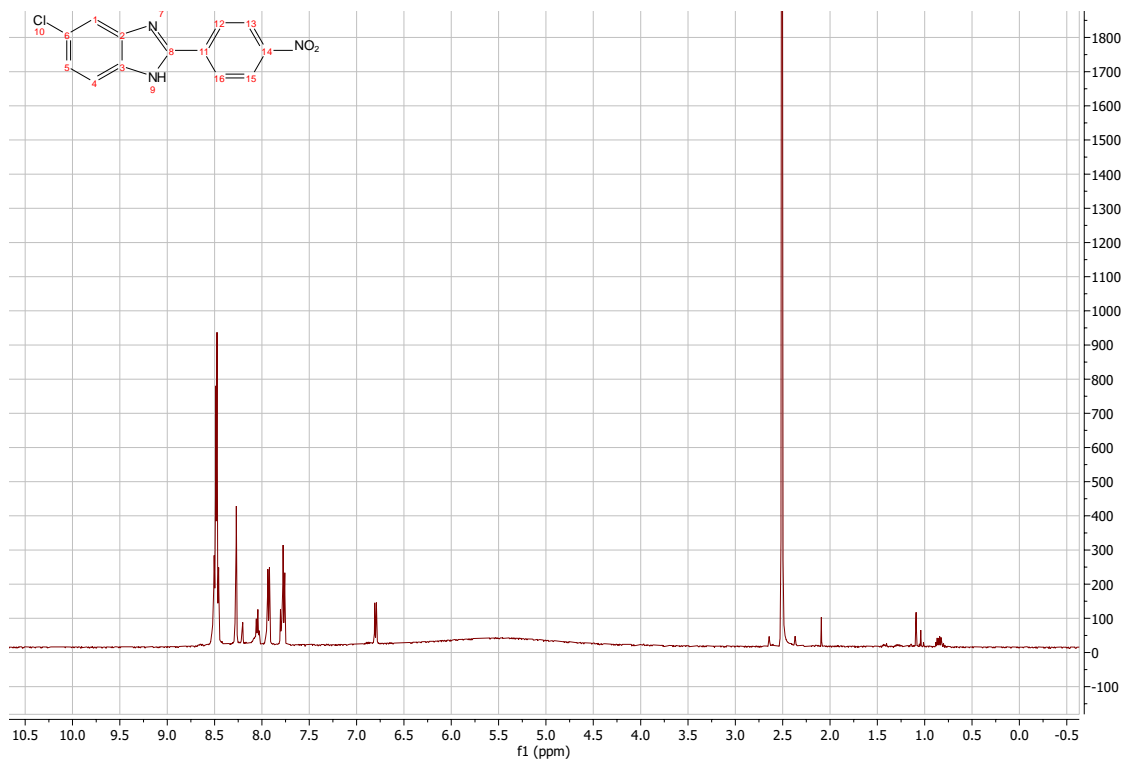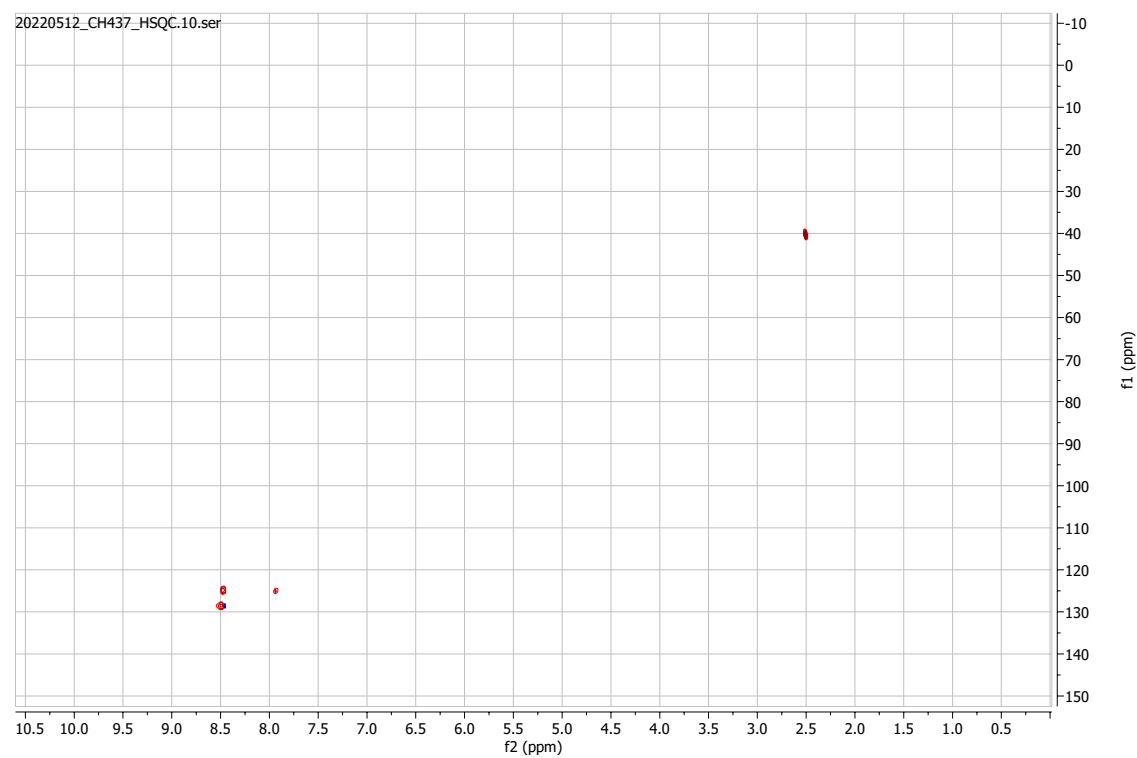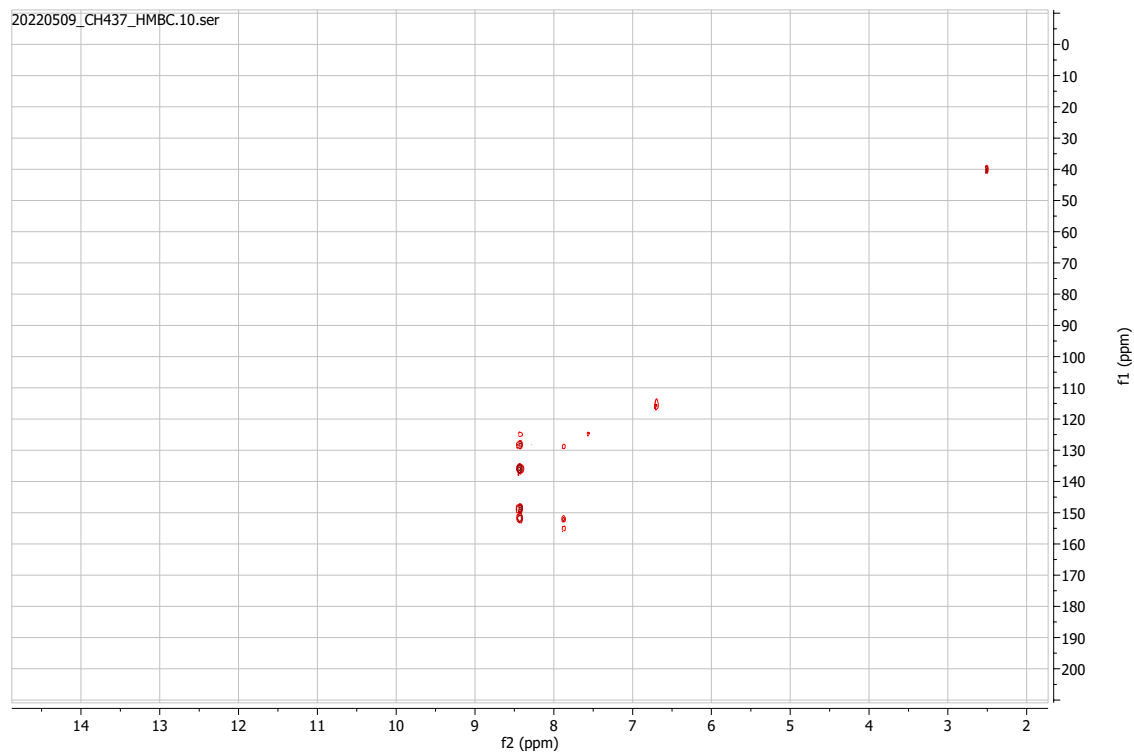
2-(4-nitrophenyl)-5-phenyl-1H-1,3-benzodiazole:
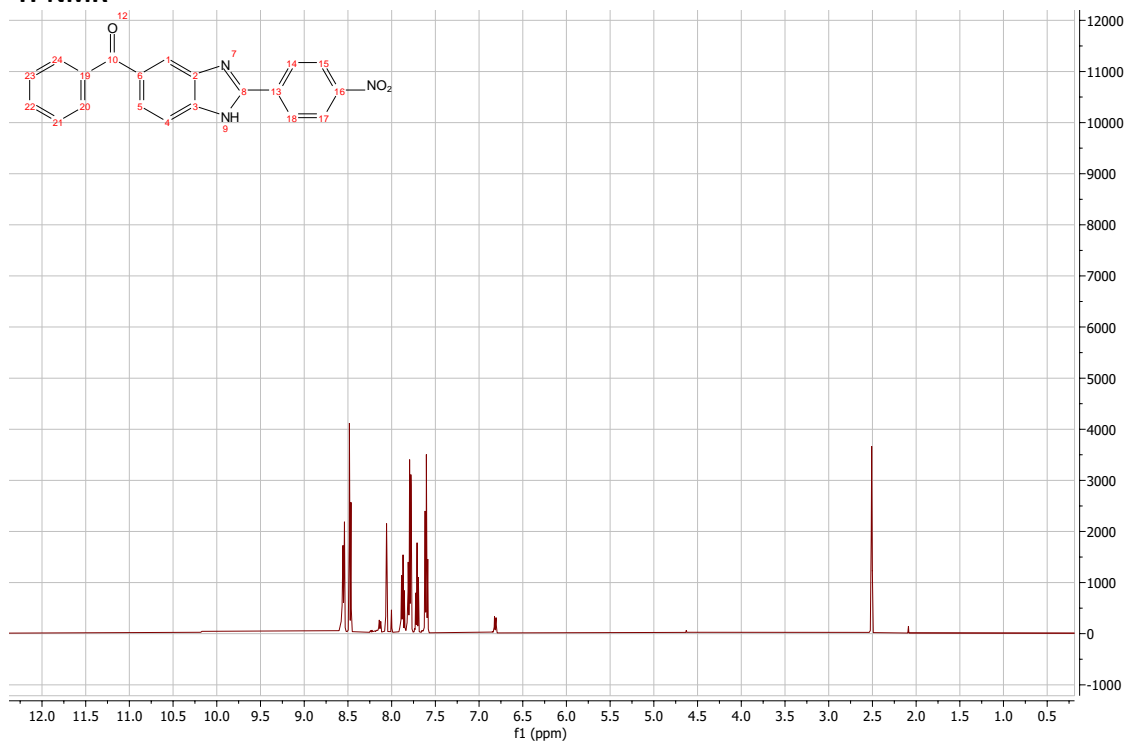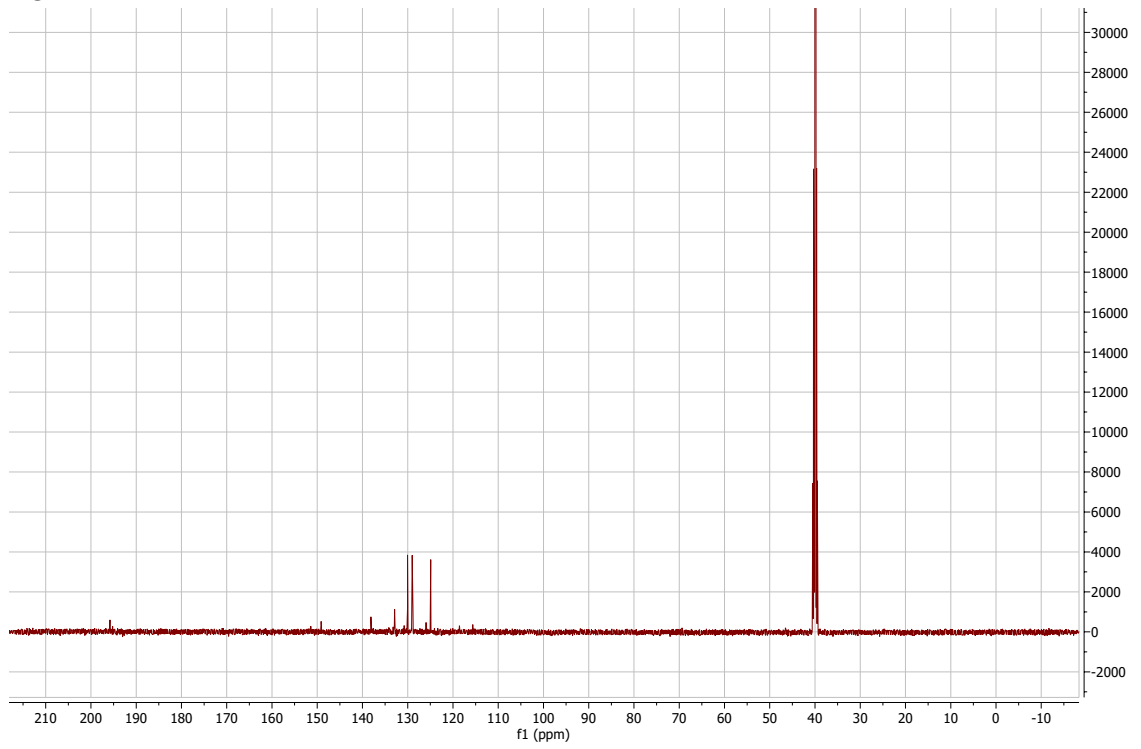
¹H-NMR

¹³C-NMR

HSQC

20220512_CH438_HSQC.10.ser
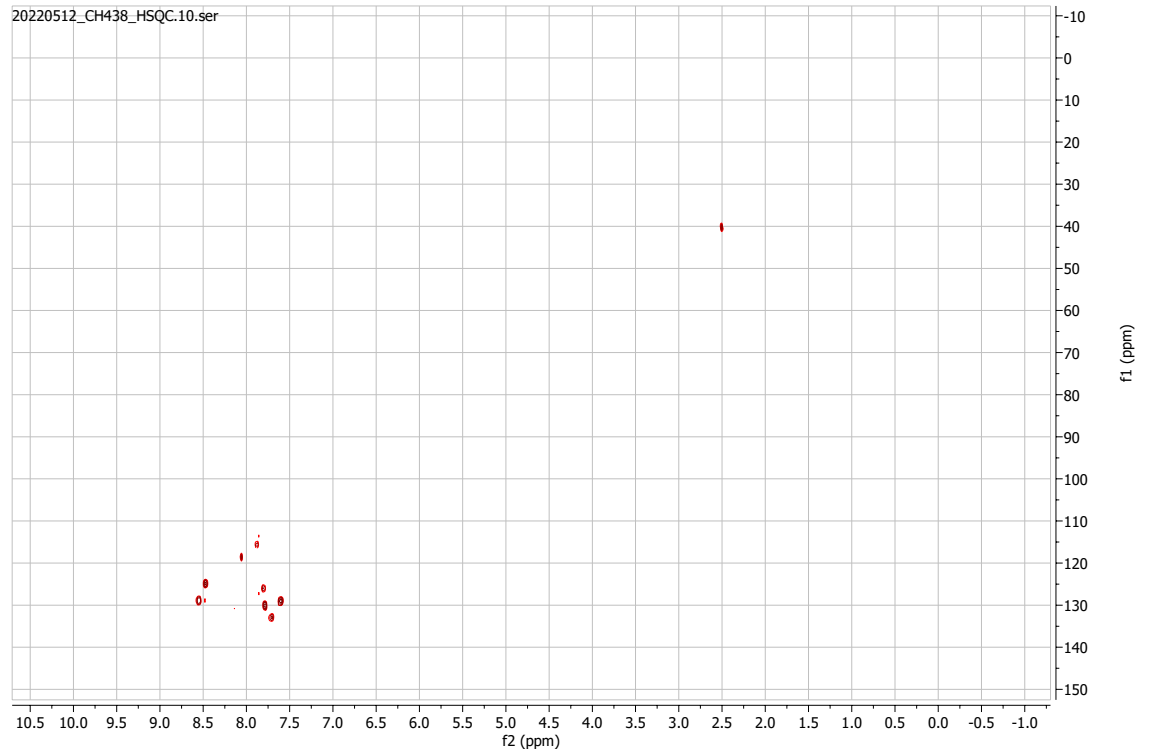
HMBC

2-(4-nitrophenyl)-1H-1,3-benzodiazole-5-carboxylic acid:
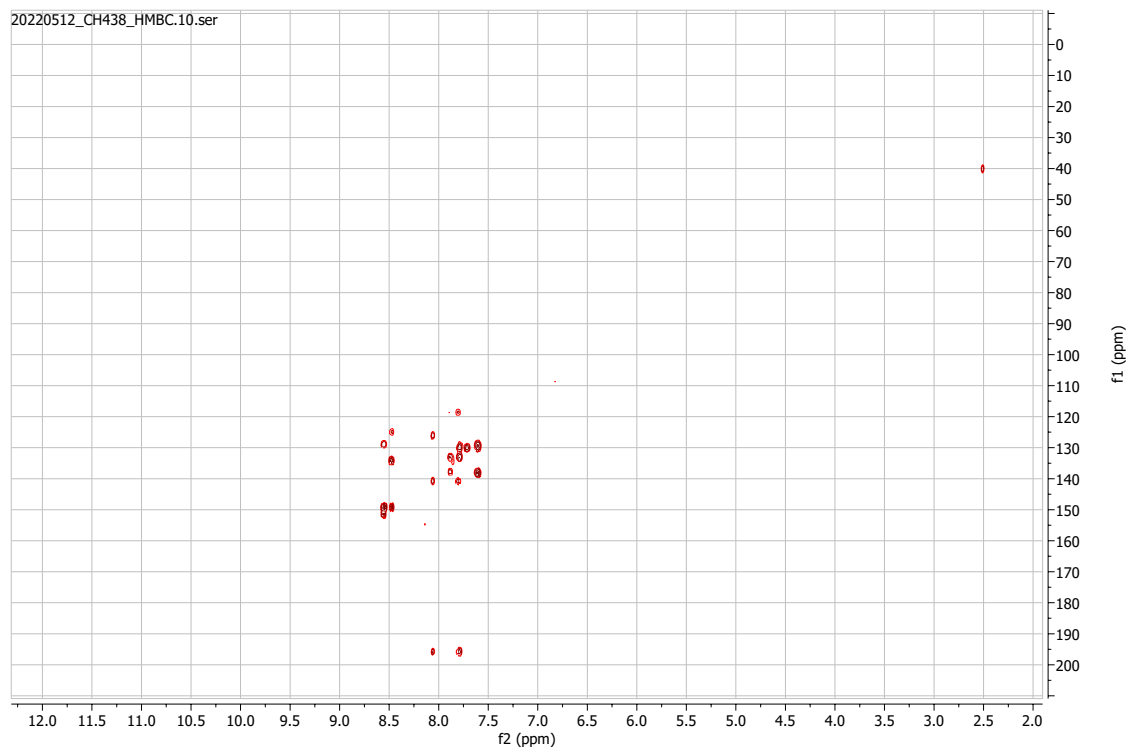
¹H-NMR

390

HSQC

20220512_CH439_HSQC.10.ser

HMBC
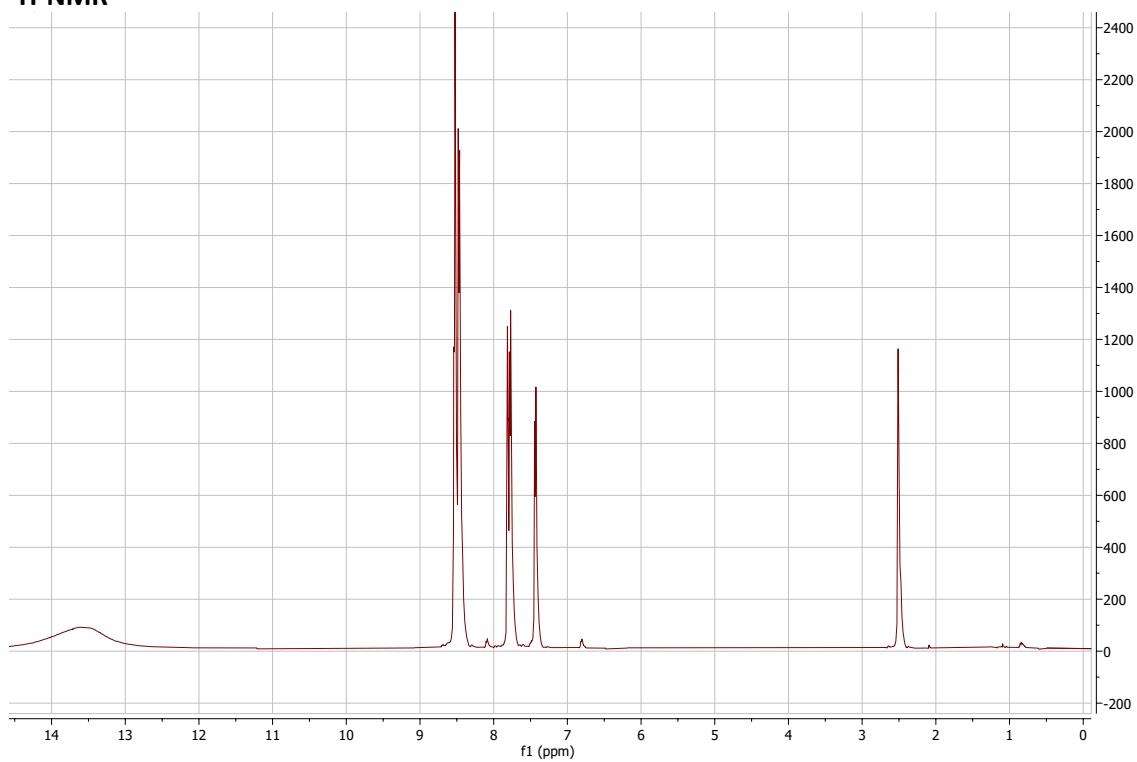
20220512_CH439_HMBC.10.ser
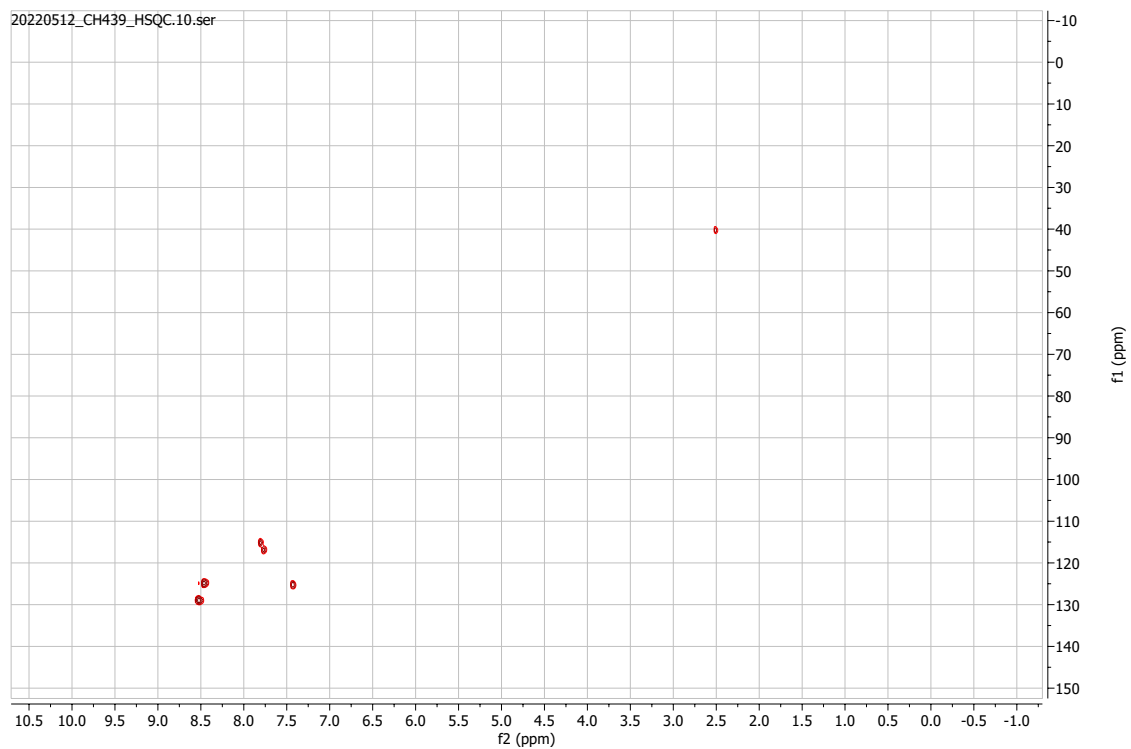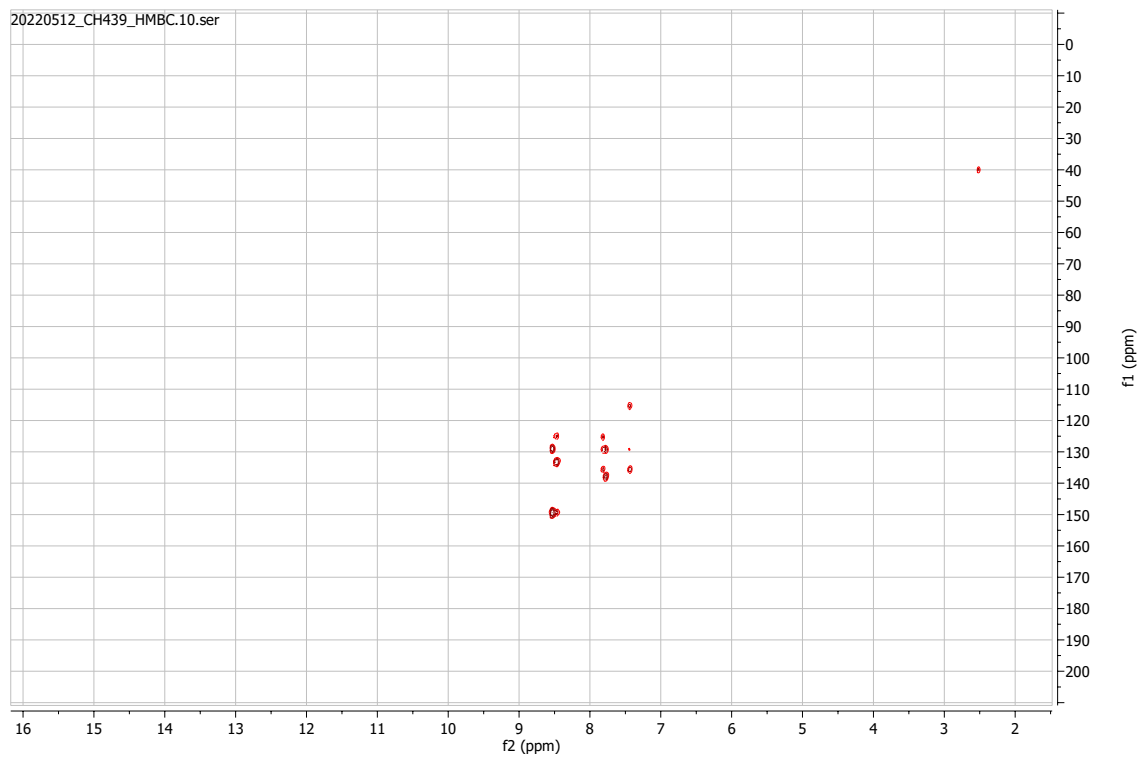
2-(4-methylphenyl)-1H-1,3-benzodiazole:
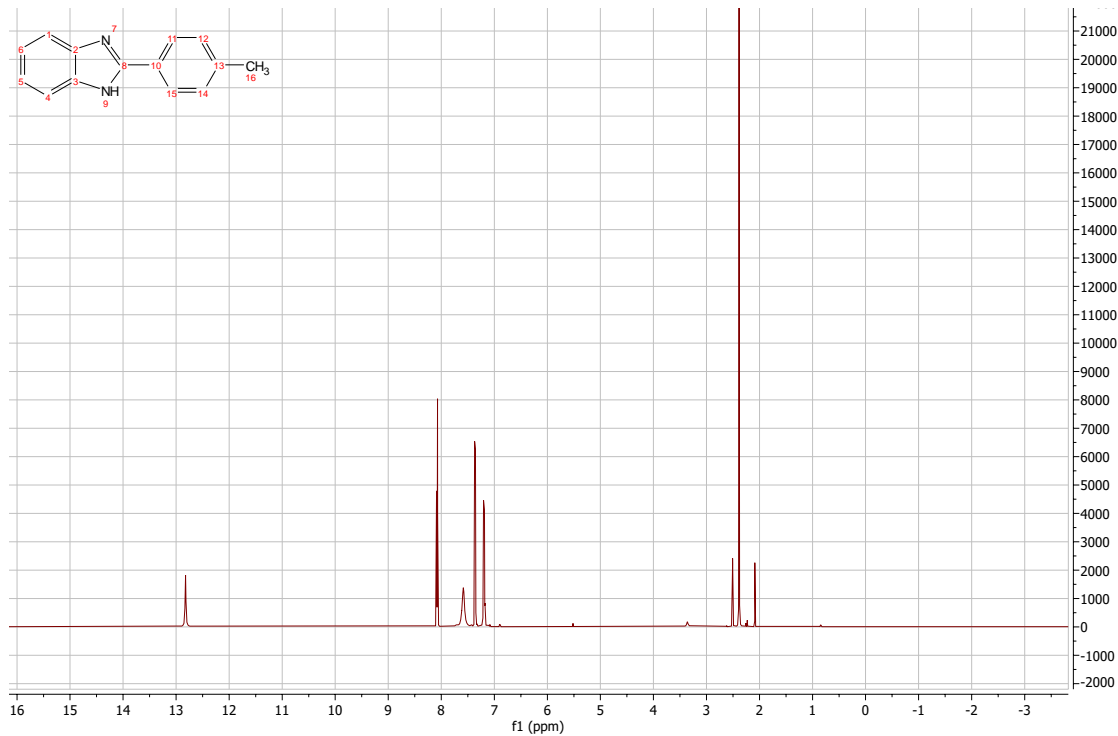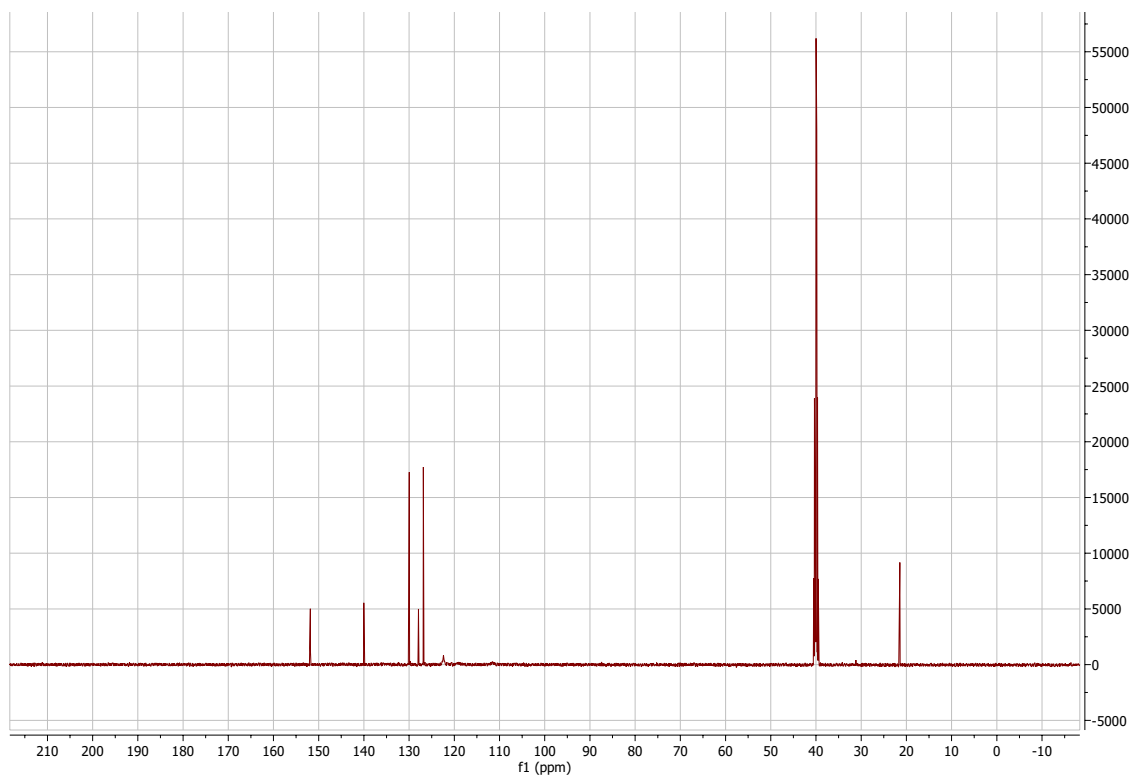
¹H-NMR

¹³C-NMR

HSQC

20220512_CH440_clean_HSQC.10.ser
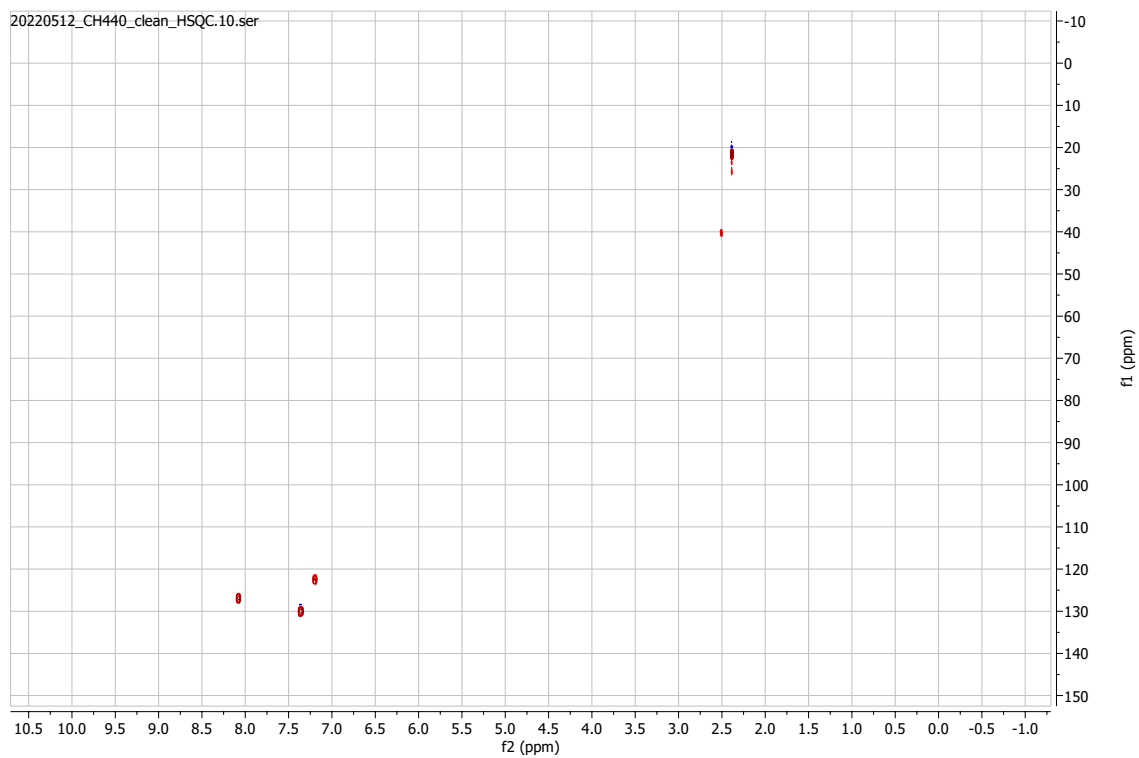
HMBC

20220512_CH440_clean_HMBC.10.ser
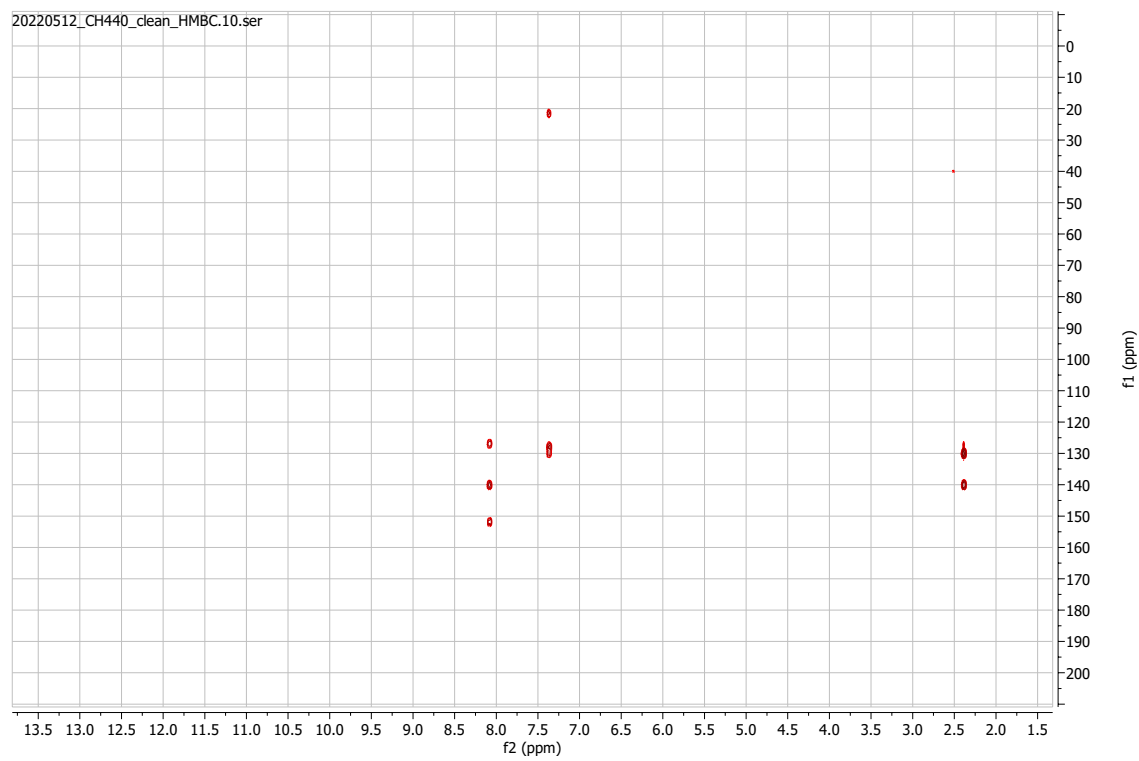
5-chloro-2-(4-methylphenyl)-1H-1,3-benzodiazole:
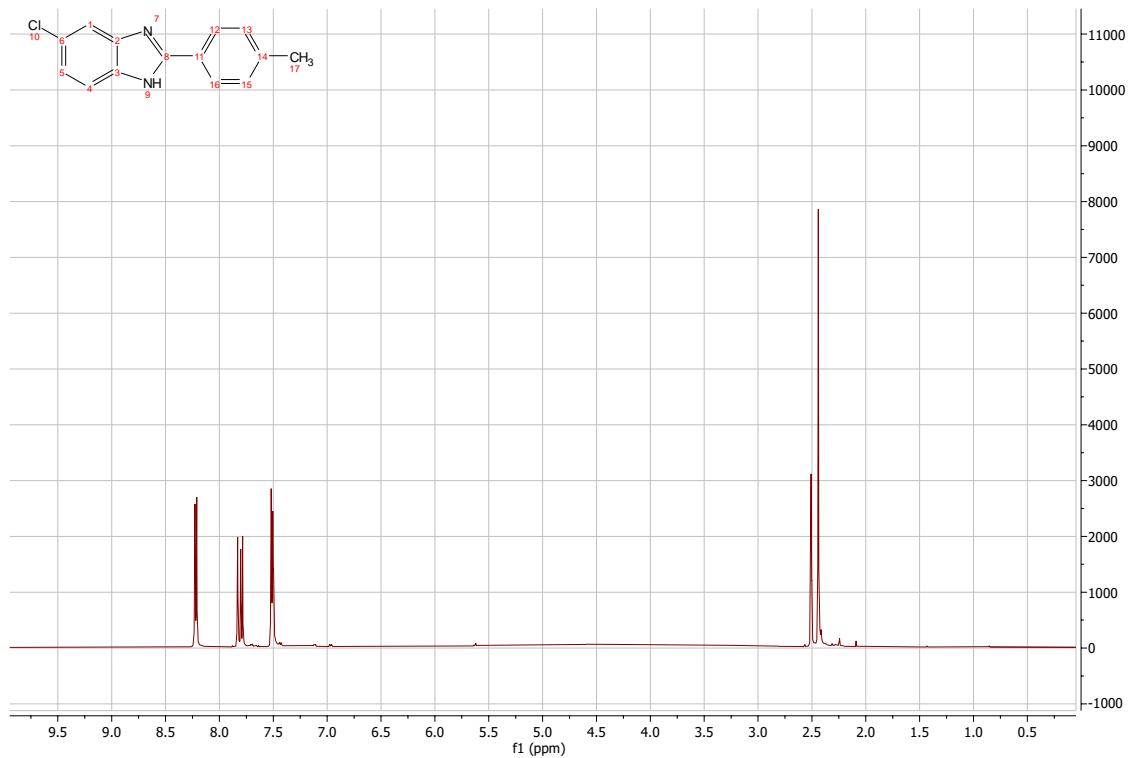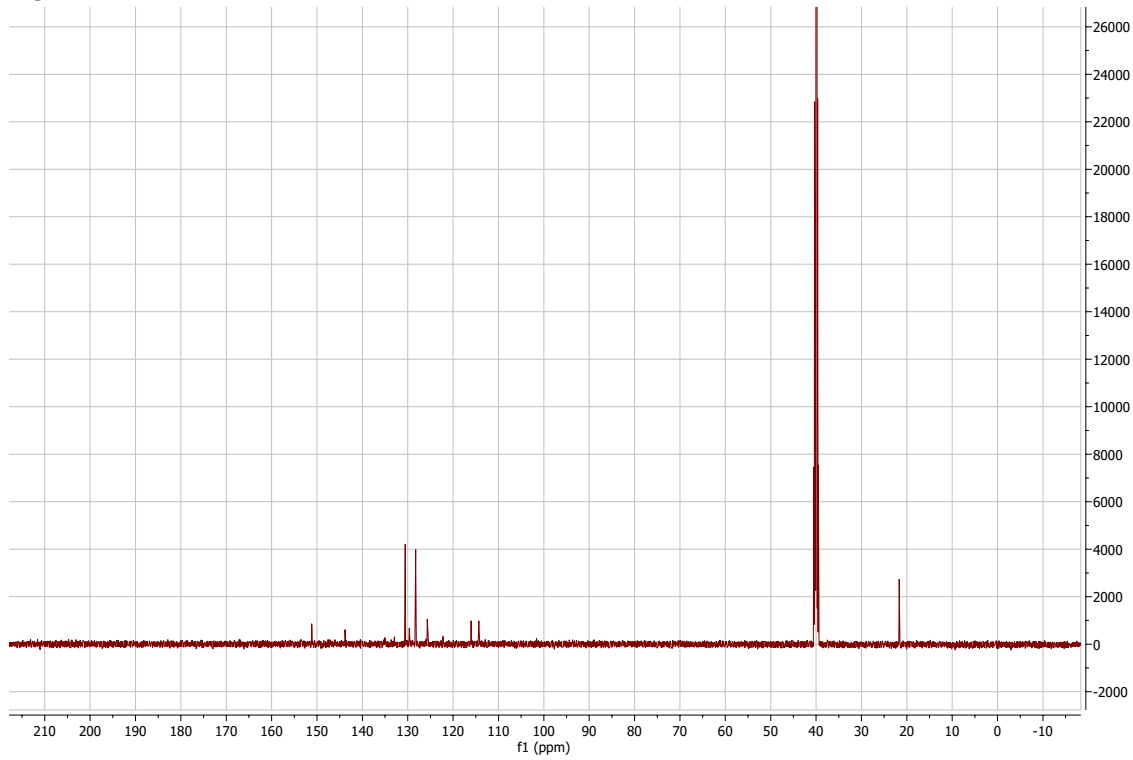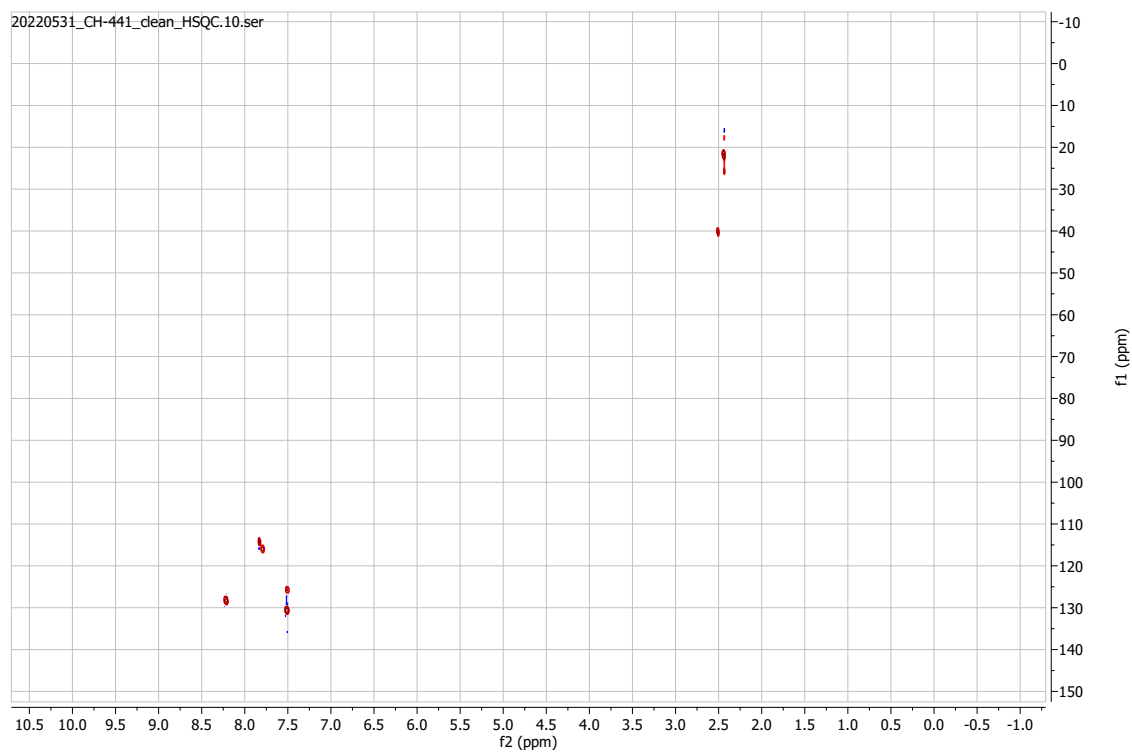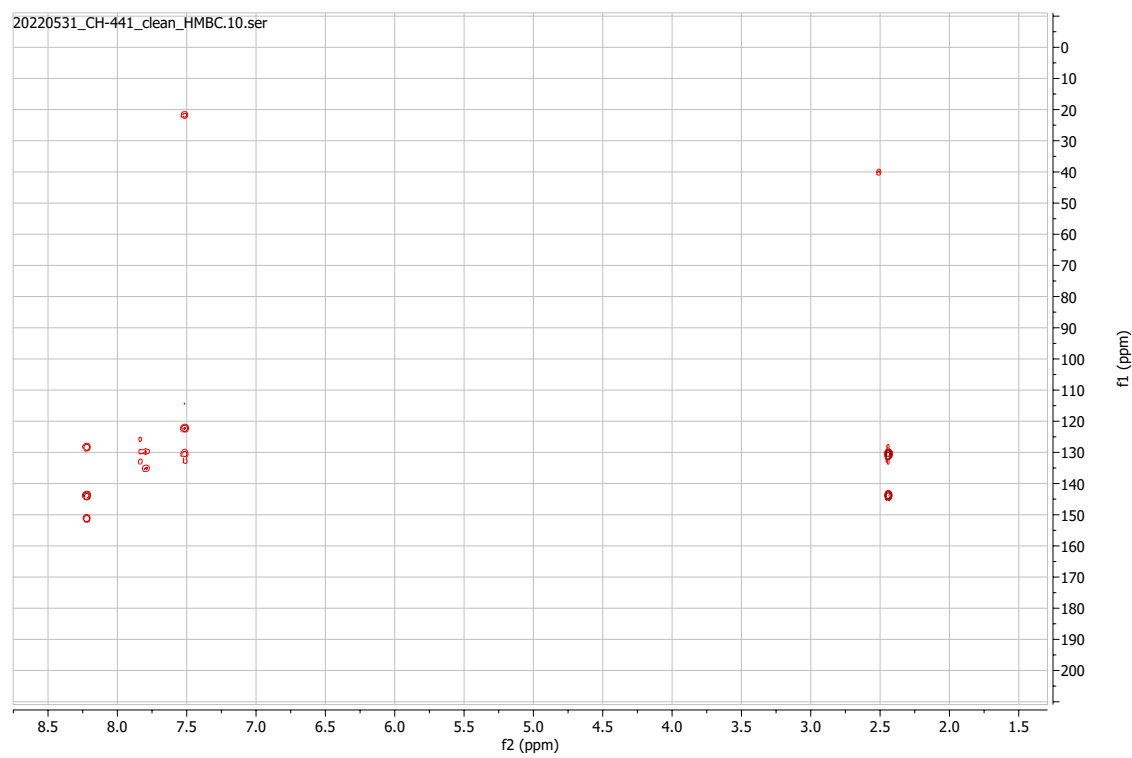
¹H-NMR

¹³C-NMR

HSQC

20220531_CH-441_clean_HSQC.10.ser

HMBC

20220531_CH-441_clean_HMBC.10.ser

5-fluoro-2-(thiophen-2-yl)-1H-1,3-benzodiazole:

¹H-NMR

HSQC

20220520_CH444_cleaned_HSQC.10.ser

HMBC

20220520_CH444_cleaned_HMBC.10.ser

5-nitro-2-(thiophen-2-yl)-1H-1,3-benzodiazole:

¹H-NMR

¹³C-NMR

HSQC

20220520_CH445_cleaned_HSQC.10.ser

HMBC

20220520_CH445_cleaned_HMBC.10.ser

5-benzoyl-2-(1H-pyrrol-2-yl)-1H-1,3-benzodiazole:

¹H-NMR

399
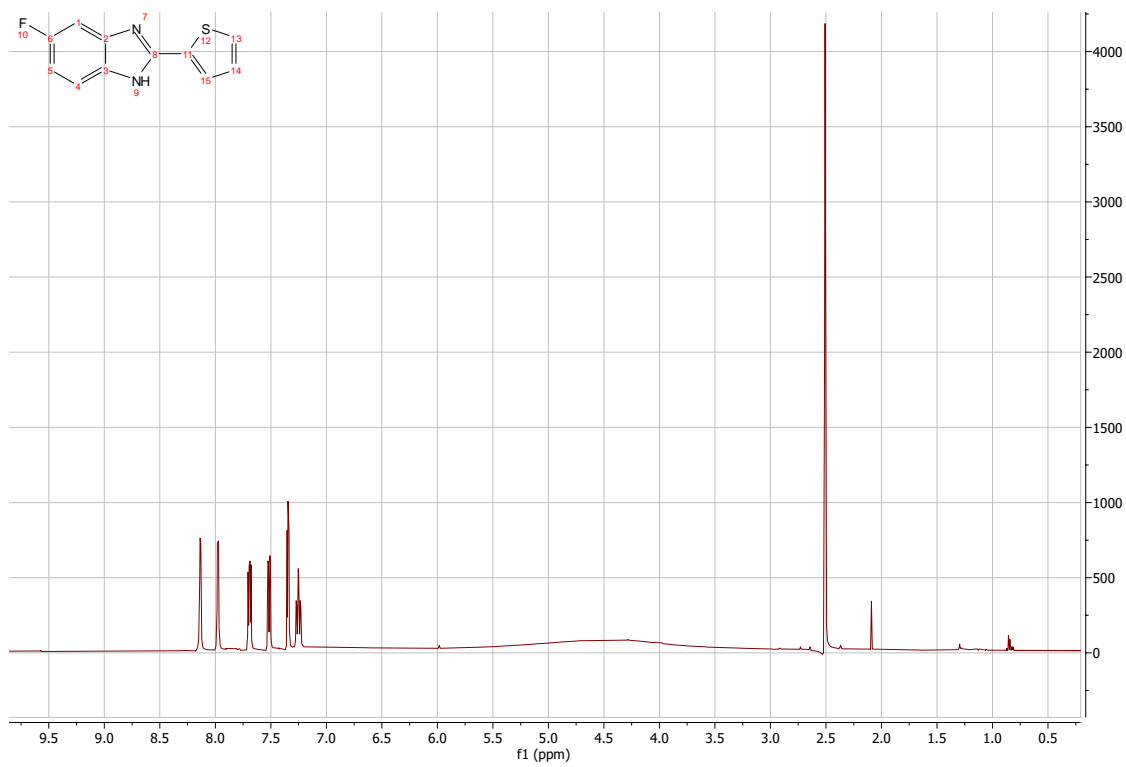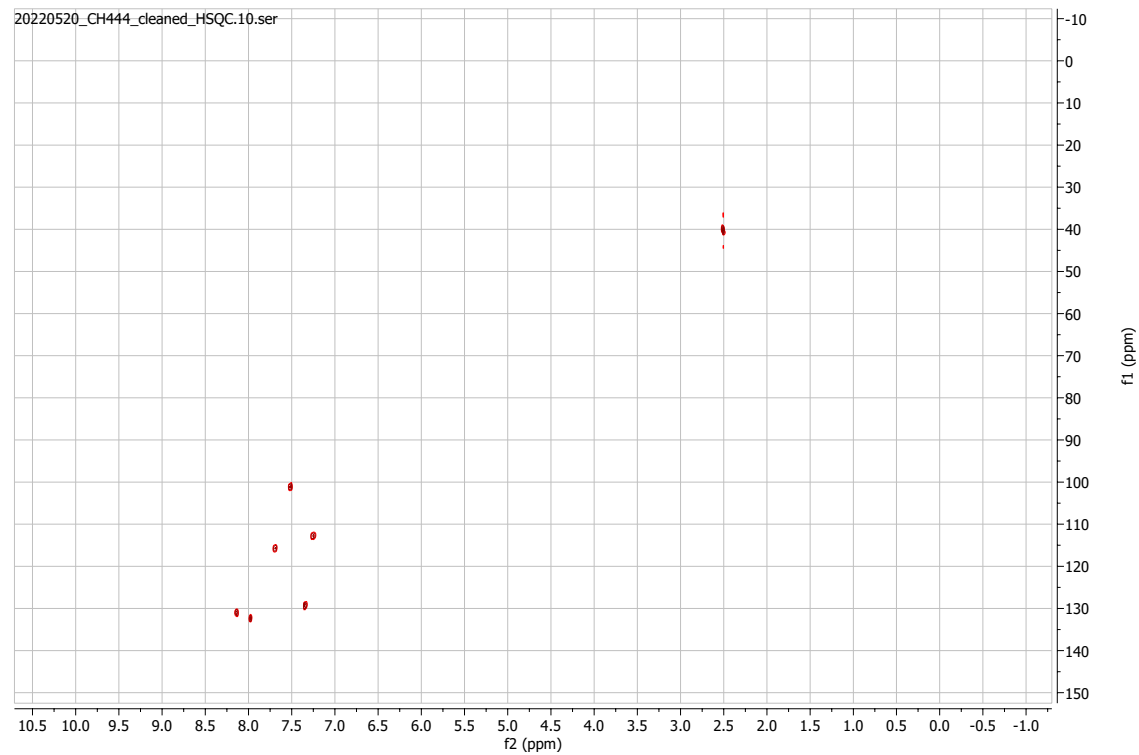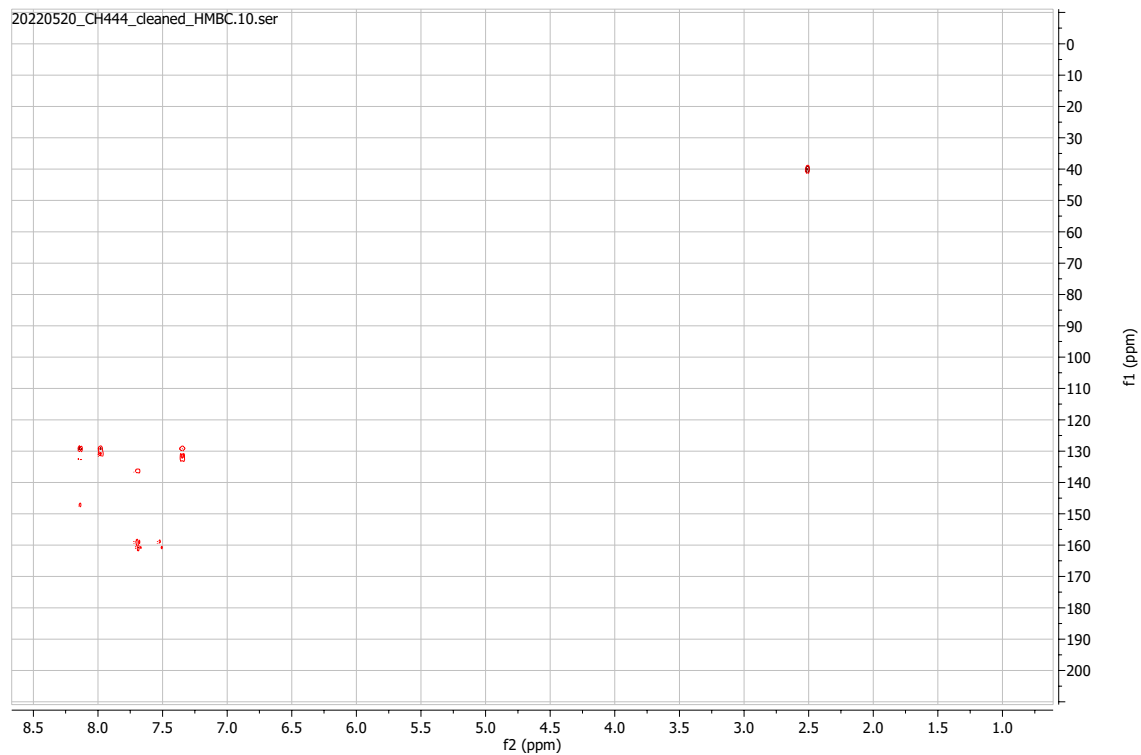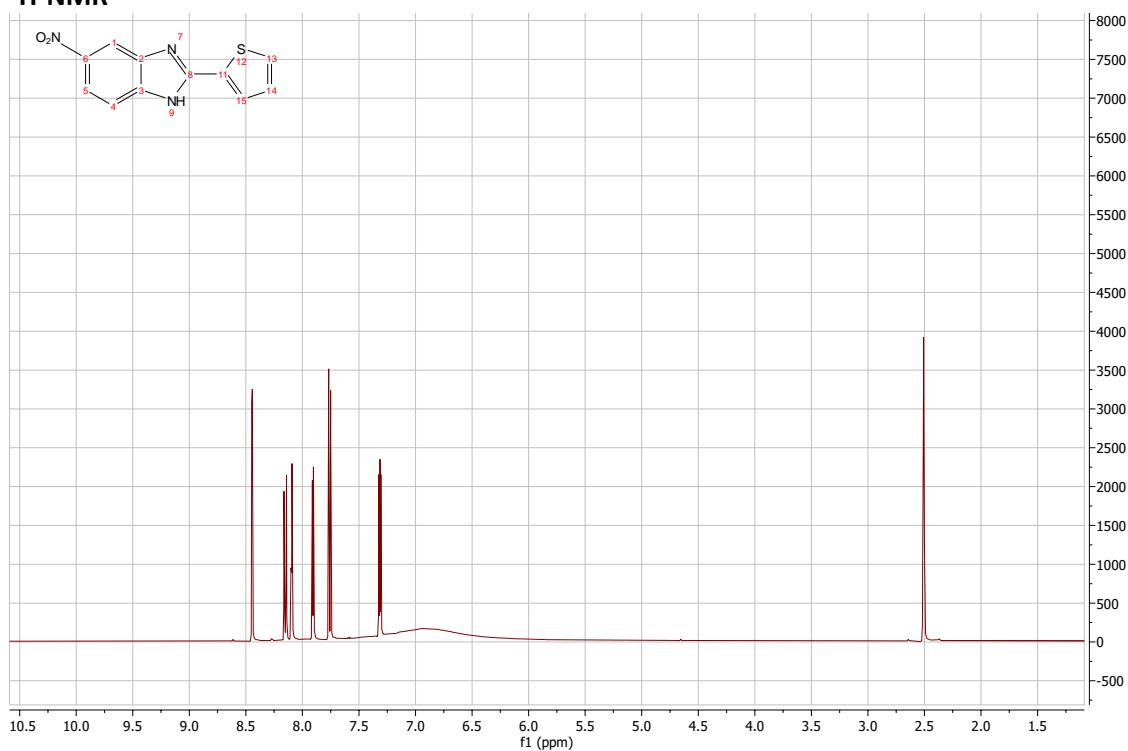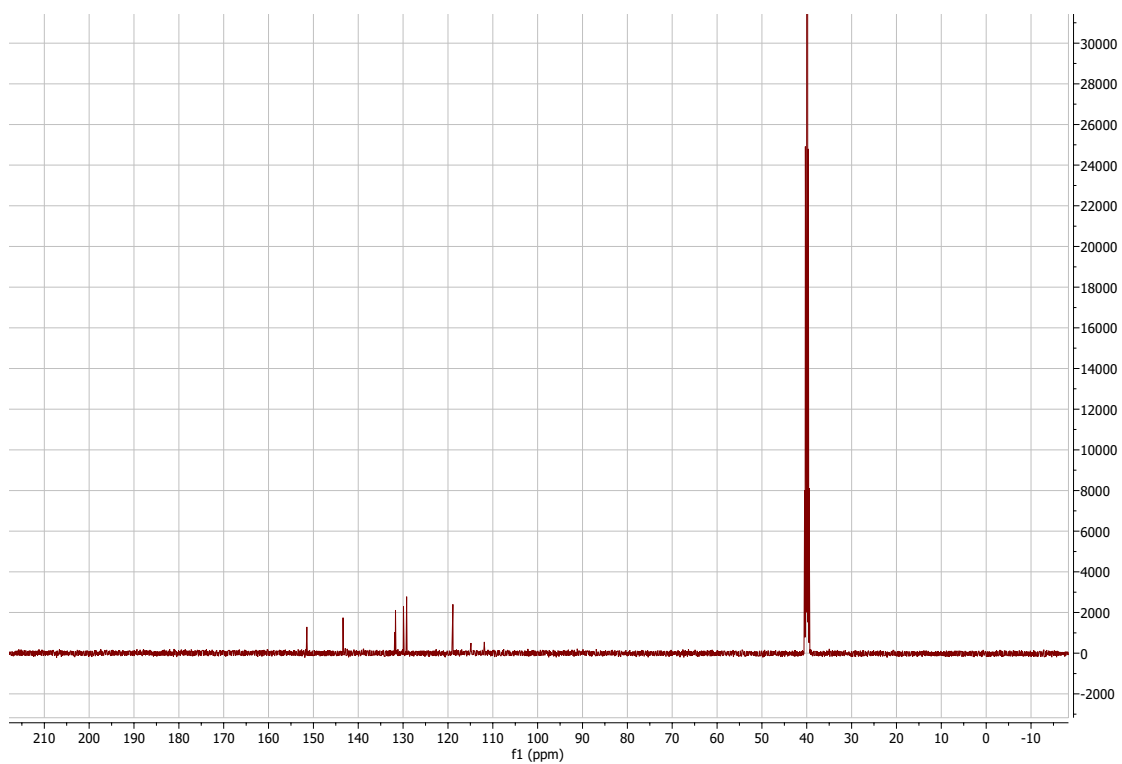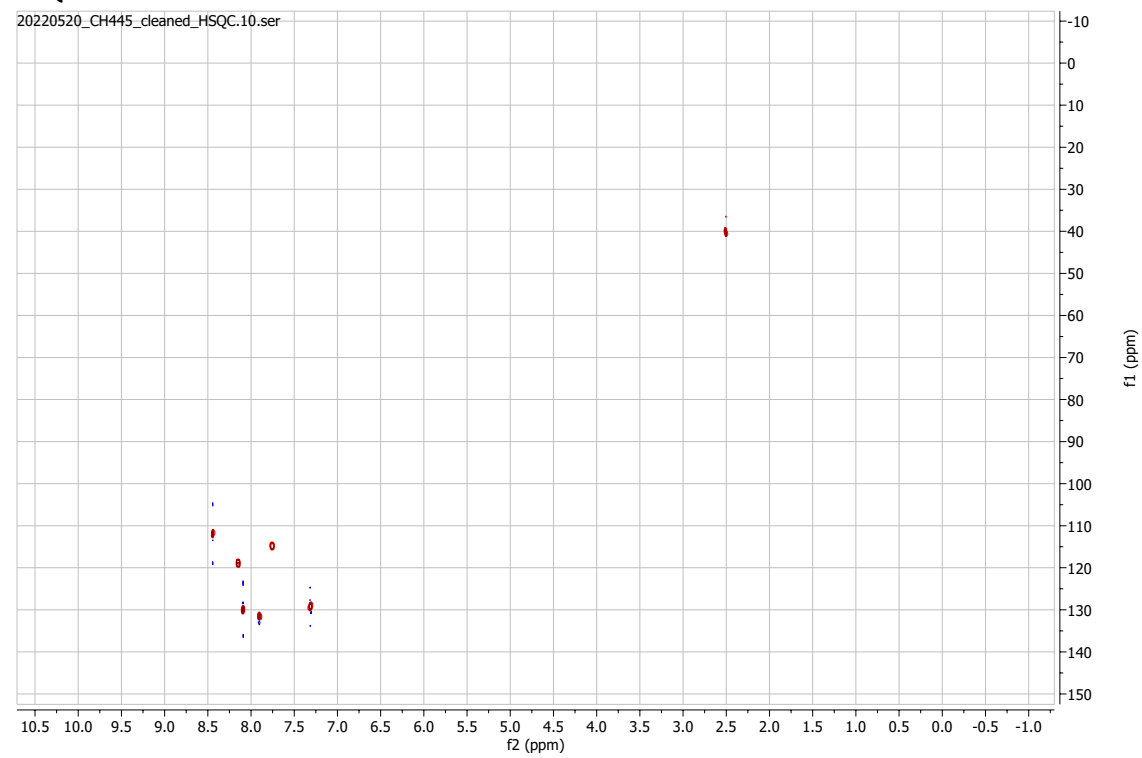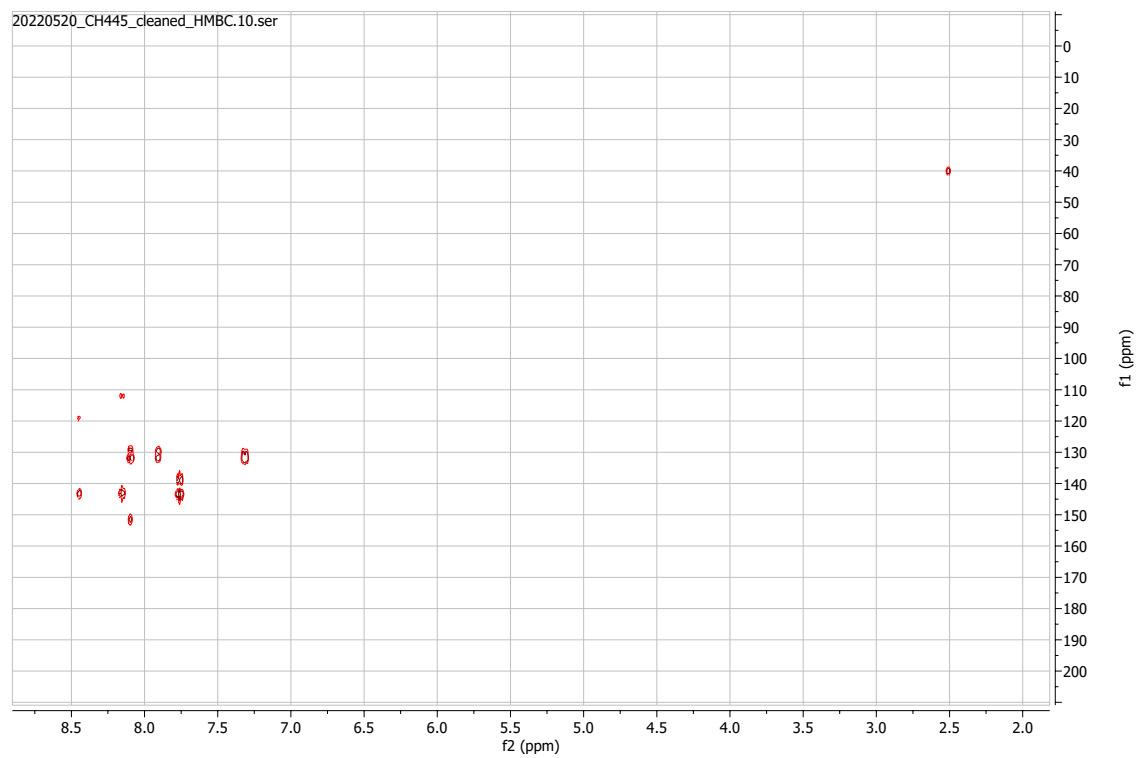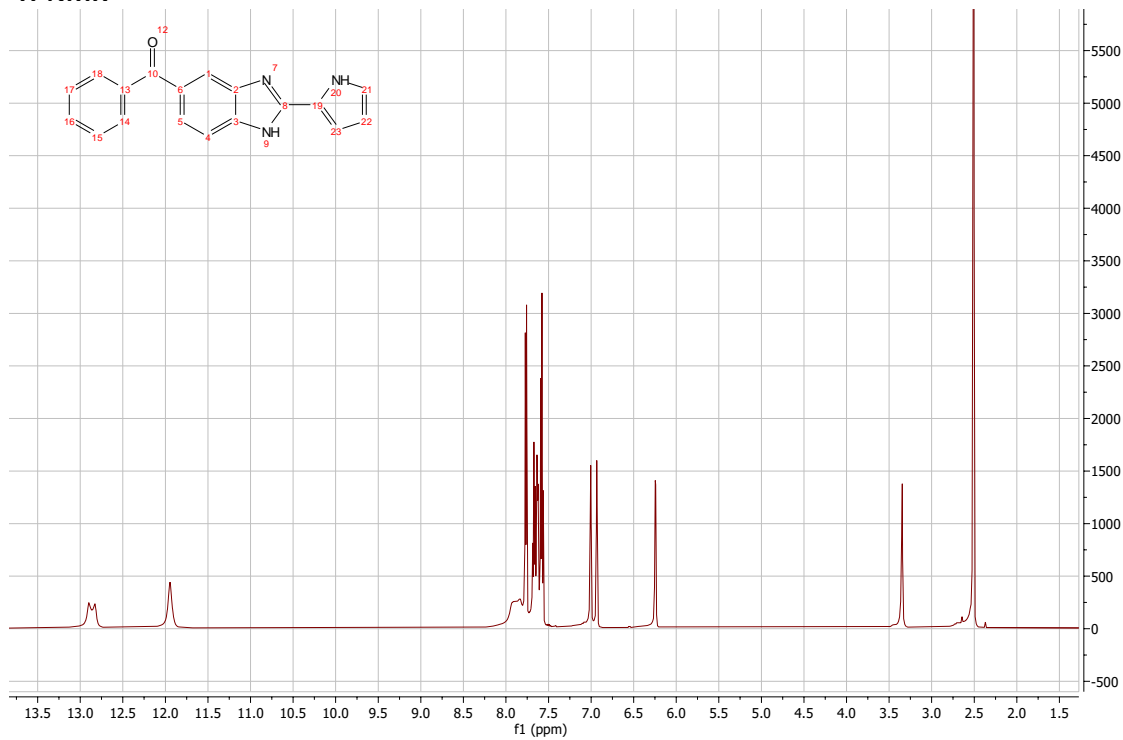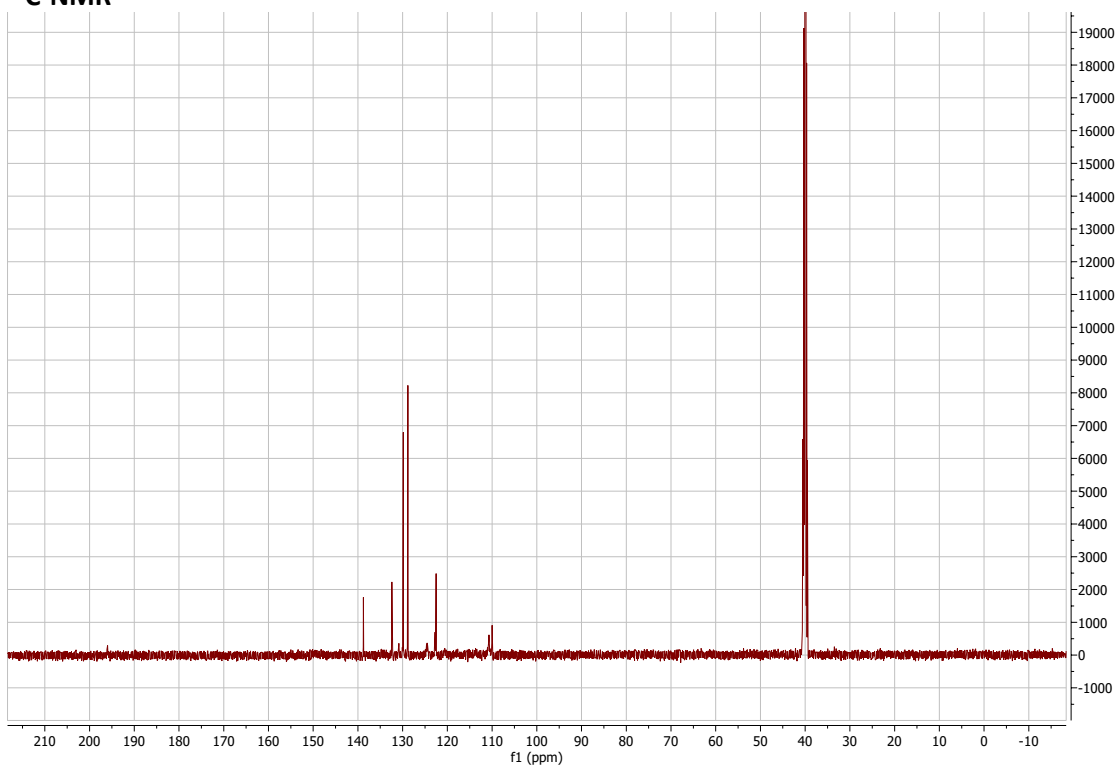
¹³C-NMR

HSQC

20230325_BZI72_HSQC.10.ser

400

HMBC

20230325_BZI72_HMBC.10.ser
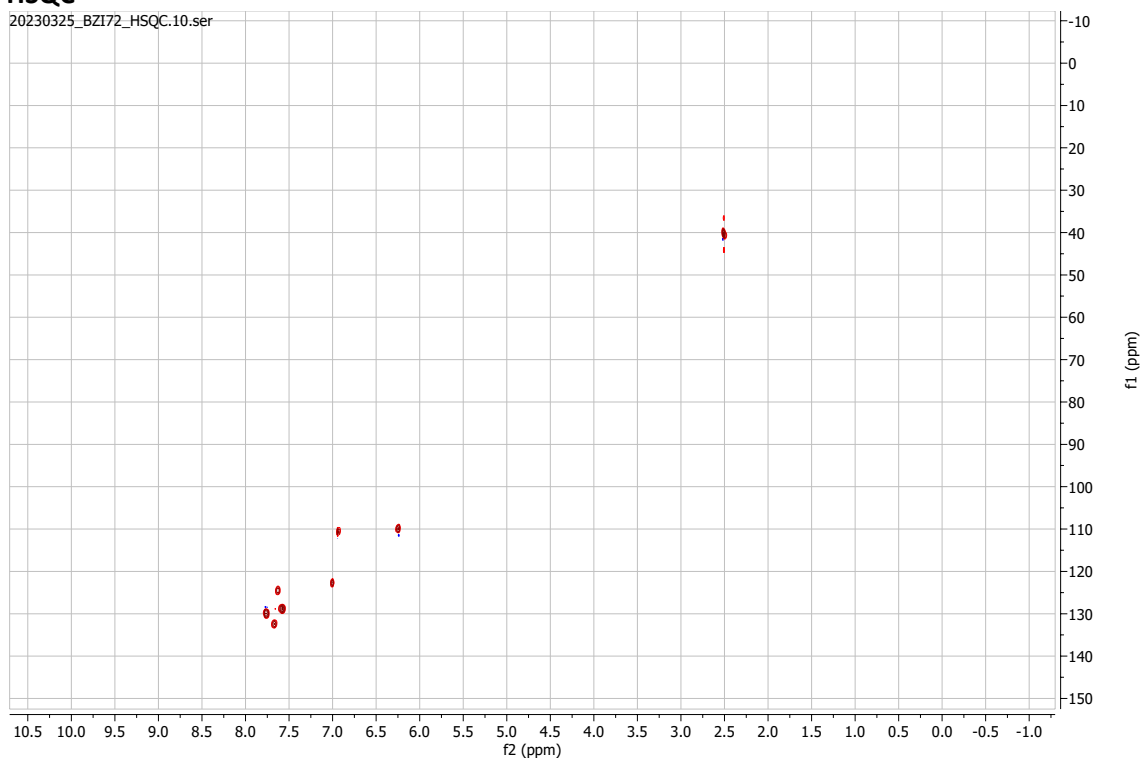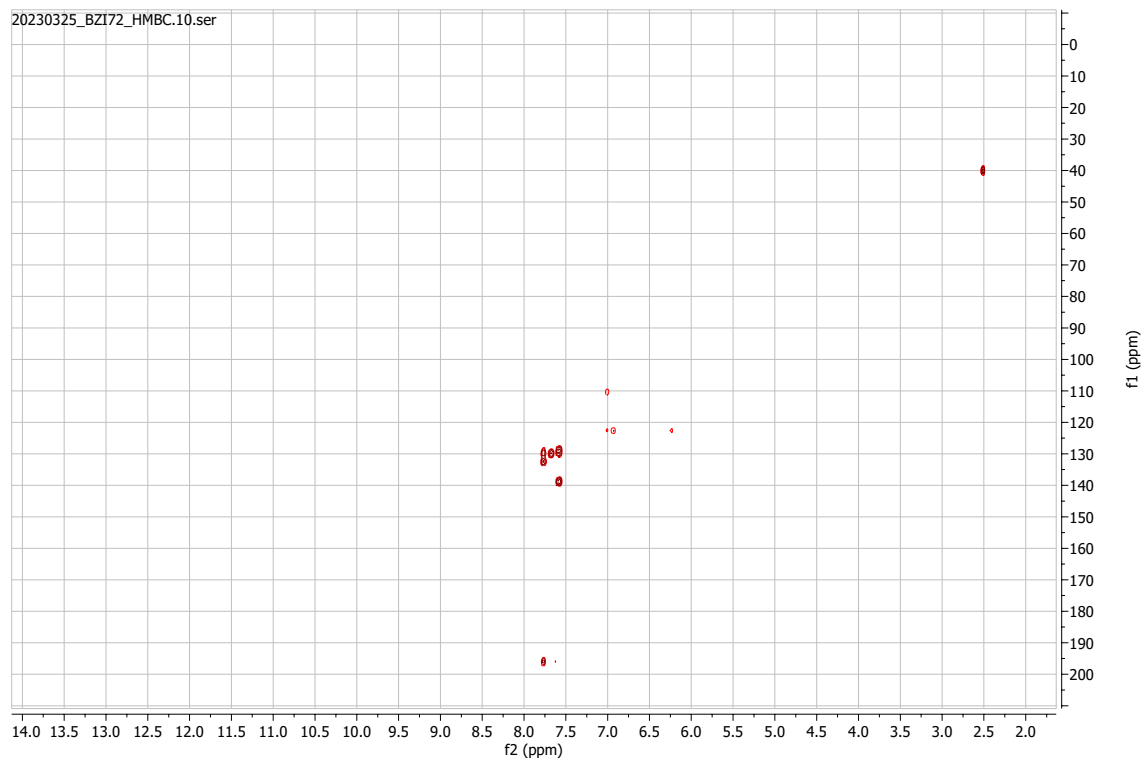
5-fluoro-2-(1H-pyrrol-2-yl)-1H-1,3-benzodiazole:
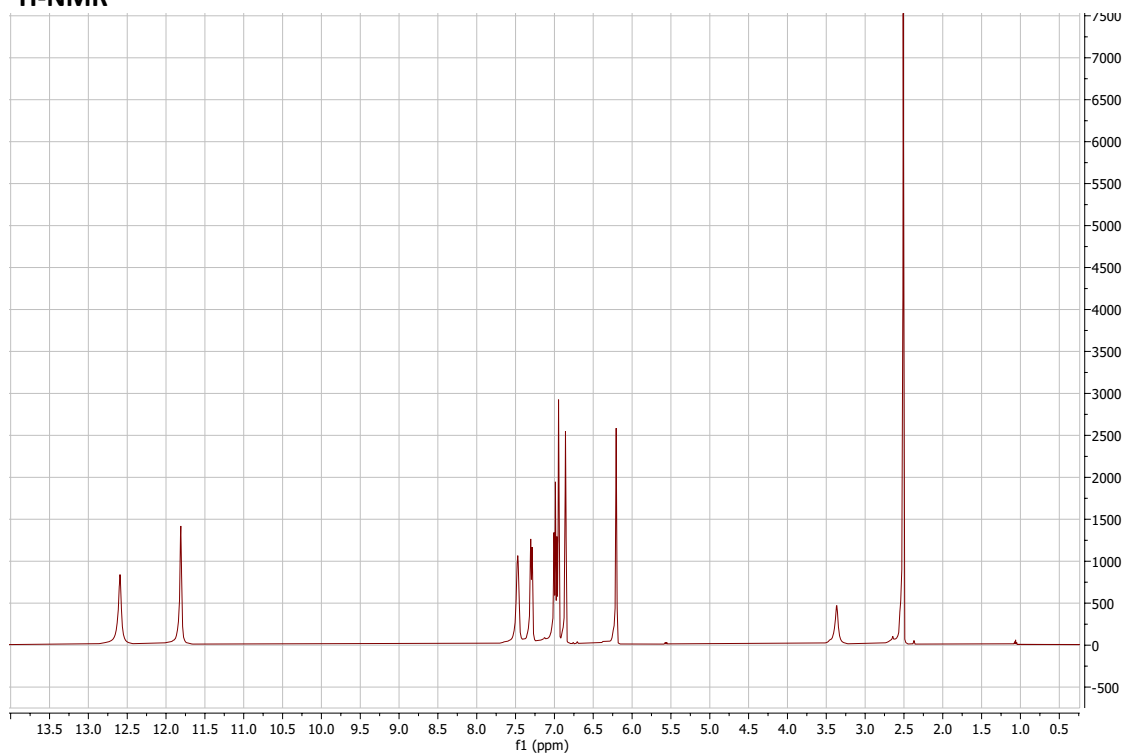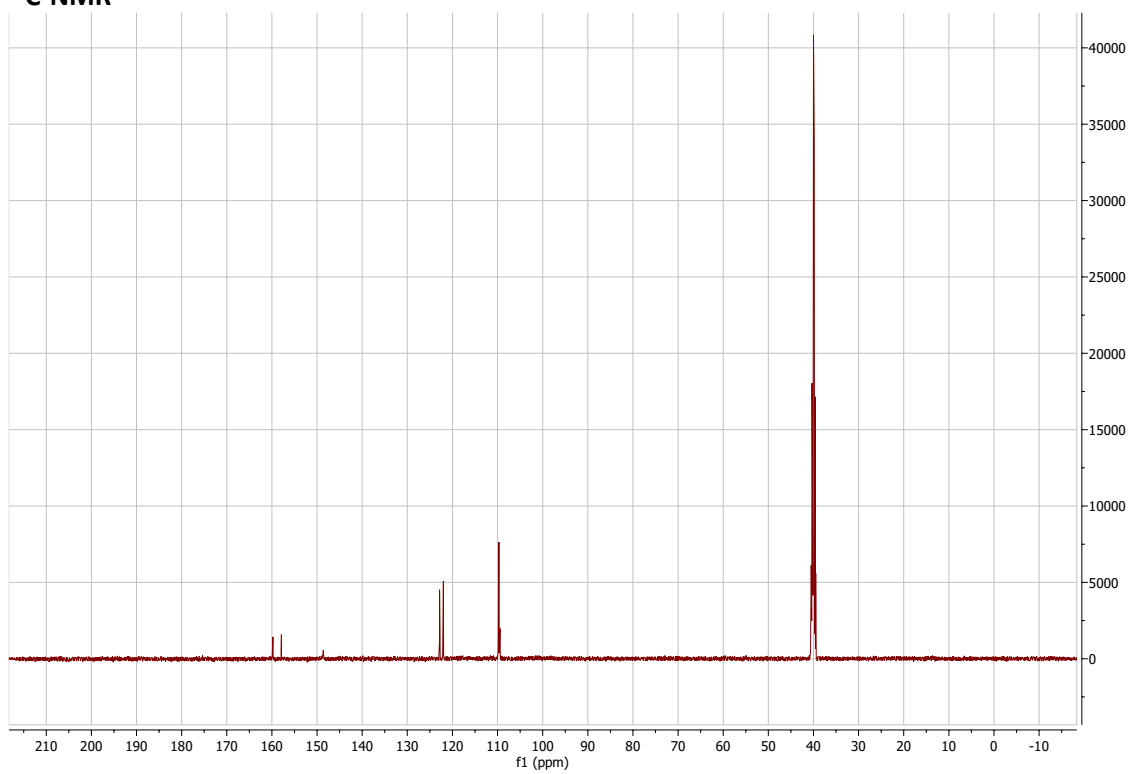
¹H-NMR

¹³C-NMR

HSQC

20230325_BZI96_HSQC.10.ser
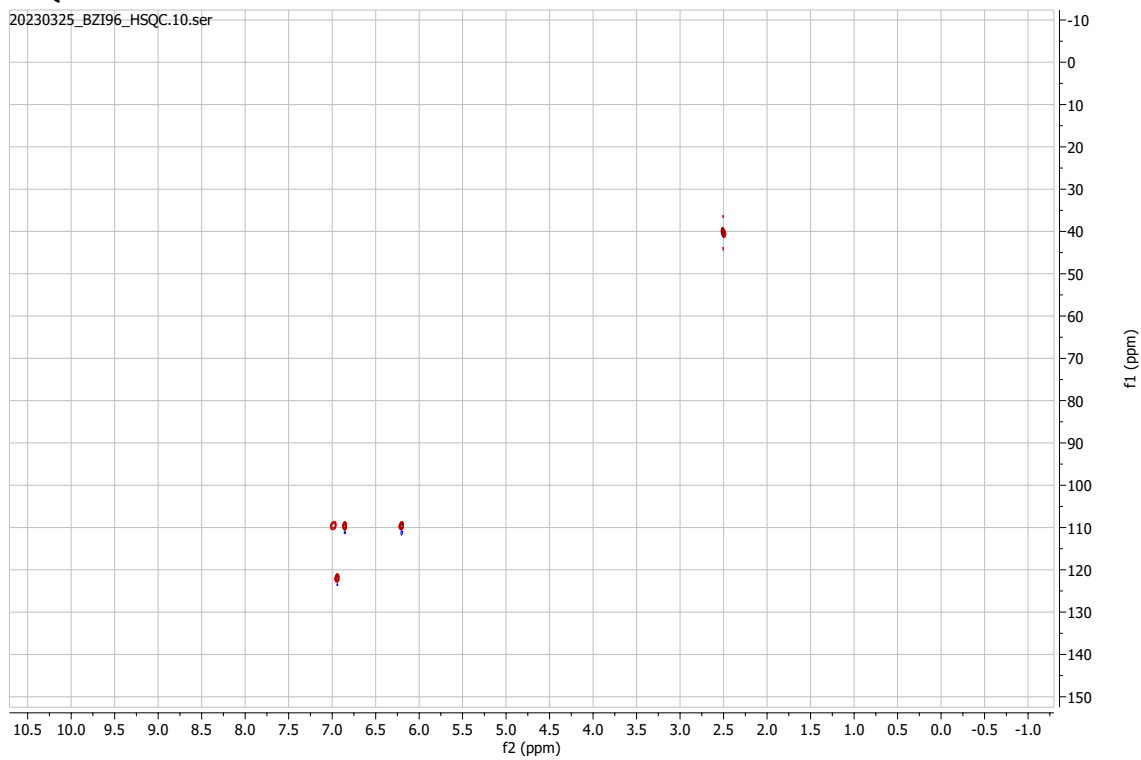
HMBC

20230325_BZI96_HMBC.10.ser
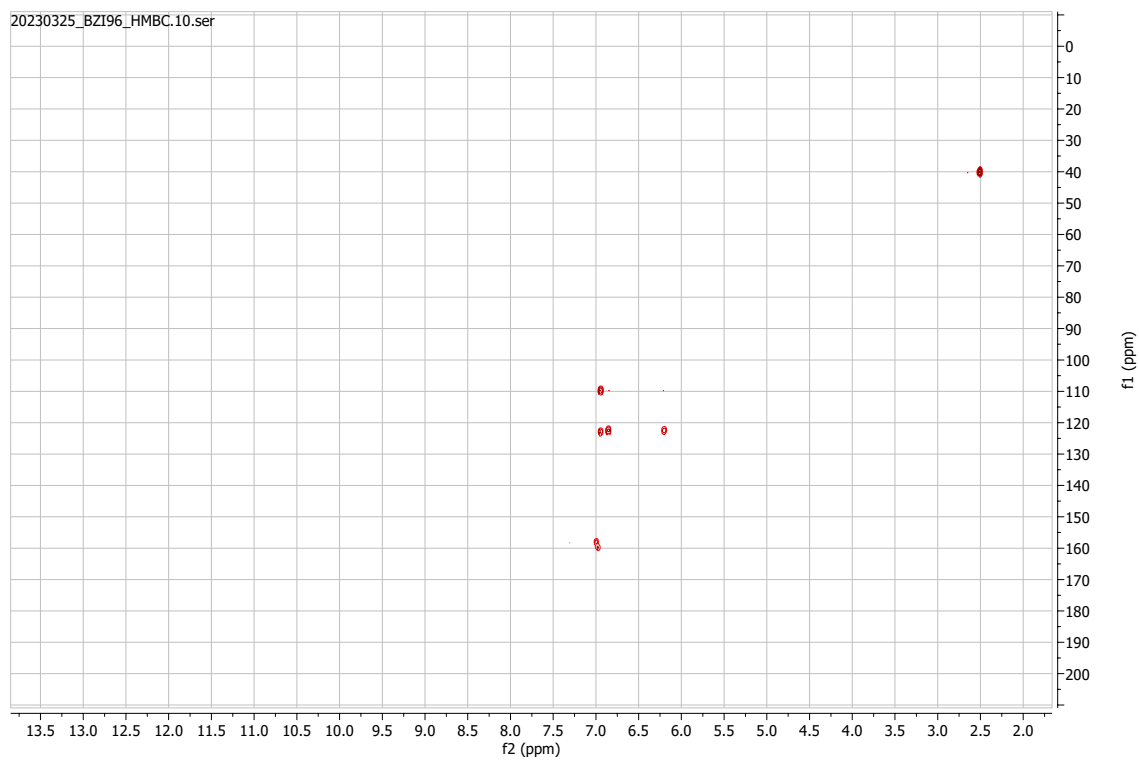
5-benzoyl-2-(3-nitrophenyl)-1H-1,3-benzodiazole:
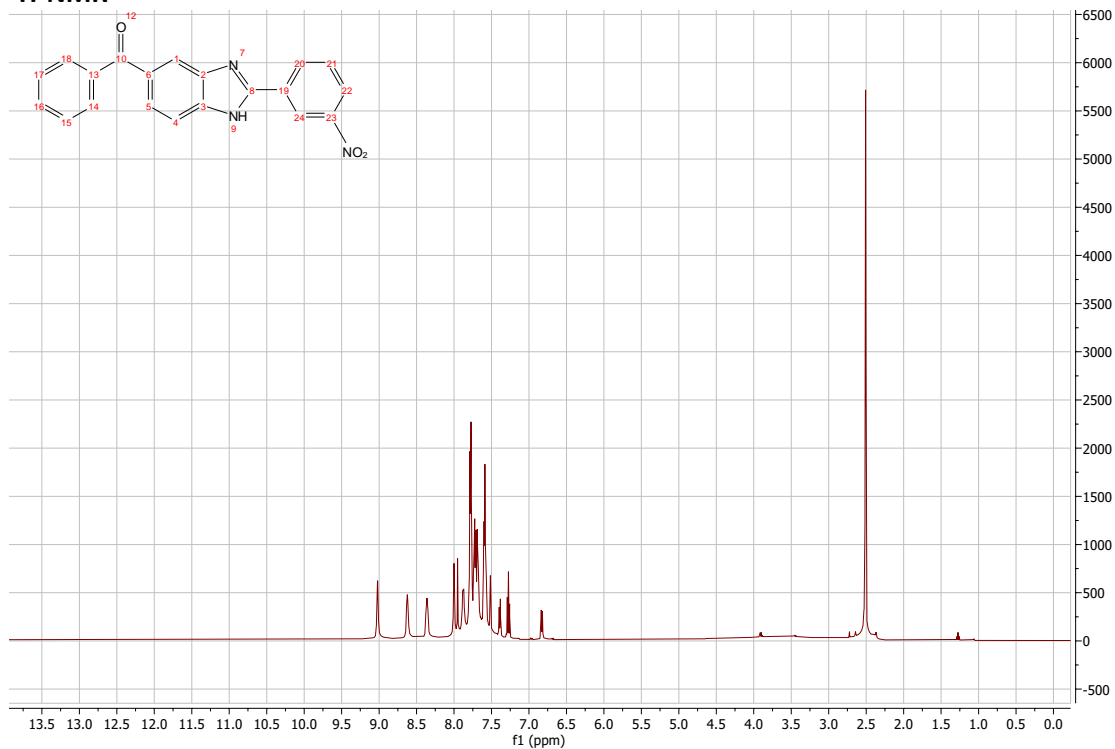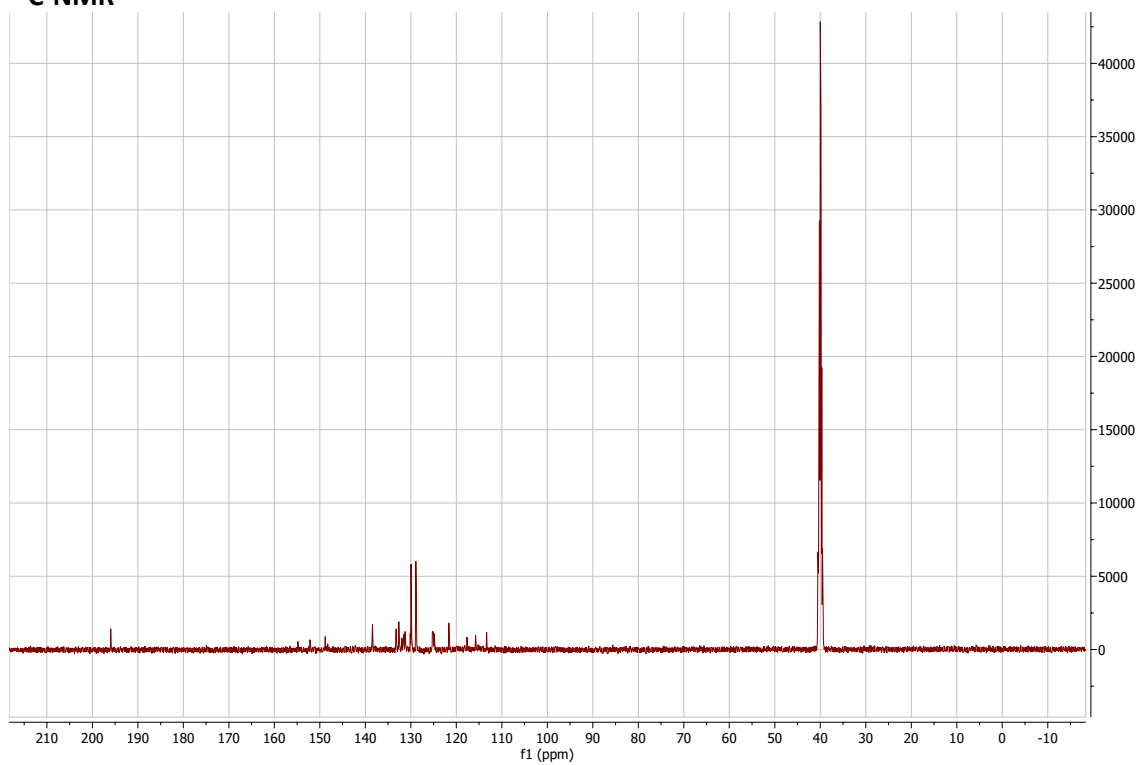
¹H-NMR

¹³C-NMR

HSQC

20230321_BZI-70.12.ser
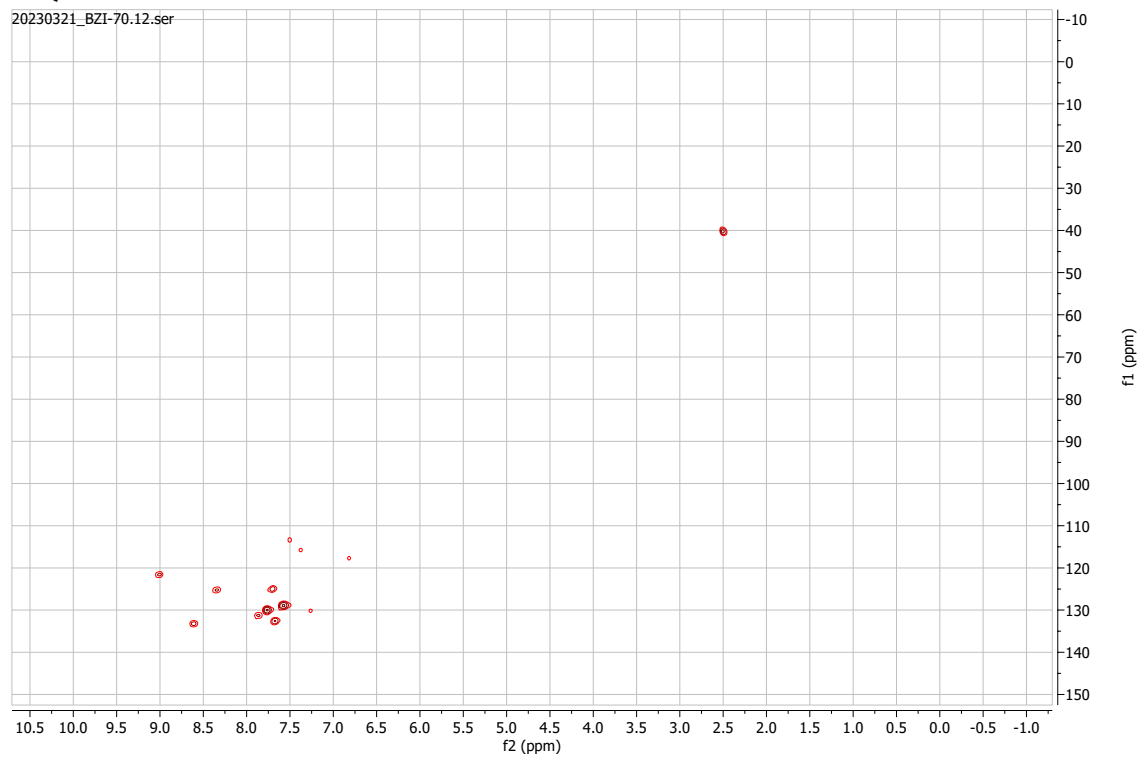
HMBC

20230321_BZI-70.13.ser

5-chloro-2-(1H-pyrrol-2-yl)-1H-1,3-benzodiazole:

¹H-NMR

¹³C-NMR

HSQC

20230320_BZI39_HSQC.10.ser

406
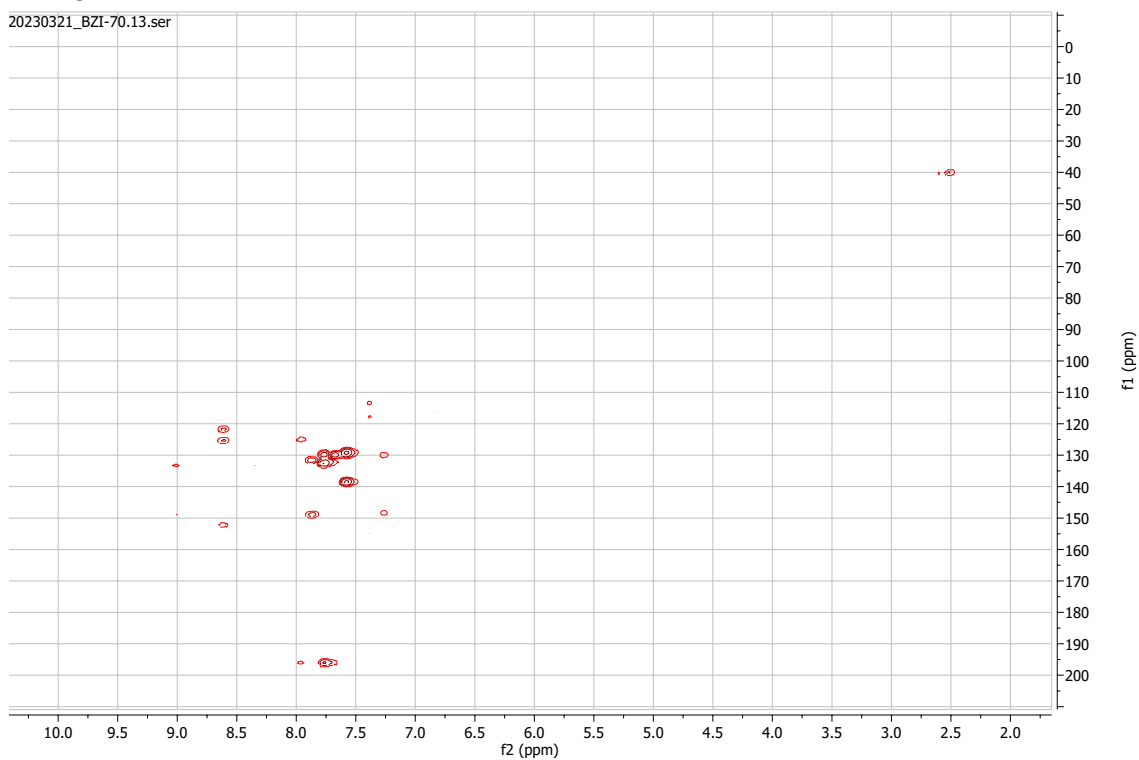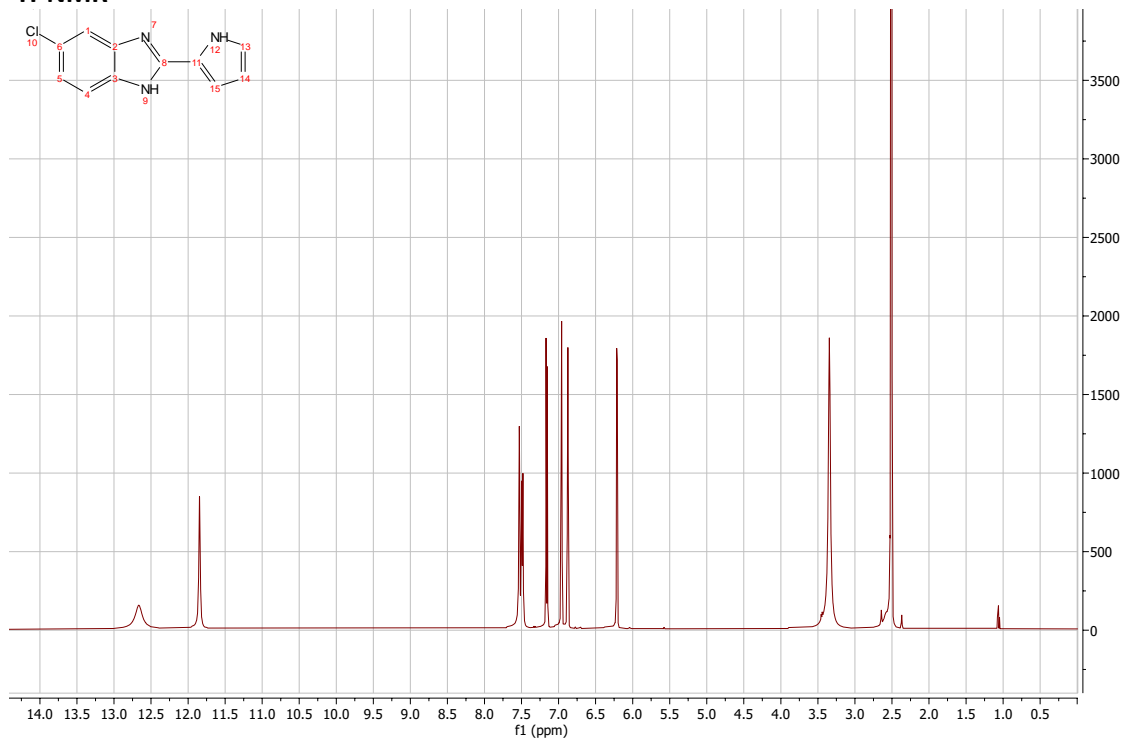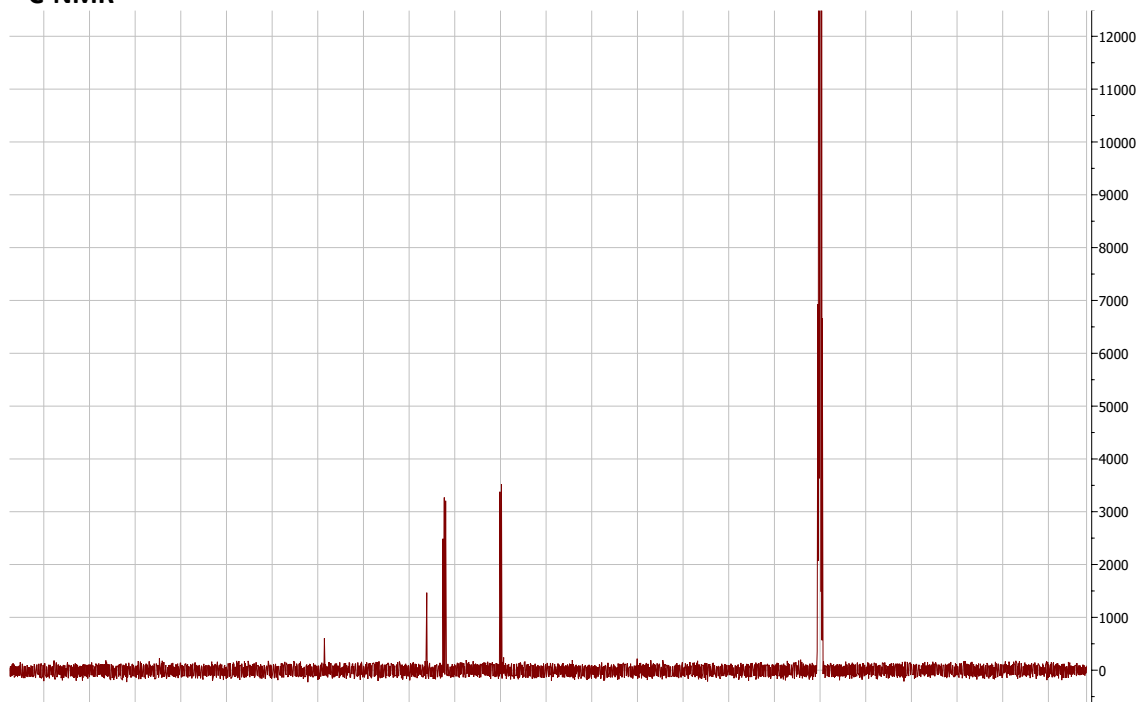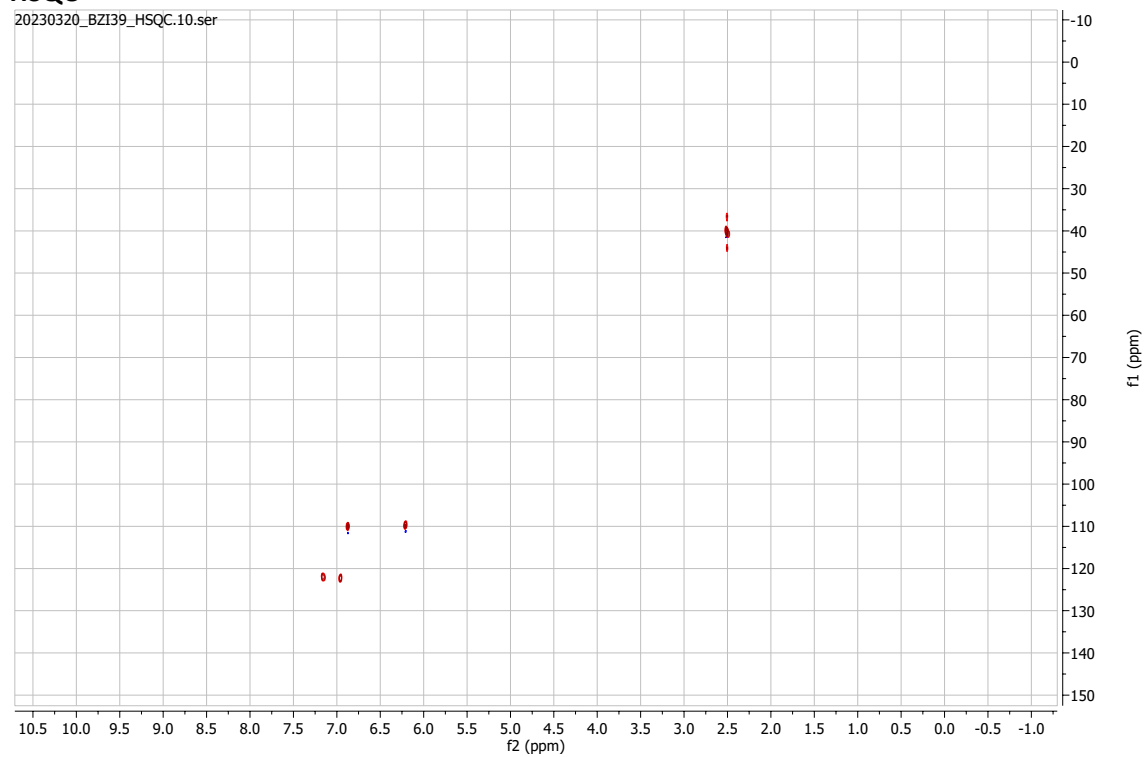
HMBC

20230320_BZI39_HMBC.10.ser
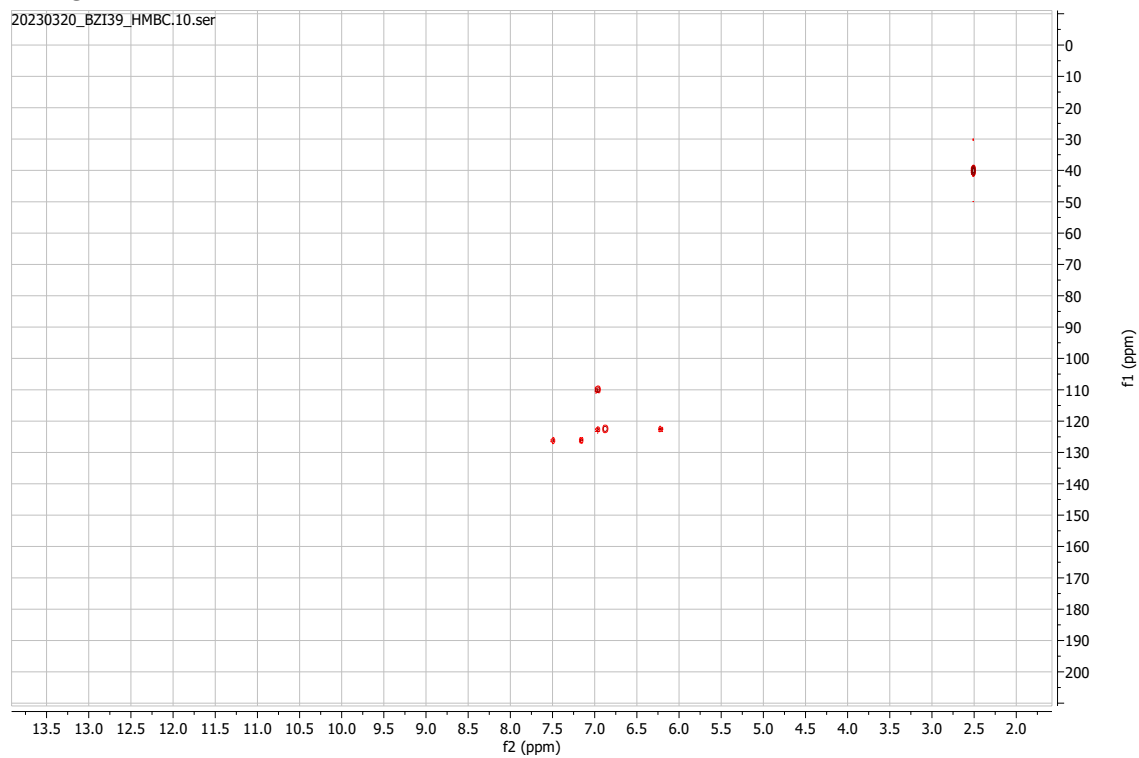
5-nitro-2-(1H-pyrrol-2-yl)-1H-1,3-benzodiazole:
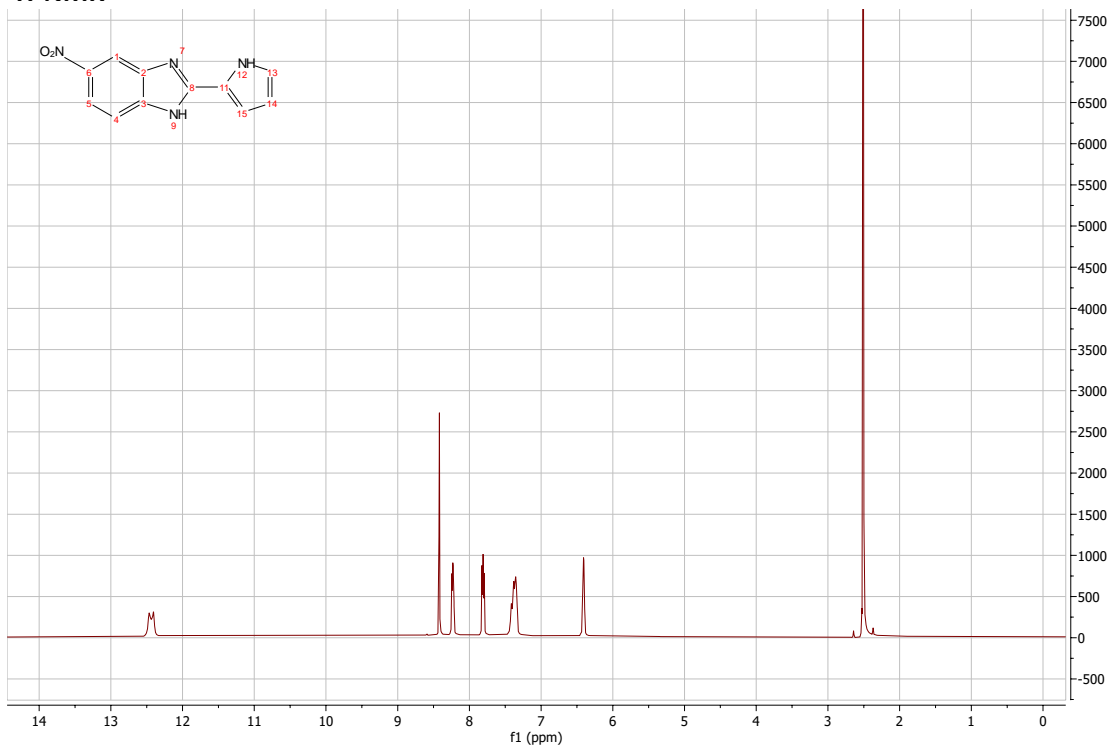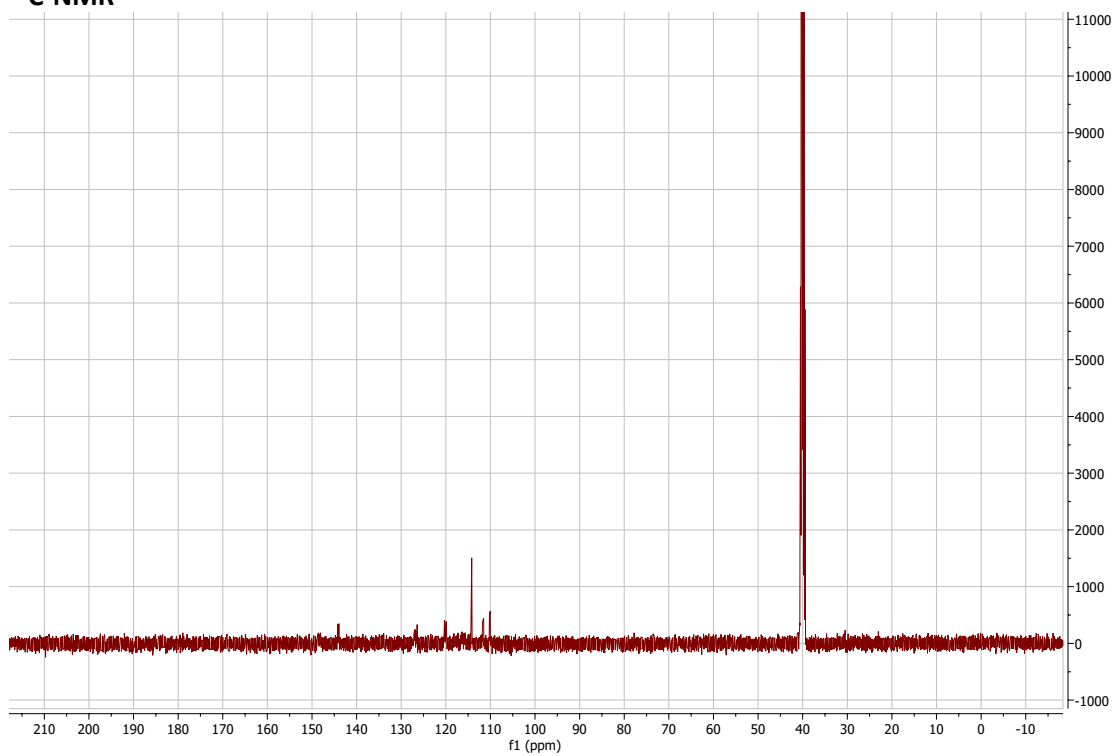
¹H-NMR

¹³C-NMR

HSQC

20230320_BZI50_HSQC.10.ser
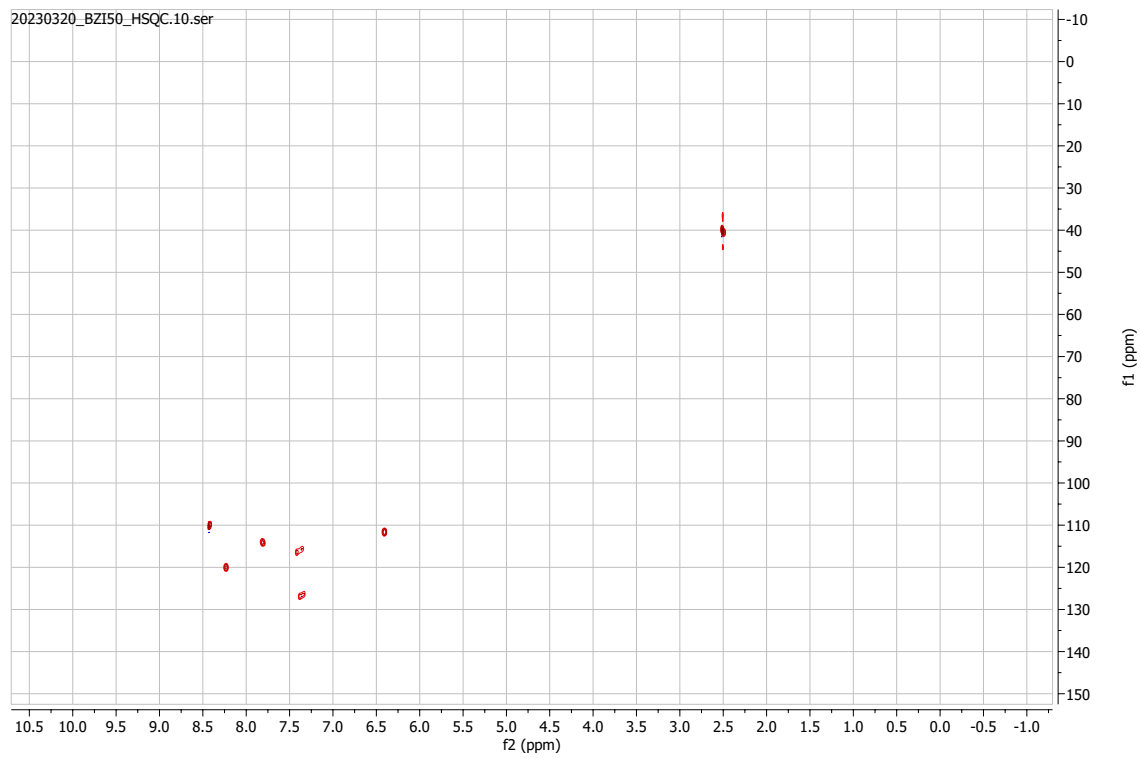
HMBC

20230320_BZI50_HMBC.10.ser

2-phenyl-1H-1,3-benzodiazole-5-carboxylic acid:

¹H-NMR

409
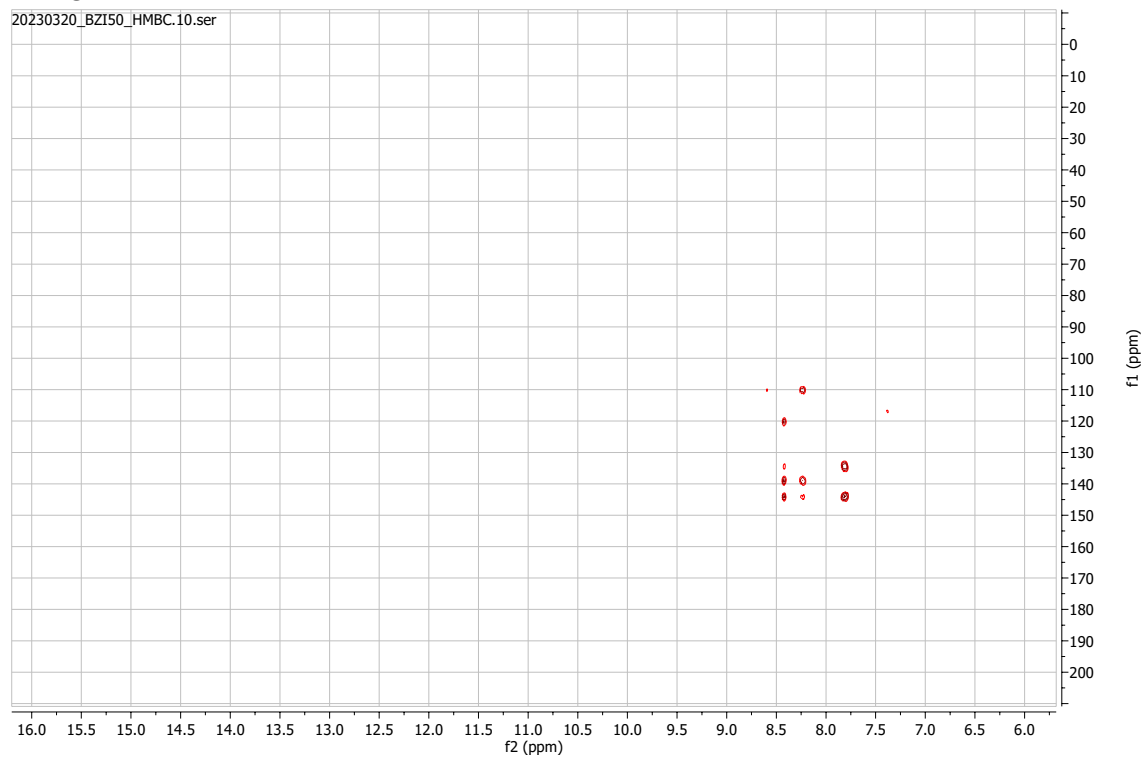
^{13}C-NMR
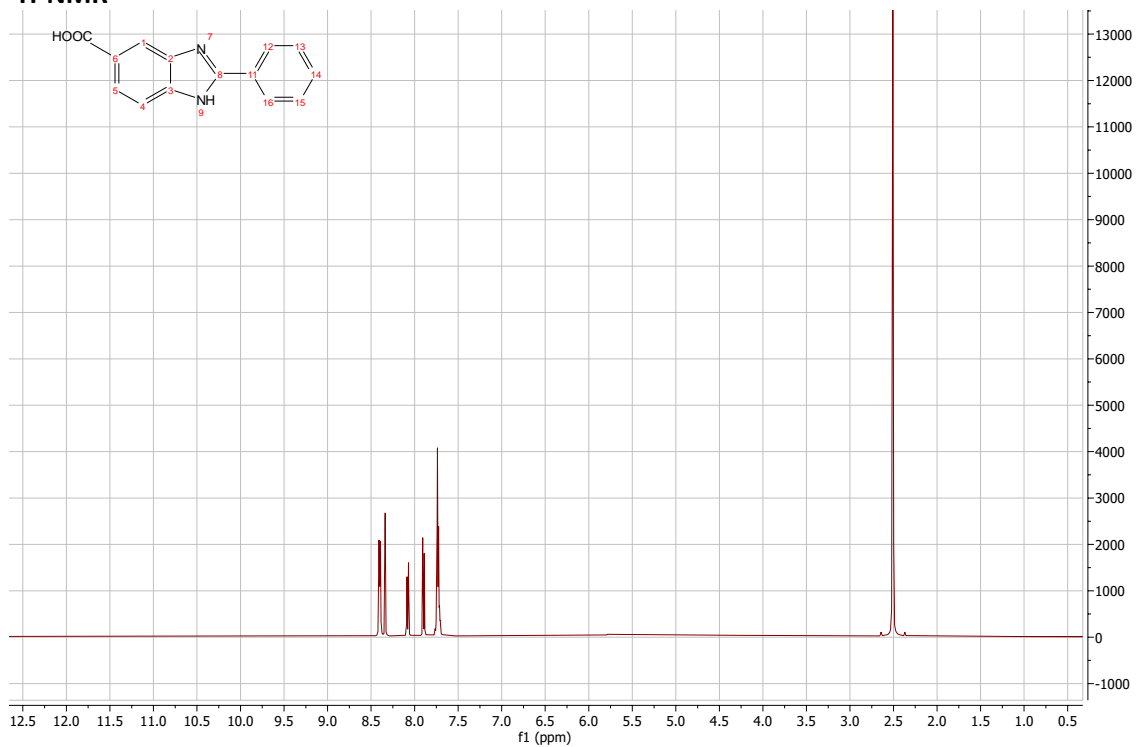
HSQC

20230320_BZI51_HSQC.10.ser
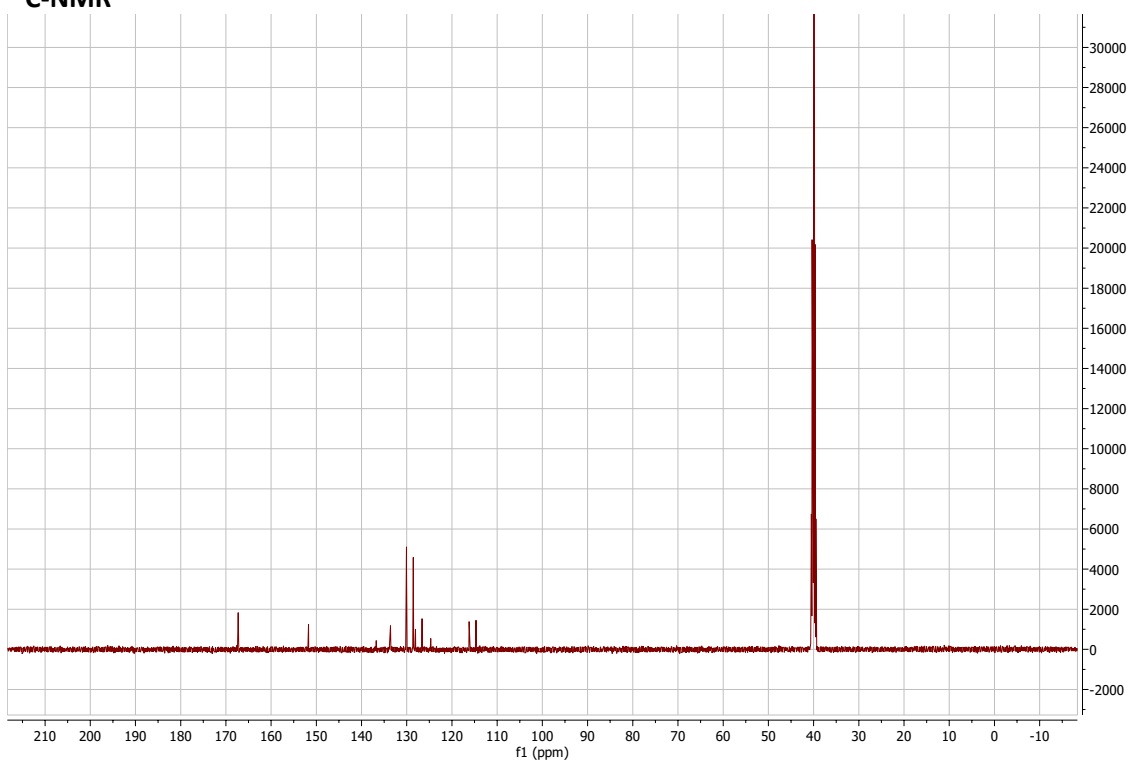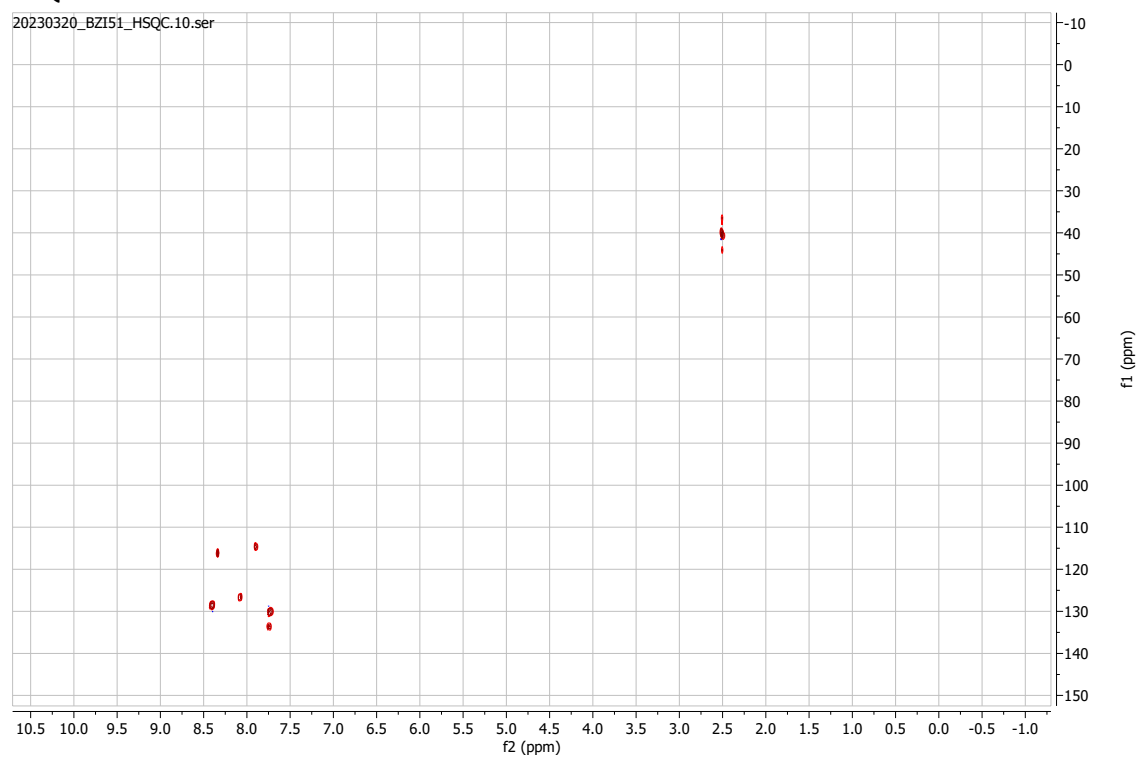
HMBC

20230320_BZI51_HMBC.10.ser

2-(3-hydroxyphenyl)-1H-1,3-benzodiazole-5-carboxylic acid:

¹H-NMR

411

HSQC

20230320_BZI57_HSQC.10.ser

HMBC

20230320_BZI57_HMBC.10.ser
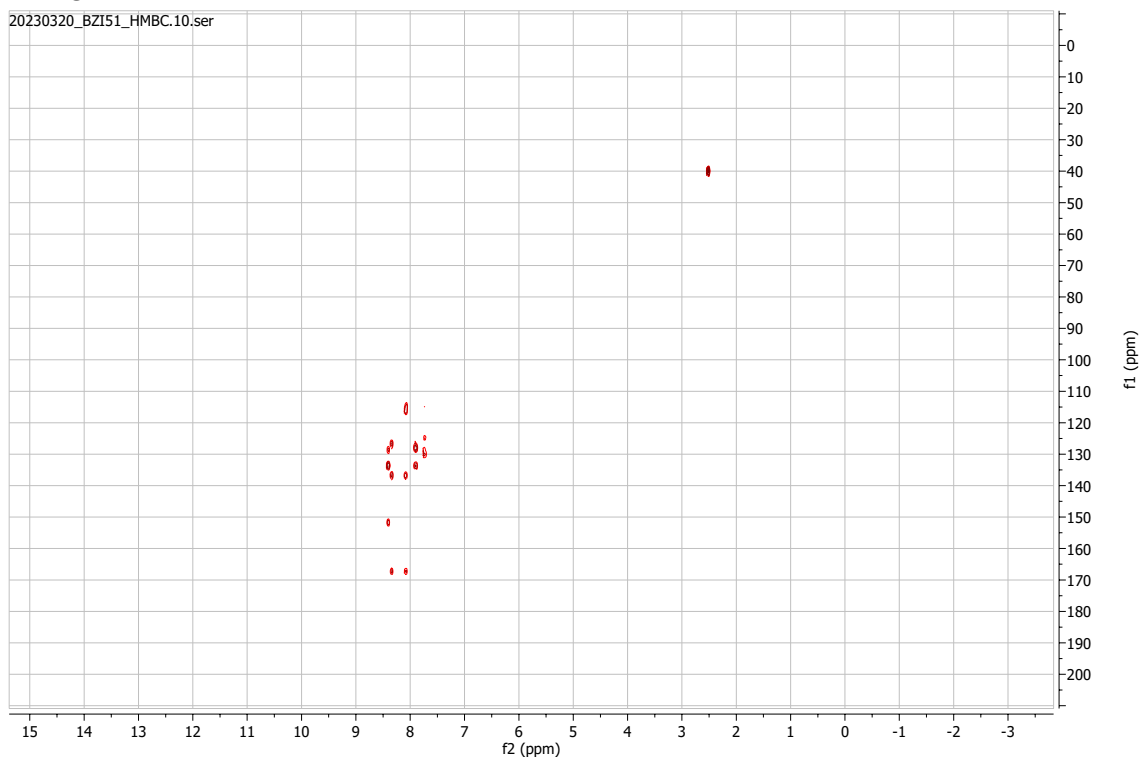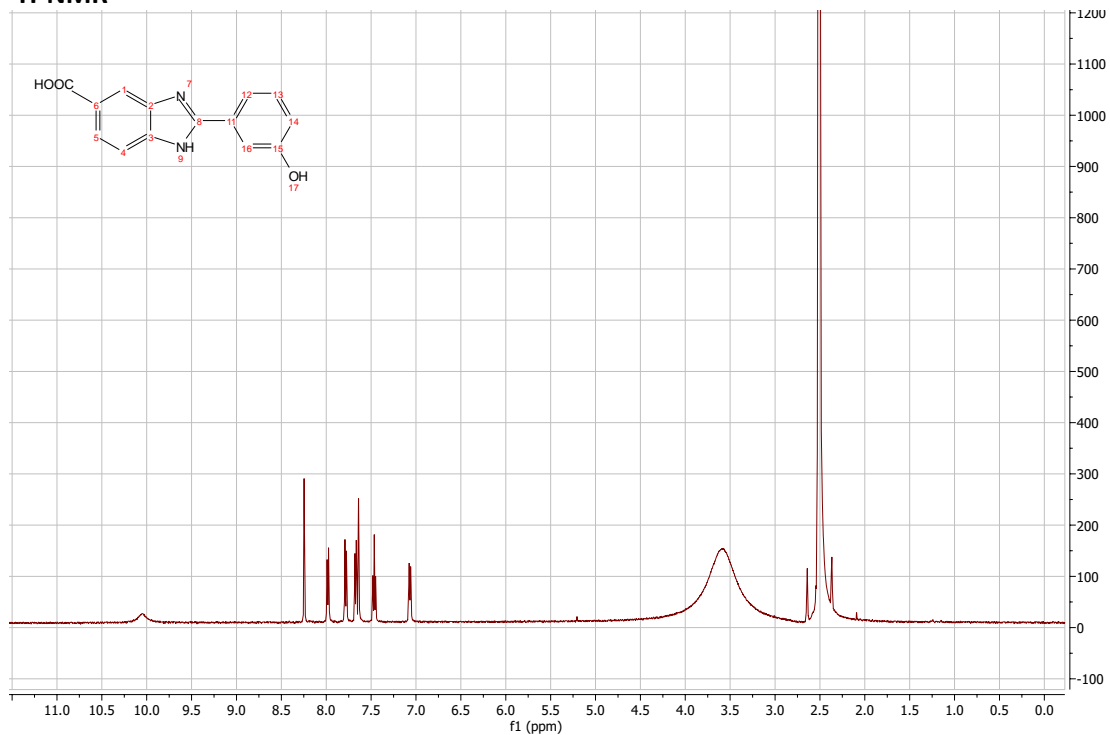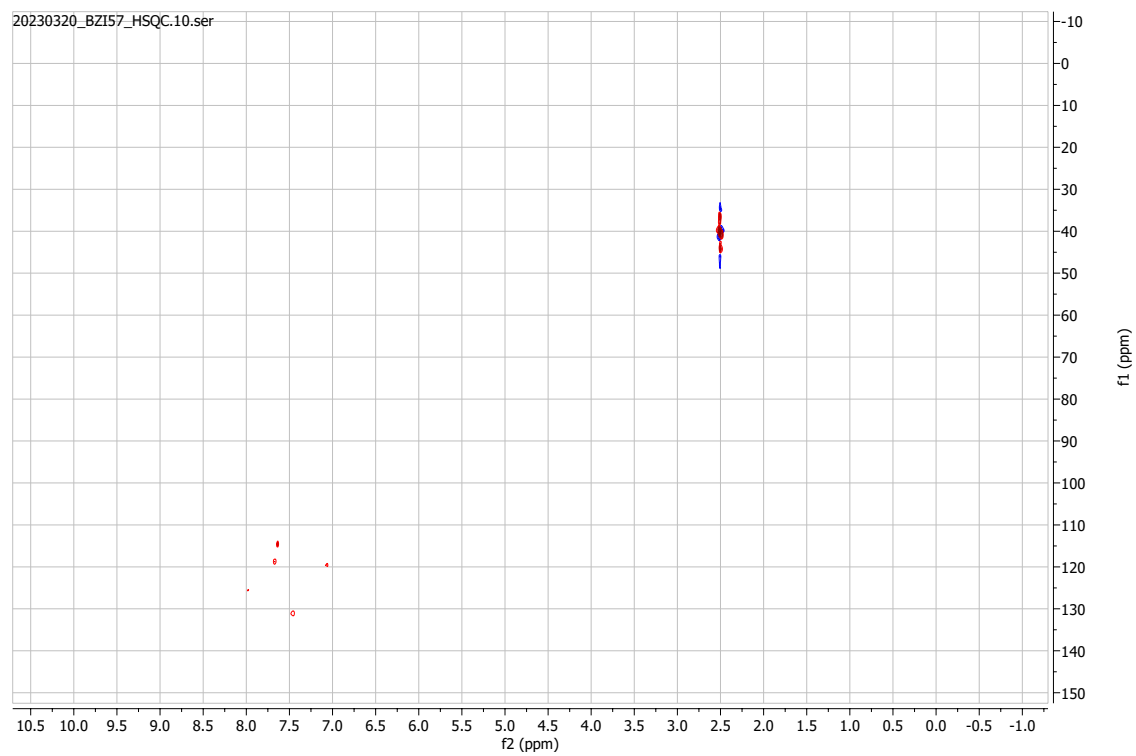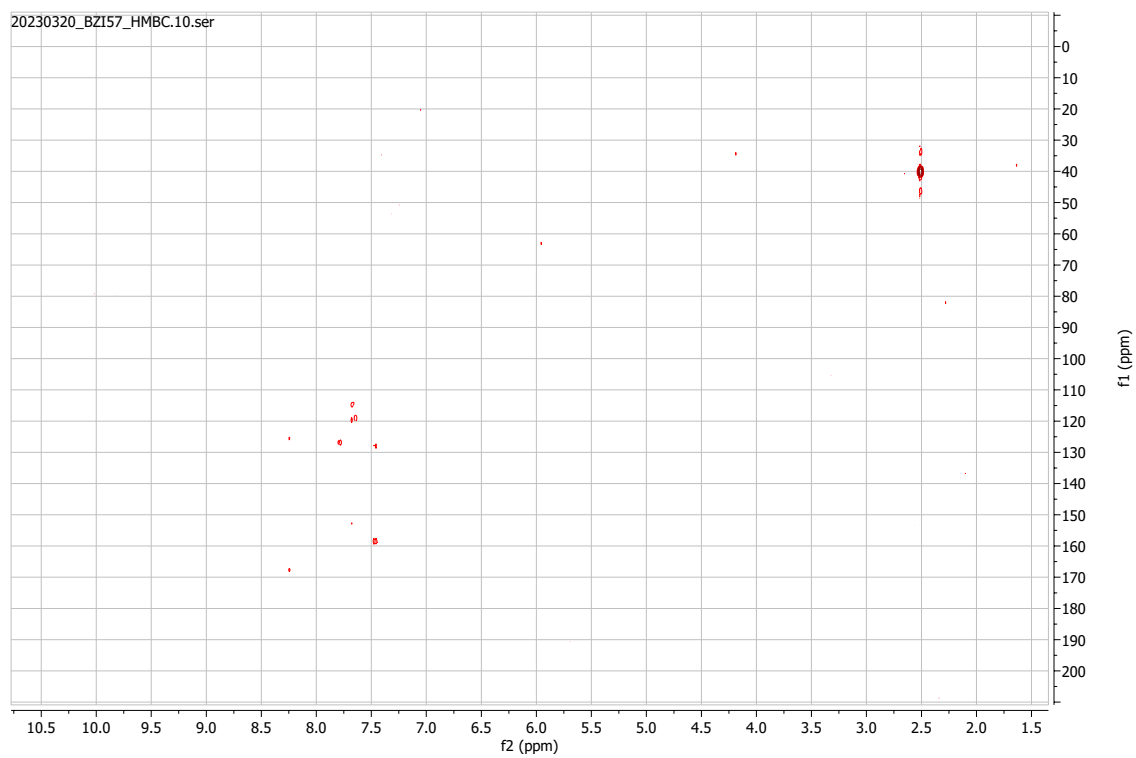
Structures of indole-benzimidazole hybrids:
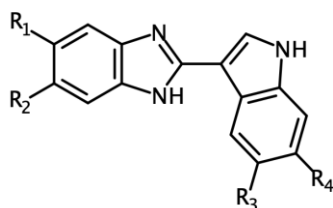
ID	R_1	R_1	R_1	R_1
HY-1	-H	-H	-H	-Cl
HY-2	-H	-H	-H	-H
HY-3	-H	-H	-Br	-H
HY-5	-H	-Cl	-H	-Cl
HY-6	-H	-Cl	-Br	-H
HY-7	-H	-Cl	-H	-H
HY-8	C_6H_5CO-	-H	-H	-H
HY-9	C_6H_5CO-	-H	-H	-Cl
HY-10	C_6H_5CO-	-H	-Br	-H
HY-11	-H	-F	-H	-H
HY-12	-H	-F	-H	-Cl
HY-13	-H	-F	-Br	-H
HY-14	-COOH	-H	-H	-H
HY-15	-COOH	-H	-H	-Cl
HY-16	-COOH	-H	-Br	-H
HY-17	-H	$-NO_2$	-H	-H
HY-18	-H	$-NO_2$	-H	-Cl
HY-19	-H	$-NO_2$	-Br	-H
HY-20	$-CH_3$	$-CH_3$	-H	-H
HY-21	$-CH_3$	$-CH_3$	-Br	-H
HY-22	$-CH_3$	$-CH_3$	-H	-Cl

Chapter 8

Bibliography

8. Bibliography

1. A. M. Valdes, J. Walter, E. Segal and T. D. Spector, Role of the gut microbiota in nutrition and health, *BMJ*, 2018, **361**, 36–44.

2. A. C. Ouwehand, S. Salminen and E. Isolauri, Probiotics: an overview of beneficial effects, *Lact. Acid Bact. Genet. Metab. Appl.*, 2002, 279–289.

3. H. Zhang, J. B. Sparks, S. V. Karyala, R. Settlage and X. M. Luo, Host adaptive immunity alters gut microbiota, *ISME J. 2015 93*, 2014, **9**, 770–781.

4. A. Hakansson and G. Molin, Gut Microbiota and Inflammation, *Nutr. 2011, Vol. 3, Pages 637-682*, 2011, **3**, 637–682.

5. A. I. Álvarez-Mercado, M. Navarro-Oliveros, C. Robles-Sánchez, J. Plaza-Díaz, M. J. Sáez-Lara, S. Muñoz-Quezada, L. Fontana and F. Abadía-Molina, Microbial Population Changes and Their Relationship with Human Health and Disease, *Microorg. 2019, Vol. 7, Page 68*, 2019, **7**, 68.

6. J. F. Zachary, Mechanisms of Microbial Infections, *Pathol. Basis Vet. Dis.*, 2017, 132.

7. J. H. Powers, Antimicrobial drug development – the past, the present, and the future, *Clin. Microbiol. Infect.*, 2004, **10**, 23–31.

8. Giguère Steeve, John F. Prescott and Patricia M. Dowling, *Antimicrobial Therapy in Veterinary Medicine - Google Libri*, John Wiley & Sons, 2013, vol. 3.

9. M. L. Kaplan and L. Kaplan, The Gram Stain and Differential Staining, *J. Bacteriol.*, 1933, **25**, 309–321.

10. S. Elmore, Apoptosis: A Review of Programmed Cell Death, *Toxicol. Pathol.*, 2007, **35**, 495.

11. M. Hutchings, A. Truman and B. Wilkinson, Antibiotics: past, present and future, *Curr. Opin. Microbiol.*, 2019, **51**, 72–80.

12. S. Doron and S. L. Gorbach, Bacterial Infections: Overview, *Int. Encycl. Public Heal.*, 2008, 273.

13. I. M. Kompis, K. Islam and R. L. Then, DNA and RNA synthesis: Antifolates, *Chem. Rev.*, 2005, **105**, 593–620.

14. V. T. Andriole, The Quinolones: Past, Present, and Future, *Clin. Infect. Dis.*, 2005, **41**, S113–S119.

15. W. Wehrli, Rifampin: Mechanisms of Action and Resistance, *Rev. Infect. Dis.*, 1983, **5**, S407–S411.

16. F. Nguyen, A. L. Starosta, S. Arenz, D. Sohmen, A. Dönhöfer and D. N. Wilson, Tetracycline antibiotics and resistance mechanisms, *Biol. Chem.*, 2014, **395**, 559–575.

17   K. Bush and P. A. Bradford, β-Lactams and β-Lactamase Inhibitors: An Overview, *Cold Spring Harb. Perspect. Med.*, 2016, **6**, a025247.

18   D. P. Levine, Vancomycin: A History, *Clin. Infect. Dis.*, 2006, **42**, S5–S12.

19   W. A. Toscano and D. R. Storm, Bacitracin, *Pharmacol. Ther.*, 1982, **16**, 199–210.

20   M. L. Rodrigues, *The multifunctional fungal ergosterol*, American Society for Microbiology, 2018, vol. 9.

21   G. Garber, An overview of fungal infections, *Drugs*, 2001, **61**, 1–12.

22   J. Berman and L. Hadany, *Trends Genet.*, 2012, 28, 197–203.

23   V. J. Fraser, M. Jones, J. Dunkel, S. Storfer, G. Medoff and W. Claiborne Dunagan, Candidemia in a Tertiary Care Hospital: Epidemiology, Risk Factors, and Predictors of Mortality, *Clin. Infect. Dis.*, 1992, **15**, 414–421.

24   M. V. Martin, The use of fluconazole and itraconazole in the treatment of Candida albicans infections: a review, *J. Antimicrob. Chemother.*, 1999, **44**, 429–437.

25   S. Campbell and K. Soman-Faulkner, Antiparasitic Drugs, *StatPearls*.

26   R. G. Yaeger, Protozoa: Structure, Classification, Growth, and Development, *Med. Microbiol.*

27   A. Rassi, A. Rassi and J. A. Marin-Neto, Chagas disease, *Lancet*, 2010, **375**, 1388–1402.

28   C. Bern, S. Kjos, M. J. Yabsley and S. P. Montgomery, Trypanosoma cruzi and Chagas' Disease in the United States, *Clin. Microbiol. Rev.*, 2011, **24**, 655.

29   L. Zekar and T. Sharman, Plasmodium Falciparum Malaria, *StatPearls*.

30   T. E. Wellems and C. V. Plowe, Chloroquine-Resistant Malaria, *J. Infect. Dis.*, 2001, **184**, 770–776.

31   G. A. Castro, Helminths: Structure, Classification, Growth, and Development, *Med. Microbiol.*

32   C. E. Hopla, L. A. Durden and J. E. Keirans, Ectoparasites and classification, *Rev. sci. tech. Off. int. Epiz*, 1994, **13**, 985–1017.

33   J. Heukelbach and H. Feldmeier, Scabies, *Lancet*, 2006, **367**, 1767–1774.

34   S. Sundar and J. Chakravarty, Paromomycin in the treatment of leishmaniasis, *Expert Opin. Investig. Drugs*, 2008, **17**, 787–794.

35   J. D. Maya, B. K. Cassels, P. Iturriaga-Vásquez, J. Ferreira, M. Faúndez, N. Galanti, A. Ferreira and A. Morello, Mode of action of natural and synthetic drugs against Trypanosoma cruzi and their interaction with the mammalian host, *Comp. Biochem. Physiol. Part A Mol. Integr. Physiol.*, 2007, **146**, 601–620.

36   J. Y. Chai, B. K. Jung and S. J. Hong, Albendazole and Mebendazole as Anti-Parasitic and Anti-Cancer Agents: an Update, *Korean J. Parasitol.*, 2021, **59**, 189.

37   H. V. Goodson and E. M. Jonasson, Microtubules and Microtubule-Associated Proteins, *Cold Spring Harb. Perspect. Biol.*, 2018, **10**, a022608.

38   M. W. Robinson, N. McFerran, A. Trudgett, L. Hoey and I. Fairweather, A possible model of benzimidazole binding to beta-tubulin disclosed by invoking an inter-domain movement, *J. Mol. Graph. Model.*, 2004, **23**, 275–284.

39   Y. Wang, H. Zhang, B. Gigant, Y. Yu, Y. Wu, X. Chen, Q. Lai, Z. Yang, Q. Chen and J. Yang, Structures of a diverse set of colchicine binding site inhibitors in complex with tubulin provide a rationale for drug discovery, *FEBS J.*, 2016, **283**, 102–111.

40   M. Á. Oliva, C. Tosat-Bitrián, L. Barrado-Gil, F. Bonato, I. Galindo, U. Garaigorta, B. Álvarez-Bernad, R. París-Ogáyar, D. Lucena-Agell, J. F. Giménez-Abián, I. García-Dorival, J. Urquiza, P. Gastaminza, J. F. Díaz, V. Palomo and C. Alonso, Effect of Clinically Used Microtubule Targeting Drugs on Viral Infection and Transport Function, *Int. J. Mol. Sci.*, 2022, **23**, 3448.

41   R. N. Jones and M. A. Pfaller, Bacterial Resistance: A Worldwide Problem, *Diagn. Microbiol. Infect. Dis.*, 1998, **31**, 379–388.

42   L. E. Cowen, D. Sanglard, S. J. Howard, P. D. Rogers and D. S. Perlin, Mechanisms of Antifungal Drug Resistance, *Cold Spring Harb. Perspect. Med.*

43   R. Pink, A. Hudson, M. A. Mouriès and M. Bendig, Opportunities and Challenges in Antiparasitic Drug Discovery, *Nat. Rev. Drug Discov. 2005 49*, 2005, **4**, 727–740.

44   A. Jeffery-Smith, S. K. Taori, S. Schelenz, K. Jeffery, E. M. Johnson, A. Borman, R. Manuel and C. S. Browna, Candida auris: A review of the literature, *Clin. Microbiol. Rev.*

45   J. Rhodes and M. C. Fisher, Global epidemiology of emerging Candida auris, *Curr. Opin. Microbiol.*, 2019, **52**, 84–89.

46   M. D. Conrad and P. J. Rosenthal, Antimalarial drug resistance in Africa: the calm before the storm?, *Lancet Infect. Dis.*, 2019, **19**, e338–e351.

47   W. Fissiha and M. Z. Kinde, Anthelmintic Resistance and Its Mechanism: A Review, *Infect. Drug Resist.*, 2021, **14**, 5403–5410.

48   L. A. Dever and T. S. Dermody, Mechanisms of Bacterial Resistance to Antibiotics, *Arch. Intern. Med.*, 1991, **151**, 886–895.

49   G. Cheng, M. Dai, S. Ahmed, H. Hao, X. Wang and Z. Yuan, Antimicrobial drugs in fighting against antimicrobial resistance, *Front. Microbiol.*, 2016, **7**, 470.

50   R. J. Worthington and C. Melander, Combination approaches to combat multidrug-resistant bacteria, *Trends Biotechnol.*, 2013, **31**, 177–184.

51   S. Chanda, K. D. Rakholiya and K. Rakholiya, Combination therapy: Synergism between natural plant extracts and antibiotics against infectious diseases Toxicity View project

Combination therapy: Synergism between natural plant extracts and antibiotics against infectious diseases.

52 J. D. Williams, β-Lactamases and β-lactamase inhibitors, *Int. J. Antimicrob. Agents*, 1999, **12**, S3–S7.

53 M. Mora-Ochomogo and C. T. Lohans, β-Lactam antibiotic targets and resistance mechanisms: from covalent inhibitors to substrates, *RSC Med. Chem.*, 2021, **12**, 1623–1639.

54 G. Kalkut, Sulfonamides and Trimethoprim, 2009, **16**, 612–615.

55 N. Cassir, J. M. Rolain and P. Brouqui, A new strategy to fight antimicrobial resistance: The revival of old antibiotics, *Front. Microbiol.*, 2014, **5**, 551.

56 K. Heinz and O. Kandler, Peptidoglycan .Types of Bacterial Cell Walls and their Taxonomic Implications, *Bacteriol. Rev.*, 1972, **36**, 407–477.

57 J. W. Johnson, J. F. Fisher and S. Mobashery, Bacterial cell-wall recycling, *Ann. N. Y. Acad. Sci.*, 2013, **1277**, 54–75.

58 J. W. Johnson, J. F. Fisher and S. Mobashery, Bacterial cell-wall recycling, *Ann. N. Y. Acad. Sci.*, 2013, **1277**, 54–75.

59 D. A. Dik, D. R. Marous, J. F. Fisher and S. Mobashery, Lytic transglycosylases: concinnity in concision of the bacterial cell wall, 2017, **52**, 503–542.

60 M. Lee, D. Hesek, D. A. Dik, J. Fishovitz, E. Lastochkin, B. Boggess, J. F. Fisher and S. Mobashery, From Genome to Proteome to Elucidation of Reactions for All Eleven Known Lytic Transglycosylases from Pseudomonas aeruginosa, *Angew. Chemie Int. Ed.*, 2017, **56**, 2735–2739.

61 M. Lee, D. Hesek, L. I. Llarrull, E. Lastochkin, H. Pi, B. Boggess and S. Mobashery, Reactions of all escherichia coli lytic transglycosylases with bacterial cell wall, *J. Am. Chem. Soc.*, 2013, **135**, 3311–3314.

62 D. M. Chipman and N. Sharon, Mechanism of lysozyme action, *Science (80-.).*, 1969, **165**, 454–465.

63 A.-M. M. W. H. Thunnissen, H. J. Rozeboom, K. H. Kalk and B. W. Dijkstra, Structure of the 70-kDa Soluble Lytic Transglycosylase Complexed with Bulgecin A. Implications for the Enzymatic Mechanism, *Biochemistry*, 1995, **34**, 12729–12737.

64 N. T. Blackburn and A. J. Clarke, Assay for Lytic Transglycosylases: A Family of Peptidoglycan Lyases, *Anal. Biochem.*, 2000, **284**, 388–393.

65 E. Scheurwater, C. W. Reid and A. J. Clarke, Lytic transglycosylases: Bacterial space-making autolysins, *Int. J. Biochem. Cell Biol.*, 2008, **40**, 586–591.

66 E. J. Van Asselt, A. M. W. H. Thunnissen and B. W. Dijkstra, High resolution crystal

structures of the Escherichia coli lytic transglycosylase slt70 and its complex with a peptidoglycan fragment, *J. Mol. Biol.*, 1999, **291**, 877–898.

67   E. J. Van Asselt, K. H. Kalk and B. W. Dijkstra, Crystallographic Studies of the Interactions of Escherichia coli Lytic Transglycosylase Slt35 with Peptidoglycan†,‡, *Biochemistry*, 2000, **39**, 1924–1934.

68   A. H. Williams, R. Wheeler, C. Thiriau, A. Haouz, M. K. Taha and I. G. Boneca, Bulgecin A: The Key to a Broad-Spectrum Inhibitor That Targets Lytic Transglycosylases, *Antibiotics*.

69   STRUCTURE OF THE 70-KDA SOLUBLE LYTIC TRANSGLYCOSYLASE COMPLEXED WITH BULGECIN-A-IMPLICATIONS FOR THE ENZYMATIC MECHANISM.

70   C. W. Reid, N. T. Blackburn, B. A. Legaree, F. I. Auzanneau and A. J. Clarke, Inhibition of membrane-bound lytic transglycosylase B by NAG-thiazoline, *FEBS Lett.*, 2004, **574**, 73–79.

71   S. Tomoshige, D. A. Dik, M. Akabane-Nakata, C. S. Madukoma, J. F. Fisher, J. D. Shrout and S. Mobashery, Total Syntheses of Bulgecins A, B, and C and Their Bactericidal Potentiation of the β-Lactam Antibiotics, *ACS Infect. Dis.*, 2018, **4**, 860–867.

72   R. Cooper and S. Unger, Novel Potentiators of ß-Lactam Antibiotics. Structures of SQ 28504 and SQ 28546, *J. Org. Chem.*, 1986, **51**, 3942–3946.

73   A.-M. W. H. Thunnissen, H. J. Rozeboom, K. H. Kalk and B. W. Dijkstra, Structure of the 70-kDa Soluble Lytic Transglycosylase Complexed with Bulgecin A. Implications for the Enzymic Mechanism.

74   J. B. Wright, The Chemistry of the Benzimidazoles, *Chem. Rev.*, 1951, **48**, 397–541.

75   S. I. Alaqeel, Synthetic approaches to benzimidazoles from o-phenylenediamine: A literature review, *J. Saudi Chem. Soc.*, 2017, **21**, 229–237.

76   Z. Wang, Phillips-Ladenburg Benzimidazole Synthesis, *Compr. Org. Name React. Reagents*, 2010, 2197–2199.

77   S. R. Rithe, R.S. Jagtap, S.S Ubarhande, One pot synthesis of substituted benzimidazole derivatives and their charcterization, *Rasayan Journal of Chemistry*, **8**, 213-217.

78   S. Lin and L. Yang, A simple and efficient procedure for the synthesis of benzimidazoles using air as the oxidant, *Tetrahedron Lett.*, 2005, **46**, 4315–4319.

79   F. Odame, E. Hosten, R. Betz, K. Lobb and Z. R. Tshentu, Benzimidazole or Diamide From a Reaction of Diamines and Carboxylic Acids or Acid Chlorides: Crystal Structures and Theoretical Studies, *Acta Chim. Slov*, 2015, **62**, 986–994.

80   H. Malipeddi, Synthesis and anthelmintic activity studies of 1-substituted benzimidazole derivatives Development of an Efficient Bacterial Consortium for the Remediation of Hydrocarbons from Contaminated Sites View project Biosurfactant Mediated Green

Synthesis Of Eco-Friendly Metal Nanoparticles And Their Application In Bioremediation Of Petroleum Hydrocarbon Pollutants View project, *Artic. J. Indian Chem. Soc.*

81   F. Bellina, C. Calandri, S. Cauteruccio and R. Rossi, Efficient and highly regioselective direct C-2 arylation of azoles, including free (NH)-imidazole, -benzimidazole and -indole, with aryl halides, *Tetrahedron*, 2007, **63**, 1970–1980.

82   B. Das, K. Venkateswarlu, M. Krishnaiah and H. Holla, An efficient, rapid and regioselective nuclear bromination of aromatics and heteroaromatics with NBS using sulfonic-acid-functionalized silica as a heterogeneous recyclable catalyst, *Tetrahedron Lett.*, 2006, **47**, 8693–8697.

83   C. T. Walsh, Nature loves nitrogen heterocycles, *Tetrahedron Lett.*, 2015, **56**, 3075–3081.

84   D. W. Woolley, SOME BIOLOGICAL EFFECTS PRODUCED BY BENZIMIDAZOLE AND THEIR REVERSAL BY PURINES, *J. Biol. Chem.*, 1944, **152**, 225–232.

85   A. A. Spasov, I. N. Yozhitsa, L. I. Bugaeva and V. A. Anisimova, Benzimidazole derivatives: Spectrum of pharmacological activity and toxicological properties (a review), *Pharm. Chem. J.*, 1999, **33**, 232–243.

86   R. Walia, S. Farha Naaz, K. Iqbal and H. S. Lamba, INTERNATIONAL JOURNAL OF RESEARCH IN PHARMACY AND CHEMISTRY BENZIMIDAZOLE DERIVATIVES-AN OVERVIEW, *IJRPC*.

87   N. G. Brink and K. Folkers, Vitamin B12. VI. 5,6-dimethylbenzimidazole, a degradation product of vitamin B12, *J. Am. Chem. Soc.*, 1949, **71**, 2951.

88   M. J. Warren, Finding the final pieces of the vitamin B12 biosynthetic jigsaw, *Proc. Natl. Acad. Sci. U. S. A.*, 2006, **103**, 4799–4800.

89   A. B. Hazra, A. W. Han, A. P. Mehta, K. C. Mok, V. Osadchiy, T. P. Begley and M. E. Taga, Anaerobic biosynthesis of the lower ligand of vitamin B12, *Proc. Natl. Acad. Sci. U. S. A.*, 2015, **112**, 10792–10797.

90   A. Grassi, J. Ippen, M. Bruno and G. Thomas, BAY P 1455, a thiazolylaminobenzimidazole derivative with gastroprotective properties in the rat, *Eur. J. Pharmacol.*, 1991, **195**, 251–259.

91   R. Walia, S. Farha Naaz, K. Iqbal and H. S. Lamba, INTERNATIONAL JOURNAL OF RESEARCH IN PHARMACY AND CHEMISTRY BENZIMIDAZOLE DERIVATIVES-AN OVERVIEW, *IJRPC*.

92   Y. Bansal and O. Silakari, The therapeutic journey of benzimidazoles: A review, *Bioorg. Med. Chem.*, 2012, **20**, 6208–6236.

93   S. Tahlan, S. Kumar and B. Narasimhan, Pharmacological significance of heterocyclic 1H-

benzimidazole scaffolds: a review, *BMC Chem. 2019 131*, 2019, **13**, 1–21.

94   M. Boiani and M. Gonzalez, Imidazole and Benzimidazole Derivatives as Chemotherapeutic Agents, *Mini-Reviews Med. Chem.*, 2005, **5**, 409–424.

95   N. Singh, A. Pandurangan, K. Rana, P. Anand, A. Ahamad and A. K. Tiwari, Benzimidazole: A short review of their antimicrobial activities, *Int. Curr. Pharm. J.*, 2012, **1**, 110–118.

96   G. Cammarota, A. Gallo, G. Ianiro and M. Montalto, Emerging drugs for the treatment of clostridium difficile, 2019, **24**, 17–28.

97   J. C. Cho, M. P. Crotty and J. Pardo, Ridinilazole: a novel antimicrobial for Clostridium difficile infection, *Ann. Gastroenterol.*, 2019, **32**, 134.

98   M. Gaba and C. Mohan, Development of drugs based on imidazole and benzimidazole bioactive heterocycles: recent advances and future directions, *Med. Chem. Res. 2015 252*, 2015, **25**, 173–210.

99   W. P. E. Raab, Broad-Spectrum Antimicrobials for Local Application, *Treat. Mycosis with Imidazole Deriv.*, 1980, 6–18.

100   R. Musiol and W. Kowalczyk, Azole Antimycotics - A Highway to New Drugs or a Dead End?, *Curr. Med. Chem.*, 2012, **19**, 1378–1388.

101   P. D. Crowley and H. C. Gallagher, Clotrimazole as a pharmaceutical: past, present and future., *J. Appl. Microbiol.*, 2014, **117**, 611–617.

102   P. R. Sawyer, R. N. Brogden, R. M. Pinder, T. M. Speight and G. S. Avery, Miconazole: A Review of its Antifungal Activity and Therapeutic Efficacy, *Drugs*, 1975, **9**, 406–423.

103   R. A. Fromtling, Overview of medically important antifungal azole derivatives, *Clin. Microbiol. Rev.*, 1988, **1**, 187–217.

104   J. Zhang, L. Li, Q. Lv, L. Yan, Y. Wang and Y. Jiang, The fungal CYP51s: Their functions, structures, related drug resistance, and inhibitors, *Front. Microbiol.*, 2019, **10**, 691.

105   Y. Zhou, J. Xu, Y. Zhu, Y. Duan and M. Zhou, Mechanism of action of the benzimidazole fungicide on Fusarium graminearum: Interfering with polymerization of monomeric tubulin but not polymerized microtubule, *Phytopathology*, 2016, **106**, 807–813.

106   R. M. Hauptmann, J. M. Widholm and J. D. Paxton, Benomyl: A broad spectrum fungicide for use in plant cell and protoplast culture, *Plant Cell Rep.*, 1985, **4**, 129–132.

107   H. Morinaga, T. Yanase, M. Nomura, T. Okabe, K. Goto, N. Harada and H. Nawata, A Benzimidazole Fungicide, Benomyl, and Its Metabolite, Carbendazim, Induce Aromatase Activity in a Human Ovarian Granulose-Like Tumor Cell Line (KGN), *Endocrinology*, 2004, **145**, 1860–1869.

108   N. F. Aftab, K. S. Ahmad and M. M. Gul, Sorptive and degradative assessments of

environmentally pestilential Benzimidazole fungicide Fuberidazole in pedosphere.

109   K. G. Desai and K. R. Desai, Green route for the heterocyclization of 2-mercaptobenzimidazole into β-lactum segment derivatives containing –CONH– bridge with benzimidazole: Screening in vitro antimicrobial activity with various microorganisms, *Bioorg. Med. Chem.*, 2006, **14**, 8271–8279.

110   K. P. Barot, S. Nikolova, I. Ivanov and M. D. Ghate, Novel Research Strategies of Benzimidazole Derivatives: A Review.

111   O. O. Ajani, O. O. Tolu-Bolaji, S. J. Olorunshola, Y. Zhao and D. V. Aderohunmu, Structure-based design of functionalized 2-substituted and 1,2-disubstituted benzimidazole derivatives and their in vitro antibacterial efficacy, *J. Adv. Res.*, 2017, **8**, 703–712.

112   M. Boiani and M. Gonzalez, Imidazole and benzimidazole derivatives as chemotherapeutic agents., *Mini Rev. Med. Chem.*, 2005, **5**, 409–424.

113   K. F. Ansari and C. Lal, Synthesis and evaluation of some new benzimidazole derivatives as potential antimicrobial agents, *Eur. J. Med. Chem.*, 2009, **44**, 2294–2299.

114   P. Bandyopadhyay, M. Sathe, S. Ponmariappan, A. Sharma, P. Sharma, A. K. Srivastava and M. P. Kaushik, Exploration of in vitro time point quantitative evaluation of newly synthesized benzimidazole and benzothiazole derivatives as potential antibacterial agents, *Bioorg. Med. Chem. Lett.*, 2011, **21**, 7306–7309.

115   K. Kumar, D. Awasthi, S. Y. Lee, I. Zanardi, B. Ruzsicska, S. Knudson, P. J. Tonge, R. A. Slayden and I. Ojima, Novel trisubstituted benzimidazoles, targeting Mtb FtsZ, as a new class of antitubercular agents, *J. Med. Chem.*, 2011, **54**, 374–381.

116   H. H. Jardosh, C. B. Sangani, M. P. Patel and R. G. Patel, One step synthesis of pyrido[1,2-a]benzimidazole derivatives of aryloxypyrazole and their antimicrobial evaluation, *Chinese Chem. Lett.*, 2013, **24**, 123–126.

117   B. Arslan, C. Kazak, H. Karataş and S. Özden, Methyl 1-n-butyl-2-(3,4-dichlorophenyl)-1H-benzimidazole-5-carboxylate, *Acta Crystallogr. Sect. E Struct. Reports Online*, 2004, **60**, o1535–o1537.

118   S. Bansal, U. Tawar, M. Singh, A. Nikravesh, L. Good and V. Tandon, Old class but new dimethoxy analogue of benzimidazole: a bacterial topoisomerase I inhibitor, *Int. J. Antimicrob. Agents*, 2010, **35**, 186–190.

119   J. B. Moreira, J. Mann, S. Neidle, T. D. McHugh and P. W. Taylor, Antibacterial activity of head-to-head bis-benzimidazoles, *Int. J. Antimicrob. Agents*, 2013, **42**, 361–366.

120   L. Hu, M. L. Kully, D. W. Boykin and N. Abood, Optimization of the central linker of dicationic bis-benzimidazole anti-MRSA and anti-VRE agents, *Bioorg. Med. Chem. Lett.*,

2009, **19**, 3374–3377.

121   D. Seenaiah, P. R. Reddy, G. M. Reddy, A. Padmaja, V. Padmavathi and N. Siva Krishna, Synthesis, antimicrobial and cytotoxic activities of pyrimidinyl benzoxazole, benzothiazole and benzimidazole, *Eur. J. Med. Chem.*, 2014, **77**, 1–7.

122   D. R. Shah, R. P. Modh and K. H. Chikhalia, Privileged s-triazines: Structure and pharmacological applications, *Future Med. Chem.*, 2014, **6**, 463–477.

123   Z. E. Koc, H. Bingol, A. O. Saf, E. Torlak and A. Coskun, Synthesis of novel tripodal-benzimidazole from 2,4,6-tris(p-formylphenoxy)-1,3,5-triazine: Structural, electrochemical and antimicrobial studies, *J. Hazard. Mater.*, 2010, **183**, 251–255.

124   R. R. Crichton, An overview of the role of metals in biology, *Pract. Approaches to Biol. Inorg. Chem.*, 2020, 1–16.

125   A. Tavman, Zn(II) and Cu(II) complexes of 2-(2-hydroxy-5-methylphenyl)-1H-benzimidazole and crystal structure of 2-(2-hydroxy-5-methylphenyl)-1H-benzimidazolium chloride, *Russ. J. Inorg. Chem.*, 2010, **55**, 377–383.

126   S. A. Stanley, S. S. Grant, T. Kawate, N. Iwase, M. Shimizu, C. Wivagg, M. Silvis, E. Kazyanskaya, J. Aquadro, A. Golas, M. Fitzgerald, H. Dai, L. Zhang and D. T. Hung, Identification of novel inhibitors of M. tuberculosis growth using whole cell based high-throughput screening, *ACS Chem. Biol.*, 2012, **7**, 1377–1384.

127   J. Ramprasad, N. Nayak, U. Dalimba, P. Yogeeswari, D. Sriram, S. K. Peethambar, R. Achur and H. S. S. Kumar, Synthesis and biological evaluation of new imidazo[2,1-b][1,3,4]thiadiazole-benzimidazole derivatives, *Eur. J. Med. Chem.*, 2015, **95**, 49–63.

128   J. Camacho, A. Barazarte, N. Gamboa, J. Rodrigues, R. Rojas, A. Vaisberg, R. Gilman and J. Charris, Synthesis and biological evaluation of benzimidazole-5-carbohydrazide derivatives as antimalarial, cytotoxic and antitubercular agents, *Bioorg. Med. Chem.*, 2011, **19**, 2023–2029.

129   B. Park, D. Awasthi, S. R. Chowdhury, E. H. Melief, K. Kumar, S. E. Knudson, R. A. Slayden and I. Ojima, Design, synthesis and evaluation of novel 2,5,6-trisubstituted benzimidazoles targeting FtsZ as antitubercular agents, *Bioorg. Med. Chem.*, 2014, **22**, 2602–2612.

130   M. Pieroni, S. K. Tipparaju, S. Lun, Y. Song, A. W. Sturm, W. R. Bishai and A. P. Kozikowski, Pyrido[1,2-a]benzimidazole-Based Agents Active Against Tuberculosis (TB), Multidrug-Resistant (MDR) TB and Extensively Drug-Resistant (XDR) TB, *ChemMedChem*, 2011, **6**, 334–342.

131   Q. A. McKELLAR and E. W. SCOTT, The benzimidazole anthelmintic agents-a review, *J. Vet. Pharmacol. Ther.*, 1990, **13**, 223–247.

132   J. W. G. Leiper and J. Crowley, The activity of thiabendazole against gastrointestinal nematodes of sheep in Great Britain. I. Dose response., *Br. Vet. J.*, 1963, **119**, 64–72.

133   W.-H. Huang and H. W. Brown, The Efficacy of Thiabendazole against Hookworm and Ascaris of Man, *J. Parasitol.*, 1963, **49**, 1014.

134   F. Battistini, N. Zaias, R. Sierra and G. Rebell, Clinical Antifungal Activity of Thiabendazole, *Arch. Dermatol.*, 1974, **109**, 695–699.

135   P. Pene, M. Mojon, J. P. Garin, J. P. Coulaud and J. F. Rossignol, Albendazole: a new broad spectrum anthelmintic. Double-blind multicenter clinical trial., *Am. J. Trop. Med. Hyg.*, 1982, **31**, 263–266.

136   J. Horton, Albendazole: a review of anthelmintic efficacy and safety in humans, *Parasitology*, 2000, **121**, S113–S132.

137   M. J. Miller, I. M. Krupp, M. D. Little and C. Santos, Mebendazole: An Effective Anthelmintic for Trichuriasis and Enterobiasis, *JAMA*, 1974, **230**, 1412–1414.

138   M. L. Colglazier, F. D. Enzie and K. C. Kates, Critical anthelmintic trials in ponies with four benzimidazoles: mebendazole, cambendazole, fenbendazole, and albendazole, *J. Parasitol.*, 1977, **63**, 724–727.

139   A. T. Mavrova, D. Vuchev, K. Anichina and N. Vassilev, Synthesis, antitrichinnellosis and antiprotozoal activity of some novel thieno[2,3-d]pyrimidin-4(3H)-ones containing benzimidazole ring, *Eur. J. Med. Chem.*, 2010, **45**, 5856–5861.

140   K. Kopańska, A. Najda, J. Zebrowska, L. Chomicz, J. Piekarczyk, P. Myjak and M. Bretner, Synthesis and activity of 1H-benzimidazole and 1H-benzotriazole derivatives as inhibitors of Acanthamoeba castellanii, *Bioorg. Med. Chem.*, 2004, **12**, 2617–2624.

141   M. Andrzejewska, L. Yepez-Mulia, A. Tapia, R. Cedillo-Rivera, A. E. Laudy, B. J. Starościak and Z. Kazimierczuk, Synthesis, and antiprotozoal and antibacterial activities of S-substituted 4,6-dibromo- and 4,6-dichloro-2-mercaptobenzimidazoles, *Eur. J. Pharm. Sci.*, 2004, **21**, 323–329.

142   J. M. Velázquez-López, A. Hernández-Campos, L. Yépez-Mulia, A. Téllez-Valencia, P. Flores-Carrillo, R. Nieto-Meneses and R. Castillo, Synthesis and trypanocidal activity of novel benzimidazole derivatives, *Bioorg. Med. Chem. Lett.*, 2016, **26**, 4377–4381.

143   C. Hernández-Covarrubias, M. A. Vilchis-Reyes, L. Yépez-Mulia, R. Sánchez-Díaz, G. Navarrete-Vázquez, A. Hernández-Campos, R. Castillo and F. Hernández-Luis, Exploring the interplay of physicochemical properties, membrane permeability and giardicidal activity of some benzimidazole derivatives, *Eur. J. Med. Chem.*, 2012, **52**, 193–204.

144   F. Hernández-Luis, A. Hernández-Campos, R. Castillo, G. Navarrete-Vázquez, O. Soria-Arteche, M. Hernández-Hernández and L. Yépez-Mulia, Synthesis and biological activity

of 2-(trifluoromethyl)-1H-benzimidazole derivatives against some protozoa and Trichinella spiralis, *Eur. J. Med. Chem.*, 2010, **45**, 3135–3141.

145   A. Márquez-Navarro, B. Nogueda-Torres, A. Hernández-Campos, O. Soria-Arteche, R. Castillo, S. Rodríguez-Morales, L. Yépez-Mulia and F. Hernández-Luis, Anthelmintic activity of benzimidazole derivatives against Toxocara canis second-stage larvae and Hymenolepis nana adults, *Acta Trop.*, 2009, **109**, 232–235.

146   C. Hernández-Covarrubias, M. A. Vilchis-Reyes, L. Yépez-Mulia, R. Sánchez-Díaz, G. Navarrete-Vázquez, A. Hernández-Campos, R. Castillo and F. Hernández-Luis, Exploring the interplay of physicochemical properties, membrane permeability and giardicidal activity of some benzimidazole derivatives, *Eur. J. Med. Chem.*, 2012, **52**, 193–204.

147   G. Aguirre, M. Boiani, H. Cerecetto, A. Gerpe, M. González, Y. F. Sainz, A. Denicola, C. O. De Ocáriz, J. J. Nogal, D. Montero and J. A. Escario, Novel Antiprotozoal Products: Imidazole and Benzimidazole N-Oxide Derivatives and Related Compounds, *Arch. Pharm. (Weinheim).*, 2004, **337**, 259–270.

148   G. Navarrete-Vázquez, M. D. M. Rojano-Vilchis, L. Yépez-Mulia, V. Meléndez, L. Gerena, A. Hernández-Campos, R. Castillo and F. Hernández-Luis, Synthesis and antiprotozoal activity of some 2-(trifluoromethyl)-1H-benzimidazole bioisosteres, *Eur. J. Med. Chem.*, 2006, **41**, 135–141.

149   B. A. Heinz and L. M. Vance, The antiviral compound enviroxime targets the 3A coding region of rhinovirus and poliovirus, *J. Virol.*, 1995, **69**, 4189–4197.

150   N. Shrivastava, M. J. Naim, M. J. Alam, F. Nawaz, S. Ahmed and O. Alam, Benzimidazole Scaffold as Anticancer Agent: Synthetic Approaches and Structure–Activity Relationship, *Arch. Pharm. (Weinheim).*, 2017, **350**, e201700040.

151   L. M. Wagner, Profile of veliparib and its potential in the treatment of solid tumors, *Onco. Targets. Ther.*, 2015, **8**, 1931–1939.

152   R. L. Coleman, G. F. Fleming, M. F. Brady, E. M. Swisher, K. D. Steffensen, M. Friedlander, A. Okamoto, K. N. Moore, N. Efrat Ben-Baruch, T. L. Werner, N. G. Cloven, A. Oaknin, P. A. DiSilvestro, M. A. Morgan, J.-H. Nam, C. A. Leath, S. Nicum, A. R. Hagemann, R. D. Littell, D. Cella, S. Baron-Hay, J. Garcia-Donas, M. Mizuno, K. Bell-McGuinn, D. M. Sullivan, B. A. Bach, S. Bhattacharya, C. K. Ratajczak, P. J. Ansell, M. H. Dinh, C. Aghajanian and M. A. Bookman, Veliparib with First-Line Chemotherapy and as Maintenance Therapy in Ovarian Cancer, *N. Engl. J. Med.*, 2019, **381**, 2403–2415.

153   F. Massoomi, J. Savage and C. J. Destache, Omeprazole: A Comprehensive Review, *Pharmacother. J. Hum. Pharmacol. Drug Ther.*, 1993, **13**, 46–59.

154   L. Bielory, K. W. Lien and S. Bigelsen, Efficacy and tolerability of newer antihistamines in

the treatment of allergic conjunctivitis, *Drugs*, 2005, **65**, 215–228.

155   W. L. Baker and W. B. White, Azilsartan Medoxomil: A New Angiotensin II Receptor Antagonist for Treatment of Hypertension.

156   C. M. Perry and W. L. Baker, Azilsartan Medoxomil, *Clin. Drug Investig. 2012 329*, 2012, **32**, 621–639.

157   S. Kanda, R. Nakashima, K. Takahashi, J. Tanaka, J. Ogawa, T. Ogata, M. Yachi, K. Araki and J. Ohsumi, Potent Antidiabetic Effects of Rivoglitazone, a Novel Peroxisome Proliferator–Activated Receptor-γ Agonist, in Obese Diabetic Rodent Models, *J. Pharmacol. Sci.*, 2009, **111**, 155–166.

158   R. L. Koffarnus, K. A. Wargo and H. M. Phillippe, Rivoglitazone: a new thiazolidinedione for the treatment of type 2 diabetes mellitus., *Ann. Pharmacother.*, 2013, **47**, 877–885.

159   M. Ganetsky, K. M. Babu, S. D. Salhanick, R. S. Brown and E. W. Boyer, Dabigatran: Review of Pharmacology and Management of Bleeding Complications of This Novel Oral Anticoagulant, *J. Med. Toxicol.*, 2011, **7**, 281–287.

160   M. Tonelli, G. Paglietti, V. Boido, F. Sparatore, F. Marongiu, E. Marongiu, P. La Colla and R. Loddo, Antiviral Activity of Benzimidazole Derivatives. I. Antiviral Activity of 1-Substituted-2-[(Benzotriazol-1/2-yl)methyl]benzimidazoles, *Chem. Biodivers.*, 2008, **5**, 2386–2401.

161   A. Husain, M. Rashid, M. Shaharyar, A. A. Siddiqui and R. Mishra, Benzimidazole clubbed with triazolo-thiadiazoles and triazolo-thiadiazines: New anticancer agents, *Eur. J. Med. Chem.*, 2013, **62**, 785–798.

162   A. Noor, N. G. Qazi, H. Nadeem, A. ullah Khan, R. Z. Paracha, F. Ali and A. Saeed, Synthesis, characterization, anti-ulcer action and molecular docking evaluation of novel benzimidazole-pyrazole hybrids, *Chem. Cent. J.*, 2017, **11**, 1–13.

163   K. C. S. Achar, K. M. Hosamani and H. R. Seetharamareddy, In-vivo analgesic and anti-inflammatory activities of newly synthesized benzimidazole derivatives, *Eur. J. Med. Chem.*, 2010, **45**, 2048–2054.

164   X. J. Wang, M. Y. Xi, J. H. Fu, F. R. Zhang, G. F. Cheng, D. L. Yin and Q. D. You, Synthesis, biological evaluation and SAR studies of benzimidazole derivatives as H1-antihistamine agents, *Chinese Chem. Lett.*, 2012, **23**, 707–710.

165   N. O. Anastassova, A. T. Mavrova, D. Y. Yancheva, M. S. Kondeva-Burdina, V. I. Tzankova, S. S. Stoyanov, B. L. Shivachev and R. P. Nikolova, Hepatotoxicity and antioxidant activity of some new N,N′-disubstituted benzimidazole-2-thiones, radical scavenging mechanism and structure-activity relationship, *Arab. J. Chem.*, 2018, **11**, 353–369.

166   R. V. Shingalapur, K. M. Hosamani, R. S. Keri and M. H. Hugar, Derivatives of benzimidazole pharmacophore: Synthesis, anticonvulsant, antidiabetic and DNA cleavage studies, *Eur. J. Med. Chem.*, 2010, **45**, 1753–1759.

167   U. Acar Cevik, B. N. Saglik, S. Levent, D. Osmaniye, B. Kaya Cavuşoglu, Y. Ozkay and Z. A. Kaplancikli, Synthesis and AChE-Inhibitory Activity of New Benzimidazole Derivatives, *Mol. 2019, Vol. 24, Page 861*, 2019, **24**, 861.

168   A. Bali, Y. Bansal, M. Sugumaran, J. S. Saggu, P. Balakumar, G. Kaur, G. Bansal, A. Sharma and M. Singh, Design, synthesis, and evaluation of novelly substituted benzimidazole compounds as angiotensin II receptor antagonists, *Bioorg. Med. Chem. Lett.*, 2005, **15**, 3962–3965.

169   W. Hamaguchi, N. Masuda, M. Isomura, S. Miyamoto, S. Kikuchi, Y. Amano, K. Honbou, T. Mihara and T. Watanabe, Design and synthesis of novel benzimidazole derivatives as phosphodiesterase 10A inhibitors with reduced CYP1A2 inhibition, *Bioorg. Med. Chem.*, 2013, **21**, 7612–7623.

170   J. M. Travins, R. C. Bernotas, D. H. Kaufman, E. Quinet, P. Nambi, I. Feingold, C. Huselton, A. Wilhelmsson, A. Goos-Nilsson and J. Wrobel, 1-(3-Aryloxyaryl)benzimidazole sulfones are liver X receptor agonists, *Bioorg. Med. Chem. Lett.*, 2010, **20**, 526–530.

171   H. Yang, Y. Ren, X. Gao and Y. Gao, Synthesis and anticoagulant bioactivity evaluation of 1,2,5-trisubstituted benzimidazole fluorinated derivatives, *Chem. Res. Chinese Univ.*, 2016, **32**, 973–978.

172   G. Surineni, Y. Gao, M. Hussain, Z. Liu, Z. Lu, C. Chhotaray, M. M. Islam, H. M. A. Hameed and T. Zhang, Design, synthesis, and in vitro biological evaluation of novel benzimidazole tethered allylidenehydrazinylmethylthiazole derivatives as potent inhibitors of Mycobacterium tuberculosis, *Medchemcomm*, 2019, **10**, 49–60.

173   G. Parker, Cardiff University, 2016.

174   C. M. Costanzo, La Sapienza, Rome University, 2018.

175   M. F. Templin, D. H. Edwards and J. V. Holtje, A murein hydrolase is the specific target of bulgecin in Escherichia coli., *J. Biol. Chem.*, 1992, **267**, 20039–20043.

176   A.-M. W. H. Thunnissen, H. J. Rozeboom, K. H. Kalk and B. W. Dijkstra, Structure of the 70-kDa Soluble Lytic Transglycosylase Complexed with Bulgecin A. Implications for the Enzymatic Mechanism1, *Biochemistry*, 1995, **34**, 12729–12737.

177   F. A. S. Alasmary, A. M. Snelling, M. E. Zain, A. M. Alafeefy, A. S. Awaad and N. Karodia, Synthesis and Evaluation of Selected Benzimidazole Derivatives as Potential Antimicrobial Agents, *Molecules*, 2015, **20**, 15206–15223.

178 M. Sako, H. Suzuki, N. Yamamoto, K. Hirota and Y. Maki, Convenient methods for regio-
and/or chemo-selective O-deacylation of taxinine, a naturally occurring taxane
diterpenoid, *J. Chem. Soc. Perkin Trans. 1*, 1998, **0**, 417–422.

179 A. Bandyopadhyay, Target product profile: A planning tool for the drug development.

180 J. P. Hughes, S. S. Rees, S. B. Kalindjian and K. L. Philpott, Principles of early drug
discovery, *Br. J. Pharmacol.*, 2011, **162**, 1239–1249.

181 T. Kaur, A. Madgulkar, M. Bhalekar and K. Asgaonkar, Molecular Docking in Formulation
and Development, *Curr. Drug Discov. Technol.*, 2018, **16**, 30–39.

182 L. G. Ferreira, R. N. Dos Santos, G. Oliva and A. D. Andricopulo, Molecular Docking and
Structure-Based Drug Design Strategies, *Mol. 2015, Vol. 20, Pages 13384-13421*, 2015,
20, 13384–13421.

183 H. Arya and M. S. Coumarb, Lead identification and optimization, *Des. Dev. Nov. Drugs
Vaccines Princ. Protoc.*, 2021, 31–63.

184 V. L. Mahan, Clinical Trial Phases, *Int. J. Clin. Med.*, 2014, **05**, 1374–1383.

185 S. M. Paul, D. S. Mytelka, C. T. Dunwiddie, C. C. Persinger, B. H. Munos, S. R. Lindborg
and A. L. Schacht, How to improve R&D productivity: the pharmaceutical industry's
grand challenge, *Nat. Rev. Drug Discov. 2010 93*, 2010, **9**, 203–214.

186 D. B. Fogel, Factors associated with clinical trials that fail and opportunities for
improving the likelihood of success: A review, *Contemp. Clin. Trials Commun.*, 2018, **11**,
156–164.

187 I. D. Kuntz, J. M. Blaney, S. J. Oatley, R. Langridge and T. E. Ferrin, A geometric approach
to macromolecule-ligand interactions, *J. Mol. Biol.*, 1982, **161**, 269–288.

188 W. Patrick Walters, M. T. Stahl and M. A. Murcko, Virtual screening—an overview, *Drug
Discov. Today*, 1998, **3**, 160–178.

189 F. Lopez-Vallejo, T. Caulfield, K. Martinez-Mayorga, M. A. Giulianotti, A. Nefzi, R. A.
Houghten and J. L. Medina-Franco, Integrating Virtual Screening and Combinatorial
Chemistry for Accelerated Drug Discovery, *Comb. Chem. & High Throughput
Screen.*, 2011, **14**, 475–487.

190 C. Acharya, A. Coop, J. E. Polli and J. Alexander D. MacKerell, Recent Advances in
Ligand-Based Drug Design: Relevance and Utility of the Conformationally Sampled
Pharmacophore Approach, *Curr. Comput. Aided. Drug Des.*, 2011, **7**, 10.

191 A. Andricopulo, L. Salum and D. Abraham, Structure-based drug design strategies in
medicinal chemistry, *Curr. Top. Med. Chem.*, 2009, **9**, 771–790.

192 S. M. Ajjarapu, A. Tiwari, P. W. Ramteke, D. B. Singh and S. Kumar, Ligand-based drug
designing, *Bioinformatics*, 2022, 233–252.

193   G. M. Morris and M. Lim-Wilby, Molecular docking, *Methods Mol. Biol.*, 2008, **443**, 365–382.

194   R. Ferreira De Freitas and M. Schapira, A systematic analysis of atomic protein–ligand interactions in the PDB, *Medchemcomm*, 2017, **8**, 1970–1981.

195   N. Foloppe and R. Hubbard, Towards predictive ligand design with free-energy based computational methods?, *Curr. Med. Chem.*, 2006, **13**, 3583–3608.

196   X. Du, Y. Li, Y. L. Xia, S. M. Ai, J. Liang, P. Sang, X. L. Ji and S. Q. Liu, Insights into Protein-Ligand Interactions: Mechanisms, Models, and Methods, *Int. J. Mol. Sci.*

197   D. B. Kitchen, H. Decornez, J. R. Furr and J. Bajorath, Docking and scoring in virtual screening for drug discovery: methods and applications, *Nat. Rev. Drug Discov. 2004 311*, 2004, **3**, 935–949.

198   E. C. Hulme and M. A. Trevethick, Ligand binding assays at equilibrium: validation and interpretation, *Br. J. Pharmacol.*, 2010, **161**, 1219–1237.

199   L. G. Ferreira, R. N. Dos Santos, G. Oliva and A. D. Andricopulo, Molecular docking and structure-based drug design strategies, *Molecules*, 2015, **20**, 13384–13421.

200   A. Scarpino, G. G. Ferenczy and G. M. Keserü, Comparative Evaluation of Covalent Docking Tools, *J. Chem. Inf. Model.*, 2018, **58**, 1441–1458.

201   C. Sotriffer, Docking of Covalent Ligands: Challenges and Approaches, *Mol. Inform.*, 2018, **37**, 1800062.

202   A. Q. K. Oyedele, A. T. Ogunlana, I. D. Boyenle, A. O. Adeyemi, T. O. Rita, T. I. Adelusi, M. Abdul-Hammed, O. E. Elegbeleye and T. T. Odunitan, Docking covalent targets for drug discovery: stimulating the computer-aided drug design community of possible pitfalls and erroneous practices, *Mol. Divers. 2022*, 2022, **1**, 1–25.

203   H. M. Kumalo, S. Bhakat and M. E. S. Soliman, Theory and applications of covalent docking in drug discovery: merits and pitfalls, *Molecules*, 2015, **20**, 1984–2000.

204   G. Klebe, Virtual ligand screening: strategies, perspectives and limitations, *Drug Discov. Today*, 2006, **11**, 580–594.

205   D. E. Koshland, The Key–Lock Theory and the Induced Fit Theory, *Angew. Chemie Int. Ed. English*, 1995, **33**, 2375–2378.

206   D. E. Koshland, CORRELATION OF STRUCTURE AND FUNCTION IN ENZYME ACTION, *Science*, 1963, **142**, 1533–1541.

207   J. D. Durrant and J. A. McCammon, Computer-Aided Drug-Discovery Techniques that Account for Receptor Flexibility, *Curr. Opin. Pharmacol.*, 2010, **10**, 770.

208   V. Salmaso and S. Moro, Bridging Molecular Docking to Molecular Dynamics in Exploring Ligand-Protein Recognition Process: An Overview, *Front. Pharmacol.*

209   F. Jiang and S. H. Kim, 'Soft docking': matching of molecular surface cubes, *J. Mol. Biol.*, 1991, **219**, 79–102.

210   J. D. Durrant and J. A. McCammon, Molecular dynamics simulations and drug discovery, *BMC Biol.*, 2011, **9**, 1–9.

211   O. Trott and A. J. Olson, AutoDock Vina: improving the speed and accuracy of docking with a new scoring function, efficient optimization, and multithreading, *J. Comput. Chem.*, 2010, **31**, NA-NA.

212   Y. Lu, Y. Wang and W. Zhu, Nonbonding interactions of organic halogens in biological systems: implications for drug discovery and biomolecular design, *Phys. Chem. Chem. Phys.*, 2010, **12**, 4543–4551.

213   E. F. Pettersen, T. D. Goddard, C. C. Huang, G. S. Couch, D. M. Greenblatt, E. C. Meng and T. E. Ferrin, UCSF Chimera—A visualization system for exploratory research and analysis, *J. Comput. Chem.*, 2004, **25**, 1605–1612.

214   E. J. Van Asselt, K. H. Kalk and B. W. Dijkstra, Crystallographic Studies of the Interactions of Escherichia coli Lytic Transglycosylase Slt35 with Peptidoglycan†,‡, *Biochemistry*, 2000, **39**, 1924–1934.

215   L. G. Ferreira, R. N. Dos Santos, G. Oliva and A. D. Andricopulo, Molecular Docking and Structure-Based Drug Design Strategies, *Mol. 2015, Vol. 20,* 2015, **20**, 13384–13421.

216   K. Schöning-Stierand, K. Diedrich, C. Ehrt, F. Flachsenberg, J. Graef, J. Sieg, P. Penner, M. Poppinga, A. Ungethüm and M. Rarey, ProteinsPlus: a comprehensive collection of web-based molecular modeling tools, *Nucleic Acids Res.*, 2022, **50**, W611–W615.

217   G. Wu, Functional amino acids in nutrition and health, *Amino Acids*, 2013, **45**, 407–411.

218   S. Naik, G. Bhattacharjya, B. Talukdar and B. K. Patel, Chemoselective Acylation of Amines in Aqueous Media, *European J. Org. Chem.*, 2004, **2004**, 1254–1260.

219   R. Hirt, F. T. King, R. G. Schmitt, F. E. Jenkins and A. N. Hambly, Acid-Catalyzed Acetylation of Organic Hydroxyl Groups, *Aust. J. Chem*, 1947, **69**, 318–338.

220   C. C. Barker, 91. The dehydration and racemisation of N-acyl-L-aspartic acids by acetic anhydride, *J. Chem. Soc.*, 1953, 453–456.

221   R. Bischoff and H. Schlüter, Amino acids: Chemistry, functionality and selected non-enzymatic post-translational modifications, *J. Proteomics*, 2012, **75**, 2275–2296.

222   J. Ivkovic, C. Lembacher-Fadum and R. Breinbauer, A rapid and efficient one-pot method for the reduction of N -protected α-amino acids to chiral α-amino aldehydes using CDI/DIBAL-H, *Org. Biomol. Chem.*, 2015, **13**, 10456–10460.

223   H. C. Brown, R. Liotta and L. Brener, Hydroboration. 46. The Regio- and Stereochemistry of the Hydroboration of Representative Cyclic Olefins with 9-Borabicyclo[3.3.1]nonane,

J. Am. Chem. Soc., 1977, **99**, 3427–3432.

224   R. Ding, Y. He, X. Wang, J. Xu, Y. Chen, M. Feng and C. Qi, molecules Treatment of Alcohols with Tosyl Chloride Does Not always Lead to the Formation of Tosylates, *Molecules*, 2011, **16**, 5665–5673.

225   E. Raczuk, B. Dmochowska, J. Samaszko-Fiertek and J. Madaj, Different Schiff Bases-Structure, Importance and Classification, *Molecules*.

226   J. Matthews, Swansea University, 2021.

227   J. H. Billman and A. C. Diesing, Reduction of Schiff Bases with Sodium Borohydride, *J. Org. Chem.*, 1957, **22**, 1068–1070.

228   M. Bartle, Swansea University, 2021.

229   M. Kumar, S. K. Pandey, N. Chaudhary, A. Mishra and D. Gupta, Highly efficient method for the synthesis of substituted benzimidazoles using sodium metabisulfite adsorbed on silica gel, *Results Chem.*, 2022, **4**, 100403.

230   C. Johnson-Hortop, Swansea University, 2022.

231   Z. Bell, J. M. Bell, D. G. Kubler, P. Sartwell and R. G. Zepp2<í, Acetal Formation for Ketones and Aromatic Aldehydes with Methanol1.

232   P. Mitchell, Swansea University, 2020.

233   Disk Diffusion Testing | Antimicrobial Susceptibility Test Methods: Dilution and Disk Diffusion Methods.

234   J. H. Hash, Measurement of bacteriolytic enzymes., *J. Bacteriol.*, 1967, **93**, 1201.

235   J. M. Andrews, Determination of minimum inhibitory concentrations, *J. Antimicrob. Chemother.*, 2001, **48 Suppl 1**, 5–16.

236   Life Sciences Research Network Wales » Roboworm – Increasing the speed of anthelmintic drug discovery Platform, https://www.lsrnw.ac.uk/platform-technologies/roboworm-increasing-the-speed-of-anthelmintic-drug-discovery.

237   K. C. L. Whatley, G. Padalino, H. Whiteland, K. K. Geyer, B. J. Hulme, I. W. Chalmers, J. Forde-Thomas, S. Ferla, A. Brancale and K. F. Hoffmann, The repositioning of epigenetic probes/inhibitors identifies new anti-schistosomal lead compounds and chemotherapeutic targets, *PLoS Negl. Trop. Dis.*, 2019, **13**, e0007693.

238   H. Whitelandid, A. Crusco, L. W. Bloembergid, J. Tibble-Howlings, J. Forde-Thomasid, A. Coghlanid, P. J. Murphy and K. F. Hoffmannid, Quorum sensing N-Acyl homoserine lactones are a new class of anti-schistosomal.

239   B. Ramirez, Q. Bickle, F. Yousif, F. Fakorede, M. A. Mouries and S. Nwaka, Schistosomes: challenges in compound screening.

240   G. Padalino, N. El-Sakkary, L. J. Liu, C. Liu, D. S. G. Harte, R. E. Barnes, E. Sayers, J. Forde-

Thomas, H. Whiteland, M. Bassetto, S. Ferla, G. Johnson, A. T. Jones, C. R. Caffrey, I. Chalmers, A. Brancale and K. F. Hoffmann, Anti-schistosomal activities of quinoxaline-containing compounds: From hit identification to lead optimisation, *Eur. J. Med. Chem.*, 2021, **226**, 113823.

241   H. Whiteland, A. Crusco, L. W. Bloemberg, J. Tibble-Howlings, J. Forde-Thomas, A. Coghlan, P. J. Murphy and K. F. Hoffmann, Quorum sensing N-Acyl homoserine lactones are a new class of anti-schistosomal, *PLoS Negl. Trop. Dis.*, 2020, **14**, e0008630.

242   A. Crusco, C. Bordoni, A. Chakroborty, K. C. L. Whatley, H. Whiteland, A. D. Westwell and K. F. Hoffmann, Design, synthesis and anthelmintic activity of 7-keto-sempervirol analogues, *Eur. J. Med. Chem.*, 2018, **152**, 87–100.

243   A. Viegas, J. Manso, F. L. Nobrega and E. J. Cabrita, Saturation-transfer difference (STD) NMR: A simple and fast method for ligand screening and characterization of protein binding, *J. Chem. Educ.*, 2011, **88**, 990–994.

244   S. Tayyab and S. R. Feroz, Serum albumin: clinical significance of drug binding and development as drug delivery vehicle, *Adv. Protein Chem. Struct. Biol.*, 2021, **123**, 193–218.

245   A. Makriyannis and S. Pavlopoulos, Structural Chemistry Using NMR Spectroscopy, Pharmaceuticals, *Encycl. Spectrosc. Spectrom.*, 2017, 306–315.

246   A. N. L. Batista, J. M. Batista, L. Ashton, V. S. Bolzani, M. Furlan and E. W. Blanch, Investigation of DMSO-induced conformational transitions in human serum albumin using two-dimensional Raman optical activity spectroscopy, *Chirality*, 2014, **26**, 497–501.

247   T. Magsumov, A. Fatkhutdinova, T. Mukhametzyanov and I. Sedov, The Effect of Dimethyl Sulfoxide on the Lysozyme Unfolding Kinetics, Thermodynamics, and Mechanism, *Biomolecules*.

248   E. F. Pettersen, T. D. Goddard, C. C. Huang, G. S. Couch, D. M. Greenblatt, E. C. Meng and T. E. Ferrin, UCSF Chimera--a visualization system for exploratory research and analysis., *J. Comput. Chem.*, 2004, **25**, 1605–1612.

249   W. D. Ihlenfeldt, E. E. Bolton and S. H. Bryant, The PubChem chemical structure sketcher.

250   O. Trott and A. J. Olson, AutoDock Vina: improving the speed and accuracy of docking with a new scoring function, efficient optimization and multithreading, *J. Comput. Chem.*, 2010, **31**, 455.

251   A. H. Williams, R. Wheeler, C. Thiriau, A. Haouz, M. K. Taha and I. G. Boneca, Bulgecin A: The Key to a Broad-Spectrum Inhibitor That Targets Lytic Transglycosylases, *Antibiotics*.

252   A. Fischer, M. Smieško, M. Sellner and M. A. Lill, Decision Making in Structure-Based Drug Discovery: Visual Inspection of Docking Results, *J. Med. Chem.*, 2021, **64**, 2489–2500.

253   M. Friedman, REVIEWS Applications of the Ninhydrin Reaction for Analysis of Amino Acids, Peptides, and Proteins to Agricultural and Biomedical Sciences.

254   R. A. Paveley, N. R. Mansour, I. Hallyburton, L. S. Bleicher, A. E. Benn, I. Mikic, A. Guidi, I. H. Gilbert, A. L. Hopkins and Q. D. Bickle, Whole Organism High-Content Screening by Label-Free, Image-Based Bayesian Classification for Parasitic Diseases, *PLoS Negl. Trop. Dis.*, 2012, **6**, e1762.

255   G. Padalino, I. W. Chalmers, K. F. Hoffmann, A. Crusco, H. Whiteland, R. Baptista, J. E. Forde-Thomas, M. Beckmann, L. A. J. Mur, R. J. Nash, A. D. Westwell and K. F. Hoffmann, Antischistosomal Properties of Sclareol and Its Heck-Coupled Derivatives: Design, Synthesis, Biological Evaluation, and Untargeted Metabolomics, *ACS Infect. Dis.*, 2019, **5**, 1188–1199.

256   H. L. Whiteland, A. Chakroborty, J. E. Forde-Thomas, A. Crusco, A. Cookson, J. Hollinshead, C. A. Fenn, B. Bartholomew, P. A. Holdsworth, M. Fisher, R. J. Nash and K. F. Hoffmann, An Abeis procera-derived tetracyclic triterpene containing a steroid-like nucleus core and a lactone side chain attenuates in vitro survival of both Fasciola hepatica and Schistosoma mansoni, *Int. J. Parasitol. Drugs Drug Resist.*